Aus dem

Universitätsklinikum Düsseldorf

Poliklinik und Funktionsbereich für Rheumatologie

(Direktor: Univ.-Prof. Dr. med. Matthias Schneider)

# Der Stellenwert der Magnet-Resonanz Tomographie für Diagnose, Therapiemonitoring und Prädiktion entzündlich-rheumatischer Gelenkerkrankungen

Habilitationsschrift zur Erlangung der venia legendi für

das Fach Innere Medizin des Fachbereichs Medizin

der Heinrich-Heine-Universität Düsseldorf

vorgelegt von

Dr. med. Philipp Sewerin

Mai 2019

## Inhaltsverzeichnis

# 1 Abkürzungen

| | |
|---|---|
| Anti-CCP AK | Antikörpern gegen zyklische citrullinierte Peptid |
| bDMARD | biological synthetic Disease Modifying Antirheumatic Drug |
| BME | Bone Marrow oedema |
| BSG | Blutsenkungsgeschwindigkeit |
| CRP | C-reaktives Protein |
| CDAI | Clinical Disease Activity Index |
| csDMARD | conventional synthetic Disease Modifying Antirheumatic Drug |
| DAS-28 | Disease Activity Score of 28 Joints |
| KM | Kontrastmittel |
| MRT | Magnet-Resonanz-Tomographie |
| MTX | Methotrexat |
| PD | Power-Doppler |
| RA | Rheumatoide Arthritis |
| RAMRIS | Rheumatoid Arthritis Magnetic Resonance Imaging Score |
| RANKL | Receptor Activator of NF-κB Ligand |
| SDAI | Simple Disease Activity Index |
| T2T | *treat-to-target* |
| tsDMARD | targeted synthetic Disease Modifying Antirheumatic Drug |

## 2 Zusammenfassung

Durch neue Wirkstoffe und Therapiekonzepte haben sich die Möglichkeiten entzündlich-rheumatische Erkrankungen zu behandeln dramatisch geändert. Stand noch vor wenigen Dekaden das Hinauszögern der unvermeidbaren Gelenkzerstörung und der drohenden Invalidität im Vordergrund, so ist heute bei Arthritiden die Krankheitsremission erklärtes Therapieziel. Mit Therapieprinzipien wie „*treat-to-target*" (T2T) werden bereits bei Diagnosestellung klare Therapieziele (in der Regel klinische Remission oder zumindest minimale Krankheitsaktivität) definiert, ihr Erreichen kurzzeitig überprüft, und bei unzureichendem Ansprechen die Therapie nach definierten kurzen (3 – max. sechs Monaten) Zeitintervallen angepasst.

In einem nächsten Schritt sollen die bisher eher global angewandten Therapiestrategien individualisiert werden, das Ziel ist somit eine „personalisierte" Medizin. Dafür haben sich zahlreiche Forschergruppen auf den Weg gemacht prädiktive Faktoren, wenn möglich bereits bei der Diagnosestellung, zu identifizieren. Damit sollen die Patienten, die mit einer sehr hohen Wahrscheinlichkeit nicht auf konventionelle Basistherapien (*conventional synthetic disease modifying antirheumatic drugs* (*csDMARDs*); wie beispielsweise MTX) ansprechen, bereits von Beginn an z.B. mit *b* (*biological*) oder *ts (targeted synthetic) DMARD* behandelt werden und andere, die auch mit *csDMARDs* gut kontrolliert sind, so zu belassen. Auch im Hinblick auf Kosten und Risiken, welche mit modernen antientzündlichen Therapien in der Rheumatologie einhergehen, scheint dieser Ansatz wichtig und unersetzlich.

Neben zahlreichen klinischen und serologischen Parametern, welche in prädiktiven Modellen Therapieansprechen vorher- und voraussagen sollen, rücken insbesondere bildgebende Verfahren in den wissenschaftlichen Fokus. Neben der Sonographie gewinnt dabei die Magnet-Resonanz-Tomographie (MRT) zunehmend an Bedeutung. Gründe hierfür sind zum einen die immer bessere Verfügbarkeit und die damit verbundenen sinkenden Kosten, zum anderen aber auch zahlreiche Möglichkeiten Pathologien verschiedener Kompartimente ohne ionisierende Strahlung erfassen zu können.

Die vorliegende Habilitationsschrift stellt eigene Untersuchungen zusammen, die die Wertigkeit der MRT bei Patienten mit entzündlich-rheumatischen Gelenkerkrankungen für Diagnose, Therapieverlauf und Ansprechen sowie deren prädiktiven Wert erfassen, um diese im Sinne einer personalisierten Behandlung möglichst effektiv und ressourcenschonend einzusetzen.

Die grundlegenden Arbeiten beschäftigten sich mit dem Stellenwert der MRT zur Krankheitseinschätzung bei Patienten mit Arthritiden. Mittels der MRT konnte ich mit meiner Arbeitsgruppe nachweisen, dass bei Patienten mit einer rheumatoiden Arthritis (RA) weiterhin Krankheitsaktivität bestehen kann, sowohl an den Händen als auch an den Füßen, obwohl gutes klinisches Ansprechen dokumentiert wird. Diese stille Krankheitsprogression (*silent progression*) trat bei unerwartet vielen Patienten auf, trotz erreichter guter klinischer Response oder gar Remission. Anhand der MRT Untersuchungen vor Einleitung einer krankheitsmodifizierenden Therapie konnten wir ein Prädiktionsmodel für Patienten mit früher sowie für etablierter RA vor Therapieeskalation entwickeln und publizieren. Dieser von mir initiierte und maßgeblich gestaltete Ansatz war Teil einer neuen Idee der Bewertung der Krankheitsaktivität bei RA Patienten, da klinisch stumme Krankheitsprogression bisher so nicht nachgewiesen wurde, insbesondere nicht bei gutem klinischem Ansprechen. Durch die Arbeiten gewann die MRT für wissenschaftliche Fragestellungen aber auch für die individuelle Prognoseabschätzung eine weiterführende Bedeutung.

Ein weiterer Fokus lag auf der Einführung verkürzter Scoring-Systeme für MRT Untersuchungen bei RA Patienten, da diese trotz zahlreicher Validierungsstudien aufgrund des hohen zeitlichen und personellen Aufwands kaum im klinischen Alltag eingesetzt werden. Darüber hinaus evaluierten wir den Nutzen molekularer MRT-Verfahren, um den Zusammenhang zwischen Knorpelqualität und der lokalen Inflammation bei Patienten mit entzündlich-rheumatischen Gelenkerkrankungen zu beurteilen. Hier konnten wir nachweisen, dass früher Verlust der Knorpelqualität, gemessen mittels molekularer MRT-Sequenzen, prädiktiv für das spätere Therapieansprechen ist und dass das Fortschreiten des Knorpelverlustes durch krankheitsmodifizierende Therapien aufgehalten werden kann. Dynamische MRT-Verfahren, welche das An- und Abflutverhalten von MRT Kontrastmitteln als Marker für das Ausmaß

der lokalen Inflammation abbilden, zeigten, dass dieses mit der Krankheitsaktivität korreliert und ebenfalls prädiktiv für das spätere Therapieansprechen sind. Durch die enge Kooperation, auch im Rahmen von BMBF-geförderten Projekten, konnte ich die bisher nicht in der Rheumatologie etablierten, molekularen MRT-Verfahren erstmals bei RA Patienten einsetzen und evaluieren und habe so bedeutend zur Implementierung der Techniken in wissenschaftliche Protokolle beigetragen.

Die Arbeiten untermauern die Wertigkeit der MRT für Prädiktion und Therapiekontrolle entzündlicher Gelenkerkrankungen; sie leisten einen wichtigen Beitrag für die Implementierung der MRT in den klinischen Algorithmus in der Rheumatologie. Darüber hinaus ergeben sich zahlreiche Ansätze für zukünftige Anwendungsmöglichkeiten der MRT in der Diagnose, der Personalisierung und Therapiekontrolle der RA und anderen entzündlichen Gelenkerkrankungen.

## 3 Literaturangaben der zugrundeliegenden Forschungsarbeiten


1. Buchbender C, **Sewerin P**, Mattes-György K, Miese F, Wittsack H-J, Specker C, Antoch G, Müller HW, Schneider M, Scherer A, Ostendorf B. Utility of combined high-resolution bone SPECT and MRI for the identification of rheumatoid arthritis patients with high-risk for erosive progression. Eur J Radiol. 2013 Feb;82(2):374–9. **Impact Factor 2013: 2.530**

2. Buchbender C, Scherer A, Miese F, **Sewerin P**, Haferkamp A, Brinks R, Wittsack HJ, Antoch G, Schneider M, Ostendorf B. Patterns of magnetic resonance imaging of the foot in rheumatoid arthritis: which joints are most frequently involved? Rheumatol Int. Jul;33(7):1731-6; Impact **Factor 2013: 1.782**

3. Vordenbäumen S, **Sewerin P**, Lögters T, Miese F, Schleich C, Bleck E, Philippski P, Schädel-Höpfner M, Pauly T, Schneider M, Ostendorf B. Inflammation and vascularisation markers of arthroscopically-guided finger joint synovial biospies reflect global disease activity in rheumatoid arthritis. Clin Exp Rheumatol. 2014 Jan 3; Jan-Feb;32(1):117-20. **Impact Factor 2014: 3.046**

4. **Sewerin P,** Buchbender C, Vordenbäumen S, Scherer A, Miese F, Brinks R, Wittsack HJ, Klein S, Schneider M, Antoch G, Ostendorf B. Advantages of a combined rheumatoid arthritis magnetic resonance imaging score (RAMRIS) for hand and feet: Does the RAMRIS of the hand alone underestimate disease activity and progression? BMC Musculoskelet Disord. 2014 Mar 26;15(1):104. **Impact Factor 2014: 2.92**

5. **Sewerin P**, Ostendorf B. New imaging procedures in rheumatology: from bench to bedside. Dtsch Med Wochenschr 1946. 2014 Sep;139(37):1835–41. **Impact Factor 2014: 0.653**

**6.** Vordenbäumen S, Schleich C, Lögters T, **Sewerin P**, Bleck E, Pauly T, Müller-Lutz A, Antoch G, Schneider M, Miese F, Ostendorf B. Dynamic contrast-enhanced magnetic resonance imaging of metacarpophalangeal joints reflects histological signs of synovitis in rheumatoid arthritis. Arthritis Res Ther. 2014 Oct 1; 16(5):452. **Impact Factor 2014: 4.302**

**7.** Müller-Lutz A, Schleich C**, Sewerin P**, Gro J, Pentang G, Wittsack H-J, Antoch G, Schneider M, Ostendorf B, Miese F. Comparison of Quantitative and Semiquantitative Dynamic Contrast-Enhanced MRI With Respect to Their Correlation to Delayed Gadolinium-Enhanced MRI of the Cartilage in Patients With Early Rheumatoid Arthritis. J Comput Assist Tomogr. 2014; Jan-Feb;39(1):64-9. **Impact 2014: 1.744**

**8.** Schleich C, Müller-Lutz A, **Sewerin P**, Ostendorf B, Buchbender C, Schneider M, Antoch G, Ostendorf B. Intra-individual assessment of inflammatory severity and cartilage composition of finger joints in rheumatoid arthritis. Skeletal Radiol. 2015 Apr;44(4):513–8. **Impact 2015: 1.767**

**9.** Schleich C, Buchbender C, **Sewerin P**, Miese F, Aissa J, Brinks R, Schneider M, Antoch G, Ostendorf B. Evaluation of a simplified version of the Rheumatoid Arthritis Magnetic Resonance Imaging Score (RAMRIS) comprising 5 joints (RAMRIS5). Clin Exp Rheumatol. 2015 Mar-Apr;33(2):209-15. **Impact Factor 2015: 2.517**

**10.** Schleich C, Müller-Lutz A, Matuschke F, **Sewerin P**, Sengewein R, Schmitt B, Ostendorf B, Wittsack HJ, Stanke K, Antoch G, Miese F. Glycosaminoglycan chemical exchange saturation transfer of lumbar intervertebral discs in patients with spondyloarthritis. J Magn Reson Imaging. 2015 Oct;42(4):1057-63. **Impact Factor 2015: 3.209**

11. **Sewerin P**, Schleich C, Ostendorf B. Magnetresonanztomografie peripherer Gelenke – up-date 2016. Aktuelle Rheumatol [Internet]. 2016 Aug 11; 42: 399–403 **Impact 2016 0.136**

12. **Sewerin P,** Vordenbaeumen S, Brinks R, Ostendorf B. Prospective MRI score to predict negative EULAR response in patients with rheumatoid arthritis (RA) before therapy-escalation to a biological therapy. Ann Rheum Dis. 2017 Nov;76(11):e44. **Impact Factor 2017: 12.81**

13. **Sewerin P,** Klein S, Brinks R, Hoyer A, Schleich C, Miese F, Blaschke S, Edelmann E, Gao IK, Georgi J, Kellner H, Keyßer G, Lorenz HM, Müller-Ladner U, Pott HG, Schulze-Koops H, Walther M, Schmidt WA, Schneider M, Ostendorf B. REMISSIONPLUS eine Initiative zur Integration moderner Bildgebung in die rheumatologische Versorgung Rückblick, Einblick, Ausblick: Auswertung der Niederfeld-MRT Daten. Aktuelle Rheumatol. 2017 Oct;42(05):432–41. **Impact 2017 0.134**

14. **Sewerin P,** Vordenbaeumen S, Hoyer A, Brinks R, Buchbender C, Miese F, Schleich C, Klein S, Schneider M, Ostendorf B. Silent progression in patients with rheumatoid arthritis: is DAS28 remission an insufficient goal in RA? Results from the German Remission-plus cohort. BMC Musculoskelet Disord. 2017 Apr 19;18(1):163. **Impact Factor 2017: 1.739**

15. **Sewerin P,** Hoyer A, Schneider M, Ostendorf B, Brinks R. Important but incomplete data analysis? Ann Rheum Dis. 2018 Apr;77(4):e18–e18.; Letter; **Impact Factor 2017: 12.81**

16. **Sewerin P,** Hoyer A, Schneider M, Ostendorf B, Brinks R. Inconsistency between Danish incidence and prevalence data about psoriatic arthritis (PsA). Ann Rheum Dis. 2018 Jan 2; annrheumdis-2017-212817.; Letter; **Impact Factor 2018: 12.35**

17. **Sewerin P**, Ostendorf B, Hueber AJ, Kleyer A. Big Data in der Bildgebung. Z Rheumatol. 2018 Apr;77(3):203–8. **Impact Factor 2018: 0.697**

18. **Sewerin P**, Le L, Vordenbäumen S, Schleich C, Sengewein R, Brinks R, Pongratz G, Bleck E, Lesch J, Mansmann U, Schneider M, Ostendorf B. Rheumatoid Arthritis Magnetic Resonance Imaging Score Predicts Therapy Response: Results of the German ArthroMark Cohort. J Rheumatol. 2018 Jun;45(6):753-759. **Impact Factor 2018: 3.470**

19. **Sewerin P,** Müller-Lutz A, Abrar D, Odendahl S, Eichner, M, Schneider, M, Ostendorf B, Schleich C, Prevention of the Progressive Biochemical Cartilage Destruction under Methotrexate Therapy in Early Rheumatoid Arthritis. Clin Exp Rheumatol 2019 Mar-Apr;37(2):179-185. **Impact Factor 2018: 3.201**

20. **Sewerin, P**., Ostendorf, B., Schleich, C. MRI diagnostics in inflammatory joint and spinal diseases: protocols and special sequences: when and for what? Z. Rheumatol. 2018 Aug;77(6):538-548. **Impact Factor 2018: 0.697**

21. **Sewerin P,** Brinks R, Schneider M, Haase I, Vordenbäumen S. Prevalence and incidence of psoriasis and psoriatic arthritis. Ann Rheum Dis. 2019 Feb;78(2):286-287. **Impact Factor 2018: 12.35**

22. **Sewerin P**, Schleich C, Vordenbäumen S, Ostendorf B. Update on imaging in rheumatic diseases: cartilage. Clin Exp Rheumatol. 2018 Sep-Oct;36 Suppl 114(5):139-144. Epub 2018 Oct 1. Review. **Impact Factor 2018: 3.201**

23. Mori V, Sawicki LM, **Sewerin P**, Eichner M, Schaarschmidt BM, Oezel L, Gehrmann S, Bittersohl B, Antoch G, Schleich C. Differences of radiocarpal cartilage alterations in arthritis and osteoarthritis using morphological and biochemical magnetic resonance imaging without gadolinium-based contrast agent administration. Eur Radiol. 2019 May;29(5):2581-2588. doi: 10.1007/s00330-018-5880-6. Epub 2018 Dec 12. **Impact Factor 2018: 4.027**

24. Pongratz G, Lowin T, **Sewerin P**, Zaucke F, Jenei-Lanzl Z, Pauly T, Ostendorf B, Schneider M. Tryptophan metabolism in rheumatoid arthritis is associated with rheumatoid factor and predicts joint pathology evaluated by the Rheumatoid Arthritis MRI Score (RAMRIS). Clin Exp Rheumatol. 2018 Nov 16. [Epub ahead of print] **Impact Factor 2018: 3.201**

25. Frenken M, Schleich C, Brinks R, Abrar DB, Goertz C, Schneider M, Ostendorf B, **Sewerin P.** The value of the simplified RAMRIS-5 in early RA patients under methotrexate therapy using high-field MRI. Arthritis Res Ther. 2019 Jan 14;21(1):21. **Impact Factor 2018: 4.269**

26. **Sewerin P,** Schleich C, Brinks R, Müller-Lutz A, Fichter F, Eichner M, Schneider M, Ostendorf B, Vordenbäumen S. Synovial perfusion assessed by dynamic contrast-enhanced MRI is associated to treatment response, remission, and cartilage quality in rheumatoid arthritis. J Rheumatol. 2019 Mar 15. pii: jrheum.180832. doi: 10.3899/jrheum.180832. **Impact Factor 2018: 3.470**

# 4 Ausführliche Zusammenfassung und Diskussion

## 4.1 Einleitung

In der vorliegenden Habilitationsschrift werden die Möglichkeiten der Magnet-Resonanz-Tomographie (MRT) für die Diagnose, individuellen Risikostratifizierung und Therapiekontrolle mittels spezifischer Scoringsysteme unter der Zuhilfenahme molekularer Bildgebung des Knorpels und der Synovialitis evaluiert.

In den letzten zwei Dekaden haben sich die Möglichkeiten Patienten mit entzündlich-rheumatischen Erkrankungen zu therapieren deutlich verbessert. Durch neue Therapiestrategien (*treat-to-target;* T2T[1]) und neue Wirkprinzipien[2] erreichen unsere Patienten heute früher und häufiger ein adäquates Therapieansprechen und haben langfristig weniger Funktionseinschränkungen, wobei eine stabile Krankheitsremission nur bei vergleichsweise wenigen Patienten erreicht werden kann[3–5]. Gründe hierfür sind häufig eine weiterhin verzögerte Diagnosestellung und fehlende Möglichleiten einer suffizienten Risikostratifizierung[5]. Zahlreiche Studien konnten zeigten, dass eine sehr frühe Therapie (z.B. innerhalb von 6 Wochen nach Symptombeginn) das Outcome und die Remissionsraten deutlich verbessern können[1,6,7].

Eine weitere Bürde stellt die noch unzureichende individuelle Risikostratifizierung von Patienten mit entzündlichen Gelenkerkrankungen dar. So werden in den aktuellen Leitlinien der *European League Against Rheumatism* (EULAR) und des *American College of Rheumatology* (ACR) Patienten mit einer rheumatoiden Arthritis (RA) weiterhin „uniform“ zu Beginn der Therapie (sollten keine entsprechenden Kontraindikationen vorliegen) mit einer *conventional synthetic disease modifying drug* (*csDMARD*; in der Regel Methotrexat (MTX)) behandelt und idealerweise nach einem Zeitintervall von drei bzw. 6 Monaten bei klinischem Nichtansprechen therapieeskaliert (anderes *csDMARD*, Kombinationstherapie aus zwei oder mehreren *csDMARDs* oder *targeted synthetic / biologic (ts/b) DMARDs*; siehe oben)[8]. Hierbei spielt es primär keine Rolle, ob Risikofaktoren für einen ungünstigen Krankheitsverlauf (wie z.B. das Vorliegen

von Erosionen im konventionellen Röntgenbild oder hochtitrige, spezifische Autoantikörper) vorliegen oder nicht.

Wichtige Bausteine für die individuelle Diagnosestellung, Risikostratifizierung und Therapiekontrolle sind dabei bildgebende Verfahren. Die konventionelle Röntgendiagnostik stellt auch heute noch den Goldstandard dar. Sie ist Teil des primären diagnostischen Algorithmus und sollte vor Einleitung der Therapie zur Sicherung der Diagnose (wenngleich sie heute nicht mehr Teil der Klassifikationskriterien ist[9,10]) und Risikostratifizierung (Erosionen im konventionellen Röntgenbild sind prädiktiv für einen progredient-erosiven Krankheitsverlauf[11,12]) durchgeführt werden. Es ist allerdings bekannt, dass konventionelle Röntgenbilder Erosionen erst spät (im Vergleich zu anderen bildgebenden Verfahren wie der MRT oder Sonographie) erkennen und somit für die Frühdiagnostik und für die frühe Einleitung einer Therapie weitestgehend ungeeignet erscheinen[12–14]. Die MRT kann die diagnostische Lücke gerade zu Beginn der Erkrankung schließen und darüber hinaus prognostische Wertigkeit für den weiteren, individuellen Verlauf der Erkrankung bieten, sodass sich die folgenden Forschungsarbeiten primär auf die Evaluation der MRT gerichtet haben.

Die vorliegenden Arbeiten leisten in der aktuellen Diskussion um den sinnvollen und zielgerichteten Einsatz bildgebender Verfahren, insbesondere der MRT, einen wichtigen Beitrag für das Erkennen des Stellenwertes der Verfahren bei Patienten mit entzündlichen Gelenkerkrankungen. Die zugrundeliegenden Publikationen haben das Verständnis neuer Techniken in der MRT peripherer Gelenke und der Implementierung in den klinischen Alltag nachhaltig gefördert.

### 4.1.1 MRT als Instrument zur Therapiekontrolle und Risikostratifizierung

Die MRT ist heute in der Lage hochauflösend, reliabel und valide entzündliche, Knochen-, Knorpel- und Weichteil-Veränderungen bei Patienten mit einer entzündlichen Gelenkerkrankung zu erkennen und abzubilden[15]. Die MRT ist das einzige Verfahren, welches in der Lage ist, Knochenmarködeme zu detektieren, die hochprädiktiv für die Entstehung von Erosionen im Verlauf der Erkrankung sind[16,17]. Durch ihre vielen Vorteile (insbesondere der Verzicht auf ionisierende Strahlung), abnehmende Kosten und die immer bessere und flächendeckendere Verfügbarkeit wird die MRT heute zunehmend auch im klinischen Alltag eingesetzt[18].

Bereits in den frühen 2000er Jahren wurden semiquantitative Scoring-Systeme etabliert, die es erlauben, Untersuchungen, welche an verschiedenen Standorten akquiriert wurden, standardisiert auszuwerten und vergleichbar zu machen[19]. So wurde von Ostergaard *et al*. 2003 der *Rheumatoid Arthritis Magnetic Resonance Imaging Score* (*RAMRIS*)-Score entwickelt und validiert. Dieser erfasst an 23 Gelenkregionen der Hand mit den Subdomänen Synovialitis (Grad 0-3), Knochenmarködeme (Grad 0-3) und Erosionen (Grad 0-3) sowie die Tenovaginitis und „*scored*" diese. In den RAMRIS wurden die Auswertungen der MCP-Gelenke Digitus 2–5, der Carpo-Metacarpophalangealgelenk Digitus 1–5, der Intercarpalgelenke der Handwurzel und das Radiocarpal- und Radioulnargelenk eingeschlossen. Hieraus errechnet sich ein Summenscore, der vergleichbar floride Krankheitsaktivität (Synovialitis und Knochenmarködeme) und Krankheitslast (Erosionen) erfasst[19].

Wie auch viele gängige klinische Scoring-Systeme, zum Beispiel der *Disease Activity Score of 28 Joints* (*DAS-28*), der *Simplified Disease Activity Score* (*SDAI*) oder *Clincal Disease Activity Score* (*CDAI*), erfasst der RAMRIS nicht alle potentiell durch eine RA betroffenen Gelenke, insbesondere nicht die Füße[20]. Es allerdings bekannt, dass gerade die Füße sehr häufig von Folgen entzündlicher Gelenkveränderungen im Rahmen der RA betroffen sind[21–23]. Dies führt dazu, dass heute im klinischen Alltag die Füße, trotz ggf. persistierender Krankheitsaktivität, nicht immer valide erfasst und bewertet werden und so die

Krankheitsaktivität möglicherweise unterschätzt wird[24,25]. Der Stellenwert eines MRT *Scores*, der auch die Füße mit einbezieht, ist hingegen in der MRT nicht validiert worden.

Der RAMRIS hat sich heute in zahlreichen klinischen Studien als valides Instrument zur Erfassung der Krankheitsaktivität etabliert und wurde hierfür bereits in klinischen Studien eingesetzt[26,27]. Wegen des hohen zeitlichen und personellen Aufwandes wird dieser im klinischen Alltag nicht standardmäßig eingesetzt. Dies galt wegen des zeitlichen Aufwands auch für Arthrosonographie. Deshalb wurden verkürzte Scorings-Systeme (US-7 *Score*; auf sieben der klinisch dominanten Hand reduzierter Ultraschall *Score*) entwickelt, welche gut mit einem Ultraschall Gesamtscore aller Finger- und Handgelenke korrelieren[28,29]. Für MRT Untersuchungen wurden bisher keine verkürzten und somit ggf. im klinischen Alltag besser anwendbaren Scoringsysteme validiert, obwohl der hohe Aufwand immer wieder als einer der wichtigsten Gründe für die nicht flächendeckende Implementierung genannt wird.

Darüber hinaus wurde der RAMRIS-*Score* bisher hauptsächlich zur Erfassung der Krankheitsaktivität bzw. zu deren Verlaufskontrolle eingesetzt[30]. Der prädiktive Wert einer ersten MRT Untersuchung vor Einleitung einer krankheitsmodifizierenden Therapie wurde bis dato nicht evaluiert. Dies erscheint in der Zusammenschau der bisher bekannten, bildmorphologisch-prädiktiven Faktoren allerdings sinnvoll. So konnte bereits gezeigt werden, dass die ossäre Destruktion im konventionellen Röntgenbild bei RA-Patienten eng mit einem schlechteren Therapieansprechen bzw. mit einem Fortschreiten der radiologischen Progression korreliert[11,12]. Erosive Veränderungen können allerdings in der MRT deutlich früher erkannt werden und die MRT kann darüber hinaus zahlreiche andere Kompartimente und potentiell von der RA betroffenen Strukturen (artikulär und periartulär) abbilden, die mit dem konventionellen Röntgenbild nicht erfasst werden können[31]. Die Evaluierung der MRT als prädiktives Instrument bei entzündlich-rheumatischen Gelenkerkrankungen war somit naheliegend und ist ein Schwerpunkt der vorgestellten Arbeiten.

### 4.1.2 MRT Sequenzen zur Erfassung der Knorpelqualität

Neben den MRT-Scannern entwickeln sich auch MRT-Techniken selbst stetig weiter. So wurden zahlreiche molekulare bildgebende Verfahren entwickelt und evaluiert. Erste molekulare Messungen der Knorpelqualität wurden bereits in den späten 80er Jahren in MRT-Untersuchungen durchgeführt[32]. In der Folge wurde durch die technische Weiterentwicklung von Scannern und Spulen eine immer detailgenauere, molekulare Darstellung des Gelenkknorpels möglich. Besonders die *Delayed Gadolinium-Enhanced Magnetic Resonance Imaging of Cartilage* (dGEMRIC) Technik ermöglichte eine genaue Evaluation des Knorpels selbst sowie dessen Integrität und wurde durch histologische Validierungsstudien zu einem anerkannten Standard der molekularen Darstellung des Knorpels in der MRT[33,34]. Ein Hauptbestandteil der extrazellulären Matrix des Faser- und hyalinen Gelenkknorpels sind Proteoglykane (PG) sowie Glykosaminoglykane (GAG). Ein verringerter Glykosaminoglykan- bzw. Proteoglykangehalt im Knorpel ist als eines der ersten Zeichen eines manifesten Knorpelschadens zu werten. Dieser Nachweis gelang erstmals an Bandscheiben[35,36]. In der Folge wurde die Technik auch an kleinen Fingergelenken eingesetzt und nachgewiesen, dass hier ebenfalls ein erster, molekularer GAG Verlust bei einer entzündlichen Arthritis einem späteren ossären Schaden vorausgeht[37].

Welche Bedeutung allerdings der molekulare GAG-Verlust für den Krankheitsverlauf bei RA Patienten selbst hat, war bisher unklar und somit ebenfalls Teil der publizierten Studien.

### 4.1.3 Dynamische MRT Sequenzen

Ferner rückten neben der molekularen Darstellung des Gelenkknorpels auch dynamische MRT Sequenzen in den Fokus wissenschaftlicher Untersuchungen, da diese, ähnliche wie die Power-Doppler (PD) Sonographie[38], lokale Perfusion durch die Messung des An- und Abflutverhalten von Kontrastmitteln (KM) in der MRT, und somit indirekt die Vaskularisierung der Synovialis erfassen und abbilden können[39]. So konnte gezeigt werden, dass Gelenke von RA-Patienten mit positivem PD-Signal in der Sonographie und somit einer lokalen Hyperämie durch die vorliegende proliferative Synovialitis eher Krankheitsschübe

erleiden und die betroffenen Gelenke in der Folge ein höheres Risiko für Erosionen aufwiesen[25,38,40]. Die Bedeutung der innovativen dynamischen MRT Sequenzen war hingegen bisher nicht untersucht. Ziel unserer Arbeiten war es nun wiederum den prognostischen Wert der dynamischen MRT-Untersuchung bei Patienten mit einer RA zu untersuchen, um diese als Teil einer personalisierten Risikostratifizierung einsetzten zu können.

## 4.2 Untersuchungen und Ergebnisse

### 4.2.1 MRT als Instrument zur Therapiekontrolle und Risikostratifizierung

Durch die Einführung und Validierung neuer Therapiestrategien ist klargeworden, dass eine frühe Therapieeinleitung und Kontrolle der Krankheitsaktivität essentiell für das Outcome der Patienten mit entzündlichen Gelenkerkrankungen ist[1,6]. Die MRT kann sowohl bei einer frühen Differenzierung einer Arthritis unterstützen, bei Kontrolluntersuchungen Veränderungen valide abbilden, aber auch als prognostisches Instrument dienen. Die folgenden Arbeiten haben daher in verschiedenen Ansätzen die MRT mit der Frage nach Prädiktion untersucht. Darüber hinaus sollte durch die Einführung verkürzter Scoring-System der Einsatz im klinischen Alltag erleichtert werden, um die Vorteile dieser Technik auch außerhalb von Klinischen Studien nutzen zu können.

1.) **Sewerin P,** Buchbender C, Vordenbäumen S, Scherer A, Miese F, Brinks R, Wittsack HJ, Klein S, Schneider M, Antoch G, Ostendorf B. Advantages of a combined rheumatoid arthritis magnetic resonance imaging score (RAMRIS) for hand and feet: Does the RAMRIS of the hand alone underestimate disease activity and progression? BMC Musculoskelet Disord. 2014 Mar 26;15(1):104. **Impact Factor 2014: 2.92**

Aus zahlreichen Studien und dem klinischen Alltag war bekannt, dass bei Patienten mit einer RA häufig im Rahmen der Polyarthritis neben den Hand- und Fingergelenken auch die kleinen Fußgelenke betroffen seien können, wobei die lokale Aktivität der Arthritis der Füße nicht zwingend mit der der Hände oder Finger korreliert[21–23].

Ziel der Arbeit war es daher den Stellenwert eines kombiniertes Hand- und Fuß-MRT Protokolls bei Patienten mit einer RA zu untersuchen. Insgesamt wurden 26 seropositive RA Patienten (Nachweis von CCP-AK und/oder RF) in einem Niederfeld-MRT (0,2 Tesla) vor Beginn einer Methotrexat (MTX)-Therapie und nach 12 Monaten untersucht und nach RAMRIS-Kriterien ausgewertet. Zusätzlich zur Untersuchung der klinisch dominanten Hand wurde der klinisch dominante Fuß mittels MRT untersucht, analog dem RAMRIS-Scorings-System bewertet (MTP I-V) und anschließend als gemeinsamer Hand-Fuß-MRT-Score (HaF-Score) ausgewertet. Ergänzend wurden klinisch die Krankheitsaktivität mittels des *Composite Scores Disease activity Score of 28-Joints* (DAS-28) erfasst und deren Veränderung zwischen 0 Monaten (T0) und 6 Monaten (T1) bewertet.

Wir konnten zeigen, dass Veränderungen (Δ) im kombinierten HaF-MRT-Score signifikant mit Veränderungen dem klinischen Therapieansprechen (ΔDAS-28) korrelierten (r = 0.820; 95%-CI 0.633-0.916). Korrelationen zu ΔDAS-28 waren am besten für Veränderungen im Synovitis-Subscore (0.648) und für das Knochenmarködem (0.703). Darüber hinaus korrelierte das ΔDAS-28 signifikant besser mit dem ΔHaF-Score als mit dem klassischen ΔRAMRIS (0.499; 0.139-0.743, p = 0.0368). Alle Patienten mit mindestens moderatem klinischen Therapieansprechen (nach EULAR[41]) (n = 11) wiesen anhaltende MR-

morphologische Zeichen persistierender Krankheitsaktivität auf, darunter fünf Patienten mit neuen Erosionen, drei davon an den Füßen. Obwohl sich klinisch die geschwollenen und druckschmerzhaften Gelenke an den Händen (n=16) und Füßen (n=15) verbesserten, konnte dies nur bei 10 bzw. 9 Patienten im MRT bestätigt werden.

Zusammenfassend konnten wir bei einem großen Anteil der Patienten mit klinischem Therapieansprechen weiterhin MR-morphologische Zeichen einer Arthritis nachweisen. Persistierende Krankheitsaktivität, insbesondere der Füße, wurden in der klinischen Untersuchung mittels DAS-28, aber auch durch den „klassischen" RAMRIS der klinisch dominanten Hand, häufig unterschätzt. Es ist zu beachten, dass es nicht nur zu persistierenden Synovilitiden, sondern auch zu neuen, unwiderruflichen und potentiell funktionsschränkenden ossären Läsionen (Erosionen), vornehmlich der Füße, gekommen war. Die Arbeit unterstreicht den hohen Stellwert der klinischen (und ggf. MR-morphologischen) Untersuchung sowohl der Hände als auch der Füße bei Patienten mit einer RA, da es ansonsten unter Berücksichtigung der routinemäßig eingesetzten Messinstrumente (sei es im klinischen Alltag oder in Studienprotokollen) zu einer Unterschätzung der Krankheitsaktivität und ggf. sogar zu einer Zunahme der Erosions- bzw. Krankheitslast kommen könnte.

2.) Schleich C, Buchbender C, **Sewerin P**, Miese F, Aissa J, Brinks R, Schneider M, Antoch G, Ostendorf B. Evaluation of a simplified version of the Rheumatoid Arthritis Magnetic Resonance Imaging Score (RAMRIS) comprising 5 joints (RAMRIS5). Clin Exp Rheumatol. 2015 Mar-Apr;33(2):209-15. **Impact Factor 2015: 2.517**

Aus den klinischen *Composite-Scores* (z.B. DAS-28[20]) war bekannt, dass verkürzte klinische Scores gut den Krankheitsverlauf der RA erfassen können[42]. Ziel der Arbeit war es daher die Wertigkeit eines auf nur noch 5 Gelenkregionen verkürzten RAMRIS-Scores (RAMRIS-5) zu untersuchten.

In der vorliegenden Arbeit wurden retrospektiv 94 Patienten mit einer RA (62 Frauen; Alter 59 ± 12 Jahren, zwischen 25 - 83 Jahren; Krankheitsdauer 60 ± 90 Monate, mediane Krankheitsdauer: 22 Monate) der REMISSION$^{PLUS}$ Kohorte mittels MRT untersucht[43]. Der verkürzte RAMRIS-5 umfasst fünf Gelenkregionen der klinisch dominanten Hand: MCP-2 und 3, Os capitatum, Os triquetrum und die distale Ulna. In allen Gelenkregionen wurden die aus dem RAMRIS bekannten *Subscores* Knochenmarködem (Grad: 0 - 3), Erosion (Grad: 0 - 10) und Synovialitis (Grad: 0 - 3) bestimmt, lediglich der Synovialitis-*Subscore* der Handwurzelknochen und der distalen Ulna wurde zu einem *Score* zusammengefasst unter Berücksichtigung der interkarpalen und radio-/ulnokarpalen Gelenke. Der RAMRIS-5 wurde zu zwei MRT-Zeitpunkten (Baseline und Verlaufskontrolle 12 Monaten nach Einleitung einer MTX-Therapie) mit dem etablierten RAMRIS verglichen. Die Auswertung ergab eine signifikante Korrelation zwischen RAMRIS-5 und RAMRIS ($r = 0.87$; $p < 0{,}001$) in der Baseline-Untersuchung und Verlaufskontrolle ($r = 0.87$; $p < 0.001$). In der Betrachtung der Subscores zeigte sich eine signifikante Korrelation zwischen RAMRIS-5 und RAMRIS-MCP (Baseline: $r = 0.66$; $p < 0.001$; Verlaufskontrolle: $r = 0.74$; $p < 0.001$) sowie zwischen RAMRIS5 und RAMRIS-Handgelenk (Baseline: $r = 0.72$; $p < 0.001$, Verlaufskontrolle: $r = 0.69$; $p < 0.001$) zu beiden Untersuchungszeitpunkten. Die Zeitdauer der RAMRIS-5 Auswertung betrug zwischen 28 - 55 Sekunden (39.4 ± 9.0) und zwischen 242 - 312 Sekunden für die Analyse des klassischen RAMRIS (278.8

± 20.3; p = 0.001) in der Baseline-Untersuchung. In der Verlaufskontrolle wurden für die RAMRIS5-Auswertung 30 - 53 Sekunden (38.3 ± 8.6) benötigt, für die RAMRIS-Auswertung 240 - 315 Sekunden (277.8 ± 21.0; p = 0.001)[44].

Zusammenfassend konnten wir erstmals einen verkürzten MRT-Score der Hand bei RA Patienten vorstellen, welche sehr gut mit dem klassischen RAMRIS aller 23 untersuchten Gelenkregionen korrelierte. Es zeigte sich eine deutliche Zeitersparnis auf durchschnittlich ca. 39 Sekunden pro Untersuchung. Der neue *Score* könnte die Nutzung und Implementierung der MRT in klinischen Alltag deutlich vorantreiben.

3.) **Sewerin P,** Klein S, Brinks R, Hoyer A, Schleich C, Miese F, Blaschke S, Edelmann E, Gao IK, Georgi J, Kellner H, Keyßer G, Lorenz HM, Müller-Ladner U, Pott HG, Schulze-Koops H, Walther M, Schmidt WA, Schneider M, Ostendorf B. REMISSIONPLUS eine Initiative zur Integration moderner Bildgebung in die rheumatologische Versorgung Rückblick, Einblick, Ausblick: Auswertung der Niederfeld-MRT Daten. Aktuelle Rheumatol. 2017 Oct;42(05):432–41. **Impact 2017 0.134**

Die Initiative Remission$^{PLUS}$ untersuchte multizentrisch den Stellenwert einer Niederfeld-MRT für die für die Therapiekontrolle bei Patienten mit einer RA vor Einleitung oder Umstellung einer antientzündlichen Systemtherapie. Bis heute wird die Therapie von Patienten mit einer RA primär an klinischen Parametern wie druckschmerzhaften und geschwollen Gelenken, häufig im Rahmen von *Composite-Scores* wie dem DAS-28, CDAI oder SDAI untersucht und bewertet. Bereits in Vorarbeiten konnten wir zeigen, dass die klinische Untersuchung allein häufig die Krankheitsaktivität unterschätzt[45].

Insgesamt wurden an acht Zentren in Deutschland Niederfeld-MRT Untersuchungen (0,2 Tesla) der klinischen dominanten Hand von 145 RA-Patienten zu zwei Zeitpunkten (bei Therapieeinleitung oder -umstellung und nach 12 Monaten) durchgeführt. Neben der Bewertung der residuellen Krankheitsaktivität[46] untersuchen wir hier in einer Subgruppe prädiktive Faktoren für das Ansprechen auf eine Biologika-Therapie.

Wir untersuchten mögliche prädiktive Faktoren für das Ansprechen auf einen TNF-Inhibitor bei Patienten mit einer RA (n=29). Fünf dieser 29 Patienten waren nach einem Jahr bezüglich der EULAR-Response Kriterien im Status „poor-responder“ (DAS-28 > 3,2 und/oder Verbesserung des DAS-28 von ≤ 0,6), 24 erzielten einen moderaten oder guten DAS-28 Response[47]. Mit Hilfe eines logistischen Regressionsmodells, welches das Alter, das Vorhandensein von Rheumafaktoren, das Geschlecht und den RAMRIS Gesamtscore zu Studienbeginn berücksichtigte, wurde ein Prädiktionswert errechnet. Aufgrund der kleinen Zahl auswertbarer Patienten wurde ein „bootstrapping“ Verfahren angewendet, bei

welchen die Berechnung 5000-mal simuliert wurde. Es zeigte sich, dass mit einer „area under the curve“ (AUC) von knapp 90 % ein negativer Response mit dem MRT Befund zu T0 voraussagen lässt. Überraschenderweise war eine hohe Krankheitsaktivität (klinisch mittels DAS-28 oder MR-morphologisch mittels RAMRIS) zu Beginn der bDMARD-Therapie protektiv gegen ein mögliches Nichtansprechen (non-response). Niedrige RAMRIS-Scores und somit niedrige MR-morphologisch erkennbare Krankheitsaktivität war mit einer hohen Wahrscheinlichkeit für ein klinischen Nichtansprechen (low- oder non-response) nach 12 Monaten verbunden. Klinisch ist die Voraussetzung für eine Therapieeskalation in der Regel eine hohe klinische Krankheitsaktivität welche mit den beschriebenen *Composite Scores* gemessen werden. Die Ergebnisse deuten an, dass eine Teilgruppe der Patienten mit klinisch hoher Krankheitsaktivität primär über eher „subjektive Parameter“, wie etwa das eigene Krankheitsempfinden oder Schmerz (*Patients global*; Teil der o.g. Kompositscores[20]) eine hohe Krankheitsaktivität aufweist, die sich allerdings nicht zwingend in „objektiveren Verfahren“, wie etwa der MRT, wiederspiegelt. Hierbei ist zu beachten, dass eine bDMARD-Therapie heute nach wie vor 15-20.000€/Jahr kostet. Sollten somit mit nur einem primären MRT die Patienten, die mit einer Wahrscheinlichkeit von über 90% schlecht oder gar nicht auf eine solche hochpreisige Therapie ansprechen, erkannt und damit eine nicht angemessene Therapieeskalation vermieden werden, hätte dies klinisch und ökonomisch einen hohen Impact.

4.) **Sewerin P,** Vordenbaeumen S, Hoyer A, Brinks R, Buchbender C, Miese F, Schleich C, Klein S, Schneider M, Ostendorf B. Silent progression in patients with rheumatoid arthritis: is DAS28 remission an insufficient goal in RA? Results from the German Remission-plus cohort. BMC Musculoskelet Disord. 2017 Apr 19;18(1):163. **Impact Factor 2017: 1.739**

Klinische Remission ist heute das erklärte Therapieziel für Patienten mit einer RA[1]. Für das Erfassen klinischer Remission existieren verschiedene Instrumente, wobei alle Remissionskriterien nahezu keine geschwollenen oder druckschmerzhaften Gelenke sowie ein gutes bis sehr gutes Wohlbefinden des Patienten (*Patients Global*) und nicht (oder kaum) messbare humorale Entzündungszeichen (CRP oder BSG) voraussetzen[5,48,49]. Trotz deutlicher Verbesserungen der therapeutischen Optionen erreichen weiterhin nur vergleichsweise wenige Patienten eine klinische Remission[3,4]. Selbst wenn diese erreicht wird, sichert das keineswegs, dass es hierunter zu keiner (radiologischen) Progression durch die RA kommt[50,51].

Aus diesem Grund haben wir im Rahmen der Remssion$^{PLUS}$ Kohorte Patienten mit einer RA vor Therapieumstellung sowie nach 12 Monaten klinisch (DAS-28 und CRP) und mittels MRT der klinisch dominanten Hand untersucht. Nach 12 Monaten zeigten 71 von 80 Patienten unter einer neu eingeleiteten oder eskalierten antientzündlichen Therapie eine klinische Besserung der Krankheitsaktivität (DAS-28) (T0 Durchschnitt (Ø) 4.96; SD 1.2; DAS28 T4 (12 Monate) Ø 2.6; SD 1.0). 73% der Patienten verbesserten sich ebenfalls im RAMRIS-*Score* (MRT), wobei 24% der Patienten ein Anstieg des RAMRIS *Scores* (somit mehr MR-morphologische Entzündungsaktivität) trotz DAS-28 Verbesserung zeigten.

48% der Patienten, die sich im DAS-28 verbesserten, erreichten eine EULAR-Remission[41]. 41% dieser Patienten (klinische Verbesserung) wiesen nach 12 Monaten mehr Erosionen (RAMRIS Erosions-Subscores) auf als zu Beginn.

Patienten, die sich klinisch verbesserten, aber keinen EULAR-response erreichten (Non-Response (n = 7)), wiesen zu 71.4% mehr Erosionen als zu Therapiebeginn auf. Moderate klinische Responder (n=19) zu 52.6% und selbst Patienten, die gut klinisch respondierten (good Resonder (n=45)), zeigten zu 31.1% mehr Erosionen als zu T0. Betrachtet man selbst die Untergruppe der Patienten die EULAR-Remission und somit das klinisch bestmögliche Therapieansprechen erreichten (n=34), so konnten hier nach 12 Monaten bei 41% der Patienten mehr erosive Veränderungen im Vergleich zu T0 dokumentiert werden[46]. Die vorliegende Arbeit untermauert sehr eindrücklich den Zusammenhang zwischen lokaler Inflammation und einem progressiven Krankheitsverlauf. Hier konnten wir erstmals zeigen, dass ggf. selbst das Therapieziel der klinischen Remission nicht zwingend einen (MR-morphologischen) Stillstand der Erkrankung bedeuten muss. Betrachtet man Patienten die sich klinisch verbesserten aber keine klinischen Response erreichten (was im klinischen Alltag sicher häufig so vorkommt), so weisen 71.4% der Patienten nach einem Jahr mehr erosive Veränderungen auf. Diese beeindruckend hohe Zahl macht sehr deutlich, dass Remission zukünftig nicht nur klinisch definiert werden sollte, sondern ggf. auch andere Parameter, wie etwa die MRT, zu deren Überprüfung hinzugezogen werden sollten.

5.) **Sewerin P**, Le L, Vordenbäumen S, Schleich C, Sengewein R, Brinks R, Pongratz G, Bleck E, Lesch J, Mansmann U, Schneider M, Ostendorf B. Rheumatoid Arthritis Magnetic Resonance Imaging Score Predicts Therapy Response: Results of the German ArthroMark Cohort. J Rheumatol. 2018 Apr 1;jrheum.170797. **Impact Factor 2018: 3.470**

Im Rahmen des multizentrischen, BMBF-geförderten Forschungsverbundes ArthroMark (01EC1009) wurden am Standort Düsseldorf insgesamt 28 Patienten mit einer frühen, seropositiven RA (erfüllten die ACR/EULAR Kriterien für eine RA[10], Krankheitsdauer < 6 Monate (2 – 23 Wochen)) mit dem Nachweis von CCP-AK und/oder RF klinisch (DAS-28/CRP) und mittels Hochfeld MRT (3T) vor, 3 und sechs Monate nach Einleitung einer MTX-Therapie untersucht und mittels RAMRIS „gescored". Ergänzend wurden die serologischen Biomarker RANKL, DKK-1, Osteoprotegrin, MMP-3 und Neuropeptide-Y bei jeder Visite untersucht. Ziel war es den prädiktiven Wert der MRT sowie der o.g. Biomarker für das Erreichen klinischer Response bzw. Remission (DAS-28/CRP) zu untersuchen.

In der Auswertung war Therapieansprechen (klinischer Response nach DAS-28) mit niedrigen Gesamt-RAMRIS-Scores zur T0 sowie mit einem niedrigen RAMRIS-Erosionen-Subscore assoziiert (p=0.03 und 0.019). Somit hatten Patienten mit einem niedrigen RAMRIS-Score und somit geringer MR-morphologisch detektierbarer Inflammation zu T0 höhere Chance nach 3 Monaten klinischen Response zu erreichen. Zudem waren niedrige RANKL-Spiegel vor Einleitung der Therapie prädiktiv für Krankheitsremission nach 6 Monaten. In einer erweiterten multivariaten Analyse waren dann erneut sowohl niedrige RAMRIS-Gesamt-Scores als auch niedrige Synovitis-Subscores im MCP-2 sowie die Kombination aus beiden Parametern prädiktiv für das Erreichen klinischer Response nach drei und sechs Monaten (p-Wert LR-test = 0.035, 0.035 und 0.042). Auch in diesem Modell waren niedrige RANKL-Spiegel mit einer höheren Wahrscheinlichkeit für das Erreichen klinischer Remission assoziiert.

Insgesamt konnten wir erstmals in einer prospektiven Studie demonstrieren, dass der Nachweis von entzündlichen Läsionen im MRT der klinischen dominanten Hand (ausgewertet mittels RAMRIS) mit

einem schlechteren klinischen Therapieansprechen nach drei und sechs Monaten verbunden ist. In unseren Vorarbeiten fanden wir Hinweise dafür, dass genau diese Patienten hingegen mit einer hohen Wahrscheinlichkeit gut eine bDMARD-Therapie mit einen TNF-Inhibitor ansprechen. Die Arbeit belegt somit den hohen Stellenwert einer frühen MRT Untersuchung der Hand für das Erkennen von Patienten mit einem hohen Risiko für eine schlechtes Therapieansprechen, die ggf. zukünftig frühzeitig mit bDMARDs therapiert werden sollten.

6.) Frenken M, Schleich C, Brinks R, Abrar DB, Goertz C, Schneider M, Ostendorf B, **Sewerin P.** The value of the simplified RAMRIS-5 in early RA patients under methotrexate therapy using high-field MRI. Arthritis Res Ther. 2019 Jan 14;21(1):21. doi: 10.1186/s13075-018-1789-3. **Impact Factor 2018: 4.269**

In unseren Vorarbeiten konnten wir bereits den verkürzten RAMRIS-5 Score einführen und evaluieren[44], wobei hierfür eine Niederfeld-MRT Kohorte mit einer bereits etablierten RA diente. Die Wertigkeit des verkürzten Scores für Patienten mit früher RA in den heute nahezu standartmäßig eingesetzten Hochfeld-MRT war hingegen bisher unklar.

Ziel der Arbeit war es daher frühe RA Patienten der BMBF-geförderten ArthroMark Kohorte vor und nach Einleitung einer MTX-Therapie mittels Hochfeld-MRT zu untersuchen[52]. Insgesamt kam es unter der MTX-Therapie erwartungsgemäß sowohl zu einem signifikanten Abfall der klinischen Parameter (DAS-28 und CRP) als auch des RAMRIS-Scores und somit der lokalen Inflammation der Gelenke. Wir konnten dabei eine hohe Korrelation zum verkürzten RAMRIS-5 Scores zu Baseline ($r = 0.838$; $P < 0.001$) und bei den Follow-up Untersuchungen (3 Monate: $r = 0.876$; $P < 0.001$; 6 Monate: $r = 0.897$; $P < 0.001$) nachweisen. Betrachtet man die Subscores des RAMRIS/RAMRIS-5 so zeigte sich stetig eine hohe Korrelation der Parameter Knochenmarködem und Erosion, wobei bei der Domäne Synovialitis eine etwas höhere Veränderung über die Zeit beim RAMRIS-5 erkannt wurde (SRM (RAMRIS) = $0.07 \pm 0.14$; SRM (RAMRIS-5) = $0.34 \pm 0.06$).

In Konklusion konnten wir nachweisen, dass der RAMRIS-5 auch in dieser unabhängigen Kohorte ein geeignetes Instrument ist um Krankheitsaktivität zur erkennen und zu Monitoren und gut mit dem etablierten RAMRIS Gesamtscore korreliert. Gerade im Hinblick auf den steigenden Einsatz der MRT im klinischen Alltag könnte dieser daher ein praxisnahes Tool zur standardisierten Auswertung von MRT Untersuchungen der Hand bei RA Patienten werden.

### 4.2.2 MRT Sequenzen zur Erfassung der Knorpelqualität

Neben dem prognostischen Wert der Scoringsysteme bzw. deren Subscore untersuchten wir die Wertigkeit der Knorpelbildgebung kleiner Fingergelenke bei Patienten mit entzündlichen Gelenkerkrankungen. Die RA geht als potentiell destruktiv-entzündliche Gelenkerkrankung häufig im Verlauf mit erosiven Veränderungen einher[42]. Es ist bekannt, dass diese Erosionen eng mit einer Verschlechterung des Funktionsstatus der betroffenen Patienten verknüpft sind[40,53]. Aus Studien zu degenerativen Gelenkerkrankungen (Arthrose, Osteoarthritis) war bereits bekannt, dass Knorpelschäden häufig manifesten ossären Läsionen vorausgehen[54]. Durch die technische Weiterentwicklung ist es heute möglich im MRT Gelenkknorpel auch an kleinen Gelenken suffizient darzustellen. Der Glykosaminoglykan (GAG) und Proteoglykangehalt des Knorpels kann somit mittels dGEMRIC- oder gagCEST-Technik reliabel und zuverlässig abgebildet werden[55,56]. Ziel der folgenden Arbeiten war es daher den Stellenwert der Knorpelbildgebung bei Patienten mit entzündlichen Gelenkerkrankungen zu untersuchen mögliche klinische Indikationen zu erkennen.

7.) **Sewerin P,** Müller-Lutz A, Abrar D, Odendahl S, Eichner, M, Schneider, M, Ostendorf B, Schleich C, Prevention of the Progressive Biochemical Cartilage Destruction under Methotrexate Therapy in Early Rheumatoid Arthritis. Clin Exp Rheumatol. (Clin Exp Rheumatol. 2018 Jun 7. [Epub ahead of print]; PMID: 29998824)) **Impact Factor 2017: 2.311**

In der vorliegenden Studie wurden 28 Patienten mit einer frühen RA aus der ArthroMark Kohorte prospektiv mittels Hochfeld-MRT (3T) der klinisch dominanten Hand vor Einleitung einer MTX Therapie sowie nach drei und sechs Monaten untersucht und nach RAMRIS ausgewertet. Ergänzend wurden zu allen Zeitpunkt CRP und DAS-28 erhoben. In der Folge wurden die MCP Gelenke 2 und 3 nach der Schwere des Synovialitis-Subscores in das schwerer und weniger schwer betroffene Gelenk dichotomisiert, wobei Gelenke mit höheren Synovialitis Subscores (im RAMRIS) mit geringen dGEMRIC-Indices und somit einem geringen GAG und Proteoglykan Gehalt in Verbindung standen ($p = 0.002$). In der Folge wurde bei allen Patienten eine MTX-Therapie eingeleitet. In den Follow-up Untersuchungen zeigte sich ein signifikanter Rückgang der lokalen Inflammation (Synovialitis-Subscore) und des DAS-28. Die dGEMRIC Werte blieben konstant, wobei sich die initial erniedrigten Werte des stärker betroffenen Gelenkes denen des weniger schwer betroffenen Gelenkes anglichen[57].

Die Arbeit unterstrich somit das Konzept der frühen Verschlechterung der Knorpelqualität auch bei entzündlichen Gelenkerkrankungen, wobei diese im direkten Zusammenhang zur lokalen Inflammation stehen. Hinzukommend konnten wir erstmals zeigen, dass MTX bei dieser Kohorte von Patienten mit sehr früher RA sowohl klinisch (DAS-28) als auch MR-morphologisch (RAMRIS) und auf molekularer MR-Ebene (dGEMRIC) in der Lage ist, Inflammation zu stoppen und sogar die Knorpelintegrität zu verbessern. Die Arbeit untermauert somit das Konzept einer möglichst frühen Therapie der RA, um ossären Spätfolgen und damit verbundener, drohender Funktionseinschränkung entgegen zu wirken.

8.) **Sewerin, P**., Schleich, C., Vordenbäumen, S., Ostendorf, B. Update on imaging in rheumatic diseases: cartilage. Clin. Exp. Rheumatol. 36 114, 139–144 (2018). **Impact Factor 2018: 3.201**

Vorarbeiten wurde nachgewiesen, dass der Verlust von Knorpelqualität eine sehr frühe Pathologie bei der RA darstellt[37,58]. In der Folge konnten wir ebenfalls zeigen, dass dieser Verlust durch den sehr frühen Einsatz von MTX gestoppt werden konnte[57]. Die dGEMRIC-Technik ist, um die Knorpelintegrität abbilden zu können, auf den Einsatz von KM angewiesen[33]. Um nun in einem klinischen Protokoll, in welchem ebenfalls der Einsatz von KM nötig ist, um die entzündliche Synovialitis quantifizieren zu können, ergänzend dGEMRIC Techniken anwenden zu können, musste somit KM in doppelter Dosis angewendet werden. Durch neue Erkenntnisse aus *post-mortem* Studien, in welchen bei Patienten mit zahlreichen MRT Untersuchungen (mit KM) im Gehirn Gadolinium (welcher essentieller Bestandteil der gängigen KM ist) nachgewiesen und das Ausmaß der Ablagerungen mit der des verabreichten KM korrelierte, geriet der Einsatz von KM in Diskussion[59]. Der Einsatz der für die Knorpelbildgebung notwendigen doppelten KM-Dosis wurde somit obsolet. Aus diesem Grund stellten wir hier KM-freie Sequenzen, sogenannte gagCEST (*Chemical exchange saturation transfer imaging on glycosaminoglycans*) Sequenzen vor, welche erstmals in der Lage waren KM-frei Knorpel auch an kleinen Fingergelenken zu erfassen[56]. Hierbei wird spezifisch die Radiofrequenzstrahlung von gelösten Protonen durch zunehmende Sättigung des Wassersignals als Folge des chemischen Austausches detektiert. Bei diesem Austausch kommt es zu einem Magnetisierungstransfer. Die austauschbaren Protonen befinden sich an den Glycosamingylcanen (GAG) des Knorpels sowohl als Hydroxyd-(OH) als auch als Amid-(NH) Gruppen. Die Spins dieser Protonen werden gesättigt und die Sättigung mittels chemischen und elektromagnetischen Austausches auf die Wasserprotonen übertragen. Es folgt eine Erhöhung des Kontrastes um ca. den Faktor 100. Da jede GAG-Einheit eine NH- und drei OH-Gruppen besitzt, kann die GAG-Konzentration im Knorpel mittels CEST bestimmt werden (*gagCEST*).

Neben der peripheren Arthritis konnten wir diese Technik ebenfalls an den Bandscheibenfächern der Wirbelsäule einführen[56,60,61], wobei bei Patienten mit degenerativen Wirbelsäulenveränderungen bereits signifikant reduzierter GAG Gehalt festgestellt werden konnte.

Die Arbeit konnte zusammenfassend die Bedeutung der Knorpelintegrität bei entzündlichen und teilweise auch degenerativen Gelenk- und Wirbelsäulenerkrankungen herausarbeiten, wobei im Rahmen der aktuellen Diskussion um den Einsatz von KM auch Techniken eingeführt wurden, die zukünftig eine KM-freie Darstellung von Knorpel- und Bandscheibenfächern möglich machen.

### 4.2.3 Dynamische MRT Sequenzen

Moderne MRT Scanner können mit entsprechenden, spezifischen Sequenzen nicht nur hochauflösend morphologische Strukturen, sondern auch auf molekularer Ebene Knorpelqualität darstellen. Ergänzend können heute dynamische MRT Sequenzen eingesetzt werden, welche durch eine Vielzahl von Bildern in sehr kurzen Zeitintervallen das An- und Abflutverhalten von KM zur Darstellung bringen[62]. So konnte nachgewiesen werden, dass ähnlich wie bei der Powerdoppler (PD) Sonographie das Perfusions-Signal der dynamischen MRT mit dem Ausmaß der Synovialtis (auch histologisch) korreliert[63]. Auf Grundlage dieser Erkenntnisse untersuchten wir die Wertigkeit solcher, dynamischer MRT-Sequenzen und deren Korrelation zur Krankheitsaktivität zum einen und einer möglichen Korrelation zum Therapieansprechen zu anderen zu validieren.

**9.)** Müller-Lutz A, Schleich C**, Sewerin P**, Gro J, Pentang G, Wittsack H-J, Antoch G, Schneider M, Ostendorf B, Miese F. Comparison of Quantitative and Semiquantitative Dynamic Contrast-Enhanced MRI With Respect to Their Correlation to Delayed Gadolinium-Enhanced MRI of the Cartilage in Patients With Early Rheumatoid Arthritis. J Comput Assist Tomogr. 2014; **Impact 2015: 1.744**

In der vorliegenden Studie haben wir den Zusammenhang der lokalen Synovialitis (Synovialtis-Subscore des RAMRIS und der dynamischen MRT) mit dem lokalen Knorpelverlust der MCP Gelenke bei Patienten mit einer frühen RA analysiert. Hierfür wurden 15 Patienten mit einer führen RA (Krankheitsdauer <6 Monate) aus der ArthroMark Kohorte (BMBF-gefördertes Konsortium) vor Einleitung einer MTX-Therapie mittels Hochfeld-MRT der klinischen dominanten Hand untersucht und nach RAMRIS ausgewertet[19]. Ergänzend wurden dynamische MRT Untersuchungen mittels *dynamic contrast-enhanced* (DCE) angefertigt und mit der dGEMRIC-Technik die Knorpelqualität evaluiert. Hierbei zeigte sich eine signifikante Korrelation der dynamischen MRT Parameter und der Synovialitis-Subscore (MCP-2 als Surrogat-Gelenk). Zudem bestand eine negative Korrelation zwischen dem Ausmaß der lokalen Inflammation (dynamische Sequenzen) und der lokalen Knorpelqualität der MCP Gelenke. Die gewonnenen Erkenntnisse konnten erstmals MR-morphologisch den Zusammenhang zwischen einer quantifizierbaren Auswertung der Synovialitis mit der Knorpelqualität nachweisen, der pathophysiologisch angenommen wird. Neu war zudem, dass unterschiedliche bei gleichen Synovialitis Subscore im RAMRIS unterschiedliche An- und Abflutverhalten mittels der dynamischen MRT erkannt wurden, was bedeutet, dass die gleiche Synovialtis (Grade) somit unterschiedlich stark vaskularisiert seien kann. Welchen prognostischen Wert diese Unterschiede haben lässt sich allerdings noch nicht sagen[64].

Somit konnten wir einen direkten morphologischen Zusammenhang zwischen der Inflammation in der dynamischen MRT und der Knorpelqualität der MCP Gelenke bei frühen RA Patienten nachweisen. Die

Daten unterstreichen das Konzept eines primären Knorpelschadens noch deutlich vor ossären Läsionen, welche direkt mit der MR-morphologisch nachweisbaren Entzündungsaktivität zusammenhängen.

10.) **Sewerin P,** Schleich C, Brinks R, Müller-Lutz A, Fichter F, Eichner M, Schneider M, Ostendorf B, Vordenbäumen S. Synovial perfusion assessed by dynamic contrast-enhanced MRI is associated to treatment response, remission, and cartilage quality in rheumatoid arthritis. J Rheumatol. 2019 Mar 15. pii: jrheum.180832. doi: 10.3899/jrheum.180832. **Impact Factor 2018: 3.470**

In unseren Vorarbeiten zur dynamischen MRT bei RA Patienten konnten wir bereits einen signifikanten Zusammenhang zwischen dem Ab- und Abflutverhalten der KM und der lokalen Inflammation in der MRT der Hand nachweisen[63,64]. Der prognostische Wert der Untersuchung war allerdings bisher nicht bekannt. Das Ziel war es daher den diesen zu untersuchen. Hierfür wurden frühe RA Patienten vor sowie 3 und sechs Monate nach Einleitung einer MTX-Therapie mittels Hochfeld-MRT der klinisch dominanten Hand untersucht. Wir konnten zeigen, dass das Ausmaß der lokalen Inflammation in den MCP Gelenken II und III gemessen mittels dynamischer MRT signifikant mit dem klinischen Therapieansprechen (Response und Remission) nach 3 und sechs Monaten korrelierte ($p<0.05$). Gleiches galt für die Knorpelqualität gemessen mittels dGEMRIC MRT. Auch hier ließ sich eine signifikante Assoziation zwischen der dynamischen MRT und der Knorpelqualität nach 3 und sechs Monaten erkennen ($p<0.004$), wobei eine erhöhte lokale Perfusion prädiktiv für einen Knorpelverlust war[65].

Wir konnten somit erstmals nachweisen, dass die dynamischen MRT Sequenzen nicht nur suffizient die lokale Inflammation wiederspiegeln können, sondern auch prädiktiv für das Therapieansprechen nach 3 und sechs Monaten bei frühen RA Patienten sind. Neben den klinischen und laborchemischen Parametern sind somit dynamische MRT Sequenzen ein mögliches Instrument um Hochrisiko Patienten frühzeitig zu erkennen und möglicherweise zukünftig angepasst zu therapieren.

# 5 Diskussion

Die MRT ist in Deutschland fast überall verfügbar und kann, soweit klinisch indiziert, bei zahlreichen Indikationen eingesetzt werden. Die vorliegende Arbeit stellt die zahlreichen Möglichkeiten der MRT für die Diagnose und Therapiekontrolle bei RA Patienten dar. Die hiermit aufkommende Frage ist somit, ob nicht jeder RA Patient bei der Diagnosestellung ein MRT bekommen sollte, um das persönliche Risiko und somit auch den therapeutischen Algorithmus vorzugeben. Diese Aussage ist sicher gewagt, soll aber in der folgenden Diskussion erhärtet werden.

Bildgebende Verfahren haben heute in der Rheumatologie sowohl bei der Diagnosestellung als auch bei der Verlaufskontrolle und zunehmend auch der Risikostratifizierung ihren festen Stellenwert. In den 1987 veröffentlichen Klassifikationskriterien der RA waren typische Erosionen im konventionellen Röntgenbild Teil des diagnostischen Algorithmus[66], wobei diese unwiderruflichen ossären Schaden dokumentieren und somit für die Früherkennung ungeeignet sind. In der Folge wurde erkannt, dass erosive Veränderungen in der MRT solchen im konventionellen Röntgenbild viele Jahre vorausgehen[31,67].

## 5.1 MRT als Instrument zur Prädiktion und Therapiekontrolle

Unsere Arbeiten konnten die Bedeutung der MRT als prädiktives Instrument bei RA Patienten in zahlreichen Studien untermauern. Den Stellenwert einer frühen MRT Untersuchung der Hand konnten wir im Hochfeld-MRT in einer prospektiven, BMBF-geförderten Studie (ArthroMark) untersuchen und publizieren. Durch die stetige Weiterentwicklung der MRT-Scanner selbst und auch der Auswertungstools werden die Untersuchungen heute immer sensitiver, auch da meistens als „Hochfeld-MRT“ (1,5-3 Tesla) durchgeführt. Dies gilt auch für Patienten mit einer sehr frühen RA, wobei der prospektive Wert einer MRT der Hand bei diesen Patienten vor Einleitung einer MTX-Therapie durch uns fokussiert untersucht wurde. Die Auswertung konnte nachweisen, dass zu Beginn der Therapie hohe RAMRIS-Gesamt-*Scores* und hohe Synovialitis-*Scores* des MCP-2 Gelenkes mit einer geringen Wahrscheinlichkeit für klinischen Response (DAS-28) assoziiert sind, solche Patienten also mit einer hohen Wahrscheinlichkeit

unzureichend gut auf eine *csDMARD* Therapie (wie beispielweise MTX) ansprechen. Wir konnten konkordant dazu nachweisen, dass lokale Inflammation, gemessen mittels dynamischer MRT, ebenfalls mit einem schlechten Therapieoutcome bei *csDMARDs* assoziiert war[65]. Patienten, die hohe Perfusionswerte der MCP Gelenke in der MRT und somit viel lokale Inflammation aufwiesen, hatten eine signifikant schlechtere Chance klinische Remission zu erreichen, welche heute sicher das klare Therapieziel darstellt. Dies galt auch für die Knorpelqualität, welche erstens mit der lokalen Inflammation negativ assoziiert war und zweitens zu einem schlechteren Therapieoutcome führte[57], wobei alle drei beschriebenen Domänen (morphologische Parameter des RAMRIS, dynamische MRT und Knorpelbildgebung) in einer einzigen Sitzung durchgeführt wurden. Vergleichbare Ergebnisse konnten auch andere Forschungsgruppen präsentieren. So wiesen Tamai *et al*. jüngst nach, dass hohe RAMRIS-*Scores* prädiktiv für ein negatives radiologisches Outcome und somit höhere Erosionslast nach einem Jahr waren[68]. Gleiches gilt für sehr frühe oder gar noch undifferenzierte Arthritiden. Mankia *et al.* wiesen nach, dass frühe lokale Inflammation in der MRT der Hand bei noch undifferenzierten Patienten mit einer erheblichen Steigerung des Risikos für die Entwicklung einer RA einhergehen[69].

Im Gegensatz dazu konnten wir in der REMISSION$^{PLUS}$ Kohorte zeigen, dass niedrige RAMRIS Gesamtwerte prädiktiv für ein schlechtes Therapieansprechen auf TNF-alpha Inhibitoren waren[70]. Dies bedeutet, dass solche Patienten ggf. erst gar nicht mit hochpreisigen *b*- oder *tsDMARDs* therapiert werden sollten, da die Chance ein adäquates Ansprechen zu erreichen gering ist. Diese Erkenntnisse lassen den Rückschluss zu, dass Patienten mit hoher Krankheitsaktivität sehr frühzeitig mit einen *bDMARD* (z.B. TNF-alpha Inhibitoren) oder ggf. auch mit einem *tsDMARD* therapiert werden sollten, da die Chancen auf ein *csDMARD* anzusprechen gering, auf ein *bDMARD* jedoch vergleichsweise gut sind. Darüber hinaus muss erwähnt werden, dass eine Verzögerung des Erreichens eines guten klinischen Ansprechens wiederum mit einem schlechteren, langfristigen Therapieansprechen in Verbindung steht. Eine frühe und zielgerichtete Therapie ist somit unabdingbar[71].

Neben dem prädiktiven Wert einer frühen MRT Untersuchung zu Diagnosestellung konnten wir nachweisen, dass die MRT im Verlauf ein wichtiges Tool ist um die Krankheitsaktivität zu dokumentieren. Wir wissen, dass persistierende lokale Inflammation mit einem progressiven Krankheitsverlauf einhergeht[1,6]. Das Erreichen klinischer Remission ist daher klares Ziel unserer Therapie[6]. In unseren Arbeiten konnten wir nachweisen, dass trotz klinischer Remission weiterhin in der sensitiven MRT Inflammation nachweisbar blieb, welche im Verlauf zu einer zunehmenden Erosionslast führte. Dies galt sowohl beim Einsatz der Niederfeld-MRT[72] als auch der Hochfeld-MRT[46]. Bis zu 40% der Patienten in klinischer Remission (also dem klar formulierten Therapieziel) wiesen nach 6 bzw. 12 Monaten weiterhin (subklinische) Inflammation in der MRT auf und entwickelten neue Erosionen. Diese Befunde unterstreichen, dass die MRT nicht nur initial zur Prognoseabschätzung, sondern auch im Verlauf zur Kontrolle der eigenen klinischen Einschätzung eingesetzt werden kann. Auch andere Gruppen konnten nachweisen, dass sensitive bildgebende Verfahren, wie etwa die Sonographie, Patienten mit subklinischer und im Verlauf progressiver RA erkennen[73], sodass der regelhafte Einsatz sicherlich erwogen werden sollte.

Die Relevanz dieser Befunde ist in der aktuellen Diskussion um den zielgerichteten Einsatz der teilweise sehr hochpreisigen *b*- und *tsDMARDs* (bis 25.000€ Jahrestherapiekosten) von höchster Relevanz. Dies gilt zum einen individuell für den Patienten, da alle Therapie mit potentiellen Nebenwirkungen und Gefahren verknüpft sind und nur dann angewendet werden sollten, wenn eine angemessene Chance für ein gutes Therapieansprechen vorliegt. Zum anderen sind solche Verfahren auch ganz ohne Frage für einen suffizienten und somit wirtschaftlichen Einsatz der Ressourcen unabdingbar. Somit ist es unter Berücksichtigung der vorliegenden Daten heute sinnvoll und zielführend vor der Einleitung einer ersten Therapie bei früher RA ein MRT der Hand und somit das Risiko für schlechtes Therapieansprechen zu quantifizieren und auch im Verlauf das Therapieansprechen bildmorphologisch zu überprüfen.

## 5.2 MRT des Fußes

Das Phänomen der subklinischen Inflammation lässt sich ebenfalls am Fuß erkennen. Das Therapieziel ist die klinische Remission, welche in der Regel mit klinischen *Composite-Scores* gemessen wird. Fast alle validierten *Scorings*-Systeme sparen die Füße , welche vergleichbar häufig und schwer wie die Hände und Finger von der RA betroffen sind, aus[42,74]. Aus früheren MRT Arbeiten unserer Arbeitsgruppe war bekannt, dass bis zu 20% der RA Patienten entzündliche Korrelate an den Füßen in der MRT aufwiesen[23]. Aus diesem Grund untersuchten wir den Stellenwert eines kombinierten Hand- und Fuß-MRT-*Scores* bei RA Patienten. Hierbei konnten wir nachweisen, dass bei Patienten trotz klinischem Ansprechen oder gar klinischer Remission, vor allem an den Füßen weiterhin entzündliche Korrelate nachweisbar waren. Im Verlauf kam es bei persistierender Inflammation zu einer Zunahme der Erosionslast, wiederum insbesondere der Füße[45]. In der Folge konnten auch andere Arbeitsgruppen publizieren, dass Patienten, insbesondere mit dem Nachweis von CCP-AK und Rheumafaktoren, häufig trotz klinischem Ansprechen im Verlauf weiterhin Zeichen einer Arthritis der Füße aufwiesen[75]. Dies ist umso wichtiger, da bekannt ist, dass Funktionseinschränkungen der Füße einen bedeutsamen Einfluss auf die Lebensqualität haben[76], diese allerdings im klinischen Alltag nicht immer suffizient beachtet werden. Hier können bildgebende Verfahren zukünftig eine herausragende Rolle einnehmen, auch und gerade da die klinische Untersuchung der Sprung- und Zehengelenke häufig herausfordernd ist. Gerade die Diskrepanz der Befunde (Hände vs. Füße) zeigt deutlich, dass hier zwingend Handlungsbedarf besteht um unsere Patienten mit den uns zur Verfügung stehenden therapeutischen Möglichkeiten bestmöglich zu versorgen. Der regelhafte Einsatz der MRT zur weiterführenden Beurteilung der Krankheitsaktivität sollte daher insbesondere bei den Füßen nachhaltig diskutiert werden.

## 5.3 Implementierung durch verkürzte Scoringsysteme

Neben der Sinnhaftigkeit und der klinischen Relevanz sind häufig auch zeitliche bzw. personelle Ressourcen Gründe für den vergleichsweise sparsamen Einsatz der MRT bei RA Patienten. Um eine

bessere Vergleichbarkeit bei einem überschaubaren zeitlichen Aufwand zu erreichen, stellten wir ein verkürztes Scoring-System für MRT Untersuchungen der Hand vor. Schon von der Arthrosonographie war bekannt, dass verkürzte Scoring-Systeme gut mit einem Gesamt-*Score* aller Gelenke der Hand korrelieren, wenn die wesentlichen Regionen erfasst werden. So wurde der US-7 (Ultrasound-*Score* of 7 *Joints*) eingeführt und heute neben klinischen Studien[25,77] auch regelhaft in der Routine eingesetzt[28]. Wir konnten für die MRT einen verkürzten *Score* vorstellen (RAMRIS-5), welcher gut mit dem Gesamt-RAMRIS korreliert und die Auswertungszeit der Untersuchung signifikant von 278 auf 38 Sekunden reduzieren[44]. Dies galt auch für Patienten mit einer frühen RA unter Verwendung der Hochfeld-MRT. Hier konnten wir nachweisen, dass mit dem RAMRIS-5 auch im Verlauf (nach 3 und sechs Monaten) hohe Korrelationen erreicht werden konnten[52]. Die Möglichkeiten dieser verkürzten Scoringsysteme scheinen gerade für den klinischen Alltag sehr wichtig zu sein. So berichteten Kgoebane *et al.,* dass für den regelhaften Einsatz der MRT außerhalb klinischer Studien der RAMRIS-5 ein sehr wertvolles Tool sein könnte[78]. Gerade in der longitudinalen Beurteilung der Krankheitsaktivität mittels der MRT ist eine Vergleichbarkeit der Untersuchungen essentiell, auch im klinischen Alltag. Somit könnte der RAMRIS-5, gerade im Verlauf um auch möglicherweise vorliegende subklinische Inflammation zu erkennen, ein wichtiger Baustein sein um die Versorgung unserer Patienten weiter zu verbessern. Die immer besseren MRT Techniken könnten sogar dazu führen, dass zukünftig die Betrachtung eines einzelnen Gelenkes durch die Vielzahl der möglichen Informationen einer einzigen MRT Untersuchung die Krankheitsaktivität des gesamten Patienten wiederspiegeln - *Pars pro toto* - und ggf. sogar eine Prognoseabschätzung möglich machen könnte.

## 5.4 Innovative MRT-Techniken

Neben dem grundsätzlichen Einsatz der MRT im klinischen Alltag zur Risikostratifizierung und Therapiekontrolle konnten wir innovative Techniken einführen und evaluieren. So konnten wir standardisierte Protokolle für den klinischen Alltag und die direkte Anwendbarkeit vorstellen[56,79]. Neben der hochsensitiven morphologischen Darstellung der Arthritis durch die MRT rückten molekulare bildgebende Verfahren im MRT in den wissenschaftlichen und zum Teil auch klinischen Fokus. So kann die *dGEMRIC*-Technik heute zuverlässig die Knorpelqualität darstellen, wobei dies auch histologisch verifiziert wurde[33,80,81]. Nimmt der Anteil der GAGs und Proteoglykane ab, führt dies zu einer verringerten lokalen Anlagerung des KM und somit zu einem schwächeren Signal in der *dGEMRIC*[37]. In Vorarbeiten konnten wir zeigen, dass eine frühe Arthritis bereits vor ossären Destruktionen durch die lokale Inflammation zu einem Verlust der Knorpelqualität (*dGEMRIC*-Index) führte[55]. Ob dieser frühe Verlust unter einer immunsuppressiven Therapie mit einem *csDMARD* aufgehalten werden kann, war hingegen bisher nicht untersucht. Im Rahmen der ArthroMark Studie konnten wir nachweisen, dass Patienten bereits zur Diagnosestellung an Gelenken mit einer Synovialitis (Synovialtis-Subscore des *RAMRIS*) signifikant geringe *dGEMRIC*-Indices auswiesen als an solchen mit weniger stark ausgeprägter lokaler Inflammation. Alle Patienten erhielten unmittelbar nach der Diagnose und dem ersten MRT eine *csDMARD*-Therapie mit MTX. Die *dGEMRIC*-Indices blieben unter dieser Therapie im Verlauf (MRTs nach 3 und sechs Monaten) stabil und fielen nicht weiter ab[57]. Diese Erkenntnisse passen gut zu den publizierten Daten von Herz *et al.* Diese konnten auch unter Verwendung der *dGEMRIC*-Technik bei RA Patienten zeigen, dass insbesondere die akut-entzündlichen Parameter in der MRT der Hand (Synovialitis und Knochenmarködeme) mit der Knorpelqualität korrelieren[82]. Hingegen konnten keine Zusammenhänge zwischen bereits bestehenden Erosionen und dem *dGEMRIC*-Index festgestellt werden, sodass auch hier die Knorpelqualität primär durch anhaltende lokale Inflammation beeinträchtigt wird. Neben der *dGEMRIC*-Technik konnten wir auch KM-freie Techniken einführen, die sicherlich zukünftig immer häufiger auch im klinischen Kontext genutzt werden[56,83]. Diese Techniken können

zukünftig bei prädiktiven Modellen ein wichtiger Baustein werden um das individuelle Risiko des Patienten zu quantifizieren und Therapien entsprechend auszurichten.

Hierzu können auch weitere technische Entwicklungen, wie die dynamischen MRT, beitragen. Wir konnten zeigen, dass das Ausmaß der lokalen Synovialitis der MCP Gelenke valide mit der dynamischen MRT quantifiziert werden kann[62]. In einer Pilotstudie konnten wir nachweisen, dass diese dynamischen MRT-Sequenzen auch histologisch mit dem Grad der Synovialitis korrlieren[63]. Die Möglichkeit einen direkten Zusammenhang zwischen dem Ausmaß der Inflammation in der dynamischen MRT mit der Knorpelqualität der MCP Gelenke zu vergleichen war neu. Insbesondere bei den untersuchten, sehr frühen RA Patienten (Krankheitsdauer <6 Monate) konnten wir demonstrieren, dass bereits ein molekularer Knorpelschaden eingetreten war. Darüber hinaus konnten wir sogar intraindividuelle Unterschiede bei gleichen Patienten zum gleichen Zeitpunkt nachweisen. MCP Gelenke mit mehr lokaler Inflammation (dynamisches MRT/ Synovialitis-Subscore) wiesen zum gleichen Zeitpunkt bereits signifikant geringe *dGEMRIC*-Indices und somit eine verminderte Knorpelqualität auf[84]. Darüber hinaus konnten wir in Folgearbeiten wiederum den hohen prädiktiven Wert der dynamischen MRT Sequenzen für das Ziel der klinischen Remission nachweisen[65]. Dabei war eine gesteigerte lokale Perfusion mit einen schlechteren Therapieansprechen nach drei und 6 Monaten assoziiert.

Es wird immer deutlicher, dass ossäre Läsionen im konventionellen Röntgenbild vergleichsweise spät im Krankheitsverlauf auftreten und zahlreiche Zeichen der Erkrankung, sei es in sensitiven morphologischen oder molekularen MRT Techniken, weit vor den knöchernen Pathologien auftreten. Die von uns publizierten Daten waren ein wichtiger Beitrag für die klinische Anwendung molekularer bildgebender Verfahren in der Rheumatologie. Sie waren für viele, auch internationale, Studiengruppen Grundlage für den Einsatz solcher Verfahren zum besseren Verständnis der Pathogenese entzündlicher Gelenkerkrankungen aber auch in klinischen Studien.

## 6 Ausblick

Die vorliegenden Daten und Arbeiten unterstreichen den hohen Stellenwert der MRT bei Patienten mit entzündlichen Gelenkerkrankungen. Sie wird heute zunehmend (wenn auch nicht immer standardisiert) im klinischen Alltag eingesetzt. Die Möglichkeiten, die sie bietet, sind enorm und nahezu überall verfügbar. Was hindert uns daran die MRT vor jeder relevanten Entscheidung einzusetzen? Die vorgestellten Untersuchungen zeigen klar, dass die MRT einen sehr hohen prädiktiven Wert für unsere Patienten aufweist, sei es bei der Diagnosestellung oder auch im Therapieverlauf. Sie kann über die Vielzahl der morphologischen (RAMRIS) und molekularen (Knorpeltechniken und dynamische Sequenzen) Parameter auf verschiedenen Ebenen nicht nur die lokale Inflammation abbilden, sondern auch voraussagen, welche Patienten mit hoher Wahrscheinlichkeit progressiv verlaufen. Wir verstehen sogar, dass sie uns bei konkreten Therapieentscheidungen helfen kann, sei es bei der Frage der Eskalation der Therapie oder ggf. zukünftig auch bei der Frage einer möglichen Deeskalation. Sie kann individuell Patienten identifizieren, die schon frühzeitig eine „höherwertige (-preisige)“ Therapie benötigen. Sie erkennt mit hoher Wahrscheinlichkeit RA-Patienten, die nicht von einer (teils sehr kostenintensiven) Eskalation der Therapie profitieren, ohne das Röntgenstrahlung benötigt wird. Sie ist in der Lage schon bei klinisch noch undifferenzierten Arthritiden Patienten zu erkennen, die mit sehr hohem Risiko eine manifeste RA entwickeln werden.

Künstliche Intelligenz und computerbasierte Algorithmen werden in naher Zukunft den Einsatz und die Informationen bildgebender Verfahren und der MRT nachhaltig verändern. Bereits heute können trainierte Systeme mit einer hohen Präzision schnittbildgebende Verfahren bewerten[85]. Auch in der Rheumatologie werden zeitnah computergesteuerte Algorithmen spezifische Untersuchungen (seien es konventionelle Röntgenbilder oder Schnittbildverfahren) beurteilen[86]. Neben der klinischen Anwendung werden auch in der Forschung neue, nicht mehr zwingend hypothesengetriebene Forschungsansätze möglich. Durch die großen Datenmengen können computerbasiert Muster erkannt werden, die Teil unseres Prädiktionsmodels werden[85–87].

Hier lohnt sich ein Blick über den Tellerrand. In der Onkologie wird heute bereits in vielen Fällen eine personalisierte medizinische Versorgung gewährleistet. Durch spezifische serologische, genetische und bildmorphologische Biomarker werden in vielen Fällen bereits maßgeschneiderte Therapien angeboten. Dies ist sicherlich ein wichtiger nächster Schritt in der Versorgung von Patienten mit entzündlich-rheumatischen Erkrankungen, um einen optimalen Einsatz der zahlreichen therapeutischen Optionen gewährleisten zu können. Dafür werden in der Rheumatologie die Bildgebung und dabei insbesondere dir MRT unverzichtbar sein, da sie schon heute non-invasiv entscheidende Informationen liefert, die auch der geschulte Untersucher in der klinischen Evaluation nicht bekommen kann.

Dennoch müssen einige Aspekte kritisch beleuchtet werden. Bisher sind die meisten Techniken und Protokolle auf den Einsatz von Kontrastmitteln angewiesen. Gerade im Hinblick auf die aktuell sehr kontroverse Diskussion über die Bedeutung der jüngst entdeckten Ablagerungen des Gadolinums im Gehirn in *post-mortem* Studien machen eine kritische Prüfung für jede Untersuchung zwingend notwendig[59], wobei aktuell mit Hochdruck an KM-freien Sequenzen (sei es für morphologische oder molekulare Verfahren) geforscht wird.

Zudem ist ebenfalls sehr klar geworden, dass eine alleinige Entscheidung über die Therapie aufgrund von bildgebenden Verfahren keinen Vorteil gegenüber der klinischen Entscheidung bietet. So wurden verschiedene Studien publiziert, die keinen Vorteil einer sonographisch gesteuerten *treat-to-target* Strategie gegenüber einer klinischen Entscheidung im Verlauf feststellen konnte[88]. Das alleinige Verlassen auf den bildmorphologischen Befund ohne das Hinzuziehen klinischer Expertise scheint hier keinen Vorteil zu bieten, beides sollte daher immer im Zusammenhang interpretiert werden.

Die von mir publizierten Arbeiten waren ein wichtiger Grundstein für nationale und internationale Kooperationen und Anträge. Sie soll Grundlage für die weitere Implementierung aber auch die (Weiter-) Entwicklung innovativer Verfahren sein.

17. McQueen, F. M. & Ostendorf, B. What is MRI bone oedema in rheumatoid arthritis and why does it matter? *Arthritis Res. Ther.* **8,** 222 (2006).
18. Colebatch, A. N. *et al.* EULAR recommendations for the use of imaging of the joints in the clinical management of rheumatoid arthritis. *Ann. Rheum. Dis.* **72,** 804–814 (2013).
19. Østergaard, M. *et al.* OMERACT Rheumatoid Arthritis Magnetic Resonance Imaging Studies. Core set of MRI acquisitions, joint pathology definitions, and the OMERACT RA-MRI scoring system. *J. Rheumatol.* **30,** 1385–1386 (2003).
20. Heegaard, C., Dreyer, L., Egsmose, C. & Madsen, O. R. Test-retest reliability of the disease activity score 28 CRP (DAS28-CRP), the simplified disease activity index (SDAI) and the clinical disease activity index (CDAI) in rheumatoid arthritis when based on patient self-assessment of tender and swollen joints. *Clin. Rheumatol.* **32,** 1493–1500 (2013).
21. McNally, E. G. Ultrasound of the small joints of the hands and feet: current status. *Skeletal Radiol.* **37,** 99–113 (2008).
22. Ostendorf, B., Scherer, A., Mödder, U. & Schneider, M. Diagnostic value of magnetic resonance imaging of the forefeet in early rheumatoid arthritis when findings on imaging of the metacarpophalangeal joints of the hands remain normal. *Arthritis Rheum.* **50,** 2094–2102 (2004).
23. Buchbender, C. *et al.* Patterns of magnetic resonance imaging of the foot in rheumatoid arthritis: which joints are most frequently involved? *Rheumatol. Int.* (2013). doi:10.1007/s00296-012-2648-1
24. Gandjbakhch, F. *et al.* Determining a magnetic resonance imaging inflammatory activity acceptable state without subsequent radiographic progression in rheumatoid arthritis: results from a followup MRI study of 254 patients in clinical remission or low disease activity. *J. Rheumatol.* **41,** 398–406 (2014).
25. Foltz, V. *et al.* Power Doppler ultrasound, but not low-field magnetic resonance imaging, predicts relapse and radiographic disease progression in rheumatoid arthritis patients with low levels of disease activity. *Arthritis Rheum.* **64,** 67–76 (2012).
26. Østergaard, M. *et al.* Significant improvement in synovitis, osteitis, and bone erosion following golimumab and methotrexate combination therapy as compared with methotrexate alone: a magnetic resonance imaging study of 318 methotrexate-naive rheumatoid arthritis patients. *Arthritis Rheum.* **63,** 3712–3722 (2011).
27. Hetland, M. L. *et al.* MRI bone oedema is the strongest predictor of subsequent radiographic progression in early rheumatoid arthritis. Results from a 2-year randomised controlled trial (CIMESTRA). *Ann. Rheum. Dis.* **68,** 384–390 (2009).
28. Backhaus, M. *et al.* Evaluation of a novel 7-joint ultrasound score in daily rheumatologic practice: a pilot project. *Arthritis Rheum.* **61,** 1194–1201 (2009).
29. Backhaus, T. M. *et al.* The US7 score is sensitive to change in a large cohort of patients with rheumatoid arthritis over 12 months of therapy. *Ann. Rheum. Dis.* **72,** 1163–1169 (2013).
30. Østergaard, M. *et al.* The OMERACT Rheumatoid Arthritis Magnetic Resonance Imaging (MRI) Scoring System: Updated Recommendations by the OMERACT MRI in Arthritis Working Group. *J. Rheumatol.* **44,** 1706–1712 (2017).
31. Ejbjerg, B. J., Narvestad, E., Jacobsen, S., Thomsen, H. S. & Østergaard, M. Optimised, low cost, low field dedicated extremity MRI is highly specific and sensitive for synovitis and bone erosions in rheumatoid arthritis wrist and finger joints: comparison with conventional high field MRI and radiography. *Ann. Rheum. Dis.* **64,** 1280–1287 (2005).
32. Lehner, K. B. *et al.* Structure, function, and degeneration of bovine hyaline cartilage: assessment with MR imaging in vitro. *Radiology* **170,** 495–499 (1989).

33. Burstein, D. *et al.* Protocol issues for delayed Gd(DTPA)(2-)-enhanced MRI (dGEMRIC) for clinical evaluation of articular cartilage. *Magn. Reson. Med.* **45,** 36–41 (2001).
34. Burstein, D., Gray, M., Mosher, T. & Dardzinski, B. Measures of molecular composition and structure in osteoarthritis. *Radiol. Clin. North Am.* **47,** 675–686 (2009).
35. Urban, J. P. & McMullin, J. F. Swelling pressure of the inervertebral disc: influence of proteoglycan and collagen contents. *Biorheology* **22,** 145–157 (1985).
36. Urban, J. P. G. & Winlove, C. P. Pathophysiology of the intervertebral disc and the challenges for MRI. *J. Magn. Reson. Imaging JMRI* **25,** 419–432 (2007).
37. Miese, F. *et al.* Molecular imaging of cartilage damage of finger joints in early rheumatoid arthritis with delayed gadolinium-enhanced magnetic resonance imaging. *Arthritis Rheum.* **64,** 394–399 (2012).
38. Jindal, S., Kaushik, R., Raghuvanshi, S., Kaushik, R. M. & Kakkar, R. Gray scale and power Doppler ultrasonographic findings in the assessment of disease activity and their correlation with disease activity parameters in rheumatoid arthritis. *Curr. Rheumatol. Rev.* (2017).
39. Martín Noguerol, T., Luna, A., Gómez Cabrera, M. & Riofrio, A. D. Clinical applications of advanced magnetic resonance imaging techniques for arthritis evaluation. *World J. Orthop.* **8,** 660–673 (2017).
40. Funck-Brentano, T. *et al.* Prediction of radiographic damage in early arthritis by sonographic erosions and power Doppler signal: a longitudinal observational study. *Arthritis Care Res.* **65,** 896–902 (2013).
41. Hetland, M. L. *et al.* Direct comparison of treatment responses, remission rates, and drug adherence in patients with rheumatoid arthritis treated with adalimumab, etanercept, or infliximab: results from eight years of surveillance of clinical practice in the nationwide Danish DANBIO registry. *Arthritis Rheum.* **62,** 22–32 (2010).
42. McInnes, I. B. & Schett, G. The pathogenesis of rheumatoid arthritis. *N. Engl. J. Med.* **365,** 2205–2219 (2011).
43. Ostendorf, B., Scherer, A., Kellner, H. & Backhaus, M. [Project REMISSION(PLUS): clinical and radiological remission : new treatment goals in the management of rheumatoid arthritis]. *Z. Für Rheumatol.* **67,** 707–710, 712–715 (2008).
44. Schleich, C. *et al.* Evaluation of a simplified version of the Rheumatoid Arthritis Magnetic Resonance Imaging Score (RAMRIS) comprising 5 joints (RAMRIS5). *Clin. Exp. Rheumatol.* (2015).
45. Sewerin, P. *et al.* Advantages of a combined rheumatoid arthritis magnetic resonance imaging score (RAMRIS) for hand and feet: Does the RAMRIS of the hand alone underestimate disease activity and progression? *BMC Musculoskelet. Disord.* **15,** 104 (2014).
46. Sewerin, P. *et al.* Silent progression in patients with rheumatoid arthritis: is DAS28 remission an insufficient goal in RA? Results from the German Remission-plus cohort. *BMC Musculoskelet. Disord.* **18,** 163 (2017).
47. Fransen, J., Creemers, M. C. W. & Van Riel, P. L. C. M. Remission in rheumatoid arthritis: agreement of the disease activity score (DAS28) with the ARA preliminary remission criteria. *Rheumatol. Oxf. Engl.* **43,** 1252–1255 (2004).
48. Felson, D. T. *et al.* American College of Rheumatology/European League Against Rheumatism provisional definition of remission in rheumatoid arthritis for clinical trials. *Arthritis Rheum.* **63,** 573–586 (2011).
49. Mierau, M. *et al.* Assessing remission in clinical practice. *Rheumatol. Oxf. Engl.* **46,** 975–979 (2007).
50. Hetland, M. L. *et al.* Radiographic progression and remission rates in early rheumatoid arthritis - MRI bone oedema and anti-CCP predicted radiographic progression in the 5-year

extension of the double-blind randomised CIMESTRA trial. *Ann. Rheum. Dis.* **69,** 1789–1795 (2010).
51. Gandjbakhch, F., Foltz, V., Mallet, A., Bourgeois, P. & Fautrel, B. Bone marrow oedema predicts structural progression in a 1-year follow-up of 85 patients with RA in remission or with low disease activity with low-field MRI. *Ann. Rheum. Dis.* **70,** 2159–2162 (2011).
52. Frenken, M. *et al.* The value of the simplified RAMRIS-5 in early RA patients under methotrexate therapy using high-field MRI. *Arthritis Res. Ther.* **21,** 21 (2019).
53. Bejarano, V. *et al.* Relationship between early bone mineral density changes and long-term function and radiographic progression in rheumatoid arthritis. *Arthritis Care Res.* **64,** 66–70 (2012).
54. Zilkens, C. *et al.* Magnetic resonance imaging and histology of ovine hip joint cartilage in two age populations: a sheep model with assumed healthy cartilage. *Skeletal Radiol.* **42,** 699–705 (2013).
55. Buchbender, C. *et al.* Cartilage quality in rheumatoid arthritis: comparison of T2* mapping, native T1 mapping, dGEMRIC, ΔR1 and value of pre-contrast imaging. *Skeletal Radiol.* **41,** 685–692 (2012).
56. Sewerin, P., Schleich, C., Vordenbäumen, S. & Ostendorf, B. Update on imaging in rheumatic diseases: cartilage. *Clin. Exp. Rheumatol.* **36 Suppl 114,** 139–144 (2018).
57. Sewerin, P. *et al.* Prevention of the progressive biochemical cartilage destruction under methotrexate therapy in early rheumatoid arthritis. *Clin. Exp. Rheumatol.* (2018).
58. Miese, F. R. *et al.* Metacarpophalangeal joints in rheumatoid arthritis: delayed gadolinium-enhanced MR imaging of cartilage--a feasibility study. *Radiology* **257,** 441–447 (2010).
59. Gulani, V. *et al.* Gadolinium deposition in the brain: summary of evidence and recommendations. *Lancet Neurol.* **16,** 564–570 (2017).
60. Schleich, C. *et al.* Value of delayed gadolinium-enhanced magnetic resonance imaging of cartilage for the pre-operative assessment of cervical intervertebral discs: dGEMRIC IN CERVICAL IVDs. *J. Orthop. Res.* **35,** 1824–1830 (2017).
61. Müller-Lutz, A. *et al.* Comparison of B0 versus B0 and B1 field inhomogeneity correction for glycosaminoglycan chemical exchange saturation transfer imaging. *Magma N. Y. N* (2018). doi:10.1007/s10334-018-0689-5
62. Ostergaard, M. *et al.* Quantification of synovistis by MRI: correlation between dynamic and static gadolinium-enhanced magnetic resonance imaging and microscopic and macroscopic signs of synovial inflammation. *Magn. Reson. Imaging* **16,** 743–754 (1998).
63. Vordenbäumen, S. *et al.* Dynamic contrast-enhanced magnetic resonance imaging of metacarpophalangeal joints reflects histological signs of synovitis in rheumatoid arthritis. *Arthritis Res. Ther.* **16,** 452 (2014).
64. Müller-Lutz, A. *et al.* Comparison of Quantitative and Semiquantitative Dynamic Contrast-Enhanced MRI With Respect to Their Correlation to Delayed Gadolinium-Enhanced MRI of the Cartilage in Patients With Early Rheumatoid Arthritis. *J. Comput. Assist. Tomogr.* (2014). doi:10.1097/RCT.0000000000000164
65. Sewerin, P. *et al.* Synovial perfusion assessed by dynamic contrast-enhanced MRI is associated to treatment response, remission, and cartilage quality in rheumatoid arthritis. *J. Rheumatol.* (2019). doi:10.3899/jrheum.180832
66. Arnett, F. C. *et al.* The American Rheumatism Association 1987 revised criteria for the classification of rheumatoid arthritis. *Arthritis Rheum.* **31,** 315–324 (1988).
67. Vlychou, M., Koutroumpas, A., Alexiou, I., Fezoulidis, I. & Sakkas, L. I. High-resolution ultrasonography and 3.0 T magnetic resonance imaging in erosive and nodal hand

osteoarthritis: high frequency of erosions in nodal osteoarthritis. *Clin. Rheumatol.* **32,** 755–762 (2013).
68. Tamai, M. *et al.* Baseline MRI bone erosion predicts the subsequent radiographic progression in early rheumatoid arthritis patients who achieved sustained good clinical response. *Mod. Rheumatol.* **27,** 961–966 (2017).
69. Mankia, K. *et al.* MRI inflammation of the hand interosseous tendons occurs in anti-CCP-positive at-risk individuals and may precede the development of clinical synovitis. *Ann. Rheum. Dis.* (2019). doi:10.1136/annrheumdis-2018-214331
70. Sewerin, P., Vordenbaeumen, S., Brinks, R. & Ostendorf, B. Prospective MRI score to predict negative EULAR response in patients with rheumatoid arthritis (RA) before therapy-escalation to a biological therapy. *Ann. Rheum. Dis.* (2017). doi:10.1136/annrheumdis-2017-211257
71. Verhoeven, M. M. A. *et al.* Effectiveness of Remission Induction Strategies for Early Rheumatoid Arthritis: a Systematic Literature Review. *Curr. Rheumatol. Rep.* **21,** 24 (2019).
72. Sewerin, P. *et al.* REMISSIONPLUS eine Initiative zur Integration moderner Bildgebung in die rheumatologische Versorgung Rückblick, Einblick, Ausblick: Auswertung der Niederfeld-MRT Daten. *Aktuelle Rheumatol.* **42,** 432–441 (2017).
73. de Miguel, E. *et al.* A reduced 12-joint ultrasound examination predicts lack of X-ray progression better than clinical remission criteria in patients with rheumatoid arthritis. *Rheumatol. Int.* **37,** 1347–1356 (2017).
74. Felson, D. T. *et al.* American College of Rheumatology. Preliminary definition of improvement in rheumatoid arthritis. *Arthritis Rheum.* **38,** 727–735 (1995).
75. van Steenbergen, H. W., van Nies, Jessica A. B., Huizinga, T. W. J., Reijnierse, M. & van der Helm-van Mil, Annette H. M. Subclinical inflammation on MRI of hand and foot of anticitrullinated peptide antibody-negative arthralgia patients at risk for rheumatoid arthritis. *Arthritis Res. Ther.* **16,** R92 (2014).
76. Wickman, A. M., Pinzur, M. S., Kadanoff, R. & Juknelis, D. Health-related quality of life for patients with rheumatoid arthritis foot involvement. *Foot Ankle Int.* **25,** 19–26 (2004).
77. Ohrndorf, S. *et al.* Reliability of the novel 7-joint ultrasound score: results from an inter- and intraobserver study performed by rheumatologists. *Arthritis Care Res.* **64,** 1238–1243 (2012).
78. Kgoebane, K., Ally, M. M. T. M., Duim-Beytell, M. C. & Suleman, F. E. The role of imaging in rheumatoid arthritis. *South Afr. J. Radiol.* **22,** (2018).
79. Sewerin, P., Ostendorf, B. & Schleich, C. MRT-Diagnostik bei entzündlichen Gelenk- und Wirbelsäulenerkrankungen: Protokolle und Spezialsequenzen: Wann und wozu? *Z. Für Rheumatol.* **77,** 538–548 (2018).
80. Bashir, A., Gray, M. L., Boutin, R. D. & Burstein, D. Glycosaminoglycan in articular cartilage: in vivo assessment with delayed Gd(DTPA)(2-)-enhanced MR imaging. *Radiology* **205,** 551–558 (1997).
81. Zilkens, C. *et al.* Delayed gadolinium-enhanced magnetic resonance imaging of cartilage (dGEMRIC), after slipped capital femoral epiphysis. *Eur. J. Radiol.* **79,** 400–406 (2011).
82. Herz, B. *et al.* Osteitis and synovitis, but not bone erosion, is associated with proteoglycan loss and microstructure damage in the cartilage of patients with rheumatoid arthritis. *Ann. Rheum. Dis.* **73,** 1101–1106 (2014).
83. Schleich, C. *et al.* Glycosaminoglycan chemical exchange saturation transfer of lumbar intervertebral discs in patients with spondyloarthritis. *J. Magn. Reson. Imaging JMRI* (2015). doi:10.1002/jmri.24877
84. Schleich, C. *et al.* Intra-individual assessment of inflammatory severity and cartilage composition of finger joints in rheumatoid arthritis. *Skeletal Radiol.* **44,** 513–518 (2015).

85. Kansagra, A. P. *et al.* Big Data and the Future of Radiology Informatics. *Acad. Radiol.* **23,** 30–42 (2016).
86. Sewerin, P., Ostendorf, B., Hueber, A. J. & Kleyer, A. Big Data in der Bildgebung. *Z. Für Rheumatol.* **77,** 203–208 (2018).
87. Baron, P. *Big Data für IT-Entscheider: riesige Datenmengen und moderne Technologien gewinnbringend nutzen*. (Hanser, 2013).
88. Haavardsholm, E. A. *et al.* Ultrasound in management of rheumatoid arthritis: ARCTIC randomised controlled strategy trial. *BMJ* **354,** i4205 (2016).

## 8 Danksagung

Ich möchte mich an dieser Stelle bei allen bedanken, die mich auf dem Weg zum Gelingen dieser Arbeit unterstützt haben.

Mein besonderer Dank gilt Herrn Univ.-Prof. Dr. med. Matthias Schneider für die uneingeschränkte Unterstützung und Förderung bei meinen wissenschaftlichen Arbeiten und seine hervorragende klinische Ausbildung.

Außerdem danke ich meinem Freund und Mentor Herrn Prof. Dr. med. Benedikt Ostendorf, der mich von Anfang an begleitet und gefördert hat. Ohne seine Unterstützung wäre diese Arbeit nicht möglich gewesen.

Darüber hinaus danke ich meinen Kolleginnen und Kollegen der Poliklinik und des Funktionsbereiches für Rheumatologie an der hiesigen Uniklinik an der HHU, die meine klinische und wissenschaftliche Ausbildung nachhaltig unterstützt haben. Hier sind insbesondere Herr PD Dr. med. Stefan Vordenbäumen, Herr PD Dr. rer. nat. Ralph Brinks und Frau Dr. med. Johanna Mucke zu nennen, welche mir stets mit Rat und Tat zur Seite standen.

Zudem danke ich den Kollegen des Instituts für diagnostische und interventionelle Radiologie. Neben Herrn Univ.-Prof. Dr. med. Gerald Antoch sind hier insbesondere meine Freunde und Kollegen PD Dr. med. Christoph Schleich, PD Dr. med. Falk Miese, PD Dr. med. Christian Buchbender, Frau Dr. rer. nat. Anja Müller-Lutz und Herr Dr. med. Daniel Benjamin Abrar zu nennen.

Mein ganz besonderer Dank gilt meiner Familie. Diese Arbeit ist meiner Mutter Ursula Sewerin gewidmet, die mich leider nicht auf meinen gesamten Weg begleiten konnte. Meinem Vater Peter Sewerin, der mich von Anfang an außergewöhnlich unterstützt hat, möchte ich an dieser Stelle von ganzem Herzen danken. Du warst und bist meine Heimat. Gleiches gilt für meine

Schwester Lisa Freitag und ihrer wundervollen Familie, die einen großen Teil an dem Gelingen der Arbeit hatten. Dies gilt auch für meine Freunde, die mir immer zur Seite standen.

Der größte Dank gilt meiner Freundin Manuela Maus, die immer eine Stütze und mein Anker war und ist. Du warst und bist mein bedingungsloser Rückhalt und mein Zuhause. Ohne dich wäre diese Arbeit nicht möglich gewesen.

European Journal of Radiology 82 (2013) 374–379

Contents lists available at SciVerse ScienceDirect

European Journal of Radiology

journal homepage: www.elsevier.com/locate/ejrad

# Utility of combined high-resolution bone SPECT and MRI for the identification of rheumatoid arthritis patients with high-risk for erosive progression

Christian Buchbender[a,*,1], Philipp Sewerin[b,1,2], Katalin Mattes-György[c,3], Falk Miese[a,4], Hans-Joerg Wittsack[a,5], Christof Specker[d,6], Gerald Antoch[a,7], Hans-Wilhelm Müller[c,8], Matthias Schneider[b,9], Axel Scherer[a,1,10], Benedikt Ostendorf[b,11]

[a] Univ Dusseldorf, Medical Faculty, Department of Diagnostic and Interventional Radiology, Moorenstr. 5, D-40225 Dusseldorf, Germany
[b] Univ Dusseldorf, Medical Faculty, Department of Rheumatology, Moorenstr. 5, D-40225 Dusseldorf, Germany
[c] Univ Dusseldorf, Medical Faculty, Department of Nuclear Medicine, Moorenstr. 5, D-40225 Dusseldorf, Germany
[d] Department of Rheumatology & Clinical Immunology, Kliniken Essen-Sud, Propsteistrasse 2, D-45239 Essen, Germany

ARTICLE INFO

*Article history:*
Received 11 September 2012
Received in revised form 16 October 2012
Accepted 17 October 2012

*Keywords:*
Rheumatoid arthritis
Single photon emission computertomography
DPD bone scanning
Magnetic resonance imaging
Joint
Erosion

ABSTRACT

*Objectives:* To evaluate the utility of sequentially acquired, post hoc fused, magnetic resonance imaging (MRI) and multi-pinhole single photon emission computed tomography (MPH-SPECT) with technetium-99m-labeled disphosphonates (Tc99m-DPD) for the identification of finger joints with later erosive progression in early rheumatoid arthritis (ERA) patients.
*Methods:* Ten consecutive ERA patients prospectively underwent MPH-SPECT and MRI of metacarpophalangeal (MCP) joints prior to and after 6 months methotrexate therapy. Tc99m-DPD uptake was measured at proximal and distal MCP sites using regional analysis. The course of joint pathologies was scored according to the Rheumatoid Arthritis MRI Score (RAMRIS) criteria.
*Results:* The frequency of increased Tc99m-DPD uptake, synovitis and bone marrow edemadecreased under MTX therapy; but the number of bone erosions increased. Joints with progressive and new erosions on follow-up had a higher baseline Tc99m-DPD uptake ($2.64 \pm 1.23$ vs. $1.43 \pm 0.91$) ($p = 0.02$).
*Conclusions:* Joints with erosive progression are characterized by an early increased Tc99m-DPD uptake, even in absence of MRI bone pathologies. Tc99m-DPD MPH-SPECT might thus be of additional value to morphological MRI for the identification of RA patients with a high risk for erosive progression.


* Corresponding author. Tel.: +49 211 81 17752.
*E-mail addresses:* christian.buchbender@med.uni-duesseldorf.de (C. Buchbender), philipp.sewerin@med.uni-duesseldorf.de (P. Sewerin), katalin.mattes@med.uni-duesseldorf.de (K. Mattes-György), falk.miese@med.uni-duesseldorf.de (F. Miese), hans-joerg.wittsack@med.uni-duesseldorf.de (H.-J. Wittsack), c.specker@kliniken-essen-sued.de (C. Specker), antoch@med.uni-duesseldorf.de (G. Antoch), HansW.Mueller@med.uni-duesseldorf.de (H.-W. Müller), matthias.schneider@med.uni-duesseldorf.de (M. Schneider), scherer@med.uni-duesseldorf.de (A. Scherer), ostendorf@med.uni-duesseldorf.de (B. Ostendorf).
[1] These authors contributed equally to this study.
[2] Tel.: +49 211 81 17817.
[3] Tel.: +49 211 81 18540.
[4] Tel.: +49 211 81 17752.
[5] Tel.: +49 211 81 17752.
[6] Tel.: +49 201 84 081214.
[7] Tel.: +49 211 81 17752.
[8] Tel.: +49 211 81 18540.
[9] Tel.: +49 211 81 17817.
[10] Tel.: +49 211 81 17752.
[11] Tel.: +49 211 811 781 7.

0720-048X/$ – see front matter © 2012 Elsevier Ireland Ltd. All rights reserved.
http://dx.doi.org/10.1016/j.ejrad.2012.10.011

## 1. Introduction

### 1.1. Background: therapy monitoring in rheumatoid arthritis

In rheumatoid arthritis (RA) the degree of long-term functional joint impairment depends on the disease activity and consecutive joint damage [1,2]. Today, clinical remission – constituting the main therapy target in RA [3–6] – can be achieved by using early and tightly controlled treatment regimes and potent disease modifying anti-rheumatic drugs. Clinical scores such as the disease activity score 28 (DAS28) are broadly applied for therapy monitoring and moderately reflect disease activity [4]. However, given that 19–30% of the patients in disease remission experienced radiographic progression [7,8], the discussion on the sufficiency of disease monitoring based on clinical scores is ongoing.

### 1.2. MRI in rheumatoid arthritis

Additional information on inflammatory activity can be gained by magnetic resonance imaging (MRI), a sensitive tool for the assessment of inflammatory changes in the soft tissue and bony structures, which is therefore broadly used for therapy monitoring. Bone marrow edema, which is detectable by MRI only, has been shown to be a strong predictor for erosive disease [9–11]. But the use of MRI for therapy monitoring in RA has also brought up new challenges. There is evidence of persistent inflammation (synovitis) despite clinical remission [12,13]. On the other hand, despite persistent synovitis in MRI, healing of erosions in X-ray has been reported [14]. This gap between clinical and morphological remission discloses the need for an extension of imaging methods in RA to identify patients who are at a high risk for extensive joint destruction and who would potentially benefit from a primary biological therapy or early therapy escalation.

### 1.3. Functional imaging in rheumatoid arthritis

Functional imaging techniques that collect metabolic information from the tissues involved in the inflammatory processes in RA are promising to provide the desired additional information. F18 Fluordeoxyglucose-Positron emission tomography is a sensitive method [15] for metabolic imaging of soft tissue inflammation in RA, even for subclinical arthritis [16] and it has also been used for therapy monitoring [17]. Inflammatory changes of the bone metabolism can be depicted by Single photon emission computed tomography (SPECT) using technetium-99m-labeled disphosphonates (Tc-99m DPD) SPECT [18,19]. A recent approach in imaging joint inflammation in RA has been the combination of functional imaging and high-resolution cross-sectional imaging [20,21]. MRI and multi-pinhole SPECT (MPH-SPECT), a high-resolution SPECT variant [22,23], were successfully combined for the assessment of inflammatory changes in finger joints of RA and osteoarthritis patients [24,25]. MPH-SPECT allows the depiction of very initial bone alterations in finger joints of early RA (ERA) patients which were not detectable on MRI scans [26]. An earlier preliminary analysis had already indicated that MPH-SPECT might represent a valuable tool for the monitoring of initial bony alterations in ERA patients under DMARD therapy [27]. Up to now no other longitudinal studies using MPH-SPECT for therapy monitoring under DMARD therapy are available and the predictive value of increased tracer uptake in SPECT is undetermined.

### 1.4. Objectives

The primary objective of this study was to evaluate whether Tc99m-DPD- MPH-SPECT in addition to MRI could identify metacarpophalangeal joints with erosive progression in ERA patients under methotrexate therapy. The secondary objective was to investigate the relationship between Tc99m-DPD uptake, persistence of synovitis and the development of erosion.

## 2. Patients and methods

### 2.1. Patients

This study was approved by the local ethical-committee (study number 3129). Written informed consent was obtained from all patients. 10 consecutive patients (8 female, 2 male; $49 \pm 13$ years [mean $\pm$ SD], range: 24–68) with early RA based on the 2010 American College of Rheumatology/European League Against Rheumatism RA classification criteria [28], with a disease duration < 6 months, no prior disease-modifying anti-rheumatic drug treatment and absence of bone erosions of the MCP joints on standard radiographs of the hands were enrolled in this study. Patients were recruited from the Department of Endocrinology, Diabetology and Rheumatology, University Dusseldorf, Dusseldorf, Germany and the Department of Rheumatology & Clinical Immunology, Kliniken Essen-Sud, Essen, Germany. The general exclusion criteria for MR imaging and SPECT imaging with Tc99m-DPD (cardiac or other pacemaker/device, metallic foreign bodies (e.g. ocular, brain vascular clip), renal insufficiency, claustrophobia, pregnancy) were applied. After baseline MR imaging all patients were treated with a standard MTX dose of 15 mg/week. All patients were imaged and revisited after 6 months methotrexate therapy. The following disease activity related parameters were collected at both time points: C-reactive protein (CRP) (mg/dl), erythrocyte sedimentation rate (ESR) (mm/h) and DAS28.

### 2.2. MPH-SPECT imaging

MPH-SPECT imaging of the clinical dominant hand was performed three hours after injection of a bodyweight adapted dose (approximately 550 MBq) of technetium-99m dicarboxypropanedisphosphonate (Tc-99m DPD) We used a Picker PRISM 2000 S camera (Philips Medical Systems) fitted with a multi-pinhole (MPH) pyramidal collimator, as decribed elsewhere [25]. The field of view (FoV) of $110 \times 100$ mm covered the metacarpophalangeal and the proximal interphalangeal joints of the imaged hand. The rotation radius was 90 mm, seven projections/180° were acquired with 250 s/projection and 100–400 counts per second (cps), resulting in a total acqusition time of 29 min. Each aperture had a sensitivity of 150 cps/MBq across the FoV. MPH-SPECT images were reconstructed at 1.33 mm using a $100 \times 100 \times 110$ mm matrix and 9 iterations. Image distortion was prevented by daily quality checks using a snake phantom (3.7 MBq, 12 projection a 100 s) and calculation of the reconstruction shift of the apertures, which was then used for correction of the MPH-SPECT hand studies.

### 2.3. MR imaging

Immediately after MPH-SPECT imaging, MRI of the clinically dominant hand (same as MPH-SPECT) was performed on the same day using a 3 Tesla MR system (Magnetom Trio; Siemens Healthcare, Germany). Patients were bedded in prone position. The arm was extended overhead, palm down to center the imaged hand in the magnetic field. The imaged hand was wrapped in a 4- channel flex coil (366 mm $\times$ 174 mm). The following sequences were acquired: (1) coronal fat-suppressed short tau inversion recovery (STIR) sequence (repetition time (TR) 5560 ms, echo time (TE) 31 ms, inversion time (TI) 150 ms, slice thickness 3 mm, field of view (FoV) $120 \times 120$ mm, matrix size $256 \times 182$ pixels), (2) coronal T1 weighed turbo spin-echo (TSE) sequence (TR 860 ms, TE 25 ms,

**Table 1**
The mean values of the erythrocyte sedimentation rate (ESR), c-reactive protein (CRP) and the disease activity score 28 (DAS28) were significantly reduced after 6 months methotrexate therapy (*t*1) compared to baseline (*t*0).

| | Mean ± SD | | *p*-value |
|---|---|---|---|
| | t0 | t1 | |
| ESR (mm/h) | 38.40 ± 24.1 | 17.2 ± 9.0 | 0.037 |
| CRP (mg/dl) | 1.96 ± 1.64 | 0.31 ± 0.25 | 0.002 |
| DAS28 | 4.63 ± 1.27 | 1.95 ± 0.81 | <0.001 |

FoV 120 × 120 mm), (3) dynamic contrast enhanced T1 weighed sequence (TR 333 ms, TE 1.46 ms, FoV 120 × 120 mm), (4) contrast enhanced coronal t1 weighed turbo spin-echo (TSE) sequence (TR 860 ms, TE 25 ms, FoV 120 × 120 mm), axial contrast enhanced T1 weighed fat suppressed spin-echo sequence (TR 765 ms, TE 12 ms, FoV 60 × 20 mm). The FoV of all sequences was adjusted to the MCP joints, being the most affected primary joint sites in ERA.

### 2.4. Image data analysis

Image analysis was focused on the MCP joints. Because of the known high prevalence of osteoarthritis of the thumb, the first MCP was excluded. MR images were read in consensus by two radiologists trained for RAMRIS scoring (AS, FM) and one physician specialized in nuclear medicine (KM) (all readers had a minimum of 5 years experience in musculosceletal imaging). In all ten patients the MCP joints II–V ($n = 40$) were scored for severity of synovitis Bone marrow edemausing the relevant subscore of the Rheumatoid Arthritis MRI Score (RAMRIS) [29]. Further, according to RAMRIS criteria, erosion and bone marrow edema subscores were assessed separately for the proximal and distal portions of the MCP joints II–V (referred to as MCP joint sites (JS), $n = 80$).

MPH-SPECT images were read by the same team of three readers (AS, FM, KM), in consensus. Because there are no reference standards available for the Tc99m-DPD uptake in normal and inflammatory MCP-joints, the number of joint sites with increased Tc99m-DPD uptake could not be assessed by absolute quantification. In order to identify the number of MCP JS with increased Tc99m-DPD uptake, therefore a 4 point grading system (0 = no increased uptake, 1 = slightly increased uptake, 2 = moderately increased uptake, 3 = severely increased uptake) was applied. In addition, a region of interest (ROI) analysis was performed for the quantitative comparison of the mean Tc99m-DPD uptake in JS with different courses of the RA related MRI pathologies. For this purpose one reader (KM) drew three-dimensional ROIs fitted to cover the head of the metacarpal bone (proximal JS) and basis of the phalangeal bone (distal JS) into the MCP joint II to V. In each patient a reference bone site in the proximal phalangeal bones, with visually normal Tc99m-DPD uptake, was chosen. In this bone site a reference ROI was placed. The mean counts in the reference ROIs were 628 ± 1090 at baseline and 1910 ± 856 at follow-up. In order to achieve comparability between patients, Tc99m-DPD uptake at MCP JS was then divided by the Tc99m-DPD uptake measure of this reference bone site, resulting in normalized Tc99m-DPD uptake ratios.

### 2.5. Statistics

Since Kolmogorov–Smirnov test indicated that measured Tc99m-DPD uptake ratios were normally distributed, parametrical statistic was used for analysis. For comparison of continuous data between groups, Student's *t*-test and analysis of variance (ANOVA) were used as appropriate. For repeated measurements of continuous variables, variants of these tests appropriate for paired samples were used; for categorical data, the Wilcoxon signed-rank test for paired-samples was used. Correlations of categorical data were calculated using Cramer's V ($\Phi_c$). Values are presented as mean value ± standard deviation. A critical *p*-value of <0.05 was used as significance level. Statistical analysis was performed using SPSS software (SPSS, version 19, SPSS, Chicago, Il).

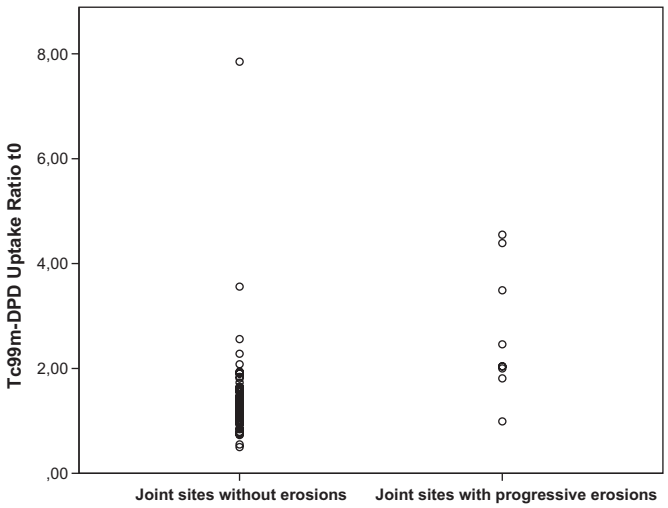


**Fig. 1.** Dot plot showing the distribution of the measured baseline Tc99m-DPD uptake ratios (all values were included in the analysis) in joint sites (JS) with and without progression or development of bone erosions on follow-up. The baseline values of the Tc99m-DPD ratios were significantly higher in joint sites with progressive or newly developed erosions ($p < 0.001$).

## 3. Results

### 3.1. Clinical disease course

Clinically, all patients responded to methotrexate. The mean values for ESR, CRP and DAS28 were significantly lower after 6 months compared to baseline (Table 1).

### 3.2. MRI

The number MCP joints affected by synovitis decreased from baseline ($n = 24$) to follow-up ($n = 18$) MRI. The severity of the RAMRIS synovitis score significantly decreased from baseline to follow-up ($p < 0.001$). Bone marrow edema was a very infrequent finding (2 JS at baseline; 1 JS at follow-up) at both time points. Seven erosions were found at baseline, 9 erosions at follow-up MRI. 6 out of 7 erosions detected at baseline were progressive on follow-up, 1 baseline erosion completely regressed and 3 erosions were newly developed.

### 3.3. MPH-SPECT Imaging

The number of JS with increased Tc99m-DPD uptake decreased from baseline ($n = 47$) to follow-up ($n = 39$). At baseline, JS that had erosions on baseline MRI had a higher Tc99m-DPD uptake (2.53 ± 1.45) than JS without erosions (1.47 ± 0.93) ($p = 0.03$) (Fig. 1). JS with progressive and newly developed erosions on follow-up MRI had a higher baseline Tc99m-DPD uptake (2.64 ± 1.23) compared to JS that did not show erosions on follow-up (1.43 ± 0.91) ($p < 0.02$) (Fig. 2). The Tc99m-DPD uptake at baseline significantly increased with the erosion size on follow-up ($p = 0.005$) (Fig. 3).

There was no significant difference in the mean Tc99m-DPD uptake between MCP joints with persistent synovitis on MRI (1.56 ± 1.27) and MCP joints without persistence of synovitis

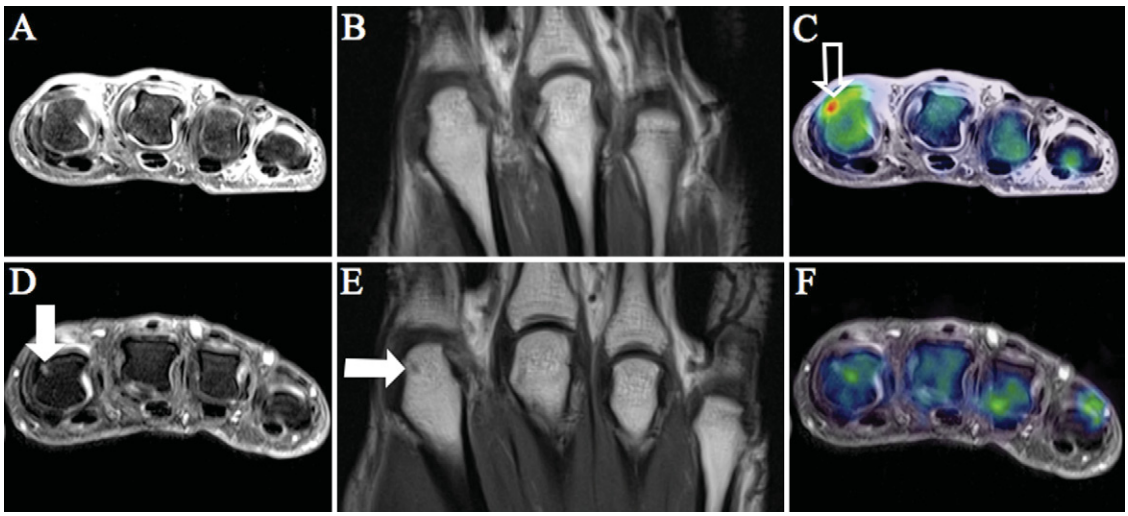


**Fig. 2.** Example disease course of a 51 years old ERA patient under MTX therapy: Baseline axial contrast enhanced T1w MR-Image (A) and coronal native T1w MR-Image (B) showing synovitis of the index, middle and fifth finger but no erosions. The fusion image of baseline MR-Image and baseline SPECT (C) depicts a focal Tc99-DPD uptake (open arrow) in the metacarpal head of the index finger. Follow-up axial (D) and coronal T1w MR-Image (E) after 6 months MTX therapy showing that a small bone defect (white arrows) was developed in location of the focal uptake. The corresponding MR-SPECT fusion image (F) documents the regression of the former focal Tc99-DPD uptake in the metacarpal head of the index finger.

($1.47 \pm 0.75$) ($p = 0.38$). There was no significant correlation between persistence of synovitis and the development of erosions on follow-up MRI ($\Phi_c = 0.3$, $p = 0.12$).

## 4. Discussion

In this study we report the first results on combined high-resolution MPH-SPECT and MRI of the MCP joints for therapy monitoring in RA. We found that high-resolution MPH-SPECT is sensitive to changes of inflammatory bone metabolism and it generally reflects the trends of inflammatory activity in MRI and the patient's disease course measured by ESR, CRP and DAS28. In advancement to conventional scintigraphy and SPECT, the given higher resolution of the MPH-SPECT technique and the image fusion of MPH-SPECT and MRI allowed for the correlation of the course of MR pathologies of the MCP joints and the bone metabolism of the corresponding JS. In our ERA study cohort, bone marrow edema, a known strong predictor for the development of bone erosions and the earliest MR finding of osteitis in RA [30], was a rare finding. Thus the course of bone marrow edema only reflected the therapy response in a small number of JS (3/80 JS; 4%). At the same time increased Tc99m-DPD uptake was frequently found in MCP JS and decreased under methotrexate therapy. This data corroborate the finding of an earlier study that reported on earliest inflammatory bone affections in RA detected by MPH-SPECT and a synchronous lack of bone marrow edema [26]. In RA, increased Tc99m-DPD uptake may reflect increased osteoblastic activity due to stimulation by proinflammatory cytokines such as TNFα, IL-1 and IL-6 [19]. Histopathological studies on RA patients who underwent joint-surgery revealed that bone marrow edema represents an accumulation of pro-inflammatory cells [31]. Further, there is evidence that proinflammatory cytokines such as TNFα, IL-1 and IL-6 strongly inhibit the differentiation of multi-potent mesenchymal stem cells to adipocytes, which are abundant in the bone marrow. It was shown that in inflamed joints not only the invasion of inflammatory cells but also the higher number of undifferentiated mesenchymal stem cells are responsible for the development of a detectable bone marrow edema in MRI [32]. The presence of elevated Tc99m-DPD uptake prior to visible bone marrow edema could reflect this time-course from direct stimulation of osteoblasts and the delayed drift of the cell composition (MSC to adipocytes) leading to bone marrow edema. On the contrary, other authors reported that Tc99m-DPD binding in the bone may be independent from osteoblast numbers but proportional to the amount of bone-forming minerals, entering the bone by chemical resorption [32,33]. The hypotheses reported above, which is based only on a small patient cohort, therefore has to be interpreted with care. Future studies on imaging findings (SPECT, MRI) with histopathological reference (e.g. utilizing mini-arthroscopy [34]) are desirable in order to investigate the true correlate of joint pathologies depicted by MRI and SPECT. Despite the clinical response of all patients and an overall reduction of inflammatory joint pathologies on MRI, primarily synovitis, we found a progression of erosions in 9 JS. Prior larger studies hypothesized that persistent synovitis despite clinical remission might be causal for a progress of joint erosions. In our small study cohort, synovitis persisted in 18 MCP joints without significant correlation between the persistence of synovitis and the progress and development of erosions on follow-up MRI. These findings conflict with hypotheses that persistent synovitis, despite

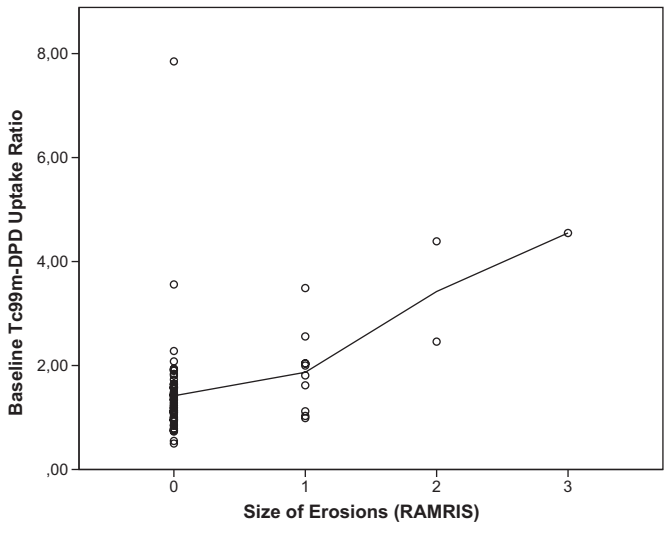


**Fig. 3.** The baseline Tc99m-DPD uptake ratio values significantly increased over the RAMRIS categories of erosion size on follow-up ($p = 0.005$).

clinical remission, might be causal for a progress of joint erosions. Supporting our data, an MRI, CT and ultrasonography controlled study on a larger RA patient cohort receiving a combined adalimumab and MTX treatment reported no progression and even occasional healing of joint erosions despite persisting synovitis [14]. One explanation for this finding is that Tc99m-DPD uptake of JS adjacent to persistent synovitis was not increased compared to JS in joints without persistence of synovitis. According to this explanation, the persistence of synovitis might be an MR imaging feature without a direct link to the bony joint compartment. For JS that showed a progression of the size of erosions or new erosions, we found a significant higher Tc99m-DPD uptake in baseline SPECT compared to JS with stable or regressive erosions. Moreover, there was a linear relationship between the Tc99m-DPD uptake values measured baseline and the size of the erosions on follow-up. These findings indicate that increased Tc99m-DPD as a measure of increased bone metabolism might be predictive for the progression of joint erosions in RA. The utilization of MPH-SPECT for the early identification of high-risk patients (for an extensive joint destruction) in need of a primary biological therapy or early therapy escalation, which potentially leads to a better outcome [35], is at least imaginable. Future studies have to carefully evaluate the potential of the MPH-SPECT technique for risk stratification of ERA patients.

This study has limitations. Due to the small number of patients our results have to be considered as preliminary and further studies are needed to verify our findings. Our analysis was limited to the MCP joints, caused by restrictions in the FoV of MPH-SPECT and MR imaging, and therefore neglected inflammatory processes in other joints of the hand (e.g. the wrist). There was no reference standard (normal value of Tc99m-DPD uptake) available for the ROI analysis of MCP JS in MPH-SPECT images. Thus no thresholds regarding the risk of development of bone erosions could be reported. Due to the consensus-reading approach we did not provide inter- and intra-reader reliabilities for the assessment of MPH-SPECT and MRI joint pathologies. With regard to the clinical value of our findings, the limited availability of MPH-SPECT has to be considered a relevant limitation.

## 5. Conclusions

In RA patients, MCP joints which later show erosive progression can be identified by increased Tc99m-DPD uptake, even in absence of MRI bone pathologies. Hybrid MPH-SPECT and MRI might thus provide valuable additional information for the identification of RA patients with a high risk of erosive progression.

## Conflict of interest

The authors declare no conflict of interest.

## Acknowledgement

This study was supported by a grant (Gz. SCHE 619/3-1) of the German Research Foundation (Deutsche Forschungsgemeinschaft, DFG), which is a competitive, peer-reviewed research fund and a non-profit organization.

## References

[1] Scott DL, Pugner K, Kaarela K, et al. The links between joint damage and disability in rheumatoid arthritis. Rheumatology 2000;39(2):122–32.
[2] Scott DL, Smith C, Kingsley G. Joint damage and disability in rheumatoid arthritis: an updated systematic review. Clinical and Experimental Rheumatology 2003;21(5 Suppl. 31):S20–7.
[3] Krishnan E, Lingala B, Bruce B, Fries JF. Disability in rheumatoid arthritis in the era of biological treatments. Annals of the Rheumatic Diseases 2012;71(2):213–8.
[4] Smolen JS, Aletaha D. Monitoring rheumatoid arthritis. Current Opinion in Rheumatology 2011;23(3):252–8.
[5] Katchamart W, Bombardier C. Systematic monitoring of disease activity using an outcome measure improves outcomes in rheumatoid arthritis. Journal of Rheumatology 2010;37(7):1411–5.
[6] Smolen JS, Aletaha D, Bijlsma JW, et al. Treating rheumatoid arthritis to target: recommendations of an international task force. Annals of the Rheumatic Diseases 2010;69(4):631–7.
[7] Lillegraven S, Prince FH, Shadick NA, et al. Remission and radiographic outcome in rheumatoid arthritis: application of the 2011 ACR/EULAR remission criteria in an observational cohort. Annals of the Rheumatic Diseases 2012;71(5):681–6.
[8] Aletaha D, Smolen JS. Joint damage progresses in DAS28 remission and is driven by residual swollen joints. Arthritis and Rheumatism 2011;63(12):3702–11.
[9] Gandjbakhch F, Foltz V, Mallet A, Bourgeois P, Fautrel B. Bone marrow oedema predicts structural progression in a 1-year follow-up of 85 patients with RA in remission or with low disease activity with low-field MRI. Annals of the Rheumatic Diseases 2011;70(12):2159–62.
[10] Hetland ML, Ejbjerg B, Hørslev-Petersen K, et al. MRI bone oedema is the strongest predictor of subsequent radiographic progression in early rheumatoid arthritis, Results from a 2-year randomised controlled trial (CIMESTRA). Annals of the Rheumatic Diseases 2009;68(3):384–90.
[11] Haavardsholm EA, Bøyesen P, Østergaard M, Schildvold A, Kvien TK. Magnetic resonance imaging findings in 84 patients with early rheumatoid arthritis: bone marrow oedema predicts erosive progression. Annals of the Rheumatic Diseases 2008;67(6):794–800.
[12] Brown AK, Quinn MA, Karim Z, et al. Presence of significant synovitis in rheumatoid arthritis patients with disease-modifying antirheumatic drug-induced clinical remission: evidence from an imaging study may explain structural progression. Arthritis and Rheumatism 2006;54(12):3761–73.
[13] Gandjbakhch F, Conaghan PG, Ejbjerg B, et al. Synovitis and osteitis are very frequent in rheumatoid arthritis clinical remission: results from an MRI study of 294 patients in clinical remission or low disease activity state. Journal of Rheumatology 2011;38(9):2039–44.
[14] Døhn UM, Ejbjerg B, Boonen A, et al. No overall progression and occasional repair of erosions despite persistent inflammation in adalimumab-treated rheumatoid arthritis patients: results from a longitudinal comparative MRI, ultrasonography, CT and radiography study. Annals of the Rheumatic Diseases 2011;70(2):252–8.
[15] Goerres GW, Forster A, Uebelhart D, et al. F-18 FDG whole-body PET for the assessment of disease activity in patients with rheumatoid arthritis. Clinical Nuclear Medicine 2006;31(7):386–90.
[16] Gent YY, Voskuyl AE, Kloet RW, et al. Macrophage PET imaging as biomarker for preclinical rheumatoid arthritis. Arthritis and Rheumatism 2012;64(1):62–6.
[17] Elzinga EH, van der Laken CJ, Comans EF, et al. 18F-FDG PET as a tool to predict the clinical outcome of infliximab treatment of rheumatoid arthritis: an explorative study. Journal of Nuclear Medicine 2011;52(1):77–80.
[18] Gotthardt M, Bleeker-Rovers CP, Boerman OC, Oyen WJ. Imaging of inflammation by PET, conventional scintigraphy, and other imaging techniques. Journal of Nuclear Medicine 2010;51(12):1937–49.
[19] Sarikaya I, Sarikaya A, Holder LE. The role of single photon emission computed tomography in bone imaging. Seminars in Nuclear Medicine 2001;31(1):3–16.
[20] Kubota K, Ito K, Morooka M, et al. FDG PET for rheumatoid arthritis: basic considerations and whole-body PET/CT. Annals of the New York Academy of Sciences 2011;1228(1):29–38.
[21] Miese F, Scherer A, Ostendorf B, et al. Hybrid (18) F-FDG PET-MRI of the hand in rheumatoid arthritis: initial results. Clinical Rheumatology 2011;30(9):1247–50.
[22] Wirrwar A, Schramm N, Vosberg H, Müller-Gärtner HW. High resolution SPECT in small animal research. Reviews in the Neurosciences 2001;12(2):187–93.
[23] Wirrwar AK, Nikolaus S, Schramm NU, Arkian S, Cohnen M, Müller HW. [Tier-SPECT: performance of a dedicated small-animal-SPECT camera and first in vivo measurements]. Zeitschrift fur Medizinische Physik 2005;15(1):14–22.
[24] Ostendorf B, Scherer A, Wirrwar A, et al. High-resolution multipinhole single-photon-emission computed tomography in experimental and human arthritis. Arthritis and Rheumatism 2006;54(4):1096–104.
[25] Ostendorf B, Mattes-György K, Reichelt DC, et al. Early detection of bony alterations in rheumatoid and erosive arthritis of finger joints with high-resolution single photon emission computed tomography, and differentiation between them. Skeletal Radiology 2010;39(1):55–61.
[26] Scherer A, Wirrwar A, Mattes-György K, et al. Bony pathologies of the metacarpophalangeal joints in early rheumatoid arthritis: comparison of MRI and high-resolution SPECT. Rofo 2009;181(9):875–80.
[27] Buchbender C, Sewerin P, Scherer A, et al. Comparison of high-resolution multi-pinhole SPECT and MRI for monitoring early arthritis patients under methotrexat therapy: first results. In: ACR 2011 Chicago: Arthritis & Rheumatism. 2011. p. 370.
[28] Aletaha D, Neogi T, Silman AJ, et al. Rheumatoid arthritis classification criteria: an American College of Rheumatology/European League Against Rheumatism collaborative initiative. Arthritis and Rheumatism 2010;62(9):2569–81.

[29] Østergaard M, Peterfy C, Conaghan P, et al. OMERACT rheumatoid arthritis magnetic resonance imaging studies, core set of mri acquisitions, joint pathology definitions, and the OMERACT RA-MRI scoring system. Journal of Rheumatology 2003;30(6):1385–6.
[30] McQueen FM, Ostendorf B. What is MRI bone oedema in rheumatoid arthritis and why does it matter? Arthritis Research and Therapy 2006;8(6): 222.
[31] Jimenez-Boj E, Nöbauer-Huhmann I, Hanslik-Schnabel B, et al. Bone erosions and bone marrow edema as defined by magnetic resonance imaging reflect true bone marrow inflammation in rheumatoid arthritis. Arthritis and Rheumatism 2007;56(4):1118–24.
[32] Leitha T, Staudenherz A, Scholz U. Three-phase bone scintigraphy of hydroxyapatite ocular implants. European Journal of Nuclear Medicine 1995;22(4):308–14.
[33] Toegel S, Hoffmann O, Wadsak W, et al. Uptake of bone-seekers is solely associated with mineralisation! A study with 99mTc-MDP, 153Sm-EDTMP and 18F-fluoride on osteoblasts. European Journal of Nuclear Medicine and Molecular Imaging 2006;33(4):491–4.
[34] Ostendorf B, Peters R, Dann P, et al. Magnetic resonance imaging and miniarthroscopy of metacarpophalangeal joints: sensitive detection of morphologic changes in rheumatoid arthritis. Arthritis and Rheumatism 2001;44(11):2492–502.
[35] Breedveld FC, Weisman MH, Kavanaugh AF, et al. The PREMIER study: A multicenter, randomized, double-blind clinical trial of combination therapy with adalimumab plus methotrexate versus methotrexate alone or adalimumab alone in patients with early, aggressive rheumatoid arthritis who had not had previous methotrexate treatment. Arthritis and Rheumatism 2006;54(1):26–37.

Rheumatol Int (2013) 33:1731–1736
DOI 10.1007/s00296-012-2648-1

ORIGINAL ARTICLE

# Patterns of magnetic resonance imaging of the foot in rheumatoid arthritis: which joints are most frequently involved?

**Christian Buchbender · Axel Scherer · Falk Miese · Philipp Sewerin · Alexandra Haferkamp · Ralph Brinks · Hans-Joerg Wittsack · Gerald Antoch · Matthias Schneider · Benedikt Ostendorf**

Received: 9 May 2012 / Accepted: 15 December 2012 / Published online: 3 January 2013


**Abstract** To investigate patterns of inflammatory MRI pathologies of the fore- and midfoot in rheumatoid arthritis (RA) and early RA (ERA) and their changes under therapy. In this prospective study, MRI data of the foot of 39 RA patients (29 female, 10 male; age: 54 ± 13 years; disease duration: 35 ± 37 months; baseline DAS28: 3.0 ± 2.0; medication: 29 DMARD, 1 biological, 9 symptomatic or non-specific treatment) were evaluated for synovitis in 314 joints, bone marrow edema and erosions according to RAMRIS criteria in a total of 585 joints. The change in joint pathology intensity was evaluated on follow-up MRI (time of follow-up: 8 ± 4 months) in 25 patients. Inflammation was generally more frequent in the metatarsophalangeal (MTP) joints (221/292; 76 %) than in the proximal metatarsal (47/292; 16 %) and tarsal bones (24/292; 8 %). The overall most frequently involved joints of the foot were MTP 5 (51/292; 18 %) and 1 (49/292; 17 %). Change under therapy was most frequently seen in the MTP 1 joint. Progress of inflammation in the MTP 1 was more frequently found in ERA patients than in patients with established RA (disease duration >12 months) ($p = 0.002$). In RA, the MTP joints, primarily MTP 5 and 1, are the predominant sites of inflammatory MRI pathologies of the foot. A change of inflammatory activity under therapy can be most frequently noted in the MTP 1 joint. This information might be helpful to improve effectiveness of MRI-controlled therapy approaches and clinical trials.

**Keywords** Rheumatoid arthritis · MRI · Foot · RAMRIS · Joint

C. Buchbender (✉) · A. Scherer · F. Miese · H.-J. Wittsack · G. Antoch
Department of Diagnostic and Interventional Radiology, Medical Faculty, University Dusseldorf, Moorenstrasse 5, 40225 Dusseldorf, Germany
e-mail: christian.buchbender@med.uni-duesseldorf.de

P. Sewerin · A. Haferkamp · M. Schneider · B. Ostendorf
Department of Rheumatology, Medical Faculty, University Dusseldorf, 40225 Dusseldorf, Germany

R. Brinks
Institute of Biometry and Epidemiology, German Diabetes Center, University Dusseldorf, 40225 Dusseldorf, Germany

## Introduction

The accuracy of magnetic resonance imaging (MRI) in the prediction of radiographic joint destruction in rheumatoid arthritis (RA) has long been recognized in the literature [1, 2]. The higher sensitivity of MRI toward inflammation of the hand and forefeet (compared to standard radiography) [3] and the development of the RA-MRI scoring system (RAMRIS), which allowed for standardized semi-quantitative assessment of inflammatory soft tissue and destructive bone alterations [4–6], made a large number of MRI-controlled clinical trials in RA possible. Since most of these studies focused on the joints of the hand, little has been known about inflammatory MRI changes of the joints of the foot. One of the few studies dealing with this problem revealed that inflammatory MRI findings in the feet are as prevalent as in the hands [7] and may even be detected in the absence of inflammation of the clinical predominantly involved hand on MRI scans [8]. The latter study was the first that deployed the established RAMRIS scoring system to the feet, which recently demonstrated excellent reliability [9]. However, limited data of MRI patterns of the arthritic forefeet have been available.

The purpose of this study was to investigate the patterns of inflammatory MRI pathologies of the fore- and midfoot

in RA and early RA (ERA) patients and the patterns of change under therapy to provide an enhanced rationale for the selection of monitored joints under therapy and in the future MRI studies in RA.

## Materials and methods

### Patients

After institutional review board approval 39, RA patients (29 female, 10 male; age: 54 ± 13 years, range 23–82; disease duration: 35 ± 37 months, range 0–158; baseline DAS28: 3.0 ± 2.0; medication: 29/39 DMARD, 1/39 biological, 9/39 symptomatic or non-specific treatment) recruited from a single center were prospectively included in this study. All patients fulfilled the 2010 American College of Rheumatology/European League Against Rheumatism Rheumatoid arthritis classification criteria [10] and had documented inflammatory changes (MRI or radiography) of the hands. To evaluate potential differences between ERA and established RA, a threshold of 12-month disease duration was selected to subdivide groups. The study cohort comprised 12 ERA and 27 established RA patients, using this threshold. MRI of one forefoot (left: 21/39, 54 %; right: 18/39, 46 %) was available in all patients. If clinically apparent, the dominant side was imaged. Follow-up MRIs were available for 25 patients (mean time to follow-up 8 ± 4 month).

### MR imaging

MR imaging was performed on MR systems with field strengths from 0.2 to 3 T (Esaote C Scan (0.2 T), Esaote Italy; Siemens Avanto (1.5 T) and Siemens Magnetom Trio (3 T), Siemens Healthcare, Erlangen, Germany). No specific rules were applied for the allocation to the different MR scanners but imaging was performed upon availability. The imaging protocols comprised pre- and post-contrast (i.v. gadolinium-based MRI contrast material) T1-weighted images with a maximum slice thickness of 3 mm in at least two orthogonal planes and coronal fat-suppressed short tau inversion recovery (STIR) sequences. The field of view contained the metatarsophalangeal joints, the tarsometatarsal joints and the intertarsal joints including the cuneiform bones, the cuboid and the navicular bone. The proximal interphalangeal joints were only sporadically included in the field of view depending upon the actual foot size and therefore, were excluded from the analysis.

### Image analysis

MR images were read in consensus by two radiologists. Images were evaluated for synovitis, bone marrow edema (BME) and erosions according to the RAMRIS guidelines [4]. The presence or absence of change (progression and regression) of these inflammatory changes was noted in cases with available follow-up MRI. Joint pathologies that were newly developed on follow-up were referred to as progression. In MTP joints, the distal and proximal joint portions were analyzed separately for the presence of BME and erosions (data not shown), but were then summarized to one bone site for the evaluation of patterns of sites of inflammation. For the evaluation of synovitis, the tarsus was referred to as one joint (intertarsal synovitis).

All statistical analyses have been performed using the software R, version 2.11.1 (The R Foundation for Statistical Computing). Estimation of differences between proportions and corresponding $p$ values has been calculated with the function prop.test including continuity correction where appropriate.

## Results

### Baseline MRI

#### *Synovitis*

One hundred and ten of four hundred and twenty-nine joints showed synovitis. Synovitis was more frequent in the MTP joints (83/110; 75 %) than in the tarsometatarsal (23/110; 21 %) and intertarsal joints (4/110; 4 %), and was most frequently noted in the MTP 4 joint (19/110; 17 %) (Fig. 1a).

#### *Bone marrow edema*

Bone marrow edema was found in a total of 66 bone sites and was more frequent in MTP joints (49/66; 74 %) than in the proximal metatarsal (8/66; 12 %), and tarsal bones (9/66; 14 %). Overall, the MTP 3 joint most frequently showed BME (12/66; 18 %), closely followed by MTP joints 4 and 5 (11/66; 17 % each) (Fig. 1b).

#### *Erosions*

A total of 119 erosions were found, of which the majority (89/119; 75 %) was noted in the MTP joints. Erosions of the proximal metatarsal bones (16/119; 13 %) and the tarsal bones (14/119; 12 %) were less frequently observed. The joint sites most frequently affected by erosions were MTP 1 (25/119; 21 %) and MTP 5 (24/119; 20 %) (Fig. 1c).

#### *Inflammation (global score)*

The sum score of inflammatory findings for each site showed that inflammatory changes of the MTP joints

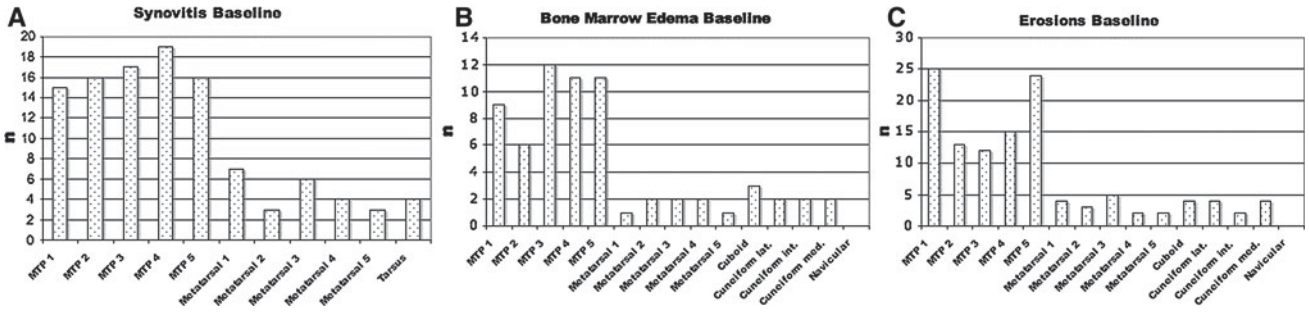


**Fig. 1** Prevalence of synovitis (**a**), bone marrow edema (**b**) and erosions (**c**) in baseline MRI of the foot

(221/292; 76 %) were more frequent than in the proximal metatarsal (47/292; 16 %) and tarsal bones (24/292; 8 %). The overall most frequently involved joints of the foot were MTP 5 (51/292; 18 %) and I (49/292; 17 %) (Fig. 2a).

*ERA versus established RA baseline*

The MTP 1 joint was more frequently affected by inflammatory changes in the ERA group (35 %) than in the established RA patient group (19 %) ($p = 0.02$). In established RA patients, MR signs of inflammation were more frequent in the MTP 4 joint ($p = 0.04$) and the proximal metatarsal bone 1 ($p = 0.01$). For baseline MRI, no significant differences between ERA and established RA patients were found in the subgroups synovitis, BME and erosions.

Follow-up MRI

*Synovitis*

On follow-up, 49 of 275 joints demonstrated an alteration of the intensity of synovitis. Of these, 35 sites showed regression and 14 were progressive. Synovitis changed more frequently in the MTP joints (29/49; 59 %) compared to the tarsometatarsal (19/49; 39 %) and intertarsal joints (1/49; 2 %). Overall, a change in the degree of synovitis was most frequently found in MTP 4 and proximal metatarsal bone 2 (7/47; 15 % each) (Fig. 3a).

*Bone marrow edema*

Thirty of three hundred and seventy-five bone sites evaluated on follow-up showed a change of BME intensity, 19 of which showed regression and 11 were progressive. An alteration of the extent of BME was more frequently noted in MTP joints (23/30; 77 %) than in proximal metatarsal (4/30; 13 %) and tarsal bones (3/30; 10 %). Regarding BME, the joint site most frequently demonstrating a change in BME was MTP 3 (8/30; 27 %) closely followed by MTP 1 (7/30; 23 %) (Fig. 3b).

*Erosions*

Fifty-seven of three hundred and seventy-five bone sites showed a change of the extent of erosions. Nineteen bone sites showed regression, 38 were progressive. Erosions of the MTP bones (39/57; 68 %) were more frequently changed compared to proximal metatarsal (11/57; 19 %) and tarsal bones (7/57; 12 %). Change of erosions of MTP 2 was predominant (11/57; 19 %) (Fig. 3c).

*Change of inflammation (global score)*

The sum score of inflammatory findings for each bone site showed that MTP joints (93/137; 25 %) were more frequently subject of change than the proximal metatarsal (34/137; 25 %) and the tarsal bones (10/137; 7 %). MTP joints 1 (21/137; 15 %) closely followed by MTP 2, 3 and 5

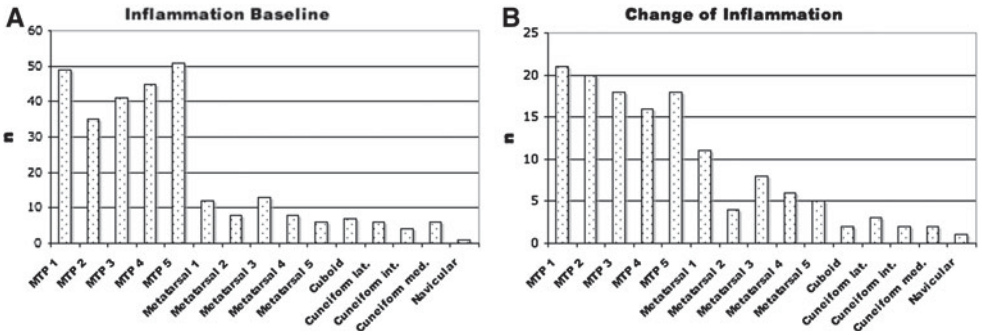


**Fig. 2** Distribution of combined inflammatory changes in baseline MRI (**a**) and change of intensity (synovitis, BME and erosions combined) on follow-up MRI (**b**)

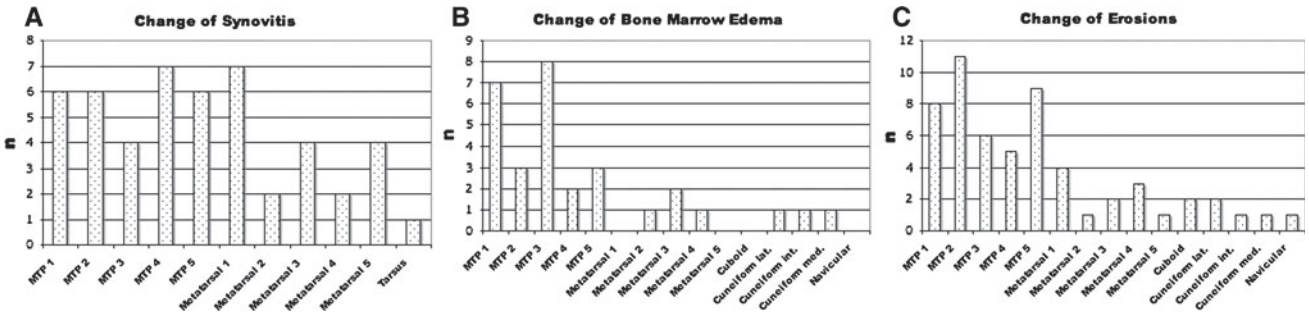


**Fig. 3** Prevalence of change in intensity of synovitis (**a**), bone marrow edema (**b**) and erosions (**c**) on follow-up MRI of the foot

(with decreasing frequency) were most frequently changed in extent of inflammation (Fig. 2b).

*ERA versus established RA follow-up*

Joint inflammation of the MTP 1 was more frequently changed under therapy ($p = 0.003$) and was more frequently progressive in the ERA group (22.5 %) than in the established RA patient group (3.5 %) ($p = 0.002$). No differences between ERA and established RA patients were found regarding the change of synovitis and BME.

## Discussion

The aim of this study was to identify the patterns of inflammation on MRI of the fore- and midfoot in RA. We found that synovitis, BME and bony erosions are common in both the forefoot (MTP joints) and the midfoot (proximal metatarsal and tarsal bones) of RA patients. Our data show that inflammatory changes are far more frequent in MTP joints than metatarsal and tarsal bones. This finding is supportive to an epidemiological study on RA patients that reported the highest burden of pain in the forefeet compared to the mid- and hindfoot [11, 12]. Our data indicate that the MTP joints 5 and 1 are the predominant sites of inflammation of the foot in RA. This finding corroborates the data from radiographic studies [13, 14] and is consistent with an MRI study that demonstrated that MTP 5 was the joint site most likely to be affected by inflammation [7].

We found that erosions are almost equally common in MTP 1 and MTP 5. Interestingly increased physical stress under the forefoot, especially MTP 1 and 4, has been discussed to cause erosions [15]. A subgroup analysis of our cohort indicates that in ERA, the MTP 1 joint is more frequently affected by inflammation ($p = 0.023$) and more frequently progresses in inflammation compared to established RA patients ($p = 0.002$). Supporting this finding, the aforementioned study on inflammation of the lower extremity in ERA patients reported that following MTP 5 the MTP 1 joint is the second most frequent site of inflammatory pathologies [7]. Based on this data, the MTP 1 joint, unlike the first metacarpophalangeal joint for the RAMRIS of the hand, should be included in the MRI score of the foot. However, the known high prevalence of joint pathologies due to coexistent osteoarthritis in MTP 1 may have biased our analysis and should be respected by evaluation of foot MRI in RA patients.

The present study is the first to systematically document the patterns of inflammation of the rheumatic fore- and midfoot on MRI. Taking into consideration that the majority of inflammatory changes can be found in the MTP joints allows for a higher precision in planning MRI-controlled clinical trials in RA. Based on our data reducing the MRI field of view and focusing on the forefoot seems to be reasonable. This bears the potential to provide shorter imaging times, which might be profitable for routine outpatient clinic care and allow for more time-efficient MRI-controlled therapy approaches. Future studies have to verify if the evaluation (e.g., RAMRIS) of the forefoot has a comparable accuracy for the estimation of disease activity as the evaluation of all foot joints. RAMRIS scoring for research purposes is also time-consuming. Because of our preliminary finding that the MTP joints 1 and 2 are most frequently affected by a change in inflammatory intensity under therapy, longitudinal studies comparing whole foot joint scores and reduced forefoot joint scores (e.g., MTP 1, 2 and 5 according to our study) for the reflection of the course of disease activity under therapy are needed.

This study gives note of a high prevalence of forefoot joint inflammation in RA patients under therapy. This finding is supported by a study reporting on MTP joint tenderness and swelling in a substantial number of RA patients who were considered to be in the state of remission [16]. Given the high burden of forefoot pain known from epidemiological studies [11, 12] and the imminence of walking disability [17], a more attentive attitude to the course of forefoot inflammation in outcome studies in RA seems worthwhile and justifiable. This applies more than ever since the favorable effect of a very early DMARD treatment on the radiographic progression has been well

documented [18]. Like the widely used DAS28 score (which does not include the feet) may misleadingly define remission in individuals [19], the exclusion of the feet in the RAMRIS eventually underestimates disease activity. In analogy to established scoring methods in conventional radiography (e.g., Sharp/van der Heijde, SENS or Ratingen score) [13, 20, 21], a combined hand and foot MRI score might state an important advancement to the present RAMRIS. In contrast, a study comparing the DAS28 and the DAS38 (which included the 10 metatarsophalangeal joints) recently showed that inclusion of the feet for evaluation of disease remission did not influence the risk for subsequent radiographic progression [22]. In the same study, 26–40 % of the patients in DAS28 remission showed disease activity on the feet [22]. Future studies have to address the prognostic value of persistent inflammation in the joints of the feet on MRI and evaluate the utility of a combined hand and foot MRI score according to the RAMRIS criteria. Also the comparison of standard radiographs of the hand and foot versus a combined hand and foot MRI protocol for their impact on the therapeutic management of RA patients has to be addressed in the future studies.

This study has limitations. The consensus reading approach does not provide inter- and intra-reader reliabilities of the RAMRIS scoring. Follow-up MRI was not available for all included individuals. The hindfoot and ankle was not imaged due to the natural field-of-view limitations of MRI. The ankle, however, is the second most frequent site (after the forefoot) of pain reported by RA patients [12] and significantly contributes to walking disability [23]. We used different MR systems upon availability. Hence, the known differences in detection rates for inflammatory joint pathologies due to different field strengths [24] may have limited the comparability of our MRI findings.

## Conclusion

In RA, the MTP joints, primarily MTP 5 and 1, are the predominant sites of inflammatory MRI pathologies of the fore- and midfoot. Under therapy, the MTP 1 joint most frequently changed in inflammatory intensity. This knowledge might be helpful to improve effectiveness of MRI-controlled therapy approaches and clinical trials.

**Conflict of interest** The authors declare that they have no conflict of interest.

## References


1. Haavardsholm EA, Bøyesen P, Østergaard M, Schildvold A, Kvien TK (2008) Magnetic resonance imaging findings in 84 patients with early rheumatoid arthritis: bone marrow oedema predicts erosive progression. Ann Rheum Dis 67:794–800
2. Bøyesen P, Haavardsholm EA, Ostergaard M, van der Heijde D, Sesseng S, Kvien TK (2011) MRI in early rheumatoid arthritis: synovitis and bone marrow oedema are independent predictors of subsequent radiographic progression. Ann Rheum Dis 70:428–433
3. Ejbjerg BJ, Vestergaard A, Jacobsen S, Thomsen HS, Østergaard M (2005) The smallest detectable difference and sensitivity to change of magnetic resonance imaging and radiographic scoring of structural joint damage in rheumatoid arthritis finger, wrist, and toe joints: a comparison of the OMERACT rheumatoid arthritis magnetic resonance imaging score applied to different joint combinations and the Sharp/van der Heijde radiographic score. Arthritis Rheum 52:2300–2306
4. Østergaard M, Peterfy C, Conaghan P, McQueen F, Bird P, Ejbjerg B et al (2003) OMERACT rheumatoid arthritis magnetic resonance imaging studies. Core set of MRI acquisitions, joint pathology definitions, and the OMERACT RA-MRI scoring system. J Rheumatol 30:1385–1386
5. Bird P, Conaghan P, Ejbjerg B, McQueen F, Lassere M, Peterfy C et al (2005) The development of the EULAR-OMERACT rheumatoid arthritis MRI reference image atlas. Ann Rheum Dis 64(Suppl):i8–i10
6. Østergaard M, Edmonds J, McQueen F, Peterfy C, Lassere M, Ejbjerg B et al (2005) An introduction to the EULAR-OMERACT rheumatoid arthritis MRI reference image atlas. Ann Rheum Dis 64(Suppl):i3–i7
7. Boutry N, Lardé A, Lapègue F, Solau-Gervais E, Flipo RM, Cotten A (2003) Magnetic resonance imaging appearance of the hands and feet in patients with early rheumatoid arthritis. J Rheumatol 30:671–679
8. Ostendorf B, Scherer A, Mödder U, Schneider M (2004) Diagnostic value of magnetic resonance imaging of the forefeet in early rheumatoid arthritis when findings on imaging of the metacarpophalangeal joints of the hands remain normal. Arthritis Rheum 50:2094–2102
9. Baan H, Bezooijen R, Avenarius JK, Dubbeldam R, Drossaers-Bakker WK, van de Laar MA (2011) Magnetic resonance imaging of the rheumatic foot according to the RAMRIS system is reliable. J Rheumatol 38:1003–1008
10. Aletaha D, Neogi T, Silman AJ, Funovits J, Felson DT, Bingham CO et al (2010) 2010 Rheumatoid arthritis classification criteria: an American college of rheumatology/European league against rheumatism collaborative initiative. Arthritis Rheum 62:2569–2581
11. Otter SJ, Lucas K, Springett K, Moore A, Davies K, Young A et al (2011) Comparison of foot pain and foot care among rheumatoid arthritis patients taking and not taking anti-TNFα therapy: an epidemiological study. Rheumatol Int 31:1515–1519
12. Otter SJ, Lucas K, Springett K, Moore A, Davies K, Cheek L et al (2010) Foot pain in rheumatoid arthritis prevalence, risk factors and management: an epidemiological study. Clin Rheumatol 29:255–271
13. van der Heijde DM, van Leeuwen MA, van Riel PL, Koster AM, van 't Hof MA, van Rijswijk MH et al (1992) Biannual radiographic assessments of hands and feet in a three-year prospective followup of patients with early rheumatoid arthritis. Arthritis Rheum 35:26–34
14. Fuchs HA, Kaye JJ, Callahan LF, Nance EP, Pincus T (1989) Evidence of significant radiographic damage in rheumatoid arthritis within the first 2 years of disease. J Rheumatol 16:585–591
15. van der Leeden M, Steultjens M, Dekker JH, Prins AP, Dekker J (2006) Forefoot joint damage, pain and disability in rheumatoid arthritis patients with foot complaints: the role of plantar pressure and gait characteristics. Rheumatology (Oxford) 45:465–469

16. van der Leeden M, Steultjens MP, van Schaardenburg D, Dekker J (2010) Forefoot disease activity in rheumatoid arthritis patients in remission: results of a cohort study. Arthritis Res Ther 12:R3
17. van der Leeden M, Steultjens MP, Ursum J, Dahmen R, Roorda LD, Schaardenburg DV et al (2008) Prevalence and course of forefoot impairments and walking disability in the first eight years of rheumatoid arthritis. Arthritis Rheum 59:1596–1602
18. Lukas C, Combe B, Ravaud P, Sibilia J, Landew R, van der Heijde D (2011) Favorable effect of very early disease-modifying antirheumatic drug treatment on radiographic progression in early inflammatory arthritis: data from the Étude et Suivi des polyarthrites indifférenciées récentes (study and followup of early undifferentiated polyarthritis). Arthritis Rheum 63:1804–1811
19. Landewé R, van der Heijde D, van der Linden S, Boers M (2006) Twenty-eight-joint counts invalidate the DAS28 remission definition owing to the omission of the lower extremity joints: a comparison with the original DAS remission. Ann Rheum Dis 65:637–641
20. Rau R, Wassenberg S, Herborn G, Stucki G, Gebler A (1998) A new method of scoring radiographic change in rheumatoid arthritis. J Rheumatol 25:2094–2107
21. van der Heijde D (1999) How to read radiographs according to the Sharp/van der Heijde method. J Rheumatol 26:743–745
22. van Tuyl LH, Britsemmer K, Wells GA, Smolen JS, Zhang B, Funovits J et al (2012) Remission in early rheumatoid arthritis defined by 28 joint counts: limited consequences of residual disease activity in the forefeet on outcome. Ann Rheum Dis 71:33–37
23. Baan H, Drossaers-Bakker W, Dubbeldam R, van de Laar M (2011) We should not forget the foot: relations between signs and symptoms, damage, and function in rheumatoid arthritis. Clin Rheumatol 30:1475–1479
24. Wieners G, Detert J, Streitparth F, Pech M, Fischbach F, Burmester G et al (2007) High-resolution MRI of the wrist and finger joints in patients with rheumatoid arthritis: comparison of 1.5 Tesla and 3.0 Tesla. Eur Radiol 17:2176–2182

# Inflammation and vascularisation markers of arthroscopically-guided finger joint synovial biopsies reflect global disease activity in rheumatoid arthritis

S. Vordenbäumen[1], P. Sewerin[1], T. Lögters[2], F. Miese[3], C. Schleich[3], E. Bleck[1], P. Philippski[1], M. Schädel-Höpfner[2], T. Pauly[4], M. Schneider[1], B. Ostendorf[1]

*[1]Department of Rheumatology, [2]Department of Trauma and Hand Surgery, and [3]Department of Diagnostic and Interventional Radiology, Medical Faculty, University of Düsseldorf, Düsseldorf, Germany; [4]Department of Orthopaedics, River Rhine Center for Rheumatology at St. Elisabeth-Hospital, Meerbusch-Lank, Germany.*

*Stefan Vordenbäumen, MD*
*Philipp Sewerin, MD*
*Tim Lögters, MD*
*Falk Miese, MD*
*Christoph Schleich, MD*
*Ellen Bleck*
*Paulina Philippski*
*Michael Schädel-Höpfner, MD*
*Thomas Pauly, MD*
*Matthias Schneider, MD*
*Benedikt Ostendorf, MD*

*Please address correspondence to:*
*Dr Stefan Vordenbäumen,*
*Dept. of Rheumatology,*
*Heinrich-Heine-University,*
*Moorenstraße 5,*
*40225 Düsseldorf, Germany.*
*E-mail: stefan.vordenbaeumen@med.uni-duesseldorf.de*

*Received on May 24, 2013; accepted in revised form on October 9, 2013.*



**Key words:** rheumatoid arthritis, arthroscopy, metacarpophalangeal joint, disease activity

*Funding: the study was supported by unconditional grants from Hiller-Stiftung, Erkrath, Germany, and the Forschungskommission of the Medical Faculty of Heinrich-Heine-University, Düsseldorf.*

*Competing interests: none declared.*

## ABSTRACT

**Objective.** *To analyse whether synovial markers of the clinically dominant metacarpophalangeal (MCP) joint reflect global disease activity measures in rheumatoid arthritis (RA).*

**Methods.** *Arthroscopically-guided synovial biopsies from the dominant metacarpophalangeal (MCP) joint of 10 patients with RA (DAS28 >3.2) were stained for determination of the synovitis score, CD68, vascular endothelial growth factor (VEGF), hypoxia-inducible factor 1α (HIF-1α). MRI and ultrasound were used to calculate the RAMRIS and US7 score respectively. Arthroscopy of the same joint was repeated in 6 patients after 6 months.*

**Results.** *The synovitis score significantly correlated to DAS28 (Spearman r=0.74), CRP (r=0.69), and US7 (r=0.66); sublining CD68 macrophages to CRP (r=0.6); HIF-1α to DAS28 (r=0.77), CRP (r=0.73); and VEGF to DAS28 (r=0.753) and RAMRIS (r=0.663). All patients showed a reduction of the DAS28 after 6 months (mean±SD: 5.2±1.5 vs. 2.75±1.1; p<0.05). There were three patients with a good EULAR response, and only these showed declining sublining CD68 macrophages in the control biopsy ($\chi^2$ test: LR 8.3, p=0.05). Two of the remaining patients with increasing CD68 sublining macrophages showed a deterioration of the RAMRIS.*

**Conclusion.** *Some histological findings in arthroscopically-guided biopsies of the dominantly affected MCP joint reflect global disease activity measures and their changes in RA patients. Moreover, repeated MCP synovial biopsy may distinguish true responders from individuals with residual disease activity, who are not readily recognised by clinical means.*

## Introduction

Synovial tissue analysis in RA has increased our understanding of disease mechanisms, and can be used in early phase trials to assess response to treatment (1, 2). Markers such as sublining CD68 macrophages have consistently been shown to be excellent disease activity parameters of rheumatoid arthritis (RA), potentially even superior to clinical composit measures such as the DAS28, which may be more liable to placebo effects (3-5). A study by Kraan *et al.* involving 9 patients suggested that comparable histological signs of inflammation in clinically inflamed joints are found irrespective of their localisation (6). This justified that synovial biopsies are usually collected from large joints such as the knee. However, the knee joint might not be affected in a considerable number of patients at the time of sampling. Thus, other large inflamed joints are recommended alternative choices (1). We noted that a number of RA patients refer to an MCP joint as their most severely affected joint in terms of pain and functional disability, especially in early disease, often in the absence of considerable clinical inflammation of larger joints. This is in accordance with systematic analyses of the topic (7). Uninflamed large joints may be biopsied, but display less severe inflammation (8), potentially not representing overall disease activity. In these cases, synovial sampling of the dominant MCP joint is an attractive option. However, to our knowledge, there are no systematic studies evaluating whether the changes observed relate to overall disease activity. Furthermore, there is theoretical concern that extensive sampling in such a small joint could preclude longitudinal analyses because of synovial scaring, or is not well tolerated by patients. Earlier studies have established the safety of singular MCP joint arthroscopy in RA (9, 10). Therefore, we assessed whether singular and repeated analysis of macroscopically inflamed synovial tissue, gathered from few targeted biopsies of MCP-joint synovial tissue, reflects measures of global disease activity such as the DAS28 or imaging procedures in RA patients.

## Patients and methods

10 consecutive patients with RA based on 2010 ACR/EULAR criteria with (1) a DAS28 >3.2, who (2) required initiation of DMARD therapy (n=4, methotrexate) or a switch of medication (n=6 patients with methotrexate additionally received adalimumab), (3) indicated an MCP joint as their most severely af-

fected and painful joint, and (4) gave their full informed written consent into the study, were recruited. All patients received an ultrasound examination with determination of the US7 score (11) and a Gadolinium-enhanced MRI (either 3.0 Tesla MRI (n=6) or alternatively 0.2 Tesla MRI in case of claustrophobia (n=4)) of the hand with determination of the RAMRIS score (12). Within one week, arthroscopy was carried out as described previously with 1.9 diameter arthroscope and local anaesthesia (Karl Storz, Tuttlingen, Germany) (9, 10). Briefly, 2 laterodorsal portals were created after skin incision for introduction of the arthroscopic camera and the biopsy forceps, respectively. A total of 6 synovial biopsies were obtained under visual control from macroscopically inflamed areas and snap frozen in Tissue-Tek (Sakura Finetek Germany, Staufen, Germany). The study was conducted according to the principles expressed in the Declaration of Helsinki and was approved by the ethics committee of the Medical Faculty of Heinrich-Heine-University (study number 3390).

*Synovial tissue*

3-5 µm serial sections were prepared from snap-frozen synovial tissue, Haematoxylin Eosion (HE) stained (Merck, Darmstadt, Germany) and evaluated prior to immunohistochemical staining of parallel sections. In each patient, a representative biopsy with the best morphology including a lining layer was selected for further analysis. Immunohistochemistry was carried out with monoclonal mouse anti-CD68 antibody (Dako, Glostrup, Denmark); anti-VEGF (Millipore, Billerica, USA), and anti-HIF-1α (Abcam, Cambridge, UK) antibody representing vascularisation; or IgG1 isotype control and secondary antibody contained within Dako Real Detection system, essentially according to manufacturer's instructions (all Dako). Stained sections were coded and evaluated at random by an observer blinded to the diagnosis and clinical data on a microscope (Axioskop 2 plus, Carl Zeiss, Jena, Germany) with digital camera (Nikon DS Vi 1, Nikon, Düsseldorf, Germany) and image acquisition software (NIS-Elements F, Nikon). HE stained sections were used for determination of the synovitis score according to Krenn (13). This is a semiquantitative 4-point sum-scale which considers lining layer hypertrophy, inflammatory infiltrate, and density of resident cells. CD68 of the sublining layer, VEGF, and HIF-1α were assessed by digital image analysis, essentially as previously described (14). Briefly, images were photographed in 100 x magnification and stored in TIF-format (resolution of 1600 x 1200). ImageJ (http://rsbweb.nih.gov/ij/index.html) was used to select regions of interest, *i.e.* sublining layer or total biopsy and the image was thresholded to highlight the stained areas, but not the respective isotype controls. For all samples stained with the same antibody, the same settings were used. After conversion of the photograph to an 8 bit binary image, the stained area was calculated as a fraction of the selected region.

**Table I.** Correlation of MCP joint synovial analyses with disease activity measures.

| | DAS28 | CRP* | US7[¥] | RAMRIS[§] |
|---|---|---|---|---|
| Synovitis score[¶] | **0.74 (*p*=0.014)** | **0.691 (*p*=0.019)** | **0.661 (*p*=0.038)** | 0.327 (NS) |
| lining layer | 0.289 (NS) | 0.410 (NS) | 0.239 (NS) | -0,200 (NS) |
| inflammatory infiltrate | **0.789 (*p*=0.007)** | **0.707 (*p*=0.015)** | 0.494 (NS.) | 0.539 (NS) |
| resident cells | 0.412 (NS) | 0.357 (NS) | 0.601 (NS) | 0.194 (NS) |
| Sublining CD68 | 0.553 (NS) | **0.599 (*p*=0.001)** | 0.455 (NS) | -0,164 (NS) |
| VEGF | **0.753 (*p*=0.012)** | 0.565 (NS) | 0.620 (NS) | **0.663 (*p*=0.037)** |
| HIF-1α | **0.766 (*p*=0.01)** | **0.73 (*p*=0.01)** | 0.564 (NS) | 0.345 (NS) |

*C-reactive protein, [¥]7 joint ultrasound score (11), [§]rheumatoid arthritis magnetic resonance imaging score (12), [¶]according to (13); NS: not significant.
Correlations of RA disease activity measures and synovial analyses of 10 MCP joint arthroscopies with the synovitis score and digital image analysis calculating the fraction of stained are of the total biopsy for vascular endothelial growth factor (VEGF) and hypoxia inducible factor 1α (HIF-1α), or the sublining region for CD68. Correlations were calculated according to Spearman, significant results are printed in bold.

**Table II.** Individual DAS28 responses of patients with follow-up synovial biopsies after 6 months ($T_0$, $T_1$) and corresponding sublining CD68 staining.

| Patient number | DAS28 | | EULAR response | sublining CD68 | | RAMRIS* | |
|---|---|---|---|---|---|---|---|
| | $T_0$ | $T_1$ | | $T_0$ | $T_1$ | $T_0$ | $T_1$ |
| 1 | 5.6 | 1.2 | good | 47 | 12 | 34 | 22 |
| 2 | 3.2 | 1.7 | good | 13 | 1 | 26 | 26 |
| 4 | 5.1 | 3.2 | good | 9 | 1 | 13 | 7 |
| 6 | 5.7 | 4.4 | moderate | 24 | 27 | 37 | 40 |
| 7 | 6.5 | 3.3 | moderate | 7 | 8 | 71 | 82 |
| 10 | 3.5 | 2.6 | moderate | 3 | 9 | 34 | 22 |

*rheumatoid arthritis magnetic resonance imaging score (12).
Disease Activity Score of 28 joints (DAS28), EULAR response based on the DAS28, digital image analysis of CD68 staining, and MRI RAMRIS score of the hand in initial ($T_0$) and control biopsies after 6 months ($T_1$). A decline in sublining CD68 was only noted in those patients with a good EULAR response ($\chi^2$ test: LR 8.3, *p*: 0.05).

*Statistical analysis*

Correlations were calculated according to Spearman. $\chi^2$ test was used for analysis of a cross table including patients with a good EULAR response and declining CD68 staining. $p<0.05$ was considered significant. SPSS 21 was used for analyses.

## Results

*Correlations of synovial markers to disease activity*

We were interested to determine whether markers of synovial inflammation relate to established measures of systemic disease activity (DAS28), and global inflammation (CRP). Table

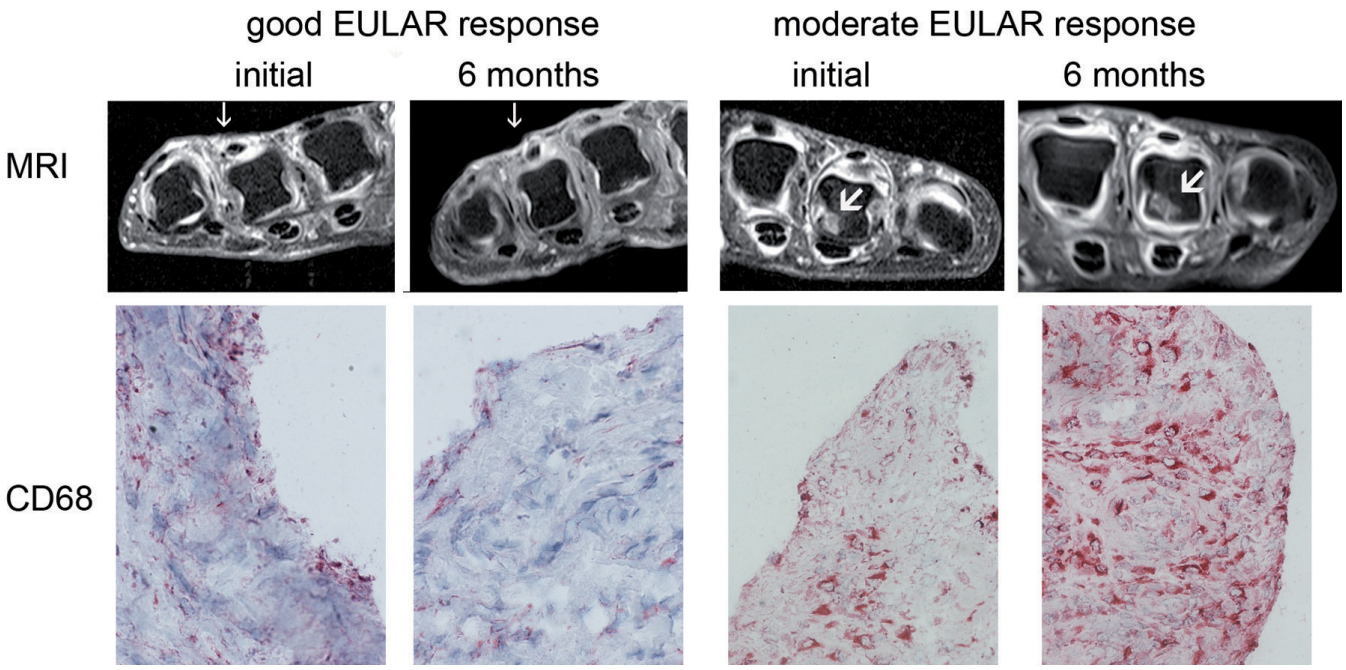


**Fig. 1.** MRI, synovial CD68 staining and EULAR response in individual patients.
Illustration of axial T1 MRI images of the hand and corresponding synovial membrane CD68 staining of one patient with a good EULAR response (P2, left panel: reduction in synovitis (arrow)) and a patient with only moderate response (P6, right panel: progressive erosions (arrow)) illustrating a progressive erosion in MRI and increasing sublining CD68 staining despite a moderate EULAR response.

I shows that the synovitis score correlated to the DAS28 and CRP. This was also true for the inflammatory infiltrate, but not for the other subscores. Similarly, CD68 staining correlated to CRP. Because vascularisation is a crucial event in RA pathophysiology and readily assessed by imaging procedures, we were interested to analyse how markers of vascularisation relate to global disease activity. As can be seen in Table I, HIF-1α and VEGF correlated to the DAS28, while only HIF-1α also related to CRP. Next, we assessed how the synovial markers related to global measures of modern imaging procedures. Correlations of the synovitis score with the US7 ultrasound score and of VEGF with the RAMIRS MRI score were observed (Table I). When considering the subscores of the respective imaging methods, VEGF staining correlated to bone marrow oedema (0.676, $p$=0.032) and erosions scores (0.695, $p$=0,026) of the RAMRIS, and synovitis (0.854, $p$=0.002) and power Doppler scores (0.676, $p$=0.032) of the US7. Correlations of the histological synovitis score to the US7 were largely due to correlations with the synovitis subscore of the US7 (0.694, $p$=0.026).

*Individual changes in synovial tissue analysis*

Furthermore, we were interested to explore the possibility that histological changes in the joint after 6 months relate to treatment response. In our cohort, 3 out of 6 patients fulfilled the criteria for a good EULAR response (P1, P2, and P4; Table II). Only these patients had declining sublining CD68 macrophages in the control biopsy, however statistical significance was not reached ($\chi^2$ test: LR 8.3, $p$=0.05). Moreover, two of the remaining patients (P6, P7) had an increase in sublining CD68 macrophages and deteriorated in the RAMRIS score (Table II, Fig. 1) despite a moderate EULAR response with a reduction of the DAS28.

*Safety of MCP biopsy*

Patients were followed-up for 14.4±5.6 months. Adverse events consisted in light to moderate pain during the arthroscopy in 2 cases, temporary swelling of the hand and impeded motion of the MCP joint for up to one week in 15 cases. There were no serious adverse events (any permanent damage, damage to nerves or vessels, infections, thrombosis, embolism). Of the 10 patients initially enrolled, 6 consented into a second arthroscopy, one patient had to be excluded due to a heart attack 5 months after the initial arthroscopy, one patient was lost to follow-up, and 2 declined a second arthroscopy, because they felt to be in remission. Scaring after the first arthroscopy was minimal and no problems were encountered introducing the arthroscope a second time into the joint.

## Conclusion

In the current study, we demonstrate that established histological assessments of the synovial membrane, e.g. sublining CD68 macrophages (3-5) and the synovitis score (13), as well as markers for vascularisation out of a single dominant MCP joint consistently relate to the DAS28, a widely used score of RA disease activity, or the serum CRP, a marker for systemic inflammation. Importantly, this was true in spite of our approach to limit the number of synovial biopsies in order to preserve enough synovial membrane for a second analysis under therapy. Arthroscopical guidance of biopsies permitted sampling of macroscopically inflamed or non-scared areas, limiting

sampling errors. This was especially important for the second biopsy, where discontinuous scaring of the synovium was observed in all cases, possibly due to the first biopsies, or effective treatment. Thus, the singular or repeated collection of few targeted MCP-joint biopsies with initial quality control of HE stained sections, may represent an alternative to more extensive sampling with pooling of biopsies from larger joints (1, 14), and still permit an adequate appraisal of overall RA disease activity. We are careful not to overinterpret these findings, because the patient number was limited and histological synovial markers were rather arbitrarily chosen and necessarily incomplete, given the small sample size out of MCP joints. Depending on the underlying question, the detection of additional markers such as CD4 and CD20 may be useful. Furthermore, high field MRI was not possible in all patients due to claustrophobia. Despite the recent demonstration of excellent sensitivity of low field MRI (15), different field strengths and the use of contrast agents have to be considered when interpreting this data. However, there are a few interesting implications. First, MCP biopsies may be used to further validate MRI or ultrasound technology, especially the concept of "silent progression", wherein patients with clinical improvement (*e.g.* DAS28) show a lack of improvement or deterioration of imaging findings. Interestingly, the global sumscores used for the assessment of ultrasound and MRI in the present study related to distinct histological markers. This reinforces the hypothesis that imaging of joint inflammation acquired by different techniques highlights distinct cellular or mechanistic aspects (16). More studies comparing histological data to imaging procedures are warranted to improve our interpretation of these images.

## References


1. VAN DE SANDE MGH, GERLAG DM, LODDE BM *et al*.: Evaluating antirheumatic treatments using synovial biopsy: a recommendation for standardisation to be used in clinical trials. *Ann Rheum Dis* 2011; 70: 423-7.
2. GOEB V, WALSH CA, REECE RJ, EMERY P, PONCHEL F: Potential role of arthroscopy in the management of inflammatory arthritis. *Clin Exp Rheumatol* 2012; 30: 429-35.
3. BAETEN D, HOUBIERS J, KRUITHOF E *et al*.: Synovial inflammation does not change in the absence of effective treatment: implications for the use of synovial histopathology as biomarkers in early phase clinical trials in rheumatoid arthritis. *Ann Rheum Dis* 2006; 65: 990-7.
4. BRESNIHAN B, PONTIFEX E, THURLINGS RM *et al*.: Synovial tissue sublining CD68 expression is a biomarker of therapeutic response in rheumatoid arthritis clinical trials: consistency across centers. *J Rheumatol* 2009; 36: 1800-2.
5. WIJBRANDTS CA, VERGUNST CE, HARINGMAN JJ, GERLAG DM, SMEETS TJ, TAK PP: Absence of changes in the number of synovial sublining macrophages after ineffective treatment for rheumatoid arthritis: impications for use of synovial sublining macrophages as a biomarker. *Arthritis Rheum* 2007; 56: 3869-71.
6. KRAAN MC, REECE RJ, SMEETS TJM, VEALE DJ, EMERY P, TAK PP: Comparison of synovial tissues from the knee joints and the small joints of rheumatoid arthritis patients. *Arthritis Rheum* 2002; 46: 2034-8.
7. MJAAVATTEN MD, HAUGEN AJ, HELGETVEIT K *et al*.: Pattern of joint involvement and other disease characteristics in 634 patients with arthritis of less than 16 weeks duration. *J Rheumatol* 2009.
8. KRAAN MC, VERSENDAAL J, JONKER M, BRESNIHAN B, POST WJ, 'T HART BA: Asymptomatic synovitis preceedes clinically manifest arthritis. *Arthritis Rheum* 1998; 41: 1281-8.
9. OSTENDORF B, DANN P, WEDEKIND F *et al*.: Miniarthroscopy of metacarpophalangeal joints in rheuamtoid arthritis. Rating of diagnostic value in synovitis staging and efficiency of synovial biopsy. *J Rheumatol* 1999; 26: 1901-8.
10. OSTENDORF B, PETERS R, DANN P *et al*.: Magnetic resonance imaging and miniarthroscopy of the metacarpophalangeal joints. *Arthritis Rheum* 2001; 44: 2492-502.
11. BACKHAUS M, OHRNDORF S, KELLNER H *et al*.: Evaluation of a novel 7-joint ultrasound scor in daily rheumatologic practice: a pilot project. *Arthritis Rheum* 2009; 61: 1194-201.
12. OSTERGAARD M, EDMONDS J, MCQUEEN F *et al*.: An introduction to the EULAR-OMERACT rheumatoid arthritis MRI reference image atlas. *Ann Rheum Dis* 2005; 64: 3-7.
13. KRENN V, MORAWIETZ L, BURMESTER G-R: Synovitis-score: discrimination between chronic low- and high-grade synovitis. *Histopathology* 2006; 49: 358-64.
14. SCIRÈ CA, EPIS O, CODULLO V *et al*.: Immunhistological assessment of the synovial tissue in small joints in rheumatoid arthritis: validation of a minimally invasive ultrasound-guided synovial biopsy procedure. *Arthritis Res Ther* 2007; 9: R101.
15. SCHMIDT WA, SCHICKE B, OSTENDORF B, SCHERER A, KRAUSE A, WALTHER M: Low-field MRI versus ultrasound: which is more sensitive in detecting inflammation and bone damage in MCP and MTP joints in mild or moderate rheumatoid arthritis. *Clin Exp Rheumatol* 2013; 31:91-6.
16. TAKASE K, OHNO S, TAKENO M *et al*.: Simultaenous evaluation of long-lasting knee synovitis in patients undergoing arthroplasty by power Doppler ultrasonography and contrast-enhanced MRI in comparison with histopathology. *Clin Exp Rheumatol* 2012; 30: 85-92.

Sewerin et al. BMC Musculoskeletal Disorders 2014, 15:104
http://www.biomedcentral.com/1471-2474/15/104

BMC Musculoskeletal Disorders

RESEARCH ARTICLE Open Access

# Advantages of a combined rheumatoid arthritis magnetic resonance imaging score (RAMRIS) for hand and feet: does the RAMRIS of the hand alone underestimate disease activity and progression?

Philipp Sewerin[1*], Christian Buchbender[2], Stefan Vordenbäumen[1], Axel Scherer[2], Falk Miese[2], Ralph Brinks[1,3], Hans-Joerg Wittsack[2], Sabine Klein[1], Matthias Schneider[1], Gerald Antoch[2] and Benedikt Ostendorf[1]

## Abstract

**Background:** To evaluate a combined rheumatoid arthritis magnetic resonance imaging score (RAMRIS) for hand and foot (HaF-score) in rheumatoid arthritis (RA).

**Methods:** Magnetic resonance imaging (MRI, 0.2 Tesla) of the dominant hand and foot of 26 ACPA positive RA patients before and 6 months after initiation of methotrexate was obtained. RAMRIS of the hand was complemented by corresponding scoring of the foot (MTP I-V; HaF-score). Disease Activity Score 28 (DAS28) and a tender and swollen joint count (JC) of the joints scored in MRI were recorded. Changes in these scores (Δ) were assessed.

**Results:** ΔHaF-score correlated significantly with ΔDAS28 (r = 0.820, 95%-CI 0.633-0.916). Correlations to ΔDAS28 were best for changes in the synovitis subscore (0.648) and bone marrow edema (0.703). Correlations to ΔDAS28 were significantly better for of the ΔHaF-score than ΔRAMRIS (0.499, 0.139-0.743, p = 0.0368).
All patients with at least moderate response (EULAR criteria, n = 11) had continuing disease activity on MRI, including five cases with new erosions, three of them at the feet. Improvements of the hand JC or foot JC were seen in 16 and 15 cases, respectively. However, MRI of the hand or feet improved in only 10 and 9 cases, respectively. No patient fulfilled SDAI remission criteria.

**Conclusions:** The HaF-score identifies patients with continuing disease activity despite clinical response that would have been missed by consideration of the traditional RAMRIS or the DAS28 alone. Response as opposed to remission may be an insufficient goal in RA as all patients showed continuing disease activity, especially at the feet.

**Keywords:** Magnetic resonance imaging, Rheumatoid arthritis, RAMRIS, Therapy monitoring, Foot

* Correspondence: philipp.sewerin@med.uni-duesseldorf.de
[1]Department of Rheumatology, Univ Duesseldorf, Medical Faculty, Moorenstrasse 5, Duesseldorf D-40225, Germany
Full list of author information is available at the end of the article

## Background

Rheumatoid Arthritis (RA) is a systemic inflammatory disease causing bone destruction and functional impairment predominantly of the small joints of hands and feet [1]. In order to impede destruction, remission became the utmost goal in the therapy of RA [2]. Beside effective treatment options including disease modifying antirheumatic drugs (DMARD) and biologicals, effective and sensitive tools for therapy monitoring are needed to reach this target. In daily practice as well as in research, therapy monitoring and response assessment are predominantly assessed by using the disease activity score 28 (DAS28) and correspondent response criteria as proposed by the American College of Rheumatology and the European League Against Rheumatism. The DAS28 comprises joints of the upper limbs, hands and the knees [3] but completely omits the feet. However, joint damage progression occur in patients considered to be in remission based on the DAS28, [4] especially in joints which are not covered by the DAS28. Consequently, there is evidence that the DAS28 might underestimate disease activity [5]. Nevertheless Smolen et *al.* demonstrated that the simplified disease activity index (SDAI), which is based on the same 28 joints used for calculation of the DAS28, has the highest predictive value for the development of new erosions [6].

In addition to clinical examination, imaging such as ultrasound and magnetic resonance imaging (MRI) play an important role in the management of RA patients. Although these high resolution imaging modalities are known to confer advantages as opposed to conventional radiographs of the hands and forefeet, the latter still state the gold standard for long-term evaluation of bone destruction. MRI, for instance, can depict earliest inflammatory joint changes such as bone marrow edema (BME), synovitis, or pre-erosion that are not visible on radiographs. Moreover, patients in clinical remission may display signs of disease activity in MRI and Power Doppler augmented ultrasound. These findings have a potential impact on therapeutic decisions, [7,8] because such findings were shown to provides a high predictive value for radiographic joint destruction and prognosis. Due to these data, MRI has become integrated part in the assessment of RA [9,10].

The RA- MRI- Scoring (RAMRIS) system, a standardized semiquantitative assessment of inflammatory soft tissue and destructive bone alteration, facilitated the use of MRI in outcome studies in RA [11-13]. Since most studies used the established RAMRIS method for the clinically dominant hand, little is known about inflammatory and radiomorphological changes of forefeet MRI regarding the relation to disease activity and response to DMARD therapy. Signs of joint inflammation of the foot on MRI were found to be as prevalent as in the hand [14]. They may even be present in the absence of inflammatory MRI findings of the clinically predominantly involved hand [15] as well as in the state of remission based on the DAS28 [16]. The latter study was the first to deploy the established RAMRIS system to the feet and has recently proofed to be highly reliable [17]. To our knowledge, there are no data available comparing the established RAMRIS score with a combined hand and foot score (HaF-score) for measurements of disease activity, radiological alteration and therapy response in RA.

The purpose of this study was to evaluate and compare the traditional RAMRIS of the hand with a new combined HaF-score in terms of clinical and serological correlation and sensitivity to change in RA patients before and after initiation of DMARD monotherapy of methotrexate (MTX), and to analyse the advantages of additional MR imaging of the foot.

## Methods

### Patients

Between November 2009 and July 2012, 26 consecutive patients were prospectively enrolled (18 female, 8 male; mean age 52.9, range ± 29.9 years, mean disease duration 8 weeks (SD 4.66, range 1–18 weeks), mean DAS28 3.5 (SD 0.78, mean CRP 0.9 mg/dl (SD 1.1)) All patients met 2010 American College of Rheumatology/European League Against Rheumatism Rheumatoid arthritis classification criteria [18] and were anticitrullinated peptide antibodies (ACPA) positive. 25 of 26 patients were positive for rheumatoid factor (RF). The general exclusion criteria for MRI imaging with gadolinium based contrast agent, were applied. Because of the dedicated open MRI system claustrophobia could be denied. Steroids were allowed up to a dose of 7.5 mg prednisolone at start and throughout the study. All patients received methotrexate at a dose of 15 mg, which could be taken orally or subcutaneously, conversions from oral to subcutaneous application were allowed. The dose of MTX was kept stable over 6 months. All patients were naïve to DMARD treatment before inclusion into the study and received MTX as part of standard care.

MRI of the dominant hand and foot was carried out prior to the initiation of MTX therapy and after 6 months. Routine parameters assessed during each visit included physical examination and routine laboratory tests including erythrocyte sedimentation rate (ESR) and C-reactive protein levels (CRP). This study was approved by the local review board and informed consent was obtained from all participating subjects.

### Magnetic resonance imaging

MR images of hands and feet were performed achieve most available comfort for patients in a low-field (0.2 T) dedicated open MR system (Esoate, C-Scan, Esaote

Biomedica Germany GmbH). A dedicated wrist and ankle coil was used for image acquisition. The clinically dominant hand and foot (determined by an experienced rheumatologist) were imaged in a single session changing dedicated coil and patient position in every patient. MRI data was obtained on two consecutive time points (T0: prior to DMARD therapy, T1: after 6 month). The image protocol for the hand comprised the following sequences: Coronal Short tau inversion recovery (STIR) sequence with a field of view (FoV) of 180* 180 mm, matrix size 192* 152, slice thickness 3 mm (Time to repetition (TR) 2420 ms, echo time (TE) 26 ms, Time to inversion (TI) 85 ms), coronal 3 dimensional T1-weighted gradient echo sequence with a FoV of 180* 180* 60 mm, matrix size 192* 192* 40, slice thickness 1 mm (TR 50 ms, TE 16 ms) prior to and after intravenous injection of contrast material (0.2 ml/kg bodyweight of Gd-DTPA (Dotarem©, Guerbet GmbH, Germany)). The following protocol was used for imaging of the foot: Coronal STIR- sequence with a FoV of 190* 190 mm, Matrix size 192* 152, slice thickness 3 mm (TR 1700 ms, TE 22 ms, TI 80 ms), coronal 3 dimensional T1- weighted gradient echo sequence with a FoV of 180* 180* 70 mm, matrix size 192* 192* 40, slice thickness 1 mm (TR 50 ms, TE 16 ms) prior to and after intravenous injection of contrast material (0.2 ml/kg bodyweight of Gd-DTPA (Dotarem©)). The 3 dimensional T1-weighted gradient echo sequences of the hand and foot were additionally reconstructed in sagittal and axial planes. The overall image acquisition time was 39 minutes (18 minutes for the hand and 21 minutes for the foot). The plasma half-life time of Dotarem© is about 90 min. Inter-reader reliability of MRI scoring was assessed by independent scoring of images at T0 by two different experienced radiologists (FM and CB) blinded to patient identity. The smalles detectable difference (SSD) according to Lassere is reported.

### Imaging data analysis

MR images were read in consensus by two board-certified radiologists with special expertise in musculoskeletal MRI and trained for RAMRIS scoring. Sites including for scoring on the hand MRI were: metacarpophalangeal joints II-V (MCP), carpal bones, distal radius, distal ulna, radiocarpal and distal radio-ulnar joint. At the foot the metatarsophalangeal (MTP) joints I-V were assessed. For each joint site, synovitis, BME and erosions were semiquantitatively graded as subscores according to the RAMRIS criteria [11]. The RAMRIS score of the hand was calculated. A combined hand and foot score (HaF-score) was calculated as a sum score of the RAMRIS and the MTP joint score including the subscores for synovitis, BME and erosions of each joint comparable to the calculation of the RAMRIS of the hand. The changes in the HaF-score or RAMRIS between the T0 and T1 (Δ) were further analyzed.

### Laboratory and clinical parameters

Laboratory and clinical parameters collected at baseline and follow-up were: ESR, CRP (mg/dl), DAS28 (based on CRP) and simplified disease activity index (SDAI). All clinical examinations were performed by an experienced rheumatologist. Changes of these parameters between T0 and T1 (Δ) were further analyzed.

### Ethic approval

The study was approved by the ethic committee of the medical faculty of the Heinrich-Heine University Duesseldorf (Study number 3226).

### Statistical analysis

Baseline and follow-up characteristics are described as proportions for categorical variables and as mean and standard deviation (SD) for continuous variables. Reported correlation coefficients are according to Spearman. Confidence intervals are two-sided 95% confidence intervals. Results with p <5% are considered to be significant. Confidence intervals for correlation coefficients have been calculated using the Fisher transform. Test for difference of two correlation coefficients has been accomplished as described previously [19]. Effect sizes are reported as standardized response means (SRMs) and are calculated according to Middle and van Sonderen [20]. Statistical analyses have been performed using R version 2.15.2 (R Development Core Team).

## Results

The mean value of DAS28 decreased from T0 (prior to MTX-therapy) to T1 (after 6 months) from 3.45 (min. 2.3; max. 4.9) to 2.9 (min. 1.8; max 4.6), the mean CRP decreased from 0.91 mg/dl (min. 0.3; max. 5.1) to 0.59 mg/dl (min. 0.3; max. 3.0). The mean RAMRIS decreased from 21.81 (min 0; max 53) to 21.69 (min 0; max 63) and the mean HaF-score from 33.58 (min 4; max 84) to 31.08 (min 2; max. 73) after 6 months (Table 1). ΔHaF-score showed the highest correlation with ΔDAS28 (T1-T0) (0.820 confidence interval (CI) 0.633-0.916) followed by Δsum score foot (0.522, CI 0.168-0.756) and ΔRAMRIS of the hand (0.662, CI 0.69-0.85) (Table 2, Figure 1). ΔHaF-score had a significantly higher correlation to ΔDAS28 than ΔRAMRIS (p = 0.0368). Correlations of ΔHaF-score to ΔSDAI values were overall slightly weaker (0.662 CI 0.369-0.835), with ΔSDAI demonstrating the highest correlations to ΔHaF-score amongst the parameters considered (Table 2). No patients reached remission based on SDAI criteria [3]. The evaluation of changes of the considered parameters (i.e. synovitis and BME) over time, employing the SRMs,

**Table 1 Comparison of radiological, laboratory and clinical scores at baseline and after 6 month**

| Score | T0 (baseline) | | | T1 (after 6 month) | | |
|---|---|---|---|---|---|---|
| | Min. | Mean | Max. | Min. | Mean | Max. |
| DAS28 | 2.3 | 3.45 | 4.90 | 1.8 | 2.90 | 4.60 |
| SDAI | 4.3 | 14.99 | 29.10 | 3.4 | 11.55 | 27.30 |
| CRP | 0.3 | 0.91 | 5.10 | 0.3 | 0.59 | 3.00 |
| BSG | 4.0 | 23.04 | 62.00 | 3.0 | 16.43 | 58.00 |
| Sum score hand | 0 | 7.59 | 22 | 0 | 6.385 | 25 |
| Sum score wrist | 0 | 14.27 | 42 | 0 | 15.31 | 59 |
| Sum score foot | 0 | 11.77 | 44 | 0 | 9.385 | 33 |
| RAMRIS | 0 | 21.81 | 53 | 0 | 21.69 | 63 |
| HaF-score | 4 | 33.58 | 84 | 2 | 31.08 | 73 |

showed a high effect size for the decrease of the DAS28 (−0.8188). In contrast, the effect size for the decrease in the HaF-score was trivial (−0.13). Similarly, based on the EULAR response criteria, eleven patients reached clinical improvement with good or moderate response. In the MRI follow-up (T1), all patients showed signs of continuing disease activity on MRI, including all good and moderate responder. Five of these showed actually new erosions (Table 3).

The analysis of the different subscores of the HaF-score with ΔDAS28 revealed that changes in synovitis (0.648 CI 0.347-0.827) and BME (0.703 CI 0.434-0.857) were best correlated. In comparison to the combined HaF-score, MRI scoring for the foot alone, showed markedly lower correlations to ΔDAS28 (Δsynovitis 0.485 (CI 0.12-0.734) and ΔBME 0.514 (CI 0.159-0.752)) (Table 4).

Next, the performance of the HaF-score against clinical examination was assessed. For this purpose, all joints considered in the HaF-score were examined on both sides and the number of swollen joints was added to the number of tender joints to create a sum score for the hand (hand joint count) and the foot (foot joint count). The hand count demonstrated worsening in six, unchanged values in four, and an improvement in sixteen patients. Despite improvement in the hand joint count on clinical examination, there was no improvement of the traditional RAMRIS in 6 of 16 patients. The foot joint count demonstrated worsening in two, unchanged values in nine, and an improvement in fifteen patients. Comparable to the traditional RAMRIS, the foot subscore of the new HaF-score uncovered 6 out of 15 patients with unchanged values or deterioration in spite of clinical improvement (i.e. foot joint count) (Table 5).

The pattern of inflammatory changes within the HaF-score was assessed. Overall, foot joints were more severely involved based on the MRI sum scores of synovitis, erosions and BME compared to the hand. Therein, MTP-2 was the single most affected joint. Furthermore, scoring of the MTP-2 showed the highest mean differences between T0 and T1 (Table 6).

Finally, inter-reader reliability of MRI scoring at T0 was assessed to estimate the generalizability of HaF-scoring. SSD were as follows: RAMRIS: 4.77, HaF score: 4.60, RAMRIS subscore hand: 2.23, RAMRIS subscore wrist: 4.10, HaF subscore foot: 1.81. In 24 of 26 patients, the HaF subscore for the foot differed by only 1 or less. In addition we analysed the inter-rater agreement at T0 for the subscores Syn, Ero and BME for MCP-2 and MTP-2 as the most frequently involved joints. SDD were as follows for MCP-2: Ero subscore 0.91, Syn subscore 1.03. BME subscore 1.91; MTP-2: Ero subscore 0.87, Syn subscore 1.29, BME scubscore 0.87.

## Discussion

This study is the first to evaluate a combined hand and foot MRI score (HaF-score) for monitoring RA patients under DMARD therapy with methotrexate. A combined assessment on hand and feet is already established for years in the assessment of conventional radiographs [21-23]. However, MRI offers the potential for visualizing synovitis and BME, which was repeatedly shown to be predictive for radiologic progression [10]. Moreover, to our knowledge, this is the first systematic report of combined hand and foot MRI in one session in RA patients. Patients had to be summoned for examination

**Table 2 Spearman-correlation between ΔDAS28 and ΔSDAI to changes in other changes scores**

| Change in score (ΔT1-T0) | Correlations between ΔDAS28 and changes in other scores | 95% confidence interval | Correlations between ΔSDAI and changes in other scores | 95% confidence interval |
|---|---|---|---|---|
| **CRP** | 0.170 | −0.232–0.523 | 0.316 | −0.082–0.626 |
| **ESR** | 0.217 | −0.186–0.558 | 0.308 | −0.09–0.621 |
| **sum score hand** | 0.368 | 0.022–0.661 | 0.280 | −0.12–0.602 |
| **sum score wrist** | 0.449 | 0.075–0.713 | 0.335 | −0.061–0.639 |
| **sum score foot** | 0.522 | 0.168–0.756 | 0.544 | 0.199–0.769 |
| **RAMRIS*** | 0.499 | 0.139–0.743 | 0.338 | −0.057–0.641 |
| **HaF–score*** | 0.820 | 0.633–0.916 | 0.662 | 0.369–0.835 |

*Significant differences between ΔRAMRIS und ΔHaF-score (p = 0.0368) in correlation to ΔDAS28.

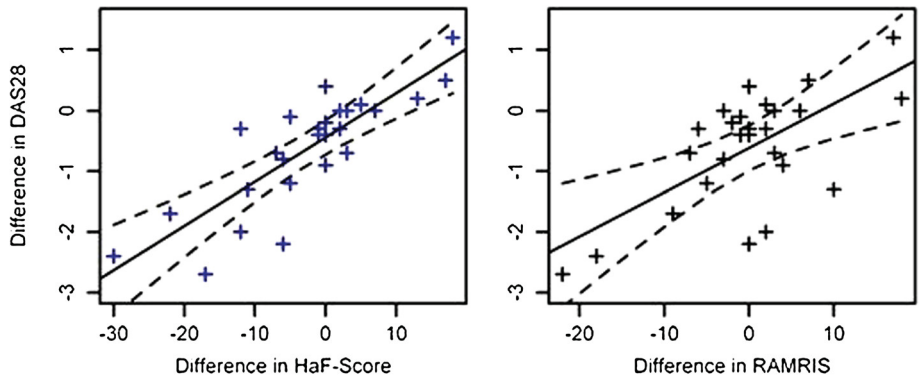


**Figure 1** Scatterplot of differences: HaF-Score (left figure) and RAMRIS (right figure) vs. DAS28.

and received contrast agents only once, resulting in a high patient satisfaction.

We found that the HaF-score correlated with clinical and laboratory measures of disease activity such as DAS28, SDAI and CRP. Analysing each component of the HaF-score separately, we found that changes in the HaF-score subscores for synovitis and BME, but not erosions, correlated with changes of the DAS28 and SDAI after therapy. This was also true if subscores for different anatomic regions were assessed separately (i.e. synovitis or BME for the hand, wrist and foot), albeit to a lesser degree. In comparison to clinical examination of the hand and the feet (hand and foot joint count), twelve patients with remarkable improvement in the joint counts after six months were uncovered by worsening or unchanged HaF-scores in MRI.

Numerous studies suggest that the DAS28 reflects disease activity [5,24]. A potential limitation to determining disease activity by the DAS28 allone is highlited by the finding of disease progression dispite clinical improvement or remission [25,26]. Krabben *et al.* have recently shown that subclinical inflammation - detected in hand and foot MRI - frequently occurs in ACPA positive patients [27]. Moreover, Wechalekar *et al.* demonstrated in a prospective study in RA-patients after six months of DMARD therapy DAS28 remisson rates of 30% (SDAI 28%), wherein 43% still showed active synovitis in the forefoot [28]. In accordance with this finding, we identified eleven RA patients as being in good or moderate response, based on the EULAR response criteria, who nevertheless showed signs of disease activity on MRI. Five of them had new erosions – and importantly, three of these erosions were located at the foot. Moreover there were seven patients with an improvement in (traditional hand) RAMRIS at T1 having new erosions, two of them in the foot. This is reflected by the effect size changes in the HaF-score, which were trivial while changes in DAS28 showed large effect sizes. Similarly, patients deemed to have improved based on the SDAI, a potentially more accurate clinical compound measure for the prediction of erosions in RA, [6] were uncovered to have continuing disease activity or deterioration based on MRI HaF-score. Importantly, in accordance with our finding that all patients had residual disease activity based on the HaF-score, no patient in the study reached remission based on SDAI criteria (SDAI < 3.3), which is

**Table 3 Delta in the sum scores of the good or moderate EULAR-responders**

| Sum score | Hand | | Wrist | | Foot | |
|---|---|---|---|---|---|---|
| | Mean | Range | Mean | Range | Mean | Range |
| **Syn** | −2.545 | −10–2 | −2.545 | −8–2 | −3.455 | −12–0 |
| **Ero** | 0.7273 | −3–4 | 0.5455 | −1–4 | 0.5455 | −1–4 |
| **BME** | −0.8182 | −5–2 | 0.5455 | −3–5 | −3.273 | −14–1 |

Syn = Synovitis, Ero = Erosion, BME = bone marrow edema.

**Table 4 Spearman-Correlation between ΔDAS28 and synovitis-, erosion- and bone marrow edema-subscore between T0 and T1**

| Score | Spearman-correlation | 95% confidence interval |
|---|---|---|
| **Syn overall** | 0.648 | 0.347–0.827 |
| **Ero overall** | 0.125 | −0.275–0.489 |
| **BME overall** | 0.703 | 0.434–0.857 |
| **Syn hand** | 0.487 | 0.123–0.736 |
| **Ero hand** | −0.296 | −0.613–0.104 |
| **BME hand** | 0.238 | −0.164–0.573 |
| **Syn wrist** | 0.349 | −0.044–0.649 |
| **Ero wrist** | 0.286 | −0.114–0.606 |
| **BME wrist** | 0.326 | −0.071–0.633 |
| **Syn foot** | 0.485 | 0.12–0.734 |
| **Ero foot** | −0.282 | −0.603–0.119 |
| **BME foot** | 0.514 | 0.159–0.752 |

Syn = Synovitis, Ero = Erosion, BME = bone marrow edema.

**Table 5 Comparison between ΔRAMRIS of the hand (a) and the foot (b) and corresponding changes in total tender joint (TJ) and swollen joint (SJ) count**

| | | Differences in hand TJ-SJ count (T1-T0) | | |
|---|---|---|---|---|
| | | **Improved** | **Equal** | **Worse** |
| **ΔRAMRIS of the hand (T1-T0)** | Improved | 10 | 1 | 0 |
| | Equal | 2 | 2 | 3 |
| | Worse | 4 | 1 | 3 |
| | | **Differences in hand TJ-SJ count (T1-T0)** | | |
| | | **Improved** | **Equal** | **Worse** |
| **ΔRAMRIS of the foot (T1-T0)** | Improved | 9 | 2 | 0 |
| | Equal | 2 | 6 | 0 |
| | Worse | 4 | 1 | 2 |

currently considered to be the best predictive measure for radiological disease progression [3]. The same was true for all patients who reached remission in DAS28 while even all of them showed residual disease activity in the HaF-score. Hence, the current study stresses the importance of reaching remission rather than a moderate or good response only.

This study is limited by small patient number. Moreover, it could be argued that a clinical compound measure including the feet such as the DAS44 would have been more suitable for comparison with the new HaF-score. However, unlike the DAS44, the DAS28 is nowadays considered to be the gold standard for determining disease activity in RA, not only in studies, but also in clinical practice. Due to national guidelines for the application of X-rays, which allow routine conventional X-rays to be obtained only once a year, a comparison between changes in MRI and X-rays was not possible in the course of 6 months. Furthermore, additional MR parameters such as scoring of tenosynovitis might be of additional value, but were not featured in our study.

Based on the present results, longitudinal studies with a longer time period evaluating the potential of a combined hand and foot MRI score (HaF-score) to predict long-term radiological and functional outcomes are clearly warranted.

There is theoretical concern that generalizability of the HaF score may be hampered by difficulties in scoring the foot. However, inter-reader realiability for the HaF-score and especially the foot subscore was excellent in the present study. Thus, the HaF may be regarded as a reliable scoring system for the assessment of hand and foot inflammation.

## Conclusion

The HaF-score identifies patients with continuing disease activity despite clinical response that would have been missed by consideration of the traditional RAMRIS or the DAS28 alone. Response as opposed to remission may be an insufficient goal in RA as all patients showed continuing disease activity, especially at the feet.

**Table 6 Most frequently affected joints**

| Affected joint | Number of patients with Syn, Ero or BME at T0 | Overall sumscore T0 | Number of patients with Syn, Ero or BME at T02 | Overall sumscore T1 | Overall difference in the sum score |
|---|---|---|---|---|---|
| **MCP2** | 19 | 63 | 17 | 56 | −7 |
| **MCP3** | 20 | 52 | 17 | 44 | −8 |
| **MCP4** | 14 | 28 | 15 | 23 | −5 |
| **MCP5** | 18 | 53 | 16 | 43 | −10 |
| **MTP1** | 18 | 67 | 16 | 63 | −4 |
| **MTP2** | 15 | 68 | 12 | 48 | −20 |
| **MTP3** | 15 | 67 | 12 | 52 | −15 |
| **MTP4** | 16 | 57 | 11 | 46 | −11 |
| **MTP5** | 13 | 47 | 13 | 35 | −12 |

MCP = metacarpophalangeal joints, MTP = metatarsophalangeal joints.

### Abbreviations

ACPA: Anti-citrullinated protein antibodies; ACR: American College of Rheumatology; BME: Bone marrow edema; CI: Confidence interval; CRP: C-reactive protein; DAS28: Disease activity score 28; DMARD: Disease modifying anti rheumatic drug; EULAR: European league against rheumatism; ESR: Erythrocyte sedimentation rate; MRI: Magnetic resonance tomography; MCP joint: Metacarpophalangeal joint; MTP joint: Metatarsophalangeal joint; MTX: Methotrexate; RA: Rheumatoid arthritis; RAMRIS: Rheumatoid arthritis magnetic resonance imaging score; SD: Standard deviation; SDAI: Simplified disease activity index; SRM: Standardized response mean.

### Competing interests

The authors declare that they have no competing interests.

### Authors' contributions

Study design: PS, CB, H-JW and BO. Study conduct: PS, CB, SV, SK, MS, GA and BO. Data collection: PS, CB, SV, AS, FM, SK and BO. Data analysis: PS, CB, SV, AS, FM, RB, SK and BO. Data interpretation: PS, SV, RB and BO. Drafting manuscript: PS. Revising manuscript content: PS, CB, SV, FM, RB, SK, MS, GA and BO. PS and RB take responsibility for the integrity of the data analysis. All authors read and approved the final manuscript.

### Acknowledgements

We would like to thank the Hiller foundation, Erkrath, Germany.

### Author details

[1]Department of Rheumatology, Univ Duesseldorf, Medical Faculty, Moorenstrasse 5, Duesseldorf D-40225, Germany. [2]Department of Diagnostic and Interventional Radiology, Univ Duesseldorf, Medical Faculty, Duesseldorf D-40225, Germany. [3]German Diabetes Center, Institute for Biometry and Epidemiology, Auf'm Hennekamp 65, Duesseldorf 40225, Germany.

Received: 20 January 2014 Accepted: 21 March 2014
Published: 26 March 2014

### References

1. Grassi W, De Angelis R, Lamanna G, Cervini C: **The clinical features of rheumatoid arthritis.** *Eur J Radiol* 1998, **1:**18–24.
2. Smolen JS, Aletaha D, Bijlsma JW, Breedveld FC, Boumpas D, Burmester G, Combe B, Cutolo M, de Wit M, Dougados M, Emery P, Gibofsky A, Gomez-Reino JJ, Haraoui B, Kalden J, Keystone EC, Kvien TK, McInnes I, Martin-Mola E, Montecucco C, Schoels M: **Treating rheumatoid arthritis to target: recommendations of an international task force.** *Ann Rheum Dis* 2010, **4:**631–637.
3. Felson DT, Smolen JS, Wells G, Zhang B, van Tuyl LH, Funovits J, Aletaha D, Allaart CF, Bathon J, Bombardieri S, Brooks P, Brown A, Matucci-Cerinic M, Choi H, Combe B, de Wit M, Dougados M, Emery P, Furst D, Gomez-Reino J, Hawker G, Keystone E, Khanna D, Kirwan J, Kvien TK, Landewé R, Listing J, Michaud K, Martin-Mola E, Montie P: **American College of Rheumatology/European League Against Rheumatism provisional definition of remission in rheumatoid arthritis for clinical trials.** *Arthritis Rheum* 2011, **3:**573–586.
4. Aletaha D, Smolen JS: **Joint damage progresses in DAS28 remission and is driven by residual swollen joints.** *Arthritis Rheum* 2011, **12:**37027–11.
5. Landewé R, van der Heijde D, van der Linden S, Boers M: **Twenty-eight-joint counts invalidate the DAS28 remission definition owing to the omission of the lower extremity joints: a comparison with the original DAS remission.** *Ann Rheum Dis* 2006, **5:**637–641.
6. Smolen JS, Breedveld FC, Schiff MH, Kalden JR, Emery P, Eberl G, van Riel PL, Tugwell P: **A simplified disease activity index for rheumatoid arthritis for use in clinical practice.** *Rheumatol Oxf Engl* 2003, **42:**244–257.
7. Brown AK, Conaghan PG, Karim Z, Quinn MA, Ikeda K, Peterfy CG, Hensor E, Wakefield RJ, O'Connor PJ, Emery P: **An explanation for the apparent dissociation between clinical remission and continued structural deterioration in rheumatoid arthritis.** *Arthritis Rheum* 2008, **58:**2958–2967.
8. Brown AK, Quinn MA, Karim Z, Conaghan PG, Peterfy CG, Hensor E, Wakefield RJ, O'Connor PJ, Emery P: **Presence of significant synovitis in rheumatoid arthritis patients with disease-modifying antirheumatic drug-induced clinical remission: evidence from an imaging study may explain structural progression.** *Arthritis Rheum* 2006, **54:**3761–3773.
9. Haavardsholm EA, Bøyesen P, Østergaard M, Schildvold A, Kvien TK: **Magnetic resonance imaging findings in 84 patients with early rheumatoid arthritis: bone marrow oedema predicts erosive progression.** *Ann Rheum Dis* 2008, **67:**794–800.
10. Bøyesen P, Haavardsholm EA, Ostergaard M, van der Heijde D, Sesseng S, Kvien TK: **MRI in early rheumatoid arthritis: synovitis and bone marrow oedema are independent predictors of subsequent radiographic progression.** *Ann Rheum Dis* 2011, **70:**428–433.
11. Østergaard M, Peterfy C, Conaghan P, McQueen F, Bird P, Ejbjerg B, Shnier R, O'Connor P, Klarlund M, Emery P, Genant H, Lassere M, Edmonds J: **OMERACT Rheumatoid Arthritis Magnetic Resonance Imaging Studies. Core set of MRI acquisitions, joint pathology definitions, and the OMERACT RA-MRI scoring system.** *J Rheumatol* 2003, **30:**1385–1386.
12. Bird P, Conaghan P, Ejbjerg B, McQueen F, Lassere M, Peterfy C, Edmonds J, Shnier R, O'Connor P, Haavardsholm E, Emery P, Genant H, Østergaard M: **The development of the EULAR-OMERACT rheumatoid arthritis MRI reference image atlas.** *Ann Rheum Dis* 2005, **64:**8–10.
13. Østergaard M, Edmonds J, McQueen F, Peterfy C, Lassere M, Ejbjerg B, Bird P, Emery P, Genant H, Conaghan P: **An introduction to the EULAR-OMERACT rheumatoid arthritis MRI reference image atlas.** *Ann Rheum Dis* 2005, **64:**3–7.
14. Boutry N, Lardé A, Lapègue F, Solau-Gervais E, Flipo RM, Cotten A: **Magnetic resonance imaging appearance of the hands and feet in patients with early rheumatoid arthritis.** *J Rheumatol* 2003, **30:**671–679.
15. Ostendorf B, Scherer A, Mödder U, Schneider M: **Diagnostic value of magnetic resonance imaging of the forefeet in early rheumatoid arthritis when findings on imaging of the metacarpophalangeal joints of the hands remain normal.** *Arthritis Rheum* 2004, **50:**2094–2102.
16. van der Leeden M, Steultjens MP, van Schaardenburg D, Dekker J: **Forefoot disease activity in rheumatoid arthritis patients in remission: results of a cohort study.** *Arthritis Res Ther* 2010, **12:**R3.
17. Baan H, Bezooijen R, Avenarius JK, Dubbeldam R, Drossaers-Bakker WK, van de Laar MA: **Magnetic resonance imaging of the rheumatic foot according to the RAMRIS system is reliable.** *J Rheumatol* 2011, **38:**1003–8.
18. Aletaha D, Neogi T, Silman AJ, Funovits J, Felson DT, Bingham CO, Birnbaum NS, Burmester GR, Bykerk VP, Cohen MD, Combe B, Costenbader KH, Dougados M, Emery P, Ferraccioli G, Hazes JM, Hobbs K, Huizinga TW, Kavanaugh A, Kay J, Kvien TK, Laing T, Mease P, Ménard HA, Moreland LW, Naden RL, Pincus T, Smolen JS, Stanislawska-Biernat E, Symmons D, *et al*: **2010 Rheumatoid arthritis classification criteria: an American College of Rheumatology/European League Against Rheumatism collaborative initiative.** *Arthritis Rheum* 2010, **62:**2569–2581.
19. Meng XL, Rosenthal R, Rubin DB: **Comparing correlated correlation coefficients.** *Psychological Bulletin* 1992, **111:**172–175.
20. Middel B, Van Sonderen E: **Statistical significant change versus relevant or important change in (quasi) experimental design: some conceptual and methodological problems in estimating magnitude of intervention-related change in health services research.** *Int J Integr Care* 2002, **2:**15–17.
21. van der Heijde DM, van Leeuwen MA, van Riel PL, Koster AM, van 't Hof MA, van Rijswijk MH, van de Putte LB: **Biannual radiographic assessments of hands and feet in a three-year prospective followup of patients with early rheumatoid arthritis.** *Arthritis Rheum* 1992, **35:**26–34.
22. van der Heijde DM, van Leeuwen MA, van Riel PL, van de Putte LB: **Radiographic progression on radiographs of hands and feet during the first 3 years of rheumatoid arthritis measured according to Sharp's method (van der Heijde modification).** *J Rheumatol* 1995, **22:**1792–1796.
23. Rau R, Wassenberg S, Herborn G, Stucki G, Gebler A: **A new method of scoring radiographic change in rheumatoid arthritis.** *J Rheumatol* 1998, **25:**2094–2107.
24. Prevoo ML, van't Hof MA, Kuper HH, van Leeuwen MA, van de Putte LB, van Riel PL: **Modified disease activity scores that include twenty-eight-joint counts. Development and validation in a prospective longitudinal study of patients with rheumatoid arthritis.** *Arthritis Rheum* 1995, **48:**3844–3848.
25. Kraan MC, Versendaal H, Jonker M, Bresnihan B, Post WJ, t Hart BA, Breedveld FC, Tak PP: **Asymptomatic synovitis precedes clinically manifest arthritis.** *Arthritis & Rheumatism* 1998, **41:**1481–1488.
26. Gandjbakhch F, Conaghan PG, Ejbjerg B, Haavardsholm EA, Foltz V, Brown AK, Møller Døhn U, Lassere M, Freeston J, Bøyesen P, Bird P, Fautrel B, Hetland ML, Emery P, Bourgeois P, Hørslev-Petersen K, Kvien TK, McQueen F, Ostergaard M: **Synovitis and osteitis are very frequent in rheumatoid arthritis clinical remission: results from an MRI study of 294 patients in clinical remission or low disease activity state.** *J Rheumatol* 2011, **38:**2039–2044.

27. Krabben A, Stomp W, van der Heijde DM, van Nies JA, Bloem JL, Huizinga TW, Reijnierse M, van der Helm-van Mil AH: **MRI of hand and foot joints of patients with anticitrullinated peptide antibody positive arthralgia without clinical arthritis.** *Ann Rheum Dis* 2013, **72:**1540–1544.
28. Wechalekar MD, Lester S, Proudman SM, Cleland LG, Whittle SL, Rischmueller M, Hill CL: **Active foot synovitis in patients with rheumatoid arthritis: applying clinical criteria for disease activity and remission may result in underestimation of foot joint involvement.** *Arthritis Rheum* 2012, **64:**1316–1322.

doi:10.1186/1471-2474-15-104
**Cite this article as:** Sewerin *et al.*: Advantages of a combined rheumatoid arthritis magnetic resonance imaging score (RAMRIS) for hand and feet: does the RAMRIS of the hand alone underestimate disease activity and progression? *BMC Musculoskeletal Disorders* 2014 **15**:104.

# Neue bildgebende Verfahren in der Rheumatologie: From bench to bedside

## New imaging procedures in rheumatology: from bench to bedside

**Autoren** P. Sewerin[1] B. Ostendorf[1]

**Institut** [1] Poliklinik für Rheumatologie, Medizinische Fakultät, Heinrich-Heine Universität Düsseldorf

## Einleitung

Moderne bildgebende Verfahren spielen in der Diagnostik und Therapiekontrolle in der Rheumatologie eine zunehmende Rolle. Gründe dafür sind unter anderem die Verbesserung und Weiterentwicklung bekannter Methoden, die Implementierung neuer Verfahren und die neuen Paradigmen und Therapieleitlinien, die auf den verbesserten therapeutischen Möglichkeiten entzündlich-rheumatischer Erkrankungen basieren. Zusätzlich zur klinischen Remission, die durch eine frühzeitige antirheumatische Therapie induziert wird, ist es inzwischen erklärtes Ziel, die radiologische Progression aufzuhalten [12]. Damit sollen Funktionalität und Arbeitsfähigkeit erhalten, die Lebensqualität verbessert und zuletzt auch die Kosten signifikant reduziert werden [24]. Die Einbindung moderner bildgebender Methoden verfeinert diese diagnostischen Algorithmen und Strategien.

Beispielhaft ist zunächst die Sonographie zu nennen, die bei Arthritis hochauflösend anatomische Strukturen und mittels Power-Doppler-Ultraschall effizient „Entzündung" darstellen kann.

Die Schnittbildgebung wie z.B. die MRT wird inzwischen systematisch zur Abklärung und Klassifikation der seronegativen Spondyloarthritis (ASAS-Klassifikationskriterien) genutzt [35].

Ferner ist es heutzutage möglich, lokale Gewebestoffwechselaktivität (z.B. Glukoseutilisation oder Knochenstoffwechsel) bei bestimmten entzündlich-rheumatischen Erkrankungen wie der Arteriitis bzw. Vaskulitis durch nuklearmedizinische Verfahren (z.B. Positronen-Emissions-Tomographie [PET]) darzustellen.

Zudem ist die Schnittbildgebung mit funktionellen Verfahren (z.B. PET oder Single Photon Emission Computed Tomography [SPECT]) zur „hybriden Bildgebung" fusioniert worden und wird zur Detektion von okkulten, entzündlichen bzw. tumorösen Prozessen immer mehr genutzt.

Eine weitere Bildgebungsmodalität sind fluoreszenzoptische Verfahren, beispielsweise mit dem Xiralite©-System. Hierbei wird der Fluoreszenzfarbstoff Indocyaningrün intravenös injiziert, welcher sich nachfolgend in hypervaskularisierten Geweben anreichert – beispielsweise bei Arthritis – und mit einer speziellen Kamera erfasst werden kann. Das Verfahren ist derzeit in der wissenschaftlichen Testung, wird aber – da zugelassen – bereits bei verschiedenen Indikationen im klinischen Alltag eingesetzt [39].

Die Kapillarmikroskopie hingegen ist eine seit Jahrzehnten etablierte Technik zur Darstellung der Mikrozirkulation der Nagelfalz, deren Zugewinn für Frühdiagnostik von Kollagenosen (z.B. bei der Systemischen Sklerose [Klassifikationsmerkmal]) aber erst seit geraumer Zeit wieder entdeckt worden ist.

Ziel aller genannter Verfahren ist die frühzeitige Erfassung des pathomorphologischen Substrates und damit die Diagnoseabsicherung der jeweiligen Erkrankung sowie die sensitive Kontrolle bzw. das exakte Monitoring des Krankheitsverlaufes. Auf diese Weise können die Frühdiagnostik, konsekutiv die frühe und gezielte Therapie und dadurch auch die Prognose verbessert werden [31].

Diese neue Vielfalt an inzwischen gut evaluierten bildgebenden Verfahren stellt den behandelnden Arzt häufig vor die Fragen: Welches Verfahren ist nun sinnvoll? Zu welchem Zeitpunkt ist es in Klinik und Praxis einzusetzen? Welchen spezifischen Mehrwert haben einzelne Methoden in der Beurteilung des individuellen Krankheitsverlaufes?

**Rheumatologie, Radiologie**

**Schlüsselwörter**
- Bildgebung
- Rheumatologie
- MRT
- Sonographie
- DECT
- Kapillarmikroskopie

**Keywords**
- imaging
- rheumatology
- MRI
- ultrasound
- DECT
- capillary microscopy

**eingereicht** 20.05.2014
**akzeptiert** 17.07.2014

**Bibliografie**
**DOI** 10.1055/s-0034-1370280
Dtsch Med Wochenschr 2014; 139: 1835–1841 · © Georg Thieme Verlag KG · Stuttgart · New York · ISSN 0012-0472

**Korrespondenz**
***Prof. Dr. med. Benedikt Ostendorf***
Poliklinik für Rheumatologie
Universitätsklinikum Düsseldorf
Heinrich-Heine-Universität
Düsseldorf
Moorenstraße 5
40225 Düsseldorf
eMail Ostendorf@med.uni-duesseldorf.de

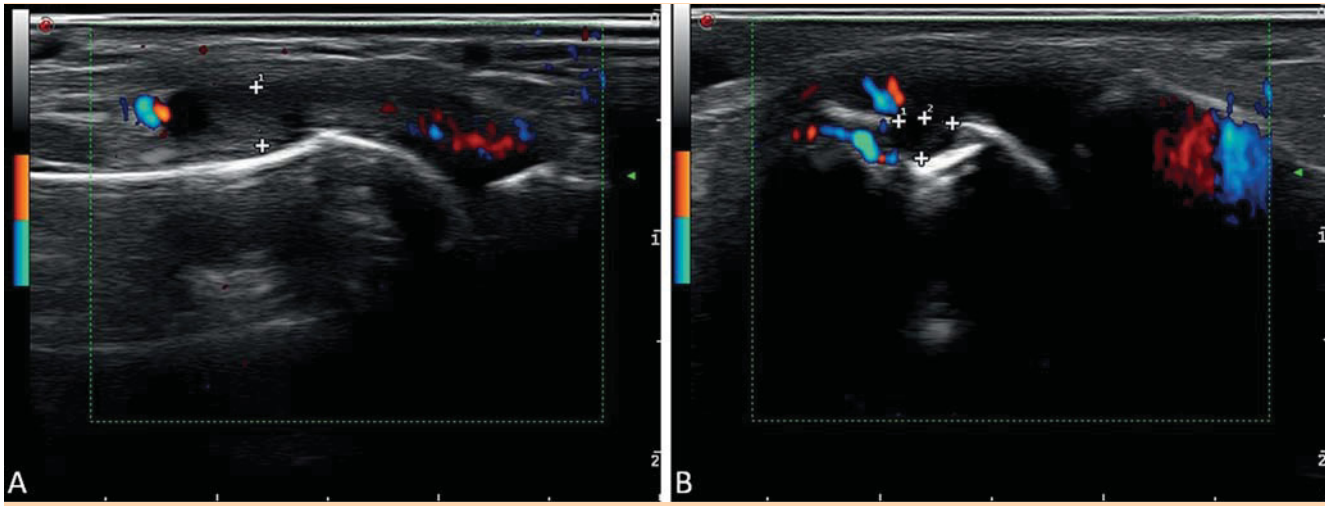


**Abb.1** Power-Doppler-Sonographie bei einer 58-jährigen Patientin mit hoch-aktiver rheumatoider Arthritis. **A)** Metacarpophalangeal-Gelenk 2 (Längsschnitt) mit einer deutlich erweiterten Gelenkkapsel und positivem Power-Doppler-Signal als Ausdruck einer Synovialitis. **B)** Power-Doppler-Sonographie des Metacarpophalangeal-Gelenkes 3 mit angrenzender Erosion (mit + 1 und + 2markiert) und Synovialitis.

## Rheumatoide Arthritis

Mit bundesweit über 800 000 Patientinnen und Patienten ist die rheumatoide Arthritis (RA) die häufigste entzündliche Gelenkerkrankung. Die Erkrankungen betreffen oft jüngere Menschen mitten im Familien- und Berufsleben, die sozialmedizinische Last ist daher eklatant hoch [40]. Die frühzeitige Diagnose und Therapie mit dem Ziel der „Remission" wird heute in Leitlinien gefordert [33]. Hierbei musste der Einsatz der Bildgebung neu diskutiert werden, da die bisher standardmäßig verwendeten konventionellen Röntgenbilder nur den Schaden bzw. die Folgen entzündlicher Gelenkveränderungen und nicht die aktuelle Krankheitsaktivität hinreichend gut erfassen können.

Mit der Arthrosonographie hingegen gelingt an kleinen sowie an großen Gelenken die sensitive Detektion von Weichteilveränderungen wie Erguss und Synovialitis. Aber auch knöcherne Alterationen wie die krankheitstypische Erosion können nachgewiesen werden – und dies deutlich sensitiver als mit dem konventionellen Röntgenbild. Aufgrund technischer Weiterentwicklungen stehen uns heutzutage hochauflösende Sonographie-Geräte zur Verfügung (Linearschallköpfe bis 5 – 7,5 – 20 MHz). Sie können aufgrund der exzellenten Ortsauflösung sowie durch Zusatz des Power-Dopplers (farbkodierte-Dopplersonographie) incipiente Gelenkaffektionen erfassen [15]. Das Ausmaß des Power-Doppler-Signals korreliert signifikant mit der Entzündungsaktivität und ist – bei unbehandelter Arthritis – prädiktiv für die Entstehung von Erosionen [17] (**Abb.1**).

Die Arthrosonographie erfolgt standardisiert entsprechend den Richtlinien der Deutschen Gesellschaft für Ultraschall in der Medizin (DEGUM) und der European League Against Rheumatism (EULAR) [12]. In diesem Zusammenhang wurde die rheumatologische Dokumentation standardisiert und vereinfacht. Etabliert hat sich für die Therapiekontrolle ein auf 7 Gelenke reduzierter US-7 Ultraschallscore, der inzwischen in rheumatologischen Kliniken und Praxen sowie auch in Studien eingesetzt wird [2, 3, 4]. Auch die semiquantitative Dokumentation und das Scoring von entzündlicher Alterationen großer Gelenke wird inzwischen standardisiert erfasst (SOLAR-Score [23]).

Mit der MRT – sei es durch die Hochfeld- oder Niederfeld-Technologie – gelingt ebenso eine detaillierte bzw. hochauflösende Darstellung von intraossären, intraartikulären oder periartikulären Gelenkstrukturen. Mittels dieser Schnittbildtechnik können Erosionen bei RA sensitiver als mit dem Röntgenbild detektiert werden; im Mittel bereits 3–4 Monate nach Krankheitsbeginn [5]. Durch die Anwendung bestimmter Wichtungen (T2-Wichtung) und die Gabe von Kontrastmittel (T1-Wichtung plus Kontrastmittel) ist die Aktivitätsbeurteilung der Entzündung (z.B. Synovialitis) möglich. Durch andere spezielle MR-Signale bzw. Wichtungen (z.B. short tau inversion recovery [STIR]) können auch subklinische Formen der Synovialitis oder die Osteitis (Knochenmarködem) erfasst werden, die hochprädiktiv für die Entstehung von Erosionen sind [25] (**Abb.2**). Die Arthrosonographie kann diese Form der Knochenentzündung bzw. Stoffwechseländerung nicht erfassen. Ebenso wie bei der Sonographie liegen für die MRT inzwischen für rheumatologische Fragestellungen zur RA standardisierte Untersuchungsprotokolle vor (z.B. RAMRIS) [29], welche in der Frühdiagnostik als auch Verlaufskontrolle eingesetzt werden, um Befunde unter gleichen Bedingungen abzubilden und vergleichen zu können. Technische Weiterentwicklungen der MRT (z.B. Niederfeld-MRT) [19] bzw. neue Sequenzprotokolle (z.B. für Knorpelmessung mittels dGEMRIC [26]) sowie neue Scoring-Protokolle für Hand und Fuß [34] haben inzwischen zu einer breiteren Anwendung der MRT und neuen Indikationen in Klinik und Praxis geführt (EULAR Recommendations [12]). Insbesondere auch bei unklarer Arthritis kann die MRT eine Hilfe bei der Differenzierung bieten und wird hierfür häufig eingesetzt.

Fluoreszenzoptische Verfahren (z.B. Xiralite©, Rheuma-Scan©) sind seit 2009 als Medizinprodukte zugelassen und werden derzeit in einigen Kliniken und Praxen zur Frühdiagnostik von Gelenkentzündungen eingesetzt. Die Technologie basiert auf dem Nachweis der charakteristischen, mit einer Arthritis assoziier-

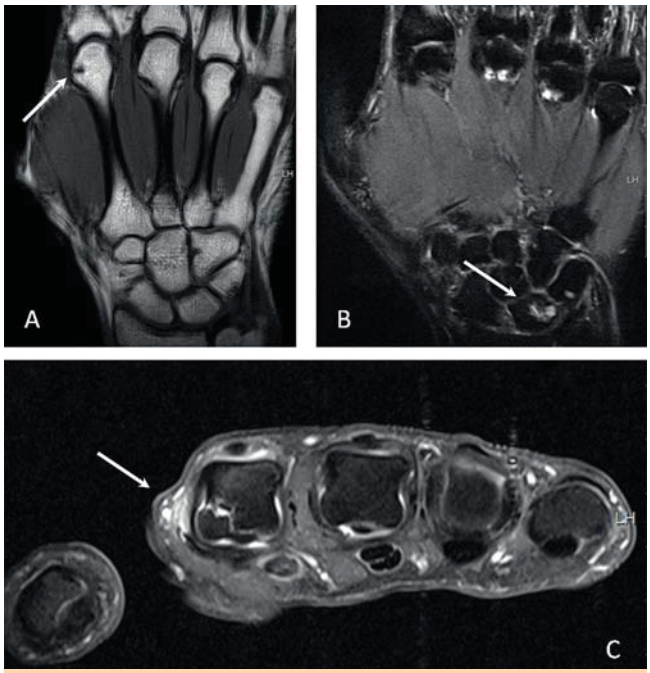


**Abb.2** Hochfeld-MRT (3-Tesla) der Hand bei einer 47-jährigen Patientin mit Rheumatoider Arthritis. **A)** T1-Wichtung nativ (ohne Kontrastmittel; coronare Schnittführung) mit einer Erosion im Kopf des Mittelhandknochens des 2. Strahles. **B)** STIR-Sequenz mit Nachweis einer Osteitis (Knochenmarködem) im Os lunatum der Handwurzel (coronare Schnittführung). **C)** T1-Wichtung nach Kontrastmittelgabe (axiale Schnittführung) mit ausgeprägter Synovialitis und Kontrastmittelanreicherung um das Metacarpophalangeal-Gelenk 2. (Abbildung: F. Miese, C. Schleich; Institut für Diagnostische und Interventionelle Radiologie, Universitätsklinikum Düsseldorf).

ten Veränderungen wie Neoangiogenese, dem daraus resultierenden erhöhten Blutfluss, der gestörten Mikrozirkulation und erhöhten Kapillarpermeabilität in Gelenken und Sehnen mithilfe des Farbstoffs Indocyaningrün und Licht im infrarotnahen Bereich. Es konnte in Studien gezeigt werden, dass die Ergebnisse (Erfassung der Hypervaskularisierung an den betroffenen Finger- und Handgelenken) mit Befunden aus Sonographie und MRT korrelieren [38, 39]. Eine Zulassung bei gesetzlich versicherten Patienten besteht noch nicht.

**kurzgefasst**

**Die Arthrosonographie ist heute aufgrund ihrer vielen Vorteile (keine Strahlung, überall verfügbar, sensitiv, u.a.) ein wichtiges und etabliertes Instrument bei der Frühdiagnostik und der Therapiekontrolle von Patienten mit z.B. einer RA. Die MRT kann, insbesondere bei komplexen Verläufen, als ergänzendes bildgebendes Verfahren eingesetzt werden, da sie suffizient und deutlich früher als die konventionelle Radiologie ossäre (insbesondere die Osteitis und Erosionen) und weichteilige, RA-spezifische Veränderungen erkennen kann.**

## Gicht

Die Gicht betrifft in westlichen Ländern 1–2% aller Erwachsenen, wobei Inzidenz und Prävalenz in den letzten Jahren und Jahrzehnten ansteigen [32]. Bei akuter und/oder rezidivierender Symptomatik mit typischer Lokalisation („Podagra“) ist die Diagnose leicht zu stellen. Der Nachweis von Harnsäurekristallen im Gelenkpunktat sichert diese schlussendlich. Bei untypischer Lokalisation und nicht eindeutigen Laborbefunden kann es aber zu Verzögerungen und Unsicherheit bei der Diagnostik kommen. Ähnlich wie bei der RA wird heute daher bei der Gichtarthritis die Sonographie ergänzend zur Diagnosestellung und Therapiekontrolle eingesetzt. So können zum einen beginnende erosive Veränderungen („knöcherner Stanzdefekt“), Synovialitis und Gichttophus sicher erkannt werden. Zum anderen kann mit Hilfe der Ultraschall-Untersuchung eine typische und pathognomonische Doppelkonturlinie im bzw. am Gelenkknorpel detektiert werden („Doppelkonturzeichen“), welche die Diagnose einer Kristallarthropathie sehr wahrscheinlich macht [11] (**Abb.3**).

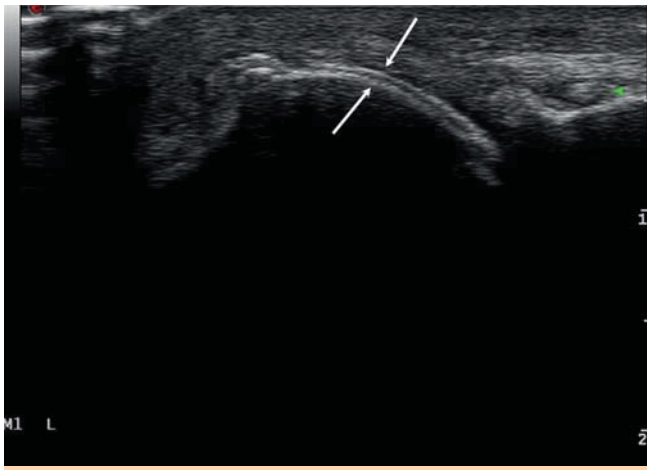

**Abb.3** Doppelkonturzeichen im hochauflösenden Ultraschall (Längsschnitt) des Knorpels des proximales Metacarpophalangealgelenkes des 2. Strahles (MCP-2) bei einem Patienten mit Gicht (Abbildung: W. Schmidt; Immanuel Krankenhaus Berlin, Standort Berlin-Buch).

Darüber hinaus besteht heute in vielen großen radiologischen Instituten und Praxen die Möglichkeit mit Hilfe der „Dual-Energy Computertomographie“-Technik (DECT) Harnsäurekristalle im CT Bild „farblich“ sichtbar zumachen. Beim Dual-Source-CT sind in einem Gerät 2 Scan-Systeme verbaut, die im Winkel von 90° angeordnet sind. Zur Detektion von Harnsäurekristallen werden die beiden Energiequellen (80 kV und 140 kV) nahezu zeitgleich gescannt. Im Gegensatz zu den meisten Geweben, welche nur geringe Schwächungsunterschiede bei der Bestrahlung aufweisen (80 kV vs. 140 kV), zeigen jodhaltige Kontrastmittel und Uratkristalle deutliche Unterschiede. Diese können im Nachhinein sichtbar gemacht und mit hoher Sensitivität Uratablagerungen erkennen, sodass in vielen Fällen auf die bisher als Goldstandard angesehene Gelenkpunktion verzichtet werden kann [13, 14]. Die Methode ist schnell umsetzbar, wenig belastend und kann auch im Bereich der gesetzlich versicherten Patientenversorgung durchgeführt werden (**Abb.4**).

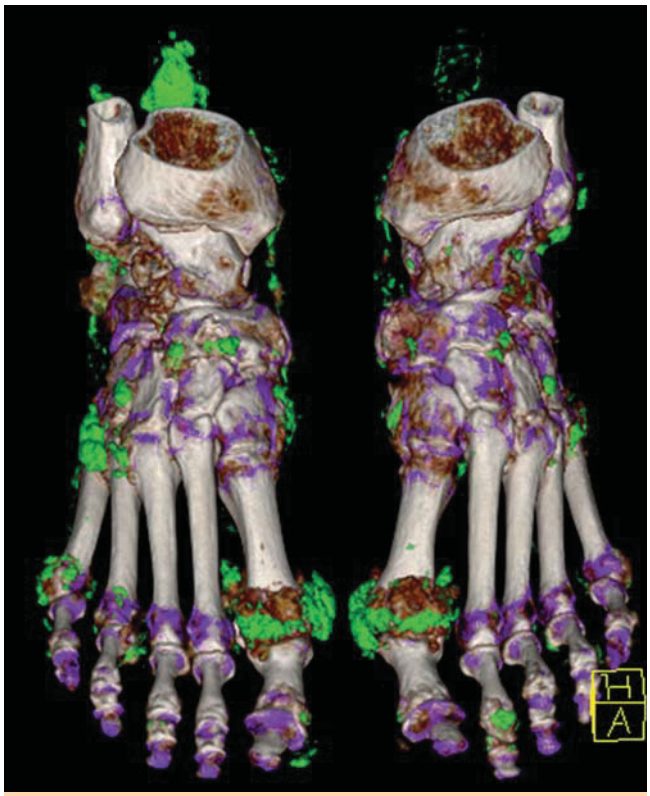

**Abb.4** DECT-Untersuchung eines 68-jährigen Patienten mit schwerer tophöser Gicht: Nachweis von Uratkristallen unter anderem an den Großzehengrundgelenken und der Achillessehne (Uratkristalle werden grün dargestellt; Abbildung: B. Manger, J. Rech; Medizinische Klinik III mit Poliklinik, Universität Erlangen-Nürnberg).

**kurzgefasst**

**Die Diagnosestellung und Therapiekontrolle einer Gicht stellt den behandelnden Arzt insbesondere bei untypischer Lokalisation und Laborkonstellation häufig vor eine große Herausforderung. Die Arthrosonographie hat durch die hohe Auflösung und der Möglichkeit typische „Doppelkonturzeichen" am Knorpel zu erfassen, einen hohen Stellenwert bei der Gichtdiagnostik erreicht. Ergänzend bietet die schon in vielen Zentren verfügbare DECT die Möglichkeit, auch kleinste Uratkristalle hochauflösend darzustellen und wird – da für den Patienten wenig belastend – in den kommenden Jahren eine wichtige Rolle im Diagnose-Algorithmus der Gicht einnehmen.**

## Spondyloarthritiden

Die seronegativen Spondyloarthritiden (SpA) sind eine heterogene Gruppe von entzündlich-rheumatischen Gelenk- und Wirbelsäulenerkrankungen. Sie werden in eine axiale und eine periphere Form (oder auch Kombination) eingeteilt [1]. In Deutschland sind knapp 1,9% der Bevölkerung hiervon betroffen [7]. Unbehandelt entwickelt sich eine zunehmende Versteifung und knöcherne Überbauung der Wirbelkörper bzw. der Wirbelsäule (Ankylos) mit massiver Einschränkung der Beweglichkeit. Daher wird heute eine frühe und effektive anti-inflammatorische Therapie (einschl. Biologika-Behandlung bei ausgewählten Fällen) empfohlen [1, 8].

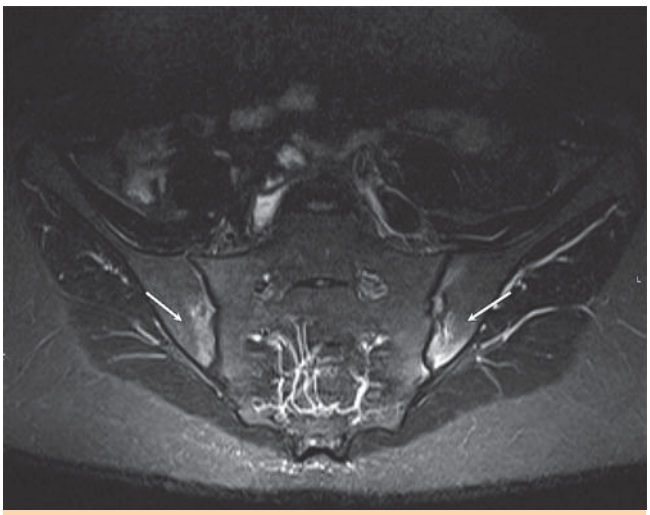

**Abb.5** MRT (STIR-Sequenz) der Iliosakralgelenke mit Nachweis einer ausgeprägten, beidseitigen Sakroiliitis mit angrenzendem Ödem bei einer 32-jährigen Patientin mit incipienter Spondyloarthritis (Röntgen der LWS o.p.B.) (Abbildung: F. Miese, C. Schleich; Institut für Diagnostische und Interventionelle Radiologie, Universitätsklinikum Düsseldorf).

Lange Jahre war die konventionelle Röntgenaufnahme der Iliosakralgelenke der Goldstandard für die Diagnosestellung und Verlaufskontrolle. In den vergangenen Jahren hat die MRT der Iliosakralgelenke und der Wirbelsäule zunehmend an Bedeutung gewonnen, da sie frühzeitiger eine Sakroiliitis bzw. Spondylitis diagnostizieren kann und somit zur Prognose-relevanten Frühdiagnose beiträgt. So wird heutzutage der Einsatz der MRT zur Detektion der Sakroiliitis von den Experten der ASAS (The Assessment of SpondyloArthritis international Society) empfohlen und hat Einzug in die aktuellen ASAS-Klassifikationskriterien gefunden [35] ( **Abb.5**).

Auch die Psoriasis-Arthritis zählt zu den seronegativen Spondyloarthritiden. Etwa ein Drittel der Patienten mit einer Psoriasis vulgaris sind im Laufe ihres Lebens von einer Psoriasis-Arthritis betroffen [10]. Ähnlich wie bei der RA ist die Sonographie ein gut evaluiertes und etabliertes diagnostisches Instrument zur Diagnosestellung und Therapie-Monitoring bei Patienten mit Psoriasis-Arthritis. So konnte gezeigt werden, dass mit Hilfe der hochauflösenden Sonographie, insbesondere unter Hinzunahme der Power-Doppler-Technik, typische entzündliche periartikuläre und ligamentäre Veränderungen wie Enthesitiden und Tenovaginitiden als auch Daktylitiden frühzeitiger im Krankheitsverlauf erfasst werden, dort wo die Röntgendiagnostik noch unauffällig ist [22].

**kurzgefasst**

**Die MRT kann heute ein wichtiges Hilfsmittel bei der Diagnosestellung bei Patienten mit SpA bzw. Spondylitis ankylosans sein und wird in den aktuellen Klassifikationskriterien der ASAS-Expertengruppe empfohlen. Die Sonographie ist ein unverzichtbarer Bestandteil der Diagnostik und Therapiekontrolle peripherer Gelenkveränderungen bei SpA (Enthesitis, Arthritis, Daktylitis) geworden.**

## Polymyalgia rheumatica und Riesenzellarteriitis/Arteriitis temporalis

Die Polymyalgia rheumatica ist eine verbreitete entzündlich-rheumatische Erkrankung, insbesondere der älteren Bevölkerung (Durchschnittsalter bei ca. 70 Jahren). In Deutschland treten jährlich zwischen 16 000 und 40 000 neue Fälle auf [21]. Die Diagnosestellung kann zu einer Herausforderung werden, da es sich um eine „Ausschlussdiagnostik" handelt. Richtungsweisend sind nur erhöhte humorale Entzündungszeichen bei typischen Muskelschmerzen im Schulter- und/oder Hüftbereich.

Auch für die Diagnostik der Polymyalgia rheumatica hat die Sonographie in den letzten Jahren zunehmend an Bedeutung gewonnen. Seit 2012 sind der sonographische Nachweis einer subacromialen Bursitis, einer Bizepssehnentendinitis oder einer Coxitis ein Klassifikations- bzw. Diagnosekriterium der Polymyalgia rheumatica geworden [16]. So konnte gezeigt werden, dass durch die Hinzunahme der Ultraschalluntersuchung (Vorliegen einer Bursitis oder Bizepssehnentendinitis eines Schultergelenkes oder einer Coxitis) die Spezifität der Diagnosestellung von 66% auf 81% sich erhöht.

Die Riesenzellarteriitis ist ähnlich wie die Polymyalgia rheumatica eine insbesondere in der älteren Bevölkerung auftretende entzündlich-rheumatische Erkrankung, die häufig mit der Polymyalgia rheumatica einhergeht. Bei bis zu zwei Drittel der Patienten kann es durch eine Minderdurchblutung des Sehnervs oder der Netzhaut zu Sehstörungen bis hin zur Erblindung kommen – eine gefürchtete Komplikation. Zahlreiche Publikationen konnten zeigen, dass die Sonographie – mit Power-Doppler-Ultraschall – typische zirkulären Wandverdickungen der betroffenen Arterien bzw. der großen abgehenden Arterien der Aorta aufzeigen kann und diese Untersuchungstechnik eine hohe Sensitivität und Spezifität aufweist, sodass eine Temporalarterienbiospie häufig nicht erforderlich ist [6, 28] (**Abb.6**). Darüber hinaus können moderne nuklearmedizinische Verfahren (z.B. PET) mit hoher Sensitivität erhöhte Glukoseutilitsation an Gefäßregionen darstellen und so eine Arteriitis – von sonographisch nicht gut zugänglichen Gefäßen (wie z.B. der thorakalen Aorta) – erfassen [30] (**Abb.7**). Zur Abklärung unklarer inflammatorischer Krankheitsbilder („Fieber unklarer Genese" DD Tumorerkrankung u.a.) werden heute an vielen Standorten bereits in der klinischen Routine hybride bildgebende Techniken (in der Regel PET-CT) eingesetzt. Hierbei wird die hohe Sensitivität für die Darstellung erhöhter Glukosestoffwechselaktivität in entzündlichen Arealen der PET mit der hohen Ortsauflösung der CT kombiniert [20].

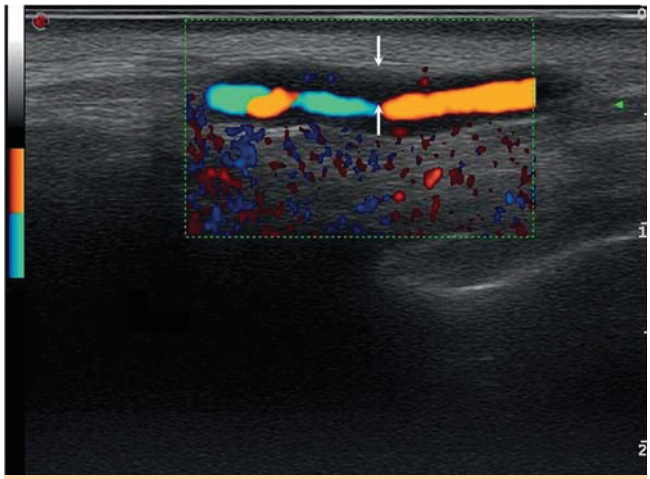

**Abb.6** Power-Doppler-Sonographie der Arteria temporalis (Längsschnitt) eines 78-jährigen Patienten mit Riesenzellarteriitis/Arteriitis temporalis mit Nachweis eines ausgeprägten Wandödems und konsekutiver Flussunregelmäßigkeit (Abbildung: O. Sander, Poliklinik für Rheumatologie, Düsseldorf).

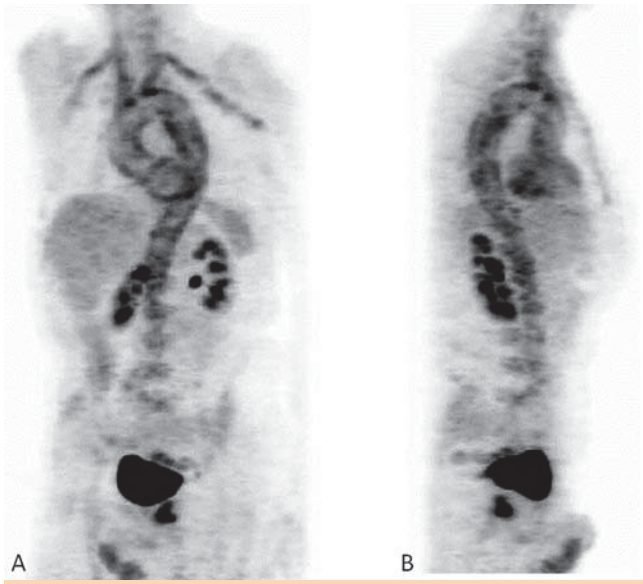


**Abb.7** Positronen-Emissions-Tomografie eines 63-jährigen Patienten mit Aortitis bei Riesenzellarteriitis und erhöhter Glukoseutilisation in der gesamten thoraklen Aorta sowie den Aa. axilares. Ansicht von frontal (**A**) und von rechtsseitig (**B**) (Abbildung H. Hautzel, Klinik für Nuklearmedizin, Düsseldorf).

**kurzgefasst**

**Die Diagnose einer Polymyalgia rheumatica bereitet aufgrund der fehlenden beweisenden Befunde nicht selten Schwierigkeiten. Die Sonographie kann durch eine einfache Untersuchung der Hüfte und des Schultergelenkes die Sensitivität der Diagnostik deutlich erhöhen. Gleiches gilt für die Arteriitis temporalis bzw. Riesenzellarteriitis, welche in der hochauflösenden Sonographie bei Krankheitsbeginn eine fast pathognomonisch zirkuläre Wandverdickung der Gefäße („entzündliches Ödem") aufweist. Bei unklaren Fällen sollte ergänzend eine Ganzkörper-PET, in Ausnahmefällen sogar ein hybrides Verfahren mit der PET-CT hinzugezogen werden, um okkulte vaskulitische Gefäßveränderungen oder andere Ursachen zu erkennen, die sonographisch nicht zugänglich sind (z.B. Aortitis u.a.).**

## Systemische Sklerose

Die systemische Sklerose ist eine systemische Bindegewebserkrankung, die sich durch eine progressive Verdickung und Verhärtung der Haut auszeichnet. Erschwerend kann es zu einer Organbeteiligung der Lunge, des Gastrointestinaltraktes und – erfreulicherweise zunehmend seltener – zu einer Beteiligung der Nieren kommen. Häufig sind periphere Durchblutungsstörungen im Sinne eines Raynaud-Syndroms ein erstes Krankheitszeichen. Die Kapillarmikroskopie ist eines der ältesten bildgebenden Verfahren, welches in den letzten Jahren wieder zunehmend in Fokus rückt. Hierbei können mit einem Mikroskop und einem handelsüblichen Öl Kapillaren der Nagelfalz vergrößert dargestellt werden. Patienten mit einer systemischen Sklerose weisen schon früh im Krankheitsverlauf typische Veränderungen der Kapillarstruktur mit Megakapillaren,

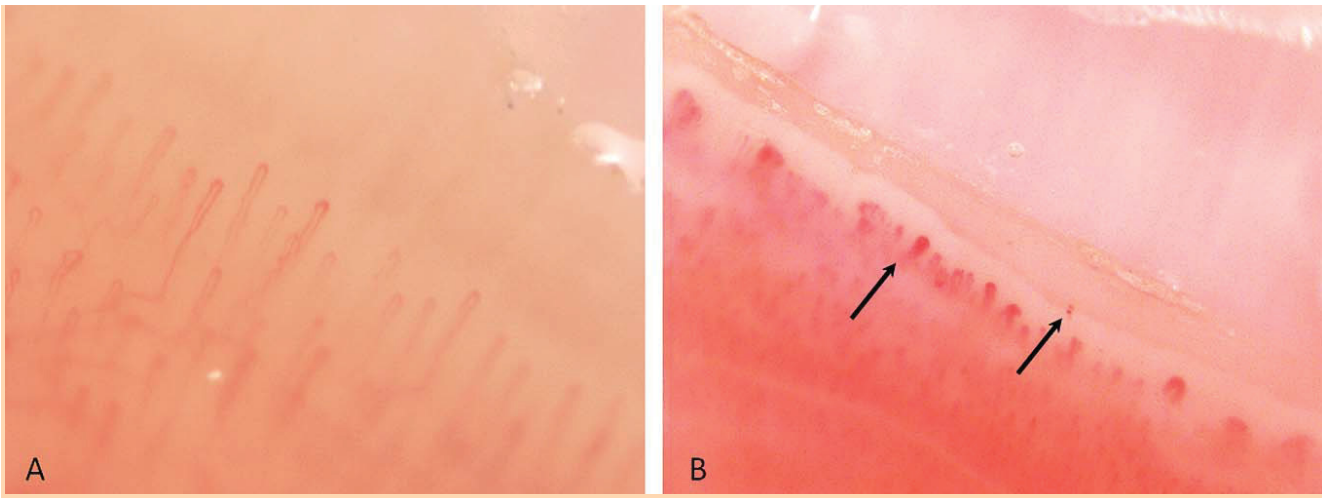


**Abb.8** Kapillarmikroskopie der Nagelfalz. **A**) Normalbefund mit typischen, haarnadelförmigen Kapillaren der Nagelfalz **B**) Kapillarektasien und Megakapillaren sowie einzelnen Blutungen bei einer 56-jährigen Patientin mit systemischer Sklerose (Abbildung: O. Sander, Poliklinik für Rheumatologie, Düsseldorf).

Ektasien, deutlichen Kaliberschwankungen sowie Einblutungen in die Nagelfalz auf [18] (**Abb.8**). 2013 wurden durch die Amerikanische und Europäische rheumatologische Fachverbände (American College of Rheumatology, ACR und die European league against rheumatism, EULAR) neue Klassifikationskriterien etabliert, in der die Kapillarmikroskopie als fester Klassifikationsparameter eingeht [37]. Kapillarmikroskopische Veränderungen können heutzutage standardisiert erfasst und dokumentiert werden [31], dies ist wichtig für die Verlaufskontrolle und Prognoseabschätzung.

**kurzgefasst**

**Die Kapillarmikroskopie ist ein kostengünstiges und etabliertes Verfahren zur Darstellung der Kapillaren an der Nagelfalz. Bereits in der Frühphase weisen Patienten mit sekundärem Raynaud-Syndrom (und ANA pos.) oder einer beginnenden systemischen Sklerose typische Veränderungen der Kapillarstruktur auf, sodass die Kapillarmikroskopie ein fester Bestandteil der Differenzialdiagnostik von Patienten mit beginnender Kollagenose bzw. Abklärung eines Raynaud-Syndroms geworden ist.**

## Ausblick

Bildgebende Verfahren wie die konventionelle Röntgendiagnostik sind seit jeher Bestandteil der Diagnostik und Therapiekontrolle rheumatischer Erkrankungen. Neue Therapiekonzepte („window of opportunity“) [9], neue Therapiestrategien („treat to target“) [27] und zunehmend die Erfordernisse für eine „personalisierte Medizin“ (Identifizierung von Risikopatienten bzw. individuelle Aktivitäts- und Prognoseabschätzung) [36] fordern und fördern sensitive moderne bildgebende Verfahren im Patientenmanagement. Die Entwicklung „from bench to bedside“ zeigt, dass viele innovative Techniken nach eingehender wissenschaftlicher und klinischer Prüfung einen bedeutenden Platz im diagnostischen Algorithmus gefunden haben. Eine Vielzahl weiterer bildgebender Methoden ist derzeit in Erprobung (Hybridbildgebung, neue MRT Sequenzen (Knorpel), kontrastmittelfreie MRT-Protokolle, molekulare Bildgebung u.a.). Sie sind noch experimentell, zeitlich aufwändig und mit höheren Kosten verbunden. Dennoch werden sie in Zukunft das Armentarium der Bildgebung deutlich erweitern können.

Als klinisch und wissenschaftlich tätige Ärzte in Praxis und Klinik sollten wir die neuen bildgebenden Methoden kritisch analysieren und ihre Vorteile – immer im Hinblick einer optimalen Patientenversorgung – sinnvoll in unsere diagnostischen Überlegungen integrieren.

**Konsequenz für Klinik und Praxis**

- Die Sonographie ist ein sensitives bildgebendes Verfahren zur Darstellung von knöchernen und weichteiligen Alterationen der Arthritis. Sie wird daher zur Frühdiagnostik und Therapiekontrolle genutzt. Darüber hinaus wird sie zunehmend zur Erfassung anderer entzündlich-rheumatischer Erkrankungen, wie z.B. Vaskulitiden oder Kristallarthropathien, genutzt.
- Die MRT kann neben der Darstellung von entzündlichen Gelenkveränderungen als einziges Verfahren Knochenmarködeme (Osteitis) detektieren, welches Prädiktiv für die Entstehung von Erosionen ist. Aufgrund ihrer Vorteile wird sie bereits zur Diagnostik der frühen Spondyloarthritis (ASAS-Diagnosekriterien) genutzt. Trotz der derzeit noch vergleichbar hohen Kosten wird dieses Verfahren aufgrund der fehlenden Strahlenbelastung und der Vorteile der Schnittbildgebung seinen festen Platz bei der Diagnostik und Therapiekontrolle entzündlich rheumatischer Erkrankungen einnehmen
- Die DECT stellt ein neues CT Verfahren zur farblichen Darstellung von Gichtkristallen dar und ist bereits heute in vielen Zentren verfügbar. Sie ist für den Patienten vergleichbar wenig belastend (keine Gelenkpunktion nötig) und wird zukünftig eine wichtige Rolle im Diagnose-Algorithmus der Gicht einnehmen.
- Die Kapillarmikroskopie wird heutzutage durch ihrer Vorteile (schnelle Durchführung, fehlende Strahlenbelastung und hohe Sensitivität) fast flächendeckend in der Rheumatologie zur Abklärung des Raynaud-Syndroms bzw. zur Frühdiagnostik und Therapiekontrolle von Kollagenose (z.B. Systemische Sklerose) genutzt.
- Hybride bildgebende Verfahren (wie z.B. PET-CT) sind innovativ und heute bereits in vielen Zentren verfügbar Die Vorteile obliegen in der hohen Sensitivität der PET und der hohen Ortsauflösung bzw. der topographischen Untermauerung durch die CT bzw. MRT (One-Stop Shop). Durch diese Vorteile werden die Verfahren zunehmend häufiger ergänzend zur Erfassung von okkulten entzündlichen- oder tumorösen Prozessen eingesetzt.

**Danksagung:** Wir danken PD Dr. F. Miese, Dr. C. Schleich, Düsseldorf und PD Dr. med. H. Hautzel, Düsseldorf, Prof. Dr. B. Manger und Dr. J. Rech, Erlangen-Nürnberg, Prof. Dr. W. Schmidt, Berlin-Buch sowie Dr. O. Sander, Düsseldorf für das Bildmaterial.

**Autorenerklärung:** Die Autoren erklären, dass sie keine finanzielle Verbindung mit einer Firma haben, deren Produkt in diesem Beitrag eine Rolle spielt (oder mit einer Firma, die ein Konkurrenzprodukt vertreibt).

## Literatur


1 AWMF. „Evidenzbasierte Leitlinie der Deutschen Gesellschaft für Rheumatologie (DGRh) und der beteiligten medizinisch-wissenschaftlichen Fachgesellschaften und weiterer Organisationen Langfassung zur S3- Leitlinie Axiale Spondyloarthritis inklusive Morbus Bechterew und Frühformen". 2013; http://www.awmf.org/uploads/tx_szleitlinien/060-003l_S3_Axiale_Spondyloarthritis_Morbus_Bechterew_2013-11.pdf

2 *Backhaus M, Burmester GR, Sandrock D et al.* Prospective Two Year Follow up Study Comparing Novel and Conventional Imaging Procedures in Patients with Arthritic Finger Joints. Ann Rheum Dis 2002; 61: 895–904

3 *Backhaus M, Ohrndorf S, Kellner H et al.* Evaluation of a Novel 7-Joint Ultrasound Score in Daily Rheumatologic Practice: A Pilot Project". Arthritis Rheum 2009; 61: 1194–1201

4 *Backhaus TM, Ohrndorf S, Kellner H et al.* The US7 Score Is Sensitive to Change in a Large Cohort of Patients with Rheumatoid Arthritis over 12 Months of Therapy". Ann Rheum Dis 2013; 72: 1163–1169

5 *Baker JF, Ostergaard M, Emery P et al.* Early MRI Measures Independently Predict 1-Year and 2-Year Radiographic Progression in Rheumatoid Arthritis: Secondary Analysis from a Large Clinical Trial. Ann Rheum Dis 2013;10.1136/annrheumdis-2013-203444

6 *Black R, Roach D, Rischmueller M et al.* The Use of Temporal Artery Ultrasound in the Diagnosis of Giant Cell Arteritis in Routine Practice". Int J Rheumc Dis 2013; 16: 352–357

7 *Braun J, Bollow M, Remlinger G.* Prevalence of Spondylarthropathies in HLA-B27 Positive and Negative Blood Donors. Arthritis Rheum 1998; 41: 58–67

8 *Braun J, van den Berg R, Baraliakos X et al.* 2010 Update of the ASAS/EULAR Recommendations for the Management of Ankylosing Spondylitis. Ann Rheum Dis 2011; 70: 896–904

9 *Breedveld F.* The Value of Early Intervention in RA – a Window of Opportunity. Clin Rheumatol 2011; 30(01): S33–39

10 *Catanoso M, Pipitone N, Salvarani C.* Epidemiology of Psoriatic Arthritis. Reumatism 2012; 64: 66–70

11 *Chowalloor PV, Keen HI.* A Systematic Review of Ultrasonography in Gout and Asymptomatic Hyperuricaemia. Ann Rheum Dis 2013; 72: 638–645

12 *Colebatch AN, Edwards CJ, Østergaard M et al.* EULAR Recommendations for the Use of Imaging of the Joints in the Clinical Management of Rheumatoid Arthritis. Ann Rheum Dis 2013; 72: 804–814

13 *Dalbeth N, Choi HK.* Dual-Energy Computed Tomography for Gout Diagnosis and Management". Curr Rheumatol Rep 2013; 15: 301

14 *Dalbeth N, Doyle A, McQueen FM.* Imaging in Gout: Insights into the Pathological Features of Disease". Current Opin Rheumatol 2012; 24: 132–138

15 *Dalvi SR, Moser DW, Samuels J.* Ultrasound and Treatment Algorithms of RA and JIA. Rheum Dis Clin North Am 2013; 39: 669–688

16 *Dasgupta B, Cimmino MA, Kremers HM et al.* 2012 Provisional Classification Criteria for Polymyalgia Rheumatica: A European League Against Rheumatism/American College of Rheumatology Collaborative Initiative. Arthritis Rheum 2012; 64: 943–954

17 *Funck-Brentano T, Gandjbakhch F, Etchepare F et al.* Prediction of Radiographic Damage in Early Arthritis by Sonographic Erosions and Power Doppler Signal: A Longitudinal Observational Study. Arthritis Care Res 2013; 65: 896–902

18 *Genth E, Krieg T.* [Systemic sclerosis – diagnosis and classification]. Z Rheumatol 2006; 65: 04 268–274

19 *Ghazinoor S, Crues JV, Crowley C.* Low-Field Musculoskeletal MRI". J Magn Reson Imaging 2007; 25: 234–244

20 *Glaudemans AWJM, de Vries EFJ, Galli F et al.* The Use of (18)F-FDG-PET/CT for Diagnosis and Treatment Monitoring of Inflammatory and Infectious Diseases. Clin Dev Immunol 2013; 2013: 623036

21 *Gonzalez-Gay MA, Vazquez-Rodriguez TR, Lopez-Diaz MJ et al.* Epidemiology of Giant Cell Arteritis and Polymyalgia Rheumatica. Arthritis Rheum 2009; 61: 1454–1461

22 *Grassi W, Gutierrez M.* Psoriatic Arthritis: Need for Ultrasound in Everyday Clinical Practice. J Rheumatol Suppl 2012; 89: 39–43

23 *Hartung W, Kellner H, Strunk J et al.* Development and Evaluation of a Novel Ultrasound Score for Large Joints in Rheumatoid Arthritis: One Year of Experience in Daily Clinical Practice. Arthritis Care Res 2012; 64: 675–682

24 *Ma MHY, Scott IC, Kingsley GH et al.* Remission in Early Rheumatoid Arthritis. J Rheumatol 2010; 37: 1444–1453

25 *McQueen FM, Ostendorf B.* What Is MRI Bone Oedema in Rheumatoid Arthritis and Why Does It Matter?. Arthritis Res Ther 2006; 8: 222

26 *Miese F, Buchbender C, Scherer A et al.* Molecular Imaging of Cartilage Damage of Finger Joints in Early Rheumatoid Arthritis with Delayed Gadolinium-Enhanced Magnetic Resonance Imaging. Arthritis Rheum 2012; 64: 394–399

27 *Nam JL, Ramiro S, Gaujoux-Viala C et al.* Efficacy of Biological Disease-Modifying Antirheumatic Drugs: A Systematic Literature Review Informing the 2013 Update of the EULAR Recommendations for the Management of Rheumatoid Arthritis. Ann Rheum Dis 2014; 73: 516–528

28 *Nesher G.* The Diagnosis and Classification of Giant Cell Arteritis". J Autoimmun 2014; 48-49: 73–75

29 *Peterfy C, Edmonds J, Lassere M et al.* OMERACT Rheumatoid Arthritis MRI Studies Module. J Rheumatol 2003; 30: 1364–1365

30 *Prieto-González S, Depetris M, García-Martínez A et al.* Positron Emission Tomography Assessment of Large Vessel Inflammation in Patients with Newly Diagnosed, Biopsy-Proven Giant Cell Arteritis: A Prospective, Case-Control Study". Ann Rheum Dis 2014; 73: 1388–1392

31 *Richter J, Iking-Konert C, Schneider M et al.* „[Capillaroscopy. An update]". Z Rheumatol 2013; 72: 145–150

32 *Roddy E, Choi HK.* Epidemiology of Gout. Rheum Dis Clin North Am 2014; 40: 155–175

33 *Schneider M, Lelgemann M, Abholz HH et al.* Interdisziplinäre Leitlinie Management der frühen rheumatoiden Arthritis. 3.: Überarbeitete Auflage. Darmstadt, Steinkopf Verlag 2011

34 *Sewerin P, Buchbender C, Vordenbäumen S et al.* Advantages of a Combined Rheumatoid Arthritis Magnetic Resonance Imaging Score (RAMRIS) for Hand and Feet: Does the RAMRIS of the Hand Alone Underestimate Disease Activity and Progression?. BMC Musculoskeletal Disorders 2014; 15: 104

35 *Sieper J, Rudwaleit M, Baraliakos X et al.* The Assessment of SpondyloArthritis International Society (ASAS) Handbook: A Guide to Assess Spondyloarthritis". Ann Rheum Dis 2009; 68(02): ii1–ii44

36 *Van den Broek M, Visser K, Allaart CF et al.* Personalized Medicine: Predicting Responses to Therapy in Patients with RA". Curr Opin Pharmacol 2013; 13: 463–469

37 *Van den Hoogen F, Khanna D, Fransen J et al.* 2013 Classification Criteria for Systemic Sclerosis: An American College of Rheumatology/European League against Rheumatism Collaborative Initiative. Arthritis Rheum 2013; 65: 2737–2747

38 *Werner SG, Langer H-E, Ohrndorf S et al.* Inflammation Assessment in Patients with Arthritis Using a Novel in Vivo Fluorescence Optical Imaging Technology. Ann Rheum Dis 2012; 71: 504–510

39 *Werner SG, Langer H-E, Schott P et al.* Indocyanine Green–Enhanced Fluorescence Optical Imaging in Patients With Early and Very Early Arthritis: A Comparative Study With Magnetic Resonance Imaging. Arthritis Rheum 2013; 65: 3036–3044

40 *Young A, Dixey J, Cox N et al.* How Does Functional Disability in Early Rheumatoid Arthritis (RA) Affect Patients and Their Lives? Results of 5 Years of Follow-up in 732 Patients from the Early RA Study (ERAS). Rheumatology (Oxford) 2000; 39: 603–611

Vordenbäumen et al. Arthritis Research & Therapy 2014, 16:452
http://arthritis-research.com/content/16/5/452

arthritis research&therapy

RESEARCH ARTICLE Open Access

# Dynamic contrast-enhanced magnetic resonance imaging of metacarpophalangeal joints reflects histological signs of synovitis in rheumatoid arthritis

Stefan Vordenbäumen[1*†], Christoph Schleich[2†], Tim Lögters[3], Philipp Sewerin[1], Ellen Bleck[1], Thomas Pauly[4], Anja Müller-Lutz[2], Gerald Antoch[2], Matthias Schneider[1], Falk Miese[2] and Benedikt Ostendorf[1]

## Abstract

**Introduction:** Synovial inflammation and joint destruction in rheumatoid arthritis (RA) may progress despite clinical remission. Dynamic contrast-enhanced magnetic resonance imaging (DCE-MRI) is increasingly used to detect synovial inflammation in RA. Although small joints such as metacarpophalangeal (MCP) joints are mainly affected by RA, MRI findings have never been directly compared to histological synovitis in MCP synovial tissue. The objective of the current study was therefore to analyse if DCE-MRI relates to histological signs of synovitis small RA joints.

**Methods:** In 9 RA patients, DCE-MRI (3 Tesla, dynamic 2D T1 weighted turbo-flash sequence) of the hand was performed prior to arthroscopically-guided synovial biopsies from the second MCP of the imaged hand. Maximum enhancement (ME), rate of early enhancement, and maximum rate of enhancement were assessed in the MCP. Synovial biopsies were stained for determination of sublining CD68 and the Synovitis Score. Correlations between MRI and histological data were calculated according to Spearman.

**Results:** ME of the MCP significantly correlated to sublining CD68 staining ($r = 0.750$, $P = 0.02$), the Synovitis Score ($r = 0.743$, $P = 0.02$), and the subscores for lining layer hypertrophy ($r = 0.789$, $P = 0.01$) and cellular density ($r = 0.842$; $P = 0.004$).

**Conclusions:** Perfusion imaging of synovial tissue in RA finger joints employing DCE-MRI reflects histological synovial inflammation. According to our study, ME is the most closely associated parameter amongst the measures considered.

## Introduction

Rheumatoid arthritis (RA) is a debilitating disease characterized by chronic inflammation and proliferation of synovial tissue with subsequent destruction of cartilage and bone [1]. The target of modern therapeutic strategies consists of complete remission, which is commonly identified based on clinical grounds in conjunction with inflammatory markers such as C-reactive protein [2]. However, joint destruction may progress in patients thus considered to be in remission [3,4]. Hence, additional tools are needed to directly assess synovitis and cartilage destruction. Magnetic resonance imaging (MRI) is increasingly used for this purpose [5]. In particular, synovitis in MRI has been shown to relate to the histological degree of synovial inflammation in human RA [6,7] and arthritis models [8,9]. Generally, most correlative studies on MRI and synovial histology in RA were performed on large joints, especially knee joints [6,7], due to more easily accessible synovial tissue [10,11]. These findings are commonly extrapolated when MRI findings of small joints are assessed that are predominantly involved in RA, particularly in early disease states [12]. Data validating MRI findings by synovial histology of metacarpophalangeal (MCP) joints are so far scarce: gadolinium

* Correspondence: stefan.vordenbaeumen@med.uni-duesseldorf.de
†Equal contributors
[1]Department of Rheumatology, Heinrich-Heine-University, Moorenstraße 5, Düsseldorf 40225, Germany
Full list of author information is available at the end of the article

enhancement in synovial tissue correlated with macroscopic findings of hyperemia and vascularity, but synovial biopsies were not systematically assessed [13]. Data on dynamic MRI of MCP joints and corresponding histological findings are lacking. In the current study, we performed contrast-enhanced dynamic MRI of the hand with determination of perfusion parameters of synovial tissue of the MCP2 joint prior to arthroscopically guided synovial sampling of the same joint with histological analysis of synovial inflammation, with the aim to correlate dynamic MRI to histological synovitis.

## Methods

### Patients and synovial sampling

Nine patients with RA based on 2010 American College of Rheumatology/European League Against Rheumatism criteria with a 28-joint disease activity score (DAS28) >3.2, who required initiation of disease-modifying antirheumatic drug therapy (three patients, methotrexate) or a switch of medication (patients with methotrexate additionally received adalimumab (four patients), tocilizumab (one patient), or rituximab (one patient)) and gave their full informed written consent, were recruited into the study. After clinical examination (including DAS28, patient-reported ratings on 10-point scales for pain of the dominant MCP2 joint and global well-being, physician-rated 68-tender and swollen joint count), all patients received MRI of the more severely affected hand up to 1 week prior to arthroscopy-guided synovial sampling as described previously [10]. A total of six synovial biopsies were obtained from each patient under visual control from macroscopically inflamed areas and were snap frozen in Tissue-Tek (Sakura Finetek Germany, Staufen, Germany). The study was conducted according to the principles expressed in the Declaration of Helsinki and was approved by the ethics committee of the Medical Faculty of Heinrich-Heine-University (study number 3390).

### Histological assessment of synovitis

The work-up and scoring of tissue sections was carried out in a blinded fashion as described previously [10]. Briefly, 3 to 5 μm sections were prepared from snap-frozen synovial tissue, hematoxylin and eosion stained (Merck, Darmstadt, Germany) and evaluated prior to immunohistochemical staining of parallel sections of a suitable biopsy including a lining layer with a monoclonal mouse anti-CD68 antibody (Dako, Glostrup, Denmark). Hematoxylin and eosion -stained sections were used for determination of the synovitis score according to Krenn and colleagues [14], which is a semiquantitative four-point sum scale considering lining layer hypertrophy, inflammatory infiltrate, and density of resident cells. For scoring of sublining CD68 staining, images were photographed at 100× magnification (Axioskop 2 plus; Carl Zeiss, Jena, Germany; and Nikon DS Vi 1; Nikon, Düsseldorf, Germany) and stored in TIF format (resolution of 1,600 × 1,200). ImageJ software [15] was used to select the sublining layer, and the image was thresholded to highlight the stained areas but not the respective isotype controls. The stained area was calculated as a fraction of the selected region.

### Magnetic resonance imaging

MRI was performed on a 3 T MRI system (Magnetom Trio; Siemens Healthcare, Erlangen, Germany). Perfusion imaging (dynamic contrast-enhanced MRI) was acquired with a dynamic two-dimensional T1-weighted turbo-flash sequence. Twenty seconds after the beginning of the sequence, the contrast agent Magnevist® (Gd-DTPA, Bayer Healthcare, Leverkusen, Germany) was injected at a dosage of 0.4 ml/kg body weight. The acquisition parameters of the dynamic contrast-enhanced MRI sequence were: repetition time = 333 milliseconds, echo time = 1.46 milliseconds, acquisition time per scan acquisition time = 1.7 seconds, flip angle = 8°, field of view = 120 × 120 mm, 200 dynamical images and five acquired slices with a slice thickness of 4 mm.

Perfusion analysis in MCP joint synovial tissue was assessed using semiquantitative analysis parameters calculated with T-One weighted Perfusion imaging Parameter CAlculation Toolkit software (TOPPCAT, Daniel P. Barboriak, Duke University School of Medicine, Durham, North Carolina, USA). In definite region of interest TOPPCAT analyses, the mean signal intensity ($S(t)$) over time was employed to calculate the maximum level of synovial enhancement (ME), the maximum rate of enhancement (MV) per second, and the rate of early enhancement (REE) 17 seconds after onset of synovial enhancement using the formulas:

$$\mathrm{ME} = \mathrm{maximum}(S(t)) - \mathrm{minimum}(S(t))$$

$$\mathrm{MV} = \mathrm{maximum}(S(i+1) - S(i-1)) \,/\, (t(i+1) - t(i-1))$$

$$\mathrm{REE} = (S2 - Si)/(Si \times 17\ \mathrm{seconds}) \times 100\%$$

where $Si$ is the signal intensity at time point $ti$, S1 is the signal intensity at onset of synovial enhancement, and S2 is the signal intensity 17 seconds after onset of synovial enhancement. In our study, REE was calculated 17 seconds after onset of synovial enhancement because we acquired a dynamic image every 1.7 seconds. Thus, we used the first 10 breakpoints for REE calculation. In all patients, the region of interest was defined as the anatomical area corresponding to the synovial membrane based on contrast-enhanced T1 images.

### Statistical analysis

Correlations between MRI parameters (ME, REE, MV) and parameters of histological synovitis (Synovitis Score, sublining CD68 staining) or clinical data were calculated

**Table 1 Correlation between dynamic MRI and histological signs of synovitis in MCP2 joints according to Spearman**

| | ME | REE | MV |
|---|---|---|---|
| Synovitis Score[a] | **0.743 (*P* = 0.02)** | 0.228 (*P* = 0.56) | 0.270 (*P* = 0.48) |
| Lining layer hypertrophy | **0.789 (*P* = 0.01)** | 0.177 (*P* = 0.65) | 0.346 (*P* = 0.36) |
| Inflammatory infiltrate | 0.249 (*P* = 0.52) | 0.053 (*P* = 0.89) | −0.107 (*P* = 0.78) |
| Cellular density | **0.842 (*P* = 0.004)** | 0.408 (*P* = 0.28) | 0.461 (*P* = 0.21) |
| Sublining CD68 | **0.750 (*P* = 0.02)** | 0.450 (*P* = 0.22) | 0.567 (*P* = 0.11) |

Significant results in bold. MCP, metacarpophalangeal; ME, maximum synovial enhancement; MRI, magnetic resonance imaging; MV maximum enhancement velocity; REE, rate of early enhancement. [a]Synovitis Score according to Krenn and colleagues [14].

according to Spearman. $P$ <0.05 was considered significant. SPSS 22 (IBM, Armonk, NY, USA) was used for analyses.

## Results

Nine patients (seven female, two male, age 57.5 ± 14.3 years) were recruited, all of whom adhered to the study protocol. Mean DAS28 at inclusion was 5.4 (range 3.5 to 7.4). In the follow-up, there were no severe adverse events within 6 months such as any permanent tissue damage, damage to nerves or vessels, infections, thrombosis, or embolisms following arthroscopy of the MCP2 joint. The median histologic Synovitis Score was 6 (range 1 to 9), corresponding to a high-grade synovitis (score >4 [14]) in seven of nine patients.

Next, we compared dynamic MRI findings with clinical characteristics of the patients. Patient-rated pain of the MCP2 joint on a 10-point scale correlated very strongly with ME ($r$ = 0.848, $P$ <0.005), and to a somewhat lesser extent with REE ($r$ = 0.681, $P$ = 0.04) and MV ($r$ = 0.695, $P$ = 0.04). No correlations were noted between the MRI parameters of the MCP2 and the global patient assessment on a 10-point scale, total tender or swollen joint count. Furthermore, a nonsignificant correlation between the DAS28 and ME ($r$ = 0.661, $P$ = 0.053) was noted.

Finally, dynamic MRI parameters were compared with histological signs of synovitis by correlation analysis. As can be seen in Table 1 and is exemplified in Figure 1, strong correlations between ME and several histological measures of synovitis were present. No such correlations were found for either REE or MV.

## Discussion

Recent developments in MRI technology are increasingly used to visualize all anatomical components of joints in RA down to a molecular level and permit functional imaging; for example, the assessment of synovial perfusion [16,17]. Findings such as bone marrow edema have prognostic value for future erosive disease [18]. Many of these findings have been validated on histological

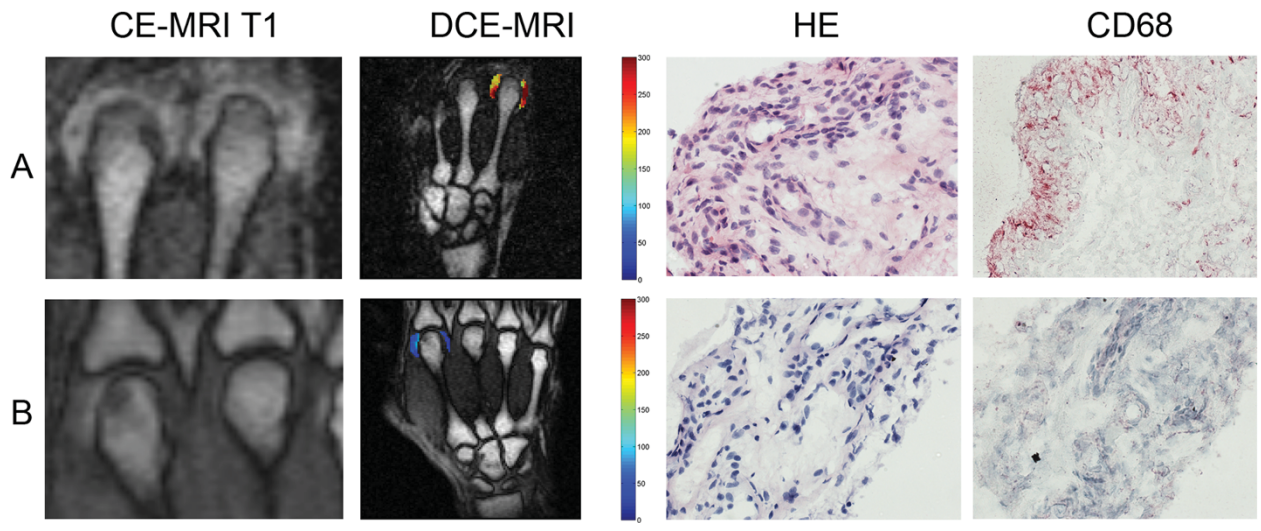


**Figure 1 Contrast-enhanced T1-weighted magnetic resonance imaging of metacarpophalangeal (MCP) joints 2 and 3 and maximum synovial enhancement of MCP 2.** Illustration of contrast-enhanced T1-weighted magnetic resonance imaging of metacarpophalangeal joint 2 and joint 3 (CE-MRI T1), fusion image of CE-MRI T1 and maximum synovial enhancement of MCP 2 measured by dynamic contrast-enhanced magnetic resonance imaging (DCE-MRI), and histological samples from the imaged joint stained with hematoxylin and eosion (HE) or immunohistochemical staining for macrophages (CD68). Patient with **(A)** a high degree of synovitis and **(B)** a low degree of synovitis. Red corresponds to a high maximum enhancement.

specimens, such as bone marrow edema and erosions [19,20], or synovial contrast enhancement and synovitis [6,7,9]. These studies have been performed in animal models or knee joints. However, RA has a predilection for small joints such as the MCP joints. Owing to a lack of other data, the validity of MRI findings of synovitis was hitherto extrapolated from large to small joints based on the abovementioned pioneering works. In the present study, we demonstrate that synovitis of MCP joints measured by ME on dynamic MRI strongly correlates to histological inflammation within the same joint. Besides conventional histological criteria, this finding extends to sublining CD68 staining, which is considered one of the best histological markers for disease activity in RA by many experts [21]. These data underscore the validity of dynamic contrast-enhanced MRI for the assessment of the degree of synovitis in small joints.

There are some limitations to this study. The small sample size is due to the invasiveness of the arthroscopic procedure and the resultant effort to keep the number of patients as small as possible with respect to the aim of the study. In spite of this, significant and consistent results were obtained. Moreover, additional synovial parameters could have been assessed such as markers of diverse cell populations and adhesion molecules. However, biopsies of MCP joints did not yield material in sufficient quality for multiple analyses in all cases. Of note, we applied a comparatively high dose of the contrast agent Magnevist® according to a standardized RA study protocol in our facility, which theoretically permits additional analyses such as delayed gadolinium-enhanced MRI [17].

## Conclusion

ME measured by dynamic MRI reflects histologic synovitis and may replace invasive sampling of synovial tissue in larger studies for the assessment of the degree of synovitis of small joints such as MCP. Our findings strongly support the use of dynamic MRI to assess synovitis in small joints of RA patients in a clinical setting.

#### Abbreviations

DAS28: 28-joint disease activity score; MCP: metacarpophalangeal; ME: maximum synovial enhancement; MRI: magnetic resonance imaging; MV: maximum rate of enhancement; RA: rheumatoid arthritis; REE: rate of early enhancement; TOPPCAT: T-One weighted perfusion imaging parameter CAlculation toolkit.

#### Competing interests

The authors declare that they have no competing interests.

#### Authors' contributions

SV participated in the conception of the study, carried out arthroscopies and synovial biopsies, read synovial histologies, interpreted data, followed-up patients, and drafted the manuscript. CS read MRI sequences and interpreted data. TL participated in the conception of the study, and carried out arthroscopies and synovial biopsies. PS participated in the conception of the study and patient follow-up. EB prepared and stained synovial tissue, and participated in data interpretation. TP carried out synovial biopsies, AM-L established and visualized dynamic MRI sequences. GA participated in the conception of the study. MS participated in the conception of the study and data interpretation. FM participated in the conception of the study, read MRI sequences and interpreted data. BO participated in the conception of the study, interpreted data, and drafted the manuscript. All authors read, revised and approved the final manuscript.

#### Acknowledgements

The authors gratefully acknowledge financial support of this study by grants from Forschungskommission of the Medical Faculty of Heinrich-Heine-University, Düsseldorf, Germany and the Hiller-Stiftung, Erkrath, Germany. The study was partially supported by a grant from Deutsche Forschungsgemeinschaft (MI 1575/1-1).

#### Author details

[1]Department of Rheumatology, Heinrich-Heine-University, Moorenstraße 5, Düsseldorf 40225, Germany. [2]Department of Diagnostic and Interventional Radiology, University Dusseldorf, Medical Faculty, Moorenstraße 5, Düsseldorf 40225, Germany. [3]Department of Trauma and Hand Surgery, Heinrich-Heine-University, Moorenstraße 5, Düsseldorf 40225, Germany. [4]Department of Orthopaedics, River Rhein Center for Rheumatology at St. Elisabeth Hospital, Hauptstraße 74, Meerbusch-Lank 40668, Germany.

Received: 17 June 2014 Accepted: 4 September 2014
Published online: 01 October 2014

#### References

1. McInnes IB, Schett G: **The pathogenesis of rheumatoid arthritis.** *N Engl J Med* 2011, **365:**2205–2219.
2. Felson DT, Smolen JS, Wells G, Zhang B, van Tuyl LHD, Funovits J, Aletaha D, Allaart CF, Bathon J, Bombardieri S, Brooks P, Brown A, Matucci-Cerinic M, Choi H, Combe B, de Wit M, Dougados M, Emery P, Furst D, Gomez-Reino J, Hawker G, Keystone E, Khanna D, Kirwan J, Kvien TK, Landewe R, Listing J, Michaud K, Martin-Mola E, Montie P, *et al*: **American College of Rheumatology/European League Against Rheumatism provisional definition of remission in rheumatoid arthritis for clinical trials.** *Ann Rheum Dis* 2011, **70:**404–413.
3. Brown AK, Quinn MA, Karim Z, Conaghan PG, Peterfy CG, Hensor E, Wakefield RJ, O'Connor PJ, Emery P: **Presence of significant synovitis in rheumatoid arthritis patients with disease-modifying antirheumatic drug–induced clinical remission: evidence from an imaging study may explain structural progression.** *Arthritis Rheum* 2006, **54:**3761–3773.
4. Brown AK, Conaghan PG, Karim Z, Quinn MA, Ikeda K, Peterfy CG, Hensor E, Wakefield RJ, O'Connor PJ, Emery P: **An explanation for the apparent dissociation between clinical remission and continued structural deterioration in rheumatoid arthritis.** *Arthritis Rheum* 2008, **58:**2958–2967.
5. Haavardsholm EA, Lie E, Lillegraven S: **Should modern imaging be part of remission criteria in rheumatoid arthritis?** *Best Pract Res Clin Rheumatol* 2012, **26:**767–785.
6. Ostergaard M, Stoltenberg M, Løvgreen-Nielsen P, Volck B, Sonne-Holm S, Lorenzen I: **Quantification of synovistis by MRI: correlation between dynamic and static gadolinium-enhanced magnetic resonance imaging and microscopic and macroscopic signs of synovial inflammation.** *Magn Reson Imaging* 1998, **16:**743–754.
7. Ostergaard M, Stoltenberg M, Løvgreen-Nielsen P, Volck B, Jensen CH, Lorenzen I: **Magnetic resonance imaging-determined synovial membrane and joint effusion volumes in rheumatoid arthritis and osteoarthritis: comparison with the macroscopic and microscopic appearance of the synovium.** *Arthritis Rheum* 1997, **40:**1856–1867.
8. Tamai K, Yamato M, Yamaguchi T, Ohno W: **Dynamic magnetic resonance imaging for the evaluation of synovitis in patients with rheumatoid arthritis.** *Arthritis Rheum* 1994, **37:**1151–1157.
9. Jacobson PB, Morgan SJ, Wilcox DM, Nguyen P, Ratajczak CA, Carlson RP, Harris RR, Nuss M: **A new spin on an old model: in vivo evaluation of disease progression by magnetic resonance imaging with respect to standard inflammatory parameters and histopathology in the adjuvant arthritic rat.** *Arthritis Rheum* 1999, **42:**2060–2073.
10. Vordenbäumen S, Sewerin P, Lögters T, Miese F, Schleich C, Bleck E, Philippski P, Schädel-Höpfner M, Pauly T, Schneider M, Ostendorf B: **Inflammation and vascularisation markers of arthroscopically-guided finger joint synovial biospies reflect global disease activity in rheumatoid arthritis.** *Clin Exp Rheumatol* 2014, **32:**117–120.

11. Vordenbäumen S, Joosten LA, Friemann J, Schneider M, Ostendorf B: **Utility of synovial biopsy.** *Arthritis Res Ther* 2009, **11:**256.
12. Mjaavatten MD, Haugen AJ, Helgetveit K, Nygaard H, Sidenvall G, Uhlig T, Kvien TK: **Pattern of joint involvement and other disease characteristics in 634 patients with arthritis of less than 16 weeks' duration.** *J Rheumatol* 2009, **36:**1401–1406.
13. Ostendorf B, Peters R, Dann P, Becker A, Scherer A, Wedekind F, Friemann J, Schulitz KP, Mödder U, Schneider M: **Magnetic resonance imaging and miniarthroscopy of metacarpophalangeal joints: sensitive detection of morphologic changes in rheumatoid arthritis.** *Arthritis Rheum* 2001, **44:**2492–2502.
14. Krenn V, Morawietz L, Burmester G-R, Kinne RW, Mueller-Ladner U, Muller B, Haupl T: **Synovitis Score: discrimination between chronic low-grade and high-grade synovitis.** *Histopathology* 2006, **49:**358–364.
15. **Image J.** [http://imagej.nih.gov/ij/]
16. McQueen FM: **Imaging in early rheumatoid arthritis.** *Best Pract Res Clin Rheumatol* 2013, **27:**499–522.
17. Miese F, Buchbender C, Scherer A, Wittsack H-J, Specker C, Schneider M, Antoch G, Ostendorf B: **Molecular imaging of cartilage damage of finger joints in early rheumatoid arthritis with delayed gadolinium-enhanced magnetic resonance imaging.** *Arthritis Rheum* 2012, **64:**394–399.
18. Bøyesen P, Haavardsholm EA, Ostergaard M, van der Heijde D, Sesseng S, Kvien TK: **MRI in early rheumatoid arthritis: synovitis and bone marrow oedema are independent predictors of subsequent radiographic progression.** *Ann Rheum Dis* 2011, **70:**428–433.
19. Albrecht A, Finzel S, Englbrecht M, Rech J, Hueber A, Schlechtweg P, Uder M, Schett G: **The structural basis of MRI bone erosions: an assessment by microCT.** *Ann Rheum Dis* 2013, **72:**1351–1357.
20. Jimenez-Boj E, Nöbauer-Huhmann I, Hanslik-Schnabel B, Dorotka R, Wanivenhaus A-H, Kainberger F, Trattnig S, Axmann R, Tsuji W, Hermann S, Smolen J, Schett G: **Bone erosions and bone marrow edema as defined by magnetic resonance imaging reflect true bone marrow inflammation in rheumatoid arthritis.** *Arthritis Rheum* 2007, **56:**1118–1124.
21. Bresnihan B, Pontifex E, Thurlings RM, Vinkenoog M, El-Gabalawy H, Fearon U, Fitzgerald O, Gerlag DM, Rooney T, van de SANDE MG, Veale D, Vos K, Tak P-P: **Synovial tissue sublining CD68 expression is a biomarker of therapeutic response in rheumatoid arthritis clinical trials: consistency across centers.** *J Rheumatol* 2009, **36:**1800–1802.

doi:10.1186/s13075-014-0452-x
**Cite this article as:** Vordenbäumen *et al.*: Dynamic contrast-enhanced magnetic resonance imaging of metacarpophalangeal joints reflects histological signs of synovitis in rheumatoid arthritis. *Arthritis Research & Therapy* 2014 **16**:452.

# Comparison of Quantitative and Semiquantitative Dynamic Contrast-Enhanced MRI With Respect to Their Correlation to Delayed Gadolinium-Enhanced MRI of the Cartilage in Patients With Early Rheumatoid Arthritis

*Anja Müller-Lutz, PhD,* Christoph Schleich, MD,* Philipp Sewerin, MD,† Janina Groß, BSc,* Gael Pentang, Msc,* Hans-Jörg Wittsack, PD,* Gerald Antoch, MD,* Matthias Schneider, MD, DDS, PhD,† Benedikt Ostendorf, PD,† and Falk Miese, PD**

**Objective:** The objective of this study was to investigate the correlation between semiquantitative and quantitative dynamic contrast-enhanced (DCE) parameters with delayed gadolinium-enhanced magnetic resonance imaging (MRI) of the cartilage (dGEMRIC).

**Methods:** Fifteen patients with early rheumatoid arthritis (RA) from the ArthroMark cohort were investigated at a 3-T MRI scanner. The metacarpophalangeal (MCP) joint of the index finger was examined with DCE-MRI and dGEMRIC. Semiquantitative and quantitative DCE perfusion parameters were calculated. The RA MRI score of the second MCP joint and the joint space width were measured.

**Results:** Significant correlations were noted between both semiquantitative and quantitative DCE parameters and the RA MRI score of the second MCP joint. There was a significant negative correlation between DCE parameters and dGEMRIC. No association between joint space width and DCE parameters was observed.

**Conclusions:** Semiquantitative and quantitative analyses of perfusion are applicable to show that cartilage damage correlates with the inflammation activity despite the absence of joint space narrowing.

**Key Words:** quantitative and semiquantitative DCE-MRI, dGEMRIC, cartilage damage, inflammation activity, early rheumatoid arthritis

(*J Comput Assist Tomogr* 2015;39: 64–69)



Rheumatoid arthritis (RA) is a chronic autoimmune disease causing inflammation and proliferation of the synovial membrane, bone erosions, bone marrow edema, and damage of tendons, menisci, and cartilage.[1–3] In particular, synovitis has been demonstrated to be associated with cartilage destruction.[4] Recently, early RA was reported to be associated with a loss of glycosaminoglycans (GAGs) in the absence of joint space narrowing.[3] However, changes in cartilage composition were also detectible in the absence of any inflammatory changes.[3]

On the other hand, it would be of interest if this loss of GAG is associated with the severity of inflammation in RA patients.

Different methods have been introduced for the biochemical assessment of cartilage composition including sodium imaging, GAG chemical exchange saturation transfer imaging, and delayed gadolinium-enhanced magnetic resonance imaging (MRI) of the cartilage (dGEMRIC).[3,5–8] Of these techniques, dGEMRIC has proven sensitivity to cartilage destruction in RA, and its applicability to assess glycosaminoglycans in small joints has been previously reported.[3,6,9,10]

The Outcome Measures in RA Clinical Trials group with the RA MRI score (RAMRIS) established a semiquantitative rating of the severity of synovitis, bone marrow edema, and erosions in the hand and wrist joints.[11] In the past, cartilage composition has been compared with the RAMRIS scoring.[4] A strong correlation between the degree of osteistis as well as synovitis with low dGEMRIC and high T2 values has been reported.[4] In their study, synovitis severity was assessed on a semiquantitative level. A validated method for the estimation of synovitis is dynamic contrast-enchanced (DCE) MRI with its proven feasibility to describe the disease activity in RA patients.[12–15] Furthermore, DCE-MRI is an established tool for the assessment of therapeutic response.[13,16] Perfusion parameters delivered by DCE-MRI can be investigated in semiquantitative and quantitative manner. The estimation of quantitative parameters can be performed by the Tofts model, which has become a standard for the analysis of DCE-MRI.[17,18] The Tofts model considers the blood plasma and the extracellular extravascular space as 2 compartments and provides information regarding the distribution of contrast agent across these 2 spaces to quantify the tissue perfusion.

To investigate the relation between synovitis and cartilage degeneration in patients with early RA, the correlation between DCE-MRI parameters and dGEMRIC was tested in the present study.

## MATERIALS AND METHODS

The study was approved by the local ethics committee, and written informed consent was obtained from all patients before the MRI examination.

### Patients

Metacarpophalangeal (MCP) joints of the index finger of 15 patients with early RA from the ArthroMark study cohort (13 females, 5 males; age, 55 [10] years) were investigated. All patients fulfilled the 2010 American College of Rheumatology/European League Against Rheumatism RA classification criteria.[19] Early RA was classified as disease duration shorter than 6 months.

### Data Acquisition

The MRI data were acquired on a whole-body 3-T MRI scanner (Magnetom Trio A Tim System; Siemens Healthcare, Erlangen, Germany). At first, the imaging protocol for estimation of inflammation was performed using a 4-channel flex coil. After a 40-minute delay, the dGEMRIC protocol was acquired using two 4-mm loop surface coils placed above and beneath the finger joint. Because of the coil sensitivity, only the second MCP (MCP2) joint was evaluated.

From the Departments of *Diagnostic and Interventional Radiology, and †Rheumatology, University Dusseldorf, Medical Faculty, Dusseldorf, Germany.
Received for publication June 19, 2013; accepted September 8, 2014.
Reprints: Christoph Schleich, Department of Diagnostic and Interventional Radiology, University of Dusseldorf, Moorenstr. 5, D-40225 Dusseldorf, Germany (e-mail: christoph.Schleich@med.uni-duesseldorf.de).
The ArthroMark project is founded by the Bundesministerium für Bildung und Forschung grant number FKZ 01EC1009A.
The authors declare no conflict of interest.

**TABLE 1.** Perfusion Parameter and Description Evaluated by The DCE Tool

| | Parameter | Description |
|---|---|---|
| Quantitative parameters | $K_{Trans}$ | Transfer constant between blood plasma and EES |
| | $k_{ep}$ | Rate constant; $K_{trans}/v_e$ where $v_e$ is the relative volume of the EES |
| Semiquantitative parameters | IAUC | Integral of the signal curve over a time $t_{IAUC}$ starting at the onset time of the bolus $t_{onset}$; $t_{IAUC}$ was set to 60 s (default value in The DCE tool) |
| | Initial slope | Slope of the signal curve determined by linear regression within the first few seconds of t after $t_{onset}$; here, 17 s were used for t |
| | Peak | Maximal signal enhancement |

IAUC, initial area under the curve.

## DCE-MRI Protocol

Before contrast media application, a coronal short tau inversion recovery (STIR) and T1-weighted turbo spin echo (TSE) sequence as well as a T1 weighted 3D fast low angle shot (T1w-3D-FLASH) sequence for T1 mapping using a dual flip-angle approach were acquired. The parameters of the coronal STIR sequence were as follows: repetition time (TR), 5560 milliseconds; echo time (TE), 31 milliseconds; flip angle, 120 degrees; field of view (FOV), 120 mm × 120 mm; and slice thickness, 2.5 mm. The parameters of the coronal T1-weighted TSE sequence were as follows: TR, 860 milliseconds; TE, 25 milliseconds; flip angle, 150 degrees; FOV, 120 mm × 120 mm; and slice thickness, 2.5 mm. The parameters of the T1w-3D-FLASH sequence were as follows: TR, 15 milliseconds; TE, 1.44 milliseconds; flip angles, 5 and 26 degrees, FOV, 160 mm × 160 mm; and slice thickness, 3 mm. Afterwards, perfusion imaging was acquired with a dynamic 2-dimensional T1-weighted turbo flash sequence. Twenty seconds after the beginning of the sequence, the contrast agent Magnevist (Gd-DTPA) was injected with a dose of 0.4 mL/kg body weight. The acquisition parameters of the DCE-MRI sequence were as follows: TR, 333 milliseconds; TE, 1.46 milliseconds; acquisition time per scan time of acquisition, 1.7 s; flip angle, 8 degrees; FOV, 120 mm × 120 mm; 200 dynamical images; and 5 acquired slices with a slice thickness of 4 mm. Thereafter, a coronal TSE and a transversal spin echo sequence with fat suppression were applied. The sequence parameters of the coronal TSE sequence were as follows: TR, 120 mm; TE, 25 milliseconds; flip angle, 150 degrees; FOV, 120 mm × 120 mm; and slice thickness, 2.5 mm. The sequence parameters of the transversal spin echo sequence were as follows: TR, 765 milliseconds; TE, 12 milliseconds; flip angles, 90 and 120 degrees; FOV, 120 mm × 60 mm; and slice thickness, 2.5 mm.

The coronal STIR sequence, coronal T1-weighted TSE sequence before and after contrast agent injection, and the spin echo sequence with fat suppression were used to determine $RAMRIS_{MCP2}$ (RAMRIS of the MCP joint of the index finger). In this study, images were evaluated for the synovitis subscore (grade 0-3). Bone marrow edema (grade 0-3) and erosions (grade 0-10) according to the RAMRIS guidelines were not evaluated.

## dGEMRIC Protocol

After a 40-minute delay, the dGEMRIC imaging sequence was applied using a dual flip-angle approach for T1 estimation. The sequence parameters were as follows: TR, 15 milliseconds; TE, 3.34 milliseconds; flip angles, 5 and 26 degrees; FOV, 90 mm × 53 mm; and slice thickness, 2 mm.

## Data Analysis

Perfusion in the MCP joint of the index finger was evaluated using semiquantitative as well as quantitative analysis using the software The DCE Tool (The DCE Tool for ClearCanvas 2.0 SP1, http://thedcetool.com). This tool is a Matlab-based plug-in for the open source PACS ClearCanvas workstation. The quantitative perfusion analysis of this program is based on the standard Tofts model.[20] For perfusion analysis, knowledge of the native T1 time is necessary. The variable flip angle T1w-3D-FLASH sequence was used for a pixel-based T1 calculation using the formula

$$T_1(x,y,z) = \frac{TR}{\ln\left[\frac{\sin(\alpha_1)\cos\alpha_2) - Q(x,y,z)\sin(\alpha_2)\cos(\alpha_1)}{\sin(\alpha_1) - Q(x,y,z)\ \sin(\alpha_2)}\right]}$$

where

$$Q(x,y,z) = \frac{S_{\alpha 1}(x,y,z)}{S_{\alpha 2}(x,y,z)}$$

and $S_{\alpha 1}(x,y,z)$ and $S_{\alpha 2}(x,y,z)$ are the pixel intensities corresponding to the 2 flip angles $\alpha_1$ and $\alpha_2$. This time was further used for semiquantitative and quantitative perfusion analysis.

A region of interest (ROI)–based perfusion analysis was performed. Two ROIs were placed on the ulnar and radial side of the MCP joint. The measured signal intensities were used to calculate the concentration time curve in the respective ROI using the formula $C_{GD}(t) = \frac{S(t) - S_0}{S_0 T_{10} R}$, where $T_{10}$ is the native T1 time, $R$ = 4.5 $s^{-1}mM^{-1}$ is the relaxivity of the contrast agent, $S_0$ is the average signal intensity in the ROI in the absence of contrast agent, and S is the average signal intensity in the ROI.

Five parameters, 3 semiquantitative and 2 quantitative parameters, were evaluated by The DCE Tool. These parameters are listed and described in Table 1.

The MCP-dGEMRIC indices of the index finger of each patient reflect the T1 time after contrast agent application. The dGEMRIC indices were determined as described elsewhere.[9] In addition, the joint space width (JSW) was determined for each patient on the T1-weighted images of the dGEMRIC protocol. The distance between MCP head and the basis of proximal phalanx in the joint space was measured.

**TABLE 2.** Mean (SD) of JSW, RAMRIS Score, dGEMRIC Index, KTrans, $k_{ep}$, IAUC, Initial Slope, and Peak

| Parameter | Mean (SD) |
|---|---|
| JSW, mm | 1.18 (0.19) |
| RAMRIS score | 2.5 (1.8) |
| dGEMRIC index, ms | 353.5 (83.9) |
| $K_{Trans}$, mL/g per min | 0.16 (0.13) |
| $K_{ep}$, 1/min | 0.25 (0.16) |
| IAUC, mM/L per s | 8.95 (6.71) |
| Initial slope, mM/L per s | 0.00778 (0.00781) |
| Peak, mM/L per s | 0.33 (0.16) |

**TABLE 3.** Correlation Between Quantitative and Semiquantitative Perfusion Parameters and JSW, RAMRIS Score, and dGEMRIC Index

| | $K_{Trans}$, mL/g per min | | $K_{ep}$, 1/min | | IAUC, mM/L per s | | Initial Slope, mM/L per s | | Peak, mM/L per s | |
|---|---|---|---|---|---|---|---|---|---|---|
| | ρ | *P* | ρ | *P* | ρ | *P* | ρ | *P* | ρ | *P* |
| JSW, mm | 0.20 | 0.46 | 0.22 | 0.44 | 0.26 | 0.35 | 0.27 | 0.34 | 0.28 | 0.31 |
| RAMRIS score | 0.85 | <0.01 | 0.62 | 0.01 | 0.86 | <0.01 | 0.86 | <0.01 | 0.75 | <0.01 |
| dGEMRIC index | −0.75 | <0.01 | −0.50 | 0.06 | −0.71 | <0.01 | −0.66 | <0.01 | −0.70 | <0.01 |

## Statistics

Correlation analysis was performed between each semiquantitative and quantitative perfusion parameter, the dGEMRIC index, $RAMRIS_{MCP2}$, and JSW using the Spearman correlation coefficient ρ. Regression lines were determined in case of significant correlation.

## RESULTS

Table 2 provides the mean (SD) of JSW, $RAMRIS_{MCP2}$, dGEMRIC index, and the semiquantitative and quantitative perfusion parameters of the MCP joint of the index finger averaged over all patients with early RA.

The correlation coefficients between all perfusion parameters and JSW, $RAMRIS_{MCP2}$, and dGEMRIC index are summarized in Table 3. No significant correlations were noted between any perfusion parameters and JSW, whereas significant positive correlations were seen between all perfusion parameters and $RAMRIS_{MCP2}$. Significant negative correlations were observed between all perfusion parameters except $k_{ep}$ and the dGEMRIC index.

The dGEMRIC and perfusion maps are shown exemplarily in 2 patients (Figs. 1, 2).

These figures substantiate the negative correlation between dGEMRIC and perfusion.

The correlation between the semiquantitative parameter peak and $RAMRIS_{MCP2}$ and dGEMRIC is displayed in Figure 3 thus visualizing the significant positive correlation between $RAMRIS_{MCP2}$ and the semiquantitative parameter peak as well as the negative correlation between dGEMRIC and the parameter peak.

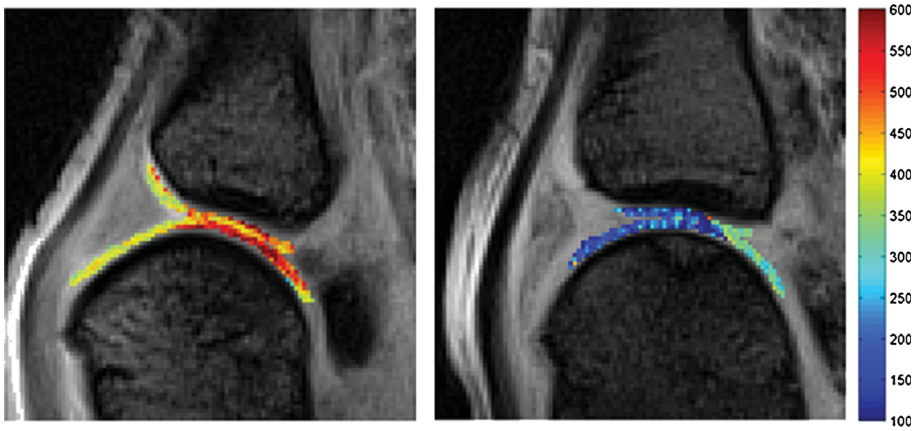


**FIGURE 1.** High-resolution dGEMRIC maps in 2 patients with early RA. Higher dGEMRIC values were obtained in the patient data on the left compared with the patient data on the right. This might indicate lower cartilage destruction in the patient on the left. Figure 1 can be viewed online in color at www.jcat.org.

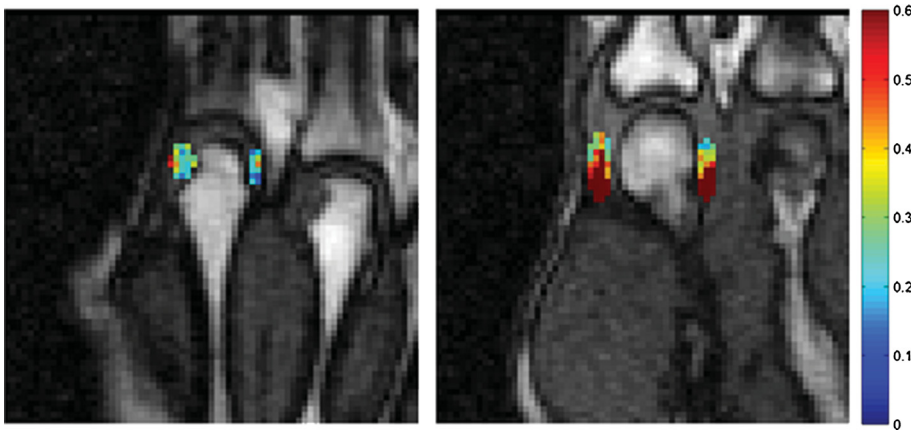


**FIGURE 2.** High-resolution perfusion maps by means of the parameter peak (mM/L per second). Low peak values were obtained in the patient on the left, whereas high values are obtained in the patient on the right. This might indicate a higher severity of synovitis in the patient on the right. Figure 2 can be viewed online in color at www.jcat.org.

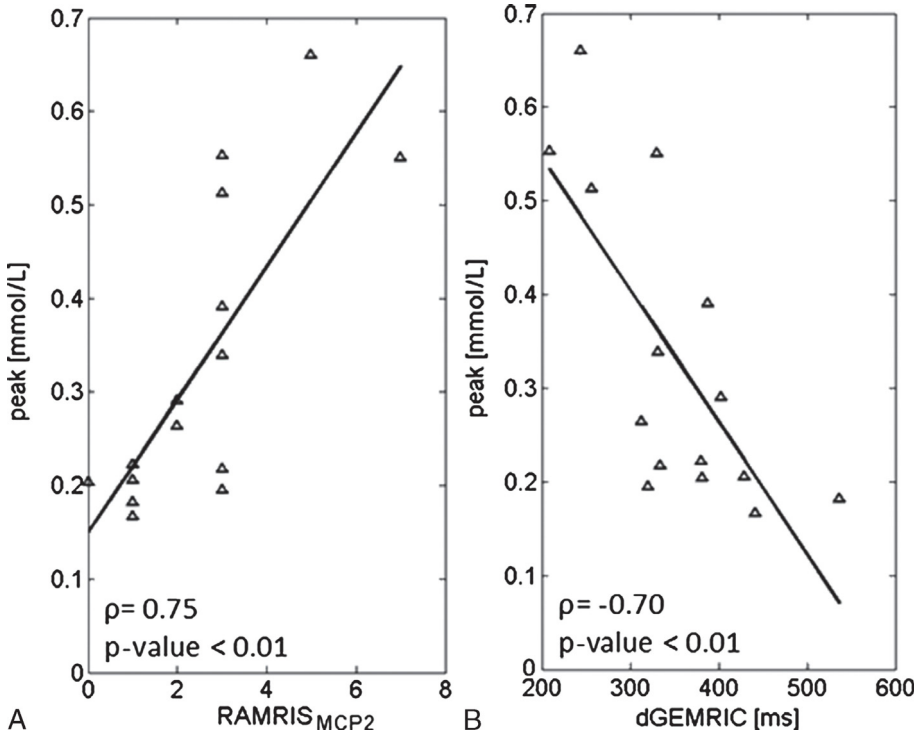


**FIGURE 3.** The correlation between the perfusion parameter peak and $RAMRIS_{MCP2}$ (A) and dGEMRIC (B) is displayed. Regression lines were determined. A significant positive correlation was noted between RAMRIS and the perfusion parameter peak, whereas a significant negative correlation was present between dGEMRIC and peak.

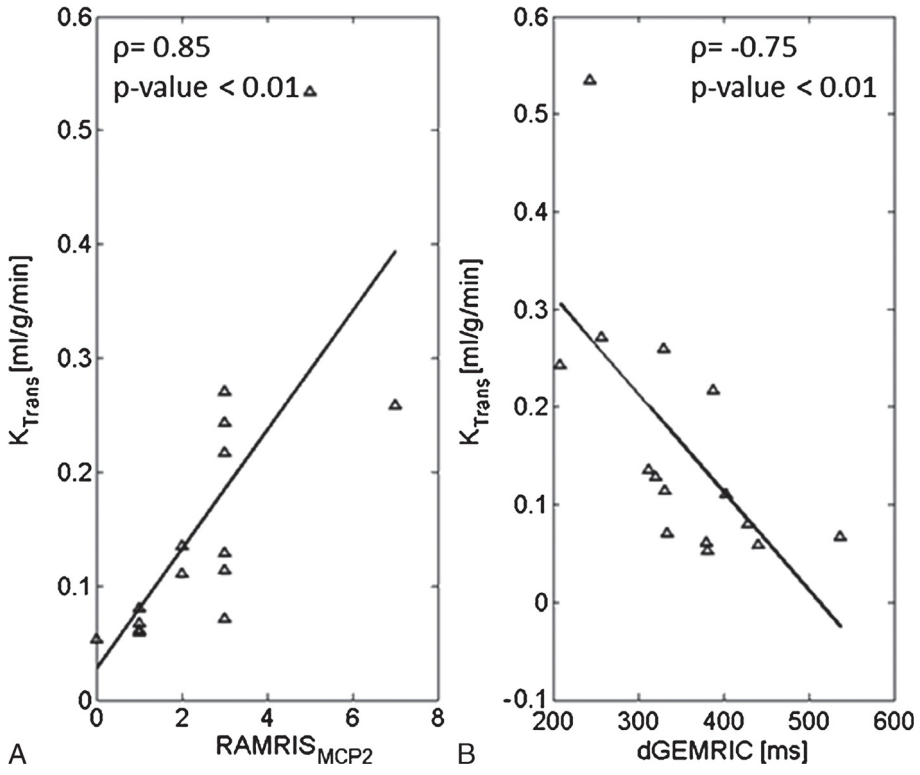


**FIGURE 4.** The correlation between the perfusion parameter $K_{Trans}$ and $RAMRIS_{MCP2}$ (A) and dGEMRIC (B) is displayed. Regression lines were determined. A significant positive correlation was noted between $RAMIS_{MCP2}$ and the perfusion parameter $K_{Trans}$, whereas a significant negative correlation was present between dGEMRIC and $K_{Trans}$.

The correlation between the quantitative parameter peak and JSW, $RAMRIS_{MCP2}$, and dGEMRIC is displayed in Figure 4 thus demonstrating the positive correlation between $RAMRIS_{MCP2}$ and $K_{Trans}$ as well as the negative correlation between dGEMRIC and $K_{Trans}$.

## DISCUSSION

The results showed a significant positive correlation between all investigated perfusion parameters and $RAMRIS_{MCP2}$ and a significant negative correlation between most perfusion parameters and dGEMRIC. This might indicate an association between synovitis severity and cartilage damage in patients with early RA. In an earlier study by Herz et al[4] an associated correlation between the RAMRIS synovitis score and dGEMRIC was noted in the MCP joints of patients with RA. In contrast to that study, we assessed synovitis with RAMRIS as well as DCE-MRI. This enables the quantitative measure of synovitis. In addition, we investigated patients with early RA before disease modifying treatment. The correlation between perfusion and dGEMRIC might indicate a potential correlation between synovitis severity and cartilage destruction at this early stage of disease.

A correlation between DCE-MRI and RAMRIS scoring has been shown in previous studies.[21,22] For example, Wojciechowski et al[22] showed a significant correlation between RAMRIS score and the number of enhancing pixels in DCE-MRI images in the wrist of 59 RA patients. Our study corroborates the correlation of RAMRIS and DCE and extends these findings to the finger joints.

The rate of diffusion depends on several factors including the vascularization of a joint, the rate of blood flow to the synovia, and wrist or finger motion. The state of equilibrium is reached faster in the small joints of the hand in comparison to large joints.[23] The change of signal intensity over time produces an S-shaped curve. This time, intensity curve can be used to measure the early enhancement rate (EER), relative enhancement, maximum enhancement, and late or static enhancement. The initial phase of the dynamic series can be used to evaluate the degree of synovial inflammation and disease activity of RA. It reflects the perfusion and permeability of the synovial tissue. Early enhancement rate is an early postcontrast measurement and is highly validated in several studies that have illustrated a high correlation with histological criteria.[2,12,24,25] In addition, EER demonstrated a good correlation with vascularity and capillary permeability that are up-regulated in RA.[2] Early enhancement rate has also been shown to correlate with erosions, pain, progression of erosions, and effectiveness of treatment in RA.[1,26] The maximum slope and relative enhancement (baseline signal subtracted from maximum increase) give information about the spread and degree of inflammation in joint. Relative enhancement seems to overestimate the degree of synovitis and thus is not the perfect parameter as a predictor for synovitis grading in RA.[27,28] Maximum enhancement and EER are comparable with our semiquantitative parameters peak and initial slope as far as differences in technical settings of dynamic MRI are taken into account.

$K_{Trans}$ analyzes the movement of contrast agent from the plasma to the extravascular extracellular space (EES) and is a parameter for vascularity and capillary permeability and thus may be sensitive to changes in inflammatory activity.[17] Depending on the software used for Toft's calculation, it is possible to receive different values for $K_{Trans}$. This makes it difficult to compare the results of different studies.[14]

The present study has some limitations. Because of the small patient collective, this study has the character of a preliminary report, and further longitudinal studies aiming at evaluating follow-ups are needed. A further limitation is the absence of synovial and cartilage biopsy as a criterion standard of synovitis severity and cartilage composition.

In summary, our data indicate a strong relation between biochemical changes in articular cartilage measured by dGEMRIC and the degree of inflammation of the synovial membrane measured by DCE-MRI in patients with early RA. Semiquantitative and quantitative analyses of perfusion are applicable to detect this correlation.

## ACKNOWLEDGMENT

*The authors thank Erika Rädisch for her expert assistance with data acquisition.*

## REFERENCES

1. Cimmino MA, Innocenti S, Livrone F, et al. Dynamic gadolinium-enhanced magnetic resonance imaging of the wrist in patients with rheumatoid arthritis can discriminate active from inactive disease. *Arthritis Rheum*. 2003;48:1207–1213.
2. Hodgson RJ, O'Connor P, Moots R. MRI of rheumatoid arthritis image quantitation for the assessment of disease activity, progression and response to therapy. *Rheumatology (Oxford)*. 2008;47:13–21.
3. Miese F, Buchbender C, Scherer A, et al. Molecular imaging of cartilage damage of finger joints in early rheumatoid arthritis with delayed gadolinium-enhanced magnetic resonance imaging. *Arthritis Rheum*. 2012; 64:394–399.
4. Herz B, Albrecht A, Englbrecht M, et al. Osteitis and synovitis, but not bone erosion, is associated with proteoglycan loss and microstructure damage in the cartilage of patients with rheumatoid arthritis. *Ann Rheum Dis*. 2014;73:1101–1106.
5. Schmitt B, Zbýň Š, Stelzeneder D, et al. Cartilage quality assessment by using glycosaminoglycan chemical exchange saturation transfer and $^{23}$Na MR imaging at 7 T. *Radiology*. 2011;260:257–264.
6. Tiderius CJ, Sandin J, Svensson J, et al. Knee cartilage quality assessed with dGEMRIC in rheumatoid arthritis patients before and after treatment with a TNF inhibitor. *Acta Radiol*. 2010;51:1034–1037.
7. Madelin G, Babb JS, Xia D, et al. Reproducibility and repeatability of quantitative sodium magnetic resonance imaging in vivo in articular cartilage at 3 T and 7 T. *Magn Reson Med*. 2012;68:841–849.
8. Borthakur A, Shapiro EM, Beers J, et al. Sensitivity of MRI to proteoglycan depletion in cartilage: comparison of sodium and proton MRI. *Osteoarthritis Cartilage*. 2000;8:288–293.
9. Miese FR, Ostendorf B, Wittsack H-J, et al. Metacarpophalangeal joints in rheumatoid arthritis: delayed gadolinium-enhanced MR imaging of cartilage—a feasibility study. *Radiology*. 2010;257:441–447.
10. Williams A, Shetty SK, Burstein D, et al. Delayed gadolinium enhanced MRI of cartilage (dGEMRIC) of the first carpometacarpal (1CMC) joint: a feasibility study. *Osteoarthritis Cartilage*. 2008;16:530–532.
11. Østergaard M, Peterfy C, Conaghan P, et al. OMERACT Rheumatoid Arthritis Magnetic Resonance Imaging Studies. Core set of MRI acquisitions, joint pathology definitions, and the OMERACT RA-MRI scoring system. *J Rheumatol*. 2003;30:1385–1386.
12. Ostergaard M, Stoltenberg M, Løvgreen-Nielsen P, et al. Quantification of synovistis by MRI: correlation between dynamic and static gadolinium-enhanced magnetic resonance imaging and microscopic and macroscopic signs of synovial inflammation. *Magn Reson Imaging*. 1998; 16:743–754.
13. Fritz J, Galeczko EK, Schwenzer N, et al. Longitudinal changes in rheumatoid arthritis after rituximab administration assessed by quantitative and dynamic contrast-enhanced 3-T MR imaging: preliminary findings. *Eur Radiol*. 2009;19:2217–2224.
14. Hodgson RJ, Barnes T, Connolly S, et al. Changes underlying the dynamic contrast-enhanced MRI response to treatment in rheumatoid arthritis. *Skeletal Radiol*. 2008;37:201–207.

15. Hodgson R, Grainger A, O'Connor P, et al. Dynamic contrast enhanced MRI of bone marrow oedema in rheumatoid arthritis. *Ann Rheum Dis*. 2008;67:270–272.
16. Kalden-Nemeth D, Grebmeier J, Antoni C, et al. NMR monitoring of rheumatoid arthritis patients receiving anti-TNF-alpha monoclonal antibody therapy. *Rheumatol Int*. 1997;16:249–255.
17. Tofts PS. Modeling tracer kinetics in dynamic Gd-DTPA MR imaging. *J Magn Reson Imaging*. 1997;7:91–101.
18. Sourbron SP, Buckley DL. On the scope and interpretation of the Tofts models for DCE-MRI. *Magn Reson Med*. 2011;66: 735–745.
19. Aletaha D, Neogi T, Silman AJ, et al. 2010 Rheumatoid arthritis classification criteria: an American College of Rheumatology/European League Against Rheumatism collaborative initiative. *Arthritis Rheum*. 2010;62:2569–2581.
20. Tofts PS. T1-weighted DCE imaging concepts: modelling, acquisition and analysis. *Magnetom Flash*. 2010;3:30–39.
21. Boesen M, Kubassova O, Bouert R, et al. Correlation between computer-aided dynamic gadolinium-enhanced MRI assessment of inflammation and semi-quantitative synovitis and bone marrow oedema scores of the wrist in patients with rheumatoid arthritis—a cohort study. *Rheumatology (Oxford)*. 2012;51:134–143.
22. Wojciechowski W, Tabor Z, Urbanik A. Assessing synovitis based on dynamic gadolinium-enhanced MRI and EULAR-OMERACT scores of the wrist in patients with rheumatoid arthritis. *Clin Exp Rheumatol*. 2013;31:850–856.
23. Peterfy CG. MR imaging. *Baillieres Clin Rheumatol*. 1996;10:635–678.
24. Reiser MF, Bongartz GP, Erlemann R, et al. Gadolinium-DTPA in rheumatoid arthritis and related diseases: first results with dynamic magnetic resonance imaging. *Skeletal Radiol*. 1989;18:591–597.
25. Gaffney K, Cookson J, Blake D, et al. Quantification of rheumatoid synovitis by magnetic resonance imaging. *Arthritis Rheum*. 1995;38: 1610–1617.
26. Kirkhus E, Bjørnerud A, Thoen J, et al. Contrast-enhanced dynamic magnetic resonance imaging of finger joints in osteoarthritis and rheumatoid arthritis: an analysis based on pharmacokinetic modeling. *Acta Radiol*. 1987. 2006;47:845–851.
27. Gaffney K, Cookson J, Blades S, et al. Quantitative assessment of the rheumatoid synovial microvascular bed by gadolinium-DTPA enhanced magnetic resonance imaging. *Ann Rheum Dis*. 1998;57:152–157.
28. Huang J, Stewart N, Crabbe J, et al. A 1-year follow-up study of dynamic magnetic resonance imaging in early rheumatoid arthritis reveals synovitis to be increased in shared epitope-positive patients and predictive of erosions at 1 year. *Rheumatology (Oxford)*. 2000;39:407–416.

Skeletal Radiol (2015) 44:513–518
DOI 10.1007/s00256-014-2045-9

SCIENTIFIC ARTICLE

# Intra-individual assessment of inflammatory severity and cartilage composition of finger joints in rheumatoid arthritis

**C. Schleich · A. Müller-Lutz · P. Sewerin · B. Ostendorf · C. Buchbender · M. Schneider · G. Antoch · F. Miese**

Received: 29 July 2014 / Revised: 22 September 2014 / Accepted: 17 October 2014 / Published online: 1 November 2014


**Abstract**
*Objective* To intra-individually assess the association of inflammation severity and cartilage composition measured by RAMRIS synovitis sub-score and delayed gadolinium-enhanced magnetic resonance imaging of the cartilage (dGEMRIC) of metacarpophalangeal (MCP) joints in patients with rheumatoid arthritis (RA).
*Methods* Forty-three patients with RA according to ACR/EULAR classification criteria (age 52.9±14.5 years, range, 18–77 years) were included in this study. All study participants received 3-T MRI scans of the metacarpophalangeal joints of the second and third finger (MCP 2 and 3). The severity of synovitis was scored according to the RAMRIS synovitis sub-score by two readers in consensus. In the cases with identical synovitis sub-scores, two radiologists decided in consensus on the joint with more severe synovitis. Cartilage composition was assessed with dGEMRIC. To test the association of inflammation severity and cartilage damage and in order to eliminate inter-patient confounders, each patient's MCP 2 and 3 were dichotomized into the joint with more severe synovitis versus the joint with less severe synovitis for a paired Wilcoxon test of dGEMRIC value.
*Results* There was a significant difference of dGEMRIC value (median of difference: 47.12, CI [16.6; 62.76]) between the dichotomized MCPs ($p$ = 0.0001). There was a significant correlation between dGEMRIC value and RAMRIS synovitis grading of the joint with more severe synovitis ($r$ = 0.5; $p$ < 0.05) and the joint with less severe synovitis ($r$ = 0.33; $p$ < 0.05).
*Conclusions* Our data concur with the concept that synovitis severity is associated with cartilage damage. The local inflammatory status on a joint level correlated significantly with the extent of cartilage degradation in biochemical MRI.

**Keywords** MRI · dGEMRIC · Rheumatoid arthritis · Inflammation

C. Schleich · A. Müller-Lutz (✉) · C. Buchbender · G. Antoch · F. Miese
Medical Faculty, Department of Diagnostic and Interventional Radiology, University Dusseldorf, D-40225 Dusseldorf, Germany
e-mail: anja.lutz@med.uni-duesseldorf.de

P. Sewerin · B. Ostendorf · M. Schneider
Medical Faculty, Department of Rheumatology, University Dusseldorf, 40225 Dusseldorf, Germany

## Introduction

Biochemical MRI of cartilage is a validated tool for assessing cartilage degradation in clinical trials of RA and osteoarthritis [1–3]. Delayed gadolinium-enhanced MRI of the cartilage (dGEMRIC) is a magnetic resonance imaging (MRI) feature to visualize proteoglycan loss in cartilage composition [4–6]. It has been demonstrated that cartilage changes measured by dGEMRIC correlate with histological analysis [7]. Based on improvements in MRI techniques, it is possible to assess cartilage composition of small joints that are frequently affected in RA [4]. A loss of proteoglycans has been demonstrated in early RA and seems to precede morphological changes in cartilage of small finger joints [2].

Uncontrolled RA is characterized by progressive joint destruction and long-term functional disability [8]. Inflammation of the synovial membrane is associated with destruction of bone and cartilage [9]. The degree of inflammation highly correlates with functional impairment and the development of joint destruction over time leads to disability [10–12].

The therapy with disease-modifying antirheumatic drugs (DMARD) and biologicals aims at disease control and can halt the progression of joint destruction [13, 14].

This has put monitoring of joint damage in the focus of radiologic attention in the follow-up of RA. In 2003, the

Outcome Measures in RA Clinical Trials (OMERACT) group with the RA MRI Score (RAMRIS) established a highly reliable sum-score based on the semi-quantitative rating of the severity of synovitis, bone marrow edema and erosions in hand and wrist joints [15]. The RAMRIS scoring system has been applied in therapy-response trials in RA [16, 17]. However, the system does not consider cartilage destruction in RA. In 33 patients with RA, Herz et al. investigated the relation between inflammation of synovia and cartilage degradation measured with biochemical MRI in an inter-individual study design. Synovitis was determined with the RAMRIS synovitis sub-score and cartilage degradation was assessed with dGEMRIC. They found a correlation between high synovitis sub-score and low dGEMRIC values, suggestive of cartilage damage [1].

Our hypothesis was that cartilage damage measured by dGEMRIC of MCP joints in patients with rheumatoid arthritis (RA) is associated with the severity of joint inflammation on a patient level.

## Materials and methods

### Patients

This study was approved by the institutional review board, and informed consent was obtained from all patients. Forty-three patients with rheumatoid arthritis, including (35 female; eight male, age 52.9±14.5 years, range, 18–77 years, disease duration 2.9±4.9 years, range, <0.5–19 years, DAS28 3.7±1.5) were enrolled in this retrospective study. All patients fulfilled the 2010 American College of Rheumatology/European League Against Rheumatism Rheumatoid arthritis classification criteria [18, 19]. All 43 patients received 3-T MRI (Magnetom Trio; Siemens Healthcare) scans of the clinically dominant hand.

### MR imaging

MRI was performed of the dominantly affected hand on a 3-T MRI system (Magnetom Trio; Siemens Healthcare) to assess synovitis T1-weighted images pre–and post-contrast were performed of the MCP joints with a maximum slice thickness of 3 mm in at least two coronal planes and a transversal fat-suppressed T1-weighted sequence [field of view (FOV) 13×18 cm, matrix size 256×182 pixels]. Gadolinium-MRI contrast agent was applied intravenously (0.4 ml/kg body weight of Gd-DTPA2-, Magnevist; Schering).

Biochemical MRI with dGEMRIC of the MCP joints of the index and middle fingers was performed with two 4-cm loop surface coils placed above and beneath the MCP joint. The size of the coils and the FOV limited the examination to two adjacent joints: MCP 2 and 3. Subjects were imaged in a prone position with the hand extended over the head. dGEMRIC was acquired 40 min after contrast agent administration.

Variable flip-angle three-dimensional gradient-echo imaging (with two flip angles) was used for T1 calculation [4]. Flip angles were set to 5° and 26°. Twenty-two sagittal slices with a thickness of 2 mm were positioned perpendicular to the joint spaces. The FOV was 73×90 mm. The matrix of 312×384 provided an in-plane resolution of 233 μm. Total acquisition time was 2.25 min.

To reduce movement artefacts, motion correction was performed on each patient's MCP joint before image analysis. For motion correction we used the software STROKETOOL (http://www.digitalimagesolutions.de, Frechen, Germany) as described elsewhere in detail [20].

### Image analysis

Standard MR images were read in consensus by two radiologists. Images were evaluated for synovitis (range, 0–3) according to the Outcome Measures in RA Clinical Trials (OMERACT) group RAMRIS guidelines established in 2003 [15]. Synovitis scoring was performed of second and third MCP. In 20 cases of identical RAMRIS synovitis sub-scores in MCP 2 and 3, a subjective gradation into the joint with more severe synovitis and the joint with less severe synovitis was undertaken by two radiologists in consensus with 2 and 8 years of experience in musculoskeletal radiology (Fig. 1). The two radiologists were blinded to the dGEMRIC values. Based on this data, the RAMRIS synovitis sub-score of second and third MCP, each patient's pair of MCP2 and MCP3 was dichotomized into the joint with more severe synovitis vs. the joint with less severe synovitis (Fig. 2). The synovitis sub-score grading in a joint with more vs. a joint with less severe synovitis refers to dichotomization. The intraindividual analyses were chosen to eliminate interindividual cofactors, such as the different inflammatory status on a joint level between different patients.

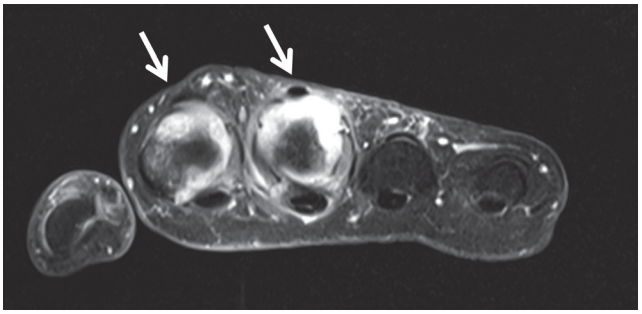

**Fig. 1** Transversal fat-suppressed T1-weighted sequence [field of view (FOV) 13 × 18 cm, matrix size 256 × 182 pixels] of a patient with RA showed identical RAMRIS synovitis sub-scores of MCP 2 and 3 (*white arrows*). In this condition, two radiologists decided in consensus on the joint with more severe synovitis and the joint with less severe synovitis. In this patient, MCP 3 was defined as the joint with more severe synovitis. Additionally, there is a tenosynovitis of the flexor tendon of the third finger

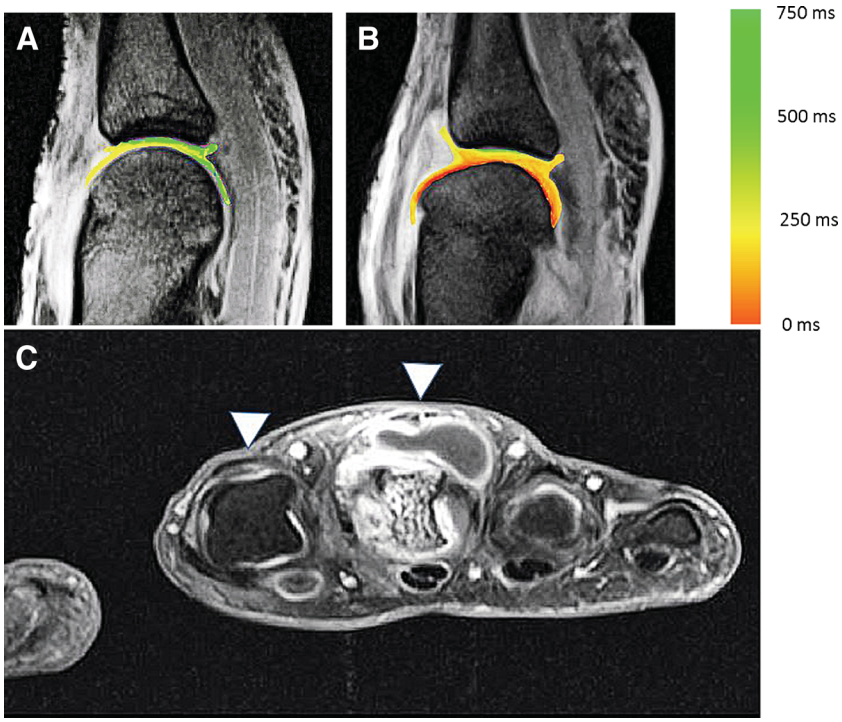


**Fig. 2** Representative dGEMRIC image of the second (**a**) and third (**b**) metacarpophalangeal joint of a patient with RA. Sagittal contrast-enhanced T1-weighted images (repetition time 15 ms, time to echo 3.34 ms, flip angle 5°) with a dGEMRIC color map overlay. Color-coding indicates high glycosaminoglycan (GAG) content (*green-blue*) to low GAG content (*red-orange*). Transversal fat-suppressed T1-weighted sequence [field of view (FOV) 13×18 cm, matrix size 256×182 pixels] of the same patient with MCP synovitis (**c**). In this patient, MCP 3 is the joint with the higher RAMRIS synovitis sub-score. dGEMRIC values demonstrate low GAG content in the joint with more severe synovitis

Molecular imaging with dGEMRIC was performed of second and third MCP. To determine cartilage quality, T1 maps were analyzed using region of interest (ROI) measurements. T1 values were calculated pixelwise using the formula

$$T1\,(x,\,y,\,z) = \frac{TR}{\ln\left[\frac{\sin\alpha1\,x\cos\alpha2 - Q(x,\,y,\,z)\,x\sin\alpha2\,x\cos\alpha1}{\sin\alpha1 - Q(x,\,y,\,z)x\sin\alpha2}\right]}$$

where

$$Q(x,\,y,\,z) = \frac{S1(x,\,y,\,z)}{S2(x,\,y,\,z)}$$

and S1(x,y,z), S2(x,y,z) are the pixel intensities corresponding to the different flip angles. Gradient-echo images with a flip angle of 5° were used as an anatomic reference for cartilage identification, and ROIs were set in the phalangeal and metacarpal cartilage of the MCP joints of the index and middle fingers. The ROIs were transferred to the co-registered T1 map. The dGEMRIC value, T1 [ms] and ROI size (number of pixels) were recorded.

### Statistical analysis

Paired Wilcoxon signed-rank test for dichotomous analyses and Spearman rho correlations between RAMRIS scores and dGEMRIC values of MCP 2 and 3 were performed using SPSS software, version 22. $p$ values less than 0.05 were considered significant. The values for dGEMRIC are presented as the mean ± SD.

## Results

dGEMRIC value of the joint with more severe synovitis was 369 ± 137 ms, dGEMRIC value of the joint with less severe synovitis was 421 ± 129 ms. RAMRIS synovitis sub-score of the joint with more severe synovitis was 2.51 (range, 1–3), synovitis sub-score of the joint with less severe synovitis MCP was 1.86 (range, 0–3). There was a significant difference between the dGEMRIC value of dichotomized MCPs ($p = 0.0001$; Fig. 3). The median of difference was 47.12, CI [16.6; 62.76].

There was a significant negative correlation between dGEMRIC value and RAMRIS synovitis sub-scores of the joint with more severe synovitis in dichotomous analysis ($r = 0.5$; $p < 0.05$; Fig. 4) as well as between dGEMRIC value and RAMRIS synovitis sub-scores of the joint with less severe synovitis ($r = 0.33$; $p < 0.05$; Fig. 5). In our patient population, only four patients showed a higher dGEMRIC value in the joint with more severe synovitis compared to the joint with less severe synovitis (Fig. 6).

## Discussion

dGEMRIC, as one method of biochemical MRI detecting cartilage degradation, is increasingly commonly used in clinical trials on cartilage changes in RA [2, 21, 22]. With dGEMRIC, it is possible to detect proteoglycan loss after the intravenous application of negatively charged contrast agent (gadolinium diethylenetriamine pentaacetate anion—Gd-

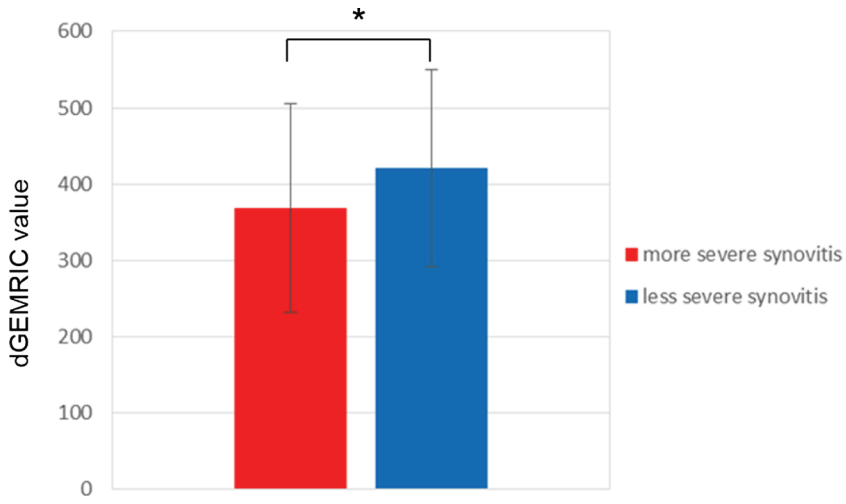


**Fig. 3** dGEMRIC values of the joint with more severe synovitis (*red*) compared to the dGEMRIC values of the joint with less severe synovitis (*blue*). There was a significant difference between both groups, indicating an association between MRI synovitis sub-score on a joint level and biochemical cartilage composition ($p = 0.0001$)

DTPA). The negatively charged Gd-DTPA penetrates cartilage in an inverse relationship to the concentration of negatively charged glycosaminoglycan side chains of proteoglycan. A depletion of proteoglycan content in degenerated cartilage results in an accumulation of the paramagnetic gadolinium ions. This consecutively accelerates T1 relaxation time [23].

Our data show that high inflammatory MRI scores were associated with cartilage proteoglycan loss on a patient level. The joint with a higher RAMRIS synovitis sub-score demonstrated a significantly lower dGEMRIC value in the intra-individual analysis representing a higher degree of cartilage destruction. In our patient population, only four patients showed a higher dGEMRIC value of the joint with more severe RAMRIS synovitis sub-score compared to the joint with a lower RAMRIS synovitis sub-score.

Clinical remission with cessation of inflammatory activity is a major aim in the treatment of RA [24]. A possible dissociation of systemic inflammatory activity from joint destruction was reported and puts preservation of joint integrity into focus of therapy [8]. MRI is a validated tool in monitoring progression of joint destruction in RA. Gandjbakhch and colleagues reported on a subclinical inflammation in RA patents in remission, which may be an explanation for structural progression despite effective treatment [24]. Tiderius et al. demonstrated that cartilage damage in biochemical MRI continues irrespective of disease activity following therapy escalation with TNF-alpha-blockers [21, 25].

Several other studies suggested a relationship between synovitis severity and joint damage [1, 24]. We found that the degree of cartilage proteoglycan loss was significantly associated with MRI sub-score of synovitis severity in a particular pair of adjacent joints.

Herz et al. showed a significant inter-individual correlation between MRI synovitis sub-score and cartilage proteoglycan loss in a cohort study design [1]. In our study we intra-individually examined MCP 2 and 3 with regard to cartilage proteoglycan loss and RAMRIS synovitis sub-score on a patient level to diminish confounders between subjects such as disease duration, age, gender, or therapy effects.

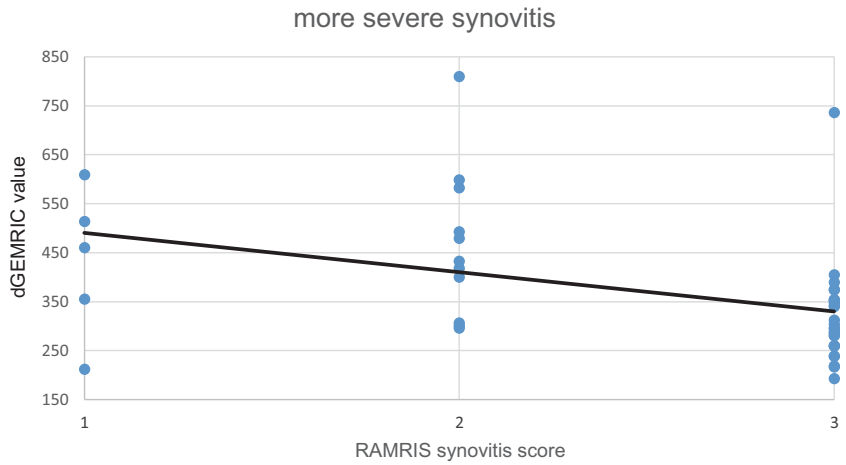


**Fig. 4** dGEMRIC value and RAMRIS synovitis sub-score of the joint with more severe synovitis. There was a significant correlation between dGEMRIC value and RAMRIS synovitis sub-score of the joint with more severe synovitis ($r = 0.5$; $p < 0.05$). MCP 2: $n = 21$; MCP 3: $n = 22$

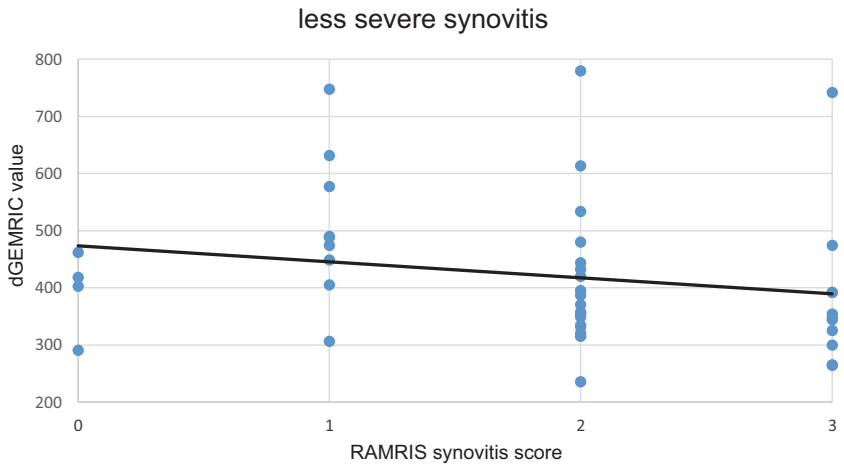


**Fig. 5** dGEMRIC value and RAMRIS synovitis sub-score of the joint with less severe synovitis. There was a significant correlation between dGEMRIC value and RAMRIS synovitis sub-score of the joint with less severe synovitis ($r = 0.33$; $p < 0.05$). MCP 2=22; MCP 3=21

Our results support the concept that inflammatory severity is associated with cartilage damage on a single joint level.

Our study has limitations. No synovial and cartilage biopsies for histological analysis as a gold standard in evaluation of joint inflammation were available. Only few studies prepared synovial biopsies as gold standard [26]. However, RAMRIS synovitis sub-score and dGEMRIC are well-established methods to assess synovial inflammation [27] and cartilage damage [7]. Additionally, the absolute values of dGEMRIC vary among different studies and protocols [1]. The lack of a standard protocol for biochemical cartilage imaging limits the comparability of dGEMRIC between individual studies.

In chondromalacia and osteoarthritis, increased cartilage perfusion in dynamic MRI has been published, suggestive of increased extracellular spaces in these conditions [28]. This finding yet awaits confirmation by other study groups. In RA, no data on cartilage perfusion are available yet. Possibly hyperperfusion leads to a bias in dGEMRIC values in RA. We found a direct correlation between high inflammatory MRI scores and low dGEMRIC values on a paired joint level, but we also detected low dGEMRIC values in patients with low or moderate synovitis.

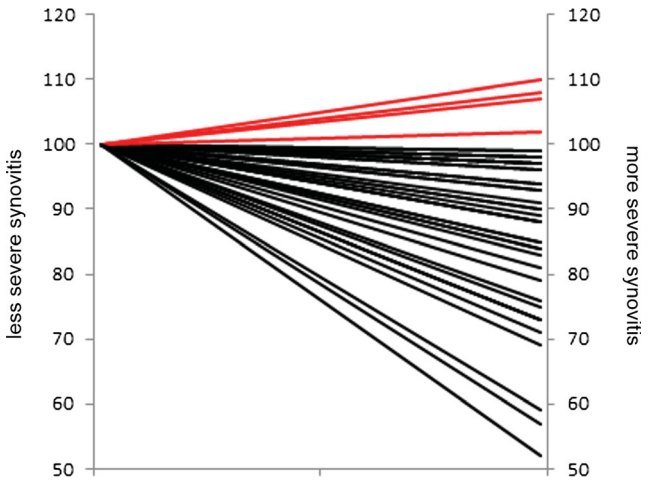


**Fig. 6** Dichotomous dGEMRIC values of MCP 2 and 3 in percent, the joint with less severe synovitis was represented as 100%. The *left side* represents the dGEMRIC value of the joint with less severe synovitis (100%). The *right side* shows the dGEMRIC value of the joint with more severe synovitis (in relation to 100% of the joint with less severe synovitis). Out of 43 examined hands, 39 MCP pairs showed lower dGEMRIC values of the joints with more severe synovitis (*black lines*)

## Conclusions

The significant association of cartilage composition and RAMRIS synovitis sub-score supports the concept that inflammation and cartilage damage are coupled on a local joint level.

**Acknowledgments** The study was supported by a grant from the Deutsche Forschungsgemeinschaft (DFG - MI 1575/1-1).

**Conflict of interest** There are no conflicts of interest to disclose.

## References

1. Herz B, Albrecht A, Englbrecht M, Welsch GH, Uder M, Renner N, Schlechtweg P, Paul D, Lauer L, Engelke K, Janka R, Rech J, Schett G, Finzel S: Osteitis and synovitis, but not bone erosion, is associated with proteoglycan loss and microstructure damage in the cartilage of patients with rheumatoid arthritis. Ann Rheum Dis 2013.
2. Miese F, Buchbender C, Scherer A, Wittsack HJ, Specker C, Schneider M, et al. Molecular imaging of cartilage damage of finger joints in early rheumatoid arthritis with delayed gadolinium-enhanced magnetic resonance imaging. Arthritis Rheum. 2012;64: 394–9.
3. Liebl H, Joseph G, Nevitt MC, Singh N, Heilmeier U, Karupppasamy S, Jungmann PM, McCulloch CE, Lynch JA, Lane NE, Link TM. Early T2 changes predict onset of radiographic knee osteoarthritis: data from the osteoarthritis initiative. Ann Rheum Dis 2014.
4. Miese FR, Ostendorf B, Wittsack HJ, Reichelt DC, Mamisch TC, Zilkens C, et al. Metacarpophalangeal joints in rheumatoid arthritis:

delayed gadolinium-enhanced MR imaging of cartilage–a feasibility study. Radiology. 2010;257:441–7.
5. Bashir A, Gray ML, Burstein D. Gd-DTPA2- as a measure of cartilage degradation. Magn Reson Med. 1996;36:665–73.
6. Burstein D, Velyvis J, Scott KT, Stock KW, Kim YJ, Jaramillo D, et al. Protocol issues for delayed Gd(DTPA)(2-)-enhanced MRI (dGEMRIC) for clinical evaluation of articular cartilage. Magn Reson Med. 2001;45:36–41.
7. Zilkens C, Miese FR, Crumbiegel C, Kim YJ, Herten M, Antoch G, et al. Magnetic resonance imaging and histology of ovine hip joint cartilage in two age populations: a sheep model with assumed healthy cartilage. Skeletal Radiol. 2013;42:699–705.
8. Lafeber FP, Van der Laan WH. Progression of joint damage despite control of inflammation in rheumatoid arthritis: a role for cartilage damage driven synovial fibroblast activity. Ann Rheum Dis. 2012;71:793–5.
9. Smolen JS, Aletaha D, Steiner G. Does damage cause inflammation? revisiting the link between joint damage and inflammation. Ann Rheum Dis. 2009;68:159–62.
10. Welsing PM, Landewé RB, van Riel PL, Boers M, van Gestel AM, van der Linden S, et al. The relationship between disease activity and radiologic progression in patients with rheumatoid arthritis: a longitudinal analysis. Arthritis Rheum. 2004;50:2082–93.
11. Aletaha D, Smolen J, Ward MM. Measuring function in rheumatoid arthritis: identifying reversible and irreversible components. Arthritis Rheum. 2006;54:2784–92.
12. Jansen LM, van der Horst-Bruinsma IE, van Schaardenburg D, Bezemer PD, Dijkmans BA. Predictors of radiographic joint damage in patients with early rheumatoid arthritis. Ann Rheum Dis. 2001;60:924–7.
13. Smolen JS, Aletaha D. Monitoring rheumatoid arthritis. Curr Opin Rheumatol. 2011;23:252–8.
14. Landewé R, van der Heijde D, Klareskog L, van Vollenhoven R, Fatenejad S. Disconnect between inflammation and joint destruction after treatment with etanercept plus methotrexate: results from the trial of etanercept and methotrexate with radiographic and patient outcomes. Arthritis Rheum. 2006;54:3119–25.
15. Ostergaard M, Peterfy C, Conaghan P, McQueen F, Bird P, Ejbjerg B, et al. OMERACT rheumatoid arthritis magnetic resonance imaging studies. Core set of MRI acquisitions, joint pathology definitions, and the OMERACT RA-MRI scoring system. J Rheumatol. 2003;30:1385–6.
16. Østergaard M, Emery P, Conaghan PG, Fleischmann R, Hsia EC, Xu W, et al. Significant improvement in synovitis, osteitis, and bone erosion following golimumab and methotrexate combination therapy as compared with methotrexate alone: a magnetic resonance imaging study of 318 methotrexate-naive rheumatoid arthritis patients. Arthritis Rheum. 2011;63:3712–22.
17. Hetland ML, Ejbjerg B, Horslev-Petersen K, Jacobsen S, Vestergaard A, Jurik AG, et al. group Cs: MRI bone oedema is the strongest predictor of subsequent radiographic progression in early rheumatoid arthritis. Results from a 2-year randomised controlled trial (CIMESTRA). Ann Rheum Dis. 2009;68:384–90.
18. van Gestel AM, Prevoo ML, Van't Hof MA, van Rijswijk MH, van de Putte LB, van Riel PL. Development and validation of the european league against rheumatism response criteria for rheumatoid arthritis. Comparison with the preliminary american college of rheumatology and the world health organization/international league against rheumatism criteria. Arthritis Rheum. 1996;39:34–40.
19. Aletaha D, Neogi T, Silman AJ, Funovits J, Felson DT, Bingham CO, et al. 2010 rheumatoid arthritis classification criteria: an american college of rheumatology/european league against rheumatism collaborative initiative. Arthritis Rheum. 2010;62:2569–2581.
20. Miese F, Kröpil P, Ostendorf B, Scherer A, Buchbender C, Quentin M, et al. Motion correction improves image quality of dGEMRIC in finger joints. Eur J Radiol. 2011;80:e427–431.
21. Tiderius CJ, Sandin J, Svensson J, Dahlberg LE, Jacobsson L. Knee cartilage quality assessed with dGEMRIC in rheumatoid arthritis patients before and after treatment with a TNF inhibitor. Acta Radiol. 2010;51:1034–7.
22. Buchbender C, Scherer A, Kröpil P, Körbl B, Quentin M, Reichelt DC, et al. Cartilage quality in rheumatoid arthritis: comparison of T2* mapping, native T1 mapping, dGEMRIC, δr1 and value of precontrast imaging. Skeletal Radiol. 2012;41:685–92.
23. Crema MD, Roemer FW, Marra MD, Burstein D, Gold GE, Eckstein F, et al. Articular cartilage in the knee: current MR imaging techniques and applications in clinical practice and research. Radiographics. 2011;31:37–61.
24. Gandjbakhch F, Conaghan PG, Ejbjerg B, Haavardsholm EA, Foltz V, Brown AK, et al. Synovitis and osteitis are very frequent in rheumatoid arthritis clinical remission: results from an MRI study of 294 patients in clinical remission or low disease activity state. J Rheumatol. 2011;38:2039–44.
25. Christensen AF, Horslev-Petersen K, Christgau S, Lindegaard HM, Lottenburger T, Junker K, et al. Uncoupling of collagen ii metabolism in newly diagnosed, untreated rheumatoid arthritis is linked to inflammation and antibodies against cyclic citrullinated peptides. J Rheumatol. 2010;37:1113–20.
26. Vordenbäumen S, Sewerin P, Lögters T, Miese F, Schleich C, Bleck E, et al. Inflammation and vascularisation markers of arthroscopically-guided finger joint synovial biopsies reflect global disease activity in rheumatoid arthritis. Clin Exp Rheumatol. 2014;32:117–20.
27. Conaghan P, Lassere M, Østergaard M, Peterfy C, McQueen F, O'Connor P, et al. OMERACT rheumatoid arthritis magnetic resonance imaging studies. Exercise 4: an international multicenter longitudinal study using the RA-MRI score. J Rheumatol. 2003;30:1376–9.
28. Sanz R, Martí-Bonmatí L, Rodrigo JL, Moratal D. MR pharmacokinetic modeling of the patellar cartilage differentiates normal from pathological conditions. J Magn Reson Imaging. 2008;27:171–7.

# Evaluation of a simplified version of the Rheumatoid Arthritis Magnetic Resonance Imaging Score (RAMRIS) comprising 5 joints (RAMRIS5)

C. Schleich[1], C. Buchbender[1], P. Sewerin[2], F. Miese[1], J. Aissa[1], R. Brinks[3], M. Schneider[2], G. Antoch[1], B. Ostendorf[2]

*[1]Department of Diagnostic and Interventional Radiology, and [2]Department of Rheumatology, University of Dusseldorf, Medical Faculty, Dusseldorf, Germany;*
*[3]Institute of Biometry and Epidemiology, German Diabetes Centre, Dusseldorf, Germany.*

## Abstract

### Objective

*The objective of this study was to evaluate a simplified version of the Rheumatoid Arthritis Magnetic Resonance Imaging Score (RAMRIS) reduced to five joints of the hand (RAMRIS5).*

### Methods

*94 patients with rheumatoid arthritis (62 female; age 59±12 years, range 25 - 83 years; disease duration 60 ± 90 months (median: 22 months, first quartile: 7 months, third quartile: 66 months) from the REMISSION PLUS study cohort who had complete files on C-reactive protein (CRP) levels and Disease Activity Score of 28 joints (DAS28) and complete MRI of the clinical dominant hand at baseline and after one year under anti-rheumatic therapy (follow-up time 12.5±1.1 months) in a dedicated extremity MRI scanner at 0.2T were included in this retrospective study.*

### Results

*There was a strong correlation between RAMRIS5 and the RAMRIS sum-score for all patients ($r=0.87$, $p<0.001$) at baseline and follow-up ($r=0.87$, $p<0.001$). Among the subscores there was a significant correlation between RAMRIS5 and RAMRIS-MCP (baseline: $r=0.66$, $p<0.001$; follow-up: $r=0.74$, $p<0.001$) as well as between RAMRIS5 and RAMRIS-wrist (baseline: $r=0.72$, $p<0.001$, follow-up: $r=0.69$, $p<0.001$) at baseline and follow-up.*

### Conclusion

*RAMRIS5, a modified shorter RAMRIS score based on five joints of the hand is a viable tool for semi-quantitative assessment of joint damage in RA. This abbreviated score might reduce the time needed for image analysis in MRI-controlled studies in RA and might facilitate the use of MRI in studies on therapy response assessment in RA.*

**Key words**

rheumatoid arthritis, RAMRIS, RAMRIS5, magnetic resonance imaging

*Christoph Schleich, MD*
*Christian Buchbender, MD*
*Philipp Sewerin, MD*
*Falk Miese, MD*
*Joel Aissa, MD*
*Ralph Brinks, Dr*
*Matthias Schneider, MD, Prof.*
*Gerald Antoch, MD, Prof.*
*Benedikt Ostendorf, MD, Prof.*

*Please address correspondence to:*
*Christoph Schleich,*
*University of Dusseldorf,*
*Medical Faculty,*
*Department of*
*Diagnostic and Interventional Radiology*
*Moorenstrasse 5,*
*40225 Düsseldorf (NRW), Germany.*
*E-mail:*
*christoph.schleich@med.uni-duesseldorf.de*

*Received on August 13, 2014; accepted in revised form on December 1, 2014.*



*Competing interests: none declared.*

## Introduction

Rheumatoid arthritis (RA) is, next to gout and psoriatic arthritis, one of the most common inflammatory rheumatic diseases with a worldwide prevalence of 0.5–0.8% (1, 2).

Untreated RA leads to chronic joint inflammation causing pain and functional disability due to swelling and joint mutilation (2, 3). To achieve a better outcome an early diagnosis and therapy with anti-rheumatic drugs aiming at the induction of disease remission is required (1, 4).

Magnetic resonance imaging (MRI) is a useful tool in detecting changes relating to RA, due to its high sensitivity to soft-tissue inflammation and bone destruction (5). In 2003 the Outcome Measures in RA Clinical Trials (OMERACT) group with the RA MRI Score (RAMRIS) established a highly reliable sum-score based on the semi-quantitative rating of the severity of synovitis, bone marrow oedema and erosions in hand (metacarpophalangeal joints) and wrist joints (6). The RAMRIS system has been shown to be a sensitive tool for the evaluation of therapy response in RA patients (7, 8). Generally, the RAMRIS score and clinical and serological disease activity parameters show a similar tendency (9). But a recent more detailed analysis on the connection between the individual changes of RAMRIS levels and the change of the well-established disease activity score for 28 joints (DAS28) and C-reactive protein (CRP) levels on the other hand by Emery and colleagues indicated only a weak correlation (10). The authors of the study interpreted this lack of correlation as an effect of the superior sensitivity of MRI for inflammation compared to clinical assessment and serological parameters.

Semi-quantitative, structured evaluation of hand-MRI using the RAMRIS system is a widely accepted and validated parameter in MRI-controlled clinical trials in RA (9, 11, 12). The RAMRIS criteria propose a sum-score of 23 joint sites of the hand (metacarpophalangeal joints 2–5, carpo-metacarpophalangeal joints 1–5, intercarpal joints, radiocarpal and radioulnar joints), yielding the sum of individual joints subscore for synovitis (grade: 0–3), bone marrow oedema (BME; grade: 0-3) and erosions (grade: 0–10). Especially in clinical studies enrolling large numbers of patients receiving MRI on multiple time-points (*e.g.* before and after treatment) this evaluation is time consuming (13) and a resource saving short score may facilitate the use of MRI, provided it offers equal sensitivity to determine changes after therapy (diagnostic performance). The aim of this study was to assess an abbreviated RAMRIS measurement encompassing 5 frequently affected joint sites, the RAMRIS5 score.

## Material and methods

*Patients*

Ethics committee vote; trial num. 3226. After institutional review board approval, the datasets of 94 RA patients [62 female; age 59±12 years, range 25-83 years; disease duration 60±90 months (median: 22 months, first quartile: 7 months, third quartile: 66 months, range 3 weeks - 44 years)] from the REMISSION PLUS study cohort (14) recruited from a single centre were retrospectively included in this study. All patients fulfilled the 2010 American College of Rheumatology/European League Against Rheumatism Rheumatoid arthritis classification criteria (15, 16). Baseline and follow-up MRI scans were acquired of the clinically dominant hand and wrist. Follow-up MRI was performed approximately 12 months (12.5±3.5 months) after the baseline scan. The DAS 28 (CRP included) was documented at both examination dates by an experienced rheumatologist (16). All patients received disease-modifying anti-rheumatic drugs (DMARD), either methotrexate/15 mg (oral)/weekly or sulfasalazine (2000mg/d)). Concomitant prednisolone was allowed up to a dose of ≤10 mg/d.

*MR imaging*

MR imaging of the clinically dominant hand and wrist was performed using an open, extremity MR-System with a fieldstrength of 0.2T (Esaote, C-Scan, Genova Italy). The system provides the most available comfort for patients with RA, resulting in a higher subjective acceptability of MRI examina-

tions (17). The imaging protocol met the OMERACT recommendations (6, 18) and included pre- and post-contrast (intravenous injection of a standard dose of 0.2 ml/kg bodyweight of Gadolinium-based MRI contrast material, Dotarem®) T1-weighted images with a maximum slice thickness of 3 mm in at least two orthogonal planes and coronal fat-supressed short tau inversion recovery (STIR) sequences.

In detail, we used the following sequences:

1. Coronal Short tau inversion recovery (STIR) sequence with a Field of view (FoV) of 180* 180 mm, matrix size 192* 152, slice thickness 3 mm, Time to repetition (TR) 2420 ms, Time to excitation (TE) 26 ms, Time to inversion (TI) 85 ms).
2. Coronal 3 dimensional T1-weighed gradient echo sequence with a FoV of 180* 180* 60 mm, matrix size 192* 192* 40, slice thickness 1 mm, TR 50 ms, TE 16 ms prior and after intravenous injection of contrast material. The 3 dimensional T1-weighed gradient echo sequence was additionally reconstructed in sagittal and axial planes.

The field of view contained the metacarpophalangeal joints, the carpometacarpal joints, carpal joints, radiocarpal and radioulnar joints. The overall image acquisition time was 18 minutes. MR images were analysed by two experienced radiologists, who have been trained for RAMRIS scoring.

*Image analysis* (Fig. 1)

MR images were read in consensus by two radiologists trained in RAMRIS-Scoring. Images were evaluated for synovitis (grade: 0–3), bone marrow oedema (BME; grade: 0–3) and erosions (grade: 0–10) according to the RAMRIS guidelines (5, 19) (Fig. 2). In MCP joints the distal and proximal joint portions were analysed separately for presence of BME and erosions. BME and erosions were also detected in the bases of metacarpal bones 1–5, intercarpal bones, distal radius and ulna. For the evaluation of synovitis MCP, carpometacarpal, intercarpal, radiocarpal and radioulnar joints of the clinically dominant hand and wrist were analysed.

**Table I.** Spearman rho correlation analysis at baseline and at follow-up measurement for C-reactive protein (CRP), Disease Activity Score 28 (DAS28), $RAMRIS_{MCP}$, $RAMRIS_{wrist}$, RAMRIS and RAMRIS 5.

| | CRP | DAS28 | RAMRIS wrist | RAMRISMCP | RAMRIS | RAMRIS5 |
|---|---|---|---|---|---|---|
| | | | Baseline | | | |
| CRP | 1.00 | 0.43 | 0.32 | 0.11 | 0.29 | 0.21 |
| DAS28 | 0.43 | 1.00 | 0.21 | 0.14 | 0.20 | 0.17 |
| $RAMRIS_{wrist}$ | 0.32 | 0.21 | 1.00 | 0.26 | 0.90 | 0.72 |
| $RAMRIS_{MCP}$ | 0.11 | 0.14 | 0.26 | 1.00 | 0.61 | 0.66 |
| RAMRIS | 0.29 | 0.20 | 0.90 | 0.61 | 1.00 | 0.87 |
| RAMRIS5 | 0.21 | 0.17 | 0.72 | 0.66 | 0.87 | 1.00 |
| | | | Follow-up | | | |
| CRP | 1.00 | 0.22 | 0.14 | -0.02 | 0.10 | 0.03 |
| DAS28 | 0.22 | 1.00 | 0.25 | 0.27 | 0.32 | 0.31 |
| $RAMRIS_{wrist}$ | 0.14 | 0.25 | 1.00 | 0.29 | 0.91 | 0.69 |
| $RAMRIS_{MCP}$ | -0.02 | 0.27 | 0.29 | 1.00 | 0.61 | 0.74 |
| RAMRIS | 0.10 | 0.32 | 0.91 | 0.61 | 1.00 | 0.87 |
| RAMRIS5 | 0.03 | 0.31 | 0.69 | 0.74 | 0.87 | 1.00 |

Prior published studies demonstrated the joints mostly affected in RA: MCP 2 and 3 in the hand and distal ulna, radius, capitate, lunate, triquetrum, scaphoid, pisiform in the wrist (20-23). Additionally we took our MRI experience in joint involvement in RA into account (14, 24) and developed a new, abbreviated score. The RAMRIS5 score included the following joints of the clinically dominant hand and wrist: MCP 2 and 3 (to evaluate synovitis, erosions and bone marrow oedema); capitate bone, triquetral bone and distal ulna (to evaluate erosions and bone marrow oedema). Synovitis of the capitate bone, triquetral bone and distal ulna was assessed as a composite wrist synovitis score comprising the intercarpal and radiocarpal joints.

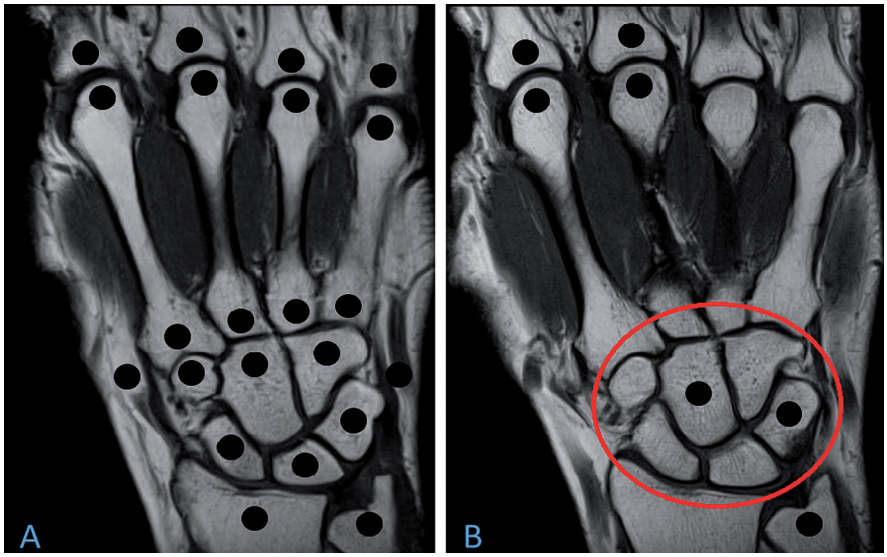


**Fig. 1.** Picture A and B show 3T MRI of the right hand. The black dots in picture A visualise areas analysed in the clinically dominant hand with RAMRIS for erosions, oedema and synovitis. For erosions 23 areas were evaluated including wrist (distal radius, distal ulna, carpal bones, metacarpal bases) and second to fifth MCP joints (metacarpal heads, phalangeal bases) with a scale from 0–10. For osteoedema the same 23 areas were evaluated as those for erosions with a scale from 0–3. For synovitis distal radioulnar joint, radiocarpal joint, intercarpal joints and second to fifth MCP joints were analysed with a scale from 0–3. Picture B shows joint sites analysed in RAMRIS5 in regard with erosions, oedema and synovitis. For erosions 5 areas were evaluated including MCP 2 and 3, carpitate bone, triquetral bone and distal ulna. We evaluated the same 5 areas for osteoedema. For synovitis we analysed MCP 2 and 3, as well as intercarpal and radiocarpal joint as one common space (red ellipse). The scale was identical in RAMRIS and RAMRIS5.

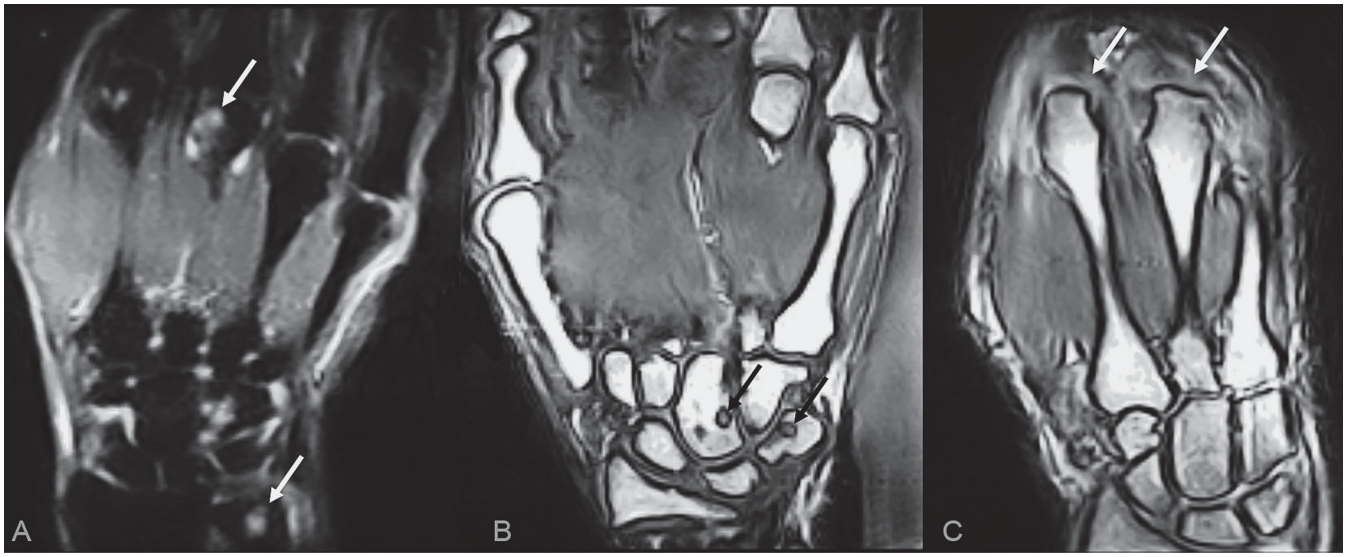


**Fig. 2.** Pictures A-C show typical MR imaging findings in RA. Picture A demonstrates a coronal STIR with bone marrow oedema in the distal ulna and in the caput of metacarpal 3 (white arrow). Coronal plane show erosion in capitate and triquetral bone (white arrows in picture BA). Picture C presents a coronal plane after contrast agent application. There is a strong enhancement of the synovitis MCP 2 and 3 (white arrow); additionally, synovitis can be seen in intercarpal and radiocarpal joints.

RAMRIS subscores were assessed for MCP joints and wrist by calculating the sumscores of inflammatory findings of the corresponding joints.

All statistical analyses were performed using the software R, version 2.11.1 (The R Foundation for Statistical Computing). For correlation analyses Spearman's rank correlation coefficient was used. A $p$-value <0.05 was chosen to demonstrate statistical significance.

## Results

*Correlation of RAMRIS, RAMRIS subscores and clinical parameters of disease activity*

There was a weak correlation between RAMRIS and CRP levels ($r$=0.29, $p$<0.01) at baseline and follow-up ($r$=0.10, $p$=0.34) as well as between RAMRIS and DAS28 (baseline: $r$=0.20, $p$=0.05, follow-up: $r$=0.32, $p$<0.01). At baseline and follow-up there was a good correlation between the subscores of $RAMRIS_{MCP}$ (baseline: $r$=0.61, $p$<0.001; follow-up: $r$=0.61, $p$<0.001) and $RAMRIS_{wrist}$ (baseline: $r$=0.90, $p$<0.001; follow-up: $r$=0.91, $p$<0.001) with RAMRIS.

*Correlation of RAMRIS5 and clinical parameters of disease activity* (Fig. 3-5)

The correlation between RAMRIS5 and CRP was weak at baseline ($r$=0.21, $p$<0.05) and follow-up ($r$=0.03, $p$=0.76). Moreover, there was a poor correlation between RAMRIS5 and DAS28 at baseline ($r$=0.17, $p$=0.11) and follow- up ($r$=0.31, $p$<0.01).

*Correlation of RAMRIS5, RAMRIS and RAMRIS subscores*

There was a strong correlation between RAMRIS5 and RAMRIS ($r$=0.87, $p$<0.001) at baseline and follow-up ($r$=0.87, $p$<0.001). There was also a good correlation between RAMRIS5 and the subscores $RAMRIS_{MCP}$ and $RAMRIS_{wrist}$ at baseline ($r_{MCP}$ = 0.66, $r_{wrist}$ = 0.72, each $p$<0.001) and follow-up ($r_{MCP}$ = 0.74, $r_{wrist}$ = 0.69, each $p$<0.001).

*Course of clinical and imaging parameters under therapy*

Under therapy DAS28 and CRP decreased from 4.87±2.94 (baseline score) to 2.88±2.18 (follow-up) and from 16.63±22.56 to 9.08±15.48, respectively. Baseline RAMRIS score was 37.65±31.06 and decreased to 25.22±17.90 in follow-up measurement (percentage change: 33.01%). Baseline RAMRIS5 score was 14.91±10.77 and decreased to 11.00±7.38 in follow-up measurement (percentage change: 26.22%).

*RAMRIS5 and RAMRIS time comparative analysis*

One radiologist tested the time which

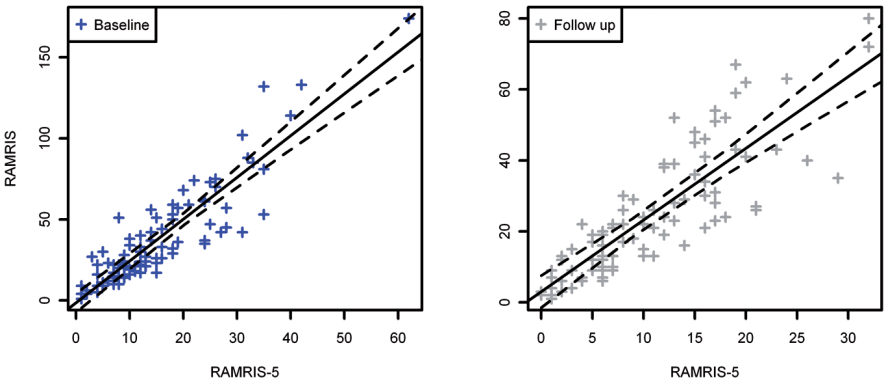


**Fig. 3.** Correlation of RAMRIS and RAMRIS5 at baseline and follow-up measurement. There was a significant and strong correlation between RAMRIS and RAMRIS 5 at baseline and follow-up measurement.

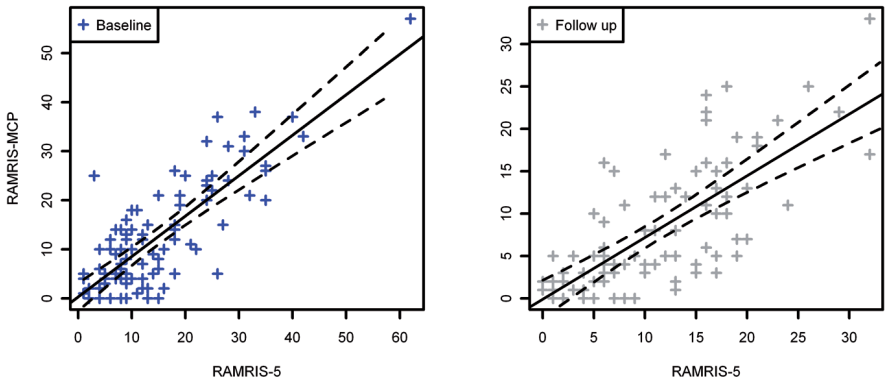


**Fig. 4.** Correlation of $RAMRIS_{MCP}$ subscore and RAMRIS5. The graphic shows a good correlation between $RAMRIS_{MCP}$ subscore and RAMRIS5.

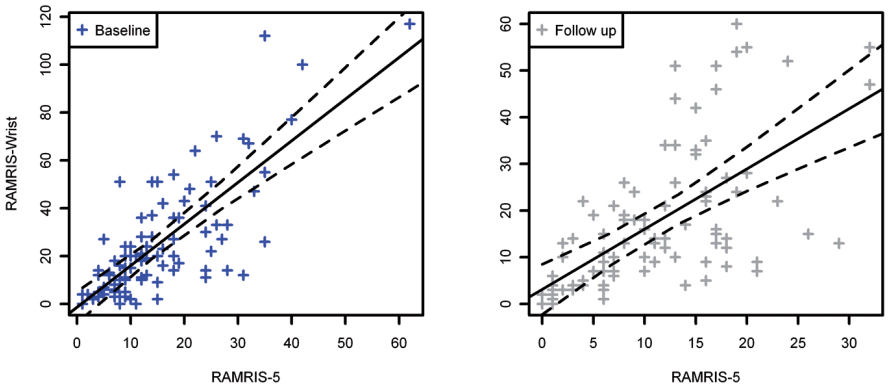


**Fig. 5.** Correlation of $RAMRIS_{WRIST}$ subscore and RAMRIS 5. The graphic shows a good correlation between $RAMRIS_{WRIST}$ subscore and RAMRIS5.

was used for both scoring methods. The examination time varied with the number of lesions present and ranged from 28 to 55 seconds (39.4±9.00) when using RAMRIS5 and from 242 to 312 seconds (278.8±20.31; $p$=0.001) when using RAMRIS. Under therapy the time period for RAMRIS5 was 30 to 53 seconds (38.3±8.63) and for RAMRIS 240 to 315 seconds (277.8±21.00; $p$=0.001).

## Discussion

The development of new therapeutic strategies for rheumatoid arthritis, aiming at the early suppression of the disease activity using DMARDs and biologicals promoted the use of MRI for the sensitive detection and monitoring of joint inflammation (25-28).

The Outcome Measures in Rheumatology Clinical Trials (OMERACT) Rheumatoid Arthritis Magnetic Resonance Imaging Score is the current standard for the structured, semi-quantitative assessment of joint alterations in rheumatoid arthritis (6). Since RAMRIS scoring is time-consuming, even after training, we evaluated an abbreviated scoring system, the RAMRIS5, comprising 5 instead of 23 joint sites. We found that the RAMRIS5 was strongly correlated to the standard RAMRIS at baseline and one year after anti-rheumatic therapy (DMARD). Additionally, RAMRIS5 and RAMRIS both showed similar tendencies under anti-rheumatic therapy and were both concordant with the clinical parameters (DAS28 or CRP) that demonstrated therapy response. RAMRIS5 showed a significant reduction of scoring time. Thus RAMRIS5 is a time and resource saving alternative for semi-quantitative scoring of inflammatory joint pathologies of the hand and their change in follow-up patients.

In contrast to the SAMIS (13), another simplification of the RAMRIS, we did not reduce the number of steps on the scales for BME, erosions and synovitis that have to be applied to all RAMRIS joint sites, in order to prevent the necessity of a new training of the readers, who are already familiar and well trained on the original scoring system. Instead, following examples of well-established ultrasound scoring systems in RA (29-31), we simplified the test by reducing the number of joint sites that have to be evaluated to five of the most frequently affected in RA. Backhaus et al. examined five joints in the hand and wrist: wrist, MCP 2 and 3, proximal interphalangeal joint (PIP) 2 and 3. In contrast to Backhaus we evaluated erosions, synovitis and bone marrow oedema according to the original RAMRIS criteria. The ultrasound scoring system cannot detect bone marrow oedema depends on technical factors. Instead, the scoring system take synovitis, tenosynovitis and bone marrow oedema into account (29).

Sharp *et al*. had previously reported that an abbreviated scoring system, using a combination of 17 joints to score erosions and 18 to score joint space narrowing, more accurately reflects the dimension of abnormalities than does the original scheme including more bones (32). Compared to the score of Sharp et al. our modified RAMRIS preserves the original RAMRIS criteria and encompassed the scoring of erosions, bone marrow oedema and synovitis. Since the latter are the dominant MRI pathologies found in RA we consider the preservation of the original RAMRIS criteria an advantage of the RAMRIS5. To save additional time for imaging and image evaluation, departing from the original RAMRIS recommendations, we only imaged and scored the clinically dominant hand. However, we do not consider this approach a relevant drawback of our study, since Ejbjerg *et al*. had previously demonstrated that there was no significant difference with respect to the detection of progressive joint destruction in rheumatoid arthritis between unilateral and bilateral MR imaging of the wrist and MCP joints (33).

Our study has limitations. We did not evaluate the inter- and intra-reader reliability of the RAMRIS5. Since the RAMRIS scoring system has a previously described high inter- and intra-reader reliability (34, 35) and due to the fact that both readers of this study were well experienced and trained for RAMRIS scoring, we consider this a minor

limitation. Additionally, the evaluation of the correlation between the RAMRIS5 and the RAMRIS when applied by readers with different levels of experience would have been desirable to establish the objective reliability of the abbreviated score. Further longitudinal studies with larger patient cohorts are needed to support our results and to answer the question if RAMRIS5 and RAMRIS lead to identical definitions of disease activity, therapeutic decisions and remission.

In conclusion, the shortened MR imaging scoring method RAMRIS5, is closely correlated with the RAMRIS for baseline and follow-up measurements. Thus RAMRIS5 can be used as a time and resource saving alternative for semi-quantitative description of inflammatory joint changes and therapy monitoring in RA.

**Acknowledgment**

The authors thank AbbVie Deutschland GmbH & Co. KG Medical Area Immunology, Wiesbaden, Germany for financially supporting this project: RemissionPLUS, which did not exert any influence on the statistical analysis or preparation of the paper.

The authors also thank Esaote Biomedica Deutschland GmbH, Köln, Germany for the technical support of the REMISSION PLUS project.

**References**

1. SCHNEIDER M, KRÜGER K: Rheumatoid arthritis--early diagnosis and disease management. *Dtsch Arztebl Int* 2013; 110: 477-84.
2. PINCUS T, SOKKA T: How can the risk of long-term consequences of rheumatoid arthritis be reduced? *Best Pract Res Clin Rheumatol* 2001; 15: 139-70.
3. SCOTT DL, SYMMONS DP, COULTON BL, POPERT AJ: Long-term outcome of treating rheumatoid arthritis: results after 20 years. *Lancet* 1987; 1: 1108-11.
4. SMOLEN JS, ALETAHA D: Monitoring rheumatoid arthritis. *Curr Opin Rheumatol* 2011; 23: 252-8.
5. ØSTERGAARD M, EDMONDS J, MCQUEEN F *et al*.: An introduction to the EULAR-OMERACT rheumatoid arthritis MRI reference image atlas. *Ann Rheum Dis* 2005; 64 (Suppl. 1): i3-7.
6. ØSTERGAARD M, PETERFY C, CONAGHAN P *et al*.: OMERACT Rheumatoid Arthritis Magnetic Resonance Imaging Studies. Core set of MRI acquisitions, joint pathology definitions, and the OMERACT RA-MRI scoring system. *J Rheumatol* 2003; 30: 1385-6.
7. ØSTERGAARD M, EMERY P, CONAGHAN PG *et al*.: Significant improvement in synovitis, osteitis, and bone erosion following golimumab and methotrexate combination therapy as compared with methotrexate alone: a magnetic resonance imaging study of 318 methotrexate-naive rheumatoid arthritis patients. *Arthritis Rheum* 2011; 63: 3712-22.
8. HETLAND ML, EJBJERG B, HØRSLEV-PETERSEN K *et al*.: MRI bone oedema is the strongest predictor of subsequent radiographic progression in early rheumatoid arthritis. Results from a 2-year randomised controlled trial (CIMESTRA). *Ann Rheum Dis* 2009; 68: 384-90.
9. HODGSON RJ, O'CONNOR P, MOOTS R: MRI of rheumatoid arthritis image quantitation for the assessment of disease activity, progression and response to therapy. *Rheumatology* (Oxford) 2008; 47: 13-21.
10. EMERY P, VAN DER HEIJDE D, OSTERGAARD M *et al*.: Exploratory analyses of the association of MRI with clinical, laboratory and radiographic findings in patients with rheumatoid arthritis. *Ann Rheum Dis* 2011; 70: 2126-30.
11. PETERFY CG, OLECH E, DICARLO JC, MERRILL JT, COUNTRYMAN PJ, GAYLIS NB: Monitoring cartilage loss in the hands and wrists in rheumatoid arthritis with magnetic resonance imaging in a multi-center clinical trial: IMPRESS (NCT00425932). *Arthritis Res Ther* 2013; 15: R44.
12. ØSTERGAARD M, DUER A, NIELSEN H *et al*.: Magnetic resonance imaging for accelerated assessment of drug effect and prediction of subsequent radiographic progression in rheumatoid arthritis: a study of patients receiving combined anakinra and methotrexate treatment. *Ann Rheum Dis* 2005; 64: 1503-6.
13. CYTEVAL C, MIQUEL A, HOA D, DAURES JP, MARIETTE X, COMBE B: Rheumatoid arthritis of the hand: monitoring with a simplified MR imaging scoring method--preliminary assessment. *Radiology* 2010; 256: 863-9.
14. OSTENDORF B, SCHERER A, KELLNER H, BACKHAUS M. [Project REMISSION (PLUS): clinical and radiological remission: new treatment goals in the management of rheumatoid arthritis]. *Z Rheumatol* 2008; 67: 707-10, 712-5.
15. VAN GESTEL AM, PREVOO ML, VAN'T HOF MA, VAN RIJSWIJK MH, VAN DE PUTTE LB, VAN RIEL PL: Development and validation of the European League Against Rheumatism response criteria for rheumatoid arthritis. Comparison with the preliminary American College of Rheumatology and the World Health Organization/International League Against Rheumatism Criteria. *Arthritis Rheum* 1996; 39: 34-40.
16. ALETAHA D, NEOGI T, SILMAN AJ *et al*.: 2010 rheumatoid arthritis classification criteria: an American College of Rheumatology/European League Against Rheumatism collaborative initiative. *Ann Rheum Dis* 2010; 69: 1580-8.
17. OSTENDORF B, EDELMANN E, KELLNER H, SCHERER A, DGRH KBVD: [Low-field magnetic resonance imaging for rheumatoid arthritis]. *Z Rheumatol* 2010; 69: 79-86.
18. LASSERE M, MCQUEEN F, ØSTERGAARD M *et al*.: OMERACT Rheumatoid Arthritis Magnetic Resonance Imaging Studies. Exercise 3: an international multicenter reliability study using the RA-MRI Score. *J Rheumatol* 2003; 30: 1366-75.
19. CONAGHAN P, BIRD P, EJBJERG B *et al*.: The EULAR-OMERACT rheumatoid arthritis MRI reference image atlas: the metacarpophalangeal joints. *Ann Rheum Dis* 2005; 64 (Suppl. 1): i11-21.
20. LARSEN A, DALE K, EEK M: Radiographic evaluation of rheumatoid arthritis and related conditions by standard reference films. *Acta Radiol Diagn* (Stockh) 1977; 18: 481-91.
21. FLEMING A, BENN RT, CORBETT M, WOOD PH: Early rheumatoid disease. II. Patterns of joint involvement. *Ann Rheum Dis* 1976; 35: 361-4.
22. BUCKLAND-WRIGHT JC, WALKER SR: Incidence and size of erosions in the wrist and hand of rheumatoid patients: a quantitative microfocal radiographic study. *Ann Rheum Dis* 1987; 46: 463-7.
23. OSTERGAARD M, MØLLER DØHN U, DUER-JENSEN A *et al*.: Patterns of magnetic resonance imaging bone erosion in rheumatoid arthritis--which bones are most frequently involved and show the most change? *J Rheumatol* 2011; 38: 2014-7.
24. SEWERIN P, BUCHBENDER C, VORDENBÄUMEN S *et al*.: Advantages of a combined rheumatoid arthritis magnetic resonance imaging score (RAMRIS) for hand and feet: does the RAMRIS of the hand alone underestimate disease activity and progression? *BMC Musculoskelet Disord* 2014; 15: 104.
25. GUIDELINES ACORSORA: Guidelines for the management of rheumatoid arthritis: 2002 Update. *Arthritis Rheum* 2002; 46: 328-46.
26. HAAVARDSHOLM EA, ØSTERGAARD M, HAMMER HB *et al*.: Monitoring anti-TNFalpha treatment in rheumatoid arthritis: responsiveness of magnetic resonance imaging and ultrasonography of the dominant wrist joint compared with conventional measures of disease activity and structural damage. *Ann Rheum Dis* 2009; 68: 1572-9.
27. HIROTA T, SUZUKI T, HAGIWARA S, OGISHIMA H, MATSUMOTO I, SUMIDA T: Analysis of the usefulness of magnetic resonance imaging evaluation for rheumatoid arthritis treated with biological agents in the early phase: retrospective observation of abatacept and infliximab. *Clin Exp Rheumatol* 2014; 32: 991.
28. CIMMINO MA, PARODI M, ZAMPOGNA G *et al*.: Dynamic contrast-enhanced, extremity-dedicated MRI identifies synovitis changes in the follow-up of rheumatoid arthritis patients treated with rituximab. *Clin Exp Rheumatol* 2014; 32: 647-52.
29. BACKHAUS M, OHRNDORF S, KELLNER H *et al*.: Evaluation of a novel 7-joint ultrasound score in daily rheumatologic practice: a pilot project. *Arthritis Rheum* 2009; 61: 1194-201.
30. OHRNDORF S, FISCHER IU, KELLNER H *et al*.: Reliability of the novel 7-joint ultrasound score: results from an inter- and intraobserver study performed by rheumatologists. *Arthritis Care Res* (Hoboken) 2012; 64: 1238-43.
31. ALEO E, BARBIERI F, SCONFIENZA L, ZAMPOGNA G, GARLASCHI G, CIMMINO MA:

Ultrasound versus low-field magnetic resonance imaging in rheumatic diseases: a systematic literature review. *Clin Exp Rheumatol* 2014; 32 (Suppl. 80): S91-98.

32. SHARP JT, YOUNG DY, BLUHM GB *et al*.: How many joints in the hands and wrists should be included in a score of radiologic abnormalities used to assess rheumatoid arthritis? *Arthritis Rheum* 1985; 28: 1326-35.
33. EJBJERG BJ, VESTERGAARD A, JACOBSEN S, THOMSEN HS, ØSTERGAARD M: The smallest detectable difference and sensitivity to change of magnetic resonance imaging and radiographic scoring of structural joint damage in rheumatoid arthritis finger, wrist, and toe joints: a comparison of the OMERACT rheumatoid arthritis magnetic resonance imaging score applied to different joint combinations and the Sharp/van der Heijde radiographic score. *Arthritis Rheum* 2005; 52: 2300-6.
34. BIRD P, EJBJERG B, MCQUEEN F, OSTERGAARD M, LASSERE M, EDMONDS J: OMERACT Rheumatoid Arthritis Magnetic Resonance Imaging Studies. Exercise 5: an international multicenter reliability study using computerized MRI erosion volume measurements. *J Rheumatol* 2003; 30: 1380-4.
35. CONAGHAN P, LASSERE M, ØSTERGAARD M *et al*.: OMERACT Rheumatoid Arthritis Magnetic Resonance Imaging Studies. Exercise 4: an international multicenter longitudinal study using the RA-MRI Score. *J Rheumatol* 2003; 30: 1376-9.

# Glycosaminoglycan Chemical Exchange Saturation Transfer of Lumbar Intervertebral Discs in Patients With Spondyloarthritis

Christoph Schleich, MD,[1] Anja Müller-Lutz, PhD,[1]* Felix Matuschke, BSc,[1] Philipp Sewerin, MD,[2] Ruben Sengewein, MD,[2] Benjamin Schmitt, PhD,[3] Benedikt Ostendorf, MD,[2] Hans-Jörg Wittsack, PhD,[1] Karolin Stanke, BSc,[1] Gerald Antoch, MD,[1] and Falk Miese, MD[1]

**Purpose:** To assess glycosaminoglycan (GAG) content of lumbar intervertebral discs (IVD) in patients with spondyloarthritis (SpA) using glycosaminoglycan chemical exchange saturation transfer (gagCEST).
**Materials and Methods:** Ninety lumbar intervertebral discs of nine patients with SpA and nine age-matched healthy controls (eight patients with ankylosing spondylitis; one patient with spondylitis related to inflammatory bowel disease; mean age: 44.1 ± 14.0 years; range: 27–72 years) were examined with a 3T magnetic resonance imaging (MRI) scanner in this prospective study. The MRI protocol included standard morphological, sagittal $T_2$-weighted ($T_2$w) images to assess Pfirrmann score of the five lumbar IVDs (L1 to S1) and biochemical imaging with gagCEST to calculate a region of interest analysis of nucleus pulposus (NP) and annulus fibrosus (AF). Prior to statistical testing of gagCEST effects ($MTR_{asym}$ values in percent) in patients and controls, IVDs were classified according to the Pfirrmann score.
**Results:** Significantly lower gagCEST values of NP and AF were found in SpA patients compared with healthy volunteers (NP: 1.41% ± 0.41%, $P = 0.001$; 95% confidence interval, CI [0.600%–2.226%]; AF: 1.19% ± 0.32%, $P < 0.001$; CI [0.560%–1.822%]) by comparing the differences of the means. Pooled nondegenerative IVDs (Pfirrmann 1 and 2) had significantly lower gagCEST effects in patients suffering from SpA compared with healthy controls in NP ($P < 0.001$; CI [1.176%–2.337%]) and AF ($P < 0.001$; CI [0.858%–1.779%]). No significant difference of $MTR_{asym}$ values was found in degenerative IVDs between patients and controls in NP ($P = 0.204$; CI [–0.504%–2.170%]).
**Conclusion:** GagCEST analysis of morphologically nondegenerative IVDs (Pfirrmann score 1 and 2) in $T_2$w images demonstrated significantly lower GAG values in patients with spondyloarthritis in NP and AF, possibly representing a depletion of GAG in spondyloarthritis in the absence of morphologic degeneration.

**J. MAGN. RESON. IMAGING 2015;42:1057–1063.**

Magnetic resonance imaging (MRI) has become an important tool in the evaluation of patients suspicious for spondyloarthritis (SpA), which was addressed by the Assessment of SpondyloArthritis international Society (ASAS) group in the SpA classification criteria.[1–4]

SpA is associated with discovertebral changes, such as spondylitis and aseptic spondylodiscitis (discovertebral erosion) representing active inflammatory lesions of the spine[5–9] or chronic spine lesions, such as syndesmophytes and ankylosis.[10] Compared to other imaging techniques, discovertebral lesions can be detected earlier with MRI.[7,11]

Biochemical imaging assesses changes of the cartilage composition on a molecular level prior to the occurrence of morphological alterations.[12,13]

Glycosaminoglycan chemical exchange saturation transfer (gagCEST) is a novel technique that allows

View this article online at wileyonlinelibrary.com. DOI: 10.1002/jmri.24877

Received Jan 6, 2015, Accepted for publication Feb 10, 2015.

*Address reprint requests to: A.M.-L., University Dusseldorf, Medical Faculty, Department of Diagnostic and Interventional Radiology, Moorenstr. 5, 40225 Dusseldorf, Germany. E-mail: anja.lutz@med.uni-duesseldorf.de

From the [1]University Dusseldorf, Medical Faculty, Department of Diagnostic and Interventional Radiology, Dusseldorf, Germany; [2]Univiversity Dusseldorf, Medical Faculty, Department of Rheumatology, Dusseldorf, Germany; and [3]Siemens Ltd. Australia, Healthcare Sector, Macquarie Park, NSW, Australia

 

visualization and quantification of biochemical components in intervertebral discs (IVD). GagCEST acquires molecule-specific saturation information on bulk water protons for the indirect detection of glycosaminoglycans (GAG) in IVDs.[14] The CEST dataset consists of multiple images acquired with presaturation impulses at different offset frequencies around the water resonance, and one reference image without saturation. The normalized signal as a function of the presaturation offset (z-spectrum) can then be used to determine and quantify CEST effects, which are asymmetric ($MTR_{asym}$) with respect to the water resonance due to the —OH protons of GAG appearing in a frequency range of 0.9 to 1.9 ppm from the water resonance. The magnitude of the measured $MTR_{asym}$ correlates directly with the underlying concentration of GAG.[15]

Initial feasibility studies report on successful differentiation of degenerative and nondegenerative IVDs with gagCEST[13,16] or cartilage quality after autologous chondrocyte transplantation.[14]

Our hypothesis was that the GAG content of IVDs in patients with SpA was decreased compared to healthy controls.

## Materials and methods

### Study Population

The study was approved by the local ethics committee and written informed consent is obtained from all participating individuals. Eighteen subjects were enrolled in this prospective study: nine patients suffering from SpA (mean age: 44.1 ± 14.0 years; range: 27–72 years) and nine age-matched healthy controls (mean age 43.5 ± 13.6 years, range 26–69 years). Patients with SpA comprised eight patients with ankylosing spondylitis (disease duration: ≥5 years; therapy: seven patients were treated with tumor necrosis factor alpha ([NFα] inhibitors, one patient with methotrexate) and one patient with spondylitis related to inflammatory bowel disease (disease duration: 1.5 years; therapy: patient was treated with methotrexate).

### MR Hardware and Sequence Protocol

MRI of the lumbar intervertebral disc was performed on a whole-body 3T MRI system (Magnetom Trio A Tim System, Siemens Healthcare, Erlangen, Germany) with a dedicated built-in spine matrix coil. All individuals were investigated in supine position. After a localizer and $T_2$-weighted ($T_2$W) sagittal imaging, CEST imaging was performed using a prototype sequence based on a 2D RF-spoiled GRE (radiofrequency-spoiled gradient-echo) readout. Therefore, two sequences were applied: a gagCEST sequence for evaluation of the CEST effect and a water saturation shift referencing (WASSR) sequence for field inhomogeneity correction.

The sagittal $T_2$W sequence consisted of 15 slices. The acquisition parameters were: TE/TR = 105/3100 msec, spatial resolution = 1.2 × 1.2 $mm^2$, slice thickness = 3 mm, flip angle = 160°, field of view = 300 × 300 $mm^2$, number of signal averages = 2, and acquisition duration of 3 minutes and 39 seconds.

**TABLE 1. Detailed Sequence Parameters of the CEST and WASSR Sequences**

| Parameters | CEST | WASSR |
|---|---|---|
| TE/TR [msec]/[msec] | 3.01/1590 | 3.01/1590 |
| Resolution [$mm^3$] | 1.6 × 1.6 × 5 | 1.6 × 1.6 × 5 |
| Flip angle [°] | 12 | 12 |
| FOV [$mm^2$] | 300 × 300 | 300 × 300 |
| Duration [min:sec] | 12:24 | 7:26 |
| Averages | 6 | 6 |
| Basic resolution | 192 × 192 | 192 × 192 |

GagCEST imaging was applied using a presaturation module consisting of six Gaussian-shaped RF pulses with a $B_1$ amplitude of 1.5 $\mu$T averaged over time using a pulse duration of 100 msec and an interpulse delay of 100 msec. The Z-spectrum was acquired from −4 ppm to 4 ppm in an interval of 0.33. The acquisition parameters of the gagCEST sequence were: TE/TR = 3.01/1590 msec, spatial resolution = 1.6 × 1.6 $mm^2$, slice thickness = 5 mm, flip angle $\alpha = 12°$, field of view = 300 × 300 $mm^2$, number of signal averages = 6, and acquisition duration of 12 minutes and 24 seconds.

WASSR imaging was performed using a presaturation module consisting of a single Gaussian-shaped RF pulse with a $B_1$ amplitude of 0.3 $\mu$T and a pulse duration of 100 msec and an interpulse delay of 100 msec. The Z-spectrum of the WASSR acquisition ranged from −1 ppm to 1 ppm in an interval of 0.05. The acquisition parameters of the WASSR sequence were: TE/TR = 3.01/590 msec, spatial resolution = 1.6 × 1.6 $mm^2$, slice thickness = 5 mm, flip angle $\alpha = 12°$, field of view = 300 × 300 $mm^2$, number of signal averages = 6 and acquisition duration of 7 minutes and 26 seconds. Table 1 provides an overview of the sequence parameters of CEST and WASSR sequences.

Suppression of bowel movement artifacts was achieved by the application of a saturation slab anterior to the spine.

### Data Analysis

All lumbar IVDs (L1 to S1; a total of 90 IVDs) were scored according to the morphological Pfirrmann classification based on sagittal $T_2$W images by a radiologist with 4 years of experience in musculoskeletal radiology.[17]

Before CEST data evaluation, both CEST and WASSR datasets were motion-corrected using a diffeomorphic registration approach incorporated in the prototype software (fMRILung Siemens).[18] Afterwards, the WASSR dataset was used to assess and correct magnetic field inhomogeneities of the CEST dataset using the WASSR maximum symmetry algorithm introduced by Kim et al.[19] Subsequently, the magnetization transfer asymmetry ratio $MTR_{asym}$ was calculated in the offset range from 1–1.5 ppm and presented in percent of the nonsaturated water signal.

The following IVD segmentation was performed using an in-house developed MatLab software (MathWorks, Natick, MA, R2012b). All lumbar IVDs were detected automatically. The disc segmentation was based on Bayes-classification to divide bone and ligament from disc tissue of the lumbar spine (Fig. 1). The segmentation area merely comprised the lumbar spine. According to the different tissue signal intensity of nonsaturated and saturated images, the segmentation tool could distinguish IVDs from the other tissues of the lumbar spine by learning on several training objects before data analysis. The defined regions of interest (ROIs) were divided into nucleus pulposus (NP) (the innermost 60% of the IVD) and annulus fibrosus (AF) (the remaining region of the IVD), as reported in the preceding studies.[20,21]

Afterwards, the results were analyzed by pairs between the patients and healthy controls for each Pfirrmann grade and disc localization (L1 to S1; Figs. 2, 3).

### *Statistical Analysis*

SPSS (v. 22; Chicago, IL) was used for statistical analysis. The mean, confidence intervals (CIs) for these mean values, median and standard deviations for NP and AF were calculated as descriptive statistics. Kolmogorov–Smirnov tests verified normal distribution of $MTR_{asym}$ values of the IVDs graded Pfirrmann score 1–3 in NP and AF. Univariate analysis of variance (ANOVA) and post-hoc Tukey test demonstrated the performance of a cluster analysis of gagCEST values between SpA patients and healthy controls according to Pfirrmann scoring (NP: $P = 0.154$, AF: $P = 0.820$; $P > 0.05$ would show a significant interaction between SpA/controls and Pfirrmann). Because of the marginal distinction of gagCEST values between Pfirrmann 1 and 2, ANOVA analyses and post-hoc Tukey test were performed to summarize gagCEST effects of Pfirrmann 1 and 2 to one group (NP: $P = 0.139$, AF: $P = 0.533$; $P > 0.05$ would show a significant interaction between SpA/controls and Pfirrmann). A paired *t*-test was used to assess statistical differences of the means of the $MTR_{asym}$ values of NP and AF between spondyloarthritis patients and healthy controls according to the Pfirrmann grade 1–3. The Wilcoxon signed-rank test was used to compare $MTR_{asym}$ values of NP and AF with a Pfirrmann score 4 and 5, which showed no normal distribution according to Kolmogorov–Smirnov tests. $P < 0.05$ was considered significant.

## Results

All measurements were technically successful. There were no dropouts. A total of 90 IVDs (45 IVDs of patients with spondyloarthritis and 45 IVDs of healthy controls) were analyzed. According to the Pfirrmann classification system[17] the 90 lumbar discs were graded into:

- 16 IVDs with Pfirrmann score 1
- 38 IVDs with Pfirrmann score 2
- 32 IVDs with Pfirrmann score 3
- 02 IVDs with Pfirrmann score 4
- 02 IVDs with Pfirrmann score 5

The descriptive statistics are summarized in Tables 2 and 3.

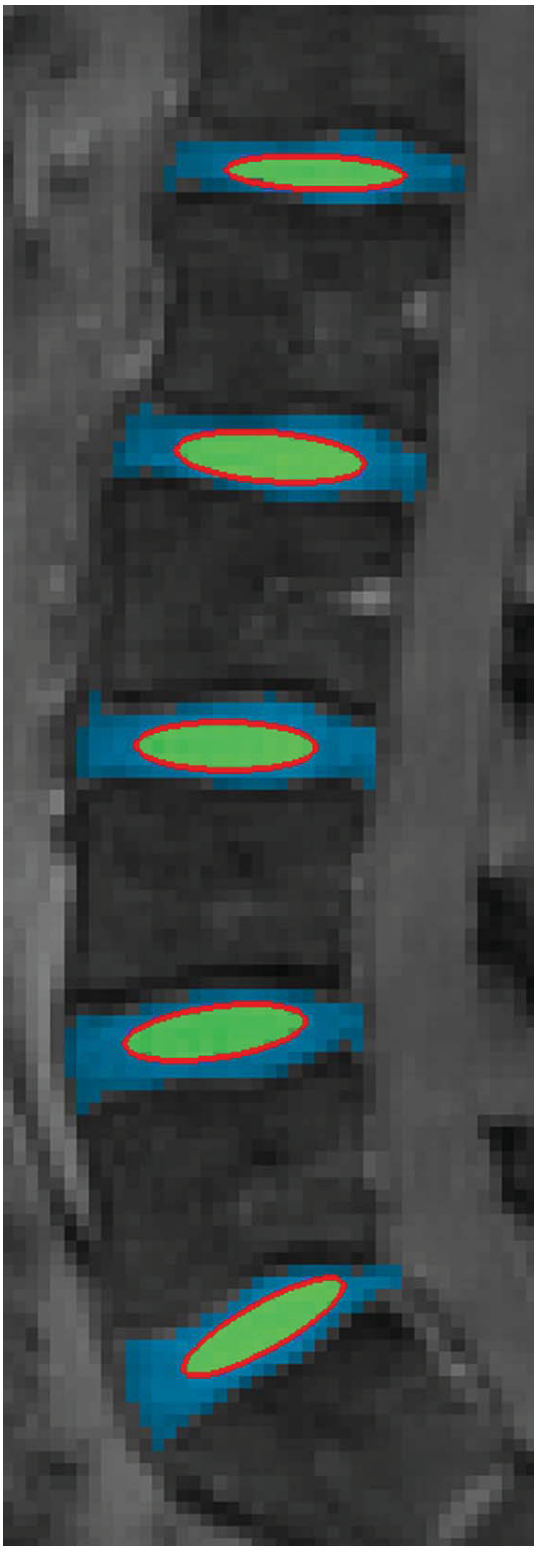

**FIGURE 1: Automatic segmentation of lumbar intervertebral discs to distinguish lumbar discs from other tissues of the lumbar spine. The segmentation was performed using an in-house-developed MatLab software being based on Bayes-classification.**

Significantly lower gagCEST values of NP and AF were found in SpA patients compared with healthy volunteers (NP: 1.41% ± 0.41%, $P = 0.001$; 95% CI [0.600%–

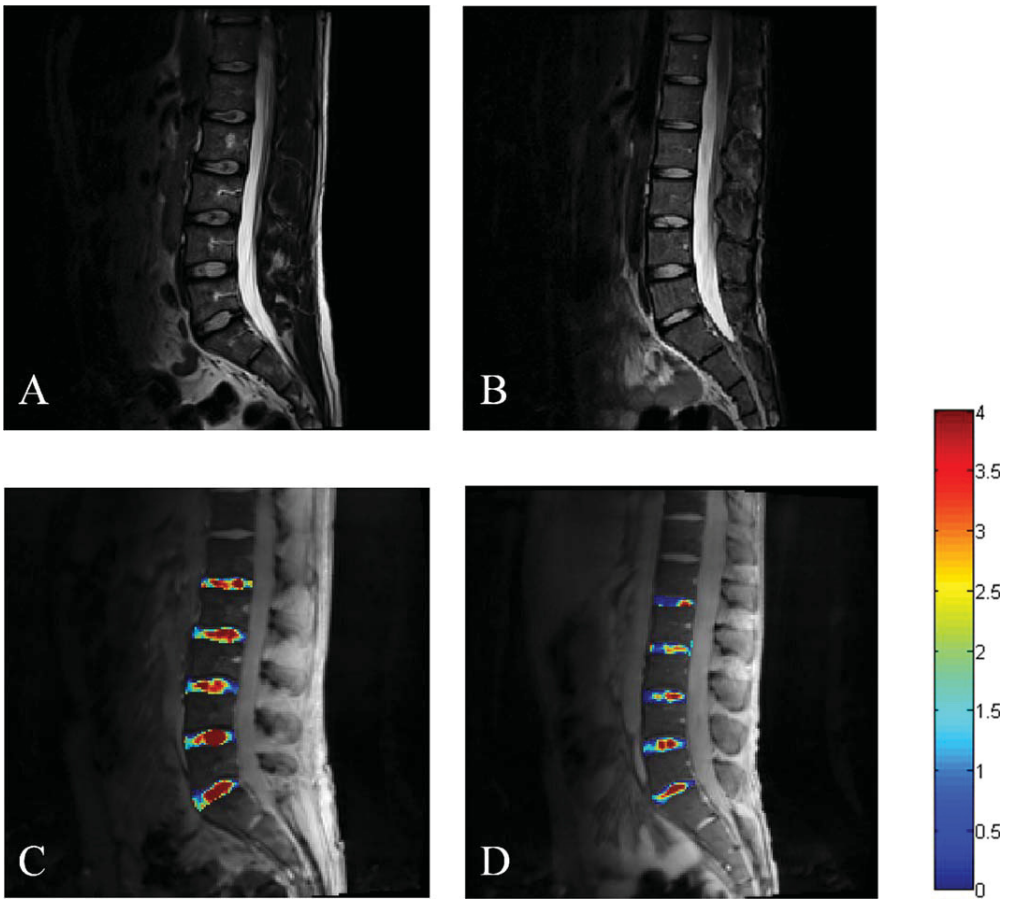


**FIGURE 2: Comparison of lumbar IVDs of a healthy volunteer (A,C) with a patient suffering from spondyloarthritis (B,D). A,B: Morphological $T_2$W images for Pfirrmann classification. Both pictures show nondegenerative IVDs with a Pfirrmann score 1 or 2. C,D: Sagittal $T_2$W images with an overlaid $MTR_{asym}$ color map illustrating the gagCEST effect in a healthy volunteer (C) and SpA patient. Color coding indicates high glycosaminoglycan (GAG) content (red) to low GAG content (blue). The pictures indicate a depletion of GAG in spondyloarthritis in the absence of morphologic degeneration.**

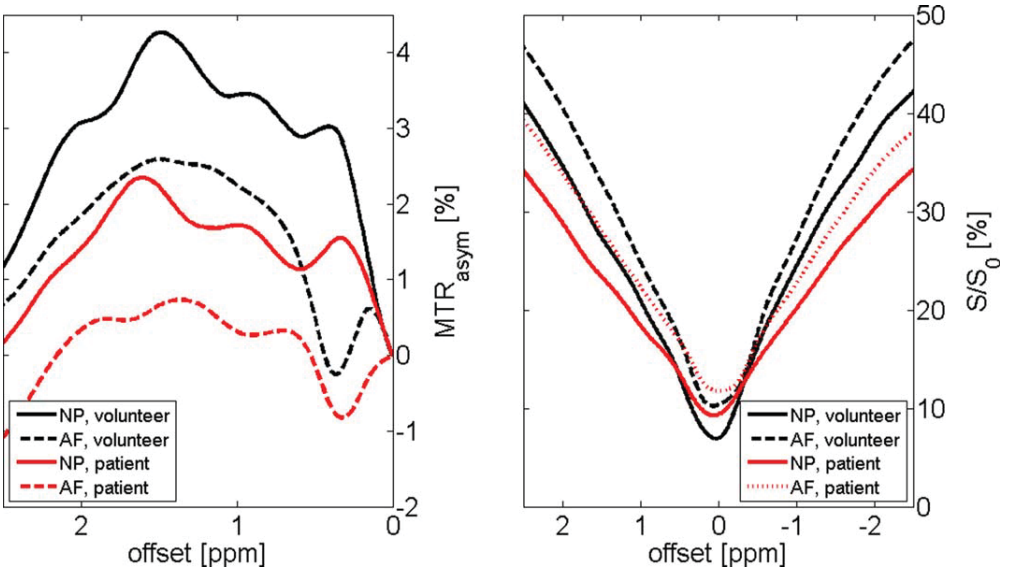


**FIGURE 3: $MTR_{asym}$ values according to different frequencies around the water resonance (left side) with the typical CEST peaks at the specific frequency range of glycosaminoglycans from 0.9 to 1.9 ppm of a patient (red) and a healthy volunteer (black). On the right side, CEST curves, Z-spectrums of the same patient and volunteer with the typical asymmetry at the specific frequency range of GAGs. $MTR_{asym}$ values, and CEST curves derived from the same patient and healthy control of Fig. 2.**

**TABLE 2. $MTR_{asym}$ Mean Values, Standard Deviation, 95% Confidence Interval, and Median of NP According to Pfirrmann Score and the Corresponding Disc Localization Between SpA Patients and Healthy Controls**

| Pfirrmann score | | Mean value | Standard deviation | 95% confidence interval | Median |
|---|---|---|---|---|---|
| 1 | SpA | 2.55 | 1.38 | 1.400−3.709 | 2.80 |
| | Con | 3.60 | 1.38 | 2.354−4.388 | 4.14 |
| 2 | SpA | 1.39 | 1.07 | 0.874−1.910 | 0.95 |
| | Con | 3.45 | 0.98 | 2.977−3.917 | 3.36 |
| 3 | SpA | −0.44 | 1.71 | −1.356−0.467 | −0.34 |
| | Con | 0.39 | 1.65 | −0.491−1.267 | 0.54 |
| 4 | SpA | −1.63 | — | — | −1.63 |
| | Con | −3.60 | — | — | −3.60 |
| 5 | SpA | −6.85 | — | — | −1.63 |
| | Con | −6.33 | — | — | −3.60 |

Pfirrmann 1: n = 16, Pfirrmann 2: n = 38, Pfirrmann 3: n = 32, Pfirrmann 4: n = 2, Pfirrmann 5: n = 2. Because of fewer IVDs graded Pfirrmann score 4 and 5 no standard deviation and CI were performed.

2.226%]; AF: 1.19% ± 0.32%, $P < 0.001$, CI [0.560%–1.822%]) by comparing the differences of the means (Fig. 4).

$MTR_{asym}$ values of NP were significantly lower in patients with spondyloarthritis compared to healthy controls at Pfirrmann score 1 (1.05% ± 1.20%; $P = 0.042$; CI [0.047%–2.049%]) and 2 (2.05% ± 1.50%; $P < 0.001$; CI [1.334%–2.775%]).

$MTR_{asym}$ values of AF were significantly lower in patients compared to controls at Pfirrmann score 1 (1.33% ±1.26%; $P = 0.020$; CI [0.280%–2.379%]), 2 (1.31% ± 1.16%; $P < 0.001$; CI [0.754%–1.872%]) and 3 (0.98% ± 1.80%; $P = 0.046$; CI [0.018%–1.936%]).

Summarizing gagCEST values of Pfirrmann 1 and 2 to one group, $MTR_{asym}$ values of NP (1.76% ± 1.47%; $P < 0.001$; CI [1.176%–2.337%]) and AF (1.32% ± 1.16%;

**TABLE 3. $MTR_{asym}$ Mean Values, Standard Deviation, 95% Confidence Interval, and Median of AF According to Pfirrmann Score and the Corresponding Disc Localization Between SpA Patients and Healthy Controls**

| Pfirrmann score | | Mean value | Standard deviation | 95% confidence interval | Median |
|---|---|---|---|---|---|
| 1 | SpA | 0.65 | 1.36 | −0.486 −1.790 | 2.80 |
| | Con | 1.98 | 0.56 | 1.511 −2.453 | 4.14 |
| 2 | SpA | −0.01 | 0.89 | −0.440 −0.415 | 0.95 |
| | Con | 1.30 | 0.97 | 0.832 −1.769 | 3.36 |
| 3 | SpA | −1.36 | 1.55 | −2.184 −0.527 | −0.34 |
| | Con | −0.38 | 1.52 | −1.190 −0.433 | 0.54 |
| 4 | SpA | −2.21 | — | — | −2.21 |
| | Con | −2.93 | — | — | −2.93 |
| 5 | SpA | −6.59 | — | — | −6.59 |
| | Con | −2.50 | — | — | −2.50 |

Pfirrmann 1: n = 16, Pfirrmann 2: n = 38, Pfirrmann 3: n = 32, Pfirrmann 4: n = 2, Pfirrmann 5: n = 2. Because of fewer IVDs graded Pfirrmann score 4 and 5 no standard deviation and CI were performed.

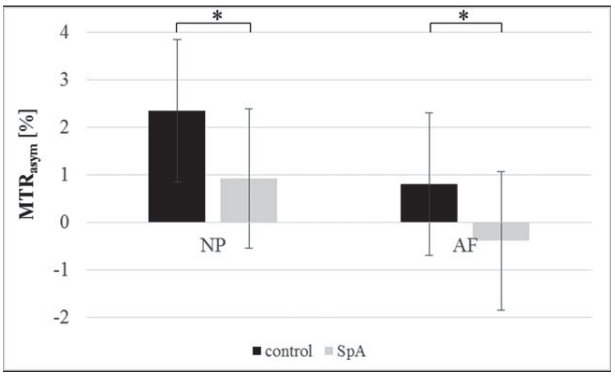


FIGURE 4: $MTR_{asym}$ values of SpA patients and healthy controls for NP and AF. In both, NP and AF, significantly lower gagCEST values were observed in patients with SpA.

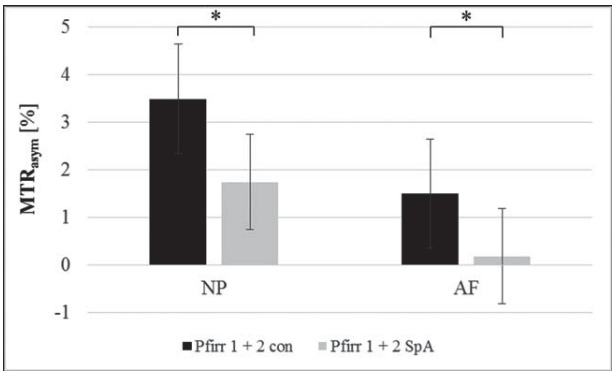


FIGURE 5: Pooled $MTR_{asym}$ values of nondegenerative IVDs (Pfirrmann 1 and 2) for NP and AF in patients with spondyloarthritis and healthy controls. In both NP and AF, significantly lower $MTR_{asym}$ values were observed in patients with SpA.

$P < 0.001$; CI [0.858%–1.779%]) were significantly lower in SpA compared to healthy controls (Fig. 5).

$MTR_{asym}$ values of NP of IVDs with a Pfirrmann score 3 showed no significant difference of the means between spondyloarthritis patients and healthy controls ($0.83\% \pm 2.51\%$; $P = 0.204$; CI [–0.504%–2.170%]). Only one IVD of patients with spondyloarthritis and healthy controls was graded Pfirrmann score 4 and 5, respectively. The $MTR_{asym}$ values of NP and AF of this IVD demonstrated negative data, which means there was no GAG content and no significant difference between patients and controls detectable.

## Discussion

Biochemical imaging with glycosaminoglycan chemical exchange saturation transfer MRI is a relatively new technique that has the ability to quantify the GAG level of IVDs.[22] In contrast to dGEMRIC, no contrast medium application, which bears the risk of side and equilibrium effects due to the dependency of the contrast medium distribution within cartilage on cofactors,[14,23] is required.

Our data indicate a significant loss of GAG in morphologically normal-appearing IVDs (Pfirrmann score 1 and 2) of patients with spondyloarthritis compared to healthy controls in NP and AF. This effect may be a result of the inflammatory and structural lesions of the spine in axial spondyloarthritis.

GAG is, next to collagen and aggrecan, a major part of the extracellular matrix.[24] The GAG content obviously varies among the different parts of the human IVD (NP, AF). In NP higher GAG concentrations were found compared to AF.[22] Earlier studies have shown that GAG is associated with the maintenance of tissue fluid content and plays a central role in degenerative disc disease.[24]

Haneder et al[16] reported on a correlation between degenerative disc alterations according to Pfirrmann score and low gagCEST effects. In the presence of degenerative disc disease (Pfirrmann 3–5 in NP and Pfirrmann 4, 5 in AF), we found no significant GAG difference between patients with spondyloarthritis and healthy controls.

Combining the gagCEST effects of discs with Pfirrmann score 1 and 2, we noted a highly significant reduction of GAG in patients with SpA compared to healthy controls.

Summarizing our data, patients suffering from SpA showed a significant loss of GAG in morphologically normal-appearing IVDs.

Our study has several limitations. The main limitation of this study is the limited number of patients with spondyloarthritis. The current results seem to be promising for evaluating the initial results in a larger population. The absence of cartilage biopsy is a further limitation. Biopsies were not performed due to ethical considerations.

Spondyloarthritis is a heterogeneous disease comprising different subtypes, such as ankylosing spondylitis, psoriatic arthritis, arthritis related to inflammatory bowel disease, reactive arthritis, or juvenile idiopathic arthritis. Our study cohort reflects this heterogeneity. In this study no data of spondylitis and spondylodiscitis activity and GAG alterations were recorded. Additionally, our study is limited to only lumbar IVDs and no gender differentiation was performed.

Furthermore, no consensus analysis by a second reader for gagCEST and Pfirrmann analysis was performed. For Pfirrmann grading, we think that this is a minor limitation because of the good intra- and interobserver agreement, given in the literature.[17] The gagCEST values for lumbar IVDs were detected automatically with the algorithm mentioned above, so this point is also considered a minor limitation.

GagCEST may be a powerful research tool to access IVD composition in spondyloarthritis and to investigate therapy effects on GAG content in advanced studies.

In conclusion, significantly lower gagCEST effects were found in SpA patients compared with healthy controls. GagCEST of nondegenerative IVDs (Pfirrmann score 1 and

2 in $T_2$w images) demonstrated significantly lower GAG values in patients with spondyloarthritis, possibly representing a depletion of GAG in spondyloarthritis in the absence of morphologic degeneration.

## Conflict of interest

No conflict of interest to report.

## References


1. Pedersen SJ, Weber U, Ostergaard M. The diagnostic utility of MRI in spondyloarthritis. Best Pract Res Clin Rheumatol 2012;26:751–766.
2. Althoff CE, Sieper J, Song IH, et al. Active inflammation and structural change in early active axial spondyloarthritis as detected by whole-body MRI. Ann Rheum Dis 2013;72:967–973.
3. Weber U, Lambert RG, Østergaard M, Hodler J, Pedersen SJ, Maksymowych WP. The diagnostic utility of magnetic resonance imaging in spondylarthritis: an international multicenter evaluation of one hundred eighty-seven subjects. Arthritis Rheum 2010;62:3048–3058.
4. Rudwaleit M, van der Heijde D, Landewé R, et al. The assessment of SpondyloArthritis International Society classification criteria for peripheral spondyloarthritis and for spondyloarthritis in general. Ann Rheum Dis 2011;70:25–31.
5. Hermann KG, Baraliakos X, van der Heijde DM, et al. Descriptions of spinal MRI lesions and definition of a positive MRI of the spine in axial spondyloarthritis: a consensual approach by the ASAS/OMERACT MRI study group. Ann Rheum Dis 2012;71:1278–1288.
6. Canella C, Schau B, Ribeiro E, Sbaffi B, Marchiori E. MRI in seronegative spondyloarthritis: imaging features and differential diagnosis in the spine and sacroiliac joints. AJR Am J Roentgenol 2013;200:149–157.
7. Bron JL, de Vries MK, Snieders MN, van der Horst-Bruinsma IE, van Royen BJ. Discovertebral (Andersson) lesions of the spine in ankylosing spondylitis revisited. Clin Rheumatol 2009;28:883–892.
8. Peluso R, DI Minno MN, Bruner V, et al. Discovertebral erosions in patients with enteropathic spondyloarthritis. J Rheumatol 2012;39: 2332–2340.
9. Langlois S, Cedoz JP, Lohse A, Toussirot E, Wendling D. Aseptic discitis in patients with ankylosing spondylitis: a retrospective study of 14 cases. Joint Bone Spine 2005;72:248–253.
10. Weber U, Hodler J, Kubik RA, et al. Sensitivity and specificity of spinal inflammatory lesions assessed by whole-body magnetic resonance imaging in patients with ankylosing spondylitis or recent-onset inflammatory back pain. Arthritis Rheum 2009;61:900–908.
11. de Vries MK, van Drumpt AS, van Royen BJ, van Denderen JC, Manoliu RA, van der Horst-Bruinsma IE. Discovertebral (Andersson) lesions in severe ankylosing spondylitis: a study using MRI and conventional radiography. Clin Rheumatol 2010;29:1433–1438.
12. Matzat SJ, van Tiel J, Gold GE, Oei EH. Quantitative MRI techniques of cartilage composition. Quant Imaging Med Surg 2013;3:162–174.
13. Rehnitz C, Kupfer J, Streich NA, et al. Comparison of biochemical cartilage imaging techniques at 3 T MRI. Osteoarthritis Cartilage 2014; 22:1732–1742.
14. Schmitt B, Zbýn S, Stelzeneder D, et al. Cartilage quality assessment by using glycosaminoglycan chemical exchange saturation transfer and (23)Na MR imaging at 7 T. Radiology 2011;260:257–264.
15. Ling W, Regatte RR, Navon G, Jerschow A. Assessment of glycosaminoglycan concentration in vivo by chemical exchange-dependent saturation transfer (gagCEST). Proc Natl Acad Sci U S A 2008;105:2266–2270.
16. Haneder S, Apprich SR, Schmitt B, et al. Assessment of glycosaminoglycan content in intervertebral discs using chemical exchange saturation transfer at 3.0 Tesla: preliminary results in patients with low-back pain. Eur Radiol 2013;23:861–868.
17. Pfirrmann CW, Metzdorf A, Zanetti M, Hodler J, Boos N. Magnetic resonance classification of lumbar intervertebral disc degeneration. Spine (Phila Pa 1976) 2001;26:1873–1878.
18. Muller-Lutz A, Schleich C, Schmitt B, et al. Improvement of gagCEST imaging in the human lumbar intervertebral disc by motion correction. Skeletal Radiol 2015;44:505–511.
19. Kim M, Gillen J, Landman BA, Zhou J, van Zijl PC. Water saturation shift referencing (WASSR) for chemical exchange saturation transfer (CEST) experiments. Magn Reson Med 2009;61:1441–1450.
20. Stelzeneder D, Welsch GH, Kovács BK, et al. Quantitative T2 evaluation at 3.0T compared to morphological grading of the lumbar intervertebral disc: a standardized evaluation approach in patients with low back pain. Eur J Radiol 2012;81:324–330.
21. Trattnig S, Stelzeneder D, Goed S, et al. Lumbar intervertebral disc abnormalities: comparison of quantitative T2 mapping with conventional MR at 3.0 T. Eur Radiol 2010;20:2715–2722.
22. Saar G, Zhang B, Ling W, Regatte RR, Navon G, Jerschow A. Assessment of glycosaminoglycan concentration changes in the intervertebral disc via chemical exchange saturation transfer. NMR Biomed 2012;25:255–261.
23. Varma G, Lenkinski RE, Vinogradov E. Keyhole chemical exchange saturation transfer. Magn Reson Med 2012;68:1228–1233.
24. Urban JP, Winlove CP. Pathophysiology of the intervertebral disc and the challenges for MRI. J Magn Reson Imaging 2007;25:419–432.

Thieme

# Magnetresonanztomografie peripherer Gelenke – up-date 2016

## Magnetic Resonance Imaging of Peripheral Joints: Update 2016

**Autoren**
**P. Sewerin[1], C. Schleich[2], B. Ostendorf[1]**

**Institute**
1 Poliklinik, Funktionsbereich & Hiller-Forschungszentrum für Rheumatologie, Heinrich-Heine-Universität Düsseldorf, Düsseldorf
2 Institut für diagnostische und interventionelle Radiologie, Heinrich-Heine-Universität Düsseldorf, Düsseldorf

**Schlüsselwörter**
Bildgebung, MRT, Rheumatoide Arthritis, Psoriasis Arthritis

**Key words**
imaging, MRI, rheumatoid arthritis, psoriasis arthritis

**Bibliografie**
**DOI** https://doi.org/10.1055/s-0042-106080
Online-Publikation: 11.8.2016
Akt Rheumatol 2017; 42: 399–403

ISSN 0341-051X

**Korrespondenzadresse**
Dr. med. Philipp Sewerin
Poliklinik, Funktionsbereich & Hiller-Forschungszentrum für Rheumatologie
Heinrich-Heine-Universität Düsseldorf
Moorenstr. 5
40225 Düsseldorf
philipp.sewerin@med.uni-duesseldorf.de

**ZUSAMMENFASSUNG**

Moderne und innovative bildgebende Verfahren spielen heute in der Rheumatologie eine zunehmend wichtige Rolle und werden dabei regelhaft bei Diagnosestellung und Therapiekontrolle eingesetzt. Neben der Sonografie, welche heute die rechte Hand des Rheumatologen darstellt, ist die Magnetresonanz-Tomografie (MRT), auch und gerade peripherer Gelenke, zunehmend in den wissenschaftlichen Fokus gerückt. Sie ist in der Lage hochsensitiv entzündliche artikuläre, periartikuläre und ossäre Veränderungen (wie die Synovialitis oder das Knochenmarködem) zu erkennen und dann darüber hinaus deutlich früher als bspw. das konventionelle Röntgen erosive Gelenkveränderungen ab zu bilden. Neben diesen Vorteilen ist es heute durch standardisierte Scoring-Systeme möglich MRT-Untersuchungen besser zu vergleichen, wobei hierfür erste vereinfachte Scores entwickelt und evaluiert wurden. Durch neue und innovative Sequenzen können frühzeitig Veränderungen des Knorpels erkannt werden. Dynamische MRT-Sequenzen versprechen eine noch genauere Darstellung lokaler Inflammation und sind neben hybriden bildgebenden Verfahren (z. B. PET-MRT oder SPECT-MRT) aktuell Gegenstand intensiver wissenschaftlicher Forschung.

**ABSTRACT**

Modern and innovative imaging techniques play an important role in the field of rheumatic diseases today and are used for diagnosis and treatment control on a regular basis. In addition to sonography, which is the “right-hand man” of a rheumatologist today, magnetic resonance imaging (MRI), especially of the peripheral joints, has moved into the focus of scientific research. Modern MRI techniques demonstrate inflammatory articular, periarticular and bony lesions (such as synovitis and bone marrow oedema) with a high level of sensitivity. Moreover they can depict erosive joint damage much earlier than conventional x-rays. In addition to these advantages, standardised scoring systems help to make MRI scans more comparable today, with some initial simplified scores having been developed and evaluated for this purpose. Due to new and innovative MRI sequences, cartilage damage can be detected at an early point in time. Dynamic MRI sequences promise an ever more precise depiction of local inflammation and, along with hybrid imaging techniques (such as PET-MRI or SPECT-MRI), they are currently the focus of intensive scientific research.

## Einleitung

Bildgebende Verfahren spielen heute eine wichtige und unverzichtbare Rolle in den diagnostischen Algorithmen und der Therapiekontrolle zahlreicher entzündlich-rheumatischer Erkrankungen. Durch die immer besseren Behandlungsmöglichkeiten und die damit verbundenen Ziele ist eine enge Therapiekontrolle neben der frühen Diagnosestellung von großer Bedeutung. So wird in den Empfehlungen der European league against rheumatism (EULAR) bei der Diagnosestellung und Therapiekontrolle die Hinzunahme bildgebender Verfahren empfohlen, da diese besser als klinische Untersuchung allein – auch subklinische – Inflammation detektieren kann [1]. Neben der Sonografie, welche heutzutage immer

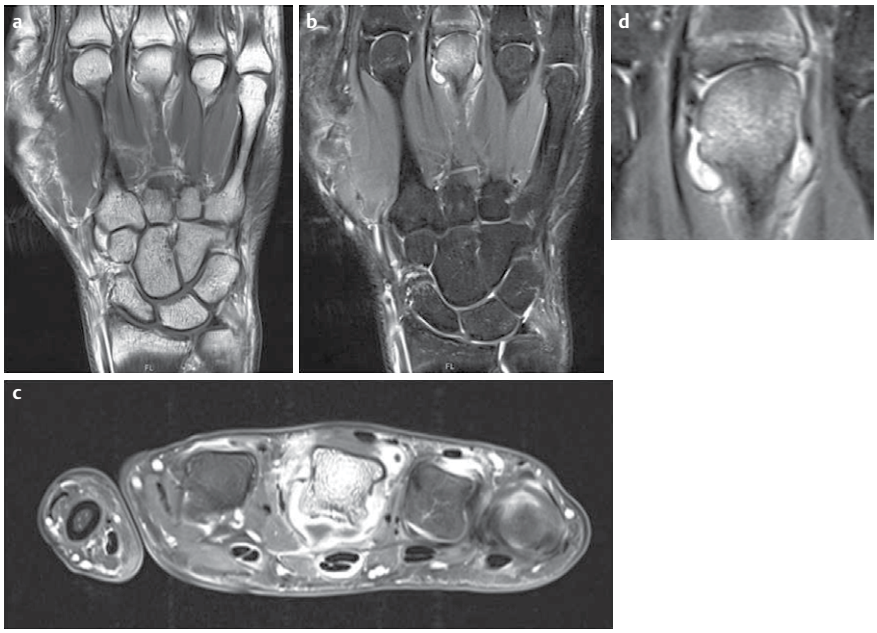


▶ **Abb. 1** 3-Tesla-Hochfeld MRT der rechten Hand eines 19-jährigen Patienten mit früher seropositiver RA (Krankheitsdauer 6 Woche). **a** T1-Sequenz mit Kontrastmittel (KM), coronare Schnittführung. **b** STIR-Sequenz, coronare Schnittführung. **c** T1-Squenz mit KM, axiale Schnittführung. **d** vergrößerte Darstellung der Synovialitis mit Nachweis eines begleitenden Knochenmarködem (MCP-3)

mehr als „bedside imaging" Verfahren die „rechte Hand" des Rheumatologen darstellt, ist auch die Magnetresonanz-Tomografie (MRT) in den letzten Jahren zunehmend in den wissenschaftlichen und auch praxisnahen Fokus gerückt, wobei die Anzahl der durchgeführten validierten Studienprotokolle stieg und deren Stellenwert zunehmend wichtiger wurde [2]. Neben dem Einsatz bei axialen Spondylarthritiden [3] wird die MRT auch in der Abklärung peripherer Arthritiden immer häufiger eingesetzt [1, 4], weil mit dieser Technik deutlich früher entzündliche Veränderungen an den Gelenken erfasst werden können, welche dem konventionellen Röntgenbild häufig entgehen. Diese zusätzlichen strukturellen Informationen über z. B. ein vorliegendes Knochenmarködem, dem Nachweis einer subklinischen Arthritis oder der klinisch oft unterschätzten Enthesitis oder Daktylitis fließen mit in die Therapieentscheidungen ein. Durch den Einsatz von standardisierten Scoring-Systemen – sei es für das Achsenskelett (Berlin-Score usw.) oder für periphere Gelenke (RAMRIS, PsAMRIS) – werden Untersuchungen immer besser vergleichbar, dies auch außerhalb von Studienprotokollen.

In der Folge sollen up-date Informationen und neue Techniken der MRT peripherer Gelenke vorgestellt werden.

## Die MRT peripherer Gelenke

Die MRT peripherer Gelenke ist heutzutage in der Lage detailliert und mit hoher Auflösung artikuläre, periartikuläre und intraossäre Strukturen abzubilden. Durch die verschiedenen Wichtungen ist es möglich o. g. Strukturen in bestmöglicher Qualität darzustellen. So kann die MRT sensitiv entzündliche Veränderungen rheumatischer Erkrankungen wie z. B. Synovialitis, Enthesitis oder das Knochemarködem darstellen. Hierfür werden regelhaft fettunterdrückte T2-Sequenzen (z. B. short tau inversion recovery [STIR]) und kontrastmittelgestützte T1 Sequenzen verwendet (▶ **Abb. 1**). Neben den akut-entzündlichen Veränderungen können durch die im Vergleich zum konventionellen Röntgen 3-dimensionale Darstellung und die hohe Ortsauflösungen sehr früh erosive Veränderungen erkannt werden. Dies gelingt bereits 2–4 Monate nach Symptombeginn einer Arthritis zu einem Zeitpunkt, wo das Röntgenbild noch völlig unauffällig erscheint [5]. Darüber hinaus ist die MRT das einzige bildgebende Verfahren, welches in der Lage ist, das Knochenmarködem mittels spezifischer Wichtungen (z. B. STIR Sequenzen) zu erfassen. Viele Studien konnten belegen, dass das Knochenmarködem einen hohen prädiktiven Wert für die spätere Entstehung von Erosionen ausweist [6, 7]. Zur besseren Darstellung und Abgrenzung entzündlicher und erosiver Läsionen sollte ein Gadolinium-haltiges Kontrastmittel (KM) eingesetzt werden. Es ist zu erwähnen, dass grundsätzlich zyklische Verbindungen eingesetzt werden sollen, da insbesondere bei linearen Gadolinium-haltigen MRT-KM dosisabhängige zerebrale Ablagerungen beobachtet wurden, wobei deren Bedeutung noch gänzlich ungeklärt ist [8]. Darüber hinaus berichten einzelne Arbeiten diese Ablagerungen auch für die inzwischen regelhaft eingesetzt, zyklischen und damit deutlich stabileren MRT-KM [9]. Es bleibt abzuwarten, ob diese neuen Erkenntnisse eine neue Einordnung der MRT-KM bedingen werden.

Die MRT wird inzwischen auch immer öfter bei der Diagnostik der Psoriasis-Arthritis (PsoA) eingesetzt. Ähnlich wie bei der RA kann die MRT im Vergleich zum konventionellen Röntgenbild deutlich früher entzündliche Veränderungen wie die Enthesitis oder die Daktylitis und entzündlich knöcherne Abbau- oder Umbauprozesse darstellen. So kann die MRT gerade bei (noch) undifferenzierten

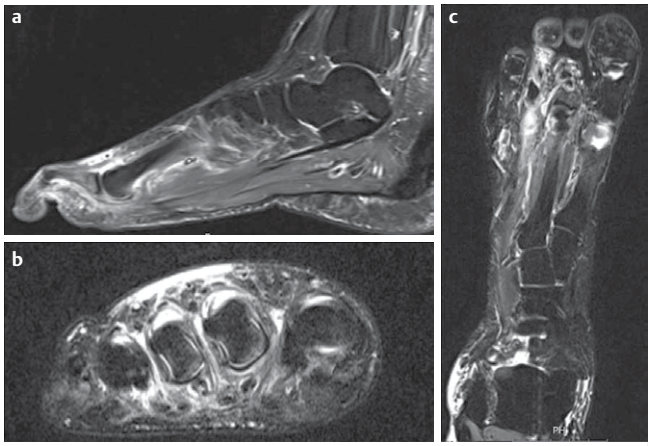


▶ **Abb. 2** 3-Tesla-Hochfeld MRT des rechten Fußes einer 39-jährigen Patientin mit Psoriasis-Arthritis und klinischem Nachweis einer Daktylitis des II und III Strahles. **a** STIR-Sequenz, sagittale Schnittführung mit dem Nachweis einer Arthritis mit periartikulärer Beteiligung und einer Daktylitis des II Strahls. **b** T2-gewichtet, fettgesättigt Sequenz, transversale Schnittführung mit einer Arthritis des II, III und IV MTP-Gelenkes, periartikuläre Mitbeteiligung sowie begleitende Beuge- und Strecksehnen Tenovaginitis. **c** STIR-Sequenz, coronare Schnittführung. Daktylitis des II und III Strahles mit periartikulärer Mitreaktion.

Arthritiden typische bildmorphologische Muster erkennen und so zur Diagnosesicherung beitragen [10]. Darüber hinaus ist sie in der Lage hochauflösend extra- und periartikuläre Beteiligungen, wie bspw. die Periarthritis und Enthesitis, welche in der klinischen Untersuchung bei diskretem Befund nicht immer sicher zu erfassen ist, abbilden [11]. Auch die DIP-Arthritis bei Nagelbeteiligung der PsoA – welche bisher isoliert auftreten in ihrem Ausmaß häufig unterschätzt wurde – rückt heute in den wissenschaftlichen Fokus. So konnten bspw. Scarpa et al. nachweisen, dass alle im MRT untersuchten PsoA-Patienten mit einer Nagelbeteiligung MR-morphologisch bereits Zeichen einer Arthritis der distalen Interphalangela-Gelenke (DIP-Gelenke) aufwiesen [12]. Ebenfalls konnte durch die MRT die Patholgenese der Daktylitis bei PsoA deutlich besser verstanden werden [13] (▶ **Abb. 2**).

## Scoring-Systeme

Zur besseren Vergleichbarkeit von MRT Untersuchungen wurde seitens der OMERACT (Outcome Measures in Rheumatology) ein standardisiertes Scoring-System entwickeltet und etabliert. Der RAMRIS (Rheumatoid Arthritis Magnetic Resonance Image Scoring System) ist ein semiquantitativer Score, welcher an den Metacarpophalangeal-Gelenken (MCP-Gelenke), den Handwurzelknochen sowie dem radiocarpalen und ulnocarpalen Übergang das Ausmaß von Synovialitis (0–3), dem Knochenmarködem (0–3) und von Erosionen (0–10) bei der rheumatoiden Arthritis bewertet [14, 15]. Der RAMRIS ist heute fester Bestandteil vieler Studienprotokolle bei der RA, welche die MRT verwenden.

Die Auswertung und das RAMRIS-Scoring ist allerdings sehr zeitaufwendig und daher nur für Studien sinnvoll, da insgesamt 23 Gelenkregionen nach oben genannten Kriterien bewertet werden müssen. Aus diesem Grund wurde ein auf fünf Gelenke reduzierter RAMRIS-5 entwickelt und in Studien evaluiert. Es konnte gezeigt werden, dass sich zwischen dem RAMRIS-5 und dem traditionellen RAMRIS für alle Patienten (n = 94) eine hohe Übereinstimmung ($r = 0{,}88$, $p < 0{,}05$) nachweisen ließ [16] und dies bei deutlich verringerter Auswertungszeit.

Neben der Vereinfachung des RAMRIS-Scores wurde ebenfalls der Stellenwert der Tenosynovitis im MRT untersucht. So konnte gezeigt werden, dass durch ein dem RAMRIS entsprechendem Punktesystem (Grad 0–3) die Tenosynovitis der Beuge- und Strecksehnen der Hand mit großer Inter- und Intrareader Reliabilität gescort werden kann und ggf. in zukünftigen Studienprotokollen als zusätzlicher Parameter verwendet und validiert werden könnte [17].

Ferne haben zahlreiche MRT-Studien bereits zeigen können, dass der Fuß in der Bewertung von Krankheitsaktivität und in der Erfassung von Frühveränderungen bei der RA nicht ausreichend berücksichtigt wird [18]. Aus diesem Grund wurde die Validität eines kombiniertes Hand-Fuß-MRT Scores (HaF-Score) untersucht. Es konnte gezeigt werden, dass Änderungen des HaF-Scores (ΔHaF-score) signifikant mit Änderungen des DAS28 (ΔDAS28) nach 6 Monaten korrelierten ($r = 0{,}820$, 95 %-CI 0,633–0,916) und das der neue HaF-Score diese besser als der traditionelle RAMRIS allein erfasst (0,499, 0,139–0,743, $p = 0{,}0368$). Bei allen Patienten, die gut oder moderat respondierten (nach EULAR-Response Kriterien [19]), konnte der HaF-Score trotz klinischen Response weiterhin entzündliche Aktivität und progressive Erosivität an den Füßen nachweisen [20].

Zur besseren Vergleichbarkeit von MRT Untersuchungen (klinisch und in Studienprotokollen) wurde dem RAMRIS angelehnt der PsAMRIS (Psoriatic Arthritis Magnetic Resonance Imaging Scoring System) für PsoA-Patienten entwickelt [21]. Neben den MCP und PIP-Gelenken wurden die häufig betroffenen distalen Interphalangeal-Gelenke (DIP-Gelenke) sowie die pathognomonische Enthesitiden und Tenovaginitiden in das Scoring System aufgenommen. Der PsAMRIS wird heute in zahlreichen MRT-Studien bei PsoA eingesetzt und evaluiert [22].

## Niederfeld-MRT

Untersuchungen im Hochfeld-MRT (1,5–3 Tesla) bieten durch die hohe Auflösung und die Vielzahl der möglichen Wichtungen viele Vorteile. Die Lagerung des Patienten ist durch den speziellen Aufbau der Magneten (mit Ausnahme der „offenen" MR-Tomografen) allerdings unkomfortabel. Der Patient muss in der Regel in Bauchlage untersucht werden (sogenannte „Supermann-Position"). Die so nötige Positionierung ist insbesondere für ältere oder Patienten mit hochaktiver Arthritis häufig schwierig bzw. nicht möglich.

Mit der Entwicklung der Niederfeld-MR-Tomografen (NF-MRT) und Klein-MR-Tomografen können Patienten deutlich einfacher und komfortabler untersucht werden, wobei Klein-MR-Tomografen mit bis zu 1,5 Tesla betrieben werden können, deren Produktion zuletzt jedoch eingestellt wurde. NF-MRT operieren meist mit einem permanenten Hauptmagnetfeld ab 0,2 Tesla. Durch diese technischen Voraussetzungen stellt die NF-MRT deutlich weniger Voraussetzungen an den zur Verfügung stehenden Raum, wobei auch Anschaffungspreis dieser Geräte deutlich hinter den klassischen Hochfeld-MR-Tomografen liegt. Verschiede Untersuchungen konnten zeigen, dass trotz im Vergleich zum Hochfeld-MRT niedrigerer Ortsauflösung mit der NF-MRT sehr gute und vergleichbare Untersuchungen

generiert werden können [23]. In Studien werden immer häufiger auch NF-MRT-Geräte eingesetzt, sei es bei der RA oder auch PsoA. So konnte gezeigt werden, dass das NF-MRT konkordant zum Hochfeld-MRT ein Therapieansprechen bildmorphologisch erfassen kann [24, 25]. Einschränkend zu erwähnen ist, dass NF-MRT bestimmte MRT-Sequenzen nicht ausreichend zu generieren vermag, insbesondere für die Erfassung des Knochenmarködems [23]. Aufgrund dieser Einschränkungen (insbesondere bei der schlechteren Auflösung) wird aktuell der Stellenwert der NF-MRT in den Gremien der EULAR und des ACR diskutiert, wobei noch keine allgemeingültige Position formuliert wurde.

## Innovative MRT-Sequenzen

In den letzten 5 Jahren haben neue MRT-Sequenzen den Anwendungs- und Indikationsbereich erweitert. Als Beispiel hierfür können neue Verfahren zur Darstellung des Gelenkknorpels an den MCP-Gelenken genannt werden. Die „Delayed gadolinium-enhanced MRI of cartilage“ (dGEMRIC)-Technik ist in der Lage Knorpelqualität, selbst an kleinen Gelenken wie den MCP-Gelenken, darzustellen. Hierfür wird die Ablagerung des Kontrastmittel Gadolinium [Gd(DTPA)2-] beobachtet, welches sich umgekehrt proportional zum Glykosaminoglykangehalt (GAG) des Knorpels verhält. Niedrige dGEMRIC Signale korrelieren mit weniger GAG Gehalt des Knorpels [26]. Es konnte gezeigt werden, dass dies auch im Knorpel der MCP Gelenke gesunder dargestellt werden kann [27]. So korreliert das Ausmaß der entzündlichen Veränderungen des RAMRIS (für Synovialitis und Knochenmarködem) deutlich besser mit der Abnahme der Knorpelqualität als der Erosionsscore [28]. Es bleibt zu erwähnen, dass diese Technik nicht flächendeckt eingesetzt wird, da aufgrund nötiger technischer und baulicher Voraussetzungen der MR-Tomografen (Hochfeld-MRT wenn möglich mit spezieller Handspule und optimierten MRT-Sequenzen) die Durchführung der Untersuchung nicht an allen Zentren möglich ist.

Um das für die dGEMRIC Sequenzen notwenige Kontrastmittel einzusparen wird aktuell an der Erstellung von kontrastmittelfreien, knorpeldarstellenden MRT Sequenzen gearbeitet. So kann mit dem glycosaminoglycan chemical exchange saturation transfer (gagCEST) Verfahren ohne Kontrastmitteln direkt durch die Abbildung des lokalen Wassergehaltes die Qualität des Knorpels erkannt werden, wobei die Umsetzung bisher nur an der Wirbelsäule machbar war [29].

Neben Wasserstoff-Ionen, welche regelhaft in allen gängigen MRT Sequenzen angeregt werden, ist insbesondere für die muskuloskeletale Bildgebung auch die Anregung von Natrium-Ionen von großem Interesse. So sind bspw. GAG als Hauptbestandteil des Gelenkknorpels negativ geladen und binden das positiv geladene Natrium. Erste MRT-Studien konnten bereits den großen Nutzen der Technik zur Beurteilung des Gelenkknorpels nachweisen, wobei dies bisher nur an großen Gelenken (bspw. Knie) gelang [30, 31].

Als weitere MR-Technik ist die Weiterentwicklung und histologische Korrelation dynamischer MRT-Sequenzen zu nennen. Hierbei wird in kurzen zeitlichen Abständen das An- und Abfluten des Kontrastmittels im und um das Gelenk gemessen. Hochentzündliche Areale weisen eine deutlich gesteigerte lokale Durchblutung auf (konkordant zur Power-Doppler Untersuchung im Ultraschall). In ersten Arbeiten wurde eine gute Korrelation des Ausmaßes der Inflammation (gemessen mittels dynamischer MRT) mit der lokalen Knorpelqualität beschrieben [32] und das die in den dynamischen MRT-Sequenzen darstellbare Inflammation mit dem histologischen Ausmaß der Entzündung korreliert [33].

## Hybride Bildgebende Verfahren

Hybride bildgebende Verfahren vereinigen 2 verschieden Techniken um Vorteile einzelner Verfahren zu kombinieren. So hat bspw. die Kombination aus der Positronen-Emissions-Tomografie (PET) und der Computertomografie (CT; PET-CT) bereits einen festen Platz im klinischen Algorithmus insbesondere bei onkologischen Fragstellungen (z. B. Staging) eingenommen. Hierbei wird die gute Ortsauflösung der CT mit der sehr hohen Sensitivität der PET kombiniert.

Auch in der Rheumatologie sind erste Untersuchungen mit hybriden bildgebenden Verfahren durchgeführt worden. So konnte gezeigt werden, dass durch die Kombination der PET mit der MRT (PET-MRT) die Sensitivität für die Detektion entzündlicher Läsionen bei der RA besser als im Einzelverfahren ist [34].

Auch die Kombination von multi-pinhole single-photon emission computed tomografy (MPH-SPECT, hochauflösende Szintigrafie) mit der MRT konnte eine höhere Sensitivität für Veränderungen des Knochenmetabolismus bei entzündlichen Arthritiden aufweisen als die MRT allein [35]. Durch die Kombination der beiden Verfahren konnten frühe Knochen-Veränderungen der RA, welche prädiktiv für die Entstehung späterer ossärer Läsionen sind, erkannt werden.

Zusammenfassend scheint die serielle oder gleichzeitige Kombination von bildgebenden Verfahren aus Radiologie und Nuklearmedizin für die Rheumatologie neue Perspektiven bei der Früherkennung von Arthritis und deren Therapiekontrolle zu ermöglichen.

## Zusammenfassung

Die MRT peripherer Gelenke wird heute immer mehr auch im klinischen Alltag eingesetzt und unterliegt einem raschen wissenschaftlichen Fortschritt. Sie ist in der Lage hoch sensitiv entzündliche und erosive Areale zu erkennen. Darüber hinaus kann die MRT als einziges Verfahren das Knochenmarködem detektieren, welches prädiktiv für die Entstehung von Erosionen ist. Durch neue Scoring-Systeme (z. B. der RAMRIS) gelingt eine immer einfacherer (RAMRIS-5) erhobene, oft komplexe MRT-Befunde zu vergleichen. Neue Sequenzen (wie z. B. dGEMRIC) erkennen frühzeitig Knorpelveränderungen, welche mit dem lokalen Ausmaß der Inflammation korrelieren. Dynamische MRT-Sequenzen registrieren das An- und Abflut-Verhalten von Kontrastmittel und könnten zukünftig bei der Bewertung von Synovialitis zusätzliche Informationen liefern.

Als Rheumatologen sind wir gefordert Innovationen kritisch zu prüfen, ihren Mehrwert zu diskutieren und die Vorteile in die klinische Anwendung zu transferieren.

### Interessenkonflikt

Teile der vorgestellten Daten wurden im Rahmen des Projektes REMISSION-PLUS erhoben, welches durch Firmen AbbVie Deutschland GmbH & Co KG und Esaote Biomedica Deutschland GmbH unterstützt wurde.

## Literatur


[1] Colebatch AN, Edwards CJ, Østergaard M et al. EULAR recommendations for the use of imaging of the joints in the clinical management of rheumatoid arthritis. Annals of the Rheumatic Diseases 2013; 72: 804–814

[2] Filippucci E, Di Geso L, Grassi W. Progress in imaging in rheumatology. Nature Reviews. Rheumatology 2014; 10: 628 –634

[3] Braun J, van Berg Rd Baraliakos X et al. 2010 update of the ASAS/EULAR recommendations for the management of ankylosing spondylitis. Annals of the Rheumatic Diseases 2011; 70: 896 –904

[4] Poggenborg RP, Sørensen IJ, Pedersen SJ et al. Magnetic resonance imaging for diagnosing, monitoring and prognostication in psoriatic arthritis. Clinical and Experimental Rheumatology 2015; 33: S66–S69

[5] Baker JF, Ostergaard M, Emery P et al. Early MRI measures independently predict 1-year and 2-year radiographic progression in rheumatoid arthritis: secondary analysis from a large clinical trial. Annals of the Rheumatic Diseases 2013

[6] McQueen FM, Ostendorf B. What is MRI bone oedema in rheumatoid arthritis and why does it matter? Arthritis Research & Therapy 2006; 8: 222

[7] Gandjbakhch F, Foltz V, Mallet A et al. Bone marrow oedema predicts structural progression in a 1-year follow-up of 85 patients with RA in remission or with low disease activity with low-field MRI. Annals of the Rheumatic Diseases 2011; 70: 2159–2162

[8] Frenzel T, Lengsfeld P, Schirmer H et al. Stability of gadolinium-based magnetic resonance imaging contrast agents in human serum at 37 degrees C. Investigative radiology 2008; 43: 817–828

[9] Radbruch A, Weberling LD, Kieslich PJ et al. Gadolinium retention in the dentate nucleus and globus pallidus is dependent on the class of contrast agent. Radiology 2015; 275: 783–791

[10] Cimmino MA, Parodi M, Innocenti S et al. Dynamic magnetic resonance of the wrist in psoriatic arthritis reveals imaging patterns similar to those of rheumatoid arthritis. Arthritis Research & Therapy 2005; 7: R725–R731

[11] Poggenborg RP, Østergaard M, Terslev L. Imaging in Psoriatic Arthritis. Rheumatic diseases clinics of North America 2015; 41: 593 –613

[12] Scarpa R, Soscia E, Peluso R et al. Nail and distal interphalangeal joint in psoriatic arthritis. The Journal of rheumatology 2006; 33: 1315 –1319

[13] Tan AL, Fukuba E, Halliday NA et al. High-resolution MRI assessment of dactylitis in psoriatic arthritis shows flexor tendon pulley and sheath-related enthesitis. Annals of the Rheumatic Diseases 2014

[14] Østergaard M, Peterfy C, Conaghan P et al. OMERACT Rheumatoid Arthritis Magnetic Resonance Imaging Studies. Core set of MRI acquisitions, joint pathology definitions, and the OMERACT RA-MRI scoring system. The Journal of rheumatology 2003; 30: 1385–1386

[15] Ostergaard M, Conaghan PG, O'Connor P et al. Reducing invasiveness, duration, and cost of magnetic resonance imaging in rheumatoid arthritis by omitting intravenous contrast injection – Does it change the assessment of inflammatory and destructive joint changes by the OMERACT RAMRIS? The Journal of rheumatology 2009; 36: 1806–1810

[16] Schleich C, Buchbender C, Sewerin P et al. Evaluation of a simplified version of the Rheumatoid Arthritis Magnetic Resonance Imaging Score (RAMRIS) comprising 5 joints (RAMRIS5). Clinical and Experimental Rheumatology 2015

[17] Haavardsholm EA, Østergaard M, Ejbjerg BJ et al. Introduction of a novel magnetic resonance imaging tenosynovitis score for rheumatoid arthritis: reliability in a multireader longitudinal study. Annals of the Rheumatic Diseases 2007; 66: 1216–1220

[18] Ostendorf B, Scherer A, Mödder U et al. Diagnostic value of magnetic resonance imaging of the forefeet in early rheumatoid arthritis when findings on imaging of the metacarpophalangeal joints of the hands remain normal. Arthritis and rheumatism 2004; 50: 2094–2102

[19] Karonitsch T, Aletaha D, Boers M et al. Methods of deriving EULAR/ACR recommendations on reporting disease activity in clinical trials of patients with rheumatoid arthritis. Annals of the Rheumatic Diseases 2008; 67: 1365–1373

[20] Sewerin P, Buchbender C, Vordenbäumen S et al. Advantages of a combined rheumatoid arthritis magnetic resonance imaging score (RAMRIS) for hand and feet: Does the RAMRIS of the hand alone underestimate disease activity and progression? BMC musculoskeletal disorders 2014; 15: 104

[21] Ostergaard M, McQueen F, Wiell C et al. The OMERACT psoriatic arthritis magnetic resonance imaging scoring system (PsAMRIS): definitions of key pathologies, suggested MRI sequences, and preliminary scoring system for PsA Hands. The Journal of rheumatology 2009; 36: 1816–1824

[22] Glinatsi D, Bird P, Gandjbakhch F et al. Validation of the OMERACT Psoriatic Arthritis Magnetic Resonance Imaging Score (PsAMRIS) for the Hand and Foot in a Randomized Placebo-controlled Trial. The Journal of rheumatology 2015; 42: 2473–2479

[23] Ejbjerg BJ, Narvestad E, Jacobsen S et al. Optimised, low cost, low field dedicated extremity MRI is highly specific and sensitive for synovitis and bone erosions in rheumatoid arthritis wrist and finger joints: comparison with conventional high field MRI and radiography. Annals of the Rheumatic Diseases 2005; 64: 1280–1287

[24] Hirota T, Suzuki T, Ogishima H et al. Evaluation of changes in magnetic resonance images following 24 and 52 weeks of treatment of rheumatoid arthritis with infliximab, tocilizumab, or abatacept. Modern Rheumatology/the Japan Rheumatism Association 2016; 26: 29–35

[25] Feletar M, Hall S, Bird P. Evaluation of Magnetic Resonance Imaging Responsiveness in Active Psoriatic Arthritis at Multiple Timepoints during the First 12 Weeks of Antitumor Necrosis Factor Therapy. The Journal of rheumatology 2016; 43: 75–80

[26] Bashir A, Gray ML, Boutin RD et al. Glycosaminoglycan in articular cartilage: in vivo assessment with delayed Gd(DTPA)(2-)-enhanced MR imaging. Radiology 1997; 205: 551–558

[27] Buchbender C, Scherer A, Kröpil P et al. Cartilage quality in rheumatoid arthritis: comparison of T2 * mapping, native T1 mapping, dGEMRIC, ΔR1 and value of pre-contrast imaging. Skeletal Radiology 2012; 41: 685–692

[28] Herz B, Albrecht A, Englbrecht M et al. Osteitis and synovitis, but not bone erosion, is associated with proteoglycan loss and microstructure damage in the cartilage of patients with rheumatoid arthritis. Annals of the Rheumatic Diseases 2014; 73: 1101–1106

[29] Schleich C, Müller-Lutz A, Matuschke F et al. Glycosaminoglycan chemical exchange saturation transfer of lumbar intervertebral discs in patients with spondyloarthritis. Journal of magnetic resonance imaging: JMRI 2015

[30] Guermazi A, Alizai H, Crema MD et al. Compositional MRI techniques for evaluation of cartilage degeneration in osteoarthritis. Osteoarthritis and cartilage/OARS, Osteoarthritis Research Society 2015; 23: 1639–1653

[31] Madelin G, Regatte RR. Biomedical applications of sodium MRI in vivo. Journal of magnetic resonance imaging: JMRI 2013; 38: 511–529

[32] Müller-Lutz A, Schleich C, Sewerin P et al. Comparison of Quantitative and Semiquantitative Dynamic Contrast-Enhanced MRI With Respect to Their Correlation to Delayed Gadolinium-Enhanced MRI of the Cartilage in Patients With Early Rheumatoid Arthritis. Journal of Computer Assisted Tomography 2014

[33] Vordenbäumen S, Schleich C, Lögters T et al. Dynamic contrast-enhanced magnetic resonance imaging of metacarpophalangeal joints reflects histological signs of synovitis in rheumatoid arthritis. Arthritis Research & Therapy 2014; 16: 452

[34] Miese F, Scherer A, Ostendorf B et al. Hybrid 18F-FDG PET-MRI of the hand in rheumatoid arthritis: initial results. Clinical rheumatology 2011; 30: 1247–1250

[35] Buchbender C, Sewerin P, Mattes-György K et al. Utility of combined high-resolution bone SPECT and MRI for the identification of rheumatoid arthritis patients with high-risk for erosive progression. European journal of radiology 2013; 82: 374–379

# Prospective MRI score to predict negative EULAR response in patients with rheumatoid arthritis (RA) before therapy-escalation to a biological therapy

Dear Editor

We read with great interest the article by Baker *et al*[1] who showed that early MRI measures independently predict erosive progression on X-ray and MRI after 1 and 2 years in therapy-naive patients with rheumatoid arthritis (RA) from the randomised-controlled GO-BEFORE trial. Due to these findings, we re-evaluated MRI data from the German REMISSION-PLUS Cohort[2 3] at our centre to verify if a MRI score may predict negative response in patients with RA before therapy-escalation to a biological therapy. MRI was performed in 257 patients before therapy-escalation (T0) and after 12 months (T1) and analysed by using the Outcome Measures in Rheumatology (OMERACT) rheumatoid arthritis MRI score (RAMRIS). In addition, clinical and laboratory parameters (Disease Activity Score 28 (DAS-28) and C-reactive protein (CRP)) were collected for each visit. Logistic regression combining clinical and MRI parameters was performed resulting in a combination of the patients' age and the RAMRIS-T0 performing best for prediction of non-response. Bootstrapping with 5000 resamples was performed to estimate the accuracy of the model.

Of the patients included, 29 were escalated to a biological therapy (20 women, median age 57 years (IQR 46–65), 95% anti-tumour necrosis factor (TNF)-alpha therapy). Poor responders (n=5) and responders (n=24) had a mean RAMRIS-T0 score of 14.4 and 52.0, respectively (Wilcoxon test $p<0.01$). High RAMRIS score showed a trend towards a protective effect against non-response (OR 0.90 per RAMRIS point, 95% CI 0.79 to 1.03, $p=0.12$). The strength of the association was stable after adjusting for age, CRP, anti citrullinated peptide antibodies (ACPA)/rheumatoid factor and DAS-28 at baseline. The median area under the curve in the bootstrap analysis was 88.9% with 95% CI 84.0% to 92.8%.

Thus, while Baker *et al* clearly demonstrated that a high inflammatory activity on MRI (ie, RAMRIS) is associated with an unfavourable prognosis (ie, radiographic progression), our observations suggest that this may be overcome by administration of a highly effective therapy, for example, a biologic agent. Indeed, patients with a prognostic unfavourable high RAMRIS were even more likely to respond, making them ideal candidates for these costly drugs.

In summary, both studies emphasise the value of an MRI before therapy initiation or escalation. Hence, further studies are needed to improve our data in established patients with RA before escalating the therapy to biological disease-modifying anti-rheumatic drug (bDMARD).

**Philipp Sewerin, Stefan Vordenbaeumen, Ralph Brinks, Benedikt Ostendorf**

Department of Policlinic of Rheumatology and Hiller Research Unit Rheumatology University Hospital (UKD), Duesseldorf, Germany

**Correspondence to** Dr Philipp Sewerin, Department and Hiller Research Unit for Rheumatology, University Hospital Duesseldorf (UKD), Moorenstreet 5, 40225 Duesseldorf, Germany; philipp.sewerin@med.uni-duesseldorf.de

**Competing interests** None declared.

**Provenance and peer review** Not commissioned; internally peer reviewed.

CrossMark

**To cite** Sewerin P, Vordenbaeumen S, Brinks R, *et al*. *Ann Rheum Dis* 2017;**76**:e44.

Received 3 February 2017
Accepted 4 February 2017
Published Online First 10 March 2017

Linked

► http://dx.doi. org/10.1136/annrheumdis-2017-211265

*Ann Rheum Dis* 2017;**76**:e44. doi:10.1136/annrheumdis-2017-211257

## REFERENCES

1 Baker JF, Ostergaard M, Emery P, *et al*. Early MRI measures independently predict 1-year and 2-year radiographic progression in rheumatoid arthritis: secondary analysis from a large clinical trial. *Ann Rheum Dis* 2014;73:1968–74.
2 Ostendorf B, Scherer A, Kellner H, *et al*. Project REMISSION(PLUS): clinical and radiological remission: new treatment goals in the management of rheumatoid arthritis. *Z Rheumatol* 2008;67:707–10, 712–15.
3 Sewerin P, Klein S, Brinks R, *et al*. REMISSIONPLUS, an Initiative to Integrate Modern Imaging into Rheumatologic Care – Review, Appraisal and Outlook: Evaluation of Low-Field MRI Data. *Akt Rheumatol* 2017;42:1–10 (2017, in press).

Thieme

# REMISSION$^{PLUS}$ eine Initiative zur Integration moderner Bildgebung in die rheumatologische Versorgung Rückblick, Einblick, Ausblick: Auswertung der Niederfeld-MRT Daten

## REMISSION$^{PLUS}$, an Initiative to Integrate Modern Imaging into Rheumatologic Care – Review, Appraisal and Outlook: Evaluation of Low-Field MRI Data

Autoren

**Philipp Sewerin[1], Sabine Klein[1], Ralph Brinks[1], Annika Hoyer[3], Christoph Schleich[2], Falk Miese[2], Sabine Blaschke[4], Edmund Edelmann[5], Ino K. Gao[6], Joachim Georgi[7], Herbert Kellner[8], Gernot Keyßer[9], Hanns-Martin Lorenz[10], Ulf Müller-Ladner[11], Hans-Georg Pott[12], Hendrik Schulze-Koops[13], Marisa Walther[14], Wolfgang A. Schmidt[14], Matthias Schneider[1], Benedikt Ostendorf[1]**

Institute

1 Poliklinik, Funktionsbereich und Hiller-Forschungszentrum für Rheumatologie, Heinrich-Heine-Universität Düsseldorf, Düsseldorf
2 Institut für diagnostische und interventionelle Radiologie, Heinrich-Heine-Universität Düsseldorf, Düsseldorf
3 Deutsches Diabetes Zentrum, Heinrich-Heine-Universität Düsseldorf, Düsseldorf
4 Rheumatologie, Universitätsklinikum Göttingen, Göttingen
5 Rheumazentrum Bad Aibling Erding, Bad Aibling Erding
6 Rheumapraxis Heidelberg, Heidelberg
7 Abteilung Innere Medizin/ Rheumatologie, Helios Ostseeklinik Damp, Damp
8 Schwerpunktpraxis für Rheumatologie und Gastroenterologie, Ärztlicher Leiter der Abteilung Rheumatologie im Krankenhaus Neuwittelsbach, München
9 Klinik und Poliklinik für Innere Medizin I, Universitätsklinikum Halle, Halle/Saale
10 Med. Klinik V, Sektion Rheumatologie, Universität Heidelberg, Heidelberg
11 Kerckhoff-Klinik, Abteilung für Rheumatologie und klinische Immunologie, Justus-Liebig-Universität Gießen, Bad Nauheim
12 Schwerpunktpraxis für Rheumatologie, Physikalische Medizin und klinische Immunologie, Rheumatologikum Hannover, Hannover
13 Rheuma-Einheit, Medizinische Poliklinik, Universitätsklinikum München – Campus Innenstadt, München
14 Immanuel-Krankenhaus Rheumaklinik Berlin-Buch, Innere Medizin, Rheumatologie und Klinische Immunologie, Berlin

Schlüsselwörter

Bildgebung, MRT, Rheumatoide Arthritis

Key words

imaging, MRI, rheumatoid arthritis

Bibliografie

**DOI** http://dx.doi.org/10.1055/s-0042-124184
Online-Publikation: 24.4.2017
Akt Rheumatol 2017; 42: 432–441

ISSN 0341-051X

Korrespondenzadresse

Dr. med. Philipp Sewerin
Poliklinik, Funktionsbereich
und Hiller-Forschungszentrum für
Rheumatologie, Heinrich-Heine-Universität Düsseldorf
Moorenstraße 5
40225 Düsseldorf
Tel.: +49/211/81/17817, Fax: +49/211/81 16 455
philipp.sewerin@med.uni-duesseldorf.de

### ZUSAMMENFASSUNG

Bildgebende Verfahren nehmen heute bei der Diagnosestellung und Therapiekontrolle der Rheumatoiden Arthritis (RA) eine unverzichtbare Rolle ein. Die Initiative REMISSION$^{PLUS}$ hat seit 2006 über 10 Jahre das Ziel verfolgt, moderne bildgebende Verfahren wie die Arthrosonografie und die Magnetresonanztomografie (MRT) in den klinischen Alltag des Rheumatologen zu implementieren. Neben Schulungen (über 3 000 Rheumatologen in über 200 Veranstaltungen) wurden zahlreiche Bildgebungs- Studien durchgeführt. Erstmals werden jetzt zusammenhängend alle Niederfeld-MRT Daten aus der Initiative vorgestellt. Die Ergebnisse dieser multizentrischen Studie zeigen, dass die Niederfeld-MRT für RA Patienten eine komfortable Untersuchungsmethode darstellt und für den Rheumatologen die Möglichkeit bietet, effektiv und sehr genau Thera-

pieeffekte (DMARD, Biologika) zu kontrollieren. Die MRT-Daten korrelierten hierbei signifikant mit Klinik und Labor. Mit der Methode ist es ferner möglich bei RA-Patienten subklinische Arthritiszeichen zu detektieren, zum anderen konnte fortschreitende radiologische Progression (Erosivität), trotz klinischer Remission („silent progression") erkannt werden. Diese Ergebnisse sind konventionell radiologisch nicht zu gewinnen, sodass der Einsatz der MRT neue Einblicke in die Pathogenese und konsekutiv neue Informationen für das Management der RA liefert. Die Bewertung dieser Vorteile und der Benefit für den Patienten im klinischen Alltag muss in weiteren Studien untersucht und diskutiert werden.

**ABSTRACT**

Imaging plays a vital role in the diagnosis and treatment control of rheumatoid arthritis (RA). Since 2006, the initiative REMISSION$^{PLUS}$ has aimed to implement modern imaging tools like arthrosonography and magnetic resonance imaging (MRI) into the routine clinical practice of rheumatologists. In addition to training sessions (over 3 000 rheumatologists in over 200 sessions), numerous sonography and MRI studies have been conducted to assess the value of these techniques for treatment control in RA. The following study summarises the results of the low-field MRI-studies. The results of this multicenter study demonstrate that low-field MRI is a comfortable examination for RA patients and enables rheumatologists to effectively and very carefully monitor treatment outcomes (DMARDs, biologics). MRI data significantly correlate with clinical and laboratory parameters. In addition, this method allows clinicians to detect subclinical indicators for arthritis as well as advancing radiological progression despite clinical remission ("silent progression"). These findings cannot be obtained in conventional X-rays. The use of MRI thus provides new insights into the pathogenesis and will consecutively deliver new informations for RA management. The assessment of these advantages and the benefits for patients in daily clinical routine need to be further examined and discussed in future studies.

## Einleitung

Das Management der rheumatoiden Arthritis (RA) hat in den letzten Jahren einen entscheidenden Paradigmenwechsel erfahren. Diese Entwicklung basierte zum einen auf dem Aufkommen neuer therapeutischen Möglichkeiten (z. B. Biologika), zum Anderen auf der Verfügbarkeit neuer Klassifikationskriterien (2010) bzw. Therapiestrategien („hit hard and early", „treat-to-target", interdisziplinäre Leitlinie) [1–3].

Ein ähnlicher Wandel hat bei der bildgebenden Diagnostik der RA stattgefunden. Hat man sich bisher auf die konventionelle Röntgendiagnostik gestützt (bis 2009 war die Erosion auch American Rheumatism Association (ARA) Klassifikationskriterium), so ist dieser alleinige Ansatz nicht mehr zeitgemäß [4, 5]. Die Tatsache, dass radiologische Veränderungen oft erst 6 Monate nach einer Gelenkentzündung mittels konventioneller Röntgenuntersuchung sichtbar werden, macht diese Technik für die Frühdiagnostik weitestgehend unbrauchbar. Da ein vorrangiges Therapieziel die möglichst vollständige Verhinderung von „Schaden" am Gelenk ist, steht das Kriterium „Erosivität" zur Diagnosestellung und Prognoseabschätzung der RA oft nicht mehr zur Verfügung. Dennoch, ein frühes Auftreten von Erosionen bleibt ein unabhängiger Prädiktor der weiteren radiologischen Progression und zeigt damit eine zwingende Therapiebedürftigkeit an [6].

Aus diesen Gründen wurden in den letzten Jahren intensiv neue sensitivere bildgebende Verfahren entwickelt und analysiert, die eine frühere Erfassung entzündlicher Gelenkveränderungen erlauben [7]. Bildgebende Techniken – wie der hochauflösende Ultraschall (US) und die Magnetresonanztomografie (MRT) – decken dieses Anforderungsprofil ab. Sie bieten eine Vielzahl von Möglichkeiten zur Visualisierung pathologischer bzw. funktioneller Frühveränderungen entzündlicher Gelenkerkrankungen wie z. B. Synovialitis, Tenosynovialitis und das Knochenmarködem, welche durch das Röntgenbild nicht erfasst werden [7–9].

Diese zusätzlich gewonnenen Informationen dienen dem Rheumatologen sowohl bei der Sicherung der frühen Diagnose als auch bei der Therapiestratifizierung, denn die Gelenkdestruktion schreitet zu Beginn der Erkrankung nicht nur am stärksten fort (meist innerhalb der ersten 2 Jahre), sondern ist zu diesem Zeitpunkt auch am besten durch krankheitsmodifizierende Therapie (DMARDs) zu hemmen. Des Weiteren werden diese bildgebenden Techniken inzwischen zur Prädiktion und Prognoseabschätzung eingesetzt. Bereits nachweisbare Erosionen im Ultraschall (US) und in der MRT, erhöhte Krankheitsaktivität – gemessen am Grad der Synovialitis, als auch der Nachweis des Knochenmarködems (nur in der MRT darstellbar) werden als entsprechende Signale für eine schlechtere Prognose gewertet [10]. Studiendaten an großen RA-Patientenkollektiven konnten zeigen, dass trotz einer messbaren klinischen Remission (DAS 28 ≤ 2,6) eine Vielzahl von RA-Patienten eine radiologische Progression („silent progression") bzw. persistierende, subklinische Krankheitsaktivität zeigt [11].

An diesen neuen Entwicklungen zum Management der frühen RA hat sich die Initiative REMISSION$^{PLUS}$ ausgerichtet, welche 2006 von deutschen Experten bildgebender Diagnostik in der Rheumatologie in Kooperation mit den Firmen AbbVie Deutschland GmbH & Co. KG (seinerzeit Abbott Immunology) und Esaote Biomedica Deutschland GmbH ins Leben gerufen wurde. Dies geschah mit der Maßgabe, dem klinisch interessierten Rheumatologen ein „Forum für Fortbildung und Diskussion" zu bieten und durch praxisnahe wissenschaftliche Studien den „diagnostischen Stellenwert der Bildgebung" in der modernen Rheumatologie zu festigen [12].

Unter Leitung von Herrn Prof. Dr. Herbert Kellner (München) – verantwortlich für die Entwicklung und Ausrichtung von Fortbildungskursen – , Frau Prof. Dr. Marina Backhaus (Berlin) – Leiterin der Ultraschall-Studien und Herrn Prof. Dr. Benedikt Ostendorf (Düsseldorf) – Leiter der Niederfeld-MRT-Studien wurden in Kooperation mit den unterstützenden Partnern das Konsortium „REMISSION$^{PLUS}$" etabliert.

Um den Einsatz der Niederfeld-MRT-Technologie zu fördern und diese Methode praxisnah auch anwenden zu können, wurden bundesweit 12 MRT-Zentren benannt und mit den entsprechenden bildgebenden Gerätschaften (Niederfeld-MRT C-Scan, Fa. Esaote Biomedica Deutschland GmbH) ausgestattet.

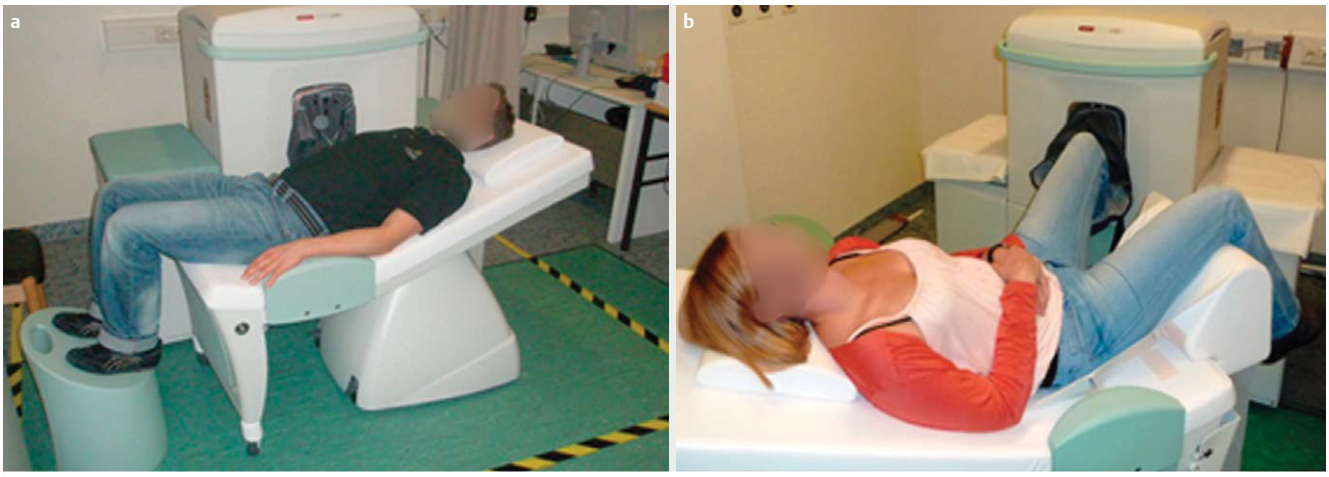

▶ **Abb. 1** Niederfeld-MRT 0.2 Tesla Extremity Unit (Esoate, C-Scan, Esaote Biomedica Deutschland GmbH). **a** Lagerung eines Patienten für eine MRT-Untersuchung der Hand; **b** Lagerung einer Patientin für die MRTUntersuchung des Fußes.

Die Vorteile der Niederfeld-MRT-Technologie sind vielfältig. Die Tomografen sind halb- bzw. offen und deutlich kleiner als die Standard-MR Tomografen, weshalb sie sich leichter in Klinik und Praxis räumlich integrieren lassen. Sie verfügen heutzutage über eine hohe Bildqualität und sind daher auch für rheumatologische Fragestellungen geeignet, die bislang den Hochfeld-MRT-Systemen vorbehalten waren [13]. Durch das offene Design können klaustrophobe Personen problemlos untersucht werden, denn bei den gelenkorientierten Verfahren ist der Patient während der Untersuchung außerhalb des Magneten und nur die zu untersuchende Extremität wird im Gerät positioniert (Isozentrum). Dieser Lagerungskomfort und die bessere Akzeptanz durch den Patienten selbst erlauben wiederholte Nachuntersuchungen zur Therapiekontrolle, wie durch die Initiative REMISSION$^{PLUS}$ vorgeschlagen, wobei dies mit deutlich verkürzten MRT-Protokollen und damit erhöhtem Komfort für die Patienten gelingt [14, 15].

Vor bzw. zu Beginn der Initiative wurden Trainingskurse zu US und MRT an den am Projekt REMISSION$^{PLUS}$ beteiligten Kliniken bzw. Praxen („Centers of Excellence“) durchgeführt. Ferner wurden Dokumentationsbögen und Scores entwickelt (US 7, SOLAR-Score, Niederfeld-MRT Score, RAMRIS 5), um US- und MRT-Befunde semiquantitativ und standardisiert zu erfassen. Dadurch wurden die Grundlagen geschaffen, Bildgebungsdaten für wissenschaftliche Zwecke zu erfassen und hinsichtlich bestimmter Fragestellungen auszuwerten [12, 16–18].

8 von 12 Zentren haben sich an der Niederfeld-MRT-Studie beteiligt, bei der zu festgelegten Messzeitpunkten MRT-Hand-Untersuchungen bei RA-Patienten vor und unter Therapie durchgeführt wurden.

Ziel dieser Niederfeld-MRT-Studie war es, zu prüfen, ob MRT-Befunde von Hand, ggf. Fuß mit der Klinik (z. B. DAS 28) und dem Labor (z. B. CRP) korrelieren und ob intensivierte Therapie die RA Gelenkentzündung bzw. – destruktion zu beeinflussen bzw. sogar zu hemmen vermag. Zudem sollte geprüft werden, ob – trotz klinischer Remission – sich weiterhin MR-morphologisch noch Entzündungszeichen darstellen lassen („subklinische Arthritis“) bzw. ein radiologischer Progress trotz klinischer Remission zu erfassen ist („silent progression“).

Mit dieser zusammenfassenden Darstellung werden komprimiert nun erstmals – unter dem Leitsatz „Rückblick, Einblick und Ausblick“ – alle Niederfeld-MRT Daten, die im Zeitraum von 2006 bis max. 2010 im Rahmen der Initiative REMISSION$^{PLUS}$ an den beteiligten MRT-Zentren erfasst worden sind, vorgestellt und hinsichtlich definierter Fragestellungen analysiert und diskutiert.

## Rückblick

Von 2006–2011 wurden 10 MRT-Befundungskurse und von 2008–2009 sieben MRT-US-Kombinationskurse durchgeführt, welche beide inhaltlich die Interpretation und das Scoring von US- und MRT-Befunden zum Gegenstand hatten. Insgesamt wurden hier mehr als 300 Rheumatologen geschult. Diese Fortbildung diente als Grundlage für die Teilnahme und Durchführung der MRT-Studie. Von 2008 bis 2013 wurden ferner 5 weitere Intensivseminare für Bildgebung mit MRT-Workshops durchgeführt. Hier wurden ca. 400 Rheumatologen über MRT fortgebildet. Als Schulungs- und Fortbildungsmaterialien wurden ein MRT-Poster und ein Atlas mit Bild- und Scoring-Beispielen für die Niederfeld-MRT entwickelt und eingesetzt.

Alle bildgebende Verfahren eingeschlossen, wurden insgesamt in den vergangenen 10 Jahren im Rahmen der Initiative REMISSION$^{PLUS}$ mehr als 200 Fortbildungsveranstaltungen mit über 3 000 Teilnehmern deutschlandweit durchgeführt. Aus 5 großen klinischen Studien (Niederfeld-MRT-Studie, US7, IMPERA, SOLAR, MUSE [17–19]) mit mehr als 3 000 dokumentierten Patienten (insbesondere US) und unter Beteiligung von weit über 100 Studienzentren (insbesondere US) wurden bis heute über 50 wissenschaftliche Kongressbeiträge und Vollpublikationen veröffentlicht.

## Einblick (Material und Methoden)

8 Niederfeld-MRT-Zentren („Center of Excellence“) beteiligten sich aktiv an der Niederfeld-MRT Studie (Bad Aibling: Praxis Dr. E. Edelmann; Halle: Universitätsklinik Halle a. d. Saale, Rheumatologie: Prof. Dr. G. Keyßer; Berlin: Immanuel Klinik Berlin-Buch, Prof. Dr. A. Krause; Heidelberg: Universitätsklinikum Heidelberg, Rheumatologie: Prof. Dr. H.-M. Lorenz und Rheumatologische Schwerpunktpraxis

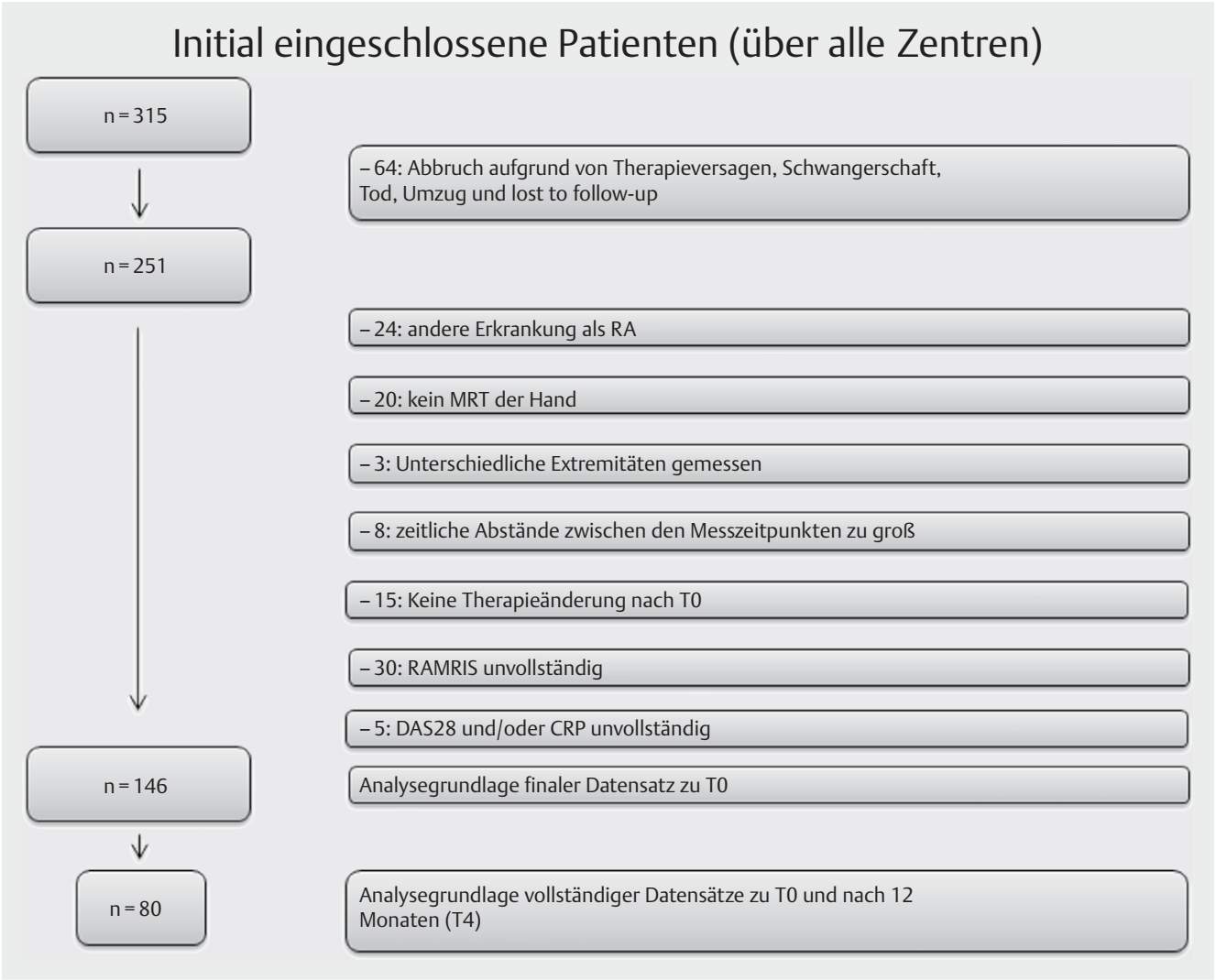


▶ **Abb. 2** Darstellung und Verlauf der primär eingeschlossen und final ausgewerteten RA-Patienten der REMISSION$^{PLUS}$ Kohorte.

Heidelberg: Dr. I. Gao; Göttingen: (Universitätsmedizin Göttingen, Rheumatologie, Frau Prof. Dr. S. Blaschke; Bad Nauheim: Kerckhoff Klinik, Prof. Dr. U. Müller-Ladner und Düsseldorf: Universitätsklinikum Düsseldorf, Poliklinik und Funktionsbereich für Rheumatologie und Hiller Forschungszentrum: Prof. Dr. M. Schneider).

**Studiendesign:** Alle RA-Patienten, welche die ACR-Klassifikationskriterien von 1987 erfüllten und bei denen eine bzw. eine neue DMARD-Therapie initiiert werden sollte (Ersteinstellung oder Therapiewechsel) bzw. eine Neueinstellung auf ein Biologikum geplant war und keine Kontraindikationen zur Durchführung eines MRT mit Kontrastmittel vorlagen (z. B. höhergradige Nierenfunktionsstörungen, Schwangerschaft oder Stillzeit, Metalle im Körper usw.) konnten in die prospektive Kohorten MRT-Studie eingeschlossen werden. Geplant waren Niederfeld-MRT Untersuchen der klinisch dominanten Hand und wenn möglich des klinisch dominanten Fußes (▶ **Abb. 1a, b**). Hierzu wurden dedizierte Niederfeld-MRT Spulen genutzt. Die MRT-Untersuchungen waren zu Beginn und zu den Monaten 3, 6, 9 und 12 geplant. Eine strikte Vorgabe war nicht gestellt. Zu jeder Visite sollten klinische und Labor-Parameter (insbesondere DAS28 und CRP) erhoben werden. Soweit konventionelle Röntgenuntersuchungen der Hände und Füße, die nicht älter als 6 Monate waren, vorlagen wurde auf dem Dokumentationsbogen zu Beginn (T0) erfasst und die Aufnahmen nach "erosiv" und "nicht-erosiv" unterteilt.

Vor Studienbeginn wurden alle Patienten gemäß der Deklaration von Helsinki mündlich und schriftlich aufgeklärt. Ein übergeordnetes Ethikvotum der Ethikkommission der Heinrich-Heine Düsseldorf lag vor (Nummer 3226).

**Rheumatoid Arthritis Magnetic Resonance Image Scoring System (RAMRIS):** Unter Leitung der OMERACT-Gruppe (Outcome MEasures in Rheumatoid Arthritis Clinical Trials) der European League Against Rheumatism (EULAR) wurde bereits 2003 der RAMRIS-Score entwickelt und evaluiert. Mit diesem Score werden das Ausmaß und die Intensität der MRT-Parameter Synovialitis (SYN), Erosion (ERO) und Knochenmarködem ( = bone marrow edema (BME)) bewertet. Dieser semiquantiative MRT-Score erlaubt eine vergleichbare Graduierung der MRT-Befunde (Hand) bei Patienten mit RA. Gescored werden an der Hand die metacarpophalangealen (MCP)-Gelenke 2–5, das Handgelenk mit allen Handwurzelknochen sowie dem radioulnaren-, dem ulnocarpalen- und dem radiocarpalen Übergang.

▶ **Tab. 1** Epidemiologische Daten der 146 eingeschlossenen Patienten zu Studienbeginn.

| | n = 146 |
|---|---|
| Männlich | 107 (73 %) |
| Weiblich | 39 (27 %) |
| Krankheitsdauer < 6 Monate | 37 (25 %) |
| Krankheitsdauer < 24 Monate | 82 (56 %) |
| Krankheitsdauer ≥ 24 Monate | 64 (44 %) |
| Rheumafaktor positiv | 79 (54 %) |
| CCP-AK positiv | 81 (56 %) (1 missings) |
| Erosiv im konventionellen Röntgen der Hände | 44 (34 %) pos. 85 (66 %) neg. (17 missings) |
| C-reaktives Protein (mg/l) | ∅ 14,36 mg/l (min. 1; max. 105) |
| DAS28 | ∅ 4,82 (min. 2,1; max.7,8) |
| Therapienaiv (keine Basis- oder Biologika-Therapie zu Studienbeginn) | 70 (48 %) |

Eingeteilt werden die Synovialitis und das Knochenmarködem in Grade von 0–3, sowie die Erosionen von 0–10 [20]. Maximal kann ein Gesamt-RAMRIS-Score von 320 Punkten erreicht werden.

**NF-MRT-Protokoll:** Alle MRT-Untersuchungen wurden an den unterschiedlen Zenten mit dem gleichen Niederfeld-MRT durchgeführt (0.2 Tesla Extremity Unit, C-Scan, Esaote Biomedica Deutschland GmbH). Das MRT-Protokoll der gesamten Hand (ggf. Fuß) lautete wie folgt: Koronare STIR-Sequenz (STIR = short tau inversion recovery), koronare 3-dimensionale T1- gewichtete Gradientenecho-Sequenz vor und nach intravenöser Injektion des Kontrastmittels (Gd-DTPA (Dotarem©, Guerbet GmbH, Germany)), das ergänzende Untersuchungsprotokoll des Fußes: Koronare STIR-Sequenz, koronare 3-dimensionale T1- gewichtete Sequenz vor und nach intravenöser Injektion vom Kontrastmittel (s. o.). Die 3-dimensionale T1-gewichtete Gradientenecho-Sequenz von Hand und Fuß wurden zusätzlich sagittal und axial rekonstruiert.

Die Auswertung bzw. Befundung der MRT-Bilder erfolgte am Zentrum selbst durch MRT-geschulten Rheumatologen. Die ausgefüllten MRT-Bögen (kein Name, aber Identifikationsnummer (pseudonymisiert)) wurden in eine zentrale Datenbank am Standort Düsseldorf eingegeben.

**Statistik/Methodik:** Eine Plausibilitätskontrolle der Datenbank nach Studienschluss erfolgte durch R.B. und S.K. Die statistische Analyse wurde mit der Software SAS Version 9.3 durchgeführt (SAS Corporation, Cary, North Carolina). Errechnet wurden Anteile, Mittelwerte, Standardabweichungen, Minima und Maxima. Fehlende Werte wurden nicht imputiert.

## Fragestellungen und Zielsetzung

Die Niederfeld-MRT-Studie wurde im Rahmen der Initiative REMISSION$^{PLUS}$ initiiert, um den Stellenwert dieses neuen bildgebenden Verfahrens als Instrument der Verlaufsbeurteilung bzw. des Therapiemonitoring bei RA an einem breiten Patientenkollektiv in einer prospektiven Kohorten-Studie – also aus der täglichen Praxis (real-life-Studie = prospektive Kohortenstudie) – zu evaluieren.

In diesem Zusammenhang sollte geprüft werden, ob die Niederfeld-MRT ein taugliches bildgebendes Verfahren für die Praxis darstellt und ein semiquantitatives Scoringverfahren wie der RAMRIS umsetzbar ist.

Mit der Auswertung der RAMRIS-Daten sollte geprüft werden, ob es ein Änderungsverhalten der MRT – vor und nach Therapie – gibt und Assoziationen von MRT-Befund mit der klinischen (DAS28) und der laborserologischen Krankheitsaktivität (BSG, CRP) zu finden sind.

In diesem Kontext stellte sich die Frage, inwiefern Patienten, die das Therapieziel „klinische und radiologische Remission“ erreichen und sich von jenen Patienten unterscheiden, die entweder nur radiologisch bzw. nur laborserologisch und/oder über den DAS28 ein Therapieansprechen zeigen. Zum anderen sollte versucht werden, mögliche „MRT-Prognoseparameter” zu identifizieren, die ein erhöhtes Risiko für z. B. einen radiologisch-progressiven Krankheitsverlauf vorhersagen können, mit der dadurch entstehenden Möglichkeit, einen auf wenige Gelenke reduzierten RAMRIS-Score entwickeln zu können.

## Ergebnisse

### Demografische Daten

Insgesamt wurden im Studienzeitraum (von 2006 bis April 2010) 315 Patienten in die REMISSION$^{PLUS}$–Niederfeld-MRT-Studie eingeschlossen. Hiervon schieden nach der ersten Visite (Screening, T0-Viste) 64 Patienten wegen Therapienebenwirkungen, Schwangerschaft, Tod, Umzug u.ä. aus. 105 weitere Patienten konnten nicht in die endgültige Auswertung aufgenommen werden, da die zur Auswertung vorgelegenen Datensätze (Dokumentationsbögen) unvollständig oder fehlerhaft waren (▶ **Abb. 2**) oder der Abstand der Messzeitpunkte um mehr als 4 Wochen überschritten wurde.

146 Patienten standen mit vollständigen Datensätzen und mindestens 2 MRT-Messzeitpunkten für die abschließende Analyse zur Verfügung. 73 % dieser Patienten waren männlich, bei 54 % konnten Rheumafaktoren und bei 56 % CCP-Antikörper nachgewiesen werden. Das durchschnittliche Alter betrug bei Studieneinschluss 59 Jahre (min. 27–max. 82 Jahre), die durchschnittliche Krankheitsdauer 63 Monate (= 5,3 Jahre; min. 2 Monate–max. 44 Jahre), wobei bei 25 % der Fälle eine Krankheitsdauer < 6, bei 56 % aller Patienten < 24 Monate und bei 44 % eine Krankheitsdauer von ≥ 24 Monaten vor-

lag. Der DAS28 betrug im Mittel bei Studienbeginn 4,9 (min. 2,2–max. 7,8), 48 % der Patienten waren therapienaiv, hatten also weder eine Basis- noch eine Biologika-Therapie erhalten (▶ **Tab. 1**).

▶ **Tab. 2** Gesamt-RAMRIS und RAMRIS-Subscores zu T0 (n = 146).

| | Mittelwert | Standardabweichung | MIN | MAX |
|---|---|---|---|---|
| Gesamt RAMRIS | 13,76 | 12,06 | 0 | 57 |
| SYN-Subscore | 4,73 | 3,19 | 0 | 12 |
| ERO-Subscore | 6,41 | 7,24 | 0 | 38 |
| BME-Subscore | 2,62 | 3,76 | 0 | 16 |

▶ **Tab. 3** Epidemiologische Daten der 80 eingeschlossenen Patienten zu Studienbeginn.

| | N |
|---|---|
| Männlich | 24 (30 %) |
| Weiblich | 56 (70 %) |
| Krankheitsdauer < 6 Monate | 15 (19 %) |
| Krankheitsdauer < 24 Monate | 42 (53 %) |
| Krankheitsdauer ≥ 24 Monate | 38 (47 %) |
| Rheumafaktor pos. | 47 (59 %) |
| CCP-AK positiv | 49 (62 %) |
| Erosiv im konventionellen Röntgen der Hände | 23 (32 %) (missings n = 9) |

### MRT-Basisdaten (n = 146)

Zu T0 (Screening bzw. Studieneinschluss) wurden protokollgemäß Niederfeld-MRT Untersuchungen von Hand/Fuß durchgeführt. Zu Studienbeginn wurde bei einem mittleren DAS28 von 4,9 ein durchschnittlicher Gesamt-RAMRIS von 13,8 gemessen (min. 0–max. 57). An ca. 5 (4,7) Gelenkregionen an der Hand wurden synovialitische Veränderungen festgestellt (SYN-Subscore). In ca. 6 (6,4) Gelenkregionen des RAMRIS konnten MR-morphologisch Erosionen nachgewiesen werden (ERO-Subscore) wobei durchschnittlich pro Patient im Niederfeld-MRT ca. 3 (2,6) Regionen mit Knochenmarködemen (BME-Subscore) an Finger- bzw. Handgelenkregionen detektiert wurden. Die MCP-Gelenke II, III und V waren hier am häufigsten betroffen (▶ **Tab. 2**).

Die konventionellen Röntgenbilder der Hände zeigten zu T0 bereits bei 34 % (n = 44) der Patienten Erosionen (positiver Nachweis mindestens einer Erosion an der Hand), 66 % (n = 85; 17) zeigten hier keine erosiven Veränderungen. Patienten ohne erosive Veränderungen waren durchschnittlich 58,9 Jahre, Patienten mit erosiven Veränderungen 61,2 Jahre (p = 0,92). Bei 80 dieser 85 Patienten (94 %) konnten im MRT Erosionen nachgewiesen werden (ERO-Subscore ≥ 1).

## Klinische Response und radiologische Progression (n = 80)

### Demografische Daten

Im Mittelpunkt dieser Auswertung stand der Vergleich des klinischen Therapieansprechens mit den seriellen Niederfeld-MRT-Untersuchungen der Hand. Es wurden 80 Patienten, bei denen vollständige Datensätze und MRT-Untersuchungen zum Zeitpunkt 0 (T0) und 12 Monate (T4) vorlagen, ausgewertet (▶ **Tab. 3**).

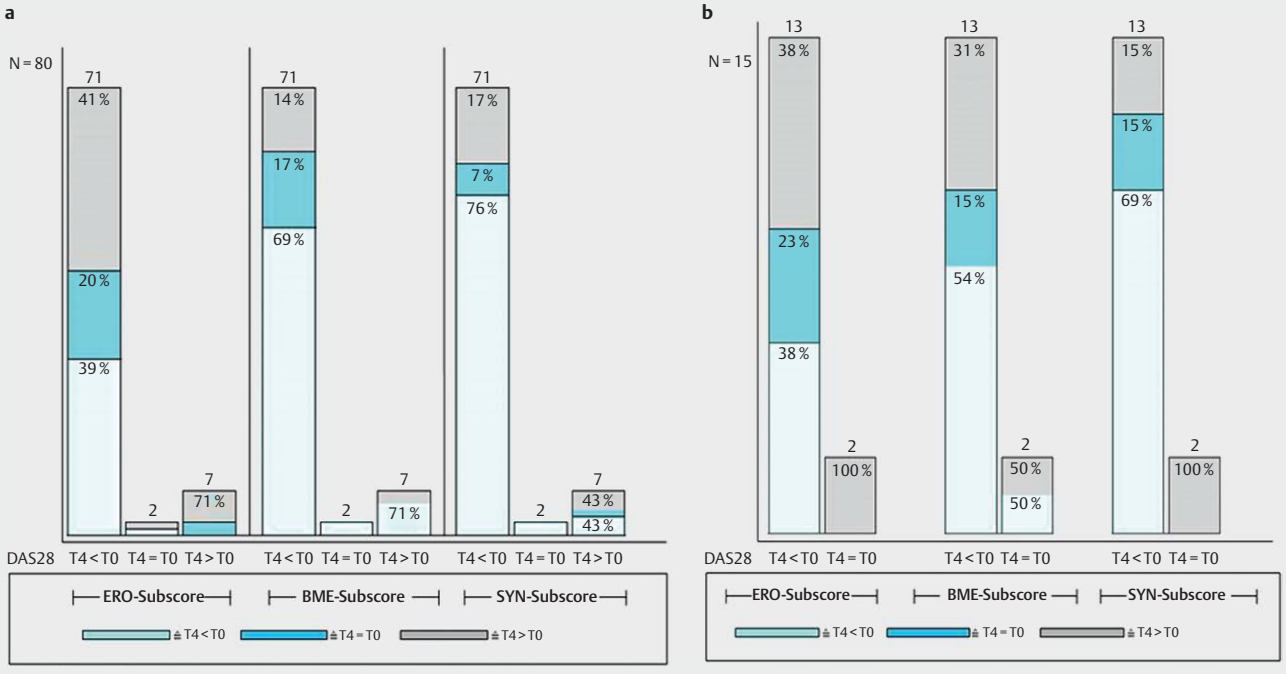


▶ **Abb. 3** Dargestellte Veranderungen im DAS28 (Saulen) und in den ERO-, BME- und SYN-Subscores (T4). **a** bei allen Patienten (n = 80) **b** bei allen Patienten mit einer kurzen Krankheitsdauer (≤ 6 Monate; n = 15).

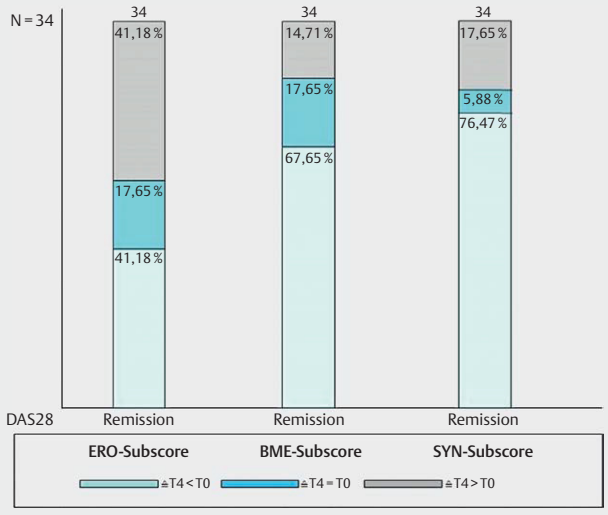


▶ **Abb. 4** Dargestellt werden Patienten in DAS28-Remission (n = 34) und die Veränderungen der Subscores SYN, BME und ERO.

## Klinische Daten im Verlauf

Insgesamt verbesserte sich der DAS28 bei 71 der 80 Patienten (jeweils links Säule ▶ **Abb. 3a/b**, **4**) im oben genannten Zeitraum. 2 Patienten zeigten einen konstanten DAS28 (mittlere Säulen) und 7 Patienten verschlechterten sich in der DAS-Bewertung (rechte Säulen). 45 Patienten erreichten low-disease activity (DAS28 < 3,2) und 34 Patienten erreichen Remission nach EULAR-response Kriterien (DAS28 ≤ 2,6). 66 % dieser 71 Patienten (DAS28 T4 < T0) hatten nach 12 Monaten (T4) einen niedrigeren CRP-Wert als zu T0, 17 % einen unveränderten Verlauf und 17 % ein höheren CRP-Wert als zu T0. Vergleichbare Werte finden sich bei der BSG.

## Niederfeld-MRT-Daten im Verlauf

Betrachtet man die RAMRIS-Scores der 71 Patienten, welche sich im DAS28 verbesserten (klinische Response, ≙ jeweils linke Säulen ▶ **Abb. 3**), so zeigten sich im MRT bei 39 % der Patienten nach 12 Monaten (T4) weniger Erosionen (ERO-Subscore) als bei Einschluss, 20 % wiesen eine gleichbleibende Erosionslast auf und 41 % der Patienten wiesen nach 12 Monaten mehr Erosionen auf als zu Studienbeginn. Betrachtet man das Knochenmarködem (BME-Subscore) so verbesserten sich 69 %, 17 % hatten nach 12 Monaten einen gleichbleibenden BME-Subscore, in 14 % der Fälle ließen sich mehr Knochenmarködeme als zu Beginn (T0) nachweisen. Vergleichbare Werte finden sich für den SYN-Subscore (▶ **Abb. 3a**). Vergleichbare Werte zeigen sich, wenn man nur die 15 Patienten mit einer Krankheitsdauer von ≤ 6 Monaten betrachtet. 38 % der Patienten entwickeln trotz Verbesserung im DAS28 nach 12 Monaten mehr Erosionen als zu T0 (▶ **Abb. 3b**).

## EULAR-Response und „silent progression“

Zur Frage der weiteren radiologischen Progression trotz DAS28-Remission wurden die MRT-Datensätze von 34 Patienten untersucht, die sich nach den EULAR-Kriterien in klinischer Remission (2) zu T4 befanden (n = 34).

Betrachtet man die RAMRIS-Subscores dieser 34 Patienten, so zeigten sich bei 41 % nach 12 Monaten MR-morphologisch mehr Erosionen als zu Beginn der Studie („silent progression“). 18 % der Patienten hatten eine konstante Erosionslast, und bei 41 % konnten nach 12 Monaten weniger Erosionen nachgewiesen werden als zu Beginn. Die Subscores für BME und SYN waren bei 15 % (BME) bzw. 18 % (SYN) der Patienten nach 12 Monaten – trotz klinischer Remission – schlechter als zu T0 (▶ **Abb. 4**).

## RAMRIS-5 (n = 94)

Der traditionelle RAMRIS umfasst 23 Gelenkregionen, wobei die Auswertung des Scores durch die Komplexität sehr zeitaufwändig ist. Aus diesem Grund wurde aus der REMISSION$^{PLUS}$ Kohorte die Wertigkeit eines auf nur noch 5 Gelenke reduzierten RAMRIS-5-Scores evaluiert. Hierbei wurden die Metacarpophalangeal-Gelenke 2–5 dem RAMRIS entsprechend für Erosionen, Knochenmarködeme und Synovialitis gescored. Das Handgelenk selbst floss nur mit dem Parameter Synovialitis als ein zusammengefasstes Gelenk in die Auswertung ein.

Zwischen RAMRIS-5 und dem traditionellen RAMRIS ließen sich für alle Patienten (n = 94) eine hohe Übereinstimmung (r = 0,9, p < 0,05) zu Studienbeginn und nach 12 Monaten (r = 0,8, p < 0,05) nachweisen [21].

## Fuß-MRT (n = 39)

Zur Frage welche Gelenke am Fuß bei der RA am häufigsten betroffen sind ("MRI-pattern"), wurden alle auswertbaren Fuß-MRTs der Gesamtkohorte analysiert. Am häufigsten konnten am MTP5 entzündliche Veränderungen nachgewiesen werden (SYN, BME und/oder ERO). Hier wurden bei 18 % (51 von 292 untersuchten Gelenken) aller untersuchten Gelenke MR-morphologische Zeichen einer Arthritis, gefolgt von entsprechenden Veränderungen am MTP1 (17 %; 49/292), gefunden. Beim SYN-Subscore war das MTP4 Gelenk (19 %) gefolgt vom MTP3 (17 %) und MTP5 (16 %) am häufigsten betroffen. Ähnliche Werte ließen sich beim BME-Subscore nachweisen: MTP3 12 %, MTP4 und MTP5 jeweils 11 % mit Nachweis eines Knochenmarködems. Erosionen (ERO-Subscore) ließen sich am häufigsten am MTP1 (25 %) gefolgt vom MTP5 (24 %) nachweisen. Die Fußwurzelknochen waren deutlich seltener betroffen. Insgesamt waren 71 % aller untersuchten Gelenke MR-morphologisch entzündlich verändert (wiesen also einen positiven SYN-, BME oder ERO-Subscore auf) [22].

## Kombinierter MRT-Hand- und Fuß-Score (n = 26)

Die Auswertung der untersuchten Patienten, welche ein Hand- und Fuß MRT erhielten, CCP-AK positiv waren und Methotrexat (MTX) erhielten, zeigte, dass Änderungen eines kombinierten MRT-Scores (ΔHaF-score) signifikant mit Änderungen des DAS28 (ΔDAS28) nach 6 Monaten korrelierten (r = 0,820, 95 %-CI 0,633–0,916). Darüber hinaus waren die Korrelationen zu Änderungen des DAS28 signifikant besser als solche zum traditionellen RAMRIS (0,5, 0,14–0,74, p = 0,036).

11 der 26 untersuchten Patienten erreichten nach 6 Monaten gutes oder moderates Therapieansprechen nach EULAR-Kriterien. Bei diesen Patienten verbesserte sich der SYN-Subscore deutlich (Hand -2,5; Handgelenk -2,5; Fuß -3,5). Der BME-Subscore verbesserte sich am Fuß stärker als an der Hand und dem Handgelenk (Hand

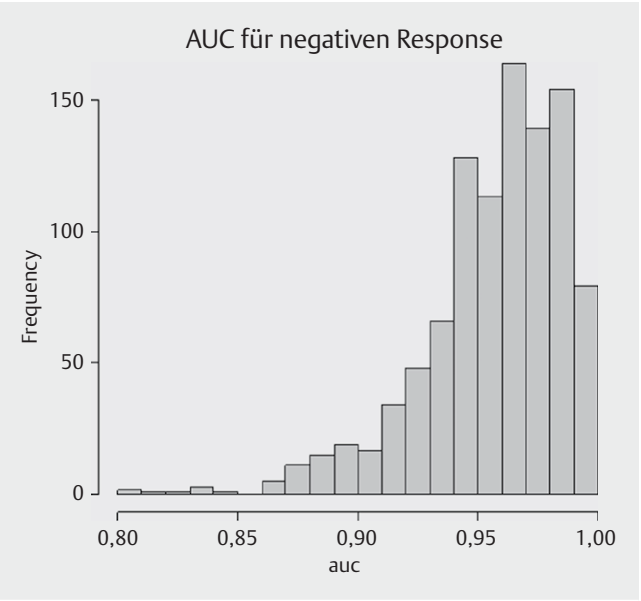


▶ **Abb. 5** Area under the curve (AUC) nach Bootstrap-Verfahren (5 000 simulierte Studien) für negative Response auf Biologika.

-0,8; Handgelenk 0,5; Fuß -3,3), wobei die Erosionslast (ERO-Subscore) in Händen und Füßen eine Verschlechterung zeigte (Hand 0,7; Handgelenk 0,5; Fuß 0,5). Bei allen o.g. Patienten mit moderatem oder guten Therapieansprechen (n = 11) konnten MR-morphologisch weiterhin entzündliche Aktivitäten (SYN- oder BME- Subscore) am Fuß nachgewiesen werden. 5 Patienten entwickelten neue Erosionen, wobei 3 dieser Erosionen an den Füßen lokalisiert waren [23].

### Prädiktions-Score (n = 29) für „Biologika-Non-Responder“

Zur Evaluation eines prädiktiven MRT-Scores wurden Datensätze von 29 Patienten, bei welchen zu Studienbeginn eine Biologika-Therapie begonnen wurde, ausgewertet. 5 dieser 29 Patienten erreichten nach einem Jahr bezüglich EULAR-Response Kriterien den Status „poor-responder“ (DAS28 > 3,2 und/oder Verbesserung des DAS28 von ≤ 0,6) und 24 hatten einen DAS Response (moderat oder gut) erreicht. Mit Hilfe eines logistischen Regressionsmodells welche das Alter, das Vorliegen von Rheumafaktoren, das Geschlecht und den RAMRIS-Gesamtscore zu Studienbeginn einschließt, wurde ein Prädiktionswert errechnet. Aufgrund der geringen Anzahl der auswertbaren Patienten wendeten wir ein „bootstramping“ Verfahren an, bei welchen die Berechnung 5 000-mal simuliert wurde. Es zeigte sich, dass mit einer AUC von 89 % ein negativer Response mit einem MRT zu T0 (Studienbeginn) vorausgesagt werden konnte (▶ **Abb. 5**). Hohe Krankheitsaktivität (klinisch und MR-morphologisch (RAMRIS)) zu Beginn der Biologika-Therapie war hierbei ein protektiver Faktor gegen ein mögliches Nichtansprechen (non-response), wobei niedrige RAMRIS-Scores zu T0 für ein Nichtansprechen prädisponieren [24].

## Diskussion ▪ Ausblick

Die Entwicklung „from bench to bedside“ zeigt, dass viele innovative bildgebende Techniken nach eingehender wissenschaftlicher und klinischer Prüfung ihre Berechtigung und Platz in der Rheumatologie gefunden haben. Die MRT – sei es in der Hochfeld- oder in der Niederfeldtechnik – ist zwar zeitlich noch aufwändig und mit höheren Kosten verbunden, aber aufgrund ihrer vielen Vorteile, d. h. der hohen Sensitivität und auch Spezifität, sowie der Möglichkeit der semiquantitativen Auswertung bzw. des Scorings, ist der Einsatz dieser Methode für den klinischen Alltag als auch für Studien sinnvoll und von Nutzen.

Die Niederfeld-MRT-Studie REMISSION$^{PLUS}$ hat diese Überlegungen bestätigt und gezeigt, dass diese bildgebende Methode gleichwohl in den diagnostischen Algorithmus des Rheumatologen implementierbar ist, vorausgesetzt, entsprechende MRT-Fort- und Weiterbildungen sind vorgeschaltet. REMISSION$^{PLUS}$ hat mit dem Einsatz der Niederfeld-MRT zur Diagnostik und Therapiekontrolle bei RA zu neuen und frühzeitigeren Einblicken in die Gelenkpathologie dieser Erkrankung geführt und eine Vielzahl von neuen Erkenntnissen, aber auch neuen Fragen aufgebracht.

In der REMISSION$^{PLUS}$ MRT-Studie wurden über 300 Patienten untersucht und 146 in die finale Auswertung aufgenommen, sodass erstmals Niederfeld-MRT Daten einer großen deutschen RA-Kohorte für entsprechende Fragestellungen und Auswertung zur Verfügung standen.

Als größte Limitation dieser Studie ist das Studiendesign (offene prospektive Kohorten-Studie) zu nennen, welches über den Studienverlauf ohne regelmäßiges Studienmonitoring, respektive anderen Kontrollmechanismen stattgefunden hat. Hierdurch bemassen sich die Zeiträume der MRT-Verlaufskontrollen eher zentrumsspezifisch und nicht einheitlich. Die finalen MRT-Datensätze müssen daher als inkonsistent heterogen eingestuft werden. Aus diesen Gründen standen nicht alle Datensätze (n = 300), die eingeschlossen wurden, für die finale Auswertung zur Verfügung (n = 146). Ferner wurden die MRT-Untersuchungen von geschulten Rheumatologen befundet und gescored und nicht von Radiologen, auch gab es keine Interreader- oder Intrareader-Analysen an den jeweiligen Zentren. Das einzige Zentrum, welches MRT-Befunde an Hand und Füßen erhoben hat und dies mit Doppelbefundung in Einklang der ortsansässigen Radiologen war der Standort Düsseldorf.

Betrachtet man die MRT-Basisdaten (n = 146) so konnten bei 34 % der Patienten bereits konventionell-radiologisch mindestens eine Erosion erkannt werden. Im Vergleich hierzu ließ sich ein durchschnittlicher RAMRIS von 14 nachweisen, was bedeutet, dass durchschnittlich ca. 14 Gelenkregionen eine Synovialitis, ein Knochenmarködem oder eine Erosion aufwiesen. Zu Studienbeginn waren somit MR-morphologisch bereits im Mittel ca. 6 Erosionen zu finden. Bei 94 % (80 von 85) aller Patienten, welche im konventionellen Röntgenbild keine Erosionen aufwiesen, konnte ein positiver ERO-Subscore im MRT und somit mindestens eine Erosion nachgewiesen werden. Die vorliegenden Daten unterstreichen damit die hohe Sensitivität der MRT auch und gerade im Hinblick auf erosive Veränderungen. Insbesondere bei diesen, konventionell-radiologisch (noch) nicht erosiven Patienten, bietet die MRT einen deutlichen Mehrwert für die individuelle Therapiestratifizierung.

Betrachtet man die REMISSION$^{PLUS}$ Kohorte zu T0 und nach 12 Monaten (n = 80), so zeigte sich bei 71 der 80 Patienten (89 %) zwar eine Verbesserung des DAS28. In den korrespondierenden Niederfeld-MRT-Untersuchungen wiesen aber 41 % dieser 71 Patienten mehr Erosionen als zu T0 auf. 14 % hatten trotz eines verbesserten

DAS28 mehr BME, 17 % mehr Synovialitiden. Vergleichbare Werte ließen sich ebenfalls in der Kohorte mit sehr kurzer Krankheitsdauer ( ≤ 6 Monate) nachweisen. Auch hier waren trotz einer DAS28 Verbesserung 38 % aller Patienten MR-morphologisch progredient erosiv, 31 % wiesen mehr BME und 17 % mehr Synovialitiden auf.

Bereits Brown et al. konnten früher zeigen, dass selbst bei klinisch asymptomatischen Gelenken im MRT bei 96 % der Patienten MR-morphologisch eine Synovialitis und bei 46 % ein Knochenmarködem nachgewiesen werden konnte [25]. In der Folge zeigten die Autoren, dass diese, sogar klinisch asymptomatischen Gelenke bei Vorliegen eines positiven SYN-Subscores oder eines positiven Power-Doppler-Signals in der Gelenksonografie im betroffenen Gelenk ein signifikant erhöhtes Erosionsrisiko aufwiesen [26].

Nach den aktuellen Empfehlungen der EULAR [3] ist eine Verbesserung des DAS28 kein ausreichendes Therapieziel, sodass DAS28 Remission gefordert wird. In den vorliegenden Daten konnten wir zeigen, dass es auch in der Gruppe, welche nach 12 Monaten eine klinische Remission erreichten (n = 34), bei einem nicht unerheblichen Anteil (41 %) der Patienten zu einer MR-morphologischen Progredienz der Erosionslast kommt. Dieses Phänomen radiologischer Progression bei klinischer Remission darf als „silent progression“ bewertet werden und hat für die Therapiestratifizierung als auch Therapieeskalation eine immense Bedeutung. Therapie-Konzepte wie das „step-down tapering“ bei stabiler RA würden auf dem Boden von rein klinischen Remissionskriterien in Kenntnis dieser Bildgebungsdaten mutmaßlich nicht funktionieren. Weitere follow-up Studien mit sensitiver Bildgebung – sei es MRT und/oder US in der Kontrolle – sind hier gefordert.

Vergleichbare Ergebnisse konnten wir im Düsseldorfer Hand/Fuß-MRT-Protokoll bzw. -Score zeigen. Bei allen RA-Patienten, die zumindest ein moderates Ansprechen nach EULAR-Kriterien aufwiesen, konnten MR-morphologisch weiterhin entzündliche Aktivitäten (Synovialitis oder Knochenmarködem/Osteitis) im Fuß-MRT (11 von 11) nachgewiesen werden. Mit dem Düsseldorfer Hand/Fuß-MRT-Score gelang somit die Identifikation von Patienten mit subklinischer Aktivität besser als mit dem klassischen RAMRIS der Hand oder des DAS28 allein. Die Daten unterstreichen, dass klinische Response kein ausreichendes Therapieziel ist, da bei allen Patienten weiterhin entzündliche Aktivität nachgewiesen werden konnte und dass der DAS28 ohne Einschluss der Bewertung der Füße, nicht das alleinige Instrument der Verlaufskontrolle sein kann [23].

Darüber hinaus konnte die Initiative REMISSION$^{PLUS}$ durch standardisierte Dokumentationsbögen national und aufgrund der Einmaligkeit der Untersuchungen und des untersuchten Patientenkollektivs international zur Festigung der Sonografie – und MRT – Diagnostik in der Rheumatologie beitragen. Durch die Beschreibung eines vereinfachten MRT-Scores (RAMRIS-5) konnte ein neues und vereinfachtes Tool evaluiert werden. Die deutliche Zeitersparnis und die gute Vergleichbarkeit mit dem klassischen RAMRIS können dazu beitragen, dass vermehrt standardisiert und somit vergleichbare Untersuchungsbefunde erhoben werden können [21].

Mit dem Düsseldorfer „MRT-Prädiktions-Score” gelang es erstmals, mit nur einem MRT zu T0 mit einer Wahrscheinlichkeit von knapp 90 % ein negatives Therapieansprechen vor Beginn einer Anti-TNF-Therapie vorauszusagen. Eingeflossen in diesen logarithmischen Score sind neben dem Geschlecht das Alter, der Nachweis von Rheumafaktoren bzw. CCP-AK („Seropositivität“) und der RAMRIS-Score zu T0. Insgesamt zeigte sich, dass niedrige RAMRIS-Werte, also wenig MR-morphologisch detektierbare Inflammation/Erosion, mit einem schlechten Therapieansprechen und somit einem höheren Risiko für Therapieversagen einhergeht. In der Literatur sind zahlreiche Faktoren beschrieben, welche negatives Therapieansprechen wahrscheinlicher machen. Hierzu zählen Seropositivität, höheres Alter, bereits eingeschränkter Funktionsstatus sowie die begleitende Prednisolon-Dosis [27]. Niedrigere RAMRIS-Scores sind bisher nicht als ein prädiktiver Faktor für ein schlechtes Therapieansprechen beschrieben. Hingegen konnten Gandjbakhch et al. zeigen, dass persistierende MR-morphologisch erkennbare Synovialitis selbst bei niedriger Krankheitsaktivität radiologisch Progression wahrscheinlicher macht [28].

Die Initiative REMISSION$^{PLUS}$ hat gezeigt, dass nach Schulung von Durchführung und Befundung, die Niederfeld-MRT ein geeignetes Tool in der Therapiekontrolle der RA darstellt. Die Auswertung der MRT-Daten zeigte, dass die Befunde häufig signifikant mit der Klinik und dem Labor korrelieren und somit den Krankheitsstatus gut reflektieren können. Dennoch zeigten viele Patienten, die sich in klinischer Remission befanden, MR-morphologisch noch Aktivitätszeichen. Studien bzw. Folgeuntersuchungen sind hierzu gefragt, um zu entscheiden, wie mit solchen MRT-Ergebnissen im klinischen Alltag umzugehen ist. Des Weiteren sind Anpassungen und Modifikationen beim Einsatz der MRT-Diagnostik sowie die Implementierung in den klinischen Alltag bzw. in den diagnostischen Algorithmus notwendig und zu prüfen. Dazu gehören einfachere Untersuchungsprotokolle und reduzierte Scoring-Methoden, wie von uns vorgestellt. Mit dem RAMRIS-5 konnte durch REMISSION$^{PLUS}$ ein reduzierter MRT-Score etabliert werden, der ähnlich bzw. in Anlehnung an den US7-Score bei der Sonografie folgerichtig prospektiv in einer größeren Kohorte geprüft werden müsste. Dass nicht nur Therapiekontrolle mit der Niederfeld-MRT gelingt, sondern auch eine Prognoseabschätzung, das konnte die Entwicklung bzw. Analyse eines Prädiktionsscore zeigen, der ein Nichtansprechen auf eine Biologika-Therapie vorhersagen kann. Dieser Informationsvorsprung könnte einen relevanten Beitrag zur „personalisierten Medizin” leisten.

Zusammenfassend hat REMISSION$^{PLUS}$ erstmals die Möglichkeit geschaffen, die Methode „Niederfeld-MRT“ praxisnah kennenzulernen, dies nach eingehender selbständiger Bewertung und Studienerfahrung. Da viele Praxen und Kliniken bisher nur beschränkten Zugang zu dieser bildgebenden Technik hatten, konnte hier ein entscheidender Beitrag zur Fort- und Weiterbildung von moderner bildgebender Diagnostik in der Rheumatologie für viele praktizierende Rheumatologen in Deutschland geleistet werden.

## Interessenkonflikt

PS erhielt Referenten und Beratungshonorare der Firma AbbVie Deutschland GmbH & Co. KG;

EE erhielt Referenten- und Beraterhonorare von den Firmen AbbVie Deutschland GmbH & Co. KG und Esaote Biomedica Deutschland GmbH

UML erhielt Referenten und Beratungshonorare der Firma AbbVie Deutschland GmbH & Co. KG

BO erhielt Referenten- und Beraterhonorare von den Firmen AbbVie Deutschland GmbH & Co. KG und Esaote Biomedica Deutschland GmbH

HK erhielt Referenten und Beratungshonorare der Firma AbbVie Deutschland GmbH & Co. KG

WAS erhielt Referenten und Beratungshonorare der Firma AbbVie Deutschland GmbH & Co. KG

SK, RB, AH, CS, FM, SB, GI, GJ, KG, LHM, HGP, HSK, MW, und MS geben an, keine Interessenkonflikte zu haben.

Abbvie Deutschland GmbH & Co. KG finanzierte die zitierten Studien und unterstützte logistisch bei der Durchführung der Datenerfassung.

Abbvie unterstützte Prüfertreffen, Fortbildungen und Expertentreffen der Initiative REMISSION$^{PLUS}$ finanziell und stimmte der Publikation der Ergebnisse zu.

Studendesign, Datenanalysen und Manuskripterstellung lagen ausschließlich in der Hand der Studienleiter und Autoren.

## Literatur


[1] Haraoui B, Smolen JS, Aletaha D et al. Treating Rheumatoid Arthritis to Target: Multinational recommendations assessment questionnaire. Ann Rheum Dis 2011; 70: 1999–2002

[2] Felson DT, Smolen JS, Wells G et al. American College of Rheumatology/European League Against Rheumatism provisional definition of remission in rheumatoid arthritis for clinical trials. Arthritis Rheum 2011; 63: 573–586

[3] Smolen JS, Aletaha D, Bijlsma JWJ et al. Treating rheumatoid arthritis to target: Recommendations of an international task force. Ann Rheum Dis 2010; 69: 631–637

[4] Aletaha D, Neogi T, Silman AJ et al. Rheumatoid arthritis classification criteria: An American College of Rheumatology/European League Against Rheumatism collaborative initiative. Ann Rheum Dis 2010; 69: 1580–1588

[5] Arnett FC, Edworthy SM, Bloch DA et al. The American Rheumatism Association 1987 revised criteria for the classification of rheumatoid arthritis. Arthritis Rheum 1988; 31: 315–324

[6] Bejarano V, Hensor E, Green M et al. Relationship between early bone mineral density changes and long-term function and radiographic progression in rheumatoid arthritis. Arthritis Care Res 2012; 64: 66–70

[7] Baker JF, Ostergaard M, Emery P et al. Early MRI measures independently predict 1-year and 2-year radiographic progression in rheumatoid arthritis: Secondary analysis from a large clinical trial. Ann Rheum Dis 2014; 73: 1968–1974

[8] Gandjbakhch F, Foltz V, Mallet A et al. Bone marrow oedema predicts structural progression in a 1-year follow-up of 85 patients with RA in remission or with low disease activity with low-field MRI. Ann Rheum Dis 2011; 70: 2159–2162

[9] Schmidt WA, Schicke B, Ostendorf B et al. Low-field MRI versus ultrasound: Which is more sensitive in detecting inflammation and bone damage in MCP and MTP joints in mild or moderate rheumatoid arthritis? Clin Exp Rheumatol 2013; 31: 91–96

[10] McQueen FM, Ostendorf B. What is MRI bone oedema in rheumatoid arthritis and why does it matter? Arthritis Res Ther 2006; 8: 222

[11] Møller-Bisgaard S, Hørslev-Petersen K, Ejbjerg BJ et al. Impact of a magnetic resonance imaging-guided treat-to-target strategy on disease activity and progression in patients with rheumatoid arthritis (the IMAGINE-RA trial): Study protocol for a randomized controlled trial. Trials 2015; 16: 178

[12] Ostendorf B, Scherer A, Kellner H et al. Project REMISSION(PLUS): Clinical and radiological remission: New treatment goals in the management of rheumatoid arthritis. Z Rheumatol 2008; 67: 707–710, 712–715

[13] Ejbjerg BJ, Narvestad E, Jacobsen S et al. Optimised, low cost, low field dedicated extremity MRI is highly specific and sensitive for synovitis and bone erosions in rheumatoid arthritis wrist and finger joints: Comparison with conventional high field MRI and radiography. Ann Rheum Dis 2005; 64: 1280–1287

[14] Duer-Jensen A, Vestergaard A, Døhn UM et al. Detection of rheumatoid arthritis bone erosions by two different dedicated extremity MRI units and conventional radiography. Ann Rheum Dis 2008; 67: 998–1003

[15] Ostendorf B, Edelmann E, Kellner H et al. Low-field magnetic resonance imaging for rheumatoid arthritis. Z Rheumatol 2010; 69: 79–86

[16] Backhaus M, Ohrndorf S, Kellner H et al. Evaluation of a novel 7-joint ultrasound score in daily rheumatologic practice: A pilot project. Arthritis Rheum 2009; 61: 1194–1201

[17] Backhaus TM, Ohrndorf S, Kellner H et al. The US7 score is sensitive to change in a large cohort of patients with rheumatoid arthritis over 12 months of therapy. Ann Rheum Dis 2013; 72: 1163–1169

[18] Hartung W, Kellner H, Strunk J et al. Development and evaluation of a novel ultrasound score for large joints in rheumatoid arthritis: one year of experience in daily clinical practice. Arthritis Care Res 2012; 64: 675–682

[19] Ohrndorf S, Fischer IU, Kellner H et al. Reliability of the novel 7-joint ultrasound score: Results from an inter- and intraobserver study performed by rheumatologists. Arthritis Care Res 2012; 64: 1238–1243

[20] Østergaard M, Peterfy C, Conaghan P et al. OMERACT Rheumatoid Arthritis Magnetic Resonance Imaging Studies. Core set of MRI acquisitions, joint pathology definitions, and the OMERACT RA-MRI scoring system. J Rheumatol 2003; 30: 1385–1386

[21] Schleich C, Buchbender C, Sewerin P et al. Evaluation of a simplified version of the Rheumatoid Arthritis Magnetic Resonance Imaging Score (RAMRIS) comprising 5 joints (RAMRIS5). Clin Exp Rheumatol 2015; 33: 209–215

[22] Buchbender C, Scherer A, Miese F et al. Patterns of magnetic resonance imaging of the foot in rheumatoid arthritis: Which joints are most frequently involved? Rheumatol Int 2013; 33: 1731–1736

[23] Sewerin P, Buchbender C, Vordenbäumen S et al. Advantages of a combined rheumatoid arthritis magnetic resonance imaging score (RAMRIS) for hand and feet: Does the RAMRIS of the hand alone underestimate disease activity and progression? BMC Musculoskelet Disord 2014; 15: 104

[24] Sewerin P, Brinks R, Schleich C et al. FRI0028 Gazing into the Crystal Ball? Prospective MRI Score to Predict Negative Eular-Response in Patients with Rheumatoid Arthritis (RA) Before Therapy-Escalation to a Biological Therapy. Ann Rheum Dis 2015; 74 (Suppl 2): 428

[25] Brown AK, Quinn MA, Karim Z et al. Presence of significant synovitis in rheumatoid arthritis patients with disease-modifying antirheumatic drug-induced clinical remission: Evidence from an imaging study may explain structural progression. Arthritis Rheum 2006; 54: 3761–3773

[26] Brown AK, Conaghan PG, Karim Z et al. An explanation for the apparent dissociation between clinical remission and continued structural deterioration in rheumatoid arthritis. Arthritis Rheum 2008; 58: 2958–2967

[27] Hetland ML, Christensen IJ, Tarp U et al. Direct comparison of treatment responses, remission rates, and drug adherence in patients with rheumatoid arthritis treated with adalimumab, etanercept, or infliximab: Results from eight years of surveillance of clinical practice in the nationwide Danish DANBIO registry. Arthritis Rheum 2010; 62: 22–32

[28] Gandjbakhch F, Haavardsholm EA, Conaghan PG et al. Determining a magnetic resonance imaging inflammatory activity acceptable state without subsequent radiographic progression in rheumatoid arthritis: Results from a followup MRI study of 254 patients in clinical remission or low disease activity. J Rheumatol 2014; 41: 398–406

Sewerin et al. BMC Musculoskeletal Disorders (2017) 18:163
DOI 10.1186/s12891-017-1528-y

BMC Musculoskeletal Disorders

RESEARCH ARTICLE Open Access

# Silent progression in patients with rheumatoid arthritis: is DAS28 remission an insufficient goal in RA? Results from the German Remission-plus cohort

Philipp Sewerin[1*], Stefan Vordenbaeumen[1], Annika Hoyer[2], Ralph Brinks[1], Christian Buchbender[3], Falk Miese[3], Christoph Schleich[3], Sabine Klein[1], Matthias Schneider[1] and Benedikt Ostendorf[1]

## Abstract

**Background:** Remission is arguably the ultimate therapeutic goal in rheumatoid arthritis (RA). Applying modern strategies, clinical remission can be achieved in a substantial number of patients with early RA (ERA). Even in those patients, the number and scope of erosions can increase. We, therefore, investigated the value of MRI for the detection of radiological progression in patients with DAS28 improvement and/or clinical remission of the German Remission-plus cohort.

**Methods:** Data-sets of 80 RA patients (according to 2010 ACR/EULAR criteria) from the Remission-plus study cohort, who fulfilled the following criteria, were retrospectively analysed: availability of two consecutive MRI scans (low-field MRI, follow-up interval 1 year) of the clinically dominant hand and wrist, and the presence of DAS28 (CRP) scores at both time points, which was used to assess disease activity.

**Results:** Seventy-one of the 80 investigated patients presented a numerical improvement of the DAS28 (CRP) after 12 months (DAS28(CRP) T0 average (Ø) 4.96, SD 1.2; DAS28 T4 (12 month) Ø 2.6, SD 1.0), 73% of them also improved in the RAMRIS-Score, while 24% demonstrated an increase despite DAS28 improvement and 3% showed equal values. 48% of patients who improved in the DAS28 reached EULAR remission. 41% of these patients had an increase in the RAMRIS Erosion-subscore after 12 months. When considering EULAR response criteria (non-response ($n = 7$), moderate response ($n = 19$), good response ($n = 45$)), an increase of erosions was found in 71.4% of non-responders, 52.6% of moderate responders, and 31.1% of good responders after 12 months, all compared to baseline.

**Conclusion:** Up to 40% of patients in this study demonstrated a progressive erosive disease detected by MRI despite DAS28 improvement or EULAR remission. Future studies are needed to determine the prognostic clinical impact of disease progression in MRI despite clinical remission, and to investigate if DAS28 remission may be an insufficient therapeutic goal and should be accompanied by MRI remission criteria.

**Keywords:** Magnetic resonance imaging, Rheumatoid arthritis, RAMRIS, Therapy monitoring, Remission, Silent progression

* Correspondence: philipp.sewerin@med.uni-duesseldorf.de
[1]Department of Rheumatology & Hiller Research Unit, University Hospital Düsseldorf, Moorenstreet 5, Duesseldorf 40225, Germany
Full list of author information is available at the end of the article

## Background

Remission in rheumatoid arthritis [RA] is arguably the ultimate goal of an anti-rheumatic therapy [1, 2]. With modern therapeutic strategies, this goal can be achieved in the majority (up to 80%) of patients with early RA (ERA) [3]. In this context, remission has been defined as a "state of absent disease activity". In contrast, flares are defined as "a substantial increase of disease activity" associated with more radiological progression and worse functional outcome [4]. Hence, continuous remission is the desired target state. A variety of response scores for RA patients based on clinical and serological data have been proposed and applied in clinical trials [5]. Among these, the American College of Rheumatology (ACR) response criteria, which rely on a relative change of five core set variables [6], and the European League Against Rheumatism (EULAR) response criteria, which are based on an absolute change of the composite Disease Activity Score in 28 joints (DAS28) including the ACR/EULAR remission criteria [7–9], are most common.

In 2002, the OMERACT (Outcome Measures in RA Clinical Trials) magnetic resonance imaging (MR)I-group introduced a highly reliable sum-score (RA MRI Score (RAMRIS)) [10] based on the semi-quantitative rating of the severity of synovitis, bone marrow edema and bone erosions in the joints of the hand and wrist [10, 11]. The RAMRIS system has been shown to be a sensitive tool for the evaluation of therapy in patients receiving conventional synthetic and biologic DMARDs (Disease-modifying anti-rheumatic drugs) [12, 13] similar to scores measuring clinical and serological parameters [14]. However, Emery et al. reported a weak correlation between the individual change of the RAMRIS and the change of the DAS28 and C-reactive protein (CRP) levels, respectively. This was thought to be due to superior sensitivity of MRI compared to DAS28 and CRP [15]. It is additionally known that the number and scope of erosions can increase instead of clinically low disease activity or remission (measured by DAS28). In particular, the existence and continuous presence of bone marrow edema as depicted by MRI is the strongest predictor for bony erosiveness in RA patients [16, 17]: Imaging studies with ultrasound and MRI revealed signs of synovitis and/or bone marrow edema in patients with clinical remission (i.e. according to ACR or EULAR criteria). This phenomenon, often denominated "silent progression", thus came into scientific focus [18, 19]. Consequently, the question was raised whether extended remission criteria which incorporate modern imaging tools could be of superior value compared to clinical composite indices [20].

We, therefore, investigated the value of MRI for the detection of erosive changes in patients with DAS28 improvement and/or remission of the German Remssion-plus cohort [21].

## Methods

### Study design

Retrospective analysis was done on the Remission-plus cohort in which the data had been prospectively evaluated [21].

### Patients cohort

Datasets of 146 RA patients from the Remission-plus study cohort who fulfilled the ACR/EULAR 2010 Criteria for RA [21] were retrospectively analysed in this study. Moreover, 80 patients who fulfilled advanced inclusion criteria consisting of (1) availability of two consecutive MRI scans (follow-up interval 1 year) of the clinically dominant hand and wrist, (2) the presence of DAS28 (CRP) scores at both time points and (3) had an DAS28 > 3,2 at T0 were investigated.

### Clinical assessment

The following EULAR core set of variables was recorded: patient's global assessment of overall disease activity, number of tender and swollen joints, erythrocyte sedimentation rate (ESR) and C-reactive protein (CRP (<5 mg/l)).

The DAS28 [22] was used to assess disease activity. Changes of disease activity were graded by the following classification criteria: DAS28 < 2.6 = clinical remission, ≤ 3.2 mild disease activity < 5.2 moderate disease activity and > 5.2 severe disease activity [23, 24].

**Table 1** Patient's characteristics at T0 (begin of the study) including the sex, disease duration, seropositivity, conventional x-rays, clinical and laboratory parameters and MRI scores (RAMRIS and RAMRIS-Subscores)

| *N* = 80 | |
|---|---|
| Male | 24 [30%] |
| Female | 56 [70%] |
| Disease-duration <6 month | 15 [19%] |
| Disease-duration <24 month | 42 [53%] |
| Disease-duration ≥24 month | 38 [47%] |
| RF pos. | 47 [59%] |
| CCP antibody pos. | 49 [62%] |
| Erosiv x-rays | 23 [32%] [missings *n* = 9] |
| CRP [mg/l] | 9.35 [SD 15.61; Min 1, Max 88] |
| DAS28 | 2.98 [SD 1.2; Min 1, Max 6,8] |
| RAMRIS | 7,78 [SD 7.16; Min 0, Max 33] |
| SYN-subscore | 2,34 [SD 2.54; Min 0, Max 11] |
| ERO-subscore | 4,39 [SD 4.74; Min 0, Max 19] |
| BME-subscore | 1,05 [SD 1.96; Min 0, Max 12] |

### EULAR response assessment

Therapy response was graded by the following improvement criteria proposed by the EULAR committee [7, 8]: DAS28 decrease >1.2 units and endpoint score <3.2 = good response, DAS28 decrease >1.2 units and endpoint score >3.2 or DAS28 decrease 0.6–1.2 units and endpoint score <5.1 = moderate response, DAS28 decrease <0.6 or DAS28 decrease 0.6–1.2 units and endpoint score >5.1 = poor response.

### Imaging procedure [low-field MRI examination]

All examination were performed with the same low-field strength 0.2-T dedicated extremity MRI unit (Esoate, C-Scan, Esaote Biomedica Germany GmbH), and the same dedicated, dual phased-array coil. The clinically dominant hand was examined. Patients with renal dysfunction and known allergic reactions to gadolinium-diethylenetriaminepentaacetic acid (Gd-DTPA) were excluded from the study. The imaging protocol comprised pre- and post-contrast (i.v. gadolinium-based MRI contrast material, e.g. Magnevist, Schering AG, Berlin) T1-weighted images with a maximum slice thickness of 3 mm in at least two orthogonal planes and coronal fat-suppressed short tau inversion recovery (STIR) sequences [in detail coronar T1-weighted before contrast agent, coronar fat-suppressed STIR before contrast agent, 3-D GE T1-weighted after contrast agent with multiplanar reconstruction in three slide positions, coronar T1- weighted after contrast agent, axial T1-weighted after contrast agent].

### MRI-scoring (RAMRIS)

MRI images were scored in each centre by MRI trained rheumatology specialists according to the RAMRIS based on OMERACT recommendations [10]. MR images were read in consensus by two board-certified radiologists with special expertise in musculoskeletal MRI and trained for RAMRIS scoring.

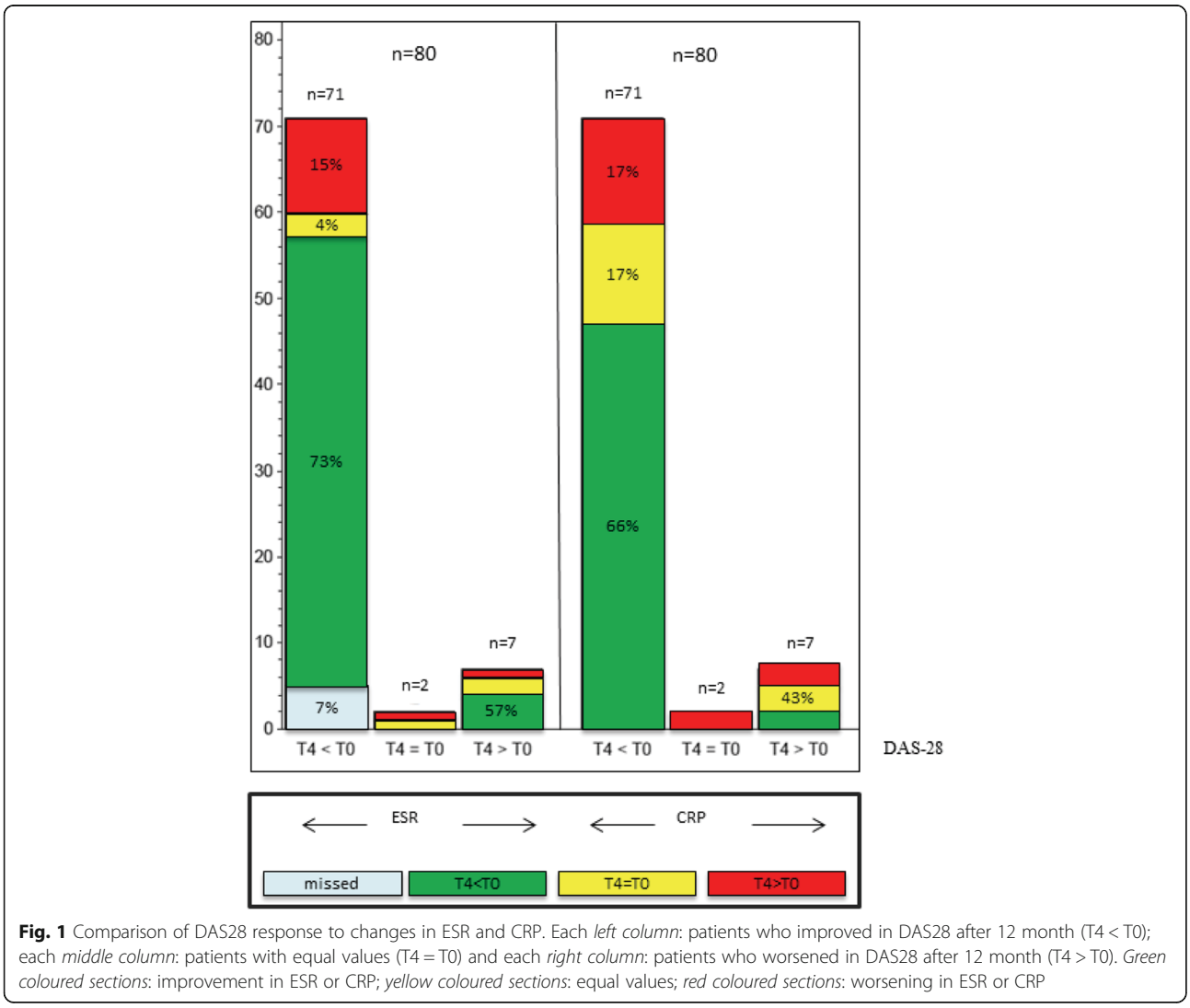


**Fig. 1** Comparison of DAS28 response to changes in ESR and CRP. Each *left column*: patients who improved in DAS28 after 12 month (T4 < T0); each *middle column*: patients with equal values (T4 = T0) and each *right column*: patients who worsened in DAS28 after 12 month (T4 > T0). *Green coloured sections*: improvement in ESR or CRP; *yellow coloured sections*: equal values; *red coloured sections*: worsening in ESR or CRP

### Statistical analysis

Results of the analyses were reported as absolute numbers and percentages where appropriate. Data management and analysis was performed with SAS, version 9.3 (SAS Institute, Cary, North Carolina).

## Results

### Characteristics of patients

Overall, 146 patients were included in the Remission-plus cohort. 64 patients were excluded due to pregnancy, death, movement or loss to follow-up. Finally, 80 patients were included in the final evaluation (30% male, 70% female). 19% showed a disease duration of less than 6 months, while 53% presented disease duration of less than 24 months, and 47% showed a disease duration of more than 24 months. The entry patient characteristics are outlined in Table 1.

### Erosiveness at TO

At T0 (begin of the study) conventional x-rays of the hands were performed. 23 of the 71 patients (32%, 9 missings) already showed at least one erosion in plane x-rays of the hand while 48 patients had no detectable erosions. Regarding the concordant MRI scans, 44 of these 48 patients [92%] showed at least one single erosion in the MRI scans (Erosion (ERO)-subscore ≥ 1).

### Clinical improvement and MRI results

Seventy-one of the 80 analysed patients presented a clinical improvement of the DAS28 after 12 months (T4), while two showed a stable disease activity and 7 worsened (DAS28(CRP) T0 average (Ø) 4.96; SD 1.2; DAS28 T4 (12 month) Ø 2.6; SD 1.0) (Fig. 1).

After 12 months, 73% of the 71 patients who improved in DAS28 showed a lower RAMRIS-Score, while 24% worsened despite DAS28 improvement, 3% showed equal values (Fig. 2). When considering RAMRIS-Subscores, 41% ($n = 29$) of these 71 patients had more erosions on MRI compared to baseline (ERO-subscore T4 > T0), while 39% showed less erosions (T4 < T0) after 12 months. Hence, 8 of 29 patients who worsened in ERO-subscore showed a difference of 1 point while 21 (approximately 72%) patients changed by at least 2 points. Regarding the affected joints, the proximal metacarpophalangeal (MCP) 2-joint was most frequently affected by worsening in ERO-subscore (9/29) followed by the trapezoid bone (6/29), the proximal MCP-3 (4/29) and proximal MCP-4 joint (4/29). Only 1/29 patients worsened in the PIP joints. We studied in addition the impact of age, sex, antibody status, systemic inflammation (CRP) and RAMRIS-subscores and found no relevant association.

In contrast, the intensity of Bone Marrow Edema (BME) and Synovitis (SYN) in MRI decreased in accordance to clinical improvement in 69% (BME) and 76% (SYN) (Fig. 3).

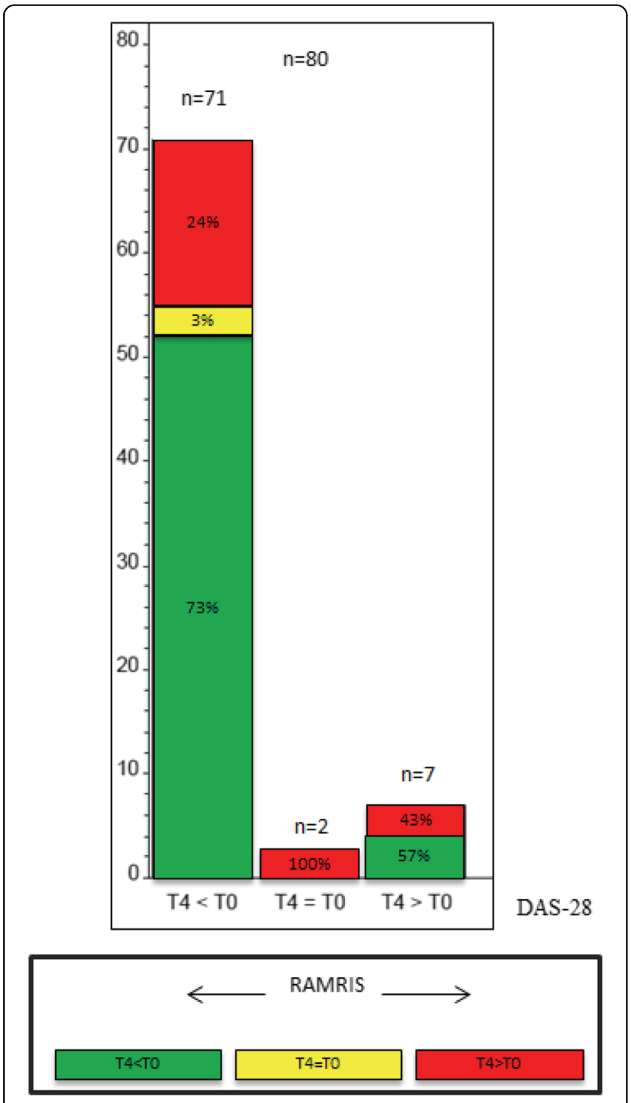


**Fig. 2** Comparison of DAS28 response to changes in RAMRIS. *Left column*: patients who improved in DAS28 after 12 month (T4 < T0); *middle column*: patients with equal values (T4 = T0); *right column*: patients who worsened in DAS28 after 12 month (T4 > T0). *Green coloured sections*: improvement in RAMRIS; *yellow coloured sections*: equal values; *red coloured sections*: worsening in RAMRIS

In a subgroup of patients with a short disease duration (<6 month, $n = 15$), tantamount results were found: 38% showed less erosions after 12 months of treatment, 23% a stable erosion score and 38% increased erosions score despite DAS28 improvement (Fig. 4).

### MRI criteria with respect to EULAR remission

Thirty four of the 71 patients who improved in DAS28 reached EULAR remission. Despite remission, 41% of all patients who attained remission showed an increased ERO-subscore after 12 months (T4) (Fig. 5).

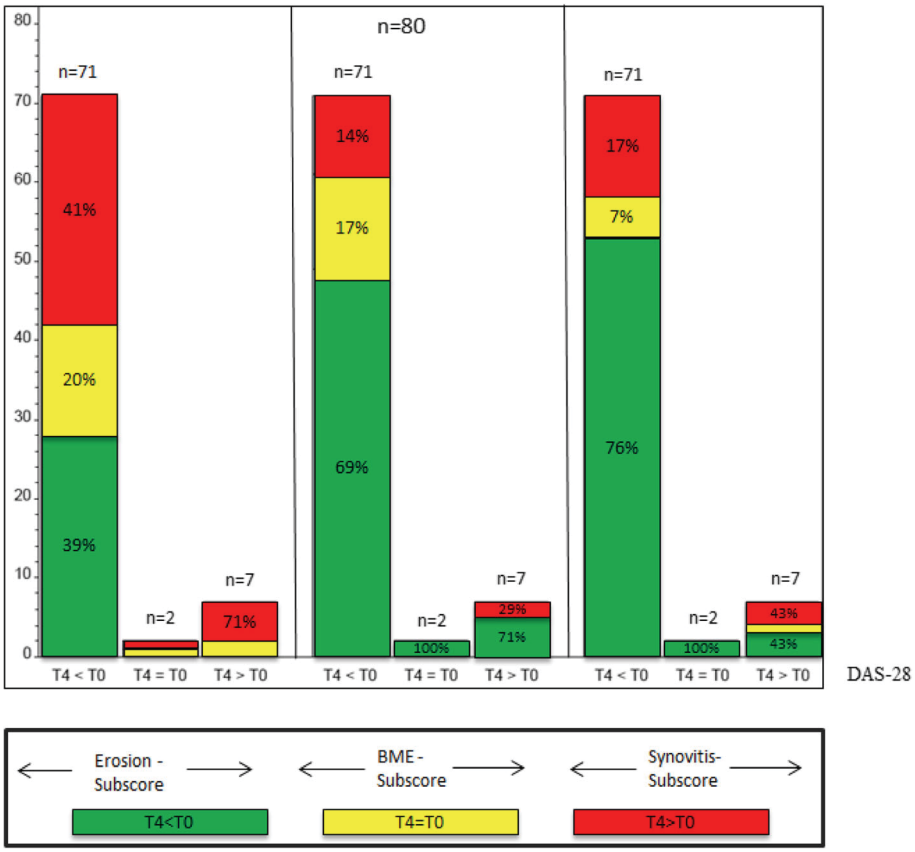


**Fig. 3** Comparison of DAS28 response to changes in Erosion-subscore, Bone-Marrow Edema (BME)-subscore and Synovitis-subscore of the RAMRIS Score. Each *left column*: patients who improved in DAS28 after 12 month (T4 < T0); each *middle column*: patients with equal values (T4 = T0); each *right column*: patients who worsened in DAS28 after 12 month (T4 > T0). *Green coloured sections*: improvement in the RAMRIS-subscores; *yellow coloured sections*: equal values; *red coloured sections*: worsening in RAMRIS-subscores

### MRI changes with respect to EULAR response

Of the 71 patients who improved in DAS28 after 12 months, 7 showed EULAR non-response, 19 had moderate and 45 good EULAR responses. An increase of erosions was found in 71.4% of non-responders, 52.6% of moderate responders, and 31.1% of good responders at T4, all compared to baseline (Fig. 6). Representative MR-Images are shown in Fig. 7.

## Discussion

Remission is the ultimate goal in RA-therapy. This has been underscored by successful applications of the Treat-to-Target (T2T)-strategies in studies and clinical practice in the last few years [2]. Interestingly, MRI does not always reflect clinical improvement, but on the contrary, does show persisting or progressive joint pathologies in a considerable number of cases in most studies [25, 26]. However, the presence of erosions is associated with a high risk of progression of the disease, while this was only shown for erosions in conventional x-rays, yet [27, 28]. Up until now, therapy response criteria like the well-established EULAR response criteria are based on different constellations of clinical data, while matching MRI criteria are not available. In our study, a high number of 94% of patients showed erosions on MRI in at least one region. Importantly, roughly 40% of all patients who improved in DAS28 or who were in EULAR-defined remission, showed an increase of MR-detectable erosions after 12 months. Approximately 72% of these patients who worsened in ERO-subscore showed a subscore-deterioration of at least 2 points, so that an inaccuracy of the measurement is unlikely and a veritable increase of the MR-detectable erosivness must be assumed. Moreover, there was no relevant distinction between early and late RA, as even patients with a short disease-duration (less than 6 months) progressed.

The course of erosive changes depended on EULAR response in the current study: patients showing DAS28 improvement but EULAR non-response presented an increase of erosiveness in almost 72% of the patients, while only 31% of patients with good EULAR response had progressive erosions in MRI. Thus, our data is in accordance with a study by Van Gestel et al. who demonstrated that the improvement regarding the

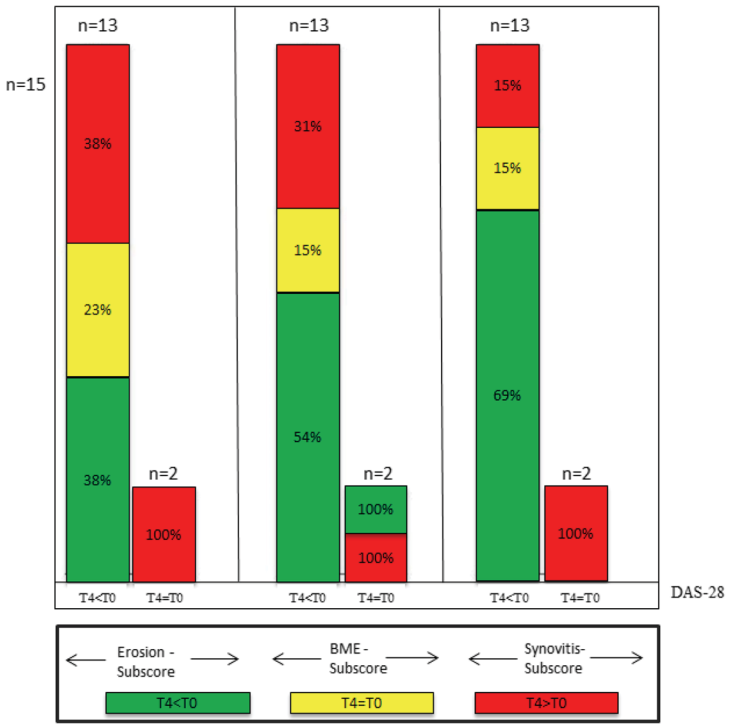


**Fig. 4** Comparison of DAS28 response to changes in Erosion-subscore, Bone-Marrow Edema (BME)-subscore and Synovitis-subscore of the RAMRIS Score of patients with short disease duration (less than six month). Each *left column*: patients who improved in DAS28 after 12 month (T4 < T0); each *right column*: patients with equal values (T4 = T0). *Green coloured sections*: improvement in the RAMRIS-subscores; *yellow coloured sections*: equal values; *red coloured sections*: worsening in RAMRIS-subscores

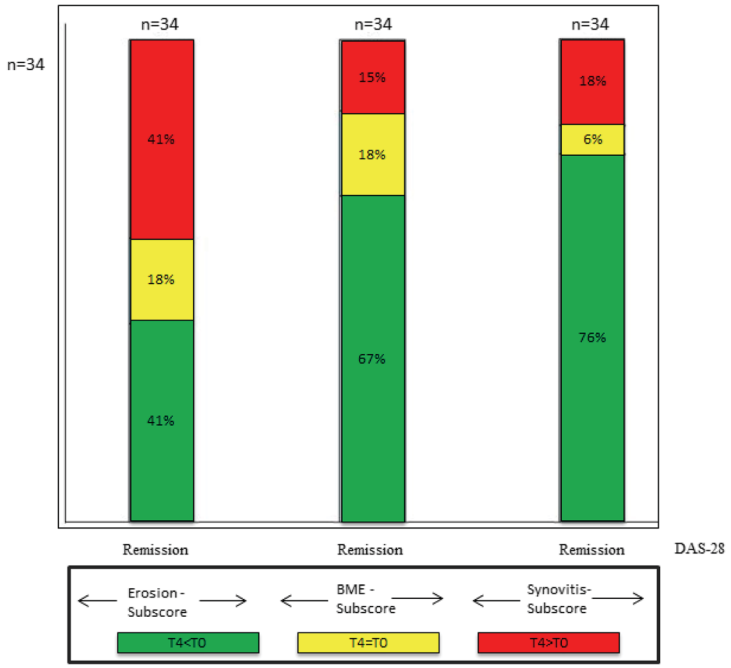


**Fig. 5** Comparison of patients who reached DAS28-remission to changes in Erosion-subscore, Bone-Marrow Edema (BME)-subscore and Synovitis-subscore of the RAMRIS Score. *Green coloured sections*: improvement in the RAMRIS-subscores; *yellow coloured sections*: equal values; *red coloured sections*: worsening in RAMRIS-subscores

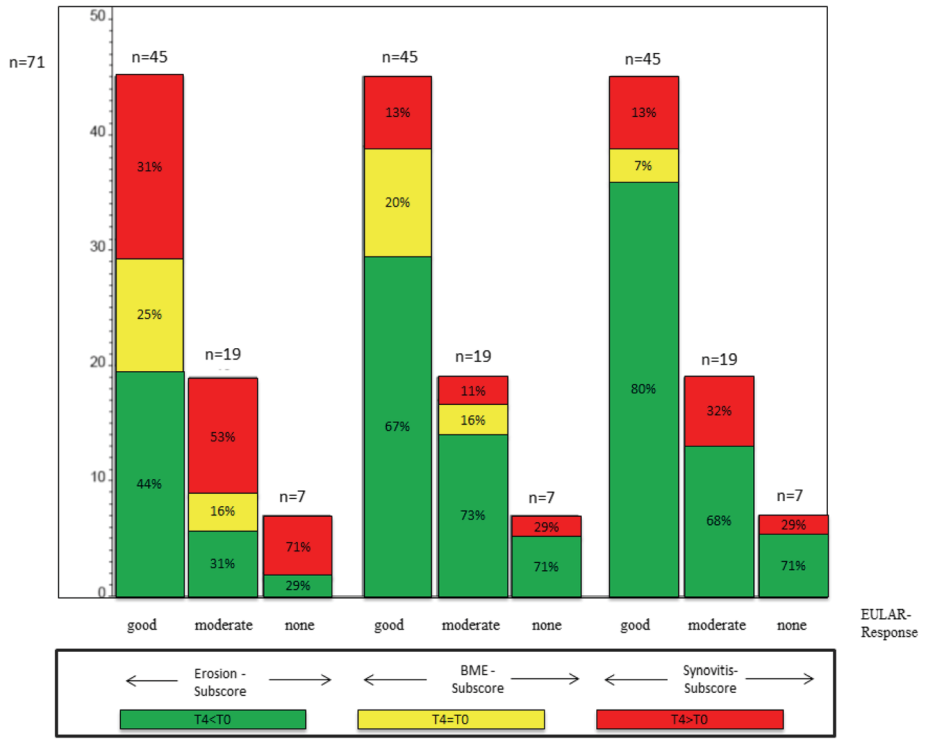


**Fig. 6** Comparison of patients who improved in DAS28 after 12 month to changes in Erosion-subscore, Bone-Marrow Edema (BME)-subscore and Synovitis-subscore of the RAMRIS Score. *Each left column*: patients who reached good EULAR-response regarding the EULAR response criteria (DAS28) after 12 month (T4 < T0); each middle column:patients moderate EULAR-response (T4 = T0); each *right column*: patients who reached none EULAR-response but improved in DAS28 after 12 month (T4 > T0). *Green coloured sections*: improvement in the RAMRIS-subscores (ERO, BME or SYN); *yellow coloured sections*: equal values; *red coloured sections*: worsening in RAMRIS-subscores

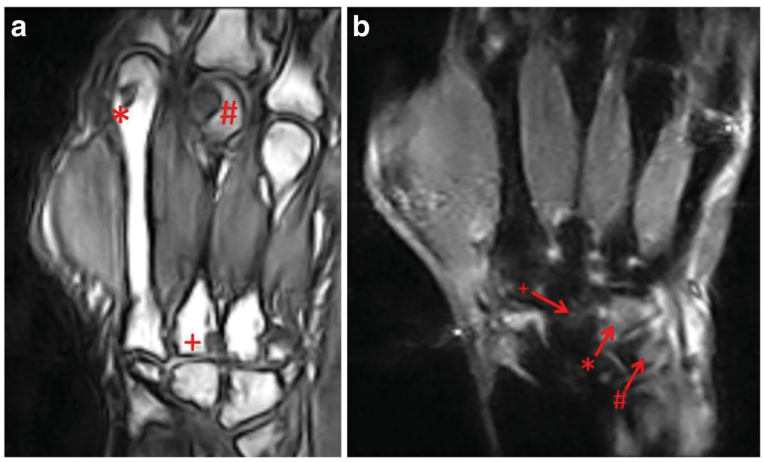


**Fig. 7 a** Nativ T1-weighted image in coronal orientation. Erosion grade 1 in the head of metacarpus D2 (*), erosion grade 3 in the head of metacarpus 3 (#). Additionally, erosion of the basis of metacarpus 3 (+). The RAMRIS score of this patient was 48. **b** Short-Tau-Inversion-Recovery Sequenz (STIR) in coronal orientation: Osteoedema in Os hamatum (*arrow with* *) and Os triquetrum (*arrow with #*) grade 3. Additionally grade 2 osteodema in Os scaphoideum (*arrow with* +). The whole RAMRIS score was 43

EULAR-response criteria is associated with less disease progression considering the clinical and conventional radiological course (highly sensitive imaging tools like MRI were not considered in this study) [8]. In contrast, it has been demonstrated that up to 20–30% of patients reaching clinical remission showed progressive erosive joint damage (silent progression) [9, 29]. Regarding the presented data, the proximal MCP-2 joints were most frequently affected by worsening in the ERO-subscore followed by the trapezoid bone and the proximal MCP-joints 3 and 4. The PIP joints were almost not affected (1/29). Regarding our additional analyses for possible predictive markers for silent progression (age, sex, antibody status, systemic inflammation (CRP) and RAMRIS-subscores), there were no statistical significant associations. However, we note that the study was not powered for specific subgroup analysis. It is known that erosive changes and BME detected by MRI lead to bone erosions which can be depict by conventional x-rays later on [16]. There is a lot of evidence that erosive progression in conventional x-rays is related to functional loss in the course of disease [30–32], while there is a lack of long term MRI data investigating the functional meaning of MR-detectable erosions, yet. Regarding that, long-term studies focused on this question are urgently needed.

Due to these issues, supplementary use of MRI scans could be of additional value to evaluate the therapy response, for example by using a smaller field of view to achieve a shorter examination time. In summary, MRI data in clinical routine confirm a high rate of silent progression despite DAS28 improvement or remission.

This study has some limitations. First, low-field MRI is used which is known to have a poorer local resolution in comparison to high-field MRI. Moreover, this multicentre study was a "real life" study without a static protocol, so that some patients were lost to follow-up or were excluded due to incomplete data. The study is not controlled for confounders such as RF, CCP-status, smoking or ethnicity. Moreover, we cannot completely exclude that progressive erosiveness detected by low-field MRI overestimates the risk of progression. In addition to that, it must be recognized that erosions were scored by MRI which is known as a very sensitive tool and could lead to occasionally over-interpretation. Hence, some sequences (for example STIR-sequences) are not fully comparable to high-field MR-scans due to the poorer resolution. To solve this last issue, both compound scores, such as the DAS28 and MRI based scores (e.g. RAMRIS), should be evaluated against gold standards such as functional or conventional radiological outcome measures in the long term in future studies.

## Conclusion

In conclusion, approx. 40% of patients demonstrated a progressive erosive RA detected by MRI despite DAS28 improvement or EULAR remission. Data is accumulating that DAS28 remission may be an insufficient therapy goal in RA. This is the first study showing the very high number of MRI-progression in RA patients despite clinical remission. Hence, MRI should be considered as a secondary outcome measure in interventional therapeutic trials with subsequent observational extension including functional measures and conventional x-rays to systematically assess this question.

### Abbreviations

ACR: American college of rheumatology; BME: Bone marrow edema; CI: Confidence interval; CRP: C-reactive protein; DAS28: Disease activity score 28; DMARD: Disease modifying anti rheumatic drug; ERA: Early rheumatoid arthritis; ERO: Erosion; ESR: Erythrocyte sedimentation rate; EULAR: European league against rheumatism; Gd-DTPA: Gadolinium-diethylenetriami nepentaacetic acid; MCP joint: Metacarpophalangeal joint; MRI: Magnetic resonance tomography; MTX: Methotrexate; OMERACT: Outcome Measures in RA Clinical Trials; RA: Rheumatoid arthritis; RAMRIS: Rheumatoid arthritis magnetic resonance imaging score; STIR: Short tau inversion recovery; SYN: Synovitis

### Acknowledgements

We would like to thank Erika Rädisch for the assistance in receiving the MRI-scans.

### Funding

This study was supported by AbbVie Immunology Germany (Remission-plus Initiative) and Esoate GmbH Deutschland. This article presents independent research data. The views expressed are those of the author(s) and not those of the sponsors. The study funders had no role in the study design, data collection, analysis or interpretation, in the writing of the paper or in the decision to submit the paper for publication.

### Availability of data and materials

The datasets used and/or analysed during the current study are available from the corresponding author on reasonable request.

### Authors' contributions

PS, CB, MS, and BO designed the study. PS, SV, CB, FM, CS, SK, MS and BO conducted the study. PS, SV, CB, FM, CS, SK, MS and BO collected the data. PS, SV, AH and RB analysed the data. PS, SV, AH, RB, CB, FM, CS, SK, MS and BO interpreted the data. PS drafted the manuscript. PS, SV, AH, RB, CB, FM, CS, SK, MS and BO revised manuscript content. PS, AH and RB take responsibility for the integrity of the data analysis. All authors read and approved the final manuscript.

### Authors' information

Not applicable.

### Competing interests

The authors declare that they have no competing interests.

### Consent for publication

Not applicable.

### Ethics approval and consent to participate

Ethical approval for the study was received from the ethics committee of the Heinrich-Heine University of Duesseldorf (reference number: 3226) and all patients provided written informed consent.

## Publisher's Note



### Author details

[1]Department of Rheumatology & Hiller Research Unit, University Hospital Düsseldorf, Moorenstreet 5, Duesseldorf 40225, Germany. [2]German Diabetes

Centre, Institute for Biometry and Epidemiology, Auf'm Hennekamp 65, Duesseldorf 40225, Germany. [3]Department of Diagnostic and Interventional Radiology, University Hospital Düsseldorf, Moorenstreet 5, Duesseldorf 40225, Germany.

Received: 29 September 2016 Accepted: 7 April 2017
Published online: 19 April 2017

## References

1. Mierau M, Schoels M, Gonda G, Fuchs J, Aletaha D, Smolen JS. Assessing remission in clinical practice. Rheumatology (Oxford). 2007;46(6):975–9.
2. Smolen JS, Aletaha D, Bijlsma JWJ, Breedveld FC, Boumpas D, Burmester G, et al. Treating rheumatoid arthritis to target: recommendations of an international task force. Ann Rheum Dis. 2010;69(4):631–7.
3. Emery P, McInnes IB, van Vollenhoven R, Kraan MC. Clinical identification and treatment of a rapidly progressing disease state in patients with rheumatoid arthritis. Rheumatology (Oxford). 2008;47(4):392–8.
4. Felson DT, Smolen JS, Wells G, Zhang B, van Tuyl LHD, Funovits J, et al. American College of Rheumatology/European League Against Rheumatism provisional definition of remission in rheumatoid arthritis for clinical trials. Arthritis Rheum. 2011;63(3):573–86.
5. Smolen JS, Aletaha D. Monitoring rheumatoid arthritis. Curr Opin Rheumatol. 2011;23(3):252–8.
6. Felson DT, Anderson JJ, Boers M, Bombardier C, Furst D, Goldsmith C, et al. American College of Rheumatology. Preliminary definition of improvement in rheumatoid arthritis. Arthritis Rheum. 1995;38(6):727–35.
7. van Gestel AM, Prevoo ML, van' tHof MA, van Rijswijk MH, van de Putte LB, van Riel PL. Development and validation of the European League Against Rheumatism response criteria for rheumatoid arthritis. Comparison with the preliminary American College of Rheumatology and the World Health Organization/International League Against Rheumatism Criteria. Arthritis Rheum. 1996;39(1):34–40.
8. van Gestel AM, Haagsma CJ, van Riel PL. Validation of rheumatoid arthritis improvement criteria that include simplified joint counts. Arthritis Rheum. 1998;41(10):1845–50.
9. Lillegraven S, Prince FHM, Shadick NA, Bykerk VP, Lu B, Frits ML, et al. Remission and radiographic outcome in rheumatoid arthritis: application of the 2011 ACR/EULAR remission criteria in an observational cohort. Ann Rheum Dis. 2012;71(5):681–6.
10. Østergaard M, Peterfy C, Conaghan P, McQueen F, Bird P, Ejbjerg B, et al. OMERACT Rheumatoid Arthritis Magnetic Resonance Imaging Studies. Core set of MRI acquisitions, joint pathology definitions, and the OMERACT RA-MRI scoring system. J Rheumatol. 2003;30(6):1385–6.
11. Conaghan P, Lassere M, Østergaard M, Peterfy C, McQueen F, O'Connor P, et al. OMERACT Rheumatoid Arthritis Magnetic Resonance Imaging Studies. Exercise 4: an international multicenter longitudinal study using the RA-MRI Score. J Rheumatol. 2003;30(6):1376–9.
12. Østergaard M, Emery P, Conaghan PG, Fleischmann R, Hsia EC, Xu W, et al. Significant improvement in synovitis, osteitis, and bone erosion following golimumab and methotrexate combination therapy as compared with methotrexate alone: a magnetic resonance imaging study of 318 methotrexate-naive rheumatoid arthritis patients. Arthritis Rheum. 2011; 63(12):3712–22.
13. Ejbjerg BJ, Narvestad E, Jacobsen S, Thomsen HS, Østergaard M. Optimised, low cost, low field dedicated extremity MRI is highly specific and sensitive for synovitis and bone erosions in rheumatoid arthritis wrist and finger joints: comparison with conventional high field MRI and radiography. Ann Rheum Dis. 2005;64(9):1280–7.
14. Hodgson RJ, O'Connor PJ, Ridgway JP. Optimizing MRI for imaging peripheral arthritis. Semin Musculoskelet Radiol. 2012;16(5):367–76.
15. Emery P, van der Heijde D, Ostergaard M, Conaghan PG, Genovese MC, Keystone EC, et al. Exploratory analyses of the association of MRI with clinical, laboratory and radiographic findings in patients with rheumatoid arthritis. Ann Rheum Dis. 2011;70(12):2126–30.
16. McQueen FM, Ostendorf B. What is MRI bone oedema in rheumatoid arthritis and why does it matter? Arthritis Res Ther. 2006;8(6):222.
17. Gandjbakhch F, Foltz V, Mallet A, Bourgeois P, Fautrel B. Bone marrow oedema predicts structural progression in a 1-year follow-up of 85 patients with RA in remission or with low disease activity with low-field MRI. Ann Rheum Dis. 2011;70(12):2159–62.
18. Hetland ML, Stengaard-Pedersen K, Junker P, Østergaard M, Ejbjerg BJ, Jacobsen S, et al. Radiographic progression and remission rates in early rheumatoid arthritis - MRI bone oedema and anti-CCP predicted radiographic progression in the 5-year extension of the double-blind randomised CIMESTRA trial. Ann Rheum Dis. 2010;69(10):1789–95.
19. Møller-Bisgaard S, Hørslev-Petersen K, Ejbjerg BJ, Boesen M, Hetland ML, Christensen R, et al. Impact of a magnetic resonance imaging-guided treat-to-target strategy on disease activity and progression in patients with rheumatoid arthritis (the IMAGINE-RA trial): study protocol for a randomized controlled trial. Trials. 2015;16:178.
20. van der Heijde D. Remission by imaging in rheumatoid arthritis: should this be the ultimate goal? Ann Rheum Dis. 2012;71 Suppl 2:i89–92.
21. Ostendorf B, Scherer A, Kellner H, Backhaus M. Project REMISSION(PLUS): clinical and radiological remission: New treatment goals in the management of rheumatoid arthritis. Zeitschrift Für Rheumatologie. 2008; 67(8):707–710, 712–715.
22. Aletaha D, Neogi T, Silman AJ, Funovits J, Felson DT, Bingham CO, et al. 2010 rheumatoid arthritis classification criteria: an American College of Rheumatology/European League Against Rheumatism collaborative initiative. Ann Rheum Dis. 2010;69(9):1580–8.
23. Prevoo ML, van' tHof MA, Kuper HH, van Leeuwen MA, van de Putte LB, van Riel PL. Modified disease activity scores that include twenty-eight-joint counts. Development and validation in a prospective longitudinal study of patients with rheumatoid arthritis. Arthritis Rheum. 1995;38(1):44–8.
24. Aletaha D, Landewe R, Karonitsch T, Bathon J, Boers M, Bombardier C, et al. Reporting disease activity in clinical trials of patients with rheumatoid arthritis: EULAR/ACR collaborative recommendations. Arthritis Rheum. 2008; 59(10):1371–7.
25. van Tuyl LHD, Felson DT, Wells G, Smolen J, Zhang B, Boers M. Evidence for predictive validity of remission on long-term outcome in rheumatoid arthritis: a systematic review. Arthritis Care Res. 2010;62(1):108–17.
26. Gandjbakhch F, Conaghan PG, Ejbjerg B, Haavardsholm EA, Foltz V, Brown AK, et al. Synovitis and osteitis are very frequent in rheumatoid arthritis clinical remission: results from an MRI study of 294 patients in clinical remission or low disease activity state. J Rheumatol. 2011;38(9):2039–44.
27. Gandjbakhch F, Haavardsholm EA, Conaghan PG, Ejbjerg B, Foltz V, Brown AK, et al. Determining a magnetic resonance imaging inflammatory activity acceptable state without subsequent radiographic progression in rheumatoid arthritis: results from a followup MRI study of 254 patients in clinical remission or low disease activity. J Rheumatol. 2014;41(2):398–406.
28. Funck-Brentano T, Gandjbakhch F, Etchepare F, Jousse-Joulin S, Miquel A, Cyteval C, et al. Prediction of radiographic damage in early arthritis by sonographic erosions and power Doppler signal: a longitudinal observational study. Arthritis Care Res. 2013;65(6):896–902.
29. Baker JF, Ostergaard M, Emery P, Hsia EC, Lu J, Baker DG, et al. Early MRI measures independently predict 1-year and 2-year radiographic progression in rheumatoid arthritis: secondary analysis from a large clinical trial. Ann Rheum Dis. 2014;73(11):1968–74.
30. Brown AK, Conaghan PG, Karim Z, Quinn MA, Ikeda K, Peterfy CG, et al. An explanation for the apparent dissociation between clinical remission and continued structural deterioration in rheumatoid arthritis. Arthritis Rheum. 2008;58(10):2958–67.
31. Schett G, Smolen JS. New insights in the mechanism of bone loss in arthritis. Curr Pharm Des. 2005;11(23):3039–49.
32. Pincus T. The underestimated long term medical and economic consequences of rheumatoid arthritis. Drugs. 1995;50 Suppl 1:1–14.

## Important but incomplete data analysis?

We are grateful to the article about incidence and prevalence of psoriatic arthritis (PsA) in Denmark by Egeberg *et al*.[1] The comprehensive health registers from Denmark and other Nordic countries have proven to yield many insights into the epidemiology of chronic diseases. The authors of the article provide very detailed information about the age-specific incidence of PsA, including its time trend. However, we have a question about reporting the overall age-specific incidence rate, combined for both sexes. Could the authors comment on the differences between men and women? The authors report that between 41.1% and 45.9% of the incident cases are male (table 1 in the paper). Are there specific age-groups where the discrepancy between both sexes vanishes or becomes extreme? Sex differences are important to obtain insights into disease aetiology, which is largely unknown in PsA[2].

The second point is related to reporting the age-specific prevalence for men and women (table 2 in the paper). The authors provide detailed data about the increasing age-specific incidence rate. Unfortunately, the authors miss to comment on temporal trends in prevalence. Increasing incidence is likely to increase the prevalence of the disease. Do the authors observe a time trend in age-specific prevalence? Are there age groups with more pronounced trends of the prevalence in time, for example, in the older age groups? The answers to these questions on the one hand are important, and on the other hand seem possible, because the data comprises the period from 1997 to 2012.

The last point might be seen as a suggestion for a further analysis. It is well-known in chronic disease epidemiology that the prevalence, incidence and mortality (with and without disease) are related by the illness-death model.[3] If two of these three figures are known, the third can be extracted.[4] The data available to the authors allow an extraction of the excess mortality of patients with PsA compared with persons without PsA. This can be achieved by analysing the age-specific prevalence at two points in time. Observed changes of the prevalence can be attributed to the incidence (which is known from the data in this study) and the excess mortality. Details can be found in Brinks and Landwehr 2014.[4]

We think that an estimation of the excess mortality would be a very important contribution to the epidemiology of PsA and would encourage the authors to perform such an analysis.

**Philipp Sewerin,[1] Annika Hoyer,[2] Matthias Schneider,[1] Ben Ostendorf,[1] Ralph Brinks[1]**

[1]Department and Hiller Research Unit of Rheumatology, University Duesseldorf, Duesseldorf, Germany
[2]Institute for Biometry and Epidemiology, German Diabetes Center, Duesseldorf, Germany

**Correspondence to** Dr Philipp Sewerin, Department and Hiller Research Unit of Rheumatology, University Duesseldorf, Germany; philipp.sewerin@med.uni-duesseldorf.de

**Competing interests** None declared.

**Provenance and peer review** Not commissioned; internally peer reviewed.



**To cite** Sewerin P, Hoyer A, Schneider M, *et al*. *Ann Rheum Dis* 2018;**77**:e18.

Received 27 June 2017
Accepted 27 June 2017
Published Online First 14 July 2017

Linked

► http://dx.doi.org/10.1136/annrheumdis-2017-211980

*Ann Rheum Dis* 2018;**77**:e18. doi:10.1136/annrheumdis-2017-211979

## REFERENCES

1 Egeberg A, Kristensen LE, Thyssen JP, *et al*. Incidence and prevalence of psoriatic arthritis in Denmark: a nationwide register linkage study. *Ann Rheum Dis* 2017;76:1591–7.
2 Ritchlin CT, Colbert RA, Gladman DD. Psoriatic Arthritis. *N Engl J Med* 2017;376:957–70.
3 Keiding N, Incidence A-S. and Prevalence: A Statistical Perspective. *J. R. Stat. Soc. Ser. A Stat. Soc* 1991;154:371.
4 Brinks R, Landwehr S. A new relation between prevalence and incidence of a chronic disease. *Mathematical Medicine and Biology*:dqu024. Math. Med. Biol. dqu024 (2015).

# Inconsistency between Danish incidence and prevalence data about psoriatic arthritis (PsA)

We are grateful to Egeberg and Kristensen for presenting the detailed data about the prevalence and incidence of psoriatic arthritis (PsA).[1] Based on these detailed information, we tried to estimate the excess mortality of people with diagnosed PsA by uising a mathematical relation between incidence, prevalence and mortality.[2 3] During analysis of the incidence and prevalence data, we have made the following observation: if we assume that—on population average—people with PsA do not have a better survival than those without PsA, we can compute a lower bound for the incidence rate from the prevalence data (the details for the derivation of the lower bound can be found in the Appendix). We calculated this mathematical lower bound based on the prevalence data and compared the lower bound with the incidence data given in Ref 1. We found that in less than 50% of the strata where incidence data were given, the corresponding mathematical lower bounds have been reached (or exceeded). For instance, the lower bound for the incidence rate in the age group 40–49 in 2009 is 43.3 per 100 000 person-years (both sexes). The observed incidence rate in this stratum is only 29.8 per 100 000 person-years—a deviation of more than 30%. More than half of the reported incidence rates stratified by age and year are implausibly small given the observed prevalence values. Unfortunately, we do not have an explanation for the inconsistencies between the incidence and prevalence data. Possibly, in estimating the age-specific prevalence, some double counting of cases has occurred.

Appendix: Deriving a lower bound for the age-specific incidence rate

Mathematically, it can be shown that

$$\partial p = (1 - p) \times \{i - p \times (m1 - m0)\}$$

where ∂p is the temporal change of the age-specific prevalence p with respect to time and age.[1 2] The rates i, m0 and m1 are the age-specific incidence and mortality rates of the people with (m1) and without diagnosed PsA (m0).

A straightforward calculation yields that

$$\partial p/(1 - p) + p \times (m1 - m0) = i.$$

With the assumption that the mortality rate of the people without PsA is not higher than the mortality of the people with PsA, that is, $m0 \leq m1$, this equation implies

$$\partial p/(1 - p) \leq i. \quad (1)$$

This means the incidence rate (i) is always greater than the temporal change (∂p) of the prevalence over 1 minus the age-specific prevalence. Thus, we have a lower bound for the incidence rate.

The question arises, if the assumption $m0 \leq m1$ is reasonable on the population level (here: Denmark). The main reason for this assumption being true (on the population level) is that PsA often is a severe disease coming along with severe side effects and disease-specific complications. Hence, it appears reasonable to us that equation (1) yields a lower bound for the incidence rate.

**Philipp Sewerin,[1] Annika Hoyer,[2] Matthias Schneider,[1] Benedikt Ostendorf,[1] Ralph Brinks[1]**

[1]Department and Hiller Research Unit of Rheumatology, University Düsseldorf, Düsseldorf, Germany
[2]Institute for Biometry and Epidemiology, German Diabetes Center, Düsseldorf, Germany

**Correspondence to** Dr Philipp Sewerin, Department and Hiller Research Unit of Rheumatology, University Duesseldorf, Duesseldorf 40225, Germany; philipp.sewerin@med.uni-duesseldorf.de

**Handling editor** Josef S Smolen

**Competing interests** None declared.

**Provenance and peer review** Not commissioned; internally peer reviewed.



**To cite** Sewerin P, Hoyer A, Schneider M, *et al*. *Ann Rheum Dis* 2019;**78**:e44.

Received 8 December 2017
Accepted 15 December 2017
Published Online First 2 January 2018

*Ann Rheum Dis* 2019;**78**:e44. doi:10.1136/annrheumdis-2017-212817

## REFERENCES

1 Egeberg A, Kristensen LE. Impact of age and sex on the incidence and prevalence of psoriatic arthritis. *Ann Rheum Dis* 2017.
2 Brinks R, Landwehr S. Age- and time-dependent model of the prevalence of non-communicable diseases and application to dementia in Germany. *Theor Popul Biol* 2014;92:62–8.
3 Brinks R, Landwehr S. A new relation between prevalence and incidence of a chronic disease. *Math Med Biol* 2015;35:425–35.

Z Rheumatol 2018 · 77:203–208
https://doi.org/10.1007/s00393-018-0422-9
Online publiziert: 6. Februar 2018




**Philipp Sewerin[1] · Benedikt Ostendorf[1] · Axel J. Hueber[2] · Arnd Kleyer[2]**

[1] Heinrich-Heine-Universität Düsseldorf (HHU), Poliklinik, Funktionsbereich und Hiller-Forschungszentrum für Rheumatologie, Universitätskliniken Düsseldorf, Düsseldorf, Deutschland

[2] Friedrich-Alexander-Universität Erlangen-Nürnberg (FAU), Medizinische Klinik 3 – Rheumatologie und Immunologie, Universitätsklinikum Erlangen, Erlangen, Deutschland

# Big Data in der Bildgebung

Bis heute sind die wissenschaftlichen und klinischen Fortschritte in der Medizin primär durch hypothesengetriebene Forschungsansätze im Rahmen von kontrollierten klinischen Studien erreicht worden. So wird davon ausgegangen, dass eine zuvor definierte klinische Variable das Outcome beeinflusst oder gar bestimmt. Andere Störgrößen („confounder") werden dabei z. B. durch ein definiertes Patientenkollektiv oder durch Randomisierung etc. auszuschalten versucht. Trotz der enormen Errungenschaften ist ein solches Vorgehen durch die unzähligen Variablen (Demographie, Pathophysiologie, genetischer Hintergrund usw.) extrem kosten- und zeitintensiv und blendet durch den Versuch einer Homogenisierung gewisse Kollektive nachhaltig aus. Im Gegensatz zu diesen hypothesengetriebenen bieten datenbasierte (Big-Data-)Forschungsansätze die Möglichkeit, zahlreiche ungefilterte Daten zu untersuchen, die alle Effekte bei möglicherweise allen Patienten berücksichtigen [1, 9]. Big Data wird durch verschiedene Eigenschaften, die 4 „V", charakterisiert [6]:

1. „Volume": Es werden sehr große Datensätze generiert.
2. „Variety": Hierfür werden Daten aus verschiedenen Quellen benötigt.
3. „Velocity": Die Daten sollen mit hoher Geschwindigkeit zur Verfügung gestellt werden.
4. „Veracity": Eine Überprüfbarkeit der Daten fehlt gelegentlich.

Alle bildgebenden Verfahren speichern heute i.d.R. Bildmaterial digital, sodass sie prinzipiell für eine Big-Data-Lösung (zentrales Speichern, Vergleichen und Auswerten) prädestiniert wären. Während konventionelle Röntgenbilder noch bis vor wenigen Jahren in den meisten klinischen Settings als klassische Hardcopys verfügbar waren, wurden bis heute nahezu flächendeckend in ambulanten Praxen und der klinischen Radiologie digitale konventionelle Röntgenuntersuchungen eingeführt [3]. Gleiches gilt für die Computertomographie (CT) und die Magnetresonanztomographie (MRT), die heute bereits große Datensätze als Primärdaten speichern, um diese dann rekonstruieren und auswerten zu können. Gerade für schnittbildgebende Techniken werden zahlreiche digitale Auswertungsmöglichkeiten geboten, die erst durch einen schnellen und effektiven Datentransfer möglich wurden (Teleradiologie; [11]). Allerdings bestehen hierbei nach wie vor Auflagen des Datenschutzes, die überwunden werden müssen [16].

## Entwicklung und Möglichkeiten von Big Data

In den vergangenen Jahren wurden zunehmend Konzepte präsentiert, die die Möglichkeit bieten, große Datenmengen in der Bildgebung einfach und effektiv für Ärzte und Patienten zugänglich zu machen [12]. Gerade in der onkologischen Bildgebung schien hier großes Potenzial vorhanden zu sein, durch die zentrale Verarbeitung und Auswertung von Daten spezifische Auswertungsalgorithmen zu standardisieren und zu verbessern [15]. Gleiche Ideen entstanden für das sog. Neuroimaging, da hier Therapieentschei-

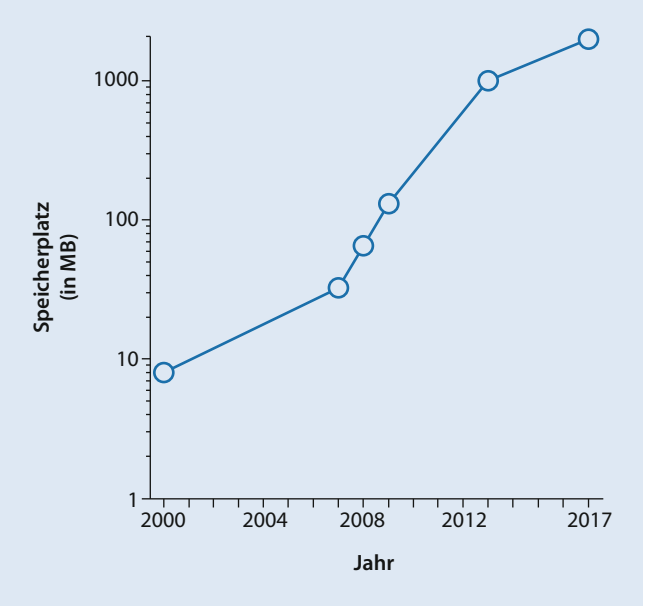


**Abb. 1** ◀ Entwicklung des USB-Speicherplatzes über die Zeit. Logarithmische Speicherkapazität in Megabyte

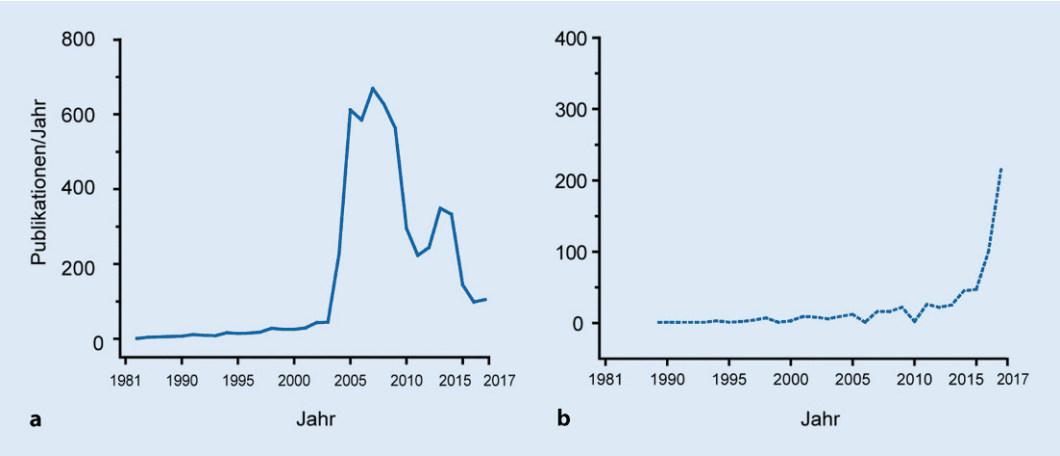


**Abb. 2** ◄ **a** PubMed-Databank-Suche zu Publikationen „artificial" AND „intelligence" AND „imaging", **b** PubMed-Databank-Suche zu Publikationen „deep" AND „machine" AND „imaging". Zeitraum von 1981 bis 2017

dungen häufig insbesondere von bildgebenden Verfahren gesteuert werden und Experten rar sind [14]. Darüber hinaus wurden in zahlreichen klinischen Studien zentrale Auswertungsverfahren angewendet, in denen die einzelnen Studienzentren anonymisierte Bildgebungsdaten einstellen, um diese dann zentrumunabhängig verblindet auswerten zu können [8]. All diese Lösungen sind häufig auf wenige Zentren beschränkt und können übergreifend nicht vereinheitlicht umgesetzt werden [7].

» Technische Weiterentwicklungen ermöglichen die einfache und schnelle Handhabung sehr großer Datenmengen

Die Entwicklung von Big Data und v. a. deren Anwendung und Bearbeitung beruhen auf dem Zutreffen des Moore-Gesetzes in der Daten- und Technologieentwicklung. Dieses besagt, dass sich Technologien über die Zeit exponentiell verbessern [2, 10]. Hierbei entstehen durch den technologischen disruptiven Fortschritt kosteneffiziente Einsatzmöglichkeiten von Medizingeräten und Anwendungen. Vor allem in der Speicherplatzentwicklung zeigte sich in den letzten Jahren, welches Potenzial die Datenverarbeitung aufweist (**Abb. 1**). So erhielt man im Jahr 2000 einen USB-Stick mit 8 Megabyte für ca. 40 € und zahlt heute für einen mit 128.000 Megabyte (128 Gigabyte) 30 €. Dem Entwicklungsfortschritt entgegengesetzt bleibt das Preisgefüge bestehen oder Kosten verringern sich in der Produktion der Hardware selbst.

Bezogen auf den Medizinmarkt, insbesondere die Entwicklung der Bildgebung, ermöglicht der Datentransport die einfache und schnelle Handhabung sehr großer Datenmengen. IBM Watson Health beispielsweise wirbt dafür, 1 Mrd. an medizinischen Bilddaten in einem Cloud-basierten Archiv zu speichern (http://www.merge.com/Blogs/Enterprise-Imaging-Blog/April-2017/One-Billion-Images-in-the-Cloud-A-Merge-Milestone.aspx). Dies ist nur aufgrund der oben beschriebenen Speicherfähigkeit, aber auch Schnelligkeit der Datenübertragung – ebenso ein wesentlicher Fortschritt der Datenverarbeitung – durchführbar. Mit solch einer Datenbasis sind nun auch eine systematische Analyse, Quantifizierung und Anwendung spezieller Algorithmen möglich. Einige Proof-of-concept-Studien wurden bereits im Bereich der CT-Bildgebung veröffentlicht: von kleinen Feldstudien zur Analyse von Bronchiektasien mit unterstützender Software bis zu künstlicher Intelligenz („artificial intelligence") mit „deep machine learning" und neuronalen Netzwerkansätzen, die an Tausenden von Bildern geschult werden [4, 5]. So zeigten beispielsweise DeBoer et al. [4], dass es anhand vorher „erlernter" Algorithmen möglich ist, automatisiert Bronchiektasen in CT-Scans von Kinder mit einer zystischen Fibrose zu quantifizieren. Hierbei wurde eine Software validiert, die durch zuvor definierte Prozesse ektatische Bronchien und „air trapping" objektiviert und möglichst untersucherunabhängig bewerten sollte. Die Autoren schlussfolgerten, dass solche automatisierten und vergleichsweise objektiven Verfahren ggf. auch für klinische Studienprogramme sinnvoll einsetzbar wären.

Der Fortschritt wird durch vielfältige Publikationen von computerunterstützten Diagnose-Tools mit einem Gipfel um 2007 belegt (**Abb. 2**). Nicht nur IBM Watson Health, sondern auch kleine Start-ups (oft Ausgliederungen aus Universitäten) entwickeln diesbezüglich Softwarelösungen, um die Arbeitsabläufe zu verbessern und durch automatisierte Bildanalyse ein Vorscreening mit hoher Spezifität und Sensitivität zu ermöglichen und damit Zeit zu sparen (z. B. http://aidence.com/). Wissenschaftlich verlagert sich das Feld zu spezifischen Softwarelösungen (z. B. „deep maching learning"), das die Publikationsleistung im Verlauf belegt („artificial intelligence" vs. „deep machine learning"; **Abb. 2**).

» Wissenschaftlich verlagert sich das Feld zu spezifischen Softwarelösungen

Ein weiteres Beispiel stellt QUIBIM S.L. dar. Auf Basis von DICOM-Bilddatensätzen sollen mittels Deep-Learning-Technologie und künstlicher Intelligenz klinische „Bildgebungsbiomarker" entschlüsselt werden (www.quibim.com). In der Osteologie fokussiert das Team dabei auf quantitative morphometrische Analysen der Knochenmikrostruktur, in der Onkologie auf Marker wie z. B. Knochenmark-

infiltrationen mittels kombinierter Positronenemissionstomographie/MRT und multiparametrischer Analysen, um nur wenige zu nennen.

Bis heute waren Kohortenanalysen in der Bildgebung nur im Rahmen von Studien zu vergleichen. Im Bereich der Osteoimmunologie entwickelte die Arbeitsgruppe um S. Boyd (University of Calgary) eine Software, die die Analyse einzelner Osteodensitometrie-Messungen (Radius, Tibia) anhand eines kanadischen Kollektivs von gesunden Probanden erlaubt (https://normative.ca/). Datensätze können anonymisiert über die Webbrowser-basierte Software einfach eingespielt und analysiert werden. Benutzt werden lediglich Alter und Geschlecht. Durch ständiges Einspielen von Daten wächst das zentral abgelegte Kontrollkollektiv, und Abfragen werden nicht gegenüber historischen Werten, wie z. B. bei der Dual-Röntgen-Absorptiometrie (DXA), sondern anhand eines dynamischen aktuellen Datensatzes abgeglichen. Dies kann im Bereich der quantitativen Knochendichtemessung als erster Schritt in Richtung einer personalisierten individuellen Empfehlung für den Patienten betrachtet werden. Dieser Ansatz stellt jedoch die Ausnahme dar, da aktuell noch regionen- und krankenhausspezifische Insellösungen heterogene Bilddatensätze generieren und so häufig noch keine gemeinsame Auswertung möglich ist (**Abb. 3**).

## Diskussion

Die hier aufgeführten Beispiele zeigen eindrucksvoll den enormen Fortschritt vornehmlich in der letzten Dekade, aber auch die damit verbundenen Herausforderungen. Zahlreiche, teilweise noch kleine Feldstudien machen darüber hinaus deutlich, welches Potenzial Big Data für die bildgebenden Verfahren haben kann. Durch die enorme Leistungsfähigkeit könnten zukünftig konventionelle Röntgenverfahren, aber auch die Schnittbildgebung wie CT oder MRT zentral und automatisiert nach zielgerichteten erlernten Algorithmen ausgewertet werden. Erste Arbeiten zeigen, mit welcher Präzision und Reliabilität dies beispielsweise bei der Bewertung von Bronchiektasen oder Screeningprogrammen in der CT möglich ist [4, 5]. Vergleichbare Verfahren wären auch in der Rheumatologie denkbar, sei es bei der Bewertung pulmonaler Beteiligung bei Systemerkrankungen oder dem Befunden und Scoring konventioneller bzw. MR-morphologischer Bildgebung der Hände und Füße (Synovialitis, Erosionen, Knochenmarködem am Beispiel automatisierter Scoringsysteme, z. B. RAMRIS [13]). Darüber hinaus könnten so neue diagnostische Informationen gewonnen werden, die bisher aufgrund der häufig nicht vergleichbaren Protokolle bzw. des fehlenden zentralen Zugriffs der Daten der klinischen und wissenschaftlichen Bewertung verborgen geblieben sind. In Zeiten, in denen gezielt gute prognostische Marker zur Therapiestratifizierung

## Zusammenfassung · Abstract

Z Rheumatol 2018 · 77:203–208 https://doi.org/10.1007/s00393-018-0422-9


P. Sewerin · B. Ostendorf · A. J. Hueber · A. Kleyer

### Big Data in der Bildgebung

**Zusammenfassung**

Die großen wissenschaftlichen Fortschritte in der Medizin wurden bis heute hauptsächlich durch hypothesengetriebene Forschungsansätze im Rahmen von kontrollierten klinischen Studien erreicht. Hierbei können allerdings aufgrund der zahlreichen Variablen nur einzelne Fragestellungen untersucht werden, sodass diese nach wie vor sehr zeit- und kostenintensiv sind. Big Data bietet durch einen neuen datenbasierten Ansatz die Möglichkeit, mit sehr großen Datenmengen alle vorhandenen Variablen zu untersuchen, und öffnet somit neue Horizonte. Die Bildgebung scheint für solche Ansätze durch die weitestgehend flächendeckende Digitalisierung der Daten und der immer besseren Hard- und Softwarelösungen prädestiniert zu sein. Einige kleine Studien wiesen bereits nach, dass automatisierte Auswertungsalgorithmen und künstliche Intelligenz Pathologien mit höchster Präzision erkennen können. Auch in der rheumatologischen Bildgebung erscheinen solche automatisierten Systeme sinnvoll, da seit Langem nach personalisierter Risikostratifizierung für die Patienten gesucht wird. Bei all den vielversprechenden Möglichkeiten muss allerdings heute noch festgestellt werden, dass die Heterogenität der Daten und die sehr komplexen Datenschutzauflagen in Deutschland eine Big-Data-Lösung in der Bildgebung noch erschweren. Die enormen Chancen in der klinischen Versorgung und der Wissenschaft sind es aber wert, diese Herausforderungen anzunehmen.

**Schlüsselwörter**

Datenanalyse · Entscheidungsfindung · Künstliche Intelligenz · Magnetresonanztomographie · Computertomographie

### Big data in imaging

**Abstract**

Until now, most major medical advancements have been achieved through hypothesis-driven research within the scope of clinical trials. However, due to a multitude of variables, only a certain number of research questions could be addressed during a single study, thus rendering these studies expensive and time consuming. Big data acquisition enables a new data-based approach in which large volumes of data can be used to investigate all variables, thus opening new horizons. Due to universal digitalization of the data as well as ever-improving hard- and software solutions, imaging would appear to be predestined for such analyses. Several small studies have already demonstrated that automated analysis algorithms and artificial intelligence can identify pathologies with high precision. Such automated systems would also seem well suited for rheumatology imaging, since a method for individualized risk stratification has long been sought for these patients. However, despite all the promising options, the heterogeneity of the data and highly complex regulations covering data protection in Germany would still render a big data solution for imaging difficult today. Overcoming these boundaries is challenging, but the enormous potential advances in clinical management and science render pursuit of this goal worthwhile.

**Keywords**

Data analysis · Decision making · Artificial intelligence · Magnetic resonance imaging · Computed tomography

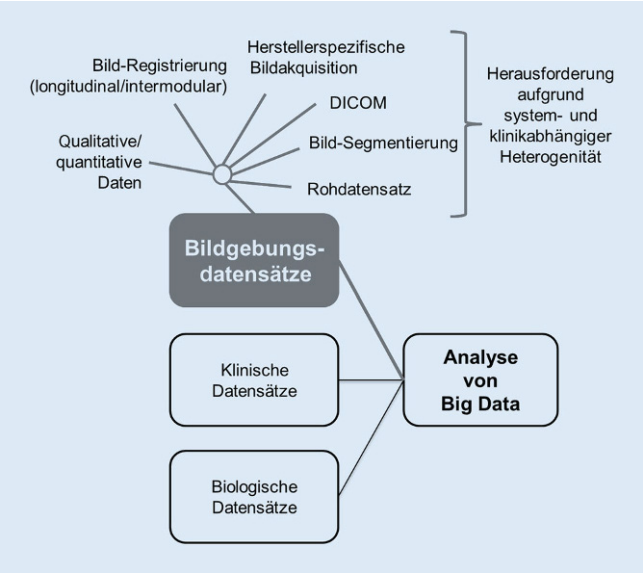


**Abb. 3** ◀ Übersicht möglicher Big-Data-Bildgebungsakquise in Anlehnung an Kansagra et al. [6]

gesucht werden, könnten aus Big Data generierte Marker (sei es in der Bildgebung oder anderweitig) eine wichtige Rolle spielen. So könnten sich durch automatisierte Prozesse und Algorithmen auch neue wissenschaftliche Fragestellungen ergeben, die aus den bisher primär hypothesengetriebenen Gedankengängen nicht entstanden wären. Ziel sollte es daher sein, die bildgebende Forschung in Deutschland zu homogenisieren (vergleichbare und austauschbare Systeme, angeglichene Protokolle, zentrale Speicherung, Cloud, „common repository") um somit zukünftig ggf. sogar digitale Bildgebungsregister („digital imaging register") etablieren zu können.

> » Die bildgebende Forschung in Deutschland muss homogenisiert werden

Die hiermit verbundenen Herausforderungen und Schwierigkeiten sollen dabei nicht unerwähnt bleiben: Bis heute sind die erhobenen Daten ohne Zweifel extrem heterogen. Wir finden Hunderte von lokalen Insellösungen, die häufig, selbst wenn gewollt, nicht vergleichbar sind. Dies beginnt bei der Aufnahmetechnik, der Hardware, der ausgespielten Bild- und Dateiformate und endet bei den hohen Datenschutzhürden. Zudem sind bildgebende Verfahren nur ein Teil der möglicherweise zahlreichen Agonisten in einer Big-Data-Lösung. Hier muss eine sinnvolle Verknüpfung zu anderen bestehenden Datensätzen angestrebt werden (klinische Daten, serologische Biomarker, ggf. Genetik). Weiter ist unklar, wer auf Daten zugreifen kann, sei es zur medizinischen oder zur wissenschaftlichen Auswertung, und welche Institution die Analyseapplikationen und Interpretation bereitstellt. Neue digitale Technologien, wie z. B. „blockchain" (ein kryptographisches Verfahren, eingesetzt im estländischen Gesundheitssystem), könnten den Datenschutz inklusive individualisierter Zugriffsrechte neu definieren. Ungelöst ist auch, wie solche Leistungen im jeweiligen Gesundheitssystem vergütet werden. All dies zeigt die zahlreichen Herausforderungen, die eine sinnvolle Verwendung von Big Data in der Bildgebung mit sich bringt. Die Möglichkeiten, die sich daraus wissenschaftlich und klinisch ergeben könnten, sind es allerdings wert, diese Herausforderungen anzunehmen.

## Fazit für die Praxis

- **Big-Data-Lösungen haben durch datenbasierte Forschungsansätze neue und innovative Möglichkeiten eröffnet.**
- **Durch die heute nahezu flächendeckende Digitalisierung ist die Bildgebung in der Medizin prädestiniert, hierbei eine Vorreiterrolle zu spielen.**
- **Automatisierte Auswertungsalgorithmen sind schon heute in Teilbereichen in der Lage, hochreliabel und präzise Pathologien zu erkennen und einzuordnen.**
- **Dies erscheint auch für bildgebende Verfahren in der Rheumatologie möglich und könnte einen wichtigen Beitrag zur personalisierten Risikostratifizierung liefern.**
- **Allerdings sind durch die sehr heterogenen Daten und strenge Datenschutzauflagen ein flächendeckender Austausch und eine Verknüpfung der Daten eingeschränkt.**
- **Die enormen Möglichkeiten, die sich aus Big Data in der Bildgebung ergeben, sollten uns motivieren, Lösungsansätze zu finden und die Herausforderungen anzunehmen.**


## Korrespondenzadresse

**Dr. P. Sewerin**
Heinrich-Heine-Universität Düsseldorf (HHU), Poliklinik, Funktionsbereich und Hiller-Forschungszentrum für Rheumatologie, Universitätskliniken Düsseldorf
Moorenstraße 5, 40225 Düsseldorf, Deutschland
philipp.sewerin@med.uni-duesseldorf.de


## Einhaltung ethischer Richtlinien

**Interessenkonflikt.** P. Sewerin, B. Ostendorf, A. J. Hueber und A. Kleyer geben an, dass kein Interessenkonflikt besteht.

Dieser Beitrag beinhaltet keine von den Autoren durchgeführten Studien an Menschen oder Tieren.

## Literatur


1. Badawi O, Brennan T, Celi LA et al (2014) Making big data useful for health care: a summary of the inaugural MIT critical data conference. JMIR Med Inform 2:e22. https://doi.org/10.2196/medinform.3447
2. Ball P (2013) Moore's law is not just for computers. Nature. https://doi.org/10.1038/nature.2013.12548
3. D'Agostino MA, Haavardsholm EA, van der Laken CJ (2016) Diagnosis and management of rheumatoid arthritis; what is the current role of established and new imaging techniques in clinical practice? Best

Pract Res Clin Rheumatol 30:586–607. https://doi.org/10.1016/j.berh.2016.10.011
4. DeBoer EM, Swiercz W, Heltshe SL et al (2014) Automated CT scan scores of bronchiectasis and air trapping in cystic fibrosis. Chest 145:593–603. https://doi.org/10.1378/chest.13-0588
5. González G, Ash SY, Vegas Sanchez-Ferrero G et al (2017) Disease staging and prognosis in smokers using deep learning in chest computed tomography. Am J Respir Crit Care Med. https://doi.org/10.1164/rccm.201705-0860OC
6. Kansagra AP, J-PJ Y, Chatterjee AR et al (2016) Big data and the future of radiology informatics. Acad Radiol 23:30–42. https://doi.org/10.1016/j.acra.2015.10.004
7. Kessel KA, Combs SE (2016) Review of developments in electronic, clinical data collection, and documentation systems over the last decade – are we ready for big data in routine health care? Front Oncol 6:75. https://doi.org/10.3389/fonc.2016.00075
8. Maitland ML, Schilsky RL (2011) Clinical trials in the era of personalized oncology. CA Cancer J Clin 61:365–381. https://doi.org/10.3322/caac.20135
9. Murdoch TB, Detsky AS (2013) The inevitable application of big data to health care. JAMA 309:1351. https://doi.org/10.1001/jama.2013.393
10. Nagy B, Farmer JD, Bui QM, Trancik JE (2013) Statistical basis for predicting technological progress. PLoS ONE 8:e52669. https://doi.org/10.1371/journal.pone.0052669
11. Nensa F, Forsting M, Wetter A (2016) The future of radiology: what can we expect within the next 10 years? Urologe A 55:350–355. https://doi.org/10.1007/s00120-016-0045-1
12. Onbay TU, Kantarcı A (2011) Design and implementation of a distributed teleradiography system: DIPACS. Comput Methods Programs Biomed 104:235–242. https://doi.org/10.1016/j.cmpb.2011.05.006
13. Østergaard M, Peterfy C, Conaghan P et al (2003) OMERACT rheumatoid arthritis magnetic resonance imaging studies. Core set of MRI acquisitions, joint pathology definitions, and the OMERACT RA-MRI scoring system. J Rheumatol 30:1385–1386
14. Poline J-B, Breeze JL, Ghosh S et al (2012) Data sharing in neuroimaging research. Front Neuroinform 6:9. https://doi.org/10.3389/fninf.2012.00009
15. Skripcak T, Belka C, Bosch W et al (2014) Creating a data exchange strategy for radiotherapy research: towards federated databases and anonymised public datasets. Radiother Oncol 113:303–309. https://doi.org/10.1016/j.radonc.2014.10.001
16. White P (2004) Privacy and security issues in teleradiology. Semin Ultrasound CT MR 25:391–395




© franckreporter / Getty Images / iStock

## Virtual Reality soll Menschen in Krankenhäusern und Heimen zu mehr Lebensqualität verhelfen

**Ein Spin-off der Uni Hohenheim entwickelt virtuelle Entspannungs-, Bewegungs- und Atemübungen, speziell für kranke, demente oder bettlägerige Menschen.**

Bewegung auf grüner Wiese oder eine entspannende Bootsfahrt auf dem Bodensee statt trister Krankenzimmerwände: Mit diesem Angebot will ein Start-up der Universität Hohenheim in Stuttgart Patienten in Krankenhäusern und Menschen mit eingeschränkter Mobilität zu mehr Lebensqualität verhelfen. Das Uni-Spin-Off ANDERS VR produziert maßgeschneiderte Visualisierungen in virtueller Realität und entwickelt eine selbstlernende App, die sich individuell auf den Nutzer einstellt.

**Psychischer Stress – hohe Folgekosten**

Patienten haben so die Möglichkeit, mit 360-Grad-Aufnahmen für eine gewisse Zeit dem Krankenzimmer zu entfliehen. Über eine App können verschiedene Szenarien gewählt werden, z.B. Naturaufnahmen, angeleitete Atemübungen oder Entspannungssequenzen und auch leichte Bewegungsübungen. Zahlreiche eigens produzierte Inhalte sollen verschiedene Fachbereiche ansprechen. Ein Fokus werde derzeit auf Krebspatienten und Patienten in der Schmerztherapie gelegt. Demnächst sei auch der Einsatz in der Orthopädie, bei Querschnittspatienten und in der Palliativmedizin vorgesehen. „Wir nehmen ein Problem mit gravierenden ökonomischen Folgen in den Fokus", so Wirtschaftswissenschaftler Dr. Andreas Haas von der ANDERS VR. „Die psychologische Belastung des Patienten kann Einfluss auf die Behandlungszeit und auch den Behandlungserfolg haben, weil Therapien abgebrochen oder nicht gut angenommen werden. Geschätzte 300 Mio. Euro Folgekosten entstehen daraus pro Jahr. Und es könnten mehr werden, wenn Krankenhäuser aus Kostengründen weniger Therapeuten beschäftigen können."

**Langfristiges Ziel: eine Plattform**

Langfristig soll das Angebot in eine Plattform umgewandelt werden, auf die auch andere Produzenten Inhalte aufspielen können. Die VR-Brille, das notwendige Handy sowie das Tablet zum Auswahl der Inhalte, als auch die Inhalte vermietet ANDERS VR als Paket an interessierte Einrichtungen.

Das Bundesministerium für Wirtschaft und Energie sowie der Europäische Sozialfonds förderten das Start-up über das EXIST-Gründerstipendium mit 145.000 Euro.

***Universität Hohenheim, www.uni-hohenheim.de/presse***

The Journal of Rheumatology Volume 45, no. 6

# Rheumatoid Arthritis Magnetic Resonance Imaging Score Predicts Therapy Response: Results of the German ArthroMark Cohort

Philipp Sewerin, Lien Le, Stefan Vordenbäumen, Christoph Schleich, Ruben Sengewein, Ralph Brinks, Georg Pongratz, Ellen Bleck, Juliane Lesch, Ulrich Mansmann, Matthias Schneider and Benedikt Ostendorf

J Rheumatol 2018;45;753-759
http://www.jrheum.org/content/45/6/753

# Rheumatoid Arthritis Magnetic Resonance Imaging Score Predicts Therapy Response: Results of the German ArthroMark Cohort

Philipp Sewerin, Lien Le, Stefan Vordenbäumen, Christoph Schleich, Ruben Sengewein, Ralph Brinks, Georg Pongratz, Ellen Bleck, Juliane Lesch, Ulrich Mansmann, Matthias Schneider, and Benedikt Ostendorf

***ABSTRACT.*** ***Objective.*** Markers for treatment response in rheumatoid arthritis (RA) are lacking. The aim of the study was to assess the performance of the RA magnetic resonance imaging (MRI) scoring system (RAMRIS) in combination with serum biomarkers to predict response to methotrexate (MTX) treatment in therapy-naive patients with early RA by using high-field MRI.

***Methods.*** Twenty-eight patients with RA were prospectively assessed with baseline 3-T MRI of the clinical dominant hand, 3 and 6 months after MTX. The patients met the 2010 American College of Rheumatology/European League Against Rheumatism (EULAR) criteria [average age 56.8 yrs (range 39–74); positive for rheumatoid factor and/or anticyclic citrullinated peptide antibodies; disease duration < 6 mos (range 2–23 weeks)]. RAMRIS and serum biomarkers consisting of various experimental proteins including receptor activator of nuclear factor-κB ligand (RANKL) were obtained. Remission or treatment response was defined according to EULAR. To adjust for intrapersonal correlation, generalized linear mixed models were used.

***Results.*** Treatment response at 3 months was associated to low RAMRIS erosion subscores and low total RAMRIS scores (p = 0.019 and 0.03, respectively). Remission at 6 months was associated to low RANKL levels (p = 0.033). In multivariate analyses, response at 3 and 6 months was predicted more accurately with the inclusion of total RAMRIS score, RAMRIS synovitis subscore at the second metacarpophalangeal (MCP) joint, or a combination of the two (p value likelihood ratio test = 0.035, 0.035, and 0.041, respectively). Remission was more accurately predicted with inclusion of RANKL, with no significant predictive effect of MRI.

***Conclusion.*** Baseline total RAMRIS can predict EULAR response. RAMRIS synovitis subscore at the second MCP joint and RANKL are associated with response and remission, respectively. (First Release April 1 2018; J Rheumatol 2018;45:753–9; doi:10.3899/jrheum.170797)

*Key Indexing Terms:*
MAGNETIC RESONANCE IMAGING RHEUMATOID ARTHRITIS
PREDICTION REMISSION THERAPY RESPONSE

Reaching remission in rheumatoid arthritis (RA) unambiguously is the goal of any antirheumatic therapy[1,2]. Treatment guidelines and recommendations published by the American College of Rheumatology (ACR) and the European League Against Rheumatism (EULAR) state that all patients diagnosed with RA should initially be treated with conven-

*From the Department and Hiller-Research-Unit for Rheumatology, and the Institute of Diagnostic and Interventional Radiology, Universitätsklinikum Düsseldorf (UKD), Heinrich-Heine-University Düsseldorf; University Düsseldorf, Medical Faculty, Department of Endocrinology, Diabetology and Rheumatology, Düsseldorf; the Institute for Medical Information Sciences, Biometry and Epidemiology, Ludwig Maximilian University, Munich, Germany.*

*Supported by a grant from the German Bundesministerium für Bildung und Forschung, ArthroMark (01EC1009).*

*P. Sewerin, MD, University Düsseldorf, Medical Faculty, Department of Endocrinology, Diabetology and Rheumatology; L. Le, Institute for Medical Information Sciences, Biometry and Epidemiology, Ludwig Maximilian University; S. Vordenbäumen, MD, PhD, Department and Hiller-Research-Unit for Rheumatology, UKD, Heinrich-Heine-University Düsseldorf; C. Schleich, MD, PhD, Department for Diagnostic and Interventional Radiology, UKD, Heinrich-Heine-University Düsseldorf; R. Sengewein, MD, Department and Hiller-Research-Unit for Rheumatology, UKD, Heinrich-Heine-University Düsseldorf; R. Brinks, PhD, Department and Hiller-Research-Unit for Rheumatology, UKD, Heinrich-Heine-University Düsseldorf; G. Pongratz, MD, PhD, Department and Hiller-Research-Unit for Rheumatology, UKD, Heinrich-Heine-University Düsseldorf; E. Bleck, Department and Hiller-Research-Unit for Rheumatology, UKD, Heinrich-Heine-University Düsseldorf; J. Lesch, Department and Hiller-Research-Unit for Rheumatology, UKD, Heinrich-Heine-University Düsseldorf; U. Mansmann, PhD, Institute for Medical Information Sciences, Biometry and Epidemiology, Ludwig Maximilian University; M. Schneider, MD, PhD, Department and Hiller-Research-Unit for Rheumatology, UKD, Heinrich-Heine-University Düsseldorf; B. Ostendorf, MD, PhD, Department and Hiller-Research-Unit for Rheumatology, UKD, Heinrich-Heine-University Düsseldorf.*

*Address correspondence to Dr. P. Sewerin, Düsseldorf University, Medical Faculty, Department and Hiller-Research-Unit for Rheumatology, Moorenstrasse 5, 40225 Düsseldorf, Germany.*
*E-mail: philipp.sewerin@med.uni-duesseldorf.de*

*Accepted for publication January 16, 2018.*

tional synthetic disease-modifying antirheumatic drugs (csDMARD) from the point of diagnosis with the ultimate aim of achieving this goal[3,4]. By using modern treat-to-target strategies, remission or at least low disease activity can be reached in up to 82% of patients[5,6].

Currently, the absence of rheumatoid factors (RF) and/or anticyclic citrullinated peptides antibodies (anti-CCP), the absence of bone erosions in conventional radiographs, the presence of low disease activity, and early intervention with csDMARD are considered good prognostic markers[5]. The sometimes poor performance of these markers might lead to under- or overtreatment of patients with early RA[7]. Owing to the more sensitive classification criteria introduced by EULAR/ACR in 2010, patients are now diagnosed and treated earlier in the course of the disease[8]. Moreover, the prognostic markers mentioned above are mostly based on randomized controlled trials including a homogeneous and preselected patient population, with generally higher prevalence of poor markers and high disease activity, so that generalizability to daily practice may be hampered. There is a lack of valid prognostic markers to help physicians to assess clinical response or remission at the onset of the disease in patients with early RA.

In clinical practice, radiographs are routinely used in most parts of the world, although their use in early RA is limited. Therefore, they are no longer part of the updated classification criteria for RA[8]. In contrast, magnetic resonance imaging (MRI) is a well-evaluated imaging technique and is used more frequently in daily practice and clinical trials for diagnosis and therapy control in patients with RA[9,10,11]. It was previously shown that MRI can depict typical pathological signs for RA such as inflammation (e.g., synovitis or tenovaginitis[12]) and bony changes early in the disease course, and with sensitivity[13,14]. These signs correlate to histological changes within the synovium[15]. In addition, MRI can reveal bone marrow edema (BME), which is known to be of high prognostic value in RA[16]. So far, the predictive role of MRI prior to initiation of csDMARD has not been systematically assessed, especially in a routine setting in patients with early RA.

Further, serological biomarkers play an increasingly important role in diagnosis, therapy control, and prognosis of early RA. Research focused especially on bone and cartilage in the last decade, with receptor activator of nuclear factor-κB ligand (RANKL) and osteoprotegerin (OPG) examined and evaluated even in RA[17,18,19]. However, no data for early arthritis and the prognostic value for reaching remission or at least clinical response have been published to date[20].

In our study, we prospectively investigated the validity of the Outcome Measures in Rheumatology (OMERACT) RA-MRI scoring system (RAMRIS) and serological biomarkers as possible prognostic markers for remission or clinical response after 3 and 6 months of methotrexate (MTX) therapy in patients with therapy-naive, seropositive (RF and/or anti-CCP antibodies) early RA with severe disease activity [28-joint count Disease Activity Score (DAS28) baseline about 4.7; C-reactive protein (CRP) about 9.6 mg/l; Table 1]. The cohort was part of the German ArthroMark initiative, which aims to assess prognostic markers for RA [supported by the German Federal Ministry of Education and Research; ArthroMark (01EC1009)].

## MATERIALS AND METHODS

ArthroMark was a multicenter consortium [Berlin (Charité, Deutsches Rheumaforschungszentrum), Frankfurt, Munich, and Düsseldorf], while the Düsseldorf location was responsible for the MRI substudy for defining predictive MRI and serological biomarkers for patients with early RA. ArthroMark Düsseldorf was a prospective MRI study of patients with seropositive early RA before initiating a therapy with MTX.

*Study design*. This was a prospective cohort study (ArthroMark) using high-field MRI (3-Tesla) of the clinically dominant hand at beginning of the study (V0) before initiating MTX therapy in patients with early RA, after 3 months (V3), and after 6 months (V6). Prednisone was allowed at the description of the treating physician, up to 10 mg per day. The study was conducted in accordance with the principles of the Declaration of Helsinki and the International Conference on Harmonisation Guidance for Good Clinical Practice and approved by ethics committees at each site (Charite Berlin EA1/193/10 and local ethic committee of Heinrich-Heine-University Düsseldorf 3483).

*Patient cohort*. Twenty-eight patients with early seropositive RA were consecutively examined [age 56.8 yrs (range 39–74 yrs); positive for RF and/or anti-CCP antibody; disease duration < 6 mos (average 16.3 weeks, range 2–23 weeks)] fulfilling the 2010 ACR/EULAR criteria for RA[8]. Patient characteristics are listed in Table 1.

*Table 1*. Patient characteristics at the beginning of the study.

| N = 28 | Values |
|---|---|
| Male | 9 (32%) |
| Female | 19 (68%) |
| Age | average 56.8 yrs (min 39 yrs, max 74 yrs) |
| Disease duration | average 16.3 weeks (min 2 weeks, max 23 weeks) |
| RF+ and/or anti-CCP antibody+ | 28 (100%): average RF 215 IU/ml (min 24, max 2314 IU/ml); average anti-CCP antibodies 131 U/ml (min 5, max > 200 U/ml) |
| CRP, baseline, mg/l | average 9.6 (SD 9.3; min 3, max 37) |
| CRP, V3 (3 mos), mg/l | average 6.5 (SD 8.6; min 3, max 37) |
| CRP, V6 (6 mos), mg/l | average 3.6 (SD 2.5; min 1, max 12) |
| DAS28 baseline | average 4.7 (SD 0.85; min 3.3, max 6.3) |
| DAS28 V3 (3 mos) | average 3.5 (SD1.3; min 1.6, max 6.2) |
| DAS28 V6 (6 mos) | average 2.6 (SD 0.83; min 1.6, max 4.8) |
| RAMRIS baseline | average 29.25 (SD 12.5; min 10, max 59) |
| RAMRIS V3 | average 27.38 (SD 11.35; min 10, max 57) |
| RAMRIS V6 | average 27.61 (SD 10.5; min 9, max 52) |
| Erosion subscore baseline | 7.93 (SD 6.7; min 0, max 21) |
| Erosion subscore V3 | 9.0 (SD 6.96; min 0, max 21) |
| Erosion subscore V6 | 9.1 (SD 7.05; min 0, max 21) |
| Erosions (radiograph), baseline | 1/28 |

RF: rheumatoid factor: anti-CCP: anticyclic citrullinated peptide antibodies; CRP: C-reactive protein; DAS28: 28-joint count Disease Activity Score; RAMRIS: rheumatoid arthritis magnetic resonance imaging scoring system.

*Clinical assessment*. The following EULAR core set of variables was recorded: patient's global assessment of overall disease activity, number of tender and swollen joints, erythrocyte sedimentation rate, and CRP (< 5 mg/l). The DAS28 was used to assess disease activity[21]. Remission was defined according to the EULAR remission criteria[22], and clinical response according to Fransen, *et al*[23].

*Biomarker assessment*. Blood serum samples were collected at every visit (0, 3, and 6 mos) on the same day as the clinical examination, and the MRI were performed and stored for posthoc analyses after the study. The following assays were carried out: human Dickkopf-1 (DKK-1; Quantikine ELISA, R&D Systems); OPG (Biomedica); free soluble RANKL high sensitivity (Biomedica); matrix metalloproteinase 3 (MMP-3; Quantikine ELISA, R&D Systems); human chitinase 3–like 1 (Quantikine ELISA, R&D Systems); neuropeptide-Y (NPY; ELISA, RAB0387 Sigma).

*Magnetic resonance imaging*. All MRI data were acquired on the same whole-body 3-Tesla MRI scanner (Magnetom Trio A Tim System; Siemens Healthcare). Images were made using a 4-channel flex coil. Before contrast media application, a coronal short-tau inversion recovery (STIR) and T1-weighted turbo spin echo sequence as well as a T1-weighted 3-D fast low angle shot sequence for T1 mapping using a dual flip-angle approach were acquired. Afterward, perfusion imaging was acquired with a dynamic 2-dimensional T1-weighted turbo flash sequence. Twenty seconds after the beginning of the sequence, the contrast agent Magnevist was injected with a dose of 0.4 ml/kg body weight.

*Protocol for delayed gadolinium-enhanced MRI of cartilage (dGEMRIC)*. After a 40-min delay, the dGEMRIC imaging sequence was applied, using a dual flip-angle approach for T1 estimation. The sequence variables were as follows: repetition time, 15 ms; echo time, 3.34 ms; flip angles, 5° and 26°; field of view, 90 mm × 53 mm; and slice thickness, 2 mm. The dGEMRIC analysis was performed by 1 radiologist with 6 years of experience in musculoskeletal imaging. The reader was blinded to RAMRIS analysis.

*RAMRIS scoring*. MRI scans were analyzed using RAMRIS[23]. According to OMERACT guidelines, RAMRIS was scored in consensus (1 radiologist with 6 years of experience in musculoskeletal imaging and 1 rheumatologist with 5 years of experience in musculoskeletal imaging). RAMRIS subscores including single joint scores were included posthoc. All scorings were performed by the same readers.

*Ethical approval and consent to participate*. Ethical approval for the study was received from the ethics committee of the Heinrich-Heine-University of Düsseldorf (reference no.: 3483) and the Charite Berlin (EA1/193/10). All patients provided written informed consent.

*Statistical testing*. The effect of biomarkers (DKK, OPG, RANKL, MMP, NPY) and MRI variables (RAMRIS and perfusion) on the outcomes EULAR response and remission at V6 have been studied in univariate analyses with the Mann-Whitney U statistical test and in multivariate analyses with logistic regression models adjusted for DAS28 at V0. Box plots are used to depict the distributions of markers in the outcome groups.

To adjust for intrapersonal correlation, we calculated generalized linear mixed models (GLMM) for the outcomes EULAR response at V6 or EULAR remission at V6. GLMM are set up with time as the independent variable and a random intercept for each study subject. Models incorporating the respective independent variables (biomarkers and MRI variables as above) were systematically assessed by likelihood ratio (LR) tests comparing with the null model (M0) that has time as the only independent variable. MRI scans (RAMRIS scoring) were blinded to the rheumatologist until the end of the study. All statistical tests are 2-sided, with a significance level of 0.05. P values are not adjusted for multiple testing.

## RESULTS

To select potential markers for further assessment, univariate logistic regression analyses were performed in the ArthroMark cohort MRI substudy, to investigate the association between these markers and clinical remission or response (according to EULAR criteria) after 3 (V3) or 6 months (V6). The RAMRIS subscore for erosions ($p = 0.019$) and total RAMRIS ($p = 0.03$) score were significantly associated with response at V3 (Figure 1). No further significant results were found for the other imaging markers assessed for response prediction at either V3 or V6 (Supplementary Material, Table 1, available from the authors on request). Of note, BME was detectable in only 4 patients of our cohort. Hence, BME was not further considered in subsequent analyses.

Concerning remission, low values of RANKL at baseline were significantly associated with EULAR remission at V6 ($p = 0.033$; Figure 2). Other markers including DKK1, OPG, MMP-3, NPY, RAMRIS and RAMRIS subscores (BME, erosions, and synovitis) did not show significant results at either V3 or V6 (Supplementary Material, Table 2, available from the authors on request).

Next, we performed multivariate analyses with the inclusion of candidate markers identified by univariate analyses, i.e., RAMRIS, RAMRIS erosion and synovitis subscore, and RANKL. Models incorporating the respective variables were systematically tested for EULAR response at V6 or EULAR remission at V6, respectively. As can be seen in Table 2, response was predicted more accurately with the inclusion of either RAMRIS (p value of LR test 0.035), RAMRIS synovitis subscore at the second MCP joint (p value of LR test 0.035), or a combination of the two (p value of LR test 0.041). Conventional potential predictors of response such as baseline DAS28 (Table 2), TJC, SJC, and CPR were assessed as well, but did not improve prediction (data not shown).

As can be seen in Table 3, remission was more accurately predicted when RANKL was considered, with increasing RANKL values worsening the chance of remission (p value of LR test 0.004). In contrast to response prediction, adding MRI markers (RAMRIS total or subscores) did not significantly improve model fit for remission.

Finally, interreader reliability of MRI scoring at T0 was assessed to estimate the generalizability of scoring. Smallest detectable differences were as follows: RAMRIS total score 4.53, RAMRIS synovitis subscore for second MCP joint 3.53, and RAMRIS erosion subscore total 4.07.

## DISCUSSION

Because treat-to-target strategies are increasingly implemented in the therapeutic algorithm and highly effective antiinflammatory therapies are available, low disease activity or even remission can be achieved in the majority of patients with RA[5,24,25]. Despite these improvements, there is a lack of valid data for prediction of therapy response or remission using clinical, serological, or radiographic variables before starting an antirheumatic therapy. ACR and EULAR recom-

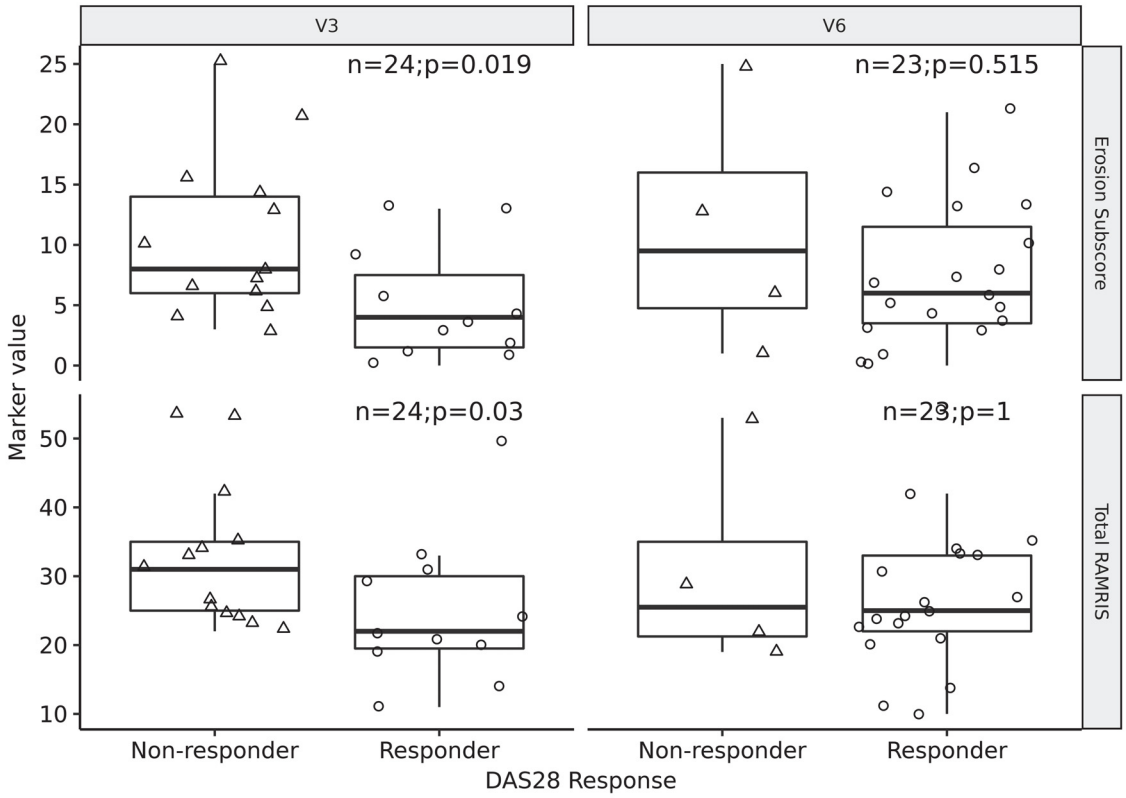


*Figure 1*. Comparison of DAS28 responders versus nonresponders (according to EULAR) at 3 months (V3, left side) and 6 months (V6, right side) depicted by box plots. Erosion subscore (upper half) and total RAMRIS (lower half) were significantly different between groups at 3 months. At 6 months no significant differences were found. DAS28: 28-joint count Disease Activity Score; EULAR: European League Against Rheumatism; RAMRIS: rheumatoid arthritis magnetic resonance imaging scoring system.

mend starting a csDMARD therapy immediately after the diagnosis of RA. Further, it is recommended that patients with a very high risk for rapid progression be treated initially with biologicals (for example, antitumor necrosis factor therapy)[3]. Accurate tools to select patients who likely profit from immediate biologic initiation rather than prior csDMARD therapy are needed. Indeed, ACR and EULAR stressed the importance of research to accomplish stratification and personalization of RA therapy in the future[4].

MRI is used increasingly in clinical trials and in daily practice[26]. It was shown that MRI is able to sensitively depict even subclinical joint inflammation[27]. To date, there are no data for the prediction of clinical outcome for high-field MRI scans of the hand before initiating an antirheumatic therapy in therapy-naive patients with early RA. RAMRIS is a validated tool that was investigated and evaluated in many studies, but was not hitherto evaluated in response or remission prediction before initiating an antirheumatoid therapy in patients with early RA[28].

In our study, high RAMRIS scores were highly associated with negative therapy response to MTX after 3 months, while low RAMRIS scores were associated with good or at least moderate therapy response (as assessed by DAS28 according to EULAR). This may indicate that RAMRIS is a potential predictive imaging marker for response. Similarly, high initial levels of the RAMRIS synovitis subscore of the second MCP joint showed association with a higher risk for poor response after 6 months, while there was no association between MRI value and remission overall. It could be demonstrated that there is sustaining inflammation in MRI despite clinical response or even remission as a sign of silent progression[10,26]. In support of this, we found that low RAMRIS or synovitis subscores of the second MCP joint were not associated with remission. Reasons for this lack of predictability may be the short therapy duration of only 6 months and the homogeneous treatment with "only" MTX. We cannot exclude that a longer followup of patients may have resulted in therapy response or remission even in those patients with a high baseline RAMRIS. However, current treatment guidelines recommend treat-to-target strategies and advise against tolerating active disease or low disease activity in biological-naive patients without contraindication[1].

We found a surprisingly low amount of BME in our study. BME is known to be highly predictive for the development of erosive disease[16]. In accordance with this observation, there was only 1 patient with erosions on conventional radiographs of the hands at baseline within the current cohort. We maintain that the low burden of BME or erosive disease

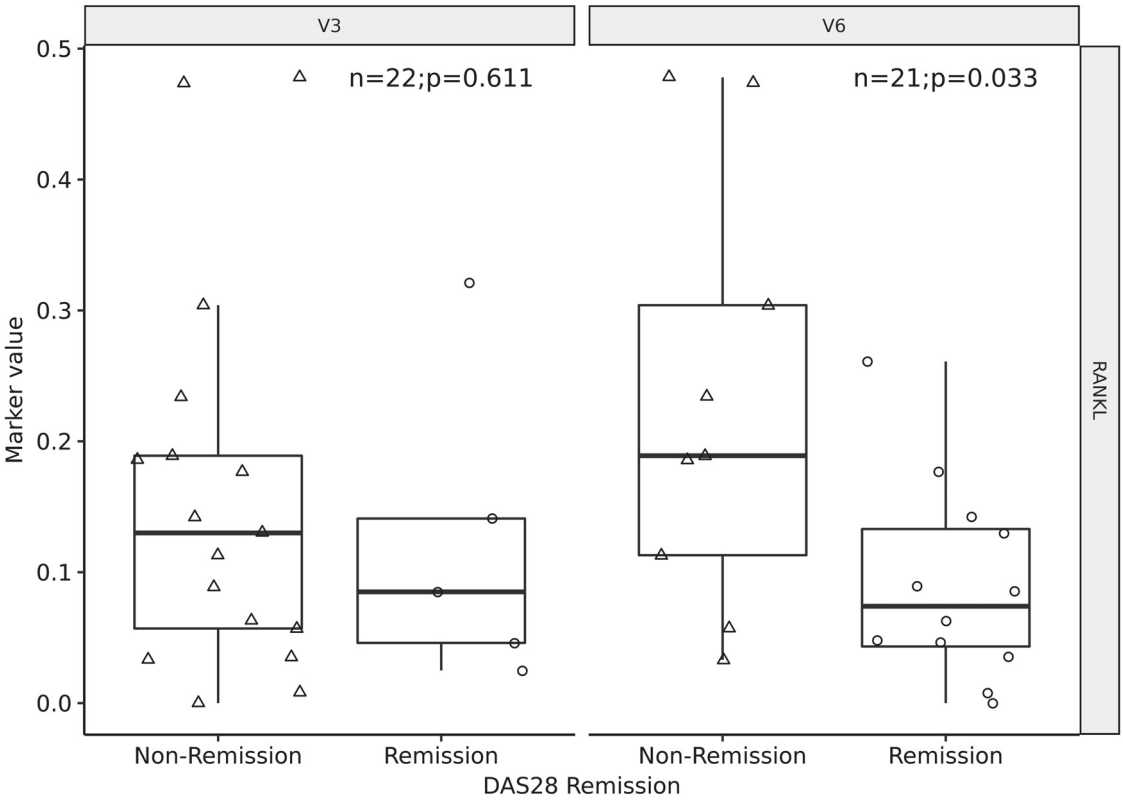


*Figure 2*. Comparison of DAS28 responders versus nonresponders (according to EULAR) at 3 months (V3, left side) and 6 months (V6, right side) depicted by box plots. RANKL was significantly different between groups at 6 months. DAS28: 28-joint count Disease Activity Score; EULAR: European League Against Rheumatism; RANKL: receptor activator of nuclear factor-κB ligand.

*Table 2*. Specifying the marker models for the outcome response.

| Y = response status (yes/no) | M1 | M2 | M3 | M4 | M5 | M6 |
|---|---|---|---|---|---|---|
| $X_i$ = | | | | | | |
| Time (in days) | x | x | x | x | x | x |
| RANKL | x | | | | | |
| RAMRIS erosion subscore total | | x | | | | |
| RAMRIS total score | | | x | | x | |
| RAMRIS synovitis subscore MCP-2 | | | | x | x | |
| DAS28 score at baseline | | | | | | x |
| AIC | 47.22 | 50.634 | 49.781 | 49.799 | 49.872 | 52.099 |
| LR test | vs M0 | vs M0 | vs M0 | vs M0 | vs M0 | vs. M0 |
| p | 0.191 | 0.0576 | **0.03473** | **0.03511** | **0.04144** | 0.1435 |

Bold face indicates significant data. RANKL: receptor activator of nuclear factor-κB ligand; RAMRIS: rheumatoid arthritis magnetic resonance imaging scoring system; MCP-2: second metacarophalangeal joint; DAS28: 28-joint count Disease Activity Score; AIC: Akaike information criterion; LR: likelihood ratio.

is a consequence of the short disease duration of only 16.3 weeks and subsequent immediate treatment. Of note, patients with BME did not appear to display higher scores in the other RAMRIS domains, potentially due to the low number of cases (n = 4).

Further and longer studies are needed to prove that RAMRIS is predictive for remission after a longer treatment period or an escalated treatment.

In contrast, baseline serum level of RANKL was significantly associated with remission in a longitudinal analysis. RANKL is known to correlate with cartilage and bony changes in degenerative or inflammatory joint diseases[17] and is considered to contribute to bone destruction in RA[29].

Our data suggest moreover that besides implemented clinical and serological markers for negative response, a high RAMRIS and a high synovitis subscore of the second MCP

*Table 3*. Specifying the marker models for the outcome remission.

| Y = remission status (yes/no) | M1 | M2 | M3 | M4 | M5 |
|---|---|---|---|---|---|
| $X_i$ = | | | | | |
| Time (in days) | x | x | x | x | x |
| RANKL | x | | | | |
| RAMRIS erosion subscore total | | x | | | |
| RAMRIS total score | | | x | | |
| RAMRIS synovitis subscore MCP-2 | | | | x | |
| DAS28 score at baseline | | | | | x |
| AIC | 36.686 | 47.183 | 47.395 | 47.232 | 47.386 |
| LR test | vs M0 | vs M0 | vs M0 | vs M0 | vs M0 |
| p | **0.0038** | 0.6362 | 0.9109 | 0.6754 | 0.8855 |

Bold face indicates significant data. RANKL: receptor activator of nuclear factor-κB ligand; RAMRIS: rheumatoid arthritis magnetic resonance imaging scoring system; MCP-2: second metacarophalangeal joint; DAS28: 28-joint count Disease Activity Score; AIC: Akaike information criterion; LR: likelihood ratio.

joint are highly predictive for poor therapy response in patients with early RA. The data also suggest that patients presenting high RAMRIS and/or synovitis subscores at a baseline MRI scan of the hand before initiating antiinflammatory therapy have a high risk of responding insufficiently to a csDMARD therapy, so that a primary biological therapy or at least a very tight therapy control could be of high value. The same applies for RANKL as a serum biomarker. Patients with high titers showed a high risk of not reaching remission after 6 months of continuous MTX therapy and may thus potentially be candidates for very tight control or immediate biological therapy.

To our knowledge, this is the first longitudinal study using GLMM showing the potential predictive value of the RAMRIS (in total and synovitis subscore of the second MCP joint) and RANKL, considering intrapersonal differences. There is a need to perform further studies to validate these findings and to define a clinically useful prediction model. Because of the number of patients, we were not able to define a cutoff value for response or remission (RAMRIS and RANKL), so that further studies are needed to gain sufficient data to justify clinical implementation.

At baseline, low RAMRIS scores were significantly associated with therapy response in our longitudinal analysis using GLMM. RAMRIS synovitis subscores at the second MCP joint and RANKL were significantly associated to response or remission, respectively. Our data suggest that MRI and biomarkers may aid response prediction and facilitate patient selection for intensified therapy in the future.


## ACKNOWLEDGMENT

We thank Erika Rädisch for assistance in gathering the MRI scans.


## REFERENCES


1. Smolen JS, Aletaha D, Bijlsma JW, Breedveld FC, Boumpas D, Burmester G, et al. Treating rheumatoid arthritis to target: recommendations of an international task force. Ann Rheum Dis 2010;69:631–7.
2. Mierau M, Schoels M, Gonda G, Fuchs J, Aletaha D, Smolen JS. Assessing remission in clinical practice. Rheumatology 2007;46:975–9.
3. Yazici H, Ozguler Y, Hatemi G, Yazici Y. Recommendations in the American College of Rheumatology guideline for the treatment of rheumatoid arthritis related to the use of biologic agents in patients with a history of cancer need reconsideration: comment on the article by Singh et al. Arthritis Rheumatol 2016;68:1315-6.
4. Colebatch AN, Edwards CJ, Østergaard M, van der Heijde D, Balint PV, D'Agostino MA, et al. EULAR recommendations for the use of imaging of the joints in the clinical management of rheumatoid arthritis. Ann Rheum Dis 2013;72:804–14.
5. Emery P, McInnes IB, van Vollenhoven R, Kraan MC. Clinical identification and treatment of a rapidly progressing disease state in patients with rheumatoid arthritis. Rheumatology 2008;47:392–8.
6. Grigor C, Capell H, Stirling A, McMahon AD, Lock P, Vallance R, et al. Effect of a treatment strategy of tight control for rheumatoid arthritis (the TICORA study): a single-blind randomised controlled trial. Lancet 2004;364:263-9.
7. De Cock D, Vanderschueren G, Meyfroidt S, Joly J, Van der Elst K, Westhovens R, et al. The performance of matrices in daily clinical practice to predict rapid radiologic progression in patients with early RA. Semin Arthritis Rheum 2014;43:627-31.
8. Aletaha D, Neogi T, Silman AJ, Funovits J, Felson DT, Bingham CO, et al. 2010 rheumatoid arthritis classification criteria: an American College of Rheumatology/European League Against Rheumatism collaborative initiative. Ann Rheum Dis 2010;69:1580–8.
9. Schleich C, Müller-Lutz A, Sewerin P, Ostendorf B, Buchbender C, Schneider M, et al. Intra-individual assessment of inflammatory severity and cartilage composition of finger joints in rheumatoid arthritis. Skeletal Radiol 2015;44:513-8.
10. Sewerin P, Buchbender C, Vordenbäumen S, Scherer A, Miese F, Brinks R, et al. Advantages of a combined rheumatoid arthritis magnetic resonance imaging score (RAMRIS) for hand and feet: Does the RAMRIS of the hand alone underestimate disease activity and progression? BMC Musculoskelet Disord 2014;15:104.
11. Møller-Bisgaard S, Hørslev-Petersen K, Ejbjerg BJ, Boesen M, Hetland ML, Christensen R, et al. Impact of a magnetic resonance imaging-guided treat-to-target strategy on disease activity and progression in patients with rheumatoid arthritis (the IMAGINE-RA trial): study protocol for a randomized controlled trial. Trials 2015;16:178.
12. McQueen FM, Chan E. Insights into rheumatoid arthritis from use of MRI. Curr Rheumatol Rep 2014;16:388.
13. McQueen FM. Imaging in early rheumatoid arthritis. Best Pract Res Clin Rheumatol 2013;27:499-522.

14. Sewerin P, Ostendorf B. [New imaging procedures in rheumatology: from bench to bedside.] [Article in German] Dtsch Med Wochenschr 2014;139:1835–41.
15. Vordenbäumen S, Sewerin P, Lögters T, Miese F, Schleich C, Bleck E, et al. Inflammation and vascularisation markers of arthroscopically-guided finger joint synovial biospies reflect global disease activity in rheumatoid arthritis. Clin Exp Rheumatol 2014;32:117-20.
16. McQueen FM, Ostendorf B. What is MRI bone oedema in rheumatoid arthritis and why does it matter? Arthritis Res Ther 2006;8:222.
17. Xu S, Wang Y, Lu J, Xu J. Osteoprotegerin and RANKL in the pathogenesis of rheumatoid arthritis-induced osteoporosis. Rheumatol Int 2012;32:3397–403.
18. Nielsen AR, Plomgaard P, Krabbe KS, Johansen JS, Pedersen BK. IL-6, but not TNF-α, increases plasma YKL-40 in human subjects. Cytokine 2011;55:152-5.
19. Alizai H, Virayavanich W, Joseph GB, Nardo L, Liu F, Liebl H, et al. Cartilage lesion score: comparison of a quantitative assessment score with established semiquantitative MR scoring systems. Radiology 2014;271:479–87.
20. Syversen SW, Goll GL, van der Heijde D, Landewé R, Gaarder PI, Odegård S, et al. Cartilage and bone biomarkers in rheumatoid arthritis: prediction of 10-year radiographic progression. J Rheumatol 2009;36:266-72.
21. Prevoo ML, van 't Hof MA, Kuper HH, van Leeuwen MA, van de Putte LB, van Riel PL. Modified disease activity scores that include twenty-eight-joint counts. Development and validation in a prospective longitudinal study of patients with rheumatoid arthritis. Arthritis Rheum 1995;38:44–8.
22. Felson DT, Smolen JS, Wells G, Zhang B, van Tuyl, Lilian HD, Funovits J, et al. American College of Rheumatology/European League Against Rheumatism provisional definition of remission in rheumatoid arthritis for clinical trials. Arthritis Rheum 2011;63:573–86.
23. Fransen J, Creemers MC, Van Riel PL. Remission in rheumatoid arthritis: agreement of the disease activity score (DAS28) with the ARA preliminary remission criteria. Rheumatology 2004; 43:1252-5.
24. Espinoza F, Fabre S, Pers YM. Remission-induction therapies for early rheumatoid arthritis: evidence to date and clinical implications. Ther Adv Musculoskelet Dis 2016;8:107-18.
25. Ma MH, Scott IC, Kingsley GH, Scott DL. Remission in early rheumatoid arthritis. J Rheumatol 2010;37:1444–53.
26. Baker JF, Ostergaard M, Emery P, Hsia EC, Lu J, Baker DG, et al. Early MRI measures independently predict 1-year and 2-year radiographic progression in rheumatoid arthritis: secondary analysis from a large clinical trial. Ann Rheum Dis 2014;73:1968–74.
27. Gandjbakhch F, Haavardsholm EA, Conaghan PG, Ejbjerg B, Foltz V, Brown AK, et al. Determining a magnetic resonance imaging inflammatory activity acceptable state without subsequent radiographic progression in rheumatoid arthritis: results from a followup MRI study of 254 patients in clinical remission or low disease activity. J Rheumatol 2014;41:398–406.
28. Østergaard M, Peterfy C, Conaghan P, McQueen F, Bird P, Ejbjerg B, et al. OMERACT rheumatoid arthritis magnetic resonance imaging studies. Core set of MRI acquisitions, joint pathology definitions, and the OMERACT RA-MRI scoring system. J Rheumatol 2003;30:1385-6.
29. Khosla S. Minireview: the OPG/RANKL/RANK system. Endocrinology 2001;142:5050–5.

# Prevention of the progressive biochemical cartilage destruction under methotrexate therapy in early rheumatoid arthritis

P. Sewerin[1], A. Müller-Lutz[2], D.B. Abrar[2], S. Odendahl[2], M. Eichner[2], M. Schneider[1], B. Ostendorf[1], C. Schleich[2]

*[1]Department and Hiller-Research Unit for Rheumatology; [2] Department of Diagnostic and Interventional Radiology, Medical Faculty, Heinrich-Heine University Düsseldorf, Germany.*

## Abstract

### Objective

*The aim of the study was to investigate biochemical cartilage composition under methotrexate (MTX) therapy and to intra-individually assess the impact of inflammation severity on cartilage composition by using dGEMRIC MRI in patients with early rheumatoid arthritis (eRA).*

### Methods

*dGEMRIC of MCP joints of the index and middle finger of 28 patients from the AthroMark cohort were examined prior to MTX-therapy as well as after 3 and 6 month. OMERACT RA MRI score and clinical parameters (CRP and DAS28) were registered at any time point. Each patient's second and third MCP joints were dichotomised into the joint with more severe synovitis versus the joint with less severe synovitis according to the RAMRIS synovitis subscore.*

### Results

*MCP joints with more severe synovitis ('bad joints') demonstrated significantly lower dGEMRIC values compared to MCP joints with less severe synovitis ('good joints') at time-points 0 and 3 months (p=0.002; p=0.019, respectively). After 6 months of MTX therapy no significant difference of dGEMRIC index was found between good and bad joint (p=0.086).*

### Conclusion

*Under MTX therapy, biochemical cartilage integrity remains stable; no further cartilage destruction occurred if patients were treated early in the course of the disease. In addition, six months of MTX therapy triggered an alignment of dGEMRIC index of MCP joints with initially severe synovitis and less severe synovitis in an intra-individual assessment. This underlines the importance of an early treatment in eRA to reduce further cartilage damage of the inflamed joints.*

**Key words**

magnetic resonance imaging, dGEMRIC, early rheumatoid arthritis, methotrexate therapy

*Philipp Sewerin, MD*
*Anja Müller-Lutz, PhD*
*Daniel Benjamin Abrar, MD*
*Sina Odendahl*
*Markus Eichner*
*Matthias Schneider, MD, PhD*
*Benedikt Ostendorf, MD, PhD*
*Christoph Schleich, MD, PhD*

*Please address correspondence to:*
*Dr Philipp Sewerin,*
*Department and Hiller-Research Unit for Rheumatology,*
*University Düsseldorf,*
*Moorenstraße 5,*
*40225 Düsseldorf, Germany.*
*E-mail:*
*philipp.sewerin@med.uni-duesseldorf.de*

*Received on February 5, 2018; accepted in revised form on April 24, 2018.*



*Funding: the ArthroMark project was founded by the Bundesministerium für Bildung und Forschung (BMBF) grant no. FKZ 01EC1009A.*
*Competing interests: none declared.*

## Introduction

Rheumatoid arthritis (RA) is characterised by inflammation of the synovia that can result in progressive joint destruction resulting in long-term functional disability (1, 2). The extent of inflammation of the synovial membrane correlates with joint destruction and functional impairment (3-5). This implies the importance of early treatment in RA reaching remission of the inflammatory joint disease achieved by therapy guidelines and recommendations of the American College of Rheumatology and the European League Against Rheumatism that recommend all patients diagnosed with RA should be treated with conventional synthetic disease-modifying drugs, ideally before erosive disease will be detected (6, 7). Although patients contemporary gave the diagnosis RA and treated by the existing guidelines, some show erosive progression of the disease (1, 8). This has put magnetic resonance imaging (MRI) of bony and cartilage damage in the focus of monitoring RA. In 2003, the Outcome Measures in RA Clinical Trials group with the RA MRI Score (RAMRIS) established a highly reliable sum-score based on the semi-quantitative rating of the severity of synovitis, bone marrow oedema and erosions in hand and wrist joints that has been applied in therapy-response trials in RA (9, 10). However, cartilage destruction has not been quantified with RAMRIS. This is all the more relevant in view of the study of Aletaha *et al*. who demonstrated that physical disability in RA is associated with cartilage damage rather than bone destruction (11). Delayed gadolinium-enhanced MRI of the cartilage (dGEMRIC) is a highly reliable, histologically controlled MRI feature to visualise proteoglycan loss in cartilage composition (12-15). With dGEMRIC, it is possible to detect proteoglycan loss after the intravenous application of negatively charged contrast agent (gadolinium diethylenetriamine pentaacetate anion – Gd-DTPA). The negatively charged Gd-DTPA penetrates cartilage in an inverse relationship to the concentration of negatively charged glycosaminoglycan side chains of proteoglycan. A depletion of proteoglycan content in degenerated cartilage results in an accumulation of the paramagnetic gadolinium ions (16, 17). This consecutively accelerates T1 relaxation time (18). Even in early RA (eRA), molecular cartilage damage could be found in this early stage of the disease while morphological alterations are not visible (19, 20). We know that structural bony destructions develop mostly at bare area, an area without cartilage coat. This protection is at stake in progressive disease and may lead to severe joint destruction. Additionally, McGonagle *et al*. found erosion formation which may not necessarily depend on the presence of a bare area (21). They found lesser bone destruction at these areas, so they conclude that cartilage coat minimise bone damage. However, cartilage damage is an important part of the disease progression in RA, and studies assessing joint space narrowing on conventional radiography have shown that joint space narrowing is independently associated with functional impairment and decreased work ability (22). The IMAGINE-RA trial showed the benefits using MR-guiding treatment in RA (23). According to the European League Against Rheumatism recommendations, therapy with methotrexate (MTX) is the anchor of the treatment management in early RA (24). The aim of our study was to investigate biochemical cartilage composition under MTX therapy and to intra-individually assess the association of inflammation severity and cartilage integrity by using dGEMRIC in patients with eRA. Our hypothesis was that MTX halts molecular cartilage degradation over time.

## Material and methods

### *Study population*

Our study was approved by two local ethics committees (study number 3828; request number EA1/193/10). Informed consent was obtained from all individual participants included in the study. Metacarpophalangeal joints of the index finger (MCP2) and the middle finger (MCP3) of 28 patients with eRA (disease duration ≤6month, Ø 16.3 weeks; min. 2 weeks, max. 23 weeks) fulfilling the ACR/EULAR 2010 criteria from the ArthroMark study cohort

**Table I.**

| Sequence/ parameter | STIR without contrast agent | T1w-TSE without contrast agent | 3 D-FLASH without contrast agent | TSE with contrast agent | SE with contrast agent | 3D-FLASH with contrast agent |
|---|---|---|---|---|---|---|
| Orientation | coronal | coronal | coronal | coronal | transversal | Sagittal |
| TE/TR (ms/ms) | 31 / 5560 | 25/ 860 | 1.44/ 15 | 25/ 120 | 12/ 765 | 3.34 / 15 |
| Flip angle (°) | 120 | 150 | 5 and 26 | 150 | 90 and 120 | 5 and 26 |
| Slice thickness (mm) | 2.5 | 2.5 | 3 | 2.5 | 2.5 | 2.0 |
| Field of view FOV (mm x mm) | 120 x 120 | 120 x 120 | 160 x 160 | 120 x 120 | 120 x 60 | 90 x 53.5 |
| Number of acquired slices | 17 | 17 | 14 | 17 | 17 | 22 |
| Time interval between two acquisitions | - | - | - | - | - | - |
| Number of images | 1 | 1 | 2 | 1 | 1 | 2 |

(mean age: 56.8 years; min. 39 years, max. 74 years; 18 females; 10 males) were enrolled in this prospective study, examined at a 3T MRI system (Magnetom Trio A Tim System; Siemens Healthcare, Erlangen, Germany) of the clinically dominant hand (hand with more pain and swollen joints compared to the other hand, scored by rheumatologist (25)). MRI was performed at baseline (prior to therapy) and three and six months after starting of MTX therapy. RAMRIS, including synovitis, oedema and erosion subscores, and clinical parameters (CRP and DAS28) were registered at all time points (26).

*MR protocol*

MRI was performed of the dominantly affected hand on a 3T MRI system (Magnetom Trio; Siemens Healthcare). Subjects were imaged in a prone position with the hand extended over the head. For anatomical imaging, a coronal short tau inversion recovery (STIR) sequence, T1-weighted turbo spin echo (TSE) sequence and two 3D fast low angle shot (3D-FLASH) sequences using two different flip angles for T1-mapping were acquired before injection of contrast agent. After contrast agent injection, a coronal TSE and a transversal SE-sequence with fat suppression were applied. Sequence parameters were chosen accordingly to a previous study (20) and are listed in Table I. Gadolinium-MRI contrast agent was applied intravenously (0.4 ml/kg body weight of Gd-DTPA2-, Magnevist; Schering). Biochemical MRI with dGEMRIC of the MCP joints of the index and middle fingers was performed with two 4-cm loop surface coils placed above and beneath the MCP joint. The size of the coils and the FOV limited the examination to two adjacent joints: MCP 2 and 3. dGEMRIC was acquired 40 min after contrast agent administration (17). Variable flip-angle three-dimensional gradient-echo imaging (with two flip angles) was used for T1calculation (17). Flip angles were set to 5° and 26°. Twenty-two sagittal slices with a thickness of 2mm were positioned perpendicular to the joint spaces. The matrix of 312×384 provided an in-plane resolution of 233 μm. Total acquisition time was 2.25 min. To reduce movement artefacts, motion correction was performed on each patient's MCP joint before image analysis using STROKETOOL (Frechen, Germany) (27).

*Image analysis*

MR images were analysed according to RAMRIS in consensus by two radiologists trained in musculoskeletal imaging to assess synovitis subscore (range 0–3), especially of MCP 2 and 3. The two readers were blinded to patients' data and dGEMRIC values. In the cases of identical RAMRIS synovitis subscores in MCP 2 and 3, a subjective gradation into the joint with more severe synovitis and the joint with less severe synovitis was undertaken by the two radiologists in consensus. Based on this data, the RAMRIS synovitis subscore of second and third MCP, each patient's pair of MCP2 and MCP3 was dichotomised into the joint with more severe synovitis *versus* the joint with less severe synovitis ('bad joint *vs*. good joint') according to a prior study of our working group (19). Molecular imaging with dGEMRIC was performed of second and third MCP. To determine cartilage quality, T1 maps were analysed using region of interest (ROI) measurements. T1 values were calculated pixelwise. Gradient-echo images with a flip angle of 5° were used as anatomic reference for cartilage identification, and ROIs were set in the phalangeal and metacarpal cartilage of the MCP joints of the index and middle fingers. The ROIs were transferred to the co-registered T1 map. The dGEMRIC index in ms was recorded.

*Statistical analysis*

Statistical analysis was performed using MATLAB (MathWorks, Natick, MA, R2015a). The mean, 95% confidence intervals for the mean values,

**Table II.**

| D2 Index Finger (ms) | General | | | Low synovitis ('good joints') | | | High synovitis ('bad joints') | | |
|---|---|---|---|---|---|---|---|---|---|
| | T0 | T3 | T6 | T0 | T3 | T6 | T0 | T3 | T6 |
| Mean | 344.07 | 361.11 | 367.23 | 381.38 | 396.63 | 393.74 | 324.90 | 376.33 | 359.45 |
| Std. | 78.32 | 79.88 | 69.73 | 74.56 | 73.48 | 50.43 | 96.44 | 111.81 | 64.08 |
| Min. | 250.78 | 189.46 | 192.28 | 290.70 | 304.27 | 320.51 | 212.05 | 217.92 | 282.14 |
| Max. | 514.22 | 528.97 | 505.29 | 493.08 | 528.97 | 439.21 | 520.07 | 566.64 | 477.87 |
| Lower Limit | 310.57 | 326.95 | 337.41 | 326.14 | 342.20 | 356.38 | 253.46 | 293.50 | 311.98 |
| Upper Limit | 377.57 | 395.28 | 397.05 | 436.61 | 451.07 | 431.10 | 396.35 | 459.16 | 406.92 |
| Median | 331.46 | 354.53 | 379.49 | 391.70 | 409.97 | 422.42 | 296.42 | 381.97 | 352.61 |

**Table III.**

| D3 Middel Finger (ms) | General | | | Low synovitis ('good joints') | | | High synovitis ('bad joints') | | |
|---|---|---|---|---|---|---|---|---|---|
| | T0 | T3 | T6 | T0 | T3 | T6 | T0 | T3 | T6 |
| Mean | 400.65 | 423.76 | 392.71 | 438.52 | 447.48 | 409.34 | 325.41 | 343.35 | 353.98 |
| StD. | 110.82 | 129.33 | 82.69 | 99.84 | 134.70 | 87.93 | 75.80 | 79.40 | 75.75 |
| Min. | 212.05 | 217.92 | 244.54 | 280.90 | 226.08 | 244.54 | 250.78 | 189.46 | 192.28 |
| Max. | 577.00 | 724.20 | 556.74 | 576.98 | 724.20 | 556.74 | 514.22 | 448.56 | 505.29 |
| Lower limit X | 353.25 | 368.44 | 357.34 | 386.23 | 376.92 | 363.28 | 285.70 | 301.76 | 314.30 |
| Upper limit X | 448.05 | 479.07 | 428.08 | 490.82 | 518.04 | 455.40 | 365.12 | 384.95 | 393.66 |
| Median (X) | 372.39 | 392.31 | 364.52 | 444.83 | 443.96 | 405.51 | 303.50 | 343.14 | 371.89 |

median and standard deviations for dGEMRIC indices were calculated as descriptive statistics (listed in Tables II-IV).

Kolmogorow-Smirnow-Lilliefors tests were used for testing normal distribution. Mann-Whitney U-test (for non-normally distributed data) was applied to show the differences of cartilage composition with the dGEMRIC index of second and third MCP joints between the different time points before and after the initiation of MTX therapy. Wilcoxon paired rank sum test for dichotomous analysis was applied to compare dGEMRIC index of the MCP joints with more severe synovitis ('bad joints') and less severe synovitis ('good joints') to illustrate if parameters are significant different at the different time points (0, 3 and 6 months). *p*-values below 0.05 were considered to be significant.

## Results

Descriptive analysis of dGEMRIC index in milliseconds (mean, standard deviation, median minimum, maximum, upper and lower limit of the 95% confidence interval) for MCP 2 and 3, as well as separated into low synovitis ('good joints) and high synovitis ('bad joints'), at the three different time points (T0 = baseline MRI before MTX treatment; T3 = three months, T6 = six months after beginning of MTX therapy) are summarised in Tables II-IV.

Additionally RAMRIS synovitis subscore demonstrated a decrease after three months of MTX therapy on MCP 2 (T0: 2.5; T3 2.0) and MCP 3 level (T0: 2.36; T3 2.04). Further, there also was a decrease in the RAMRIS oedema subscore on MCP 3 level after three and six months (T0: 0.43; T3: 0.29; T6: 0.29).

**Table IV.**

| Total D2+D3 | Low synovitis | | | High synovitis | | |
|---|---|---|---|---|---|---|
| | T0 | T3 | T6 | T0 | T3 | T6 |
| Mean | 400.65 | 423.76 | 392.71 | 344.07 | 361.11 | 367.23 |
| Std. | 110.82 | 129.33 | 82.69 | 78.32 | 79.88 | 69.73 |
| Min. | 212.05 | 217.92 | 244.54 | 250.78 | 189.46 | 192.28 |
| Max. | 576.98 | 724.20 | 556.74 | 514.22 | 528.98 | 505.29 |
| Lower Limit | 353.25 | 368.44 | 357.34 | 310.57 | 326.95 | 337.41 |
| Upper Limit | 448.05 | 479.07 | 428.08 | 377.57 | 395.28 | 397.05 |
| median | 372.39 | 392.31 | 364.52 | 331.46 | 354.53 | 379.49 |

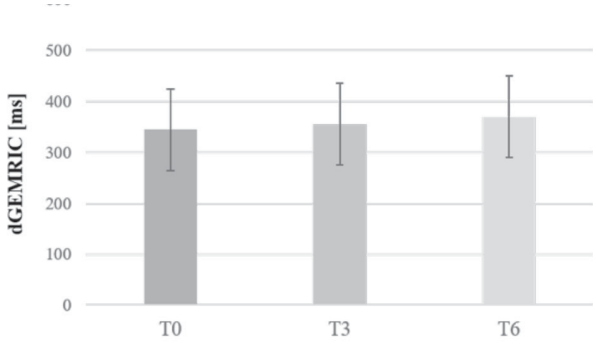


**Fig. 1.** dGEMRIC index in ms of MCP D2 of the different time points (from left to the right: T0, T3 and T6).
No significant difference was found between the different time points.

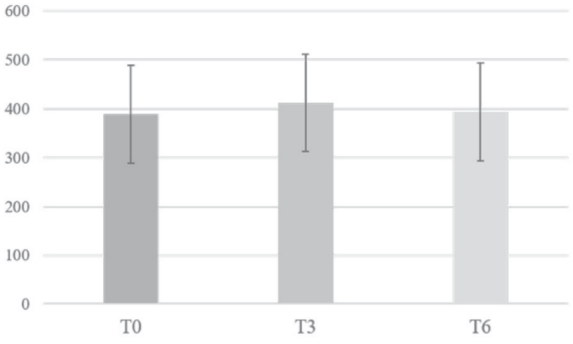


**Fig. 2.** dGEMRIC index in ms of MCP D3 of the different time points (from left to the right: T0, T3 and T6).
No significant difference could be revealed between the different time points.

*Biochemical integrity of MCP joint cartilage under MTX therapy*

dGEMRIC index of second and third MCP joint showed no significant difference between T0 and T3 (D2: $p$=0.45; D3: $p$=0.55) and between T0 and T6 (D2: $p$=0.15; D3: $p$=0.42) (Fig. 1-3).

*Cartilage assessment of lower synovitis ('bad') vs. higher synovitis ('good') in MCP joints 2 and 3 in T0, T3 and T6*

MCP joints with more severe synovitis ('bad joints') demonstrated significantly lower dGEMRIC values compared to MCP joints with less severe synovitis ('good joints') at time-point 0 and 3 months ($p$=0.002; $p$=0.019, respectively). After 6 months of MTX therapy, no significant difference of dGEMRIC index was found between good and bad joints ($p$=0.086) (Fig. 4-5). RAMRIS

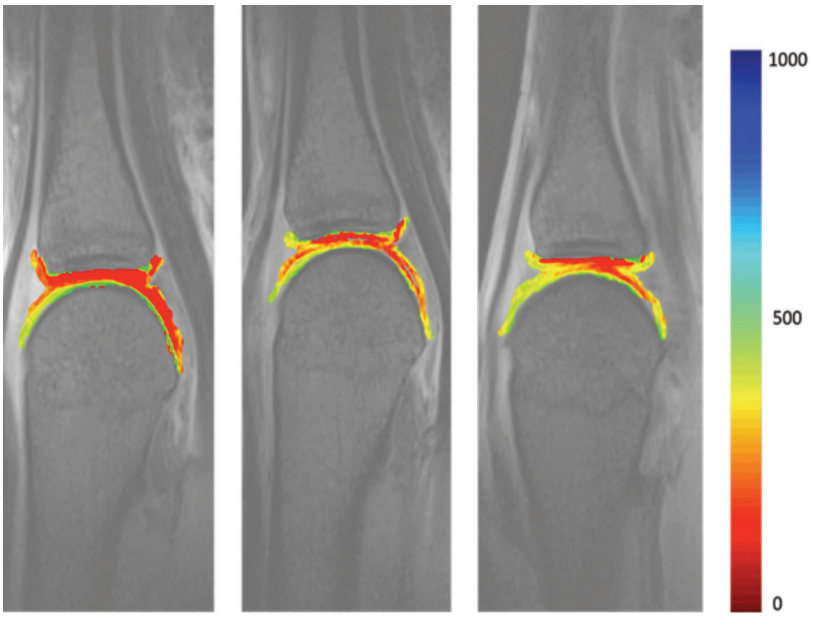


**Fig. 3.** Colour-coded dGEMRIC map with low dGEMRIC index in red and high dGEMRIC index in blue in ms. In this patient with high synovitis subscore (grade 3), no significant progression of cartilage damage could be illustrated. In contrast, subtle higher dGEMRIC index in T6 could be displayed.

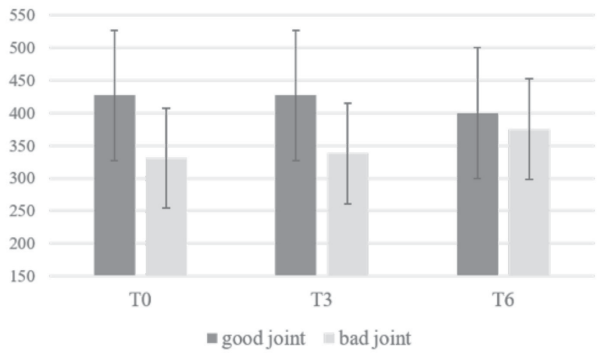


**Fig. 4.** 'Bad joints' showed significantly lower dGEMRIC index compared to 'good joints' at baseline measurements and three months after MTX therapy. Six months after the initiation of MTX therapy, no significant difference between 'bad and good joints' could be found.

synovitis subscore showed significantly higher scores in 'bad' *versus* 'good' joints ($p$=0.02; 2.64 *vs*. 2.18).

## Discussion

Treat-to-target strategies are key concepts in current RA therapy management by which achieving remission or at least low disease activity via a rapid diagnosis combined with the use of cs-DMARDs, like MTX, is possible in the majority of patients (28-31). Subclinical inflammation in RA as a possible trigger for progressive joint destruction was reported and puts preservation of joint integrity into focus of therapy (1, 8). Our results revealed a stop of cartilage degradation under MTX therapy in a six months follow up. Herz *et al*. investigated the relation between inflammation of synovia and cartilage degradation measured with biochemical and morphological MRI (32). They demonstrated an association with high synovitis and proteoglycan loss measured by dGEMRIC.

A depletion of the proteoglycan content in the inflamed cartilage leads to an increased accumulation of contrast medium and an accelerated T1 relaxation time that can be detected with dGEMRIC (13, 19). In this context, joints with a higher RAMRIS synovitis subscore demonstrated significantly lower dGEMRIC values in an intraindividual analysis. To diminish confounders between subjects such as disease duration, age, gender, or therapy effects, we compared particular pair of adjacent joints in each patient (19). Our follow up study displayed higher cartilage destruction in joints with higher synovitis subscore ('bad joints') compared to joints with lower synovitis subscore ('good joints') at baseline and three months after start of MTX therapy. Six months after initiation of MTX therapy, we found an alignment between the proteoglycan loss of the previously 'bad and good joints'. Our results support the concept that inflammatory severity is associated with cartilage damage on a single joint level and can be stopped with antirheumatic therapy. In MCP D2, dGEMRIC indices increased over time. This may be a healing effect of the cartilage with higher proteoglycan content after the initiation of therapy. This effect was already described in knee joints after exercise (33). In RA, this effect was not described yet. In our study, the dGEMRIC increase was not significant, so it is possible that artefacts of molecular imaging lead to the increase. We had no histological confirmation about this.

Our study has limitations. One limitation was the small number of patients investigated in this study. This was partly due to the strict requirements of this study including only patients with early RA which were investigated at three time points. Further longitudinal studies are needed to confirm our results. No synovial and cartilage biopsies for histological analysis as a gold standard in evaluation of joint inflammation were available. Only few studies prepared synovial biopsies as gold standard (15). However, RAMRIS synovitis sub-score and dGEMRIC are well established methods to assess synovial inflammation (34) and cartilage damage (35). Additionally, the dGEMRIC values vary among different studies and protocols (32). The lack of a standard protocol for biochemical cartilage imaging limits the comparability of dGEMRIC between individual studies. Additionally, there is major overlap when comparing the different groups and dGEMRIC indices. This has to be taken into account when interpreting the results.

In conclusion, under MTX therapy, biochemical cartilage integrity remains stable, no further cartilage destruction occurred in the six month follow up. This might be explainable through reduced inflammation on joint level. In

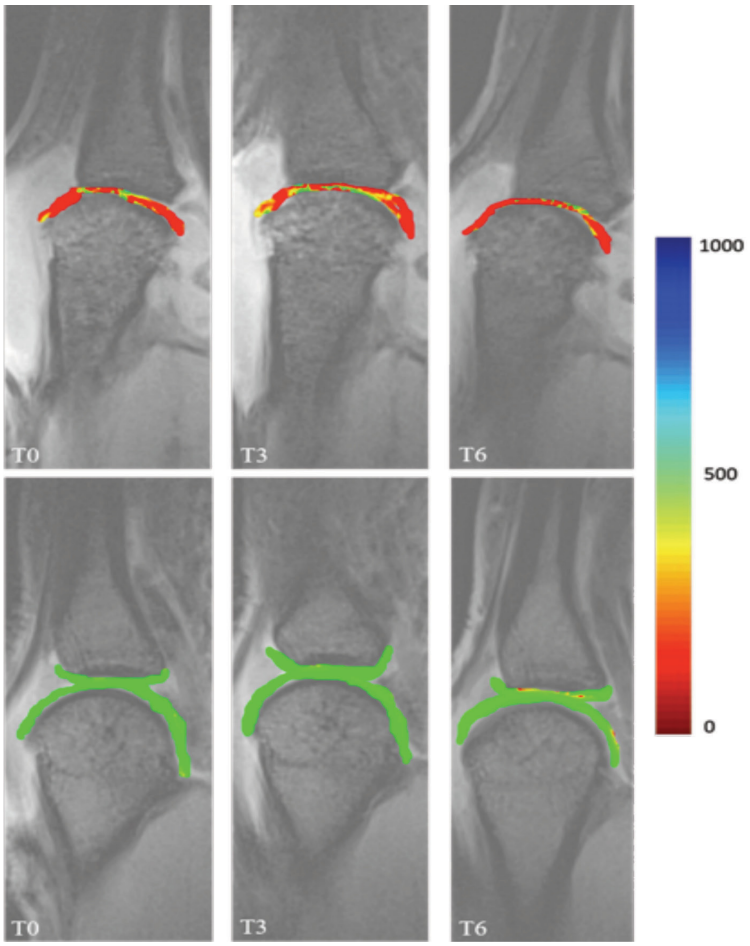


**Fig. 5.** Colour-coded dGEMRIC map with low dGEMRIC index in red and high dGEMRIC index in blue in ms. In this patient MCP joints with high synovitis subscore constantly demonstrated low dGEMRIC index across the different time points ('bad joint', upper row) compared to the 'good joint' (lower row).

addition, six months of MTX therapy triggered an alignment of dGEMRIC index of MCP joints with initially severe synovitis and less severe synovitis in an intra-individual assessment. This underlines the importance of an early treatment in eRA to reduce further cartilage damage of the inflamed joints. dGEMRIC may be an important tool to detect early molecular damage of cartilage in RA.

## References


1. LAFEBER FP, VAN DER LAAN WH: Progression of joint damage despite control of inflammation in rheumatoid arthritis: a role for cartilage damage driven synovial fibroblast activity. *Ann Rheum Dis* 2012; 71: 793-95.
2. FEX E, JONSSON K, JOHNSON U, EBERHARDT K: Development of radiographic damage during the first 5-6 yr of rheumatoid arthritis. A prospective follow-up study of a Swedish cohort. *Br J Rheumatol* 1996; 35: 1106-15.
3. ALETAHA D, SMOLEN J, WARD MM: Measuring function in rheumatoid arthritis: Identifying reversible and irreversible components. *Arthritis Rheum* 2006; 54: 2784-92.
4. SMOLEN JS, ALETAHA D, STEINER G: Does damage cause inflammation? Revisiting the link between joint damage and inflammation. *Ann Rheum Dis* 2009; 68: 159-62.
5. MACCHIONI P, MAGNANI M, MULÈ R *et al*.: Ultrasonographic predictors for the development of joint damage in rheumatoid arthritis patients: a single joint prospective study. *Clin Exp Rheumatol* 2013; 31: 8-17.
6. ALETAHA D, NEOGI T, SILMAN AJ *et al*.: 2010 rheumatoid arthritis classification criteria: an American College of Rheumatology/European League Against Rheumatism collaborative initiative. *Ann Rheum Dis* 2010; 69: 1580-88.
7. KOSTA PE, VOULGARI PV, ZIKOU AK, DROSOS AA, ARGYROPOULOU MI: The usefulness of magnetic resonance imaging of the hand and wrist in very early rheumatoid arthritis. *Arthritis Res Ther* 2011; 13: R84.
8. GANDJBAKHCH F, CONAGHAN PG, EJBJERG B *et al*.: Synovitis and osteitis are very frequent in rheumatoid arthritis clinical remission: results from an MRI study of 294 patients in clinical remission or low disease activity state. *J Rheumatol* 2011; 38: 2039-44.
9. ØSTERGAARD M, PETERFY C, CONAGHAN P *et al*.: OMERACT Rheumatoid Arthritis Magnetic Resonance Imaging Studies. Core set of MRI acquisitions, joint pathology definitions, and the OMERACT RA-MRI scoring system. *J Rheumatol* 2003; 30: 1385-86.
10. ØSTERGAARD M, EMERY P, CONAGHAN PG *et al*.: Significant improvement in synovitis, osteitis, and bone erosion following golimumab and methotrexate combination therapy as compared with methotrexate alone: a magnetic resonance imaging study of 318 methotrexate-naive rheumatoid arthritis patients. *Arthritis Rheum* 2011; 63: 3712-22.
11. ALETAHA D, FUNOVITS J, SMOLEN JS: Physical disability in rheumatoid arthritis is associated with cartilage damage rather than bone destruction. *Ann Rheum Dis* 2011; 70: 733-39.
12. ZILKENS C, MIESE F, HERTEN M *et al*.: Valid-ity of gradient-echo three-dimensional delayed gadolinium-enhanced magnetic resonance imaging of hip joint cartilage: a histologically controlled study. *Eur J Radiol* 2013; 82: e81-86.
13. MIESE F, BUCHBENDER C, SCHERER A *et al*.: Molecular imaging of cartilage damage of finger joints in early rheumatoid arthritis with delayed gadolinium-enhanced magnetic resonance imaging. *Arthritis Rheum* 2012; 64: 394-99.
14. BURSTEIN D, VELYVIS J, SCOTT KT *et al*.: Protocol issues for delayed Gd(DTPA)(2-)-enhanced MRI (dGEMRIC) for clinical evaluation of articular cartilage. *Magn Reson Med* 2001; 45: 36-41.
15. VORDENBÄUMEN S, SCHLEICH C, LÖGTERS T *et al*.: Dynamic contrast-enhanced magnetic resonance imaging of metacarpophalangeal joints reflects histological signs of synovitis in rheumatoid arthritis. *Arthritis Res Ther* 2014; 16: 452.
16. BASHIR A, GRAY ML, BURSTEIN D: Gd-DTPA2- as a measure of cartilage degradation. *Magn Reson Med* 1996; 36: 665-73.
17. MIESE FR, OSTENDORF B, WITTSACK HJ *et al*.: Metacarpophalangeal joints in rheumatoid arthritis: delayed gadolinium-enhanced MR imaging of cartilage--a feasibility study. *Radiology* 2010; 257: 441-47.
18. CREMA MD, ROEMER FW, MARRA MD *et al*.: Articular cartilage in the knee: current MR imaging techniques and applications in clinical practice and research. *Radiographics* 2011; 31: 37-61.
19. SCHLEICH C, MÜLLER-LUTZ A, SEWERIN P *et al*.: Intra-individual assessment of inflammatory severity and cartilage composition of finger joints in rheumatoid arthritis. *Skeletal Radiol* 2015; 44: 513-18.
20. MÜLLER-LUTZ A, SCHLEICH C, SEWERIN *et al*.: Comparison of quantitative and semiquantitative dynamic contrast-enhanced MRI with respect to their correlation to delayed gadolinium-enhanced MRI of the cartilage in patients with early rheumatoid arthritis. *J Comput Assist Tomogr* 2015; 39: 64-69.
21. MCGONAGLE D, TAN AL, MØLLER DØHN U, OSTERGAARD M, BENJAMIN M: Microanatomic studies to define predictive factors for the topography of periarticular erosion for-

mation in inflammatory arthritis. *Arthritis Rheum* 2009; 60: 1042-51.
22. ØSTERGAARD M, BIRD P, GANDJBAKHCH F *et al*.: The OMERACT MRI in Arthritis Working Group - update on status and future research priorities. *J Rheumatol* 2015; 42: 2470-72.
23. MØLLER-BISGAARD S, HØRSLEV-PETERSEN K, EJBJERG BJ *et al*.: Impact of a magnetic resonance imaging-guided treat-to-target strategy on disease activity and progression in patients with rheumatoid arthritis (the IMAGINE-RA trial): study protocol for a randomized controlled trial. *Trials* 2015; 16: 178.
24. COMBE B, LANDEWE R, DAIEN CI *et al*.: 2016 update of the EULAR recommendations for the management of early arthritis. *Ann Rheum Dis* 2017; 76: 948-59.
25. MCQUEEN FM, BENTON N, PERRY D *et al*.: Bone edema scored on magnetic resonance imaging scans of the dominant carpus at presentation predicts radiographic joint damage of the hands and feet six years later in patients with rheumatoid arthritis. *Arthritis Rheum* 2003; 48: 1814-27.
26. MCQUEEN F, LASSERE M, EDMONDS J *et al*.: OMERACT Rheumatoid Arthritis Magnetic Resonance Imaging Studies. Summary of OMERACT 6 MR Imaging Module. *J Rheumatol* 2003; 30: 1387-92.
27. MIESE F, KRÖPIL P, OSTENDORF B *et al*.: Motion correction improves image quality of dGEMRIC in finger joints. *Eur J Radiol* 2011; 80: e427-31.
28. EMERY P, MCINNES IB, VAN VOLLENHOVEN R, KRAAN MC: Clinical identification and treatment of a rapidly progressing disease state in patients with rheumatoid arthritis. *Rheumatology* (Oxford) 2008; 47: 392-98.
29. ESPINOZA F, FABRE S, PERS YM: Remission-induction therapies for early rheumatoid arthritis: evidence to date and clinical implications. *Ther Adv Musculoskelet Dis* 2016; 8: 107-18.
30. JACOBS JW: Optimal use of non-biologic therapy in the treatment of rheumatoid arthritis. *Rheumatology* (Oxford) 2012; 51 (Suppl. 4): iv3-8.
31. HUO Y, VELDHUIZEN RD, VAN DER HEIJDE DM *et al*.: Society for Rheumatology Research Utrecht investigators. Automated joint space width quantification of hand and wrist joints: a proof of concept study. *Clin Exp Rheumatol* 2016; 34 (Suppl. 101): S34-S39.
32. HERZ B, ALBRECHT A, ENGLBRECHT M *et al*.: Osteitis and synovitis, but not bone erosion, is associated with proteoglycan loss and microstructure damage in the cartilage of patients with rheumatoid arthritis. *Ann Rheum Dis* 2014; 73: 1101-6.
33. BURSTEIN D: Tracking longitudinal changes in knee degeneration and repair. *J Bone Joint Surg Am* 2009; 91 (Suppl. 1): 51-53.
34. ØSTERGAARD M, DUER A, NIELSEN H *et al*.: Magnetic resonance imaging for accelerated assessment of drug effect and prediction of subsequent radiographic progression in rheumatoid arthritis: a study of patients receiving combined anakinra and methotrexate treatment. *Ann Rheum Dis* 2005; 64: 1503-6.
35. TIDERIUS CJ, SANDIN J, SVENSSON J, DAHLBERG LE, JACOBSSON L: Knee cartilage quality assessed with dGEMRIC in rheumatoid arthritis patients before and after treatment with a TNF inhibitor. *Acta Radiol* 2010; 51: 1034-37.

Z Rheumatol 2018 · 77:538–548
https://doi.org/10.1007/s00393-018-0497-3
Online publiziert: 18. Juni 2018


**Redaktion**
U. Müller-Ladner, Bad Nauheim
U. Lange, Bad Nauheim

**P. Sewerin[1] · B. Ostendorf[1] · C. Schleich[2]**

[1] Poliklinik, Funktionsbereich & Hiller Forschungszentrum für Rheumatologie, Universitätsklinikum, Heinrich-Heine Universität Düsseldorf, Düsseldorf, Deutschland

[2] Institut für Diagnostische und Interventionelle Radiologie, Universitätsklinikum, Heinrich-Heine Universität Düsseldorf, Düsseldorf, Deutschland

# MRT-Diagnostik bei entzündlichen Gelenk- und Wirbelsäulenerkrankungen: Protokolle und Spezialsequenzen: Wann und wozu?

Bildgebende Untersuchungen stellen wichtige Hilfsmittel bei der Diagnostik und Differenzialdiagnostik entzündlich und degenerativ rheumatischer Gelenk- und Wirbelsäulenerkrankungen dar. Die konventionelle Röntgendiagnostik diente hierbei lange Zeit – ob ihrer vielen Vorteile – als der bildmorphologische „Goldstandard". Die Tatsache, dass radiologische Veränderungen aber oft erst Monate nach einer Gelenkentzündung mittels konventioneller Röntgenuntersuchung sichtbar werden, macht diese Technik für die Frühdiagnostik weitestgehend unbrauchbar, wobei ein primäres Röntgenbild bei der Diagnosestellung weiterhin empfohlen wird. Grund ist unter anderem, dass Erosionen im konventionellen Röntgen nach wie vor wichtig für die Prognoseabschätzung bleiben. Somit werden sensitivere bildgebende Verfahren wie hochauflösender Ultraschall und die Magnetresonanztomographie (MRT) heutzutage immer mehr in Klinik, Praxis und Studien zur frühen Diagnoseabsicherung als auch Therapiekontrolle eingesetzt.

Die MRT hat hier einen besonderen Stellenwert, denn ihr obliegt das Potenzial – aufgrund der Schnittbildtechnik und verschiedener Wichtungen und Sequenzen – Veränderungen im und um das Gelenk bzw. der Wirbelsäule frühzeitig im Krankheitsverlauf abzubilden. MR-morphologisch können so Gelenkerguss, Synovialitis, Tenovaginitis, Enthesitis, inzipiente Knorpel- und Knochenstoffwechselstörungen und die Erosion als auch Gelenkumbau und -anbau (Syndesmophyt, Osteophyt) sicher erfasst werden. Auch subklinische Entzündungen oder frühe degenerative Veränderungen z. B. auf Knorpelebene, welche dem konventionellen Röntgenbild entgehen, können mithilfe der MR-Technik eher aufgedeckt werden.

Durch die Entwicklung von MRT-Scoring-Instrumenten (z. B. RAMRIS für Hand/Fuß [1], verschiedene MRT-Scores für die Wirbelsäule [2], WORMS für Kniegelenke [3]) können MRT-Befunde semiquantitativ graduiert werden und sind somit standardisiert vergleichbar, was für Studien und wissenschaftliche Fragestellungen unabdingbar geworden ist.

Alle diese Vorteile tragen dazu bei, dass die MRT inzwischen praxistauglich regelhaft in der Rheumatologie eingesetzt, in EULAR-Empfehlungen zur Diagnostik der RA genannt wird und bei den entzündlichen Wirbelsäulenerkrankungen auch Teil der ASAS-Klassifikationskriterien geworden ist.

Es ist zu erwähnen, dass neben der MRT auch die Sonographie in der Lage ist, bildmorphologisch Pathologien, insbesondere der peripheren Gelenke, zu erfassen und zu bewerten [4]. Heute steht die Sonographie nahezu flächendeckend sowohl im klinischen als auch im ambulanten Setting zur Verfügung und wird hier regelhaft eingesetzt. Trotz der technischen Fortschritte ist die Sonographie nach wie vor nicht geeignet, um valide Pathologien des Achsenskeletts abzubilden. Hinzukommend ist bisher nur die MRT in der Lage, das prognostisch wichtige Knochenmarködem zu erfassen, was anderen bildgebenden Verfahren und somit auch der Sonographie nicht gelingt [5].

Als Rheumatologen sind wir gefordert, die Grundlagen der MRT-Technik zu verstehen, die Ergebnisse zu bewerten und mit Anamnese, Klink und Labor in einen Kontext zu setzen. Dies bedeutet, dass auch die MRT-Diagnostik Teil unserer Ausbildung ist und eine kontinuierliche Fort- und Weiterbildung nach sich zieht. Dieser Grundsatz bedingt aber auch die intensive Kommunikation und den regelhaften Austausch mit den Fachkollegen der Radiologie, welche in der Regel die MRT-Diagnostik durchführen. Nur die gezielte und überprüfte Indikation zur MRT-Diagnostik, die korrekten Angaben von Informationen zur Erkrankung und zum Patienten als auch der fachliche Austausch mit den befundenen ärztlichen Kolleginnen/en zur entsprechenden MRT-Untersuchung wird die Qualität dieser radiologischen Leistung noch weiter verbessern, was letztendlich unseren Patienten zugutekommen wird.

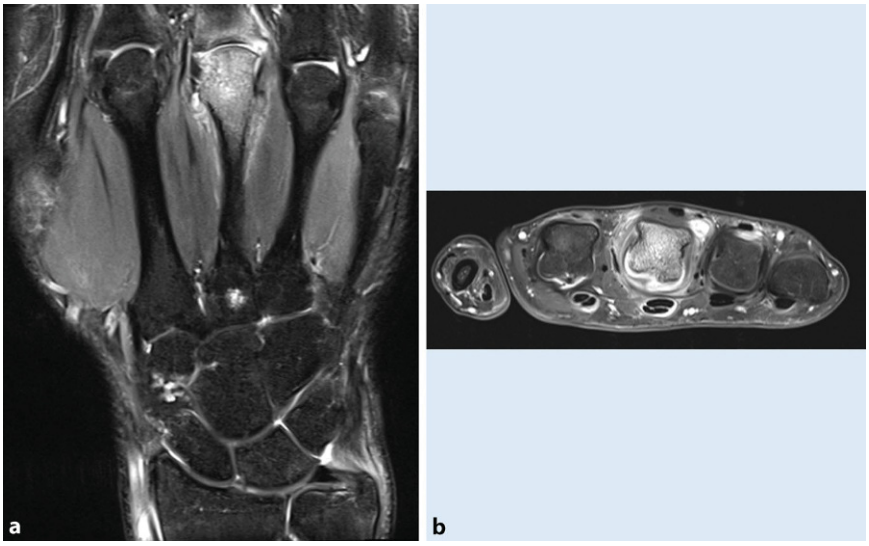


**Abb. 1** ▲ **a** STIR-Sequenz der Hand, koronare Schnittführung; Patient mit einer RA. Nachweis eines Knochenmarködems und einer Synovialitis Metacarpophalangealgelenk (MCP) Digitus (D) 3 sowie eine Erosion an der Basis des Mittelhandknochens (MHK) 3. **b** T1-Sequenz der Hand, transversale Schnittführung, fs post Kontrastmittel (KM), Nachweis einer Synovialitis und einer Tenovaginitis mit punctum maximum D3

In den folgenden Abschnitten werden die derzeit relevanten MRT-Protokolle respektive Spezialsequenzen und ergänzenden praxisnahen Empfehlungen zur MRT-Diagnostik von rheumatischen Erkrankungen peripherer Gelenke und des zentralen Achsenskeletts synoptisch und stichwortartig zusammengefasst und vorgestellt.

## Allgemeine Grundsätze in der Untersuchung von Wirbelsäule und Gelenken

Durch die immer bessere Verfügbarkeit und die sinkenden Kosten werden MRT-Untersuchungen heute auch zunehmend im klinischen Alltag eingesetzt. Untersuchungen des Bewegungsapparates werden meist in MRT-Systemen mit Magnetfeldstärken von 1,5–3 Tesla (T) durchgeführt, die eine hohe Auflösung bei relativ kurzen Untersuchungszeiten ermöglichen. Besondere Indikationen und Techniken ergeben sich für Niederfeldgeräte (0,2 T), die in einem eigenen Kapitel besprochen werden. Es muss beachtet werden, dass die Unmöglichkeit einer suffizienten Fettunterdrückung mittels kontrastunterstützter Sequenzen eine wesentliche Einschränkung für das Niederfeld-MRT darstellt, da eine frequenzselektive Fettsättigung aufgrund des nur geringen „chemical shift" zwischen Wasser und Fett bei niedriger Magnetfeldstärke nahezu unmöglich ist.

Allgemein ist zu bedenken, dass spezifische Kontraindikationen zu beachten sind, die vor einer Untersuchung besprochen werden müssen. Hierzu zählen Klaustrophobie, akute und chronische Niereninsuffizienzen (z. B. bei Dialysepatienten bzw. einer GFR von <30 ml/min wegen des erhöhten Risikos für nephrogene systemische Fibrosen [NSF]), bekannte KM-Allergien (Gadolinium) oder Schwangerschaft. Hinzukommend sollten besondere Kautelen, wie etwa Implantate (die heute häufig MRT-fähig sind), Herzschrittmacher und Stents (die nach Endothelialisierung ins MRT dürfen), ebenfalls frühzeitig diskutiert werden.

Neben dem Scanner selbst ist zu beachten, dass Gelenke mit dezidierten Spulensystemen (z. B. für Knie-, Schulter- oder Handgelenke) untersucht werden sollten um die optimale Auflösung und Signalausbeute zu garantieren. Für die Untersuchung der Wirbelsäule ist häufig bereits eine spezielle Spule im Untersuchungstisch integriert.

Zu Beginn einer Untersuchung werden immer Übersichtsbilder (sog. „localizer") mit einer T1- und einer T2-gewichteten Sequenz in 2 Ebenen aufgenommen. Das T1-Bild zeigt primär die morphologischen Details, das T2-Bild zeigt hingegen optimal pathologische Flüssigkeitsansammlungen in Gelenken, Sehnenscheiden, Knochen (Knochenmarködeme; Osteitis) und Sehnenansätzen (Enthesen). Anschließend sollte versucht werden eine kontrastmittelunterstützte (Kontrastmittel [KM]) T1-gewichtete Sequenz mit Unterdrückung des Fettsignals in 2 bis 3 Schnittebenen einzusetzen (z. B. durch „chemical shift" oder „Dixon"-Technik). Alternativ können nicht fettgesättigte T1-gewichtete Bilder nach KM-Gabe generiert werden, die in der Folge automatisiert von den nativen T1-gewichteten Bildern subtrahiert werden und dadurch eine Kontrastmittelanreicherung sichtbar macht. Durch die Unterdrückung des Fettsignals bzw. die Subtraktionstechnik kommt entzündliches Gewebe (z. B. eine entzündliche Synovialproliferate) selektiv signalreich zur Darstellung und lässt sich vom umgebenden Fettgewebe gut abgrenzen. Im Bereich der Wirbelsäule und der Iliosakralgelenke (ISG) kann alternativ zu den KM-unterstützten Sequenzen eine Short-Tau Inversion Recovery (STIR)-Sequenz eingesetzt werden, die ebenfalls eine hohe Auflösung bei guter Angrenzung von pathologischen Wasseransammlungen ermöglicht und eine Fettsuppression durch einen speziellen Anregungsimpuls erreicht. In der Diagnostik der Wirbelsäule gilt die STIR-Sequenz den KM-unterstützten T1-gew. Sequenzen als gleichwertig, in der Gelenkdiagnostik ist die STIR-Sequenz aber meist unterlegen, weil Erguss und Synovialproliferat nicht gut zu unterscheiden sind, sodass hier weiterhin der Einsatz von KM empfohlen wird. Eine weitere Möglichkeit der suffizienten Fettunterdrückung zur Darstellung von Flüssigkeitsansammlungen bietet die „turbo inversion recovery magnitude" (TIRM)-Technik, die bereits bei der Darstellung von Osteomyelitiden bei Kindern zur Anwendung gekommen ist [6].

Z Rheumatol 2018 · 77:538–548 https://doi.org/10.1007/s00393-018-0497-3


P. Sewerin · B. Ostendorf · C. Schleich

# MRT-Diagnostik bei entzündlichen Gelenk- und Wirbelsäulenerkrankungen: Protokolle und Spezialsequenzen: Wann und wozu?


## Zusammenfassung

Die Magnetresonanztomographie (MRT) stellt heutzutage in der Rheumatologie einen wichtigen Bestandteil bei der bildgebenden Diagnostik und Therapiekontrolle bei entzündlichen und nichtentzündlichen Erkrankungen der Wirbelsäule und peripherer Gelenke dar. Die richtige Wahl geeigneter und praktikabler MRT-Protokolle und Sequenzen stellen den MRT-anfordernden und indikationsstellenden Arzt aber häufig vor große Herausforderungen. In der folgenden Übersichtsarbeit werden Empfehlungen und Vorschläge für MRT-Untersuchungsprotokolle für die Anwendung in Klinik und Praxis gegeben und neue Sequenzen evaluiert und bewertet, um für die Rheumatologie so in Zukunft möglichst standardisierte und vergleichbare Untersuchungen zu generieren und die Qualität der radiologischen Leistung so zu optimieren.



## Schlüsselwörter

Magnetresonanztomographie · Protokolle · Sequenzen · Arthritis · Spondyloarthritis


# MRI diagnostics in inflammatory joint and spinal diseases: protocols and special sequences: when and for what?


## Abstract

Magnetic resonance imaging (MRI) is an important component in rheumatology for imaging diagnostics and therapy monitoring of inflammatory and non-inflammatory diseases of the spine and peripheral joints. The correct selection of suitable and practical MRI protocols and sequences represents a great challenge for physicians with respect to requesting and interpreting the indications for MRI investigations. This review article provides recommendations and suggestions for MRI investigation protocols for clinical utilization and practice. New sequences are evaluated and assessed in order to generate the best possible standardized and comparable examinations for rheumatology in the future and therefore optimize the quality of radiological interventions.



## Keywords

Magnetic resonance imaging · Protocols · Sequences · Arthritis · Spondyloarthritis


## Empfohlene MRT-Protokolle: Extremitäten

### Hand (Hochfeld-MRT)

**Gerät.** 1,5–3 T MRT (Hochfeld-MRT); 3 T ist 1,5 T oder Niederfeld-MRT (0,2–1,5 T; s. unten) vorzuziehen, da ein höheres Signal-zu-Rausch-Verhältnis (SNR) zu einer besseren räumlichen und zeitlichen Auflösung führt respektive zu einer Kontrastverstärkung.

**Indikation.** Frühdiagnostik und Therapiekontrolle der rheumatoiden Arthritis (RA)/Psoriasisarthritis (PsoA), Differenzialdiagnostik bei typischen Mustern und Studien [9].

**MRT-Pathologien.** Synovialitis, Erosion, Knochenmarködem („bone marrow edema“ [BME]), Enthesitis, Tenovaginitis, Erguss.

**Nebenbefunde.** Traumatische und degenerative Veränderungen.

**Spule.** Handspule, Oberflächenspule.

**Lagerung.** Bauchlage in „Superman“-Position oder Rückenlage, Hand über Kopf oder Hand unter Gesäß. Alternativ ist heute auch eine Off-Center-Lagerung in einer dedizierten Handspule bei modernen Geräten möglich.

**MRT-Protokoll.** Obligat sollten eine STIR/TIRM coronar (cor), T1 cor nativ und eine transversale Sequenz T2 fs („fat-saturated“/fett-unterdrückt), PD fs oder STIR/TIRM durchgeführt werden. Alternativ zur T1 nativ kann eine 3D-GRE cor (z. B. VIBE/THRIVE oder Dixon-VIBE) zur Detektion von Erosionen eingesetzt werden. Zur Abbildung der Synovialitis kann nach KM-Applikation eine T1 fs cor und ggf. transversal (tra) durchgeführt werden. Alternativ kann mittels Subtraktionstechnik eine nicht fettgesättigte T1 post-KM von der nativen T1 subtrahiert werden, vorausgesetzt die Sequenzparameter werden zwischen beiden Sequenzen nicht verändert (◘ **Abb. 1**; [7, 8]).

**Zusatzinformation.** Das „field of view“ (FOV) der koronaren Bildgebung umfasst in der Regel die komplette Hand von der Fingerspitze bis zum distalen Radius/Ulna. Zur detaillierten Analyse der arthritischen Veränderungen kann alternativ das FOV verkleinert werden, bei RA das Radiocarpalgelenk einschließlich der MCP-Gelenke umfassen, bei PsoA von der Fingerspitze bis zu den MCP-Gelenken reichen. Die transversalen Bilder umfassen bei RA die MCP-Gelenke, ggf. das Radiocarpalgelenk; bei PsoA sollten die transversalen Bilder die Fingerspitze bis inklusive die PIP-Gelenke umfassen, wobei bei der Wahl des FOV immer die Beschwerden des einzelnen Patienten als Grundlage des Protokolls dienen sollten; es sollte eine Schichtdicke von 2–3 mm gewählt werden; die Applikation von KM erfolgt gewichtsadaptiert: 0,2 ml/kg Körpergewicht (maximal 20 ml) und wird für alle weiteren Untersuchungsprotokolle in gleicher Dosierung angewendet.

**Limitationen.** Klaustrophobie, Lagerung, Dauer.

**Dauer der Untersuchung.** Untersuchungszeit einschließlich Gabe von KM: RA: 20–30 min; PsoA: 25–35 min.

**Scoring.** Rheumatoid Arthritis Magnetic Resonsance Imaging Score (RAMRIS; RA; [1]), PSAMRIS (PsoA; [10, 11]).

### Fuß (Hochfeld-MRT)

**Gerät.** 1,5–3 T MRT.

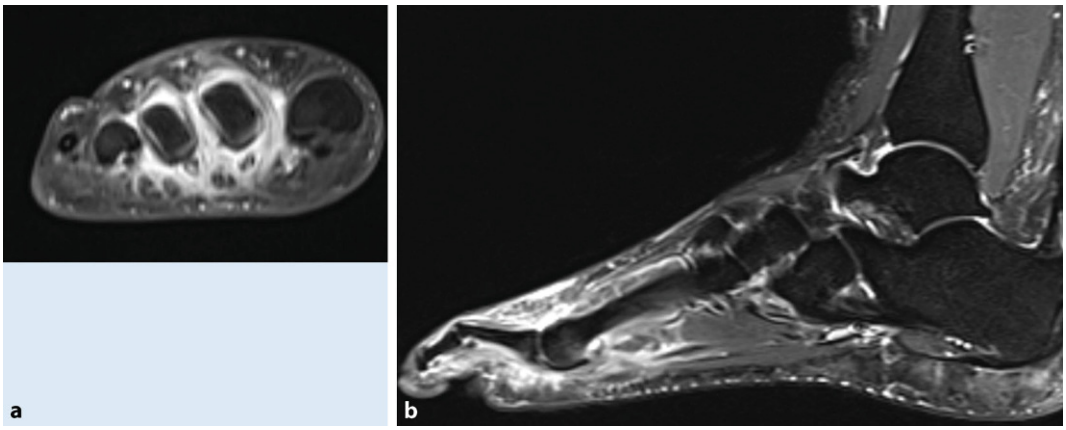


**Abb. 2** ◀ **a** T1-Sequenz des Fußes, koronare Schnittführung, Patient mit einer PsoA; fs post KM; Nachweis einer Synovialitis mit begleitender Weichteilbegleitreaktion. **b** STIR-Sequenz des Fußes, sagittale Schnittführung mit Nachweis einer Daktylitis des 3. Strahles

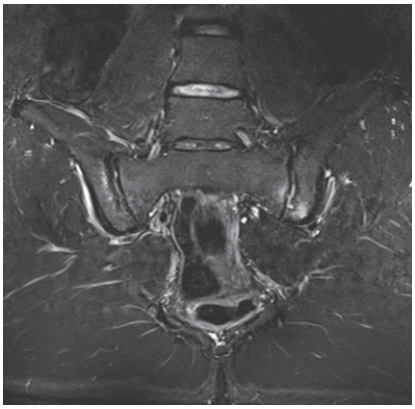

**Abb. 3** ▲ STIR-Sequenz des Os sacrum mit Nachweis einer akuten Sakroiliitis bei einem Patienten mit einer axialen Spondylitis

**Indikation.** Frühdiagnostik und Therapiekontrolle der RA/PsoA, Differenzialdiagnostik.

**MRT-Pathologien.** Synovialitis, Erosion, BME, Enthesitis, Tenovaginitis.

**Spule.** Kopfspule, bei kleinen Füßen auch Kniespule möglich.

**Lagerung.** Rückenlage, Füße voran (Neutral-Null-Stellung).

**MRT-Protokoll.** Obligat sollten koronare Sequenzen angefertigt werden: PD fs, STIR/TIRM oder T2 fs. Transversal sollten PD fs, STIR/TIRM oder T1-Sequenzen durchgeführt werden. Zusätzlich können PD fs sag oder T1 TSE cor-Sequenzen angefertigt werden. Nach KM-Applikation sollten T1 fs-Sequenzen, wenn möglich in allen 3 Raumrichtungen, ergänzt werden (◘ **Abb. 2**; [12]).

**Zusatzinformation.** Das FOV reicht von der Fußwurzel ab dem Talonavikulargelenk bis zu den Zehenspitzen für die koronare und transversale Schichtführung; die sagittalen Bilder sollten den gesamten Fuß, inklusive des oberen Sprunggelenks, umfassen; es wurden Schichtdicken von 2–3 mm gewählt.

**Limitationen.** Klaustrophobie, Lagerung, Dauer.

**Dauer der Untersuchung.** Einschließlich Gabe von KM: 30 min.

**Scoring.** Hand- und Fuß-Score [13, 14].

## Hand/Fuß (Niederfeld-MRT, Extremitäten-MRT)

**Gerät.** Niederfeld-MRT (0,2–1 T MRT).

**Indikation.** Frühdiagnostik und Therapiekontrolle der RA/PsoA, Differenzialdiagnostik, Studien.

**Spule.** Dedizierte Spule (Hand, Fuß, Knie, Ellenbogen).

**Lagerung.** Nur die zu untersuchende Extremität liegt im Isozentrum des Magneten, daher für Rheumatiker komfortabel; ideal für Klaustrophobiker.

**MRT-Protokoll.** Hand/Fuß: STIR cor, T1 GRE vor und nach KM-Applikation (FOV: in der Regel ganze Hand, wenn möglich; falls nur kleineres FOV bzw. zur Detailanalyse FOV RA: Radiocarpalgelenk – inklusive MCP-Gelenke; FOV PsoA: Fingerspitze – inklusive PIP-Gelenke), T1 GRE tra (FOV RA: CP-Gelenke; PsoA: Fingerspitze bis inklusive PIP-Gelenke); es werden Schichtdicken von 3 mm empfohlen. T2-gewichtete Sequenzen in axialer Schichtführung können fakultativ ergänzt werden [15].

**Limitationen.** Bildqualität, kleines FOV (bei großen Händen kann das geplante FOV nicht vollständig abgebildet werden), nicht alle fettgesättigten Sequenzen verfügbar.

**Dauer der Untersuchung.** Untersuchungszeit einschließlich Gabe von KM: Hand oder Fuß: ca. 20–35 min.

**Scoring.** RAMRIS, Hand- und Fuß-Score [13].

## Knie

**Gerät.** 1,5–3 T MRT.

**Indikation.** Diagnostik und Therapiekontrolle der Arthritis und Arthrose, Differenzialdiagnostik.

**MRT-Pathologien.** Synovialitis, Erosion, BME, Enthesitis, Tenovaginitis und Gelenkbinnenschaden: Meniskus, Kreuzbänder, Knorpel, Knochen, Baker-Zyste, Tumoren, Osteonekrose.

**Nebenbefunde.** Traumatische und degenerative Veränderungen.

**Spule.** Dezidierte Kniespule, Oberflächenspule.

**Tab. 1** Protokollvorschläge ausgewählter Gelenkregionen bei Arthritis

| Untersuchte Region | MRT-Protokoll |
|---|---|
| Iliosakralgelenk | *Coronar oblique*[a] *T1-gewichtet (T1)* |
| | *Coronar oblique STIR/TIRM* oder PD fs, T1 fs oder Gradientenechosequenzen |
| | *Axial*[b] *PD fs* oder STIR/TIRM |
| | *Post-KM T1 fs* zur Darstellung einer Synovialitis, Enthesitis, Kapsulitis |
| | Obligatorisch: Minimum *coronar oblique T1-gewichtet, coronar oblique STIR/TIRM;* mindestens 2 aufeinanderfolgende Schichten sollten erfasst werden |
| Wirbelsäule, SpA | *Sagittal T1-gewichtet* |
| | *Sagittal STIR/TIRM* |
| | *Axial T2 fs* oder FFE (zur Darstellung des Osteoödems der posterior gelegenen kleinen Wirbelgelenke) |
| | *Fettgesättigte T1-Post-KM-Bilder* in axialer und sagittaler Schichtführung werden häufig zur Darstellung der aktiven Inflammation benötigt |
| Wirbelsäule, RA | *Sagittal T1-gewichtet* |
| | *Sagittal STIR/TIRM* |
| | *Axial T2 fs* oder FFE des Atlantoaxial- oder Atlantookzipitalgelenks |
| | *Koronare T1* bei atlantoaxialer/atlantookzipitaler Subluxationsstellung |
| | *Fettgesättigte T1-Post-KM-Bilder* in axialer und sagittaler Schichtführung werden häufig zur Darstellung der aktiven Inflammation benötigt |
| Hand[c] | *Koronar T1-gewichtet/3D-GRE* |
| | *Koronar STIR/TIRM* oder T2 fs |
| | *Axial T2 fs* oder PD fs oder STIR/TIRM |
| | *Post-KM T1 oder T1 fs* (zur Darstellung der Synovialitis; isotrope 3-D-Sequenzen erlauben Rekonstruktionen in allen Ebenen) |
| Oberes Sprunggelenk und Fuß[d] | *Sagittal PD fs* |
| | *Koronar*[d] *T2 FS, STIR/TIRM oder PD fs* |
| | *Axial*[e] *T1-gewichtet* |
| | *Axial PD fs oder T2 STIR/TIRM* |
| | *Post-KM T1 or T1 fs* |
| Schultergelenk | *PD fs* in allen Raumrichtungen, ausgerichtet an der Skapula |
| | *Parasagittal T1-gewichtet* |
| | *Post-KM T1 fs* zur Darstellung von entzündlichen Veränderungen |
| Hüftgelenk | *Cor STIR/TIRM,* T2 fs oder PD fs |
| | *Cor T1-gewichtet* |
| | *Tra STIR/TIRM*, T2 fs oder PD fs |
| | *Post-KM T1 fs* zur Darstellung von entzündlichen Veränderungen |

***FFE*** Fast-field-Echo, ***FS*** Fettsuppression, ***PD*** protonengewichtet, ***PsoA*** Psoriasisarthritis, ***RA*** rheumatoide Arthritis, ***SpA*** Spondylarthropathie, ***STIR*** „short tau inversion recovery", ***TIRM*** „turbo inversion recovery magnitude"

[a]Coronar oblique: Schicht in koronarer Ebene der Iliosakralgelenke in Bezug auf die Tangente der posterioren Oberfläche des Wirbelkörpers SWK2

[b]Axial: eine transversale Schicht der Iliosakralgelenke senkrecht zur koronaren Schichtführung

[c]Bei RA ist die Abbildung des Handgelenks bis zu den Metakarpophalangealgelenken essenziell; die distalen Interphalangealgelenke sollten bei PsoA mit abgebildet werden

[d]Koronare Schichtführung entlang der Körperachse

[e]Axiale Schichtführung orthogonal zur Körperachse

**Lagerung.** Rückenlage, Neutral-Null-Stellung.

**MRT-Protokoll.** PD fs in cor, tra und sag Schichtführung. T1 cor vor und zur Darstellung einer möglichen Synovialitis nach KM-Applikation. Fakultativ können T2 tra, T1 fs tra nach KM-Applikation oder knorpelspezifische Sequenzen (DESS, Truefisp) ergänzt werden.

**Zusatzinformation.** Das FOV umfasst das gesamte Kniegelenk, inklusive distaler Femur und prox. Tibia/Fibula; die Schichtdicke aller Sequenzen beträgt 3 mm.

**Limitationen.** Klaustrophobie, Lagerung, Dauer.

**Dauer der Untersuchung.** Untersuchungszeit einschließlich Gabe von KM: 15–30 min.

**Scoring.** WORMS [3].

## Schulter

**Gerät.** 1,5–3 T MRT.

**Indikation.** Diagnostik und Therapiekontrolle der Arthritis und Arthrose, Differenzialdiagnostik.

**MRT-Pathologien.** Synovialitis, Erosion, BME, Enthesitis, Tenovaginitis und Gelenkbinnenschaden: Rotatorenmanschette, Bizepssehne, Knorpel, Knochen, Tumoren.

**Nebenbefunde.** Traumatische und degenerative Veränderungen.

**Spule.** Dezidierte Schulterspule, Alternative: Flexspule.

**Lagerung.** Rückenlage, Neutral-Null-Stellung.

**MRT-Protokoll.** PD fs in parakoronarer, parasagittaler und transversaler Schichtführung, alternativ STIR/TIRM, ausgerichtet an der Skapula. Mindestens eine T1-gewichtete Sequenz, zur Beurteilung der Rotatorenmanschette ist eine parasagittale Schichtführung zu bevorzugen.

Zur Darstellung einer möglichen Synovialitis T1 fs parakoronar und transversal nach KM-Applikation [16].

**Zusatzinformation.** Das FOV umfasst das gesamte Schultergelenk; die Schichtdicke aller Sequenzen beträgt 3 mm.

**Limitationen.** Klaustrophobie, Lagerung, Dauer.

**Dauer der Untersuchung.** Untersuchungszeit einschließlich Gabe von KM: 20–25 min.

### Hüftgelenk

**Indikation.** Diagnostik und Therapiekontrolle der Arthritis und Arthrose, Differenzialdiagnostik.

**MRT-Pathologien.** Synovialitis, Erosion, BME, Enthesitis, Tenovaginitis und Gelenkbinnenschaden: Labrum, Knorpel.

**Nebenbefunde.** Traumatische und degenerative Veränderungen.

**Spule.** Flexspule.

**Lagerung.** Rückenlage, Neutral-Null-Stellung.

**MRT-Protokoll.** PD fs in cor und sag Schichtführung. Alternativ können STIR/TIRM oder T2 fs-Sequenzen angefertigt werden. T1 cor vor und zur Darstellung einer möglichen Synovialitis nach KM-Applikation. Zusätzlich sollten tra-Sequenzen (PD fs, STIR/TIRM, T2 fs) angefertigt werden. Fakultativ können knorpelspezifische Sequenzen (z. B. DESS) ergänzt werden [16].

**Zusatzinformation.** Das FOV umfasst das gesamte Hüftgelenk; die Schichtdicke aller Sequenzen beträgt 3–4 mm.

**Limitationen.** Klaustrophobie, Lagerung, Dauer.

**Dauer der Untersuchung.** Untersuchungszeit einschließlich Gabe von KM: ca. 30 min

### Enthesen

**Gerät.** 1,5–3 T MRT.

**Indikation.** Frühdiagnostik und Therapiekontrolle bei der PsoA, SpA, Enthesitis, Differenzialdiagnostik.

**MRT-Pathologien.** Enthesitis, Synovialitis, BME, Bursitiserosion, Syndesmophyt, Exostose, Knochenmarködem.

**Nebenbefunde.** Traumatische (Ruptur) und degenerative Veränderungen.

**Spule.** Die Enthesitis stellt eine Entzündung des Sehnen-Knochen-Übergangs dar, die sich prinzipiell an allen Körperregionen manifestieren kann. Besonders häufig ist die Achillessehne betroffen. Je nach Topographie bzw. Befallsmuster und Vorkommen der Enthesitis können verschiedene Spulen zum Einsatz kommen; zur Darstellung der Achillessehne kann ein OSG-Protokoll mit Kopf- oder Kniespule (bei kleinen Füßen) eingesetzt werden; Enthesen am Schultergelenk können mithilfe einer dezidierten Schulterspule oder einer Oberflächenspule dargestellt werden; das Ellenbogengelenk kann mittels einer Oberflächenspule; einzelne Finger/Fußzehen können mittels Ring- oder einer dezidierten Handgelenkspule abgebildet werden.

**Lagerung.** In der Regel Neutral-Null-Position; in Rückenlage werden Schulter und OSG (z. B. für Darstellung der Achillessehne) dargestellt; das Ellenbogengelenk wird normalerweise in Bauchlage mit gestrecktem Arm untersucht (die Untersuchung ist ebenfalls in Rückenlage oder flektiertem Ellenbogengelenk möglich); die MRT-Untersuchung einzelner Finger wird in Bauchlage durchgeführt.

**MRT-Protokoll.** PD TSE cor, T1 TSE cor vor und nach KM-Applikation, T1 TSE transv. nach KM-Applikation, ggf. T2 TSE tra, PD TSE sag, T1 TSE sag nach KM-Applikation; die einzelnen Ebenen im Schulterprotokoll werden nach Glenoid/Skapula ausgerichtet, dadurch werden parakoronare und parasagittale Ebenen abgebildet; die Achillessehne wird im Rahmen des OSG-Protokolls erfasst, auf eine vollständige Abbildung nach kranial sollte geachtet werden; sollten weitere Bandstrukturen am OSG erfasst werden, muss eine entsprechende Kippung entlang der gewünschten Ligamente erfolgen; das FOV sollte stets die komplette Enthese bzw. das Gelenk umfassen; die Schichtdicke beträgt zwischen 2 und 3 mm, je kleiner die zu erfassende Struktur ist, desto kleinere Schichtdicken sollten gewählt werden [17].

**Limitationen.** Klaustrophobie, Lagerung, Dauer.

**Dauer der Untersuchung.** Untersuchungszeit einschließlich Gabe von KM: Je nach Untersuchungsregion beträgt die Untersuchungszeit zwischen 15 und 30 min.

**Scoring.** PSAMRIS.

## Empfohlene MRT-Protokolle: Wirbelsäule

### HWS

**Gerät.** 1,5–3 T MRT.

**Indikation.** Entzündliche HWS-Beteiligung bei RA, z. B. Komprimierung des Myelons, Densdestruktion, Instabilität, präoperative Abklärung.

**Spule.** Halsspule.

**Lagerung.** Rückenlage.

**MRT-Protokoll.** STIR/TIRM sag, T1 TSE sag vor und nach KM-Applikation (zur Detektion entzündlicher Veränderungen der Synovia, Enthesen). Fakultativ T2 TSE sag. Das betroffene Bewegungssegment sollte zusätzlich transversal abgebildet werden: T2 medic (alternativ T2), T1 TSE tra nach KM-Applikation; bei RA wird v. a. der Dens axis transversal abgebildet [16].

**Limitationen.** Klaustrophobie, Lagerung, Dauer; cave: Überstreckung bei Lagerung (HWS-Instabilität).

**Dauer der Untersuchung.** Dauer der Untersuchung einschließlich Gabe von KM: 20–25 min.

### Lendenwirbelsäule (LWS), Brustwirbelsäule (BWS) und ISG (Iliosakralgelenke)

#### LWS und BWS

**Gerät.** 1,5–3 T MRT.

**Indikation.** Frühdiagnostik und Therapiekontrolle Spondyloarthritis (Spondylitis, Iliosakralarthritis).

**Spule.** Körperspule.

**Lagerung.** Rückenlage.

**MRT-Protokoll.** Das WS-Protokoll umfasst eine STIR sag, T1 TSE sag vor und nach KM-Applikation, T2 TSE sag mit einer Schichtdicke von 3–4 mm; zusätzlich können die gewünschten Bewegungssegmente transversal mit einer Schichtdicke von 3 mm dargestellt werden: T2 TSE tra, T1 TSE tra nach KM-Applikation, ggf. STIR cor mit einer Schichtdicke von 4 mm; das FOV sagittal sollte den kompletten WS-Bereich umfassen. Zur Diagnosestellung Spondyloarthritis kann nach aktueller Studienlage auf Kontrastmittel verzichtet werden. Vorteile kann eine Kontrastmittelapplikation bringen bei der Suche nach weiteren entzündlichen Veränderungen im Rahmen einer Synovialitis, Enthesitis oder Kapsulitis [20].

**Limitationen.** Klaustrophobie, Lagerung, Dauer.

**Dauer der Untersuchung.** Untersuchungszeit einschließlich Gabe von KM: LWS-Protokoll: 20 min; BWS-Protokoll: 20–30 min.

**Scoring.** Z. B. Berlin-MRT-Score; ASpiMRI Score, Leeds Score, Berliner Score, SPARCC, ASAS [2, 21].

#### ISG

**Indikation.** Frühdiagnostik Arthritis, Enthesitis, Tumor.

**Spule.** Körperspule.

**Lagerung.** Rückenlage.

**MRT-Protokoll.** Das Protokoll der ISG umfasst eine STIR/TIRM (alternativ PD fs) parakoronar (ausgerichtet an der Hinterkante von SWK 2), T1 parakoronar vor und nach KM-Applikation (zur dezidierten Diagnostik einer Synovialitis, Enthesitis, Kapsulitis, ansonsten verzichtbar). Fakultativ T2 tra, PD fs oder STIR/TIRM (orthogonal zur Hinterkante von SWK 2), T1 tra nach KM-Applikation; die Schichtdicke beträgt 3–4 mm (**Abb. 3**; [18, 19]).

**Limitationen.** Klaustrophobie, Lagerung, Dauer.

**Dauer der Untersuchung.** Untersuchungszeit einschließlich Gabe von KM: 20–30 min.

**Scoring.** Z. B. Aarhus-Score, Herrmann-Bollow-Score, Leeds-Score, Rudwaleit-Sieper-Score, SPARCC, ASAS [21].

## MRT-Spezialsequenzen

### Dynamische MRT

**Indikation.** Therapiekontrolle bei RA durch KM-Dynamik (Perfusion) der Hand [22, 23].

Die dynamische MRT entspricht einer Perfusionsmessung nach KM-Applikation über die Zeit; dazu werden repetitiv 3-dimensionale T1 gewichtete Sequenzen in koronarer Schichtführung angefertigt; insgesamt werden 200 Bilder in einem Abstand von 1,7 ms angefertigt; es gibt zur dynamischen MRT herstellerseitig verschiedenste kommerzielle Anbieter für Softwareapplikationen.

**Spule.** Die Hand wird mit einer dezidierten Handgelenkspule in „Superman"-Position untersucht; alternativ kann eine Flexspule verwendet werden; eine vermehrte KM-Anreicherung eines Fingergelenkes korreliert mit der Entzündungsaktivität.

**Dauer der Untersuchung.** 5–7 min; *dGEMRIC* (Delayed Gadolinium-Enhanced Magnetic Resonance Imaging of Cartilage).

**Indikation.** Knorpelqualität/Frühdiagnostik der Arthrose [24, 25].

**Cave.** Double-dose bei intravenöser KM-Applikation notwendig.

**Protokoll.** Bei der molekularen Bildgebung mittels dGEMRIC nutzt man die chemisch-physikalischen Eigenschaften der anionischen, negativ geladenen, gadoliniumhaltigen Kontrastmittel Gadolinium, welche auch in der täglichen Routine als MRT-Kontrastmittel Verwendung finden; nach intravenöser Injektion diffundiert das Kontrastmittel umgekehrt proportional zum Anteil der ebenfalls negativ geladenen Glykosaminoglykane (Bestandteil der Knorpelmatrix; GAG) in den Knorpel; da im degenerierten Knorpel der Gehalt an GAG (negativ geladen) verringert ist, kann sich im Vergleich zum gesunden Knorpel vermehrt Kontrastmittel im Knorpelgewebe anreichern; das Gadolinium verkürzt die T1-Zeit im MRT, sodass der GAG-Gehalt durch die T1-Analyse, innerhalb eines umschriebenen Knorpelbezirks als dGEMRIC-Index berechnet werden kann.

**Spule.** Mit der dezidierten Handspule können sämtliche Knorpelflächen der kleinen Fingergelenke oder des Handgelenks dargestellt werden; alternativ können kleine „loop-coils" verwendet werden, die ober- und unterhalb des jeweiligen Gelenks platziert werden; der Patient wird, wie bereits bei der MRT-Untersuchung der Hand, in Superman-Position mit der Hand über dem Kopf untersucht; die dGEMRIC-Sequenz wird 40 min nach Kontrastmittelapplikation angefertigt; zur Berechnung des dGEMRIC-Index wird eine 3-D-Gradienten-Echo-Sequenz mit 2 unterschiedlichen Flipwinkeln und einer Schichtdicke von 2 mm aufgenommen.

**Dauer der Untersuchung.** 2:30 min nach einem Delay von 40 min nach KM-Injektion.

## Kontrastmittelfreie Sequenzen

Durch die Entdeckung von Kontrastmittel(KM; Gadolinium)-Ablagerungen

| Abkürzungen | |
|---|---|
| *ASAS* | Assessment of SpondyloArthritis international Society |
| *ASpiMRI* | AS spinal MRI Score |
| *BME* | „Bone marrow edema“ |
| *Cor* | Coronar |
| *DESS* | Double Echo Steady State |
| *DGEMRIC* | Delayed Gadolinium-Enhanced Magnetic Resonance Imaging of Cartilage |
| *DIP* | Distales Interphalangealgelenk |
| *DOTA* | (1,4,7,10-Tetraazacyclododecan-1,4,7,10-tetraessigsäure, mit Gd Gadotersäure) |
| *DTPA* | Diethylentriaminpentaessigsäure |
| *EULAR* | European League Against Rheumatism |
| *FOV* | „Field of view“ |
| *Fs* | Fettgesättigt |
| *GAG* | Glykosaminoglykane (Bestandteil der Knorpelmatrix) |
| *GagCEST* | „Glycosaminoglycan chemical exchange saturation transfer“ |
| *Gd* | Gadolinium |
| *GFR* | Glomeruläre Filtrationsrate |
| *GRE* | Gradienten-Echo-Sequenz |
| *HWS* | Halswirbelsäule |
| *ISG* | Iliosakralgelenke |
| *KM* | Kontrastmittel |
| *LWS* | Lendenwirbelsäule |
| *MCP* | Metakarpophalangealgelenk |
| *MEDIC* | „Multi echo data image combination“ |
| *NSF* | Nephrogene systemische Fibrose |
| *OSG* | Oberes Sprunggelenk |
| *PD* | Protonengewichtete Sequenz |
| *PIP* | Proximales Interphalangealgelenk |
| *PsAMRIS* | Psoriatic arthritis magnetic resonance imaging scoring system |
| *PsoA* | Psoriasisarthritis |
| *RA* | Rheumatoide Arthritis |
| *RAMRIS* | Rheumatoid arthritis MRI scoring system |
| *Sag* | Sagittal |
| *SNR* | Signal-to-Noise-Ratio |
| *SPARCC* | Spondyloarthritis Research Consortium of Canada |
| *STIR* | Short-Tau Inversion Recovery Sequenz |
| *T1* | T1-gewichtet |
| *T2* | T2-gewichtet |
| *TIRM* | „Turbo inversion recovery magnitude“ |
| *Tra* | Transversal |
| *TrueFisp* | True fast imaging with steady state precession |
| *TSE* | Turbo-Spin-Echo-Sequenz |
| *WORMS* | Whole-organ MRI scoring method |

im Gehirn in Post-mortem-Studien ist die Diskussion um einen schonenden Einsatz von MRT-Kontrastmitteln aufgenommen. So konnte gezeigt werden, dass es bei der intravenösen Applikation von KM zu Ablagerungen von Gadolinium im Gehirn kommen kann. Diese Ablagerungen treten vorwiegend bei linearen Kontrastmitteln, jedoch auch in geringen Mengen bei makrozyklischen Kontrastmitteln auf. Nach aktuellem wissenschaftlichem Kenntnisstand sind keine gesundheitlichen Auswirkungen der Ablagerungen bekannt. Als Reaktion auf die intrakraniellen Gadoliniumablagerungen verbot die European Medicines Agency (EMA) die Anwendung von einer Vielzahl linearer, Gadolinium-basierter Kontrastmittel, darunter auch das für die dGEMRIC-Technik gebräuchliche Kontrastmittel. Obwohl makrozyklische Kontrastmittel nicht verboten wurden, sollte ihre Verwendung auf notwendige Untersuchungen beschränkt sein, sodass eine „double-dose“ Anwendung zur Beurteilung des Knorpels obsolet ist [26].

Aus diesem Grund wird aktuell an zahlreichen KM-freien MRT-Protokollen gearbeitet, welche wir im folgenden Abschluss auszugsweise darstellen möchten.

## Kontrastmittelfreie MR-Perfusion zur Erfassung von Entzündung

Die ASL(„arterial spin labeling“)-Technik nutzt das Blut selbst als endogenes Kontrastmittel, das durch einen Inversionspuls vor der Datenauslese markiert wird. In ersten Studien bei Patienten mit Arthritis konnte eine gute Korrelation der ASL-Perfusion mit der etablierten kontrastmittelgestützten MRT-Perfusion ermittelt werden. Die Bedeutung der Methode kann insbesondere darin gesehen werden, dass engmaschige Verlaufskontrollen, wie sie im Rahmen von Therapiestudien gewünscht sind, zukünftig möglicherweise kontrastmittelfrei ausgeführt werden können.

## Kontrastmittelfreie MR-Sequenzen zur Erfassung von Knorpelveränderungen

**KM-freie Sequenzen.** gagCEST („glycosaminoglycan chemical exchange saturation transfer“) und Natriumbildgebung zur Evaluierung der Knorpelqualität [27, 28].

**Protokoll.** gagCEST ermöglicht die Darstellung von Molekülen mit geringer Konzentration (mM) durch Messung der Wasserstoffprotonen des Gesamtkörperwassers (M); der CEST-Kontrast basiert auf der Sättigung der Wasserstoffprotonen von Glykosaminoglykanen; diese gesättigten Wasserstoffprotonen sind in einem chemischen Austausch mit den ungesättigten Wasserstoffprotonen des Gesamtkörperwassers; die Höhe des Signalverlustes des Gesamtkörperwassers korreliert mit der Menge an austauschbaren Protonen der angesteuerten Moleküle; der gagCEST-Effekt ist bei einer Frequenzbreite von 0,9–1,9 ppm der Wasserfrequenz messbar; der in diesem Bereich detektierbare Signalverlust des Gesamtkörperwassers korreliert mit dem GAG-Gehalt des Knorpels; der Verlust an GAG geht mit einer Schädigung des Gelenkknorpels einher.

**Spule.** gagCEST kann mit einer dezidierten Handgelenkspule angefertigt werden.

**Eine weitere molekulare Bildgebungsmodalität zur Abbildung des Gelenkknorpels ist die *Natriumbildgebung*.** Ähnlich zur gagCEST-Sequenz ist es möglich, Natrium zur Bildgebung zu nutzen; der Natriumgehalt des Knorpels korreliert direkt mit dem GAG-Gehalt des Knorpels; zur Natriumbildgebung wird eine dezidierte Hardwareausrüstung benötigt.

**Dauer der Untersuchung.** 12–15 min.

**Schlussfolgerung.** Die MRT ist eine bildgebende Methode, welche aufgrund ihrer vielen Vorteile zur Diagnostik entzündlicher und nichtentzündlicher weichteiliger und knöcherner Veränderungen am Skelettsystem immer häufiger eingesetzt wird. Der hohe Stellenwert der MRT wird für die strukturelle Früh- und Differenzialdiagnostik in der Rheumatologie genutzt, welche mit anderen konventionellen bildgebenden Techniken oder Schnittbildmethoden nicht gelingt. Die korrekte Durchführung von MRT-Untersuchungen, die Vereinheitlichung von MRT-Protokollen und die Beachtung von Spezialsequenzen könnten einen Beitrag zur Qualitätsverbesserung der radiologischen Leistung für die Rheumatologie liefern.

Weitere, kontrastmittelfreie Techniken zur Darstellung des Knorpels sind T1- und T2-mapping-Verfahren.

### T1ρ imaging (T1rho)

T1ρ ist eine MRT-Technik, die Veränderungen des regionalen Proteoglykangehalts erfassen kann. Dabei können die Interaktionen zwischen den mit Makromolekülen assoziierten Protonen erfasst werden. Ein Knorpelschaden führt zu einem Verlust an Proteoglykanen und damit den Makromolekülen, was zu einer erhöhten T1ρ-Zeit führt [29].

### T2/T2* mapping

Transverse Relaxationszeiten sind von der Gewebezusammensetzung abhängig. Mit T2/T2*-Verfahren können die Kollagenstruktur und damit ein Knorpelschaden erfasst werden [30].


## Korrespondenzadresse

**Dr. P. Sewerin**
Poliklinik, Funktionsbereich & Hiller Forschungszentrum für Rheumatologie, Universitätsklinikum, Heinrich-Heine Universität Düsseldorf
Moorenstr. 5, 40225 Düsseldorf, Deutschland
philipp.sewerin@med.uni-duesseldorf.de


## Einhaltung ethischer Richtlinien

**Interessenkonflikt.** P. Sewerin, B. Ostendorf und C. Schleich geben an, dass kein Interessenkonflikt besteht.

Dieser Beitrag beinhaltet keine von den Autoren durchgeführten Studien an Menschen oder Tieren.

## Literatur


1. Østergaard M, Peterfy C, Conaghan P et al (2003) OMERACT Rheumatoid Arthritis Magnetic Resonance Imaging Studies. Core set of MRI acquisitions, joint pathology definitions, and the OMERACT RA-MRI scoring system. J Rheumatol 30(6):1385–1386
2. Baraliakos X, Braun J (2016) Imaging scoring methods in axial spondyloarthritis. Rheum Dis Clin North Am 42(4):663–678
3. Peterfy CG, Guermazi A, Zaim S et al (2004) Whole-Organ Magnetic Resonance Imaging Score (WORMS) of the knee in osteoarthritis. Osteoarthr Cartil 12(3):177–190
4. Mandl P, Naredo E, Wakefield RJ, Conaghan PG, D'Agostino MA, Force OUT (2011) A systematic literature review analysis of ultrasound joint count and scoring systems to assess synovitis in rheumatoid arthritis according to the OMERACT filter. J Rheumatol 38(9):2055–2062
5. McQueen FM, Ostendorf B (2006) What is MRI bone oedema in rheumatoid arthritis and why does it matter? Arthritis Res Ther 8(6):222
6. Hauer MP, Uhl M, Allmann KH, Laubenberger J, Zimmerhackl LB, Langer M (1998) Comparison of turbo inversion recovery magnitude (TIRM) with T2-weighted turbo spin-echo and T1-weighted spin-echo MR imaging in the early diagnosis of acute osteomyelitis in children. Pediatr Radiol 28(11):846–850
7. Nakahara R, Nishida K, Hashizume K et al (2015) MRI of rheumatoid arthritis:comparing the outcome measures in rheumatology clinical trials (OMERACT) scoring and volume of synovitis for the assessment of biologic therapy. Acta Med Okayama 69(1):29–35
8. Narváez J, Sirvent E, Narváez JA et al (2008) Usefulness of magnetic resonance imaging of the hand versus anticyclic citrullinated peptide antibody testing to confirm the diagnosis of clinically suspected early rheumatoid arthritis in the absence of rheumatoid factor and radiographic erosions. Semin. Arthritis Rheum 38(2):101–109
9. Braum LS, McGonagle D, Bruns A et al (2013) Characterisation of hand small joints arthropathy using high-resolution MRI—limited discrimination between osteoarthritis and psoriatic arthritis. Eur Radiol 23(6):1686–1693
10. Østergaard M, Bird P, Gandjbakhch F et al (2015) The OMERACT MRI in arthritis working group—update on status and future research priorities. J Rheumatol 42(12):2470–2472
11. Ostergaard M, McQueen F, Wiell C et al (2009) The OMERACT psoriatic arthritis magnetic resonance imaging scoring system (PsAMRIS): definitions of key pathologies, suggested MRI sequences, and preliminary scoring system for PsA Hands. J Rheumatol 36(8):1816–1824
12. Ostendorf B, Scherer A, Mödder U, Schneider M (2004) Diagnostic value of magnetic resonance imaging of the forefeet in early rheumatoid arthritis when findings on imaging of the metacarpophalangeal joints of the hands remain normal. Arthritis Rheum 50(7):2094–2102
13. Sewerin P, Buchbender C, Vordenbäumen S et al (2014) Advantages of a combined rheumatoid arthritis magnetic resonance imaging score (RAMRIS) for hand and feet: does the RAMRIS of the hand alone underestimate disease activity and progression? BMC Musculoskelet Disord 15:104
14. Buchbender C, Scherer A, Miese F et al (2013) Patterns of magnetic resonance imaging of the foot in rheumatoid arthritis: which joints are most frequently involved? Rheumatol Int 33(7):1731–1736
15. Ghazinoor S, Crues JV, Crowley C (2007) Low-field musculoskeletal MRI. J Magn Reson Imaging 25(2):234–244
16. Sudoł-Szopińska I, Jurik AG, Eshed I et al (2015) Recommendations of the ESSR Arthritis Subcommittee for the use of magnetic resonance imaging in musculoskeletal rheumatic diseases. Semin Musculoskelet Radiol 19(4):396–411
17. Tan AL, Fukuba E, Halliday NA, Tanner SF, Emery P, McGonagle D (2015) High-resolution MRI assessment of dactylitis in psoriatic arthritis shows flexor tendon pulley and sheath-related enthesitis. Ann Rheum Dis 74(1):185–189
18. Hermann KG, Baraliakos X, van der Heijde DM et al (2012) Descriptions of spinal MRI lesions and definition of a positive MRI of the spine in axial spondyloarthritis: a consensual approach by the ASAS/OMERACT MRI study group. Ann Rheum Dis 71(8):1278–1288
19. Baraliakos X, van der Heijde D, Braun J, Landewé RB (2011) OMERACT magnetic resonance imaging initiative on structural and inflammatory lesions in ankylosing spondylitis—report of a special interest group at OMERACT 10 on sacroiliac joint and spine lesions. J Rheumatol 38(9):2051–2054
20. Sung S, Kim HS, Kwon JW (2017) MRI assessment of sacroiliitis for the diagnosis of axial spondyloarthropathy: comparison of fat-saturated T2, STIR and contrast-enhanced sequences. Br J Radiol 90(1078):20170090
21. Sieper J, Rudwaleit M, Baraliakos X et al (2009) The Assessment of SpondyloArthritis international Society (ASAS) handbook: a guide to assess spondyloarthritis. Ann Rheum Dis 68(Suppl 2):ii1–ii44
22. Cimmino MA, Parodi M, Innocenti S et al (2005) Dynamic magnetic resonance of the wrist in psoriatic arthritis reveals imaging patterns similar to those of rheumatoid arthritis. Arthritis Res Ther 7(4):R725–31
23. Müller-Lutz A, Schleich C, Sewerin P et al (2015) Comparison of quantitative and semiquantitative dynamic contrast-enhanced MRI with respect to their correlation to delayed gadolinium-enhanced MRI of the cartilage in patients with

early rheumatoid arthritis. J Comput Assist Tomogr 39(1):64–69
24. Burstein D, Velyvis J, Scott KT et al (2001) Protocol issues for delayed Gd(DTPA)(2-)-enhanced MRI (dGEMRIC) for clinical evaluation of articular cartilage. Magn Reson Med 45(1):36–41
25. Miese FR, Ostendorf B, Wittsack HJ et al (2010) Metacarpophalangeal joints in rheumatoid arthritis: delayed gadolinium-enhanced MR imaging of cartilage—a feasibility study. Radiology 257(2):441–447
26. Gulani V, Calamante F, Shellock FG, Kanal E, Reeder SB, Medicine ISf M (2017) Gadolinium deposition in the brain: summary of evidence and recommendations. Lancet Neurol 16(7):564–570
27. Schleich C, Müller-Lutz A, Matuschke F et al (2015) Glycosaminoglycan chemical exchange saturation transfer of lumbar intervertebral discs in patients with spondyloarthritis. J Magn Reson Imaging. https://doi.org/10.1002/jmri.24877
28. Schmitt B, Zbýn S, Stelzeneder D et al (2011) Cartilage quality assessment by using glycosaminoglycan chemical exchange saturation transfer and (23)Na MR imaging at 7 T. Radiology 260(1):257–264
29. Nemeth A, Di Marco L, Boutitie F et al (2018) Reproducibility of in vivo magnetic resonance imaging T. J Magn Reson Imaging 47(4):1022–1033
30. Link TM, Neumann J, Li X (2017) Prestructural cartilage assessment using MRI. J Magn Reson Imaging 45(4):949–965




## Rauchen erhöht Risiko für Rheuma und verschlimmert rheumatische Schäden

**Raucher erkranken nicht nur häufiger an Rheuma als andere Menschen. Die Gelenkzerstörung schreitet bei ihnen auch rascher voran. Sieben Zigaretten am Tag steigern das Erkrankungsrisiko für eine rheumatoide Arthritis um mehr als das Doppelte.**

Zu den weniger bekannten Folgen des Rauchens gehört der schlechte Einfluss auf rheumatische Erkrankungen. Die Gründe sind nach Auskunft von Professor Dr. med. Hanns-Martin Lorenz, Präsident der DGRh und Leiter der Sektion Rheumatologie am Universitätsklinikum Heidelberg, nicht genau bekannt: „Wir vermuten aber, dass Rauchen Fehlfunktionen des Immunsystems hervorruft, die bei bestimmten Menschen den letzten Anstoß zur Entwicklung einer rheumatoiden Arthritis geben können." Rauchen, so der Experte, könnte die Bildung der Antikörper fördern, die die Gelenkhaut attackieren und dadurch die Zerstörung der Gelenke in die Wege leiten.

### Eindeutige Studienergebnisse

Die Studienergebnisse sind eindeutig: Starke Raucher erkranken deutlich häufiger an einer rheumatoiden Arthritis. Besonders gefährdet sind Frauen. Bereits weniger als sieben Zigaretten am Tag steigern das Erkrankungsrisiko um mehr als das Doppelte. Das Risiko steigt bereits nach wenigen Jahren an und es hält noch bis zu 15 Jahre nach dem Rauchstopp an. Zudem schlagen Therapien schlechter an: „Rauchen kann auch die Wirksamkeit von Rheumamedikamenten und hier vor allem der neueren Biologika schwächen," erklärt Lorenz: „Diese Patienten benötigen unter Umständen höhere Dosierungen und sind dadurch vermehrt den Nebenwirkungen der Rheumamittel ausgesetzt."

Frühere Untersuchungen haben auch gezeigt, dass Rauchen das Fortschreiten der Erkrankung beschleunigt. Eine neue Untersuchung aus Schweden ergab, dass es bei Rauchern bereits zu Beginn der Erkrankung häufiger zu einer raschen Zerstörung der Gelenke kommen kann [1]. Emil Rydell von der Universität in Lund und Mitarbeiter haben Rheuma-Patienten über mehr als fünf Jahre begleitet. Bei jedem fünften Patienten kam es während dieser Zeit trotz Behandlung zu einer raschen Verschlechterung, in Form einer zunehmenden Verschmälerung des Gelenkspalts oder Erosionen des Knochens. Raucher waren besonders häufig betroffen. Bei aktiven Rauchern kam es 3,6-fach häufiger zu einer schnellen Schädigung der Gelenke. Bei früheren Rauchern war das Risiko noch um den Faktor 2,79 erhöht.

Ein Rauchstopp gehört zu den wichtigsten Begleitmaßnahmen der Rheumatherapie: „Alle Patienten sollten spätestens mit der ersten Medikamenteneinnahme mit dem Rauchen aufhören." Diesen Rat müsse jeder behandelnde Rheumatologe seinen Patienten im Rahmen der Behandlung mit auf den Weg geben.

[1] Rydell, E. et al. Arthritis Res Ther (2018) 20: 82. https://doi.org/10.1186/s13075-018-1575-2

***Stephanie Priester***
***Pressestelle DGRh***

# Prevalence and incidence of psoriasis and psoriatic arthritis

Psoriasis (Pso) and psoriatic arthritis (PsA) are inflammatory disorders which can severely impair health and quality of life. For both Pso and PsA, an increasing prevalence has been reported.[1 2] Comprehensive data on the prevalence and incidence of Pso and PsA are important in order to adequately allocate specialist care and financial resources. These data are incomplete for Pso and especially PsA. In particular, no population-based study has estimated their prevalence or incidence in Germany. We obtained the statutory health insurance data of approximately 65 million people from 2009 to 2012, covering 80% of the German population. Pso and PsA age-standardised prevalence based on the International Classification of Diseases (ICD) codes was obtained and age-standardised incidence rates calculated as described previously.[3] Briefly, cross-sectional prevalence data of consecutive years were used in conjunction with different assumed mortality rates of 1.1–1.5, with assumed reductions in annual mortality rates of 0%–5% in order to estimate incidence ranges.

Depending on the year, approximately 65 million individuals were assessed. There were 1.4–1.6 million cases of Pso and 127 000–156 000 cases of PsA identified. The age-standardised prevalence for Pso was 22.2–22.9 and 21.3–22.1 per 100 000 individuals in men and women, respectively (online supplementary figure 1). The prevalence for PsA was 1.8–2.1 and 2.1–2.5 per 100 000 individuals in men and women, respectively (online supplementary figure 2). A steady increase in prevalence was observed for both Pso and PsA. The incidence of Pso in 2009 ranged from 35.4 to 50.3 and from 46.3 to 58.2 in men and women, respectively, and declined thereafter. The incidence of PsA in 2009 ranged from 13.8 to 14.9 and from 18.1 to 19.1 in men and women, respectively, and declined thereafter. All data are detailed in table 1. Based on these data we used two different scenarios to estimate the number of patients living in Germany in 2018: (1) German age pyramid of 2018 applied to prevalence in 2012, or (2) projection of prevalence extrapolated by annual per cent change, then application of the 2018 age pyramid. Concerning Pso, 959 362–1 012 167 male and 956 822–1 030 847 female patients are expected to be living in Germany in 2018. Concerning PsA, 75 376–102 320 male and 90 473–127 349 female patients are expected to be living in Germany in 2018. This calculation may serve to project future mortality in other European countries.

Thus, we summarise that roughly 2 million patients with Pso and at least 200 000 patients with PsA are currently living in Germany. The age-standardised prevalence and incidence of PsA are in line with estimates from other European countries or the USA,[4] although higher incidences have been reported.[2] The ratio of PsA/Pso prevalence in the current study was approximately 10%, which is well within the range of previous reports. The ICD-based case definition is a limitation to the study as it may result in reduced precision as opposed to diagnostic criteria.[5] Most recent observational studies report an increase[6] or at least stable incidences[2] for Pso or PsA. In the current study, we calculated incidences based on cross-sectionally observed prevalence and different assumed mortality ratios in reference to the mathematical relation between incidence, prevalence and mortality.[3] These analyses consistently resulted in a decline in the incidence of both diseases over the observed study period. However, we suggest a careful interpretation of these incidences since changed awareness for the respective diagnoses or changed coding behaviour of ICD codes may account for the differences. Thus, the results should be interpreted as possible trends in incidences.

The epidemiological data reported herein cover a substantial portion of the German population and thereby improve our understanding of the prevalence and incidence of Pso and PsA in Europe.

**Table 1** Prevalence of Pso and PsA from 2009 to 2012 in Germany

| Year | 2009 | 2010 | 2011 | 2012 |
|---|---|---|---|---|
| Population (n) | 64 637 752 | 63 962 071 | 64 988 016 | 65 792 296 |
| Female (%) | 53.5 | 53.4 | 53.3 | 53.2 |
| Pso (n) | 1 419 537 | 1 440 807 | 1 477 333 | 1 512 769 |
| Pso prevalence (n/1000) | | | | |
| Male | 22.22 | 22.59 | 22.69 | 22.86 |
| Female | 21.27 | 21.76 | 21.93 | 22.12 |
| Pso incidence (n/100 000) | | | | |
| Male | 35.38–50.27 | 26.44–39.36 | 17.32–29.31 | 17.14–26.31 |
| Female | 46.30–58.17 | 35.30–45.63 | 21.67–30.47 | 19.05–26.39 |
| PsA (n) | 127 334 | 137 763 | 146 463 | 156 182 |
| PsA prevalence (n/1000) | | | | |
| Male | 1.81 | 1.96 | 2.03 | 2.13 |
| Female | 2.07 | 2.26 | 2.37 | 2.49 |
| PsA incidence (n/100 000) | | | | |
| Male | 13.81–14.88 | 11.59–12.54 | 9.59–10.39 | 9.84–10.49 |
| Female | 18.12–19.14 | 15.23–16.14 | 12.03–12.80 | 11.76–12.38 |

Data from the German statutory health insurance system of approximately 64 million people (population) were employed to assess age-standardised prevalence of psoriasis (Pso) and psoriatic arthritis (PsA) for the male and female German population (mean values). Age-standardised incidence was calculated based on prevalence data and different assumed mortality scenarios resulting in the given ranges.

**Philipp Sewerin, Ralph Brinks, Matthias Schneider, Isabell Haase, Stefan Vordenbäumen**

Medical Faculty, Department of Rheumatology and Hiller Research Unit Rheumatology, Heinrich-Heine-University Düsseldorf, Düsseldorf, Germany

**Correspondence to** Dr Philipp Sewerin, Medical Faculty, Department Rheumatology and Hiller Research Unit Rheumatology, Heinrich-Heine-University Düsseldorf, Düsseldorf 40225, Germany; philipp.sewerin@med.uni-duesseldorf.de

**Handling editor** Josef S Smolen

**Acknowledgements** We would like to express our gratitude to DIMDI (German Institute for Medical Documentation and Information) for preparing the data sets.

**Contributors** PS, RB, MS, IH and SV contributed to the design and implementation of the research, to the analysis of the results and to the writing of the manuscript.

**Competing interests** None declared.

**Patient consent** Not required.

**Provenance and peer review** Not commissioned; externally peer reviewed.



► Additional material is published online only. To view please visit the journal online (http://dx.doi.org/10.1136/annrheumdis-2018-214065).

**To cite** Sewerin P, Brinks R, Schneider M, *et al*. *Ann Rheum Dis* 2019;**78**:286–287.

Received 6 July 2018
Revised 23 July 2018
Accepted 30 August 2018
Published Online First 21 September 2018

*Ann Rheum Dis* 2019;**78**:286–287. doi:10.1136/annrheumdis-2018-214065

## REFERENCES

1 Danielsen K, Olsen AO, Wilsgaard T, *et al*. Is the prevalence of psoriasis increasing? A 30-year follow-up of a population-based cohort. *Br J Dermatol* 2013;168:1303–10.
2 Springate DA, Parisi R, Kontopantelis E, *et al*. Incidence, prevalence and mortality of patients with psoriasis: a U.K. population-based cohort study. *Br J Dermatol* 2017;176:650–8.
3 Hoyer A, Tönnies T, Brinks R. Possible trends in incidence of diabetes in Italy. *Nutr Metab Cardiovasc Dis* 2018;28:427–8.
4 Scotti L, Franchi M, Marchesoni A, *et al*. Prevalence and incidence of psoriatic arthritis: systematic review and meta-analysis. *Semin Arthritis Rheum* 2018;48:28–34.
5 Villani AP, Rouzaud M, Sevrain M, *et al*. Prevalence of undiagnosed psoriatic arthritis among psoriasis patients: systematic review and meta-analysis. *J Am Acad Dermatol* 2015;73:242–8.
6 Egeberg A, Kristensen LE, Thyssen JP, *et al*. Incidence and prevalence of psoriatic arthritis in Denmark: a nationwide register linkage study. *Ann Rheum Dis* 2017;76:1591–7.

# Update on imaging in rheumatic diseases: cartilage

P. Sewerin[1], C. Schleich[2], S. Vordenbäumen[1], B. Ostendorf[1]

[1]*Department and Hiller Research Unit of Rheumatology,*
[2]*Department of Diagnostic and Interventional, Radiology, Heinrich-Heine University Dusseldorf, Germany.*

*Philipp Sewerin, MD**
*Christoph Schleich,**
*Stefan Vordenbäumen,*
*Benedikt Ostendorf,*

**These authors contributed equally.*

*Please address correspondence to:*
*Dr Philipp Sewerin,*
*Department and Hiller Research Unit of Rheumatology,*
*Heinrich-Heine University Dusseldorf,*
*Moorenstraße 5,*
*40225 Dusseldorf, Germany.*
*E-mail:*
*philipp.sewerin@med.uni-duesseldorf.de*

*Received on August 21, 2018; accepted in revised form on August 30, 2018.*

*Clin Exp Rheumatol 2018; 36 (Suppl. 114): S139-144.*



**Key words**: ultrasound, cartilage, rheumatic diseases

*Competing interests: none declared.*

**ABSTRACT**

*In recent years, the role of articular cartilage for understanding pathogenesis as well as for clinical research has become increasingly important. Whereas previously cartilage could only be assessed invasively, various imaging procedures are available for its evaluation now. Although still widely used, conventional radiography bears significant limitations since it assesses cartilage indirectly by joint space width. Today, the cartilage thickness and structure can be reliably evaluated using ultrasound, although the molecular structure cannot be determined, yet. Besides ultrasound, MRI offers the possibility to image morphological changes with a very high resolution. In addition, the quality and composition of joint cartilage can already be measured due to a constant technical improvement and new MRI sequences such as dGEMRIC even in small joints (e.g. MCP or MTP joints). Despite the advantages of contrast agents for the detection of inflammation, its use is reevaluated today. Regarding that contrast agent-free imaging techniques for the assessment of joint cartilage are developed with great effort to depict its quality and changes over time. These novel MRI methods such as T2/T2*- and T1ϱ-mapping, gagCEST, and sodium imaging provide promising quantitative imaging biomarkers that can detect early cartilage changes before morphological alterations occur. Hence, US and MRI will likely be of paramount importance in future clinical trials and clinical assessment of inflammatory and degenerative joint diseases not only for understanding pathogenesis but also for using its possible value in daily practice.*

## Introduction

Alterations in the composition of articular cartilage are a common feature in the pathogenesis of inflammatory and degenerative joint diseases. Cartilage is a key component of synovial joints and consists of chondrocytes, which are the exclusive cell type embedded within a dense and highly organised extracellular matrix (ECM). Cartilage ECM is synthesised by these chondrocytes and is composed of a collagenous network that contains primarily type II collagen along with glycosaminoglycans (GAGs) such as hyaluronan, and a variety of proteoglycans, *e.g.* GAG-containing proteins that are linked to the collagen network. The exact composition of cartilage ECM, its physiology, and the interactions of its individual components, are described in detail elsewhere (1).

Cartilage loss is a hallmark of osteoarthritis (OA). Indeed, chondrocyte and dysfunctional ECM production is likely paramount for the development of this widespread disorder (2). Patients experience considerable loss of joint function, pain and impaired quality of life. Unfortunately, there is currently no effective pharmacological treatment available, which significantly alters the course of the disease. An important obstacle to the development of pharmacological agents is the slowly progressive course of OA, requiring long and costly clinical trials (3). Reliable non- or minimal invasive imaging techniques of cartilage therefore have the potential to facilitate significantly the search for effective treatments options

Treatment goals for rheumatoid arthritis (RA) as defined by both American College of Rheumatology (ACR) and the European League Against Rheumatism (EULAR) are directed to include a treat to target strategy with a goal of low disease activity or remission according to an index derived from an RA core data set (4, 5). Therefore, it is recommended to initiate conventional synthetic disease modifying drugs (cs-DMARDs) immediately after the diagnosis, ideally before erosive disease of the bone is detected.

For decades, imaging has played an important role for diagnosis and therapy

control in patients with inflammatory joint diseases. It is well known that bone erosions in conventional radiographs are associated with a high likelihood for a progressive course of the disease (6, 7). Moreover, it has been shown that joint space narrowing, representing cartilage loss, is predictive for new bone erosions in follow-up and that it is independently associated with functional impairment and decreased work ability (8, 9). Joint space narrowing is observed when cartilage degradation has already occurred. Hence, more sophisticated methods to detect early cartilage injury were sought. Ultrasound (US) and Magnetic Resonance Imaging (MRI) are increasingly used in both research and clinical routine to inform diagnostic algorithms and guide therapy, especially in RA (10, 11).

This review introduces the current possibilities of ultrasound and MRI for the detection of early cartilage damage and loss of cartilage integrity using molecular imaging techniques in arthritis and osteoarthritis.

**Ultrasound**

Conventional radiographs permit indirect recognition of cartilage damage depicted as joint space narrowing. In contrast, ultrasound (US) allows a detailed visualisation of the hyaline cartilage: Small cartilage abnormalities in patients with RA can be identified sonographically from loss of the hyperechoic superficial margin of articular cartilage with reverberation artifacts (grade 1 defect) up to osteochondral defects appearing as a complete loss of the cartilage substance and a contour defect of subchondral bone, with loss of uniformity of the strongly hyperechoic subchondral bone interface (grade 4 defect) (12). US now can be considered a reliable and valid technique for cartilage assessment even at small finger joints, with excellent sensitivity compared to x-rays (13). Moreover, there is a good interobserver reproducibility when analysing the morphological changes of the cartilage at MCP joint in patients with RA (14).

Hence, there is evidence showing that ultrasound can depict cartilage defects in inflammatory joint disease. Abe et al. compared synovial histology (from 215 joints undergoing synovectomy and reconstructive surgery) with US on 177 patients with RA. Power Doppler signal grade reflected histological scores in both large and small joints, and was correlated significantly with DAS28, C-reactive protein and matrixmetalloproteinase-3, while there is no specific data for cartilage assessment up until now (15).

Moreover, ultrasound is used regularly in clinical practice to detect crystal arthropathies such as gout or calcium pyrophosphate deposition disease (CPDD) showing a typical hyperechoic spots within the hyaline cartilage layer (16, 17). Due to these opportunities ultrasound is now part of the current classifications criteria in gout (18).

In osteoarthritis (OA), current studies attempt to clarify the association between US pathologies and symptoms of patients with OA. In a recent published meta-analysis, US signs of OA including synovial hypertrophy and positive power Doppler (PD) signal were associated with knee pain and OA. These aspects were significantly less common in general population or among asymptomatic controls and were more related to structural changes of the cartilage itself than to pain (19). Furthermore, US imaging including grey-scale synovitis and PD signals could predict future risk of radiographic progression of hand OA. However, only morphological cartilage changes (not on a molecular level) were taken into consideration (20).

However, no study to date has shown that US measures permit prediction of future cartilage loss. In addition, US does not depict changes of the cartilage integrity or composition; US can capture morphological damage of the cartilage, but molecular assessment is not possible yet.

**Magnetic resonance imaging**

Magnetic resonance imaging (MRI) is a well evaluated imaging technique in RA clinical trials and is used more frequently in daily practice for early diagnosis and therapy control in RA patients (21-23). Modern MRI techniques can depict inflammatory smooth tissue (such as synovitis, enthesitis and tenovsynovitis) and bony changes and lesions (such as bone marrow oedema, erosions, and joint space narrowing) with a high level of sensitivity (24). Moreover, MRI can detect erosive joint damage much earlier than conventional x-rays (25). In addition, validated scoring systems such as Outcome Measures in RA Clinical Trials (OMERACT) RA MRI Score (RAMRIS) and simplified versions facilitate comparison of MRI readings due to standardisation (26, 27). The RAMRIS is a highly reliable sum-score based on the semi-quantitative rating of the severity of synovitis, bone marrow oedema and erosions in hand and wrist joints that has been applied in therapy-response trials in RA (22, 24). More recently, a score of joint space narrowing/cartilage thinning was added to RAMRIS (28-30). This is all the more relevant in view of the study of Aletaha *et al*. who demonstrated that physical disability in RA is associated with cartilage damage rather than bone destruction (9).

Morphological imaging of cartilage is possible mainly in proton density, proton density with fat saturation/spectral attenuated inversion recovery (SPAIR), T2-weighted, T2-weighted with fat saturation, T1 volume isotropic turbo spin echo acquisition (VISTA) 3D, and 3D fast spoiled gradient echo (FSPGR) sequences (31).

In some centres, the modified Outerbridge system (grading scale) that originally was based on arthroscopic findings, is used to classify changes in hyaline cartilage on MRI. This system is based on a grading of the depth, location, and severity of chondral injuries as follows: grade 0 – normal cartilage, grade 1 – signal intensity alterations with an intact surface of the articular cartilage compared with the surrounding normal cartilage, grade 2 – partial thickness defect of the cartilage, grade 3 – fissuring of the cartilage to the level of the subchondral bone and grade 4 – exposed subchondral bone (32). Another morphological technique is the double-echo steady state (DESS) MR sequence with water excitation that offers high-resolution, three-dimensional (3D) imaging and multiplanar reformatting. Its strong fluid signal creates an ar-

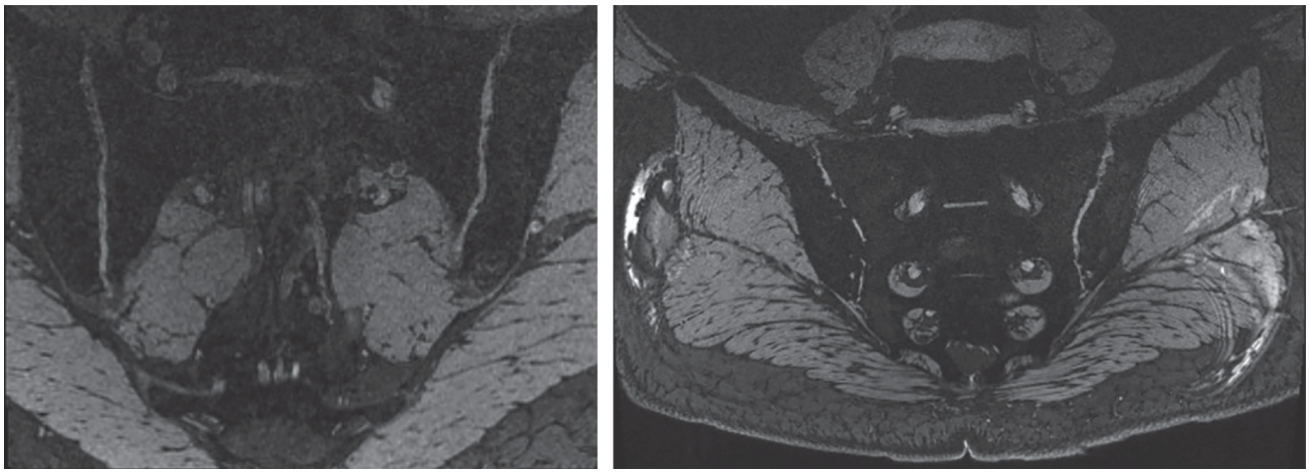

**Fig. 1.** DESS (double-echo steady state) sequence of the sacroiliac joint of a healthy control (left picture) and a patient with sacroiliitis (right image). In addition to the typical signs of sacroiliitis like erosion, ankylosis and joint space narrowing, it is possible to detect morphological alterations of the cartilage visible by signal loss of cartilage.

throgram-like effect within the joint that may increase the diagnostic possibilities in finding cartilage alterations. The radial imaging approach will further improve the visualisation the cartilage and provides information on the localisation and extent of that is essential if surgical treatment is intended. The good reliability of the DESS technique with radial imaging for evaluation of cartilage was shown by comparative analysis with intraoperative data (33) (Fig. 1).

Regarding the high impact of assessing cartilage thickness and integrity, high resolution morphological and biochemical imaging came more and more in focus of scientific research. Delayed gadolinium-enhanced MRI of the cartilage (dGEMRIC) is a high reliable, histologically controlled MRI feature to visualise proteoglycan loss in cartilage composition (34, 35). With dGEMRIC, it is possible to detect proteoglycan loss after the intravenous application of negatively charged contrast agent (gadolinium diethylenetriamine pentaacetate anion - Gd-DTPA). The negatively charged Gd-DTPA penetrates cartilage in an inverse relationship to the concentration of negatively charged glycosaminoglycan side chains of proteoglycan. A depletion of proteoglycan content in degenerated cartilage results in accumulation of the paramagnetic gadolinium ions. This progressively accelerates T1 relaxation time (36) (Fig. 2).

dGEMRIC has been performed in several joints of patients suffering from RA or OA. For example, Tiderius *et al*. demonstrated that cartilage damage in biochemical MRI continues irrespective of disease activity following therapy escalation with TNF-alpha-blockers in RA (37). Schleich *et al*. showed the capability of dGEMRIC as an additional feature in the preoperative assessment of degenerated cervical intervertebral discs (IVDs). IVDs scheduled for discectomy demonstrated significantly lower dGEMRIC values compared to IVDs who were not scheduled for surgical intervention (38).

OA is the most frequent condition associated with cartilage degeneration and dGEMRIC has been used to assess cartilage degeneration in the knee joint and hip joint with secondary osteoarthritis due to hip dysplasia (39, 40). Joint space narrowing and the development of osteophytes at the knee joints as indicators for knee OA have been reported to be associated with lower dGEMRIC values at baseline making dGEMRIC a predictor of radiologically manifest knee OA following partial meniscectomy. The first study to assess small joints proved the feasibility of dGEMRIC in the first metacarpophalangeal joint in an OA case. Follow-up dGEMRIC measurements have been used to assess the effect of cartilage repair procedures of the knee, suggesting varying degree of proteoglycan replenishment.

Cartilage repair tissue after Matrix-induced Autologous Chondrocyte Implantation (MACI) in the knee joint has been demonstrated to have a reduced zonal variation of dGEMRIC values and a decrease in the relaxation rate of the deep zone of the transplant in the 1 year follow-up was interpreted as a slow increase in GAG (41). In RA, early cartilage damage prior to macroscopic cartilage loss has been assumed based on decreased dGEMRIC in the metacarpophalangeal joints of RA patients prior to the initiation of therapy with disease modifying drugs (35).

For dGEMRIC, the application of intravenous contrast agent is obligatory. However, recent studies have brought potential adverse effects of gadolinium to international attention. Due to potential gadolinium depositions in the brain, the European Medicines Agency (EMA) banned several linear gadolinium-based contrast agents. Even though macrocyclic contrast agents have not been suspended, they should be used with care and a strict indication (42).

Hence, future research should focus more on gadolinium-free molecular MR imaging of cartilage such as glycosaminoglycan chemical exchange saturation transfer (gagCEST), sodium MRI and T1 rho mapping to visualise the GAG content, T2/T2* mapping to evaluate the water content and collagen network integrity or diffusion-weighted imaging (DWI)(43–45) (Fig. 3). In clinical studies, especially T2 and T2* mapping have been used mostly at the knee and the hip showing promising results in assessing early diseases stages

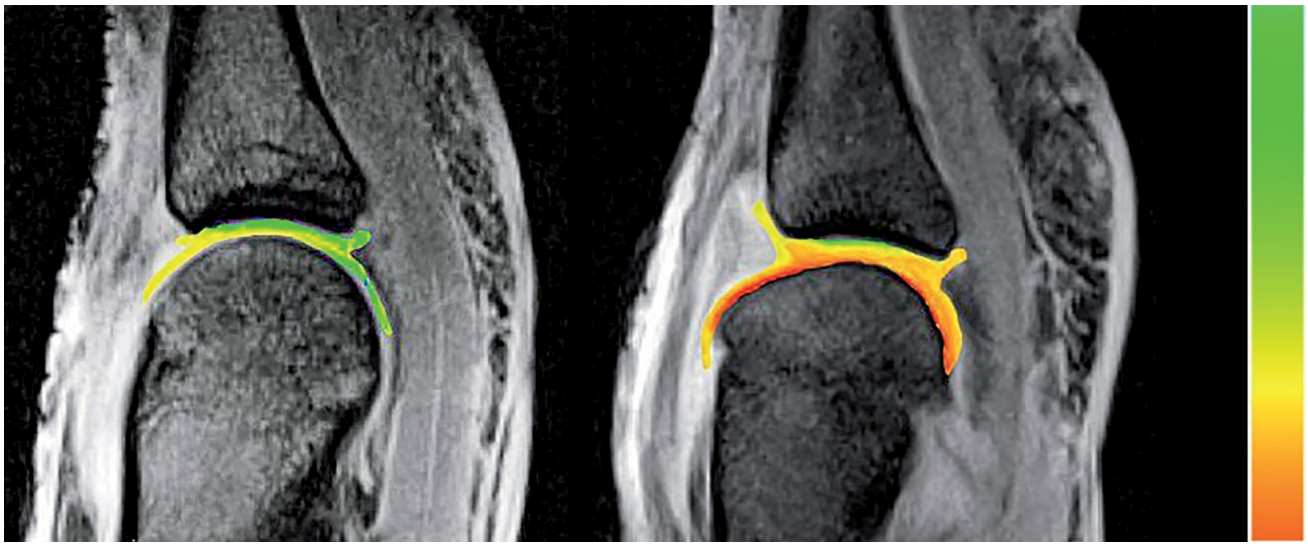

**Fig. 2.** Colour-coded dGEMRIC map with low dGEMRIC index in red and high dGEMRIC index in green in ms. The left picture shows a patient with low grade synovitis, while the right picture illustrates a patient with high grade synovitis, both patients suffering from RA. The right picture demonstrates significantly lower dGEMRIC index compared to the left picture, indicating higher cartilage alteration of the patient with higher synovitis.

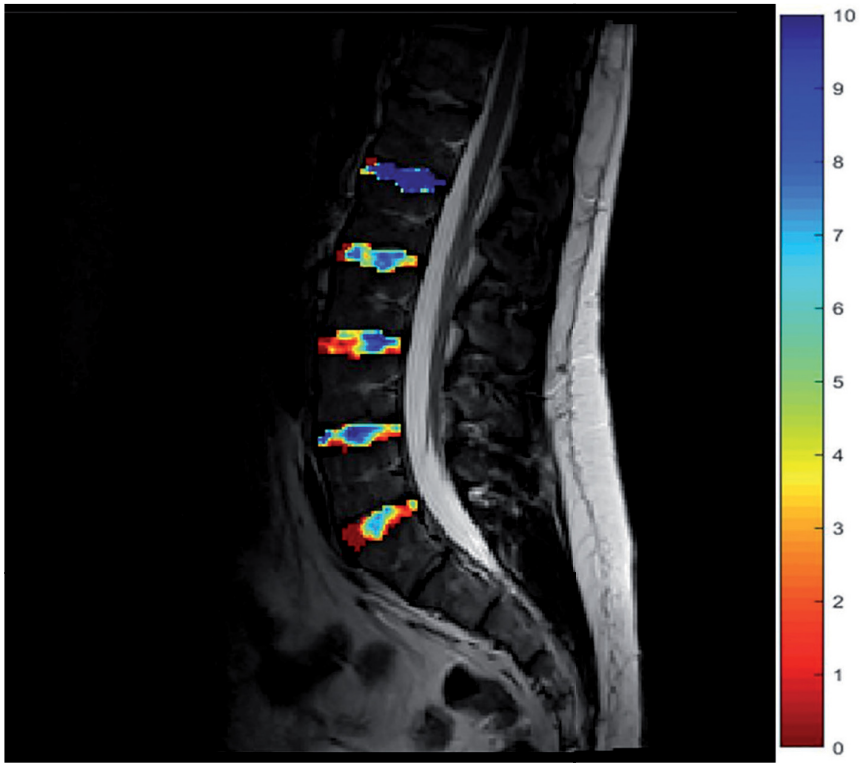


**Fig. 3.** Colour-coded gagCEST map of the lumbar spine (L1 - S1), with high GAG content in blue and low GAG content in red. This patient with radiculopathy presented significantly lower GAG content compared to controls, especially at the affected segment L5/S1.

and in monitoring cartilage changes. Kijowski *et al*. found improved sensitivity in the detection of cartilage lesions of the knee and for the identification of early cartilage degeneration(46). Ellermann *et al*. have focused on T2 and T2* mapping of the hip, showing that T2* relaxation times in normal cartilage were significantly higher than those of cartilage with early and more advanced degeneration (47).

T2 maps have also been obtained from the ankle, proximal interphalangeal joint and wrist. The association of physical activity with cartilage degeneration remains controversial and only a few studies have assessed the relationship using T2 mapping. T2-mapping has also been applied for quantitative assessment of fibrocartilage, in particular IVDs and menisci. In IVDs, T2 relaxation times are dependent on the quantity of water and the integrity of the proteoglycan (PG)-collagen matrix. During early disc degeneration, T2 mapping shows a decrease in water and collagen matrix (48).

Even in early RA (eRA), molecular cartilage damage could be found in this early stage of the disease while morphological alterations (for example joint space narrowing) are not visible (49). Herz *et al*. investigated the relation between inflammation of synovitis and cartilage degradation measured with biochemical and morphological MRI (50). They demonstrated an association with high synovitis and proteoglycan loss measured by dGEMRIC. It is known that structural bony destructions develop mostly at bare area, an area without cartilage coat. This protection is at stake in progressive disease and may lead to severe joint destruction. Additionally, McGonagle *et al*. found erosions in sites lined by cartilage (51). These authors described lesser bone destruction at these areas, so they concluded that cartilage coat minimises bone damage.

## Future directions

US is increasingly explored as a bedside tool for early diagnosis, and quantification of OA progression as well as RA cartilage damage. Conventional US techniques including PD and duplex techniques do not yet permit analysis of chemical cartilage or ECM composition. MRI has constantly been improved to obtain higher resolution images and detect cartilage injury on a molecular level, even without the need for potentially hazardous contrast agents. Both techniques are well tolerated by the patient and serious adverse events are rare, with the exception of potential side effects from contrast agents. Therefore, US and MRI will likely be of increasing importance in future clinical trials and clinical assessment of RA and OA.

## References


1. PAP T, KORB-PAP A: Cartilage damage in osteoarthritis and rheumatoid arthritis – two unequal siblings. *Nat Rev Rheumatol* 2015; 11: 606-15.
2. GUILAK F, NIMS RJ, DICKS A, WU C-L, MEULENBELT I: Osteoarthritis as a disease of the cartilage pericellular matrix. *Matrix Biol* 2018 May 22 [Epub ahead of print].
3. NELSON AE: Osteoarthritis year in review 2017: clinical. *Osteoarthritis Cartilage* 2018; 26: 319-25.
4. ALETAHA D, NEOGI T, SILMAN AJ *et al*.: 2010 rheumatoid arthritis classification criteria: an American College of Rheumatology/European League Against Rheumatism collaborative initiative. *Ann Rheum Dis* 2010; 69: 1580-8.
5. SMOLEN JS, ALETAHA D, BIJLSMA JWJ *et al*.: Treating rheumatoid arthritis to target: recommendations of an international task force. *Ann Rheum Dis* 2010; 69: 631-7.
6. DARAWANKUL B, CHAIAMNUAY S, PAKCHOTANON R, ASAVATANABODEE P, NARONGROEKNAWIN P: The good EULAR response at the first year is strongly predictive of clinical remission in rheumatoid arthritis: results from the TARAC cohort. *Clin Rheumatol* 2015; 34: 43-9.
7. FUNCK-BRENTANO T, GANDJBAKHCH F, ETCHEPARE F *et al*.: Prediction of radiographic damage in early arthritis by sonographic erosions and power Doppler signal: a longitudinal observational study. *Arthritis Care Res* 2013; 65: 896-902.
8. VAN DER HEIJDE D: Erosions versus joint space narrowing in rheumatoid arthritis: what do we know? *Ann Rheum Dis* 2011; 70 (Suppl. 1): i116-8.
9. ALETAHA D, FUNOVITS J, SMOLEN JS: Physical disability in rheumatoid arthritis is associated with cartilage damage rather than bone destruction. *Ann Rheum Dis* 2011; 70: 733-9.
10. BLIDDAL H, BOESEN M, CHRISTENSEN R, KUBASSOVA O, TORP-PEDERSEN S: Imaging as a follow-up tool in clinical trials and clinical practice. *Best Pract Res Clin Rheumatol* 2008; 22: 1109-26.
11. AMERICAN COLLEGE OF RHEUMATOLOGY RHEUMATOID ARTHRITIS CLINICAL TRIALS TASK FORCE IMAGING GROUP AND OUTCOME MEASURES IN RHEUMATOLOGY MAGNETIC RESONANCE IMAGING INFLAMMATORY ARTHRITIS WORKING GROUP. Review: The utility of magnetic resonance imaging for assessing structural damage in randomized controlled trials in rheumatoid arthritis. *Arthritis Rheum* 2013; 65: 2513-23.
12. DISLER DG, RAYMOND E, MAY DA, WAYNE JS, MCCAULEY TR: Articular cartilage defects: in vitro evaluation of accuracy and interobserver reliability for detection and grading with US. *Radiology* 2000; 215: 846-51.
13. MÖLLER B, BONEL H, ROTZETTER M, VILLIGER PM, ZISWILER H-R: Measuring finger joint cartilage by ultrasound as a promising alternative to conventional radiograph imaging. *Arthritis Rheum* 2009; 61: 435-41.
14. FILIPPUCCI E, DA LUZ KR, DI GESO L *et al*.: Interobserver reliability of ultrasonography in the assessment of cartilage damage in rheumatoid arthritis. *Ann Rheum Dis* 2010; 69: 1845-8.
15. ABE A, ISHIKAWA H, NAKAZONO K, MURASAWA A, WAKAKI K: A comparison of the ultrasonography images of the joints of patients with rheumatoid arthritis and the corresponding synovial histological findings. *Mod Rheumatol* 2016; 26: 534-9.
16. GUTIERREZ M, DI GESO L, SALAFFI F *et al*.: Ultrasound detection of cartilage calcification at knee level in calcium pyrophosphate deposition disease: ultrasound in calcium pyrophosphate deposition disease. *Arthritis Care Res* 2014; 66: 69-73.
17. TERSLEV L, GUTIERREZ M, SCHMIDT WA *et al*.: Ultrasound as an outcome measure in gout. A validation process by the OMERACT Ultrasound Working Group. *J Rheumatol* 2015; 42: 2177-81.
18. NEOGI T, JANSEN TLTA, DALBETH N *et al*.: 2015 Gout classification criteria: an American College of Rheumatology/European League Against Rheumatism collaborative initiative. *Ann Rheum Dis* 2015; 74: 1789-98.
19. SARMANOVA A, HALL M, MOSES J, DOHERTY M, ZHANG W: Synovial changes detected by ultrasound in people with knee osteoarthritis - a meta-analysis of observational studies. *Osteoarthritis Cartilage* 2016; 24: 1376-83.
20. MATHIESSEN A, SLATKOWSKY-CHRISTENSEN B, KVIEN TK, HAMMER HB, HAUGEN IK: Ultrasound-detected inflammation predicts radiographic progression in hand osteoarthritis after 5 years. *Ann Rheum Dis* 2016; 75: 825.
21. CONAGHAN P, LASSERE M, ØSTERGAARD M *et al*.: OMERACT Rheumatoid Arthritis Magnetic Resonance Imaging Studies. Exercise 4: an international multicenter longitudinal study using the RA-MRI Score. *J Rheumatol* 2003; 30: 1376-9.
22. HETLAND ML, STENGAARD-PEDERSEN K, JUNKER P *et al*.: Radiographic progression and remission rates in early rheumatoid arthritis - MRI bone oedema and anti-CCP predicted radiographic progression in the 5-year extension of the double-blind randomised CIMESTRA trial. *Ann Rheum Dis* 2010; 69: 1789-95.
23. FREESTON JE, BIRD P, CONAGHAN PG: The role of MRI in rheumatoid arthritis: research and clinical issues. *Curr Opin Rheumatol* 2009; 21: 95-101.
24. BAKER JF, OSTERGAARD M, EMERY P *et al*.: Early MRI measures independently predict 1-year and 2-year radiographic progression in rheumatoid arthritis: secondary analysis from a large clinical trial. *Ann Rheum Dis* 2014; 73: 1968-74.
25. HAAVARDSHOLM EA, BØYESEN P, ØSTERGAARD M, SCHILDVOLD A, KVIEN TK: Magnetic resonance imaging findings in 84 patients with early rheumatoid arthritis: bone marrow oedema predicts erosive progression. *Ann Rheum Dis* 2008; 67: 794-800.
26. ØSTERGAARD M, PETERFY C, CONAGHAN P *et al*.: OMERACT Rheumatoid Arthritis Magnetic Resonance Imaging Studies. Core set of MRI acquisitions, joint pathology definitions, and the OMERACT RA-MRI scoring system. *J Rheumatol* 2003; 30: 1385-6.
27. ØSTERGAARD M, EMERY P, CONAGHAN PG *et al*.: Significant improvement in synovitis, osteitis, and bone erosion following golimumab and methotrexate combination therapy as compared with methotrexate alone: a magnetic resonance imaging study of 318 methotrexate-naive rheumatoid arthritis patients. *Arthritis Rheum* 2011; 63: 3712-22.
28. OSTERGAARD M, BØYESEN P, ESHED I *et al*.: Development and preliminary validation of a magnetic resonance imaging joint space narrowing score for use in rheumatoid arthritis: potential adjunct to the OMERACT RA MRI scoring system. *J Rheumatol* 2011; 38: 2045-50.
29. GLINATSI D, BIRD P, GANDJBAKHCH F *et al*.: Validation of the OMERACT Psoriatic Arthritis Magnetic Resonance Imaging Score (PsAMRIS) for the hand and foot in a randomized placebo-controlled trial. *J Rheumatol* 2015; 42: 2473-9.
30. ØSTERGAARD M, PETERFY CG, BIRD P *et al*.: The OMERACT Rheumatoid Arthritis Magnetic Resonance Imaging (MRI) Scoring System: updated recommendations by the OMERACT MRI in Arthritis Working Group. *J Rheumatol* 2017; 44: 1706-12.
31. OSTROWSKA M, MAŚLIŃSKI W, PROCHOREC-SOBIESZEK M, NIECIECKI M, SUDOŁ-SZOPIŃSKA I: Cartilage and bone damage in rheumatoid arthritis. *Reumatologia* 2018; 56: 111-20.
32. OEI EHG, VAN TIEL J, ROBINSON WH, GOLD GE: Quantitative radiological imaging techniques for articular cartilage composition: Towards early diagnosis and development of disease-modifying therapeutics for osteoarthritis. *Arthritis Care Res* 2014; n/a-n/a.
33. SCHLEICH C, HESPER T, HOSALKAR HS *et al*.: 3D double-echo steady-state sequence assessment of hip joint cartilage and labrum at 3 Tesla: comparative analysis of magnetic resonance imaging and intraoperative data. *Eur Radiol* 2017; 27: 4360-71.
34. BURSTEIN D, VELYVIS J, SCOTT KT *et al*.: Protocol issues for delayed Gd(DTPA) (2-)-enhanced MRI (dGEMRIC) for clinical

evaluation of articular cartilage. *Magn Reson Med* 2001; 45: 36-41.
35. MIESE F, BUCHBENDER C, SCHERER A *et al*.: Molecular imaging of cartilage damage of finger joints in early rheumatoid arthritis with delayed gadolinium-enhanced magnetic resonance imaging. *Arthritis Rheum* 2012; 64: 394-9.
36. CREMA MD, ROEMER FW, MARRA MD *et al*.: Articular cartilage in the knee: current MR imaging techniques and applications in clinical practice and research. *Radiographics* 2011; 31: 37-61.
37. TIDERIUS CJ, SANDIN J, SVENSSON J, DAHLBERG LE, JACOBSSON L: Knee cartilage quality assessed with dGEMRIC in rheumatoid arthritis patients before and after treatment with a TNF inhibitor. *Acta Radiol* 2010; 51: 1034-7.
38. SCHLEICH C, MIESE F, MÜLLER-LUTZ A *et al*.: Value of delayed gadolinium-enhanced magnetic resonance imaging of cartilage for the pre-operative assessment of cervical intervertebral discs. *J Orthop Res* 2017; 35: 1824-30.
39. KIM Y-J, JARAMILLO D, MILLIS MB, GRAY ML, BURSTEIN D: Assessment of early osteoarthritis in hip dysplasia with delayed gadolinium-enhanced magnetic resonance imaging of cartilage. *J Bone Joint Surg Am* 2003; 85-A: 1987-92.
40. TIDERIUS CJ, OLSSON LE, LEANDER P, EKBERG O, DAHLBERG L: Delayed gadolinium-enhanced MRI of cartilage (dGEMRIC) in early knee osteoarthritis. *Magn Reson Med* 2003; 49: 488-92.
41. PINKER K, SZOMOLANYI P, WELSCH GC *et al*.: Longitudinal evaluation of cartilage composition of matrix-associated autologous chondrocyte transplants with 3-T delayed gadolinium-enhanced MRI of cartilage. *AJR Am J Roentgenol* 2008; 191: 1391-6.
42. GULANI V, CALAMANTE F, SHELLOCK FG, KANAL E, REEDER SB, INTERNATIONAL SOCIETY FOR MAGNETIC RESONANCE IN MEDICINE: Gadolinium deposition in the brain: summary of evidence and recommendations. *Lancet Neurol* 2017; 16: 564-70.
43. REHNITZ C, KUPFER J, STREICH NA *et al*.: Comparison of biochemical cartilage imaging techniques at 3 T MRI. *Osteoarthritis Cartilage* 2014; 22: 1732-42.
44. WELSCH GH, TRATTNIG S, PATERNOSTRO-SLUGA T *et al*.: Parametric T2 and T2* mapping techniques to visualize intervertebral disc degeneration in patients with low back pain: initial results on the clinical use of 3.0 Tesla MRI. *Skeletal Radiol* 2011; 40: 543-51.
45. SCHLEICH C, MÜLLER-LUTZ A, BLUM K *et al*.: Facet tropism and facet joint orientation: risk factors for the development of early biochemical alterations of lumbar intervertebral discs. *Osteoarthritis Cartilage* 2016; 24: 1761-8.
46. KIJOWSKI R, BLANKENBAKER DG, MUNOZ DEL RIO A, BAER GS, GRAF BK: Evaluation of the articular cartilage of the knee joint: value of adding a T2 mapping sequence to a routine MR imaging protocol. *Radiology* 2013; 267: 503-13.
47. ELLERMANN J, ZIEGLER C, NISSI MJ *et al*.: Acetabular cartilage assessment in patients with femoroacetabular impingement by using T2* mapping with arthroscopic verification. *Radiology* 2014; 271: 512-23.
48. ZHANG Y, HU J, DUAN C, HU P, LU H, PENG X: Correlation study between facet joint cartilage and intervertebral discs in early lumbar vertebral degeneration using T2, T2* and T1ρ mapping. *PLoS One* 2017; 12: e0178406.
49. SCHLEICH C, MÜLLER-LUTZ A, SEWERIN P *et al*.: Intra-individual assessment of inflammatory severity and cartilage composition of finger joints in rheumatoid arthritis. *Skeletal Radiol* 2015; 44: 513-8.
50. HERZ B, ALBRECHT A, ENGLBRECHT M *et al*.: Osteitis and synovitis, but not bone erosion, is associated with proteoglycan loss and microstructure damage in the cartilage of patients with rheumatoid arthritis. *Ann Rheum Dis* 2014; 73: 1101-6.
51. MCGONAGLE D, TAN AL, MØLLER DØHN U, OSTERGAARD M, BENJAMIN M: Microanatomic studies to define predictive factors for the topography of periarticular erosion formation in inflammatory arthritis. *Arthritis Rheum* 2009; 60: 1042-51.

European Radiology (2019) 29:2581–2588
https://doi.org/10.1007/s00330-018-5880-6

MUSCULOSKELETAL

# Differences of radiocarpal cartilage alterations in arthritis and osteoarthritis using morphological and biochemical magnetic resonance imaging without gadolinium-based contrast agent administration

Valentina Mori[1] · Lino M. Sawicki[1] · Philipp Sewerin[2] · Markus Eichner[1] · Benedikt M. Schaarschmidt[1] · Lisa Oezel[3] · Sebastian Gehrmann[3] · Bernd Bittersohl[4] · Gerald Antoch[1] · Christoph Schleich[1]

Received: 19 June 2018 / Revised: 19 October 2018 / Accepted: 8 November 2018 / Published online: 12 December 2018


## Abstract

**Objectives** To identify differences of radiocarpal cartilage alterations in osteoarthritis and arthritis using multiparametrical magnetic resonance imaging (MRI) comprising morphological and biochemical sequences without gadolinium-based contrast agent administration.

**Methods** In this prospective study, multiparametrical MRI of the radiocarpal cartilage was performed in 47 participants (mean age, 46.6 ± 17.6 years; min., 20 years; max., 79 years) on a 3 Tesla MRI. The cohort consisted of 11 patients suffering from arthritis, 10 patients with osteoarthritis, 14 patients after distal radius fracture, and 12 healthy volunteers. The radiocarpal cartilage was assessed using morphological (DESS, TrueFISP) and biochemical (T2*) MRI sequences without the application of intravenous contrast agent. The modified Outerbridge classification system for morphological and region-of-interest analyses for biochemical analysis was applied to assess the degree of cartilage damage in each patient before data were statistically tested for significant difference between the groups using a post hoc Tukey test.

**Results** In morphological imaging, cartilage damage was significantly more frequent in arthritis and osteoarthritis than in healthy volunteers (DESS: $p = 0.01$, $p = 0.0004$; TrueFISP: $p = 0.02$, $p = 0.0001$). In T2* imaging, patients with osteoarthritis showed higher cartilage damage compared to patients with arthritis ($p = 0.01$).

**Conclusion** With multiparametrical MRI, it is possible to identify differences of radiocarpal cartilage alterations of patients with arthritis and osteoarthritis using the combination of morphological and biochemical MR imaging of the radiocarpal cartilage without the application of contrast agent. Multiparametrical MRI without the usage of contrast agent may be a potential tool helping to distinguish both entities.

**Key Points**

- *Multiparametrical MRI with morphological and biochemical sequences allows the differentiation of patients with arthritis and osteoarthritis.*
- *High-resolution MRI of radiocarpal cartilage is possible without administration of contrast agent.*

**Keywords** Morphological and cartilage MR imaging · Without gadolinium-based contrast agent · Arthritis · Osteoarthritis · Radiocarpal cartilage

✉ Lino M. Sawicki
LinoMorris.Sawicki@med.uni-duesseldorf.de

[1] Department of Diagnostic and Interventional Radiology, Medical Faculty, University of Düsseldorf, 40225 Düsseldorf, Germany

[2] Department and Hiller-Research-Unit for Rheumatology, UKD, Heinrich Heine University Düsseldorf, Düsseldorf, Germany

[3] Department of Trauma and Hand Surgery, University Hospital, Moorenstrasse 5, 40225 Düsseldorf, Germany

[4] Department of Orthopedics, Medical Faculty, University of Düsseldorf, Düsseldorf, Germany

**Abbreviations**

| | |
|---|---|
| ANOVA | Analysis of variance |
| CI | Confidence interval |
| DESS | Double echo steady state |
| DGEMRIC | Delayed gadolinium-enhanced MRI of cartilage |
| DRF | Distal radius fracture |
| DWI | Diffusion-weighted imaging |
| EMA | European Medicines Agency |
| GagCEST | Glycosaminoglycan chemical exchange saturation transfer |
| ICC | Intraclass correlation coefficient |
| LC | Central lunate |
| LP | Peripheral lunate |
| MRI | Magnetic resonance imaging |
| OA | Osteoarthritis |
| PD | Proton density |
| RA | Rheumatoid arthritis |
| ROI | Region-of-interest |
| SC | Central scaphoid |
| SP | Peripheral scaphoid |
| STARD | Standards for reporting of diagnostic accuracy studies |
| TNF-α | Tumor necrosis factor α |
| TRUFI | True fast imaging with steady state precession |

## Introduction

The radiocarpal cartilage of the wrist is one of the most challenging joints for magnetic resonance imaging (MRI) due to its thin hyaline cartilage layers and multiple surfaces [1]. Wrist pain is a common clinical problem of varying etiology [2]. In many cases, articular cartilage injury or loss is suspected if other obvious clinical syndromes are excluded [3]. To guide therapy, it is essential to detect cartilage damage. Cartilage injury may result either from direct trauma or as a common end point of inflammatory or degenerative diseases [4]. In clinical practice, the differentiation of arthritis and osteoarthritis (OA) may cause diagnostic problems because of the chronic progressive nature of both entities [5, 6]. However, different treatment strategies are tracked in both diseases, which asks for better diagnostic tools to detect early stages, especially in the case of rheumatoid arthritis where an early therapy start is considered to be a decisive prognostic factor [7].

Conventional radiographs are limited in showing cartilage damage until the disease has processed to joint space narrowing [2]. For wrist imaging, MRI is the technique of choice [8]. Particularly, MRI is able to depict both focal and diffuse cartilage defects [9]. Several MR sequences are available for morphological cartilage imaging of the wrist. Among them, the TRUFI (true fast imaging with steady state precession) sequence is the most accurate method according to a current study [10]. The DESS (double echo steady state) sequence is another morphological MR sequence that has been proven useful for cartilage assessment [11, 12]. Biochemical cartilage imaging has been proposed to assess extracellular matrix components of hyaline cartilage with delayed gadolinium-enhanced MRI of cartilage (dGEMRIC) technique as the gold standard [13]. For dGEMRIC, the application of intravenous contrast agent is obligatory. However, recent studies brought potential adverse effects of gadolinium to international attention [14, 15]. Due to potential gadolinium depositions in the brain, the European Medicines Agency (EMA) banned several linear gadolinium-based contrast agents, even though macrocyclic contrast agents have not been suspended their use should be limited to those examinations where there is no alternative [16]. Hence, future research should focus on gadolinium-free molecular MR imaging of cartilage such as glycosaminoglycan chemical exchange saturation transfer (gagCEST), sodium MRI and T1 rho mapping to visualize the GAG content, T2/T2* mapping to evaluate the water content, and collagen network integrity or diffusion-weighted imaging (DWI) [17–19]. In this study, we applied T2* mapping for molecular cartilage imaging. T2* mapping is advantageous in many ways. Next to no needed application of contrast media, it allows a three-dimensional (3D), high-resolution, isotropic cartilage evaluation with a short acquisition time [20].

The purpose of this study was to identify differences in osteoarthritis and arthritis with multiparametrical MRI using morphological (DESS, TRUFI) and biochemical (T2*) sequences of radiocarpal cartilage without the usage of intravenous contrast agent.

## Materials and methods

### Study design

The study was approved by the local ethics committee. Written informed consent was obtained from all volunteers prior to inclusion for this prospective study.

### Study population

Forty-seven participants (27 male, 20 female; mean age, 46.6 ± 17.6 years; min., 20 years; max., 79 years) who underwent 3T wrist MRI during the period from October 2016 to March 2017 were prospectively enrolled in this study. The cohort consisted of 11 patients suffering from arthritis (disease duration, 2.9 ± 1.7 years; min., 1 year; max., 7 years; 5 male; 6 female; mean age, 47.3 ± 15.7 years; min., 27 years; max., 76 years), 10 patients with osteoarthritis (disease duration, 7.6 ± 4.7 years; min., 2 years; max., 19 years; 6 male; 4 female; mean age, 63.3 ± 9.6 years; min., 50 years; max., 79 years), 14 patients with a condition following distal radius fracture (trauma 4.1 ± 2.7 years ago; min., 1 year; max., 11 years; 8 male, 6 female; mean age,

**Table 1** Detailed sequence parameters

| | | T2* map 3D | DESS 3D | TrueFISP 3D |
|---|---|---|---|---|
| $T_R/T_E$ | ms/ms | 33.0/4.95 | 11.86/4.54 | 10.06/4.16 |
| Field of view | $mm^2$ | 100 × 61 | 94 × 61 | 100 × 61 |
| Slice thickness | mm | 0.42 | 0.42 | 0.42 |
| Flip angle | ° | 25 | 25 | 57 |
| Averages | | 1 | 2 | 2 |
| Basic resolution | | 256 | 128 | 256 |
| Number of slices | | 144 | 144 | 144 |
| Acquisition duration | min:sec | 5:47 | 5:41 | 5:13 |

45.5 ± 16.3 years; min., 23 years; max., 70 years) and 12 healthy controls (8 male; 4 female; mean age, 33.5 ± 13 years; min., 20 years; max., 65 years) without any wrist pain or trauma in their clinical history. The patients with condition following distal radius fracture could be divided into six patients with intraarticular fracture and eight patients without joint involvement. The group of arthritis consisted of five (three seropositive) patients with rheumatoid arthritis (RA). Among them, two patients were treated with methotrexate (one in combination with prednisolone), one patient received TNF-α inhibitors in combination with prednisolone, one patient prednisolone only, and another patient received no therapy. The other six arthritis patients were suffering from psoriatic arthritis (treated with apremilast in combination with prednisolone), spondyloarthritis (treated with TNF-α inhibitors), Stills disease (treated with prednisolone), sarcoidosis (treated with prednisolone), and systemic juvenile idiopathic arthritis (treated with methotrexate). All patients with arthritis showed signs of wrist synovitis in a clinical examination. The patients suffering from osteoarthritis received conservative therapy, such as pain medication or physical therapy. All patients with a condition following distal radial fracture had terminated disease-specific therapy and osteosynthesis equipment had been removed prior to the study. All patients were diagnosed by clinically experienced rheumatologists and trauma surgeons. Exclusion criteria were general contraindications to MR imaging, metal implants at the wrist, and undefined wrist disease.

## MR imaging protocol

All MR examinations were performed at a 3T MRI scanner (Magnetom Skyra, Siemens Healthineers) using a dedicated, 16 channel, high-resolution wrist coil. Two patients were measured with a four-channel flex coil, because they did not fit into the dedicated wrist coil due to plaster casts. All participants were examined in prone position with the arm over the head, the so-called superman position. Our sequence protocol included the morphological sequences DESS and TRUFI as well as the biochemical imaging sequence T2*, each acquired in coronal orientation. For T2* mapping, nine consecutive echoes were obtained (TE: 16.1 ms, 32.2 ms, 48.3 ms, 64.4 ms, 80.5 ms, 96.6 ms, 113.0 ms, 129.0 ms, 145.0 ms). To complete the sequence protocol, T1- and PD (proton density)-weighted images in coronal orientation were supplemented for the evaluation of bone and joint fluid in a clinical setting. These five sequences resulted in an examination duration of about 22 min. No intravenous contrast application was applied. The MR protocol details were given in Table 1.

## Data analysis

All data sets were evaluated by a board certified radiologist with 6 years of experience in musculoskeletal imaging and a medical student, trained in cartilage segmentation. Both readers were blinded to clinical diagnosis and to the other morphological analyses, respectively. The molecular image analysis was performed in consensus [21]. Analysis of the two morphological sequences and the biochemical sequence were performed separately and with 2 weeks apart to avoid recognition bias. Due to the scapholunate ligament, the radiocarpal cartilage was divided into different zones: peripheral lunate (LP), central lunate (LC), peripheral scaphoid (SP),

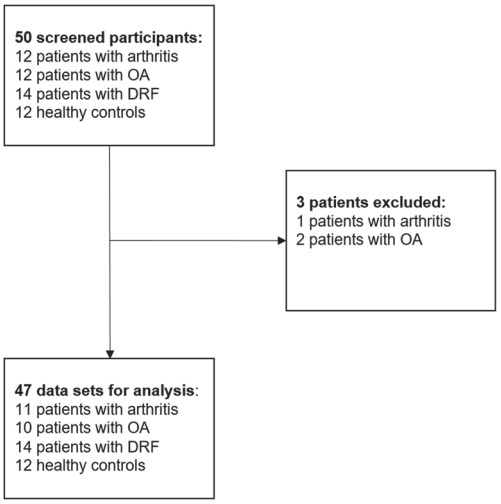


**Fig. 1** Screening flow chart of the study participants according to STARD. Three patients (one with arthritis and two with osteoarthritis) prematurely terminated the MR examination and hat to be excluded

**Table 2** Morphological and biochemical assessment of radiocarpal cartilage in healthy participants, patients with arthritis, osteoarthritis, and with a condition following distal radius fracture

| | Mean | Std | Median | Min | Max | CI (lower limit) | CI (upper limit) |
|---|---|---|---|---|---|---|---|
| Control DESS | 0.521 | 0.511 | 0.375 | 0 | 3 | 0.355 | 0.81 |
| Control TrueFISP | 0.25 | 0.433 | 0 | 0 | 3 | 0.005 | 0.495 |
| Control T2* map [ms] | 21.398 | 3.45 | 21.525 | 12.7 | 26.9 | 19.44 | 23.35 |
| Arthritis DESS | 1.625 | 1.31 | 1.125 | 0 | 4 | 0.813 | 2.437 |
| Arthritis TrueFISP | 1.475 | 1.48 | 0.875 | 0 | 4 | 0.557 | 2.393 |
| Arthritis T2* map [ms] | 19.08 | 3.579 | 19.325 | 10.2 | 27 | 16.964 | 21.195 |
| Osteoarthritis DESS | 2.639 | 1.263 | 3 | 0 | 4 | 1.814 | 3.464 |
| Osteoarthritis TrueFISP | 2.472 | 1.192 | 2.75 | 0 | 4 | 1.694 | 3.251 |
| Osteoarthritis T2* map [ms] | 14.698 | 4.478 | 14.64 | 5.8 | 23.5 | 11.922 | 17.468 |
| Trauma DESS | 1.696 | 1.035 | 1.5 | 0 | 4 | 1.154 | 2.239 |
| Trauma TrueFISP | 1.607 | 1.174 | 1.375 | 0 | 4 | 0.992 | 2.222 |
| Trauma T2* map [ms] | 18.366 | 2.913 | 17.938 | 11.3 | 28.8 | 16.84 | 19.766 |

and central scaphoid (SC). For morphological cartilage assessment, the modified Outerbridge classification [22] was used: grade 0, normal; grade 1, cartilage softening; grade 2, cartilage abrasion; grade 3, cartilage loss; grade 4, no evaluation of cartilage possible. The data sets of the molecular sequence were converted to the Leonardo® Workstation (Siemens Healthineers) and a region-of-interest (ROI) analysis was performed for each cartilage zone. T2* images with a TE time of 16.1 ms were used as an anatomic reference for cartilage identification. The ROIs were transferred to the co-registered T2* map. TE times in milliseconds of the different cartilage zones were calculated. The degree of cartilage damage correlates with decreasing TE times in the T2* map [23].

## Statistical analysis

Statistical analysis was performed using MATLAB (MathWorks). The mean, standard deviations, median, minimum, maximum, and 95% confidence interval (CI) were calculated for morphological and biochemical assessment of radiocarpal cartilage. Kolmogorow-Smirnow-Lilliefors tests were used to assess normal distribution. Univariate analysis of variance (ANOVA) and post hoc Tukey test were performed to assess statistical differences of the means of the morphological and biochemical cartilage evaluation of the different groups and subgroups. After Bonferroni correction, $p < 0.0167$ was assumed statistically significant. Intra- and interreader reliability were tested with intraclass correlation coefficient (ICC) for morphological cartilage evaluation.

## Results

The cartilage assessment of 47 participants could be used for statistical analysis. Three patients (one with arthritis and two with osteoarthritis) had prematurely terminated the MR examination (Fig. 1). The descriptive statistics were summarized in Table 2 (mean ± standard deviation; median; minimum/maximum; 95% CI [lower limit; upper limit]). Interreader (ICC = 0.91) and intrareader reliability (ICC = 0.91) were excellent.

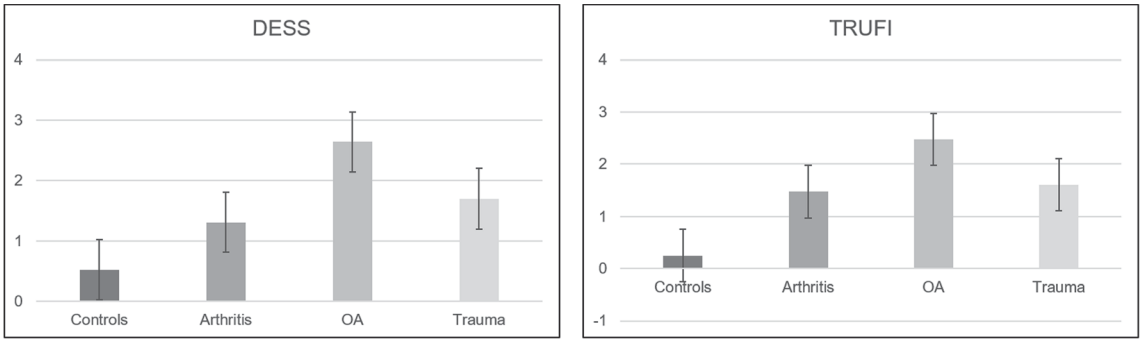


**Fig. 2** Bar chart of the morphological radiocarpal cartilage assessment according to modified Outerbridge classification for healthy controls, patients with arthritis, osteoarthritis (OA), or with a condition following distal radius fracture (trauma). Significantly higher cartilage damage was found in patients with arthritis, OA, or trauma compared to healthy controls with morphological cartilage imaging (DESS, TRUFI)

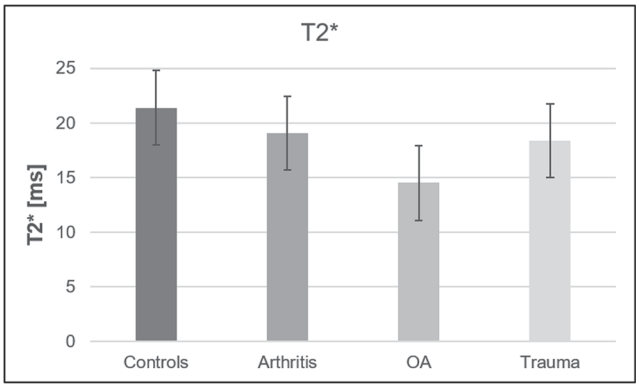


**Fig. 3** Bar chart of the biochemical radiocarpal cartilage assessment according to T2* mapping in milliseconds (ms) for healthy controls, patients with arthritis, osteoarthritis (OA), or with a condition following distal radius fracture (trauma). Significantly higher cartilage damage with lower T2* values was found in patients with OA compared to patients suffering from arthritis, patients with condition after distal radius fracture, and healthy controls

## Analysis of morphological cartilage assessment

DESS sequence showed significantly higher cartilage damage in patients with arthritis ($p = 0.018$) and osteoarthritis ($p < 0.0001$) and patients with condition after distal radius fracture ($p = 0.005$) compared with healthy controls. TRUFI revealed significantly higher cartilage degradation in patients suffering from arthritis ($p = 0.0162$), patients with osteoarthritis ($p < 0.0001$), and patients with condition after distal radius fracture ($p = 0.003$) compared with healthy controls. For both, DESS and TRUFI, patients with arthritis illustrated significantly lower cartilage damage in central zones (LC and SC) compared to osteoarthritis (DESS: $p = 0.003$; TRUFI: $p = 0.011$). For peripheral zones (LP and SP), no significant difference could be found ($p > 0.05$). In patients with arthritis, as well as in patients suffering from osteoarthritis, significantly higher cartilage loss was found in central zones (LC and SC) compared to peripheral zones (LP and SP) (arthritis: $p = 0.04$; osteoarthritis: $p = 0.02$). No significant difference between intraarticular fracture and no intraarticular fracture line could be depicted in patients with condition after distal radius fracture for DESS and TRUFI ($p > 0.05$) (Fig. 2).

## Analysis of molecular cartilage assessment

T2* sequence showed significantly higher cartilage damage in patients with osteoarthritis compared to patients with arthritis ($p = 0.005$), patients with condition after distal radius fracture

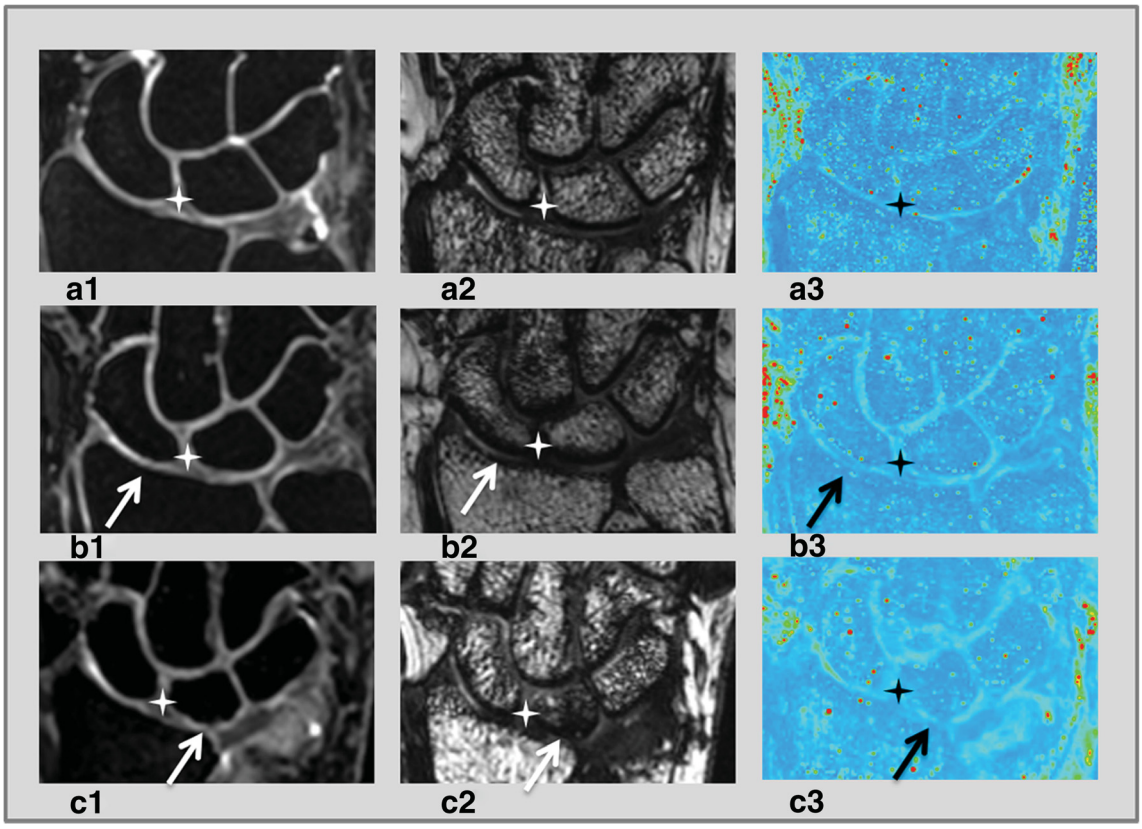


**Fig. 4** Image synopsis of a healthy participant (**a**), a patient with arthritis (**b**), and a patient suffering from osteoarthritis (**c**). For each case, the three main sequences DESS (1), TrueFISP (2), and T2* map (3) were presented. The arrows in figures **b**1–**b**3 emphasize a low-grade cartilage damage of central zone under the scaphoid of a patient with arthritis. Images **c**1–**c**3 of a patient suffering from osteoarthritis show a high-grade cartilage damage of the articular cartilage of the lunate

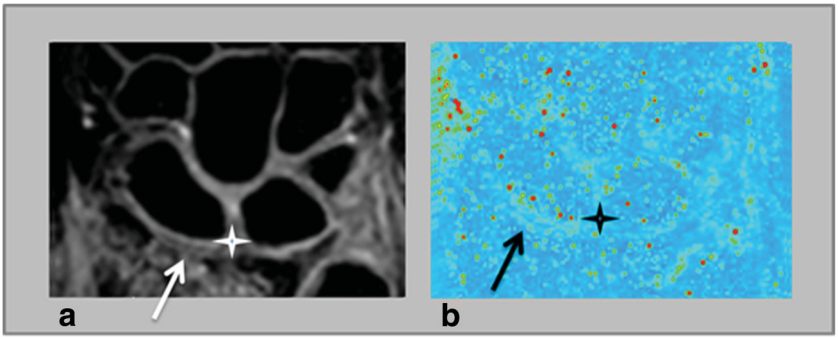


**Fig. 5** Delamination of radial articular cartilage after intraarticular distal radius fracture 19 months ago. The damage can be shown in DESS (**a**) and is also recognizable in the corresponding T2* map (**b**). A bone marrow edema in the distal radius can be illustrated in the DESS sequence (**a**)

($p = 0.014$), and healthy controls ($p < 0.0001$). For T2*, patients with arthritis illustrated significantly lower cartilage damage in central zones (LC and SC; $p = 0.005$) and peripheral zones (LP and SP; $p = 0.0002$) compared to osteoarthritis. Patients with arthritis illustrated significantly higher cartilage damage in central zones (LC and SC) compared to peripheral zones (LP and SP) ($p = 0.0004$). No significant difference between intraarticular fracture and no intraarticular fracture line could be depicted in patients with condition after distal radius fracture for T2* ($p > 0.05$) (Figs. 3, 4, 5 and 6).

## Discussion

Our data showed that multiparametrical MRI of the radiocarpal cartilage with the combination of high-resolution, morphological DESS and TRUFI sequences and biochemical T2* mapping has the potential to identify differences of cartilage alterations in patients with arthritis compared with patients with osteoarthritis. This is all the more important because it can clinically be difficult to distinguish both diseases, especially in the condition of erosive osteoarthritis [24]. Additionally, our data revealed that multiparametrical MRI of assessing radiocarpal cartilage is able to differentiate healthy participants from patients suffering from arthritis, osteoarthritis, or distal radius fracture. In many cases, articular cartilage injury or loss is suspected for wrist pain [3]. Haims et al could not demonstrate significant cartilage alterations in patients with wrist pain using indirect MR arthrograms and unenhanced MRI [2]. Our MR protocol comprised 3D, high-resolution sequences that allow the detailed illustration of the thin hyaline cartilage layers of radiocarpal cartilage [1]. For the triangular fibro-cartilaginous complex (TFCC), high-resolution MRI has shown good sensitivity in correlation with arthroscopy [25, 26]. Our multiparametrical MRI demonstrated higher cartilage degradation in central compared to peripheral zones in arthritis and osteoarthritis. In addition, significantly higher cartilage damage in central zones of radiocarpal cartilage was found in patients with osteoarthritis compared with patients suffering from arthritis. This may be explainable by force distribution over the wrist that relatively show a stronger impact on the central zones of radiocarpal cartilage in patients with osteoarthritis compared with arthritis [27]. In patients with a condition after distal radial fracture, no significant difference of cartilage alterations could be found between intraarticular fracture and no intraarticular fracture line. Both entities could lead to severe posttraumatic cartilage damage and secondary osteoarthritis [28]. The advantage of our MR protocol is that no contrast media is necessary for cartilage evaluation. With regard to the recently discovered gadolinium deposits in the brain resulting from intravenous MR contrast agent application, gadolinium-free imaging of articular cartilage is becoming a focus both for research and clinical imaging [16].

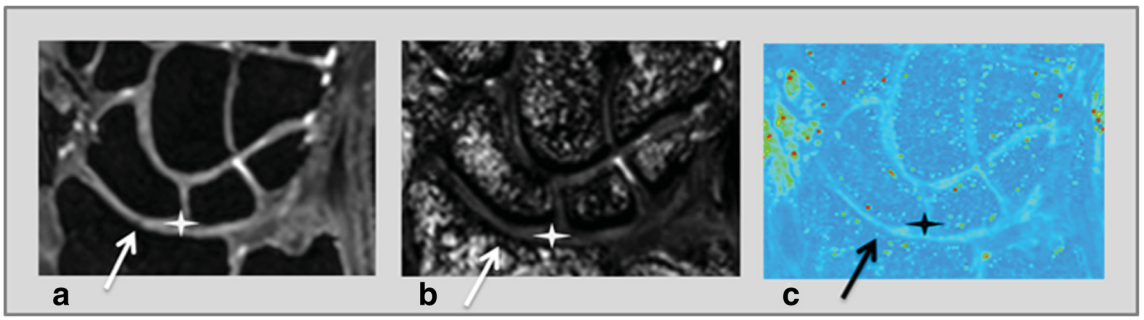


**Fig. 6** Intraarticular fracture of distal radius that was treated osteosynthesis. The current picture represents severe local cartilage damage corresponding to the former fracture line. The trauma happened 5 years ago

Our study has limitations. In spite of 47 examined participants, the main limitation is the small sample size. It should be noted that the study was performed without an arthroscopic or histological correlation. This was not possible due to ethical reasons. For patients suffering from osteoarthritis, no classification system could be specified. Conventional radiographs were not performed in this prospective study. Another limitation is the missing inter- and intrareader reliability for biochemical imaging. In our opinion, this is a minor limitation, as T2* mapping has already been proven to provide high inter- and intrareader reliability in former studies [29]. No age-matched groups between patients suffering from arthritis and patients with osteoarthritis could be applied. This is because of the different onset of the two diseases.

In conclusion, multiparametrical MRI of the radiocarpal cartilage with a combination of high-resolution morphological and biochemical sequences on a clinical 3T MRI system may be a powerful, non-invasive tool to investigate and diagnose patients with wrist pain. Our MR imaging protocol allows to identify differences in cartilage evaluation of patients with arthritis and osteoarthritis, healthy subjects could be distinguished from patients suffering from arthritis, osteoarthritis, or trauma, and zonal distribution of cartilage damage could be worked out. Moreover, we found that this is possible without the use of gadolinium-based contrast agent, that is expected to be a growing focus in future MR imaging trials of articular cartilage.

**Acknowledgements** We would like to thank Erika Rädisch for the assistance in receiving the MRI scans.

**Funding** The authors state that this work has not received any funding.

## Compliance with ethical standards

**Guarantor** The scientific guarantor of this publication is PD Dr. med. Christoph Schleich.

**Conflict of interest** The authors of this manuscript declare no relationships with any companies, whose products or services may be related to the subject matter of the article.

**Statistics and biometry** No complex statistical methods were necessary for this paper.

**Informed consent** Written informed consent was obtained from all patients in this study.

**Ethical approval** Institutional Review Board approval was obtained.

**Methodology**
- prospective
- diagnostic study
- performed at one institution

## References

1. Rehnitz C, Kuni B, Wuennemann F et al (2017) Delayed gadolinium-enhanced MRI of cartilage (dGEMRIC) and T2 mapping of talar osteochondral lesions: indicators of clinical outcomes. J Magn Reson Imaging 46:1601–1610
2. Haims AH, Moore AE, Schweitzer ME et al (2004) MRI in the diagnosis of cartilage injury in the wrist. AJR Am J Roentgenol 182:1267–1270
3. Strickland CD, Kijowski R (2011) Morphologic imaging of articular cartilage. Magn Reson Imaging Clin N Am 19:229–248
4. Hayter CL, Gold SL, Potter HG (2013) Magnetic resonance imaging of the wrist: bone and cartilage injury. J Magn Reson Imaging 37:1005–1019
5. Kouri T, Saario R, Merilahti-Palo R, Söderström KO (1987) Simplified distinction of rheumatoid synovial histopathology from that of degenerative joint diseases. Clin Rheumatol 6:98–100
6. Ehrlich GE (2001) Erosive osteoarthritis: presentation, clinical pearls, and therapy. Curr Rheumatol Rep 3:484–488
7. Schneider M, Lelgemann M, Abholz H-H et al (2011) DGRh-Leitlinie: management der frühen rheumatoiden arthritis. Springer Verlag, Berlin, Heidelberg
8. Chhabra A, Soldatos T, Thawait GK et al (2012) Current perspectives on the advantages of 3-T MR imaging of the wrist. Radiographics 32:879–896
9. Oneson SR, Scales LM, Erickson SJ, Timins ME (1996) MR imaging of the painful wrist. Radiographics 16:997–1008
10. Rehnitz C, Klaan B, von Stillfried F et al (2016) Comparison of modern 3D and 2D MR imaging sequences of the wrist at 3 Tesla. Rofo 188:753–762
11. Abraham CL, Bangerter NK, McGavin LS et al (2015) Accuracy of 3D dual echo steady state (DESS) MR arthrography to quantify acetabular cartilage thickness. J Magn Reson Imaging 42:1329–1338
12. Schleich C, Hesper T, Hosalkar HS et al (2017) 3D double-echo steady-state sequence assessment of hip joint cartilage and labrum at 3 Tesla: comparative analysis of magnetic resonance imaging and intraoperative data. Eur Radiol 27:4360–4371
13. Miese FR, Ostendorf B, Wittsack HJ et al (2010) Metacarpophalangeal joints in rheumatoid arthritis: delayed gadolinium-enhanced MR imaging of cartilage–a feasibility study. Radiology 257:441–447
14. Stojanov D, Aracki-Trenkic A, Benedeto-Stojanov D (2016) Gadolinium deposition within the dentate nucleus and globus pallidus after repeated administrations of gadolinium-based contrast agents-current status. Neuroradiology 58:433–441
15. Fingerhut S, Sperling M, Holling M et al (2018) Gadolinium-based contrast agents induce gadolinium deposits in cerebral vessel walls, while the neuropil is not affected: an autopsy study. Acta Neuropathol. https://doi.org/10.1007/s00401-018-1857-4
16. Gulani V, Calamante F, Shellock FG, Kanal E, Reeder SB (2017) Gadolinium deposition in the brain: summary of evidence and recommendations. Lancet Neurol 16:564–570
17. Rehnitz C, Kupfer J, Streich NA et al (2014) Comparison of biochemical cartilage imaging techniques at 3 T MRI. Osteoarthritis Cartilage 22:1732–1742
18. Welsch GH, Trattnig S, Paternostro-Sluga T et al (2011) Parametric T2 and T2* mapping techniques to visualize intervertebral disc degeneration in patients with low back pain: initial results on the clinical use of 3.0 Tesla MRI. Skeletal Radiol 40:543–551
19. Schleich C, Müller-Lutz A, Blum K et al (2016) Facet tropism and facet joint orientation: risk factors for the development of early biochemical alterations of lumbar intervertebral discs. Osteoarthritis Cartilage 24:1761–1768

20. Hesper T, Hosalkar HS, Bittersohl D et al (2014) T2* mapping for articular cartilage assessment: principles, current applications, and future prospects. Skeletal Radiol 43:1429–1445
21. Hesper T, Neugroda C, Schleich C et al (2017) T2*-mapping of acetabular cartilage in patients with femoroacetabular impingement at 3 Tesla: comparative analysis with arthroscopic findings. Cartilage. https://doi.org/10.1177/1947603517741168:1947603517741168
22. Holstein A, Zilkens C, Bittersohl B et al (2011) Delayed gadolinium-enhanced MRI of cartilage (dGEMRIC) and morphologic MRI of cartilage in the long-term follow-up after Legg-Calve-Perthes disease (LCPD). J Med Imaging Radiat Oncol 55:259–265
23. Bittersohl B, Miese FR, Hosalkar HS et al (2012) T2* mapping of hip joint cartilage in various histological grades of degeneration. Osteoarthritis Cartilage 20:653–660
24. Ehrlich GE (2003) Osteoarthritis beginning with inflammation. Definitions and correlations. Bull World Health Organ 81:691–693
25. Ochman S, Wieskötter B, Langer M, Vieth V, Raschke MJ, Stehling C (2017) High-resolution MRI (3T-MRI) in diagnosis of wrist pain: is diagnostic arthroscopy still necessary? Arch Orthop Trauma Surg 137:1443–1450
26. Chang AL, Yu HJ, von Borstel D et al (2017) Advanced imaging techniques of the wrist. AJR Am J Roentgenol 209:497–510
27. Hara T, Horii E, An KN, Cooney WP, Linscheid RL, Chao EY (1992) Force distribution across wrist joint: application of pressure-sensitive conductive rubber. J Hand Surg Am 17:339–347
28. Medved F, Gonser P, Lotter O, Albrecht D, Amr A, Schaller HE (2013) Severe posttraumatic radiocarpal cartilage damage: first report of autologous chondrocyte implantation. Arch Orthop Trauma Surg 133:1469–1475
29. Bittersohl B, Hosalkar HS, Hughes T et al (2009) Feasibility of T2* mapping for the evaluation of hip joint cartilage at 1.5T using a three-dimensional (3D), gradient-echo (GRE) sequence: a prospective study. Magn Reson Med 62:896–901

# Tryptophan metabolism in rheumatoid arthritis is associated with rheumatoid factor and predicts joint pathology evaluated by rheumatoid arthritis MRI Score (RAMRIS)

G. Pongratz[1], T. Lowin[1], P. Sewerin[1], F. Zaucke[2], Z. Jenei-Lanzl[2], T. Pauly[3], B. Ostendorf[1], M. Schneider[1]

*[1]Department of Rheumatology and Hiller Research Center for Rheumatology, University Hospital Düsseldorf, Germany; [2]Experimental Orthopaedics, Dept. of Orthopedics Surgery Friedrichsheim, University Hospital Frankfurt, Frankfurt, Germany; [3]Department of Orthopaedics, River Rhein Center for Rheumatology at St. Elisabeth Hospital, Meerbusch-Lank, Germany.*

## Abstract

### Objective

*Tryptophan and its metabolites have been suggested to play a role in inflammatory processes. However, studies in rheumatoid arthritis (RA) are scarce, which prompted us to investigate two cohorts of RA patients to better understand the importance of tryptophan metabolism in this disease.*

### Methods

*Tryptophan and its metabolites were characterised by ELISA in a cross-sectional cohort 1 (81 RA, 55 OA) and a longitudinal cohort 2 (25 RA, 3 visits over 6 months) to investigate discriminatory power between diseases and predicitive value for radiologic outcome, respectively. Radiologic outcome was monitored by RA MRI Score (RAMRIS), including grading of synovitis, bone oedema and erosion, as well as delayed gadolinium-enhanced MRI of cartilage (dGEMRIC) index assessing cartilage quality of the MCP II joint.*

### Results

*RA patients showed higher levels of serum serotonin (RA: 206.8 ng/ml ± 156.7; OA: 81.2 ng/ml ± 63.6) and estimated indoleamine (2,3)-dioxygenase (IDO) activity (kynurenine / tryptophan ratio; RA: 0.065±0.067; OA: 0.021±0.010). IDO activity showed similar, or better discriminatory power between RA and OA (AUC 0.914) than anti-CCP antibody level (AUC 0.922) and rheumatoid factor (RF, AUC 0.783), respectively. In cohort 2, regression analysis revealed a predictive value of baseline serotonin levels and IDO activity for changes in RAMRIS score and erosions at month six, respectively.*

### Conclusion

*This study supports the hypothesis that tryptophan and its metabolites can be used as biomarkers predicting radiologic outcome and discriminate between RA and OA patients. Overall, our results strengthen the notion that tryptophan metabolism is closely linked to RA disease mechanisms.*

**Key words**

serotonin, IDO, kynurenine, tryptophan, rheumatoid arthritis, prognostic marker, rheumatoid factor, anit-CCP, MRI, RAMRIS, dGEMRIC

*Georg Pongratz,*
*Torsten Lowin,*
*Philipp Sewerin,*
*Frank Zaucke,*
*Zsuzsa Jenei-Lanzl,*
*Thomas Pauly,*
*Benedikt Ostendorf,*
*Matthias Schneider*

*Please address correspondence to:*
*Prof. Georg Pongratz,*
*Poliklinik, Funktionsbereich und Hiller Forschungszentrum für Rheumatologie,*
*UKD, HHUD Life Science Center,*
*Merowingerplatz 1A,*
*40225 Düsseldorf. Germany.*
*E-mail:*
*georg.pongratz@med.uni-duesseldorf.de*

*Received on March 9, 2018; accepted in revised form on July 23, 2018.*



*The datasets analysed during the current study are available from the corresponding author on reasonable request.*

*Funding: this work was supported by an unlimited grant by the Hiller Foundation and by a grant from the German "Bundesministerium für Bildung und Forschung" (BMBF, ArthroMark (01EC1009))*

*Competing interests: the authors received ELISA kits to determine tryptophan and its metabolites as a gift from Neuroimmun GmbH, Karlsruhe. However, the company had no influence over the data analysis and interpretation.*

## Introduction

Rheumatoid arthritis (RA) is a chronic inflammatory disease which is characterised by autoantibody production, joint destruction and disability (1). Healthy synovial tissue is comprised of synovial fibroblasts (SF) and macrophages, whereas lymphocytes migrate to the joint in the course of RA. Pro-inflammatory cytokines transform SF into a "tumor-like" phenotype with the capacity to degrade cartilage and bone (1, 2). One major goal in caring for patients with RA is to prevent joint destruction by immunosuppressive therapy (1). Easy to determine markers that allow predicting risk for joint destruction are useful for the management of RA patients since use of more stringent immunosuppressive regimens, *e.g.* biologics could be guided by such biomarkers. Sensitive imaging modalities, like magnetic resonance imaging (MRI), support evaluation of outcome and prognostication of disease course (3). Modern techniques even allow non-invasive fine assessment of finger joint cartilage degeneration in RA using Delayed Gd(DTPA)2-enhanced MRI of cartilage (dGEMRIC) (4, 5).

Already twenty years ago, it was reported that synovial fluid of RA patients shows highest indoleamine (2,3)-dioxygenase (IDO) activity and lowest tryptophan (TRP) as compared to gout, psoriatric arthritis (PsA), or osteoarthritis (OA) (6). IDO, which metabolises tryptophan to kynurenine, was clearly increased in lining layer of inflamed RA synovial tissue (7). In serum of treatment naïve RA patients TRP levels were decreased and kynurenine (KYN) was increased suggesting an increased activity of IDO (8). These changes are persistent even after treatment (8, 9) and associated with disease stage (10) consistent with a role of IDO activity in RA pathogenesis. Inhibiting IDO activity results in aggravated collagen-induced arthritis in mice (11). It has even been speculated that one mechanism by which shared epitope contributes to pathogenesis of RA involves inhibition of IDO (12, 13). However, in the K/BxN murine RA model which is more dependent on B cell antibody response, IDO inhibition results in amelioration of disease, possibly by paradoxically inhibiting B cell responses as opposed to innate and T cell responses (14).

TRP is a limiting and essential amino acid, and deprivation of TRP by IDO is one anti-inflammatory mechanism, as observed during pregnancy to achieve tolerance of the fetus (15) or in a fibroblast co-culture system showing Th1-inhibiting potential (16). Anti-inflammatory activity of IDO is also suggested by poor prognosis of several tumors which upregulate IDO to escape immune elimination (17). Besides degradation of TRP, anti-inflammation by IDO might be mediated via its product KYN which binds to the aryl hydrocarbon receptor (AHR) stimulating anti-inflammatory pathways (18) but also increasing bone resorption (19). Therefore, rather than suggesting a mere beneficial role for IDO in autoimmunity, IDO is more viewed as context-dependent modifier.

TRP levels are not only decreased by IDO activity, since it also serves as precursor of serotonin (SER) (20), a step initiated by tryptophanhydroxylase (TPH), which generates 5-hydroxytryptophan that gets further metabolised to SER. SER is linked to mood disorders linking IDO pathway to depression and fatigue (21). In models of arthritis, *i.a.* SER results in aggravation of synovial inflammation and a SER antagonist resulted in reduced local inflammation (22). In RA patients, SER serum levels are positively associated with erosions at the temporomandibular joints (23). A direct link between bone loss and SER was established in animal models showing a direct inhibitory function of SER on osteoblast activity (24), findings that correspond with reports showing negative association of bone mass with SER in postmenopausal RA patients (25). SER also has a direct effect on immune cells, which can be anti- or proinflammatory, depending on cell type, context, and receptors involved (26).

As presented above, multiple evidence points towards an involvement of TRP and its metabolites in several aspects of RA. Therefore, we investigated the potential of these metabolites to discrimi-

nate between RA and OA and predictive outcome in RA.

## Materials and methods

*Patient cohorts*

Two cohorts of patients were analysed. Cross-sectional cohort 1 consisted of 55 patients with long-standing RA fulfilling ACR/EULAR revised criteria for RA (27) and 81 patients with long-standing OA who underwent elective joint replacement surgery.

Longitudinal cohort 2 comprised 25 patients with RA again classified according to the ACR/EULAR revised criteria for RA. This cohort was extracted from the arthromark study (28), where RA patients undergo high-field (3 Tesla) MRI (Magnetom Trio A Tim System; Siemens Healthcare, Erlangen, Germany) of the dominant hand, affected by RA at 0, 3, and 6 months using a 4-channel flex coil.

The MRI protocol includes a coronal short tau inversion recovery (STIR)-, T1-weighted turbo spin echo (TSE)-, and T1 weighted 3D fast low angle shot (T1w-3D-FLASH)-sequence for T1 mapping using a dual flip-angle approach. dGEMRIC was acquired with inversion recovery fast spin-echo sequences for 15 minutes. The application of the variable flip angle (VFA) method to dGEMRIC lead to shorter acquisition times and facilitated high resolution assessment of small joints (4, 5, 29). This dGEMRIC cartilage assessment is based on the fact that negatively charged glycosaminoglycan (GAG), a main component of hyaline cartilage, hinders the accumulation of Gd(DTPA)2-. Therefore, the T1-relaxation time of cartilage (dGEMRIC Index, [ms]) is a measure of GAG loss (30).

RAMRIS score was determined according to OMERACT guidelines, in consensus (one radiologist with at least six years' experience in musculoskeletal imaging and one rheumatologist with five years' experience in musculoskeletal imaging, both blinded to all relevant patient data) (31).

Both studies were approved by the Ethics Committee of the University of Düsseldorf (cohort 1: no. 2018-88-KFogU; cohort 2: no. 3828) and in case of cohort 2 also by the ethics committee of the Charité Berlin (EA1/193/10). The studies were conducted in accordance with the principles of the Declaration of Helsinki and the International Conference on Harmonisation Guidance for Good Clinical Practice. All patients were informed about the purpose of the study and gave written consent upfront. Patient characteristics are summarised in Table I.

*ELISA to determine anti-CCP, tryptophan, serotonin and kynurenine in serum*

Serum samples were taken at 0, 3 and 6 months before MRI readings from initially treatment naïve, active patients as described in (28), or at the time of elective surgery in a non-active state, and were stored at -80°C until further processing. L-tryptophan and L-kynurenine were detected by IDKs IDO activity ELISA kit (K7726, Neuroimmun GmbH, Karlsruhe, Germany), serotonin was detected by IDKs serotonin ELISA kit (K6880, Neuroimmun GmbH, Karlsruhe, Germany). Anti-CCP antibodies were detected using a commercially available assay (Anti-CCP hs (high sensitive)®, Orgentec diagnostic, Mainz, Germany). All assays were conducted according to the manufacturer's protocols.

*Statistical analysis*

Statistical analysis was performed with SPSS 24 (IBM, Armonk, USA). The general level of significance was $p<0.05$ and two-sided tests were performed. To minimise statistical error, non-normally distributed variables (Shapiro-Wilk test) were logarithmically transformed before parametric tests as indicated. To analyse discriminatory value of variables, ROC analysis was performed.

**Table I.** Patient characteristics of cross-sectional cohort 1 and longitudinal cohort 2.

| | Cross-sectional cohort 1 | | | | | longitudinal cohort 2 | |
|---|---|---|---|---|---|---|---|
| | OA | range | RA | range | *p*-value (MWU) | RA | range |
| number (n) / visit | 81 | | 55 | | | 25 | |
| female sex (%) | 71.6 | | 80 | | | 66.3 | |
| median age (yr) | 72 | 49 - 88 | 67 | 22 - 85 | 0.03 | 55 | |
| median RF (U/ml) | 5.8 | 0.2 - 25.3 | 29.3 | 1.2 - 567.2 | < 0.001 | | |
| cDMARD | 0 | | 36 | | | | |
| one | 0 | | 31 | | | 25 (MTX) | |
| two | 0 | | 5 | | | | |
| bDMARD | | | 15 | | | | |
| anti TNF | 0 | | 13 | | | | |
| anti IL-6R | 0 | | 2 | | | | |
| Prednisolon (mg/d) | 0 | | 5 | 2.5 - 8.0 | | | |
| median CRP (mg/dl) | | | | | | 0.3 | 0.1 - 3.7 |
| median DAS28 | | | | | | 3.7 | 1.4 - 6.3 |
| median RAMRIS | | | | | | 25 | 9 - 59 |
| median dGEMRIC | | | | | | | |
| median no. of erosions | | | | | | 7 | 0 - 26 |
| median dGEMRIC [ms] | | | | | | 360.1 | 189.5 – 529 |
| serotonin [ng/ml] | | | | | | 206.8 | 17 - 975 |
| tryptophan [µmol/l] | | | | | | 55.5 | 40 – 79.5 |
| kynurenine [µmol/l] | | | | | | 2.2 | 0 – 9.9 |

To investigate the predictive value of baseline measurements for outcomes after six month, linear regression models were fitted.

*Ethics approval and consent to participate*

Both studies were approved by the Ethics Committee of the University of Düsseldorf cohort 1: no. 2018-88-KFogU; cohort 2: no. 3828) and in case of cohort 2 also by the ethics committee of the Charité Berlin (EA1/193/10). The studies were conducted in accordance with the principles of the Declaration of Helsinki and the International Conference on Harmonisation Guidance for Good Clinical Practice. All patients were informed about the purpose of the study and gave written consent upfront

## Results

*RA patients show increased serum tryptophan / kynurenine ratio (estimated IDO activity) as compared to OA patients and association of tryptophan metabolism with rheumatoid factor (RF), but not anti-CCP*

Average SER was increased (Fig. 1A, $p<0.001$) whereas TRP levels were markedly decreased (Fig. 1B, $p<0.001$) in serum of patients with RA as compared to OA. KYN did show the least, but also significant difference, with increased serum levels in RA patients (Fig. 1C; $p=0.001$). As expected, IDO activity, estimated by TRP / KYN ratio, was also increased in RA patients as compared to OA (Fig. 1D).

Further analysis revealed a negative association between rheumatoid factor (RF) and TRP (-0.369, $p=0.006$), as well as a positive association between estimated IDO activity (KYN/TRP; r=0.385, $p=0.004$) and quantitative RF in RA patients Supplementary Table S1). In contrast, levels of KYN (r=-0.439, $p=0.001$) as well as estimated IDO activity (r=-0.276, $p=0.044$) showed negative association with RF in linear correlation analysis for OA patients (Table S1). These results might indicate a context-dependent involvement of IDO pathways in RF production. However, we could not detect any correlation of tryptophan metabolites and anti-CCP antibody levels.

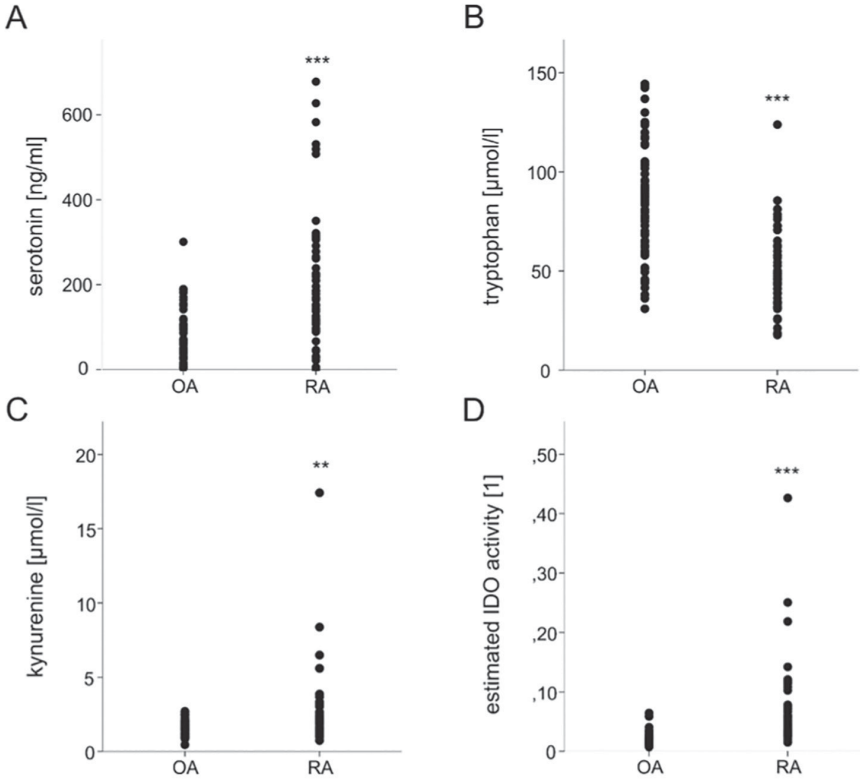


**Fig. 1.** Level of tryptophan and metabolites in serum of rheumatoid arthritis (RA) and osteoarthritis (OA) patients. Serum levels of serotonin (**A**), trypophan (**B**), kynurenine (**C**), and estimated indoleamine (2,3)-dioxygenase (IDO) activity (kynurenine / tryptophan ratio) (**D**), is depicted. Each dot corresponds to one individual patient. *p*-values were calculated by Mann-Whitney-U test. ***$p<0.0001$, **$p<0.001$.

To characterise the value of TRP and its metabolites to distinct between systemic inflammatory conditions, like RA and non-inflammatory OA, we performed ROC analysis. Estimated IDO activity (AUC 0.914, SD 0.860–0.969) showed better test characteristics than RF (AUC 0.783, SD 0.688–0.878) and even similar test characteristics to anti-CCP levels (AUC 0.922, SD 0.860–0.984) in discriminating RA from OA (Fig. 2). A cut-off value of 0.0253 for IDO activity (KYN/TRP ratio) discriminated patients with RA from OA with a specificity of 79.6% and a sensitivity of 96.3%.

In summary, these results confirm differences in RA *versus* OA regarding metabolites of the TRP metabolism with an increase in SER and IDO activity in RA patients, respectively. In contrast to anti-CCP serum levels, which did not show any correlation to tryptophan metabolites, the production of RF is positively associated with estimated IDO activity, whereas a negative association was found in OA patients.

*Association of RA parameters with tryptophan metabolism is modulated by inflammatory status*

Since levels of autoantibodies, like RF, are regarded as prognostic markers and therefore are directly related to joint destruction in RA, we further analysed association and predictive value of TRP metabolites in a second, radiologically well characterised patient cohort. These RA patients were characterised by CRP, DAS28, different radiologic scores and values (RAMRIS, dGEMRIC index) and number of radiologically detected erosions (Table I). We first performed simple correlation analysis to determine, if linear relationships exist between TRP metabolism and determined RA parameters.

Correlation analysis revealed that KYN (r=0.224, $p=0.046$), number of erosions (r=0.405, $p<0.001$), and RAMRIS (r=0.485, $p<0.001$) was associated with age and KYN (r=0.262, $p=0.020$) was also associated with sex. After controlling for age and sex by partial correlation analysis, no linear association of

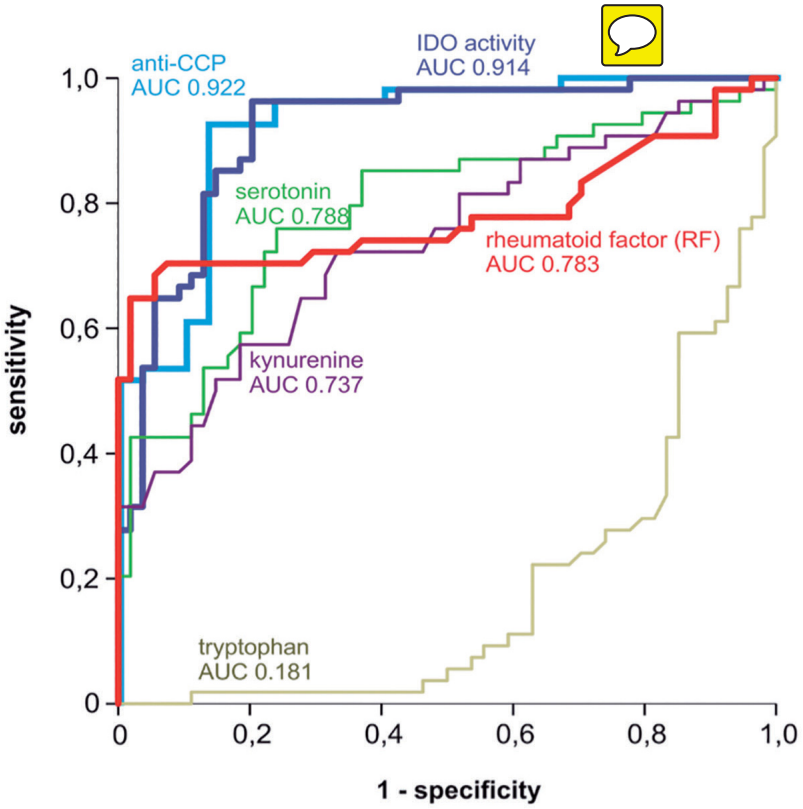


**Fig. 2.** Receiver Operator Characteristic (ROC) of tryptophan and metabolites to destinct between rheumatoid arthritis (RA) and osteoarthritis (OA). ROC of serotonin (green line), kynurenine (brown line), tryptophan (light brown line), estimated indoleamine (2,3)-dioxygenase (IDO) activity (thick blue line) are compared to rheumatoid factor (RF, thick red line) and anti-CCP antibody levels (anti-CCP, thick light blue line), respectively. Area under the curve (AUC) as a measure of the characteristic are given for each metabolite.

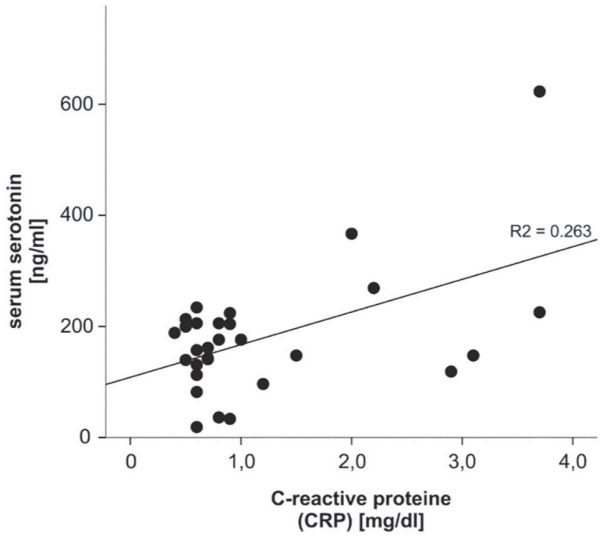


**Fig. 3.** Linear correlation of serum serotonin and c-reactive protein (CRP) in patients with increased CRP values. A dot plot of serum serotonin levels and CRP values is depicted. Every dot represents one patient. The straight line represents the linear regression of the data (r2 = 0.263).

CRP with TRP or its metabolites was evident. However, only analysing patients with increased CRP (>0.3 mg/dl) values revealed a highly significant association with serum SER levels in partial correlation analysis (r=0.527, $p$=0.006, Fig. 3), whereas RA patients with normal CRP values (<0.3 mg/dl) did not show any association with CRP (r=-0.065, $p$=0.7). This points to an association that is only evident under inflammatory conditions. For KYN and TRP such dependency on inflammation state was not deducible (data not shown).

DAS28 did show a weak linear relationship with KYN (r=0.237, $p$=0.055) and estimated IDO activity (r=0.218, $p$=0.079) in partial correlation controlled for age, sex and CRP. Relationship to radiological outcomes and parameters such as RAMRIS, dGEMRIC index, or the number of erosions could not be demonstrated in this first analysis (data not shown).

*Predictive value of tryptophan metabolism for radiologic outcome in RA*

In clinical practice, the most important question would be to determine outcome from one baseline measurement of TRP metabolites. Therefore, we investigated a possible predictive value for TRP metabolites measured at baseline regarding changes in RA outcomes at month 6 by linear regression modelling (Table S1). By backwards exclusion of predictors, serum SER level measured at baseline (standardised beta: 0.529, $p$=0.014) was shown to be the best sole predictor of percent change in RAMRIS at month six of follow-up. Controlling for age and sex weakened the role of SER in the model (standardised beta: 0.426, $p$=0.056) and the predictive value of this model was modest (corrected r2=0.245, $p$=0.074). However, since analysis above showed that associations were primarily observed in patients with increased CRP and in clinical practice this patient group would experience the highest risk of radiographic progression (32, 33), we analysed this subgroup of patients with in the same model. This markedly improved model characteristics (Table II) and best predictive value for change in RAMRIS at month 6 was calculated for a model including TRP, KYN, and SER (corrected r2=0.529, $p$=0.01) with SER being the sole significant contributor (standardised beta: 0.676, $p$=0.004) even after controlling for sex and age (Table II). On the other hand, serum KYN levels at baseline were the sole significant factor in a model (corrected r2=0.228, $p$=0.048) predicting increase in erosions at month 6 (standardised beta: -0.536, $p$=0.048), which also remained signifi-

**Table II.** Linear regression model predicting change in RAMRIS at month six in RA patients with increased CRP values.

| Model# | model chracteristics | predictor | Std beta | T | *p*-value |
|---|---|---|---|---|---|
| 1 | r=0.800 | constant | | 1.747 | 0.115 |
| | r2=0.64 | serotonin ng/ml | 0.636 | 2.805 | **0.021** |
| | corr. r2=0.44 | tryptophan µmol/l | 0.32 | 1.294 | 0.228 |
| | ANOVA *p*=0.062 | kyneurenine µmol/l | -0.198 | -0.86 | 0.412 |
| | | age | -0.12 | -0.486 | 0.638 |
| | | sex | 0.02 | 0.084 | 0.935 |
| 2 | r=0.800 | constant | | 2.047 | 0.068 |
| | r2=0.64 | serotonin ng/ml | 0.643 | 3.197 | **0.01** |
| | corr. r2=0.496 | tryptophan µmol/l | 0.315 | 1.382 | 0.197 |
| | ANOVA *p*=0.025 | kyneurenine µmol/l | -0.204 | -0.973 | 0.354 |
| | | age | -0.119 | -0.51 | 0.621 |
| 3 | r=0.794 | constant | | 3.159 | 0.009 |
| | r2=0.63 | serotonin ng/ml | 0.676 | 3.684 | **0.004** |
| | corr. r2=0.529 | tryptophan µmol/l | 0.373 | 1.958 | 0.076 |
| | ANOVA *p*=0.01 | kyneurenine µmol/l | -0.239 | -1.254 | 0.236 |
| 4 | r=0.760 | constant | | 2.848 | 0.015 |
| | r2=0.577 | serotonin ng/ml | 0.685 | 3.651 | **0.003** |
| | corr. r2=0.507 | tryptophan µmol/l | 0.308 | 1.641 | 0.127 |
| | ANOVA *p*=0.006 | | | | |
| 5 | r=0.695 | constant | | 9.32 | 0 |
| | r2=0.483 | serotonin ng/ml | 0.695 | 3.482 | **0.004** |
| | corr. r2=0.443 | | | | |
| | ANOVA *p*=0.004 | | | | |

**Table III.** Linear regression model predicting change in erosions at month six in RA patients with increased CRP values.

| Model# | model chracteristics | predictor | Std beta | T | *p*-value |
|---|---|---|---|---|---|
| 1 | r=0.779 | constant | | 2.051 | 0.07 |
| | r2=0.607 | serotonin | 0.476 | 2.052 | 0.07 |
| | corr. r2=0.432 | **IDO activity** | -0.831 | -3.184 | **0.011** |
| | ANOVA *p*=0.056 | age | 0.449 | 1.685 | 0.126 |
| | | sex | -0.186 | -0.801 | 0.444 |
| 2 | r=0.761 | constant | | 1.952 | 0.079 |
| | r2=0.579 | serotonin | 0.412 | 1.926 | 0.083 |
| | corr. r2=0.452 | **IDO activity** | -0.768 | -3.143 | **0.01** |
| | ANOVA *p*=0.029 | age | 0.393 | 1.557 | 0.151 |
| 3 | r=0.690 | constant | | 4.406 | 0.001 |
| | r2=0.477 | serotonin | 0.329 | 1.495 | 0.163 |
| | corr. r2=0.382 | **IDO activity** | -0.566 | -2.573 | **0.026** |
| | ANOVA *p*=0.028 | | | | |
| 4 | r=0.609 | constant | | 5.946 | 0 |
| | r2=0.370 | **IDO activity** | -0.609 | -2.657 | **0.021** |
| | corr. r2=0.318 | | | | |
| | ANOVA *p*=0.021 | | | | |

cant after controlling for age and sex (Table S2). Using estimated IDO activity as a predictor for developing more erosions at month six further improved the model (Table III, standardised beta -0.609, *p*=0.021, corrected r2=0.318, *p*=0.021). A predictive model could not be fit for baseline levels of TRP or its metabolites regarding changes in DAS28 or dGEMRIC index at month 6 (data not shown).

In conclusion, for patients with increased CRP at baseline, a negative association of baseline KYN serum levels with increase in erosions after six month and a positive association of baseline SER serum levels with increases in RAMRIS at month six were detected.

## Discussion

This study contributes to a better understanding of TRP and its metabolites in RA and OA patients. Basically, we found parameters of the TRP metabolism altered in RA as compared to OA, confirming already known differences described in the literature (8, 10, 34). However, to our knowledge, this is the first analysis to show a discriminatory power of IDO activity between OA and RA patients, which was even better, or similar than the established markers RF and anti-CCP, respectively. In addition, we could show that IDO is directly related to serum level of RF, pointing to a possible role of TRP metabolism in autoantibody production. This assumption is supported by reports showing a direct influence of TRP metabolites on B cell function, concluding that IDO2 activity is directly linked to autoantibody production in animal models of arthritis, and therefore proposing IDO2 as therapeutic target (14, 35, 36). Therefore, our report is the first to support such a mechanism in human RA, at least for RF, since we could not show such an association with anti-CCP antibody levels, possibly pointing to a different role of IDO in generation of RF vs. anti-CCP antibodies. However, by creating mice deficient in IDO2, a specific defect in autoantibody production with decreased pathology in model of arthritis was demonstrated (36). Interestingly, this role for IDO2 seemed to be specific for pathologic autoantibody responses and was not observed in physiologic antibody responses (35, 36). In our study, we also provide support for this hypothesis in humans, since in patients suffering from OA, a non-systemic inflammatory arthritis, the production of RF was negatively associated with IDO activity, contrasting the result in RA patients and pointing to a different role of IDO activity depending on inflammatory state.

A similar dual role, depending on inflammatory state, was established for SER, since we observed an association of SER with CRP only in patients with increased CRP values, but not in non-inflamed patients. Therefore, in contrast to KYN and TRP, SER behaved like an acute phase reactant. SER has been shown to act proinflammatory via HT2A receptors in animal models of adjuvant induced arthritis in rats (37), however

its effect on bone metabolism (38) and TNF mediated inflammation of arterial blood vessels (39) might be protective.

The measured total SER level depends more on release from thrombocytes than IDO or TPH activity and thrombocyte numbers are associated with inflammatory activity (40). Furthermore, platelets have been shown to contain less and release more SER under inflammatory conditions, like RA (41).

However, serum SER is a predictor of radiological outcome measured by RAMRIS in RA patients. RAMRIS is a MRI scoring system semiquantitatively assessing severity of synovitis, bone marrow oedema and erosions in hand and wrist joints, and was especially developed for evaluation of inflammatory and destructive changes in RA hands and wrists (31). It has been evaluated in many studies, including treatment-response trials, and a recent meta-analysis confirms validity for assessing extent of inflammatory changes and destruction in RA (42). Furthermore, subscores of the RAMRIS are directly linked to histopathological correlates, *e.g.* findings on MRI are linked to cartilage damage and reflect histological synovitis (29, 43). The predictive value of RAMRIS for RA outcome measured by DAS28 has been recently reported, and it has been suggested that RAMRIS might be a valuable parameter to predict treatment response (28). Therefore, prediction of RAMRIS by SER reflects the importance of SER as marker of inflammation, specifically for RA. In light of these findings it is not surprising that inhibitors of SER receptors were already successfully used systemically and intra-articularly in patients with RA (44).

It is unclear why cartilage integrity, measured by dGEMRIC is not associated with TRP or its metabolites in the predictive regression model. We expected that SER shows some association with dGEMRIC, since it reflects inflammation which itself is positively associated with production of metalloproteinases that are main contributors to cartilage degradation (45). However, dGEMRIC does not change considerable over time in our study within six month, although inflammation measured by CRP and DAS28 was decreased in our cohort over time (data not shown). Therefore, it is possible, that study period was too short to reflect changes in dGEMRIC due to changes in inflammation. Supporting this hypothesis is a study showing that during anti-TNF therapy, even a good response to therapy measured by clinical and laboratory parameters, did not halt further knee joint cartilage GAG loss as measured by dGEMRIC (46). Therefore, dGEMRIC seems not to reflect short term changes in inflammation and this might be the reason why it is not associated with serotonin in our study.

Interestingly, erosions itself are better predicted by a negative association with KYN or IDO activity, respectively, than SER serum baseline levels, suggesting that KYN might be particularly involved in bone pathology. Positive association of serum KYN with OCN, a marker of bone resorption, is known (47). It is also known, that TRP metabolism and KYN, respectively, are positively linked to bone mineral density (48). *In vitro* experiments show that inhibiting IDO1, and therefore decreasing KYN, decreases osteoblastogenesis and increases osteoclast activity, leading to osteopenia (19). This could be a direct, mechanistic explanation for the negative association of KYN with erosions and points out the importance of IDO activity in RA bone pathology. SER on the other hand showed no predictive value for erosions in particular. In contrast to IDO activity and KYN, in vitro experiments using murine osteoclast- and osteoblast-differentiation assays clearly demonstrated a protective role for SER via HT2A receptors, acting via increasing osteoprotegerin and decreasing RANKL (38). In addition, protective HT2A receptors are downregulated in RA tissue (49). Therefore, it might well be that increased SER levels in RA patients, despite a possible systemic proinflammatory role, are a countermeasure against bone loss and not a cause of the latter. However, this needs to be determined in future mechanistic studies.

## Conclusion

In summary, our study provides evidence for a role of SER serum level as prognostic marker of radiologic outcome in RA measured by composite RAMRIS, whereas IDO activity and KYN baseline levels predict developing erosions. Therefore, it is not surprising that IDO activity is an even better marker than RF, and equivalent to anti-CCP in discriminating between OA and RA patients. One important aspect is to take the inflammatory state of the patient into consideration while interpreting results concerning TRP metabolites. This might not only be relevant in RA, but also for other inflammatory diseases and could help solving some of the controversies regarding a pro- or anti-inflammatory role of TRP and its metabolites (50).

## Key message

RA and OA patients can be discriminated by IDO activity better than RF, serotonin acts as marker of inflammation in RA and serotonin, as well as IDO activity have prognostic value for radiologic outcome.

## Acknowledgement

We thank Ellen Bleck for her excellent technical support.

## References

1. SMOLEN JS, ALETAHA D, MCINNES IB: Rheumatoid arthritis. *Lancet* 2016; 388: 2023-38.
2. BARTOK B, FIRESTEIN GS: Fibroblast-like synoviocytes: Key effector cells in rheumatoid arthritis. *Immunol Rev* 2010; 233: 233-55.
3. MCQUEEN FM, OSTENDORF B: What is mri bone oedema in rheumatoid arthritis and why does it matter? *Arthritis research & therapy* 2006; 8: 222.
4. MIESE FR, OSTENDORF B, WITTSACK HJ *et al.*: [cartilage quality in finger joints: Delayed gd(DTPA)(2)-enhanced MRI of the cartilage (dGEMRIC) at 3t]. *RoFo* 2010; 182: 873-8.
5. MIESE FR, OSTENDORF B, WITTSACK HJ *et al.*: Metacarpophalangeal joints in rheumatoid arthritis: Delayed gadolinium-enhanced mr imaging of cartilage--a feasibility study. *Radiology* 2010; 257: 441-7.
6. BERTAZZO A, PUNZI L, BERTAZZOLO N *et al.*: Tryptophan catabolism in synovial fluid of various arthropathies and its relationship with inflammatory cytokines. *Adv Exp Med Biol* 1999; 467: 565-70.
7. PARK MK, OH HJ, HEO YM *et al.*: Myeloid differentiation primary response protein 88 blockade upregulates indoleamine 2,3-dioxygenase expression in rheumatoid synovial fibroblasts. *Exp Mol Med* 2011; 43: 446-54.
8. FORREST CM, KENNEDY A, STONE TW, STOY N, DARLINGTON LG: Kynurenine and neopterin levels in patients with rheumatoid

arthritis and osteoporosis during drug treatment. *Adv Exp Med Biol* 2003; 527: 287-95.
9. KURZ K, HEROLD M, WINKLER C, KLOTZ W, RUSSE E, FUCHS D: Effects of adalimumab therapy on disease activity and interferon-gamma-mediated biochemical pathways in patients with rheumatoid arthritis. *Autoimmunity* 2011; 44: 235-42.
10. SCHROECKSNADEL K, WINKLER C, DUFTNER C, WIRLEITNER B, SCHIRMER M, FUCHS D: Tryptophan degradation increases with stage in patients with rheumatoid arthritis. *Clin Rheumatol* 2006; 25: 334-7.
11. SZANTO S, KORENY T, MIKECZ K, GLANT TT, SZEKANECZ Z, VARGA J: Inhibition of indoleamine 2,3-dioxygenase-mediated tryptophan catabolism accelerates collagen-induced arthritis in mice. *Arthritis Res Ther* 2007; 9: R50.
12. DE ALMEIDA DE, LING S, PI X, HARTMANN-SCRUGGS AM, PUMPENS P, HOLOSHITZ J: Immune dysregulation by the rheumatoid arthritis shared epitope. *J Immunol* 2010; 185: 1927-34.
13. HOLOSHITZ J, DE ALMEIDA DE, LING S: A role for calreticulin in the pathogenesis of rheumatoid arthritis. *Ann N Y Acad Sci* 2010; 1209: 91-8.
14. SCOTT GN, DUHADAWAY J, PIGOTT E *et al*.: The immunoregulatory enzyme ido paradoxically drives b cell-mediated autoimmunity. *J Immunol* 2009; 182: 7509-17.
15. BADAWY AA, NAMBOODIRI AM, MOFFETT JR: The end of the road for the tryptophan depletion concept in pregnancy and infection. *Clin Sci* (Lond) 2016; 130: 1327-33.
16. TYKOCINSKI LO, LAUFFER AM, BOHNEN A *et al*.: Synovial fibroblasts selectively suppress th1 cell responses through ido1-mediated tryptophan catabolism. *J Immunol* 2017; 198: 3109-17.
17. PRENDERGAST GC, CHANG MY, MANDIK-NAYAK L, METZ R, MULLER AJ: Indoleamine 2,3-dioxygenase as a modifier of pathogenic inflammation in cancer and other inflammation-associated diseases. *Curr Med Chem* 2011; 18: 2257-62.
18. OPITZ CA, LITZENBURGER UM, SAHM F *et al*.: An endogenous tumour-promoting ligand of the human aryl hydrocarbon receptor. *Nature* 2011; 478: 197-203.
19. VIDAL C, LI W, SANTNER-NANAN B *et al*.: The kynurenine pathway of tryptophan degradation is activated during osteoblastogenesis. *Stem Cells* 2015; 33: 111-21.
20. SWAMI T, WEBER HC: Updates on the biology of serotonin and tryptophan hydroxylase. *Curr Opin Endocrinol Diabetes Obes* 2018; 25: 12-21.
21. KIM S, MILLER BJ, STEFANEK ME, MILLER AH: Inflammation-induced activation of the indoleamine 2,3-dioxygenase pathway: Relevance to cancer-related fatigue. *Cancer* 2015; 121: 2129-36.
22. FAKHFOURI G, RAHIMIAN R, GHIA JE, KHAN WI, DEHPOUR AR: Impact of 5-ht(3) receptor antagonists on peripheral and central diseases. *Drug Discov Today* 2012; 17: 741-7.
23. VOOG U, ALSTERGREN P, ELIASSON S, LEIBUR E, KALLIKORM R, KOPP S: Progression of radiographic changes in the temporomandibular joints of patients with rheumatoid arthritis in relation to inflammatory markers and mediators in the blood. *Acta Odontol Scand* 2004; 62: 7-13.
24. CHABBI-ACHENGLI Y, COMAN T, COLLET C *et al*.: Serotonin is involved in autoimmune arthritis through th17 immunity and bone resorption. *Am J Pathol* 2016; 186: 927-37.
25. BERNARDES M, VIEIRA T, LUCAS R *et al*.: Serum serotonin levels and bone in rheumatoid arthritis patients. *Rheumatology Int* 2017; 37: 1891-8.
26. HERR N, BODE C, DUERSCHMIED D: The effects of serotonin in immune cells. *Front Cardiovasc Med* 2017; 4: 48.
27. ALETAHA D, NEOGI T, SILMAN AJ *et al*.: 2010 rheumatoid arthritis classification criteria: An american college of rheumatology/european league against rheumatism collaborative initiative. *Arthritis Rheum* 2010; 62: 2569-81.
28. SEWERIN PL, VORDENBÄUMEN S, SCHLEICH C *et al*.: Rheumatoid arthritis magnetic resonance imaging score (RAMRIS) predicts das-28 therapy response in rheumatoid arthritis patients: Results of the German arthromark cohort. *J Rheumatol* 2018.
29. SCHLEICH C, MULLER-LUTZ A, SEWERIN P *et al*.: Intra-individual assessment of inflammatory severity and cartilage composition of finger joints in rheumatoid arthritis. *Skeletal Radiol* 2015; 44: 513-8.
30. BASHIR A, GRAY ML, BOUTIN RD, BURSTEIN D: Glycosaminoglycan in articular cartilage: In vivo assessment with delayed gd(DTPA) (2-)-enhanced MR imaging. *Radiology* 1997; 205: 551-8.
31. OSTERGAARD M, PETERFY C, CONAGHAN P *et al*.: Omeract rheumatoid arthritis magnetic resonance imaging studies. Core set of mri acquisitions, joint pathology definitions, and the omeract RA-MRI scoring system. *J Rheumatol* 2003; 30: 1385-6.
32. MIERAU R, GENTH E: Diagnosis and prognosis of early rheumatoid arthritis, with special emphasis on laboratory analysis. *Clin Chem Lab Med* 2006; 44: 138-43.
33. MARKATSELI TE, VOULGARI PV, ALAMANOS Y, DROSOS AA: Prognostic factors of radiological damage in rheumatoid arthritis: A 10-year retrospective study. *J Rheumatol* 2011; 38: 44-52.
34. CRAWFORD N: Some observations on the blood serotonin levels in rheumatoid arthritis with a study of platelet serotonin absorption. *Clin Chim Acta* 1969; 23: 139-46.
35. MERLO LMF, GRABLER S, DUHADAWAY JB *et al*.: Therapeutic antibody targeting of indoleamine-2,3-dioxygenase (ido2) inhibits autoimmune arthritis. *Clin Immunol* 2017; 179: 8-16.
36. MERLO LMF, PIGOTT E, DUHADAWAY JB *et al*.: Ido2 is a critical mediator of autoantibody production and inflammatory pathogenesis in a mouse model of autoimmune arthritis. *J Immunol* 2014; 192: 2082-90.
37. HARBUZ MS, MARTI O, LIGHTMAN SL, JESSOP DS: Alteration of central serotonin modifies onset and severity of adjuvant-induced arthritis in the rat. *Br J Rheumatol* 1998; 37: 1077-83.
38. GUSTAFSSON BI, THOMMESEN L, STUNES AK *et al*.: Serotonin and fluoxetine modulate bone cell function *in vitro*. *J Cell Biochem* 2006; 98: 139-51.
39. YU B, BECNEL J, ZERFAOUI M, ROHATGI R, BOULARES AH, NICHOLS CD: Serotonin 5-hydroxytryptamine(2a) receptor activation suppresses tumor necrosis factor-alpha-induced inflammation with extraordinary potency. *J Pharmacol Exp Ther* 2008; 327: 316-23.
40. SMITH AF, CASTOR CW: Connective tissue activation. Xii. Platelet abnormalities in patients with rheumatoid arthritis. *J Rheumatol* 1978; 5: 177-83.
41. ZELLER J, WEISSBARTH E, BARUTH B, MIELKE H, DEICHER H: Serotonin content of platelets in inflammatory rheumatic diseases. Correlation with clinical activity. *Arthritis Rheum* 1983; 26: 532-40.
42. WOODWORTH TG, MORGACHEVA O, PIMIENTA OL, TROUM OM, RANGANATH VK, FURST DE: Examining the validity of the rheumatoid arthritis magnetic resonance imaging score according to the omeract filter-a systematic literature review. *Rheumatology* (Oxford) 2017; 56: 1177-88.
43. VORDENBAUMEN S, SCHLEICH C, LOGTERS T *et al*.: Dynamic contrast-enhanced magnetic resonance imaging of metacarpophalangeal joints reflects histological signs of synovitis in rheumatoid arthritis. *Arthritis Res Ther* 2014; 16: 452.
44. SAMBORSKI W, STRATZ T, MACKIEWICZ S, MULLER W: Intra-articular treatment of arthritides and activated osteoarthritis with the 5-ht3 receptor antagonist tropisetron. A double-blind study compared with methylprednisolone. *Scand J Rheumatol Suppl* 2004; 119: 51-4.
45. GOLDRING MB, OTERO M, TSUCHIMOCHI K, IJIRI K, LI Y: Defining the roles of inflammatory and anabolic cytokines in cartilage metabolism. *Ann Rheum Dis* 2008; 67 (Suppl. 3): iii75-82.
46. TIDERIUS CJ, SANDIN J, SVENSSON J, DAHLBERG LE, JACOBSSON L: Knee cartilage quality assessed with dGEMRIC in rheumatoid arthritis patients before and after treatment with a TNF inhibitor. *Acta Radiol* 2010; 51: 1034-7.
47. ENTENMANN L, PIETZNER M, ARTATI A *et al*.: Comprehensive metabolic characterization of serum osteocalcin action in a large non-diabetic sample. *PloS one* 2017; 12: e0184721.
48. APALSET EM, GJESDAL CG, UELAND PM *et al*.: Interferon (ifn)-gamma-mediated inflammation and the kynurenine pathway in relation to bone mineral density: The hordaland health study. *Clin Exp Immunol* 2014; 176: 452-60.
49. KLING A, RANTAPAA-DAHLQVIST S, STENLUND H, MJORNDAL T: Decreased density of serotonin 5-ht2a receptors in rheumatoid arthritis. *Ann Rheum Dis* 2006; 65: 816-9.
50. FILIPPINI P, DEL PAPA N, SAMBATARO D, DEL BUFALO A, LOCATELLI F, RUTELLA S: Emerging concepts on inhibitors of indoleamine 2,3-dioxygenase in rheumatic diseases. *Curr Med Chem* 2012; 19: 5381-93.

Frenken et al. Arthritis Research & Therapy (2019) 21:21
https://doi.org/10.1186/s13075-018-1789-3

Arthritis Research & Therapy

RESEARCH ARTICLE Open Access

# The value of the simplified RAMRIS-5 in early RA patients under methotrexate therapy using high-field MRI

Miriam Frenken[1†], Christoph Schleich[1†], Ralph Brinks[2], Daniel Benjamin Abrar[1], Christine Goertz[2], Matthias Schneider[2], Benedikt Ostendorf[2] and Philipp Sewerin[2*]

## Abstract

**Background:** The aim of the study was to evaluate a simplified version of the Rheumatoid Arthritis Magnetic Resonance Imaging Score (RAMRIS) for five joints of the hand (RAMRIS-5) in patients with early rheumatoid arthritis (RA) before and after the initiation of methotrexate (MTX) therapy using high-resolution, 3-T magnetic resonance imaging (MRI).

**Methods:** Twenty-eight patients with a seropositive, early RA (disease duration of less than 6 months (range 2–23 weeks)) according to 2010 American College of Rheumatology/European League Against Rheumatism (ACR/EULAR) criteria (mean age 56.8 years, range 39–74) were prospectively assessed with a baseline investigation including clinical assessment (disease activity score of 28 joints (DAS-28) and C-reactive protein (CRP)) and 3-T MRI of the clinically dominant hand. Follow-up visits were performed 3 and 6 months after initiation of a MTX therapy at baseline. MRI scans were analyzed in accordance with RAMRIS and the simplified RAMRIS-5.

**Results:** DAS-28 and CRP decreased significantly after initiation of MTX therapy. Even though erosion scores increased over time, RAMRIS and RAMRIS-5 also decreased significantly after the start of therapy. There was a strong correlation between the total RAMRIS-5 and RAMRIS at baseline ($r = 0.838$; $P < 0.001$) and follow-up (3 months: $r = 0.876$; $P < 0.001$; 6 months: $r = 0.897$; $P < 0.001$). In the short term (3-month follow-up), RAMRIS and RAMRIS-5 demonstrated similar ability to detect changes for all subgroups (bone edema, erosion, and synovitis). In the long-term comparison (6-month follow-up), RAMRIS-5 also showed similar effectiveness when detecting changes in bone edema and erosion compared with RAMRIS. Deviations occurred regarding only synovitis, where change was slightly higher in RAMRIS-5: SRM (RAMRIS) = 0.07 ± 0.14; SRM (RAMRIS-5) = 0.34 ± 0.06.

**Conclusions:** Three-Tesla MRI-based RAMRIS-5 is a simplified and resource-saving RAMRIS score which compares favorably with the RAMRIS when detecting changes in early RA. Even though there is a slight abbreviation between RAMRIS-5 and the original score regarding the change of synovitis, it may be used for diagnosis and therapy monitoring in follow-up evaluations.

**Keywords:** High-field magnetic resonance imaging, Early rheumatoid arthritis, Prediction, RAMRIS-5, RAMRIS

* Correspondence: philipp.sewerin@med.uni-duesseldorf.de
†Miriam Frenken and Christoph Schleich contributed equally to this work.
[2]Department and Hiller Research Unit for Rheumatology, UKD, Heinrich-Heine University Düsseldorf, Moorenstrasse 5, 40225 Düsseldorf, Germany
Full list of author information is available at the end of the article

## Background

Rheumatoid arthritis (RA) is the most common inflammatory joint disease. Early diagnosis and treatment significantly improve the long-term outcome [1, 2]. Delayed treatment leads to chronic synovitis, joint destruction, pain, loss of function, and reduced quality of life [1–3]. Many studies have shown that early and rigorous treatment significantly reduces the impact of chronic inflammation and prevents radiological progression in a large proportion of patients [3, 4]. In the early stage of the disease, there is a "window of opportunity", which starts to close between the third and fourth month after symptom onset where patients have more benefits from active treatment with conventional synthetic disease-modifying anti-rheumatic drugs (csDMARDs) than in the later course of the disease. This is because irreversible joint destruction occurs more often in the later stages of the disease [5]. Therefore, the current treat-to-target approach demands therapy with csDMARDs at an interval no more than 3 months after symptom onset. Thus, early diagnosis is crucial to allow early treatment and prevent irreversible joint destruction [6]. In early stages, RA often shows non-typical and only temporary symptoms. The revised American College of Rheumatology/European League Against Rheumatism (ACR/EULAR) Classification Criteria were established to define early RA [7]. The ACR/EULAR Classification Criteria include acute-phase reactants, serology, joint distribution, and symptom duration [8]. Erosive joint destruction, detected in conventional radiography in a typical location, is proof enough to diagnose RA. However, it is not a sign of early RA. Even during a very aggressive progression of the disease, erosive joint destruction can be identified by using conventional radiography 6–24 months at the earliest following the onset of symptoms [9, 10]. Therefore, in addition to clinical examination and serological biomarkers, imaging tools—such as ultrasound or magnetic resonance imaging (MRI)—play an important role in the detection of early RA. MRI can show changes associated with early RA that are predictive for the development of bone destruction in the course of the disease, such as soft tissue inflammation and bone edema [11, 12]. As Schleich et al. [13] have already shown, RAMRIS-5 is applicable in low-field MRI scanners. Image generation speed, spatial resolution, and contrast improve with increasing field strength. This is most noticeable between low-field (≤0.3 T) and high-field (≥1.5 T) imaging [14]. In order to detect changes associated with early RA (for example, small erosions), there is a need for a high spatial resolution and thus a high field strength. As spatial resolution increases with magnetic flux density [15–17], it can be assumed that small changes in the 3-T MRI can be detected even better than in the 1.5-T MRI. Wieners et al. [17] showed the superiority of 3-T compared with 1.5-T image quality of RA hands, regarding the extent of bone edema, synovitis, small bone erosions, and the inter-reader reliability, even though image quality at 1.5 T was also acceptable.

With the RAMRIS, the Outcome Measures in RA Clinical Trials (OMERACT) group established a highly reliable, standardized, semi-quantitative instrument to evaluate therapy outcome [13, 18, 19]. This is a sum score based on the presence of synovitis, bone marrow edema, and erosions at 23 joint sites of the dominant hand and wrist (metacarpophalangeal [MCP], intercarpal, carpo-metacarpophalangeal, radiocarpal, and radioulnar) [19]. The assessment of RAMRIS is time- and resource-consuming. A streamlined MRI score, RAMRIS-5, focusing on only five joints of the hand and wrist, has been evaluated and proven to have a strong correlation in patients with established RA at low-field MRI [13]. However, it has not yet been evaluated for patients with early RA at high-field 3-T MRI. Therefore, the aim of the study is to establish RAMRIS-5 in early RA patients at baseline and under therapy at high-field MRI within the scope of the German ArthroMark cohort, which aims to identify new therapy strategies and modern imaging for diagnosis and therapy control in early RA.

## Methods

### Patients

Twenty-eight patients with early RA (mean age: 56.8 years; minimum 39 years, maximum 74 years); rheumatoid factor (RF) or anti-cyclic citrullinated peptide (anti-CCP) antibody–positive or both; disease duration of less than 6 months, mean duration: 16.3 weeks (minimum 2 weeks, maximum 23 weeks) fulfilling the 2010 ACR/EULAR criteria for RA [8] from the German ArthroMark initiative cohort were prospectively recruited from multiple centers but MRI scans were performed in Düsseldorf only. The ArthroMark consortium—Berlin (Charité, Deutsches Rheumaforschungszentrum), Frankfurt, Munich, and Düsseldorf, Germany—was funded by the Federal Ministry of Education and Research (Bundesministerium für Bildung und Forschung [BMBF], 01EC1009).

Ethics approval was given by the ethics committee of the Heinrich-Heine University of Düsseldorf (reference number 3483) and the Charité Berlin (EA1/193/10). Written informed consent was obtained from all patients before enrollment.

All patients were treated with the recommended csDMARD, methotrexate (MTX). Supplementary application of prednisone was allowed up to 10 mg per day. No patient received a dose increase. There was no change to other treatments. With high-field MRI (3 T), imaging of the clinical dominant hand was performed at baseline ($t$ = 0) before starting MTX therapy and at follow-up under MTX therapy, about 3 months ($t$ = 1)

and 6 months ($t$ = 2) after the baseline scan. At all three examination days, the disease activity score of 28 joints (DAS-28) and C-reactive protein (CRP) were recorded.

### Magnetic resonance imaging

A 3-T MRI scanner (Magnetom Trio A Tim System; Siemens Healthcare, Erlangen, Germany) with a four-channel flex coil was used for all imaging. The image protocol contained the following sequences of the clinical dominant hand: coronal short tau inversion recovery (STIR) and T1-weighted turbo spin echo (TSE). After intravenous injection of the contrast agent (0.4 mL/kg body weight of Gd-DTPA; Magnevist®), a coronal TSE and a transversal SE sequence with fat suppression were applied. The field of view covered MCP II–V, carpometacarpal, carpal, radiocarpal, and distal radioulnar joints. Sequence parameters are listed in Table 1.

### Image analyses

MRI images were read in consensus by two physicians with special expertise in musculoskeletal imaging (one radiologist and one rheumatologist). MRI scans were evaluated for synovitis in the MCP joints II–V and in the wrist joints (distal radioulnar joint, radiocarpal joint, and intercarpal-carpometacarpal joints) in accordance with the EULAR/OMERACT rheumatoid arthritis MRI scoring system (RAMRIS). Additionally, bone edema and erosions were detected in MCP joint bones II–V as well as all wrist joint bones (distal radius, distal ulna, scaphoid, lunate, triquetrum, pisiform, trapezium, trapezoid, capitate, hamate, and the proximal metacarpal bones I–V) [11]. By summarizing the subscores for synovitis, bone edema, and erosions, the semi-quantitative RAMRIS score for the clinical dominant hand was calculated. RAMRIS-5, the modified, shorter version of RAMRIS, is reduced to commonly affected bones and joints in RA [13]. In order to calculate the RAMRIS-5 score, bone edema (Fig. 1) and erosion (Fig. 2) were evaluated in the following five joint sites: MCP II and III, capitate bone, triquetral bone, and distal ulna (Fig. 3). In addition, synovitis was scored in the MCP II and III joint (Fig. 4) and in the wrist. To keep it simple, there is only one synovitis wrist score that covers all intercarpal and radiocarpal joints. This simplified score corresponded to the worst synovitis score of the three affected joints.

### Statistical analysis

Standardized response means (SRMs) were calculated for all subgroups (edema, erosion, and synovitis) of RAMRIS and RAMRIS-5 after 3 months (t0 versus t1) and after 6 months (t0 versus t2). The SRM between two points in time is defined as the mean change between the two points over the standard deviation of the change between these points in time. Baseline and follow-up analyses for the total score (sum of the subscores of edema, erosion, and synovitis) were calculated in accordance with Spearman's rank correlation coefficient. Change over time was assessed by a paired $t$ test where appropriate. Results with a $P$ value of less than 0.05 were considered significant. Inter-reader agreement was calculated by using Pearson's intraclass correlation coefficient (ICC) analysis (absolute agreement). One radiologist tested the time which was used for both scoring methods.

## Results

RAMRIS-5 and RAMRIS time-comparative analysis demonstrated significantly lower time consumption for RAMRIS-5 compared with RAMRIS at baseline (42.4 ± 8.00 s versus 277.3 ± 21.3 s; $P$ <0.05), at the 3-month follow-up (38.4 ± 8.70 s versus 270.6 ± 19.7 s; $P$ <0.05), and at the 6-month follow-up (35.7 ± 5.70 s versus 267.2 ± 17.2 s; $P$ <0.05).

RAMRIS and RAMRIS-5 were evaluated for all three subscores—bone edema, erosion, and synovitis—and for the total sum score. RAMRIS and RAMRIS-5 as a total score showed mean values at baseline (RAMRIS: 29.29; RAMRIS-5: 13.29). There was a reduction under MTX therapy already at 3-month follow-up (T0-T1 mean of differences: RAMRIS: 2.08, 95% confidence interval (CI) 0.19 to 3.98, $P$ = 0.03 (paired $t$ test); RAMRIS-5: 0.54, 95% CI −0.5 to 1.58, $P$ = 0.29) and an increase within the 6 months of follow-up (T1-T2 RAMRIS: −2.14, 95% CI −3.61 to −0.86, $P$ = 0.006, RAMRIS-5: 0.95, 95% CI −1.80 to −0.11, $P$ = 0.029). The mean values for bone edema in RAMRIS and RAMRIS-5 fell continuously

**Table 1** Sequence details

| Sequence/Parameter | STIR without contrast agent | T1w-TSE without contrast agent | TSE with contrast agent | SE with contrast agent |
|---|---|---|---|---|
| Orientation | Coronal | Coronal | Coronal | Transversal |
| TE/TR, ms/ms | 31/5560 | 25/860 | 25/120 | 12/765 |
| Flip angle, ° | 120 | 150 | 150 | 90 and 120 |
| Slice thickness, mm | 2.5 | 2.5 | 2.5 | 2.5 |
| Field of view, mm × mm | 120 × 120 | 120 × 120 | 120 × 120 | 120 × 60 |
| Number of acquired slices | 17 | 17 | 17 | 17 |

Abbreviations: *SE* spin echo, *STIR* short tau inversion recovery, *T1w-TSE* T1-weighted turbo spin echo, *TE/TR* echo time/repetition time, *TSE* turbo spin echo

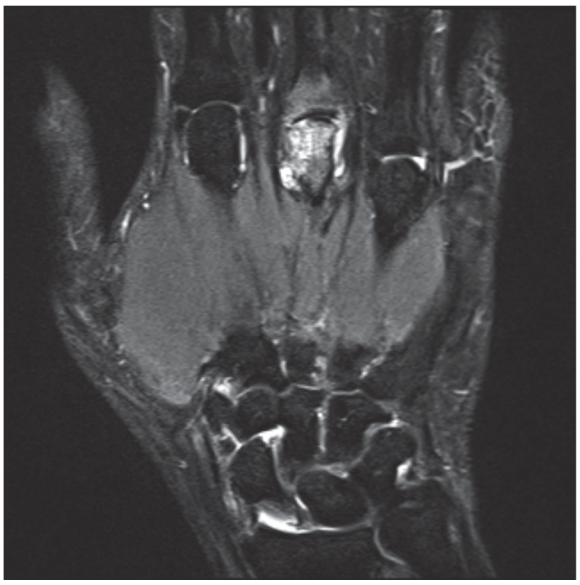

**Fig. 1** Example of a patient's hand with bone marrow edema in the metacarpophalangeal D3 joint (coronal short tau inversion recovery without contrast agent)

over time (baseline: 4.64; 1.64, 3-month follow-up: 3.21; 1.13, 6-month follow-up: 2.43; 1.04). The number of erosions increased in RAMRIS and RAMRIS-5 after 3 months and showed a further slight increase in RAMRIS-5 after 6 months (baseline: 7.96; 4.18, 3-month follow-up: 9.13; 4.92, 6-month follow-up: 9.04; 5.09). Synovitis showed a decrease after 3 months and a rise after 6 months that was below the baseline in RAMRIS and RAMRIS-5 (baseline: 16.68; 7.46, 3-month follow-up: 14.88; 6.71, 6-month follow-up: 16.26; 7.09). ICC analysis revealed a high inter-observer agreement for RAMRIS (ICC = 0.99; $P$ <0.0001) and RAMRIS-5 (ICC = 0.97; $P$ <0.0001).

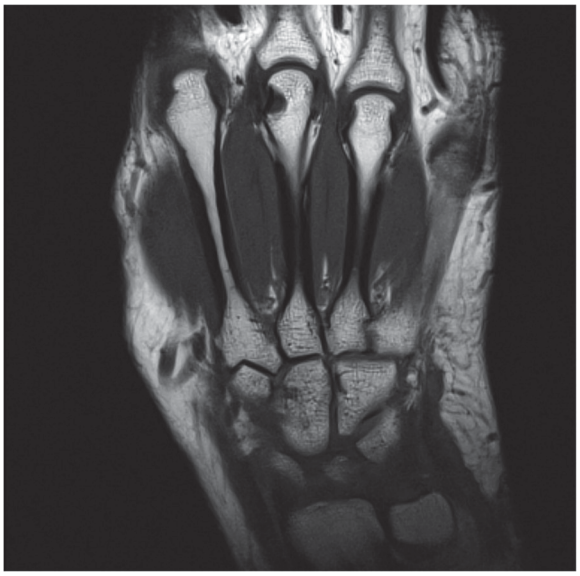

**Fig. 2** Example of a patient's hand with erosion in the metacarpophalangeal III joint (coronal T1-weighted turbo spin echo)

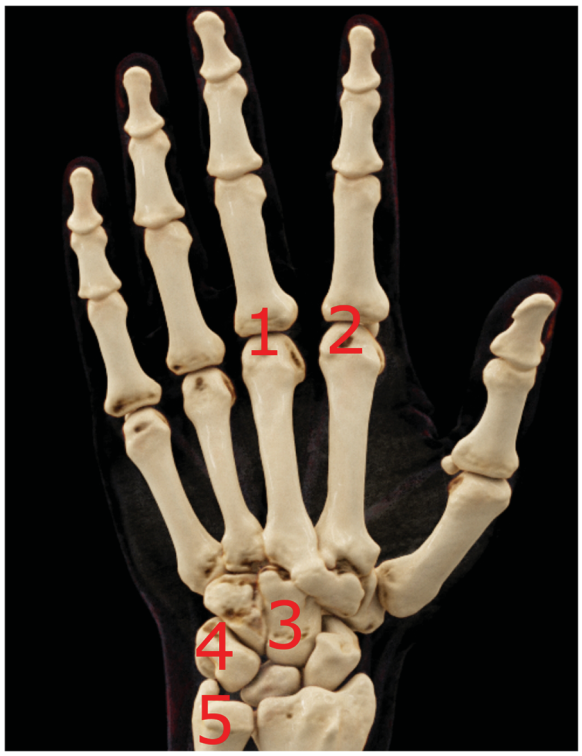


**Fig. 3** Schematic view of the five joint sites, where bone edema and erosion are evaluated for RAMRIS-5: metacarpophalangeal (MCP) III (1) and II (2) joints, capitate bone (3), triquetral bone (4), and distal ulna (5). In addition, synovitis is scored in the MCP II and III joints as well as in the wrist. Abbreviation: *RAMRIS-5* Rheumatoid Arthritis Magnetic Resonance Imaging Score for five joints of the hand

The RAMRIS-5 total score showed a high correlation with RAMRIS at all times, at baseline and under MTX therapy (baseline: $r$ = 0.838; $P$ <0.001, 3-month follow-up: $r$ = 0.876; $P$ <0.001, 6-month follow-up: $r$ = 0.897; $P$ <0.001).

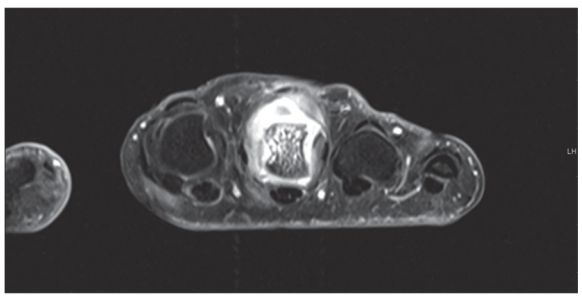

**Fig. 4** Example of a patient's hand with synovitis metacarpophalangeal III, bone marrow edema, and erosions (transversal spin echo sequence with fat suppression)

In the short term (3-month follow-up), RAMRIS and RAMRIS-5 showed a similar ability for detecting changes with overlapping standard deviations for all subgroups (bone edema, erosion, and synovitis). In the long-term comparison (6-month follow-up), the RAMRIS-5 also showed similar capabilities to detect changes regarding bone edema and erosion compared with RAMRIS. Deviations occurred only regarding synovitis, where the change is slightly higher in RAMRIS-5 (standardized response mean SRM(R) = 0.07 ± 0.14; SRM(R5) = 0.34 ± 0.06) (Table 2, Fig. 5).

CRP levels were highest at the initial measurement (9.6 mg/L) and continually decreased in the 3 and 6 months of follow-up under MTX therapy (6.5 mg/L; 3.6 mg/L). In 14 out of 24 patients, CRP levels decreased in the 3-month follow-up after MTX therapy. There were five patients with constant CRP levels and five patients with an increase. In the 6-month follow-up in 16 out of 22 patients, CRP levels decreased. There were five patients with no changes in CRP levels and one with an increase.

Corresponding to CRP levels, the DAS-28 had been highest at the initial measurement (4.69) and continually dropped in the 3 and 6 months of follow-up (3.46; 2.57). In 21 out of 24 patients, DAS-28 improved by the 3-month follow-up. There were three patients with a DAS-28 increase. By the 6-month follow-up, DAS-28 decreased in 22 out of 23 patients. There was one patient with an increase (Table 3).

Furthermore, there was a weak correlation between 6-month RAMRIS follow-up and DAS-28 at the 3-month follow-up ($r$ = 0.533; $P$ = 0.013). We did not find evidence for a correlation between RAMRIS/RAMRIS-5 and DAS-28 or CRP ($t$ = 0: DAS-28/RAMRIS $P$ = 0.657; DAS-28/RAMRIS-5 $P$ = 0.888; CRP/RAMRIS $P$ = 0.267; CRP/RAMRIS-5 $P$ = 0.303; $t$ = 1: DAS-28/RAMRIS $P$ = 0.055; DAS-28/RAMRIS-5 $r$ = 0.434; $P$ = 0.034; CRP/RAMRIS $P$ = 0.127; CRP/RAMRIS-5 $r$ = 0.496; $p$ = 0.14; $t$ = 2: DAS-28/RAMRIS $P$ = 0.629; DAS-28/RAMRIS-5 $P$ = 0.543; CRP/RAMRIS $p$ = 0.731; CRP/RAMRIS-5 $P$ = 0.816).

**Table 2** Comparison of standardized response means for the subgroups erosion, edema, and synovitis for months 3 and 6

| | SRM (3) | SD (3) | SRM (6) | SD (6) |
|---|---|---|---|---|
| Erosion | | | | |
| RAMRIS | −0.15 | 0.25 | −0.15 | 0.11 |
| RAMRIS-5 | −0.12 | 0.17 | −0.14 | 0.17 |
| Edema | | | | |
| RAMRIS | 0.17 | 0.29 | 0.09 | 0.25 |
| RAMRIS-5 | 0.15 | 0.9 | 0.07 | 0.10 |
| Synovialitis | | | | |
| RAMRIS | 0.47 | 0.14 | 0.07 | 0.14 |
| RAMRIS-5 | 0.43 | 0.06 | 0.34 | 0.06 |

*Abbreviations*: *RAMRIS* Rheumatoid Arthritis Magnetic Resonance Imaging Score, *RAMRIS-5* Rheumatoid Arthritis Magnetic Resonance Imaging Score for five joints of the hand, *SD* standard deviation, *SRM* standardized response mean

## Discussion

The OMERACT RAMRIS system is widely accepted as a reference standard in RA trials for diagnosing, staging, and follow-up [20]. Owing to its time commitment, it is barely used in clinical practice [20]. A simplified scoring system, RAMRIS-5, introduced by Schleich et al., turned out to be a time-saving alternative with close correlation to RAMRIS for patients with an established RA in low-field MRI (minimum disease duration of 5 years) [13]. Because it was unclear whether there is also a high correlation between RAMRIS and RAMRIS-5 in patients with early RA, we evaluated the shortened scoring method RAMRIS-5, reduced to only five instead of 23 joint sites, for patients earlier than 6 months after disease onset (early RA).

The selection of RAMRIS-5 joints is based on previous studies and observations of our own research group [18, 21] which demonstrated a frequent involvement of the selected joints. With regard to early RA, Fleming et al. [22] describe lesions at the MCP joints as well as at the wrist, which are partly included in the RAMRIS-5. The RAMRIS-5 therefore seemed to be suitable primarily for the early stage of RA.

Our results show a strong correlation between the total mean RAMRIS and the total mean RAMRIS-5 at baseline as well as under MTX therapy at 3 and 6 months of follow-up. This emphasizes that RAMRIS-5 is an appropriate, time-saving alternative to RAMRIS not only for patients with established RA but also for patients with early RA. It is suitable for detecting disease-typical findings and follow-up evaluation under therapy.

Furthermore, RAMRIS-5 has an equivalent performance level for detecting changes under therapy as RAMRIS does for all subgroups (edema, erosion, and synovitis) after 3 months. Even after 6 months, change is also similar between RAMRIS-5 and the original score for edema and erosion. Deviations between RAMRIS and RAMRIS-5 occurred only in the change of synovitis in the long follow-up (6 months). The change of the RAMRIS-5 synovitis score was higher than that of RAMRIS. In our case, this means a stronger reduction of RAMRIS-5 than of RAMRIS after therapy.

The fact that synovitis is measured in only three instead of five regions, in contrast to the other subgroups, increases the risk of deviating from the results of the original score. In addition, the wrist score for synovitis was deliberately chosen as a region frequently affected by

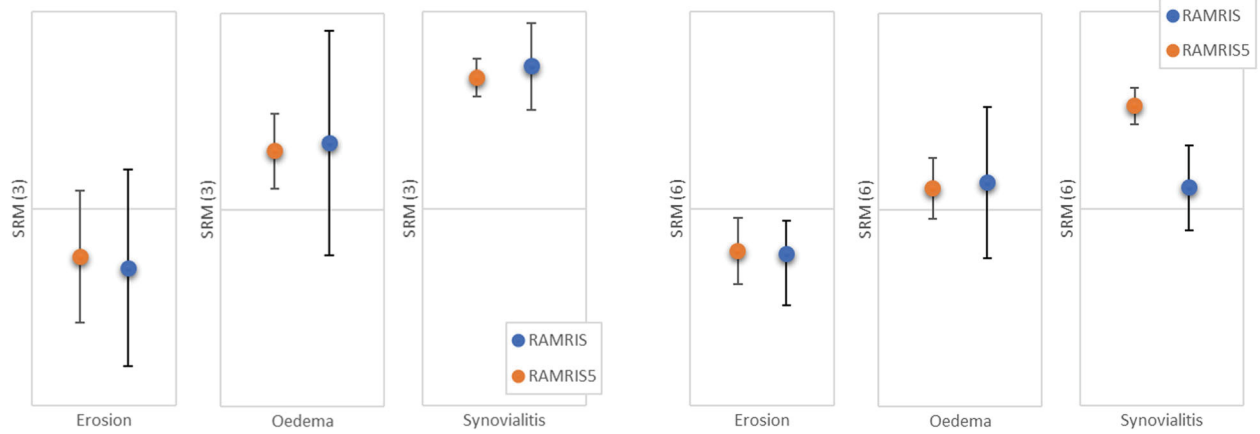


**Fig. 5** Results of the performance of detecting changes measured by the standardized response mean (SRM) for all subgroups of RAMRIS and RAMRIS-5 after 3 and 6 months of follow-up. Abbreviations: *RAMRIS* Rheumatoid Arthritis Magnetic Resonance Imaging Score, *RAMRIS-5* Rheumatoid Arthritis Magnetic Resonance Imaging Score for five joints of the hand

RA. In case of a decrease in synovitis under therapy, this leads to a stronger weighting of the improvement in RAMRIS-5 and a discrete overestimation of the improvement in the course of the disease. One might argue to refine the RAMRIS-5 synovitis score by including another joint area, but because the synovial change is overestimated and not underestimated, the RAMRIS-5 does not miss out on a possible therapy-requiring disease relapse. On the contrary, progress in synovitis could be even better perceived. Furthermore, the change in the "window of opportunity" after about 3 months is similar to that of the original RAMRIS and deviates from it only in the later course (6-month follow-up). Furthermore, since the great advantage of RAMRIS-5 is its brevity and suitability for everyday use, adding more joint sites is not recommended from our point of view for implementing MRI in daily practice. To summarize, we are convinced that the selected joints in RAMRIS-5 are still the right choice for the assessment of early RA disease activity at the beginning and during treatment, even for early RA. We could show the time-saving capabilities of RAMRIS-5, which is a further and very important step to implement an objective MRI scoring method in clinical routines.

Early diagnosis and therapy of RA are of great importance to prevent joint destruction and to reach the stated target of remission or at least low disease activity [5, 6]. Conventional x-rays of the hand and wrist are still the gold standard for diagnosing, staging, and follow-up of patients with RA. However, it is insensitive to early erosion whereas MRI is more sensitive for detecting erosions and other early changes associated to RA like bone edema and synovitis [23, 24]. Therefore, MRI has become a useful tool in the diagnostic process for arthritis, especially for early RA [17]. Regarding MRI image quality, there is a better signal-to-noise ratio and a higher spatial resolution with increasing magnetic flux density in general [15–17]. Additionally, compared with the image quality of low-field MRI (<0.3 T), that of high-field MRI (≥1.5 T) is superior because of a reduced acquisition time that leads to shorter protocols and fewer motion artifacts [15, 25]. Other technically related non-RA-specific studies showed that, compared with the image quality of low-field MRI, that of high-field MRI systems is superior when focusing on small anatomic structures, such as the posterior inter-malleolar ligament (a possible cause of the posterior ankle impingement syndrome) [16]. Therefore, it can be assumed that RA-specific small anatomical structures can also be better detected by means of high-field MRI. Moreover, there is evidence that 3-T is superior to 1.5-T MRI for the detection for bony changes [26]. Owing to the higher

**Table 3** Mean clinical and radiological measures before and after therapy (3- and 6-month follow-up)

| | DAS | CRP | RAMRIS | | | | RAMRIS-5 | | | |
|---|---|---|---|---|---|---|---|---|---|---|
| | | | Edema | Synovitis | Erosion | RAMRIS | Edema | Synovitis | Erosion | RAMRIS-5 |
| t0 | 4.69 | 0.96 | 4.64 | 16.68 | 7.96 | 29.29 | 1.64 | 7.46 | 4.18 | 13.29 |
| t1 | 3.46 | 0.65 | 3.21 | 14.88 | 9.13 | 23.32 | 1.13 | 6.71 | 4.92 | 10.93 |
| t2 | 2.57 | 0.36 | 2.43 | 16.26 | 9.04 | 22.79 | 1.04 | 7.09 | 5.09 | 10.86 |

*Abbreviations*: *CRP* C-reactive protein, *DAS* disease activity score, *RAMRIS* Rheumatoid Arthritis Magnetic Resonance Imaging Score, *RAMRIS-5* Rheumatoid Arthritis Magnetic Resonance Imaging Score for five joints of the hand

spatial resolution at 3 T, bone marrow edema was better assigned to anatomic structures [17], which might help to diagnose early RA. Even though some studies declare low-field imaging to be a good alternative [17], there is no doubt that detailed high-field MRI offers a better image quality compared with low-field imaging [17]. In summary, it can be stated that the anatomically small changes in early RA are better represented by the better spatial resolution and the higher contrast in high-field MRI. If 3-T MRI is available, the higher field strength should be preferred.

As expected, levels of CRP, DAS-28, RAMRIS, and RAMRIS-5 initially showed maximum value and dropped in the 3 months of follow-up under MTX therapy, indicating response to the therapy. Moreover, it confirms RAMRIS/RAMRIS-5 as good monitoring tools. Surprisingly, even though CRP and DAS-28 dropped in the 6 months of follow-up, there was a slight increase in RAMRIS/RAMRIS-5. Consequently (and consistent to the results of Schleich et al.), there was no significant correlation between RAMRIS/RAMRIS-5 and DAS-28 or CRP. Some authors interpret the missing correlation as a result of MRI superiority in detecting RA-associated inflammation compared with clinical assessment or serological parameters [13]. Indeed, it is known that MRI is very sensitive for the detection of even very small pathologies [24]. In fact, Sewerin et al. documented a progression in erosive bone destruction detected by MRI and an increase in the RAMRIS during improvement of DAS-28 or EULAR remission for up to 40% of patients [27]. The missing correlation between RAMRIS/RAMRIS-5 and DAS-28/CRP could demonstrate that there may be a progression of local synovial destructive reaction that is visible by MRI despite clinical response or even remission. In other words, the missing correlation could be a sign of silent progression [18, 28]. It must be mentioned that the very high sensitivity could lead to overinterpretation of MRI-detected pathologies. Hence, several studies could demonstrate high numbers of erosions, even in healthy controls. Boeters et al. recently demonstrated that MRI-detected erosions have to be assessed very carefully, as erosion scores of individual persons with and without RA were largely overlapping, and even RA-specific erosions were found in both groups. This underlines the need for re-evaluating the comparability of the RAMRIS and RAMRIS-5 in high-field MRI [29].

Our study had several limitations. We had a homogenous patient cohort but a fairly small patient number. This is partly a result of the study's strict requirement to include only patients with early RA who were investigated three times. Larger patient cohorts are needed to prove whether RAMRIS-5 is a valid and reliable alternative to the time-consuming RAMRIS for all patients. If it is not, outliers must be identified. It is also necessary to perform further studies to confirm and investigate the lack of correlation between RAMRIS/RAMRIS-5 and CRP/DAS-28 and to show whether a silent progression might be a persuasive explanation.

In summary, this study underlines the former data showing a very high correlation between RAMRIS and RAMRIS-5. It was not yet known that RAMRIS-5 is verified as a good and resource-saving tool for diagnosing and follow-up investigations even in early RA when using high-field (3-T) MRI. RAMRIS-5 presents itself as a score that detects similar changes as the original score with only a slightly higher detection of change in the synovitis subscore. Despite the limitations that a reduced score always has, the RAMRIS-5 shows very good results and is a useful tool in clinical, everyday life because of its great time efficiency.

## Conclusion

RAMRIS-5, the simplified version of the well-established RAMRIS, is a resource-saving, appropriate alternative with an accurate detection of change over time, especially for edema and erosion. It is appropriate not only for patients with established RA but also for those with early RA. In regard to its shorter expenditure of time, there may be a high potential for using RAMRIS-5 in daily clinical practice to detect and monitor RA.

### Abbreviations

ACR: American College of Rheumatology; CI: Confidence interval; CRP: C-reactive protein; csDMARD: Conventional synthetic disease-modifying antirheumatic drug; DAS-28: Disease activity score of 28 joints; EULAR: European League Against Rheumatism; ICC: Intraclass correlation coefficient; MCP: Metacarpophalangeal; MRI: Magnetic resonance imaging; MTX: Methotrexate; OMERACT: Outcome Measures in Rheumatoid Arthritis Clinical Trials; RA: Rheumatoid arthritis; RAMRIS: Rheumatoid Arthritis Magnetic Resonance Imaging Score; RAMRIS-5: Rheumatoid Arthritis Magnetic Resonance Imaging Score for five joints of the hand; SRM: Standardized response mean; TSE: Turbo spin echo

### Acknowledgments

We would like to thank Erika Rädisch for the assistance in receiving the MRI scans.

### Funding

The study was supported by a grant from the German "Bundesministerium für Bildung und Forschung" (BMBF), ArthroMark (01EC1009).

### Availability of data and materials

The datasets used or analyzed (or both) during the current study are available from the corresponding author on reasonable request.

### Authors' contributions

CS, MS, BO, and PS contributed to study design. CS, CG, MS, BO, and PS contributed to study conduct and data collection. MF, CS, RB, DBA, MS, BO, and PS contributed to data interpretation. PS contributed to drafting the manuscript. MF, CS, RB, DBA, CG, MS, BO, and PS contributed to data analysis and to revising manuscript content and they take responsibility for the integrity of the data analysis. All authors read and approved the final manuscript.

#### Ethics approval and consent to participate
Ethic approval was given by the ethics committee of the Heinrich-Heine University of Düsseldorf (reference number 3483) and the Charité Berlin (EA1/193/10). Written informed consent was obtained from all patients before enrollment.

#### Consent for publication
All authors read, revised, and approved the final manuscript.

#### Competing interests
The authors declare that they have no competing interests.

## Publisher's Note


#### Author details
[1]Department for Diagnostic and Interventional Radiology, UKD, Heinrich-Heine University Düsseldorf, Moorenstrasse 5, 40225 Düsseldorf, Germany. [2]Department and Hiller Research Unit for Rheumatology, UKD, Heinrich-Heine University Düsseldorf, Moorenstrasse 5, 40225 Düsseldorf, Germany.

Received: 11 May 2018 Accepted: 7 December 2018
Published online: 14 January 2019

#### References
1. Akdemir G, Heimans L, Bergstra SA, Goekoop RJ, van Oosterhout M, van Groenendael J, et al. Clinical and radiological outcomes of 5-year drug-free remission-steered treatment in patients with early arthritis: IMPROVED study. Ann Rheum Dis. 2018;77:111–8.
2. Combe B, Landewe R, Daien CI, Hua C, Aletaha D, Alvaro-Gracia JM, et al. 2016 update of the EULAR recommendations for the management of early arthritis. Ann Rheum Dis. 2017;76:948–59.
3. Nell VPK, Machold KP, Eberl G, Stamm TA, Uffmann M, Smolen JS. Benefit of very early referral and very early therapy with disease-modifying anti-rheumatic drugs in patients with early rheumatoid arthritis. Rheumatology. 2004;43:906–14.
4. Moura CS, Abrahamowicz M, Beauchamp ME, Lacaille D, Wang YS, Boire G, et al. Early medication use in new-onset rheumatoid arthritis may delay joint replacement: results of a large population-based study. Arthritis Res Ther. 2015;17:197.
5. Espinoza F, Fabre S, Pers YM. Remission-induction therapies for early rheumatoid arthritis: evidence to date and clinical implications. Ther Adv Musculoskelet Dis. 2016;8:107–18.
6. Smolen JS, Landewe R, Bijlsma J, Burmester G, Chatzidionysiou K, Dougados M, et al. EULAR recommendations for the management of rheumatoid arthritis with synthetic and biological disease-modifying antirheumatic drugs: 2016 update. Ann Rheum Dis. 2017;76:960–77.
7. Combe B, Landewe R, Lukas C, Bolosiu HD, Breedveld F, Dougados M, et al. EULAR recommendations for the management of early arthritis: report of a task force of the European Standing Committee for International Clinical Studies Including Therapeutics (ESCISIT). Ann Rheum Dis. 2007;66:34–45.
8. Aletaha D, Neogi T, Silman AJ, Funovits J, Felson DT, Bingham CO 3rd, et al. 2010 rheumatoid arthritis classification criteria: an American College of Rheumatology/European League Against Rheumatism collaborative initiative. Ann Rheum Dis. 2010;69:1580–8.
9. Machold KP, Stamm TA, Eberl GJ, Nell VK, Dunky A, Uffmann M, et al. Very recent onset arthritis--clinical, laboratory, and radiological findings during the first year of disease. J Rheumatol. 2002;29:2278–87.
10. Sanmarti R, Gomez-Centeno A, Ercilla G, Larrosa M, Vinas O, Vazquez I, et al. Prognostic factors of radiographic progression in early rheumatoid arthritis: a two year prospective study after a structured therapeutic strategy using DMARDs and very low doses of glucocorticoids. Clin Rheumatol. 2007;26:1111–8.
11. Ostergaard M, Edmonds J, McQueen F, Peterfy C, Lassere M, Ejbjerg B, et al. An introduction to the EULAR-OMERACT rheumatoid arthritis MRI reference image atlas. Ann Rheum Dis. 2005;64(Suppl 1):i3–7.
12. McQueen FM, Ostendorf B. What is MRI bone oedema in rheumatoid arthritis and why does it matter? Arthritis Res Ther. 2006;8:222.
13. Schleich C, Buchbender C, Sewerin P, Miese F, Aissa J, Brinks R, et al. Evaluation of a simplified version of the Rheumatoid Arthritis Magnetic Resonance Imaging Score (RAMRIS) comprising 5 joints (RAMRIS5). Clin Exp Rheumatol. 2015;33:209–15.
14. Rinck PA, Muller RN. Field strength and dose dependence of contrast enhancement by gadolinium-based MR contrast agents. Eur Radiol. 1999;9:998–1004.
15. Loew R, Kreitner KF, Runkel M, Zoellner J, Thelen M. MR arthrography of the shoulder: comparison of low-field (0.2 T) vs high-field (1.5 T) imaging. Eur Radiol. 2000;10:989–96.
16. Sutera R, Bianco A, Paoli A, Padulo J, Thomas E, Iovane A, et al. Identification of normal and pathological posterior inter-malleolar ligament with dedicated high-field vs low-field MRI. A pilot study. Muscles Ligaments Tendons J. 2015;5:12–7.
17. Wieners G, Detert J, Streitparth F, Pech M, Fischbach F, Burmester G, et al. High-resolution MRI of the wrist and finger joints in patients with rheumatoid arthritis: comparison of 1.5 Tesla and 3.0 Tesla. Eur Radiol. 2007;17:2176–82.
18. Sewerin P, Buchbender C, Vordenbaumen S, Scherer A, Miese F, Brinks R, et al. Advantages of a combined rheumatoid arthritis magnetic resonance imaging score (RAMRIS) for hand and feet: does the RAMRIS of the hand alone underestimate disease activity and progression? BMC Musculoskelet Disord. 2014;15:104.
19. Ostergaard M, Peterfy C, Conaghan P, McQueen F, Bird P, Ejbjerg B, et al. OMERACT rheumatoid arthritis magnetic resonance imaging studies. Core set of MRI acquisitions, joint pathology definitions, and the OMERACT RA-MRI scoring system. J Rheumatol. 2003;30:1385–6.
20. Cyteval C, Miquel A, Hoa D, Daures JP, Mariette X, Combe B. Rheumatoid arthritis of the hand: monitoring with a simplified MR imaging scoring method--preliminary assessment. Radiology. 2010;256:863–9.
21. Østergaard M, Emery P, Conaghan PG, Fleischmann R, Hsia EC, Xu W, et al. Significant improvement in synovitis, osteitis, and bone erosion following golimumab and methotrexate combination therapy as compared with methotrexate alone: a magnetic resonance imaging study of 318 methotrexate-naive rheumatoid arthritis patients. Arthritis Rheum. 2011;63:3712–22.
22. Fleming A, Benn RT, Corbett M, et al. Early rheumatoid disease. II. Patterns of joint involvement. Ann Rheum Dis. 1976;35:361-64.
23. Taouli B, Zaim S, Peterfy CG, Lynch JA, Stork A, Guermazi A, et al. Rheumatoid arthritis of the hand and wrist: comparison of three imaging techniques. AJR Am J Roentgenol. 2004;182:937–43.
24. Colebatch AN, Edwards CJ, Ostergaard M, van der Heijde D, Balint PV, D'Agostino MA, et al. EULAR recommendations for the use of imaging of the joints in the clinical management of rheumatoid arthritis. Ann Rheum Dis. 2013;72:804–14.
25. Ejbjerg BJ, Narvestad E, Jacobsen S, Thomsen HS, Østergaard M. Optimised, low cost, low field dedicated extremity MRI is highly specific and sensitive for synovitis and bone erosions in rheumatoid arthritis wrist and finger joints: comparison with conventional high field MRI and radiography. Ann Rheum Dis. 2005;64:1280–7.
26. Sormaala MJ, Ruohola JP, Mattila VM, Koskinen SK, Pihlajamaki HK. Comparison of 1.5T and 3T MRI scanners in evaluation of acute bone stress in the foot. Bmc Musculoskel Dis. 2011;12:128.
27. Sewerin P, Vordenbaeumen S, Hoyer A, Brinks R, Buchbender C, Miese F, et al. Silent progression in patients with rheumatoid arthritis: is DAS28 remission an insufficient goal in RA? Results from the German Remission-plus cohort. BMC Musculoskelet Disord. 2017;18:163.
28. Baker JF, Ostergaard M, Emery P, Hsia EC, Lu JD, Baker DG, et al. Early MRI measures independently predict 1-year and 2-year radiographic progression in rheumatoid arthritis: secondary analysis from a large clinical trial. Ann Rheum Dis. 2014;73:1968–74.
29. Boeters DM, Nieuwenhuis WP, van Steenbergen HW, Reijnierse M, Landewe RBM, van der Helm-van Mil AHM. Are MRI-Detected Erosions Specific for RA? a Large Explorative Cross-Sectional Study. Ann Rheum Dis. 2018;77:861–8.

The Journal of Rheumatology

# Synovial perfusion assessed by dynamic contrast-enhanced MRI is associated to treatment response, remission, and cartilage quality in rheumatoid arthritis

Philipp Sewerin, Christoph Schleich, Ralph Brinks, Anja Müller-Lutz, Florian Fichter, Markus Eichner, Matthias Schneider, Benedikt Ostendorf and Stefan Vordenbäumen

DOI: 10.3899/jrheum.180832
http://www.jrheum.org/content/early/2019/03/11/jrheum.180832

# Synovial perfusion assessed by dynamic contrast-enhanced MRI is associated to treatment response, remission, and cartilage quality in rheumatoid arthritis

Philipp Sewerin[1#], Christoph Schleich[2#], Ralph Brinks[1], Anja Müller-Lutz[2], Florian Fichter[2], Markus Eichner[2], Matthias Schneider[1], Benedikt Ostendorf[1], Stefan Vordenbäumen[1]

[1] Heinrich-Heine-University Düsseldorf, Medical Faculty, Department and Hiller-Research-Unit for Rheumatology, 40225 Dusseldorf, Germany

[2] Heinrich-Heine-University Düsseldorf, Medical Faculty, Department of Diagnostic and Interventional Radiology, 40225 Dusseldorf, Germany

# equal contribution

PS: Philipp.Sewerin@med.uni-duesseldorf.de; CS: Christoph.Schleich@med.uni-duesseldorf.de; RB: Ralph.Brinks@med.uni-duesseldorf.de; AML; Anja.Lutz@med.uni-duesseldorf.de; FF: Florian.Fichter@uni-duesseldorf.de; ME: Markus.Eichner@uni-duesseldorf.de; MS: Matthias.Schneider@med.uni-duesseldorf.de; BO: Ostendorf@med.uni-duesseldorf.de; SV: Stefan.Vordenbaeumen@med.uni-duesseldorf.de

**Corresponding author**: Dr. Philipp Sewerin, Heinrich-Heine-University Düsseldorf, Medical Faculty, Department and Hiller-Research-Unit for Rheumatology, Moorenstrasse 5, 40225 Duesseldorf, Germany, E-mail: philipp.sewerin@med.uni-duesseldorf.de, Phone: +49 211 811 7817, Fax: +49 211 811 9206

**Keywords**: Rheumatoid Arthritis, Remission, Response, Prediction, Cartilage

**Key messages**: Synovial perfusion measured by DCE-MRI relates to therapy response and remission in early RA patients. High scores in DCE-MRI perfusion were significantly associated to a lower cartilage quality.

**Abstract**

**Objective:** To assess associations of synovial perfusion, cartilage quality and outcome in rheumatoid arthritis (RA).

**Methods:** Synovial perfusion and cartilage quality were assessed by dynamic contrast-enhanced magnetic resonance imaging in metacarpophalangeal joints of 28 treatment-naïve RA patients at baseline, 3 and 6 months after methotrexate. Analysis was by linear mixed modelling.

**Results:** Synovial perfusion parameters were associated to remission ($p<0.05$) and cartilage quality ($p<0.004$). Maximum synovial enhancement was associated to EULAR response ($p<0.05$). Synovial perfusion improved in non-responders over time ($p<0.05$).

**Conclusion:** Synovial perfusion relates to remission, response, and cartilage quality in a cohort of therapy naïve, early RA patients.

**Introduction**

Dynamic contrast-enhanced magnetic resonance imaging (DCE-MRI) in rheumatoid arthritis (RA) permits assessment of synovial perfusion and reflects histological signs of synovitis in RA (1) and relate to systemic disease activity (2). Hence, DCE-MRI theoretically offers the possibility for an objective evaluation of disease activity. Current response criteria partially rely on patient reported outcomes, e.g. a patient global and reported joint pain informing the DAS28 (3). This may result in overestimation of disease activity (3), even though the subjective components are sensitive to change (4). Conversely, undertreatment of patients which show a progressive disease course despite clinical remission may also occur, a situation sometimes referred to as 'silent progression' (5). Moreover, growing evidence suggests that early and continuing cartilage damage is of paramount importance in the pathogenesis of RA (6). Cartilage damage in turn can be assessed in finger joints of RA patients by non-invasive means employing delayed Gadolinium-enhancement MRI (dGEMRIC), for instance (7).

We therefore assessed active, treatment-naïve RA patients, who were started on methotrexate therapy by MRI in order to determine how DCE-MRI relates to remission, response, and cartilage quality.

## Methods

*Patients and protocol*

Treatment-naïve patients with RA according to 2016 ACR/EULAR criteria (n = 28, mean age 55 ± 11.4 years, 19 female,disease duration ≤ 6month, Ø 16.3 weeks; min. 2 weeks, max. 23 weeks; all patients were pos. for Rheumatoid Factor (Ø RF 215 IU/ml; Min 24, Max 2314 IU/ml and CCP Antibodies (Ø CCP antibodies 131 U/ml; Min 5, Max >200 U/ml); DAS28 baseline Ø 4.7 (SD 0.85; Min 3.3, Max 6.3); DAS28 3 month Ø 3.5 (SD1.3, Min 1.6, Max 6.2); DAS28 6 month Ø 2.6 (SD 0.83,Min 1.6, Max 4.8) from the outpatient department of Heinrich-Heine-University Düsseldorf, Germany were consecutively enrolled. DAS28 with CRP, and an MRI of the dominantly involved hand were assessed at baseline, and at 3 and 6 months after initiation of methotrexate therapy (15 mg s.c. weekly). Exclusion criteria consisted in pregnancy, age < 18 years, claustrophobia, contraindications for either MRI (e.g. metal implants) or Gadolinium (e.g. allergy). Treatment response and remission were defined according to EULAR criteria. The study was approved by the Ethics Committee of the Medical Faculty of Heinrich-Heine-University Düsseldorf, Germany (study number 3828). All patients provided written informed consent.

*MRI protocol*

3-Tesla MRI (Magnetom Trio A Tim System; Siemens Healthcare, Erlangen, Germany) was used to obtain DCE-MRI and dGEMRIC scans of MCP joints 2 and 3. DCE-MRI imaging was performed with a multi-slice T1-weighted turbo-flash sequence (8). The contrast agent (Gd-DTPA, Magnevist; Schering) was applied twenty seconds after the sequence start as previously described (7). Briefly, maximum contrast enhancement (ME), maximum synovial volume (MV), and rate of contrast enhancement after 17s (RE) were calculated for further analyses.

dGEMRIC imaging sequences were obtained 40 minutes after injection of 0.4 mL/kg body weight gadolinium. 3D FLASH imaging was performed, as previously described (8). MRI protocols including data processing are detailed in supplement 1. MRI investigators (CS, AML, FF, ME) were blinded to the clinical information and other imaging information such as sonography or conventional x-rays.

*Statistical analysis*

Linear mixed modelling with a random intercept for patient identity and adjustments for age and gender were performed with DCE-MRI parameters (ME, MV, RE) as the dependent variables, and remission or response, and the time point as independent variables. Additionally, dGEMRIC values were used as dependent with DCE-MRI parameters as independent variables along with the above adjustments. A p-value $< 0.05$ was considered significant. In order to verify model assumptions, we relied on inspection of (1) plotting model residuals vs. predicted value to check for linearity, (2) qq-ploting to check for normal distribution of residuals, (3) leverage plotting with ANOVA to check for homogeneity of variance. All statistical analyses were performed with the statistical software R, version 3.4.1 (The R Foundation for Statistical Computing).

**Results**

In order to measure synovial perfusion, DCE-MRI was conducted. Distinct parameters related to contrast enhancement (MV, ME, RE) were used for further analyses. EULAR remission criteria were met by 5 patients (17.9%) at 3 months, and 12 patients (42.9%) at 6 months. Remission was associated to significantly lower values for all DCE-MRI parameters in both joints assessed, with the highest magnitude of effect for ME (table 1a) (figures 1 and 2).

EULAR moderate or good response criteria were met by 7 (25%) and 9 (32.1%) patients at 3 months, and by 2 (7.1%) and 10 (35.7%) patients at 6 months, respectively. Any treatment response (good or moderate) was associated to lower ME, but not MV or RE in both joints (table 1a). Next, cartilage quality was assessed by dGEMRIC and compared to DCE-MRI. High scores in any DCE-MRI perfusion parameter were significantly associated to a lower cartilage quality, with the highest magnitude of effect for MV and RE (table 1a).

EULAR remission and response incorporate subjective measures such as tender joint count and patient global assessment. We were therefore interested in the time course of perfusion in patients not satisfying remission or response criteria under methotrexate therapy. All DCE-MRI parameters improved over time under methotrexate therapy even in patients not satisfying remission or treatment response criteria. This association was significant for both joints and all parameters assessed with the exception of a borderline significance for ME in MCP3 joints in association to response (table 1b).

**Discussion**

Histological synovial inflammation, especially sublining CD68 macrophages range amongst the best parameters to detect treatment response in RA. These markers do not seem to be influenced by placebo effects (9). However, the determination of synovial inflammation by histological means is limited by the necessity of invasive procedures. We have previously shown that DCE-MRI reflects histological signs of synovitis in RA (1) and may therefore potentially substitute invasive techniques. Our current study expands on this knowledge by demonstrating that DCE-MRI parameters consistently relate to remission and response as defined by the compound measures DAS28 according to EULAR definition.

Of the different DCE-MRI parameters assessed, ME was the only significant predictor of response, while remission was predicted by MV and RE as well. Of note, the magnitude of effect (represented by the 'Estimate' in table 1) was consistently highest for ME which suggests that ME is the best parameter for determination of treatment response and remission. Conversely, cartilage quality (dGEMRIC) was more closely associated to RE or MV as opposed to ME ('Estimate' in the 'dGEMRIC' columns of table 1a). Thus, our data suggest that the different perfusion parameters are complementary in their information on synovial perfusion and cartilage quality.

We previously reported that patients in clinical remission or responding to therapy may show a progressive disease course when additionally analyzed by MRI, a situation also referred to as silent progression (5). Interestingly, our current results suggest that the opposite may hold true as well: patients who did not reach remission according to clinical criteria showed reduced synovial perfusion over time. We speculate that this is a consequence of treatment effectivity as opposed to the natural course of the disease. A number of subgroup analyses of randomized controlled trials with the use of DCE-MRI sequences support this notion (10–12).

In contrast, MRI may also unmask erosive disease in successfully treated patients (13) and bone marrow edema is a major risk factor for future erosive disease (14). Thus, MRI may help to prevent both over- and undertreatment of RA patients. Of note, our assumptions are based on previous literature and the results presented. The generalizability of our data is however limited due to the small sample size. Hence, more data is needed before firm conclusions can be drawn in this regard. Furthermore, whether remission defined by MRI more accurately predicts favorable outcomes (e.g. functionality, erosive disease on conventional x-rays) than established and validated clinical criteria such as the DAS28 is under debate (15). The increased costs of an MRI-based outcome criterion as opposed to a clinical criterion also have to be kept in mind. Additionally, our protocol involved the application of gadolinium as a contrast agent and concerns have been raised concerning the safety of gadolinium use (16). However, contrast free sequences are being developed and may render the use of gadolinium unnecessary for some indications of MRI in the future (17).

Growing evidence suggests that cartilage injury is paramount in the perpetuation of RA and potentially even a key inciting component in RA pathogenesis (6). The current study supports this concept by demonstrating that proteoglycan loss evidenced by a reduced dGEMRIC index is associated to increased synovial perfusion in early RA patients. We did not find improved cartilage quality in either remitting patients, responding patients, or in the time-course under methotrexate therapy, however. This may reflect a lack of cartilage repair despite effective treatment over time (18). The functional long-term impact of reduced cartilage quality is well documented (18,19), emphasizing the importance to protect cartilage integrity.

In conclusion, synovial tissue perfusion relates to remission, response, and cartilage quality assessed by MRI in a cohort of therapy-naïve, early RA patients.

**Declarations**

**Availability of supporting data:** The datasets used and/or analysed during the current study are available from the corresponding author on reasonable request.

**Competing interests:** The authors declare that they have no competing interests.

**Funding:** The study was supported by a grant from the German "Bundesministerium fur Bildung und Forschung"(BMBF), ArthroMark (01EC1009)

**Authors' contributions:** Study design: PS, CS, RB, MS, BO and SV. Study conduct: PS, CS, BO and SV. Data collection: PS, CS, RB, MS, BO and SV. Data analysis: PS, CS, RB, AML, FF, ME, MS, BO and SV. Data interpretation: PS, CS, RB, AML, FF, ME, MS, BO and SV. Drafting manuscript: PS and SV. Revising manuscript content PS, CS, RB, AML, FF, ME, MS, BO and SV take responsibility for the integrity of the data analysis. All authors read and approved the final manuscript.

**Acknowledgements:** We would like to thank Erika Radisch for the assistance in receiving the MRI-scans.

## References


1. Vordenbäumen S, Schleich C, Lögters T, Sewerin P, Bleck E, Pauly T, et al. Dynamic contrast-enhanced magnetic resonance imaging of metacarpophalangeal joints reflects histological signs of synovitis in rheumatoid arthritis. Arthritis Res Ther 2014;16:452.

2. Vordenbäumen S, Sewerin P, Lögters T, Miese F, Schleich C, Bleck E, et al. Inflammation and vascularisation markers of arthroscopically-guided finger joint synovial biospies reflect global disease activity in rheumatoid arthritis. Clin Exp Rheumatol 2014;32:117-20.

3. Son KM, Lee SY, Seo YI, Choi J-E, Kim HA. Contribution of subjective Disease Activity Score 28 (DAS28) components to the response to treatment of rheumatoid arthritis. Clin Rheumatol 2017;36:1221-7.

4. Jurgens MS, Overman CL, Jacobs JWG, Geenen R, Cuppen BVJ, Marijnissen ACA, et al. Contribution of the subjective components of the disease activity score to the response to biologic treatment in rheumatoid arthritis. Arthritis Care Res 2015;67:923-8.

5. Sewerin P, Vordenbaeumen S, Hoyer A, Brinks R, Buchbender C, Miese F, et al. Silent progression in patients with rheumatoid arthritis: is DAS28 remission an insufficient goal in RA? Results from the German Remission-plus cohort. BMC Musculoskelet Disord 2017;18:163.

6. Pap T, Korb-Pap A. Cartilage damage in osteoarthritis and rheumatoid arthritis--two unequal siblings. Nat Rev Rheumatol 2015;11:606-15.

7. Miese F, Buchbender C, Scherer A, Wittsack H-J, Specker C, Schneider M, et al. Molecular imaging of cartilage damage of finger joints in early rheumatoid arthritis with delayed gadolinium-enhanced magnetic resonance imaging. Arthritis Rheum 2012;64:394-9.

8. Schleich C, Müller-Lutz A, Sewerin P, Ostendorf B, Buchbender C, Schneider M, et al. Intra-individual assessment of inflammatory severity and cartilage composition of finger joints in rheumatoid arthritis. Skeletal Radiol 2015;44:513-8.

9. de Hair MJH, Harty LC, Gerlag DM, Pitzalis C, Veale DJ, Tak PP. Synovial tissue analysis for the discovery of diagnostic and prognostic biomarkers in patients with early arthritis. J Rheumatol 2011;38:2068-72.

10. Beals C, Baumgartner R, Peterfy C, Balanescu A, Mirea G, Harabagiu A, et al. Magnetic resonance imaging of the hand and wrist in a randomized, double-blind, multicenter, placebo-controlled trial of infliximab for rheumatoid arthritis: Comparison of dynamic contrast enhanced assessments with semi-quantitative scoring. PloS One 2017;12:e0187397.

11. Waterton JC, Ho M, Nordenmark LH, Jenkins M, DiCarlo J, Guillard G, et al. Repeatability and response to therapy of dynamic contrast-enhanced magnetic resonance imaging biomarkers in rheumatoid arthritis in a large multicentre trial setting. Eur Radiol 2017;27:3662-8.

12. Conaghan PG, Østergaard M, Bowes MA, Wu C, Fuerst T, van der Heijde D, et al. Comparing the effects of tofacitinib, methotrexate and the combination, on bone marrow oedema, synovitis and bone erosion in methotrexate-naive, early active rheumatoid arthritis: results of an exploratory randomised MRI study incorporating semiquantitative and quantitative techniques. Ann Rheum Dis 2016;75:1024-33.

13. Tamai M, Kawakami A, Uetani M, Takao S, Arima K, Iwamoto N, et al. A prediction rule for disease outcome in patients with undifferentiated arthritis using magnetic resonance imaging of the wrists and finger joints and serologic autoantibodies. Arthritis Rheum 2009;61:772-8.

14. Haavardsholm EA, Lie E, Lillegraven S. Should modern imaging be part of remission criteria in rheumatoid arthritis? Best Pract Res Clin Rheumatol 2012;26:767-85.

15. van Tuyl LHD, Felson DT, Wells G, Smolen J, Zhang B, Boers M, et al. Evidence for predictive validity of remission on long-term outcome in rheumatoid arthritis: a systematic review. Arthritis Care Res 2010;62:108-17.

16. Runge VM. Critical Questions Regarding Gadolinium Deposition in the Brain and Body After Injections of the Gadolinium-Based Contrast Agents, Safety, and Clinical Recommendations in Consideration of the EMA's Pharmacovigilance and Risk Assessment Committee Recommendation for Suspension of the Marketing Authorizations for 4 Linear Agents. Invest Radiol 2017;52:317-23.

17. Rehnitz C, Kupfer J, Streich NA, Burkholder I, Schmitt B, Lauer L, et al. Comparison of biochemical cartilage imaging techniques at 3 T MRI. Osteoarthritis Cartilage 2014;22:1732-42.

18. Schett G, Coates LC, Ash ZR, Finzel S, Conaghan PG. Structural damage in rheumatoid arthritis, psoriatic arthritis, and ankylosing spondylitis: traditional views, novel insights gained from TNF blockade, and concepts for the future. Arthritis Res Ther 2011;13 Suppl 1:S4.

19. Hayer S, Bauer G, Willburger M, Sinn K, Alasti F, Plasenzotti R, et al. Cartilage damage and bone erosion are more prominent determinants of functional impairment in longstanding experimental arthritis than synovial inflammation. Dis Model Mech 2016;9:1329-38.

**Figure 1**

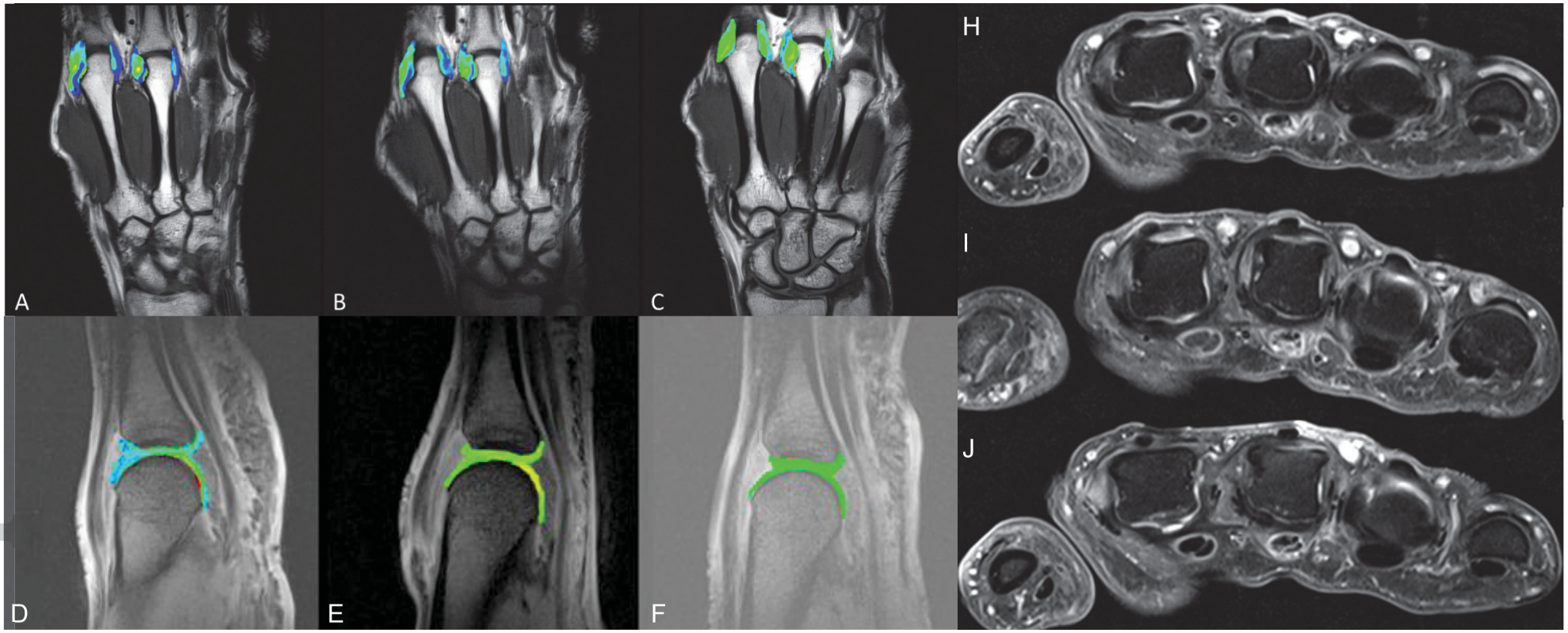

**Figure 2:**

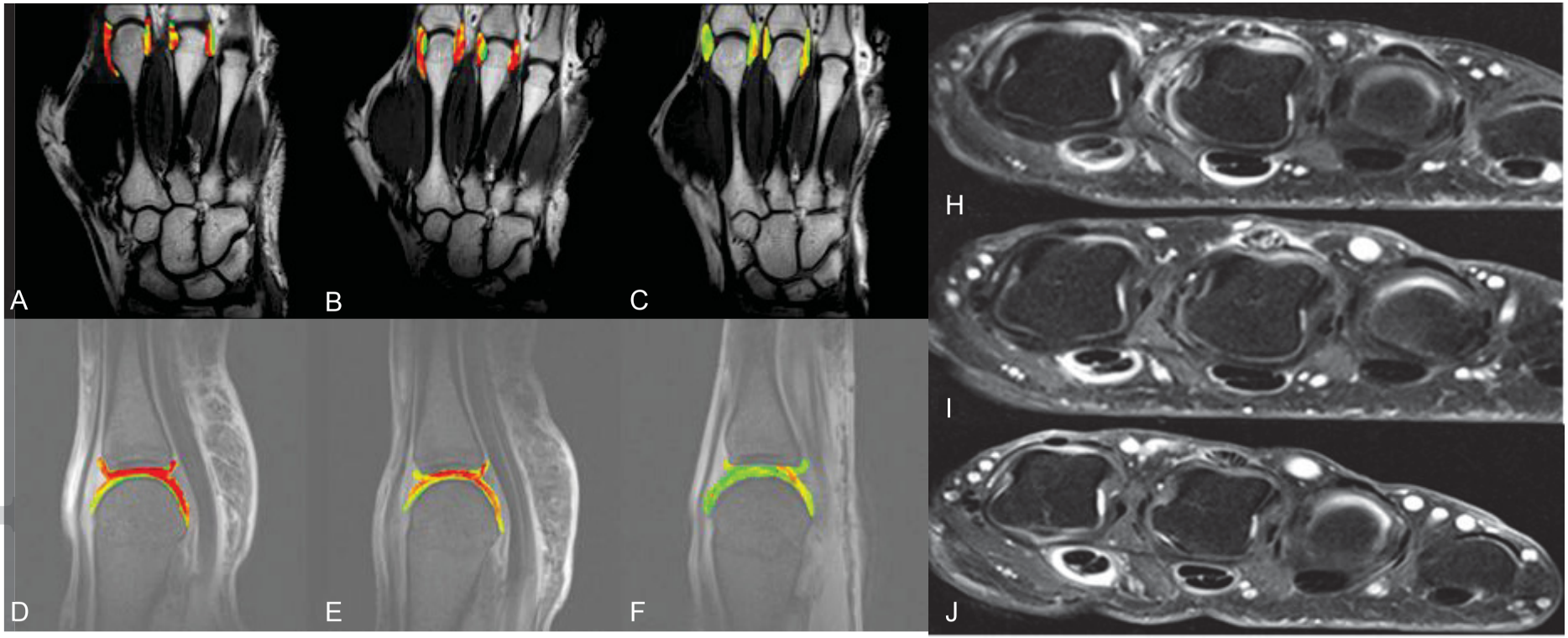

**Figure Legends**

**Fig. 1.** Picture **A - C:** Overlay of native T1 image of digitus 2 and 3 with colour-coded map of dynamic MRI from blue - low perfusion to red - high perfusion of MCP D2 and D3. Picture A demonstrated the perfusion of MCP joints at baseline MRI prior to MTX therapy, picture B and C showed the perfusion after 3 and 6 months after MTX therapy. In this example, we found higher perfusion after 3 and 6 months compared to baseline MRI for both MCP joints. Picture D - F showed a colour-coded dGEMRIC map of MCP D2 from blue - high GAG content to red - low GAG content. In correlation with dynamic MRI, dGEMRIC analysis demonstrated an increasing GAG loss after 3 and 6 months after MTX therapy (picture E and F) compared to baseline MRI (picture D) in this case. Picture H – J illustrated axial fat suppressed T1 images after application of contrast agent of MCP joints. Morphological synovitis subscore according to RAMRIS showed moderate synovitis at baseline and after 3 months MTX therapy of MCP D2 (picture H and I). 6 months after MTX therapy, we found high synovitis subscore in MCP D2 (picture J) in this patient. This is in accordance with our analysis demonstrating a significant correlation of perfusion and synovitis subscore 6 months after the beginning of MTX therapy.

**Fig. 2.** Picture A – C: Overlay of native T1 image of digitus 2 and 3 with colour-coded map of dynamic MRI from blue - low perfusion to red - high perfusion of MCP D2 and D3. Picture A demonstrated the perfusion of MCP joints at baseline MRI prior to MTX therapy, picture B and C showed the perfusion after 3 and 6 months after MTX therapy. In this example, we found higher perfusion at baseline MRI compared to follow up measurements after 3 and 6 months initiating MTX therapy. Picture D – F showed colour-coded dGEMRIC map of MCP D2 from blue - high GAG content to red - low GAG content. In correlation with dynamic

MRI, dGEMRIC analysis demonstrated lower dGEMRIC index after 3 and 6 months initiating MTX therapy (picture E and F) compared to baseline MRI (picture D) in this case. Picture H – J illustrated axial fat suppressed T1 images after application of contrast agent of MCP joints. Morphological synovitis subscore according to RAMRIS showed high synovitis of MCP D2-D4 at baseline MRI (picture H). After 3 and 6 months MTX therapy, we found lower synovitis subscore in MCP D2 - D4 (picture I and J) in this patient.

Table 1

A

| Joint | DCI-MRI | Remission | | | Response | | | dGEMRIC | | |
|---|---|---|---|---|---|---|---|---|---|---|
| | | E | SE | P | E | SE | P | E | SE | P |
| MCP2 | ME | -15.6 | 6.7 | 0.02 | -48.5 | 22.5 | 0.03 | -0.8 | 0.2 | <0.0001 |
| | MV | -0.5 | 0.2 | 0.01 | -1-3 | 0.8 | 0.09 | -18.1 | 4.9 | <0.001 |
| | RE | -0.3 | 0.2 | 0.04 | -0.9 | 0.6 | 0.11 | -31.5 | 6.3 | <0.0001 |
| MCP3 | ME | -8.7 | 3.8 | 0.02 | -28.4 | 13.5 | 0.03 | -1.1 | 0.3 | <0.0001 |
| | MV | -0.4 | 0.2 | 0.02 | -0.6 | 0.6 | 0.28 | -24.7 | 8.6 | 0.004 |
| | RE | -0.3 | 0.1 | <0.01 | -0.5 | 0.4 | 0.23 | -38.4 | 11.6 | <0.001 |

B

| Joint | DCI-MRI | Non-remission with MTX over time | | | Non-response with MTX over time | | |
|---|---|---|---|---|---|---|---|
| | | E | SE | P | E | SE | P |
| MCP2 | ME | -15.6 | 6.7 | 0.02 | -15.5 | 7.0 | 0.03 |
| | MV | -0.6 | 0.2 | 0.01 | -0.7 | 0.2 | 0.005 |
| | RE | -0.3 | 0.2 | 0.04 | -0.4 | 0.2 | 0.02 |
| MCP3 | ME | -8.7 | 3.8 | 0.02 | -7.7 | 4.0 | 0.06 |
| | MV | -0.4 | 0.2 | 0.02 | -0.4 | 0.2 | 0.02 |
| | RE | -0.3 | 0.1 | 0.009 | -0.3 | 0.1 | 0.01 |

**Table 1**

**A.** Associations of synovial perfusion imaging with outcome and cartilage quality. Dynamic contrast-enhanced MRI (DCE-MRI) was used to calculate maximum synovial enhancement (ME), maximum synovial volume (MV) and the rate of synovial enhancement (RE) in metacarpophalangeal (MCP) 2 and 3 joints of 28 rheumatoid arthritis patients. DCI-MRI parameters were associated with EULAR remission, EULAR good or moderate vs. no response, and cartilage quality (delayed Gadolinium enhancement (dGEMRIC)) by linear mixed modelling (E, estimate; SE, standard error; P, p-value).

**B** Time course of synovial perfusion in non-remitting or non-responding patients receiving methotrexate. Dynamic contrast-enhanced MRI (DCI-MRI) was used to calculate maximum synovial enhancement (ME), maximum synovial volume (MV) and the rate of synovial enhancement (RE) in metacarpophalangeal (MCP) 2 and 3 joints of non-remitting or non-responding rheumatoid arthritis patients according to EULAR criteria who received methotrexate therapy. Associations according to linear mixed modelling (E, estimate; SE, standard error; P, p-value).